



The Chemical Synthesis of Aliphatic Benzo[*b*][1,4]dioxepin-3-one Analogues Related to Synthetic Marine Odorants

A thesis submitted in fulfilment of the requirements for the degree of
Doctor of Philosophy

Christopher Mark Plummer

B. Sci. (App. Sci.)

B. Sci. (App. Sci.) (Hons)

School of Applied Sciences
College of Science Engineering and Health
RMIT University

January 2016

Declaration

I certify that except where due acknowledgement has been made, the work is that of the author alone; the work has not been submitted previously, in whole or in part, to qualify for any other academic award; the content of the thesis is the result of work which has been carried out since the official commencement date of the approved research program; any editorial work, paid or unpaid, carried out by a third party is acknowledged; and, ethics procedures and guidelines have been followed.

Christopher Mark Plummer

11/1/2016

This thesis is dedicated to my parents, Lisa and Mark.

Publications

Sections of the work presented in this thesis have appeared elsewhere:

Refereed Journal Publications:

C. M. Plummer, R. Gericke, P. Kraft, A. Raynor, J. Froese, T. Hudlický, T. J. Rook, O. A. H. Jones, H. M. Hügel, Synthesis of Saturated Benzodioxepinone Analogues: Insight into the Importance of the Aromatic Ring Binding Motif for Marine Odorants, *Eur. J. Org. Chem.* **2015**, 486-495.

C. M. Plummer, P. Kraft, J. Froese, T. Hudlický, T. J. Rook, O. A. H. Jones, H. M. Hügel, Synthesis and Olfactory Properties of 2-Substituted and 2,3-Annulated 1,4-Dioxepan-6-ones, *Asian J. Org. Chem.* **2015**, 4, 1075-1084.

Conference Poster Presentations:

2013 Flavours and Fragrances – Leipzig, Germany.

C. M. Plummer, R. Gericke, T. J. Rook, H. M. Hügel. Towards the synthesis of new marine fragrances: The synthesis of chiral aliphatic benzodioxepinone derivatives.

2014 Belgian Organic Synthesis Symposium (BOSS-XIV) – Louvain-la-Neuve, Belgium.

C. M. Plummer, R. Gericke, T. J. Rook, O. A. H. Jones, H. M. Hügel. Towards the synthesis of new fragrances: The synthesis of chiral aliphatic benzodioxepinone analogues.

2014 Royal Australian Chemical Institute (RACI) National Congress – Adelaide, Australia.

C. M. Plummer, R. Gericke, T. J. Rook, O. A. H. Jones, H. M. Hügel. Towards the synthesis of new fragrances: The synthesis of chiral aliphatic benzodioxepinone analogues.

Contents

Statement of Authenticity	I
Dedication	II
Publications.....	III
Contents.....	IV
Acknowledgements	V
Abbreviations	VII
Abstract.....	VIII
Table of Contents.....	IX
List of Figures.....	XII
List of Schemes.....	XVI
List of Tables.....	XIX
1 Introduction	1
2 Synthesis of Hexahydrobenzo[<i>b</i>][1,4]dioxepin-3-one Stereoisomers.....	48
3 Synthesis of Additional Analogues of the Aliphatic Benzo[<i>b</i>][1,4]dioxepin-3-one System	107
4 Synthesis of 2-Substituted and 2,3-Annulated 1,4-Dioxepan-6-ones.....	151
5 Studies Towards the Synthesis of Isocyclemonone Analogues	194
6 Conclusions and Recommendation for Future Research	211
Appendixes	217

Acknowledgements

I would first like to thank my parents, Mark and Lisa, for their ongoing support and love. I owe every bit of my success, past and future, to their never ending support. Without them this thesis would not even be a possibility. I would be in a very different place without their support. This thesis is dedicated to them.

I would also like to thank the rest of my family and extended family for their support. In particular; my brother Matt for always being there for me and for being the best little brother that I could have asked for, and my Uncle Kenny for always caring, supporting and keeping an eye on me. I would also like to thank my Nanna Ann, Aunty Lorraine and Cousin Madeleine for their support and love, and for getting me out of the house when things weren't so great. I also need to thank my two pets, Houdini and Spunky, as they both always managed to cheer me up every time I needed them.

A big thank you to my supervisor Associate Professor Helmut Hügel for supporting and supervising me throughout the duration of my PhD candidature, as well as my honours year and undergraduate project. Thank you for letting me make my own mistakes so that I could learn and grow as a chemist, even if I did not understand it at the time. Thank you for all your ideas and advice, and for instilling enthusiasm for organic synthesis in me. A big thank you to Dr. Oliver Jones for being the best supervisor that a PhD student could ask for and for always being there when I needed his help. A big thank you to Trevor Rook for always lending a useful ear to all of my problems, those related to chemical synthesis and also those that were not.

I also need to thank my unofficial synthesis mentors, Dr. Benjamin Alford and Dr. Anthony Lingham, as they gave me all the synthetic skills that I have today. Thanks are due to Ben for showing such patience in teaching me laboratory technique, starting all the way back in my undergraduate project. You have been exceptionally generous with your time and expertise, and I could never thank you enough. Thanks are due to Anthony for always being there to bounce ideas off, and also for showing me what it means to have real enthusiasm for chemistry, and science in general. Thanks are also due to Dr. Sheshanath Bhosale for his assistance in the laboratory and for his advice on multiple topics.

Massive thanks are due to Aaron Raynor and Scott McMaster for taking the wild ride that was a PhD degree with me. Thank you for always being there to discuss all the complicated problems that I had. This project would not have gotten anywhere near as far without your valued troubleshooting. Thanks for also sharing your mateship and your lives with me, and for making these last five years bearable.

Thanks are due to Frank Antolasic and Paul Morrison for all their hard work in making things happen at RMIT. Thank you Frank for maintaining the instruments that made my research possible and for always offering your expertise and advice whenever I had a problem. Thank you Paul for running so many spectra for me, and for always being willing to help and offer advice when things didn't look as I had planned. Thanks are also owed to Howard Anderson for his much appreciated help and troubleshooting over the years. Thanks are due to Dr. Robert Brkljaca for his help with NOESY NMR correlation, and to both Robert and Dr. Julie Niere for answering all of my odd NMR questions.

A huge thank you is due to Dr. Philip Kraft of Givaudan, Switzerland for essentially acting as an unlisted supervisor. Thank you for all the brilliant knowledge that you inputted into my project, for all your hard work and for your never ending patience. Without you this project had no purpose or conclusion. Your assistance and insight was appreciated more than you know. Thanks are also due to the staff at Givaudan; Alain Alchenberger and Dominique Lelièvre for their olfactory analysis, and to Katarina Grman and her panellists for the odour threshold determinations.

Thanks are due to Jordan Froese and Professor Tomáš Hudlický of Brock University for providing the enantiopure *cis*-diol compounds that made the pieces of this puzzle come together. Thanks are due to Robert Gericke of Technische Universität Bergakademie for the crystal structure analysis of my compounds, as well as his valued friendship. Thanks are also due to Jörg Wagler for his assistance with crystallography.

Abbreviations

Δ Heat	HSQC Heteronuclear Single Quantum Coherence
δ Chemical shift (ppm)	iBu Isobutyl
\uparrow Distillation	IPP Isopentenyl pyrophosphate
$\uparrow\downarrow$ Reflux	IR Infrared
[α] Specific rotation	LDA Lithium diisopropylamide
[O] Oxidation	LDBB Lithium 4,4'- <i>t</i> -butylbiphenylide
2D Secondary dimension	mCPBA <i>meta</i> -Chloroperoxybenzoic acid
Ac Acetyl	Me Methyl
AC Adenylate Cyclase	mp Melting point
ATP Adenosine triphosphate	Ms Mesyl
Bu Butyl	MS Molecular Sieve
Bn Benzyl	NMO <i>N</i> -Methylmorpholine <i>N</i> -Oxide
Bz Benzoyl	NMR Nuclear Magnetic Resonance
cAMP Cyclic adenosine monophosphate	NOESY Nuclear Overhauser effect spectroscopy
CDCl₃ Deuterated chloroform	Nu Nucleophile
COSY Correlated spectroscopy	PAD Potassium azodicarboxylate
D 589nm (sodium D line)	PCC Pyridinium chlorochromate
d₆-DMSO Deuterated dimethyl sulfoxide	Ph Phenyl
DBU 1,8-Diazabicycloundec-7-ene	PPA Polyphosphoric acid
DCM Dichloromethane	Pr Propyl
DHP Dihydropyran	<i>p</i>TSA <i>para</i> -Toluenesulphonic acid
DIBAL Diisobutylaluminium hydride	py Pyridine
DIPEA Diisopropylethylamine	QSAR Quantitative Structure-Activity Relationship
DMAPP Dimethylallyl pyrophosphate	SOR Structure-Odour Relationship
DME Dimethoxyethane	<i>t</i>Bu Tertiary butyl
DMF Dimethyl formamide	TDO Toluene dioxygenase
DMK Acetone	Tf Trifluoromethanesulfonyl
DMP Dess-Martin Periodinane	th Odour Threshold
DMS Methylthiomethane	THF Tetrahydrofuran
DMSO Dimethyl sulfoxide	TLC Thin Layer Chromatography
DPG Dipropylene glycol	TMS Trimethylsilyl
Et Ethyl	TPAP Tetrapropylammonium perruthenate
FPP Farnesyl pyrophosphate	Ts Tosyl
FT-IR Fourier Transform Infrared Spectroscopy	
GC Gas Chromatography	
GC-MS Gas Chromatography-Mass Spectrometry	
GC-O Gas Chromatography-Olfactometry	
GDP Guanosine diphosphate	
GPP Geranyl pyrophosphate	
GTP Guanosine triphosphate	
HMBC Heteronuclear Multiple Bond Correlation	
HRMS High Resolution Mass Spectrometry	

Abstract

Odour discrimination is a combinatorial phenomenon, as odorant molecules are known to bind to multiple olfactory receptors. It is also considered that the absolute configuration of a molecule is of crucial importance in determining the human perception of odour. Additionally, it is also recognised that a substance evokes a sense of smell provided that its molecular shape is compatible with the complementary space within the olfactory receptor.

Since the benzo[*b*][1,4]dioxepin-3-one scaffold represents the essential structural characteristics of the synthetic marine odorant family, we were therefore interested in the effect of modulating the molecular shape via an aromatic/aliphatic ring exchange. By the substitution of the aromatic functionality with a saturated ring counterpart we endeavoured to discover the molecular interactions of the carbocyclic ring systems with olfactory receptor sites, including any potential chiral interactions occurring within the receptor(s).

Our initial results revealed that an aromatic ring system was necessary for binding to the marine odorant receptor(s) and that the addition of an alkene or methyl substituent had little effect on receptor affinity. The synthesised aliphatic benzo[*b*][1,4]dioxepin-3-one analogues instead exhibited a plethora of odorant descriptors and consequently it was speculated that perhaps altogether new odorant families could be targeted by further chemical synthesis. It was also questioned if the fusion of 1,4-dioxepan-6-one heterocyclic rings onto naturally occurring terpenoid odorants could merge/synergise existing fragrance classes. The chemical synthesis and olfactory characterisation of a variety of aliphatic benzo[*b*][1,4]dioxepin-3-one analogues, as well as a series of 2-substituted and 2,3-annulated 1,4-dioxepan-6-one analogues is hereby reported.

Table of Contents

CHAPTER 1 – Introduction

1.1 – Preamble	1
1.2 – The Chemical Senses	3
1.2.1 – General Physiology of Olfaction	3
1.2.2 – Olfactory Receptors	5
1.3 – Structure-Odour Relationships (SOR)	7
1.3.1 – Quantitative and Qualitative Olfactory Descriptions	7
1.3.2 – Structure-Odour Correlation	9
1.3.3 – Osmophores and Functional Groups	11
1.3.4 – Stereochemistry and Odour Perception	14
1.4 – Marine Odorants	18
1.4.1 – Naturally Occurring Marine Odorants	18
1.4.2 – Synthetic Marine Odorants	20
1.4.3 – Benzo[<i>b</i>][1,4]dioxepin-3-one Discovery – Pfizer	22
1.4.4 – Benzo[<i>b</i>][1,4]dioxepin-3-one Structure-Odour Relationship Studies – Givaudan	23
1.4.5 – Benzo[<i>b</i>][1,4]dioxepin-3-one Structure-Odour Relationship Studies – Firmenich	28
1.4.6 – Benzo[<i>b</i>][1,4]dioxepin-3-one Structure-Odour Relationship Studies – RMIT University ..	32
1.5 – Isocyclemone Odorants	34
1.5.1 – Commercially Available Products	34
1.5.2 – Isocyclemone Structure-Odour Relationship Studies – Harvard University	36
1.5.3 – Isocyclemone Structure-Odour Relationship Studies – Givaudan	40
1.6 – References	42

CHAPTER 2 – Synthesis of Hexahydrobenzo[*b*][1,4]dioxepin-3-one Stereoisomers

2.1 – Introduction	48
2.1.1 – Project Proposal & Rationale	48
2.1.2 – Aromatic and Aliphatic Carbocyclic Rings	48
2.1.3 – Potential Synthetic Pathways to the Benzo[<i>b</i>][1,4]dioxepin-3-one Scaffold	51
2.2 – Results and Discussion	58
2.2.1 – Synthesis of Calone 1951 [®] by Dieckmann Condensation	58
2.2.2 – Synthesis of <i>threo</i> -Configured Hexahydrobenzo[<i>b</i>][1,4]dioxepin-3-one	62
2.2.3 – Synthesis of <i>erythro</i> -Configured Hexahydrobenzo[<i>b</i>][1,4]dioxepin-3-one	69
2.2.4 – Attempts at Williamson Cyclisation with 2-((1-Bromo-3-chloropropan-2-yl)oxy)tetrahydro- 2 <i>H</i> -pyran	73
2.2.5 – Attempts at Williamson Cyclisation with Alternative Reagents	76
2.2.6 – Williamson Cyclisation with 3-Chloro-2-(chloromethyl)prop-1-ene	81
2.2.7 – Comparisons of Chemical and Olfactory Properties	85
2.3 – Experimental	90
2.4 – References	101

CHAPTER 3 – Synthesis of Additional Analogues of the Aliphatic Benzo[*b*][1,4]dioxepin-3-one System

3.1 – Introduction	107
3.1.1 – Olfactory Receptors and Strategies for Addressing Weak Affinity	107
3.1.2 – Biotransformation of Aromatic Substrates	109
3.2 – Results & Discussion	111
3.2.1 – Synthesis of 7-Methylhexahydrobenzo[<i>b</i>][1,4]dioxepin-3-one Analogues.....	111
3.2.2 – Synthesis of 5a,6,9,9a-Tetrahydrobenzo[<i>b</i>][1,4]dioxepin-3-one Analogues.....	117
3.2.3 – Synthesis of 6/9-Substituted Aliphatic Benzo[<i>b</i>][1,4]dioxepin-3-one Analogues	118
3.2.4 – Synthesis of Alternative Ring Benzo[<i>b</i>][1,4]dioxepin-3-one Analogues.....	126
3.2.5 - Structure-Odour Correlations and Conclusion.....	129
3.3 – Experimental	134
3.4 – References.....	147

CHAPTER 4 – Synthesis of 2-Substituted and 2,3-Annulated 1,4-Dioxepan-6-ones

4.1 – Introduction	151
4.1.1 – Terpenoids and Molecular Fusion.....	151
4.1.2 – The <i>Seco</i> Synthetic Technique	153
4.2 – Results and Discussion.....	156
4.2.1 – Synthesis of 1,4-Dioxepan-6-one Analogues.....	156
4.2.2 – 1,4-Dioxepan-6-one/Terpenoid Odorant Fusion – (+)- α -Pinene.....	159
4.2.3 – 1,4-Dioxepan-6-one/Terpenoid Odorant Fusion – (<i>R</i>)-Camphor.....	161
4.2.4 – 1,4-Dioxepan-6-one/Terpenoid Odorant Fusion – (<i>S</i>)-Carvone and (<i>S</i>)-Carvotanacetone	164
4.2.5 – 1,4-Dioxepan-6-one/Terpenoid Odorant Fusion – (+)-Limonene	167
4.2.6 – 1,4-Dioxepan-6-one/Terpenoid Odorant Fusion – (–)-Menthol	170
4.2.7 - Structure-Odour Correlations and Conclusions.....	174
4.3 – Experimental Section	178
4.4 – References.....	190

CHAPTER 5 – Studies Towards the Synthesis of Isocyclemonone Analogues

5.1 – Introduction	194
5.2 – Results and Discussion.....	196
5.2.1 – Synthesis of Oxazaborolidine Catalyst Precursors.....	196
5.2.2 – Synthesis of Diene Precursors – Organolithium Route	197
5.2.3 – Synthesis of Diene Precursors – Grignard Reaction Route.....	198
5.2.4 – Synthesis of Diene Precursors – Stille Coupling Route.....	199
5.2.5 – Catalyst Generation and Diels–Alder Experiment	201
5.3 – Experimental	203
5.4 – References.....	208

CHAPTER 6 – Conclusions and Recommendation for Future Research

6.1 – Conclusions.....	211
6.2 – Recommendation for Future Research.....	213
6.3 – References.....	216

APPENDIXES

Table of Appendixes	217
General Experimental Conditions	220
Crystal Structure Data for Compounds 167 , 173 and 204	221
NMR Spectra.....	230

List of Figures

Figure 1.1: Camphoraceous odorants 1–4 , with different molecular structures	1
Figure 1.2: Overview of the science of olfaction	2
Figure 1.3: The mammalian olfactory system.....	3
Figure 1.4: Graphical representation of a typical neuron cell	4
Figure 1.5: Graphical representation of the cAMP mediated transduction pathway operating in olfactory receptor neurons	7
Figure 1.6: Fragrance wheel	8
Figure 1.7: Air and water odour threshold differences of <i>anti</i> -3-mercapto-2-methylpentanol diastereomers	9
Figure 1.8: Molecular shape, molecular size and functional groups affect odorant properties	11
Figure 1.9: Exchanging H-bond acceptors; almond smelling analogues of benzaldehyde (14)	12
Figure 1.10: Commercially available musk odorants 18 and 19 , and thionated analogues 20–23	13
Figure 1.11: Group 14 analogues (25–27) of benzyl(dimethyl)carbinol (24)	14
Figure 1.12: Chiral odorant pairs illustrating different odour descriptions and odour threshold (th) values	16
Figure 1.13: Odour threshold values for various stereoisomers of wine lactone (36)	16
Figure 1.14: Odour comparisons of synthetic alkoxyazines	17
Figure 1.15: Naturally occurring odorant compounds in algae	18
Figure 1.16: Bromophenol odorants from natural marine sources.	19
Figure 1.17: Naturally occurring unsaturated aldehyde compounds containing marine nuances	19
Figure 1.18: Various synthetic marine odorants	20
Figure 1.19: Marine nitro musk odorant 64 , polycyclic musk odorant 65 and target compound 66	23
Figure 1.20: Library of 7,8-annulated and 7-alkyl substituted benzo[<i>b</i>][1,4]dioxepin-3-one analogues	25
Figure 1.21: Marine odorant olfactophore model generated by Kraft <i>et al.</i>	25
Figure 1.22: Unsaturated benzo[<i>b</i>][1,4]dioxepin-3-one analogues synthesised by Kraft <i>et al.</i>	27
Figure 1.23: Mono- and <i>bis</i> -deoxygenated benzo[<i>b</i>][1,4]dioxepin-3-one analogues synthesised by Gaudin <i>et al.</i>	28
Figure 1.24: Targeted benzo[<i>b</i>][1,4]dioxepin-3-one analogue scaffolds of Gaudin <i>et al.</i>	30
Figure 1.25: Marine-ozone olfactophore model generated by Gaudin <i>et al.</i>	31
Figure 1.26: Five-membered benzo[<i>b</i>][1,4]dioxepin-3-one analogues displaying marine and lily-of-the-valley nuances.....	32
Figure 1.27: Graphical representation of the C–3 benzo[<i>b</i>][1,4]dioxepin-3-one analogues.	33
Figure 1.28: Arborone (116) analogues 138–143 prepared by Hong and Corey	39
Figure 1.29: Oxa-Georgyone analogues 144 and 145 prepared by Hicken and Corey	40
Figure 1.30: Eight-membered isocyclemonone analogues 146–148 prepared by Kraft <i>et al.</i>	40
Figure 1.31: Spirocyclic isocyclemonone analogues 149–154 synthesised by Kraft <i>et al.</i>	41
Figure 2.1: Aromatic/aliphatic ring exchange of the benzo[<i>b</i>][1,4]dioxepin-3-one molecular scaffold.	48

Figure 2.2: Top: Two resonance structures of a benzene molecule; Bottom: A more accurate visualisation of molecular resonance	49
Figure 2.3: Delocalisation of π -electrons in an aromatic cyclohexa-1,3,5-triene ring.....	49
Figure 2.4: Top: Conformational changes during the inversion of cyclohexane; Bottom: Axial and equatorial positions of a chair conformation ring	50
Figure 2.5: Minimum-energy conformation of 7-methylbenzo[<i>b</i>][1,4]dioxepin-3-one (Calone 1951 [®]) displaying pseudo-twist-boat conformation.....	51
Figure 2.6: Dieckmann condensation route leading the benzo[<i>b</i>][1,4]dioxepin-3-one scaffold	52
Figure 2.7: Thorpe-Ziegler route leading the benzo[<i>b</i>][1,4]dioxepin-3-one scaffold	53
Figure 2.8: Williamson ether synthesis routes developed by Kraft <i>et al.</i> (route a/c), Curtin <i>et al.</i> (route a/d/e), Sinou <i>et al.</i> (route b followed by d/e (one-pot)) and Gaudin <i>et al.</i> (route f) leading the benzo[<i>b</i>][1,4]dioxepin-3-one scaffold	55
Figure 2.9: Williamson ether synthesis route developed by Hgel <i>et al.</i> (route a/b/d) and Rosnati <i>et al.</i> (route c) leading the benzo[<i>b</i>][1,4]dioxepin-3-one scaffold.....	55
Figure 2.10: Methodology developed by Nerdel <i>et al.</i> leading to the 1,4-dioxepan-6-one scaffold.....	56
Figure 2.11: Epoxide cyclisation route to 2-dimethylbenzo[<i>b</i>][1,4]dioxepin-3-ol scaffold	57
Figure 2.12: Potential hydrogenation route to the saturated benzo[<i>b</i>][1,4]dioxepin-3-one scaffold	57
Figure 2.13: ¹ H, ¹³ C HSQC spectra of compound Calone 1951 [®] (50).....	59
Figure 2.14: Proposed reaction mechanism for the Dieckmann condensation reaction leading to the benzo[<i>b</i>][1,4]dioxepin-3-one scaffold	60
Figure 2.15: Graphical representation of <i>exo</i> (outside) and <i>endo</i> (inside) ring closing reactions	61
Figure 2.16: Graphical representation of <i>tet</i> , <i>trig</i> and <i>dig</i> ring closing reactions	62
Figure 2.17: Stereochemical relationships of cyclohexane-1,2-diol.....	63
Figure 2.18: Proposed catalytic cycle for a boron trifluoride (BF ₃) catalysed O–H insertion reaction with a diazo compound	66
Figure 2.19: Various spectra of compound (\pm)- 161 . Top: ¹ H NMR spectrum; Middle: ¹³ C NMR spectrum; Bottom: Mass spectrum (EI) showing molecular ion at <i>m/z</i> 288	68
Figure 2.20: ¹ H, ¹³ C HSQC spectra of compound (\pm)- 166	69
Figure 2.21: Proposed catalytic cycle of the Upjohn dihydroxylation	70
Figure 2.22: Mass spectrum (EI) of compound 173 showing molecular ion at <i>m/z</i> 170.....	72
Figure 2.23: Proposed mechanism for acid-catalysed decarboxylation of a β -ketoester intermediate to yield the saturated benzo[<i>b</i>][1,4]dioxepin-3-one analogue.....	73
Figure 2.24: GC-MS chromatograph of the permanganate oxidation of (\pm)- 175 to 182 , showing halogen exchange.....	77
Figure 2.25: Reaction mechanism for the Williamson reaction between substituted cyclohexane-1,2-diol analogues and 3-chloro-2-(chloromethyl)prop-1-ene.....	83
Figure 2.26: Catalytic cycle of a ruthenium tetroxide oxidation.....	84
Figure 2.27: ¹ H NMR overlay of the unsubstituted aromatic and aliphatic benzo[<i>b</i>][1,4]dioxepin-3-one analogues.....	86

Figure 2.28: Molecular structure of <i>rac</i> -hexahydro-2 <i>H</i> -benzo[<i>b</i>][1,4]dioxepin-3(4 <i>H</i>)-one (167) showing thermal ellipsoids at a 50% probability level	86
Figure 2.29: Molecular structure of <i>meso</i> -hexahydro-2 <i>H</i> -benzo[<i>b</i>][1,4]dioxepin-3(4 <i>H</i>)-one (173) showing thermal ellipsoids at a 50% probability level	88
Figure 3.1: Original marine olfactophore model developed by Kraft <i>et al.</i> , with bound ligands.....	107
Figure 3.2: Potent synthetic marine odorant analogues and their respective odour descriptors.....	108
Figure 3.3: Comparison of the degradation pathway of aromatic compounds by wild type <i>P. putida</i> , the knock-out mutant (Pp39D) and the bioengineered <i>E. coli</i> strain (JM109 pDTG601)	109
Figure 3.4: Dihydroxylation of toluene by the three-component toluene dioxygenase (TDO) enzymatic system	110
Figure 3.5: Mechanism of an ozonolysis reaction.....	112
Figure 3.6: ¹³ C NMR of crude compound 198 , reaction displayed in Scheme 3.1	112
Figure 3.7: ¹³ C NMR overlay of various 4-methylcyclohexane-1,2-diol samples.....	115
Figure 3.8: Molecular structure of (5 <i>aR</i> ,7 <i>R</i> ,9 <i>aR</i>)-7-methylhexahydrobenzo[<i>b</i>][1,4]dioxepin-3-one (204) showing thermal ellipsoids at a 50% probability level	116
Figure 3.9: Mass spectrum (EI) of compound 219 showing molecular ion at <i>m/z</i> 182.....	119
Figure 3.10: ¹ H, ¹ H NOESY spectra of compound 222 , showing NOE correlation between 3-Me and 1-H signals	121
Figure 3.11: Proposed catalytic cycle for Suzuki coupling reactions	125
Figure 3.12: ¹³ C NMR of crude material obtained for reaction of compound 241 , reaction displayed in Scheme 3.14	127
Figure 3.13: Product distribution during an acid-catalysed reaction of 241	128
Figure 3.14: Rigid-body superposition of the X-ray structure of 167 (blue, Figure 2.28) and the structure of 227 (magenta) derived from X-ray coordinates of 173 (Figure 2.29) on the minimum-energy conformer of Calone 1951 [®] (50 , black).....	133
Figure 4.1: Biosynthetic intermediates leading to terpene and terpenoid compounds.....	151
Figure 4.2: Various terpene and terpenoid odorants, and their natural source and abundance	152
Figure 4.3: Molecular structure amalgamation of marine odorant Calone 1951 [®] (50) and musk odorant Galaxolide [®] (65)	153
Figure 4.4: Molecular structures of 7-dehydrocholesterol (260) and cholecalciferol (vitamin D ₃ , 261).	153
Figure 4.5: <i>Seco</i> analysis of β-ionone (262) to give molecular fragment 263	154
Figure 4.6: Analogues 265–267 synthesised from <i>seco</i> analysis of the molecular structure of lead compound 264	155
Figure 4.7: <i>Seco</i> analysis of 7-methylbenzo[<i>b</i>][1,4]dioxepin-3-one (Calone 1951 [®] , 50)	155
Figure 4.8: Library of 1,4-dioxepan-6-one analogues 269 , 275–278 displaying odour descriptors and odour thresholds (th) values, where applicable	158
Figure 4.9: Proposed catalytic cycle for the dihydroxylation of alkenes by Sudalai <i>et al.</i>	159
Figure 4.10: Tertiary amine ligands accelerate the reactivity of osmium tetroxide.....	160

Figure 4.11: ^1H , ^{13}C HSQC spectra of compound 283	161
Figure 4.12: Mechanism of the Shapiro reaction of hydrazone compound 287 to give alkene 288 ..	163
Figure 4.13: GC-MS chromatograph of the oxidation reaction of (<i>S</i>)-carvone (28).....	165
Figure 4.14: GC-MS chromatograph of the oxidation reaction of (+)-limonene (299)	168
Figure 4.15: Acid-catalysed ring-opening of <i>cis</i> - and <i>trans</i> -limonene oxides to give <i>trans</i> -diol 302 ..	168
Figure 4.16: ^1H NMR spectra of dioxepanone fused (+)-limonene analogue 304	169
Figure 4.17: Mechanism for the acid-catalysed aromatisation of (<i>S</i>)-carvone to carvacrol.....	170
Figure 4.18: ^{13}C NMR spectra showing: (top) mesylate 306 ; (middle) elimination reaction of 306 with heat to give alkene 309 ; (bottom) elimination of 306 with KO t Bu to give alkene 307	171
Figure 4.19: Different elimination products of mesylate compound 306	172
Figure 4.20: Minimum-energy conformation of (1 <i>R</i> ,2 <i>R</i> ,3 <i>S</i> ,6 <i>R</i>)-3-isopropyl-6-methylcyclohexane-1,2-diol (308)	173
Figure 4.21: Biflexible alignment of the (<i>S</i>)-enantiomer of compound 276 (grey) on (<i>R</i>)-celery ketone (black, 313) and <i>cis</i> -jasnone (white, 314)	177
Figure 5.1: Commercially available isocyclemonone odorants.....	194
Figure 5.2: Proposed <i>oxa</i> -isocyclemonone analogues.....	195
Figure 5.3: Mass spectrum (EI) of compound 329 showing molecular ion at <i>m/z</i> 108.....	198
Figure 5.4: Simplified catalytic cycle of a Stille coupling reaction.....	200
Figure 5.5: ^{13}C NMR overlay of (<i>E</i>)-2-methyl-2-butenal (317 , top) and the crude material obtained from reaction displayed in Scheme 5.9 (bottom), displaying a new aldehyde peak at δ 206.4 ppm..	202
Figure 6.1: Selected benzo[<i>b</i>][1,4]dioxepin-3-one analogues	211
Figure 6.2: Aliphatic benzo[<i>b</i>][1,4]dioxepin-3-one and 1,4-dioxepan-6-one analogues	212
Figure 6.3: Proposed scaffolds for new marine odorants.	214

List of Schemes

Scheme 1.1: Original synthesis of the benzo[<i>b</i>][1,4]dioxepin-3-one and 4,5-dihydrobenzo[<i>b</i>]oxepin-3-one analogues by Beereboom, Cameron and Stephens	22
Scheme 1.2: Synthetic route employed by Kraft <i>et al.</i> in the synthesis of 7,8-annulated and 7-alkyl substituted benzo[<i>b</i>][1,4]dioxepin-3-one analogues	24
Scheme 1.3: Synthesis of analogue 89 from eugenol (87), with alkene isomerisation	26
Scheme 1.4: Synthetic route employed by Kraft <i>et al.</i> in the synthesis of conjugated seven-alkenyl substituted benzo[<i>b</i>][1,4]dioxepin-3-one analogues	27
Scheme 1.5: Synthetic route to benzo[<i>b</i>][1,4]dioxepin-3-one analogues employed by Hgel <i>et al.</i>	32
Scheme 1.6: Commercial synthesis of Iso E Super [®] (115) from myrcene (112) and (3 <i>E</i>)-3-methylpent-3-en-2-one (113)	34
Scheme 1.7: Total synthesis of racemic Arborone (116) from α -ionone (117)	35
Scheme 1.8: Commercial synthesis of Georgywood [®] (124) from homomyrcene (121) and 3-methylbut-3-en-2-one (122)	36
Scheme 1.9: Enantioselective synthesis of (–)-Georgyone (124) from homomyrcene (121) and methacrylaldehyde (126).....	37
Scheme 1.10: Enantioselective synthesis of (+)-Arborone (116) from 1,3-butadiene (130) and (<i>E</i>)-2-methylbut-2-enal (131)	38
Scheme 2.1: Synthesis of Calone 1951 [®] (50) from 4-methylcatechol (155) via Dieckmann methodology	58
Scheme 2.2: Synthesis of <i>rac</i> -cyclohexane-1,2-diol (160) from cyclohexene (158).....	63
Scheme 2.3: Failed Williamson reactions between <i>rac</i> -cyclohexane-1,2-diol (160) and ethyl bromoacetate (156)	64
Scheme 2.4: Synthesis of <i>rac</i> -1,2-bis(allyloxy)cyclohexane (163) from <i>rac</i> -cyclohexane-1,2-diol (160)	64
Scheme 2.5: Synthesis of ethyl diazoacetate (165) from ethyl glycinate hydrochloride (164)	65
Scheme 2.6: Synthesis of <i>threo</i> -configured aliphatic benzo[<i>b</i>][1,4]dioxepin-3-one (\pm)- 167 from <i>rac</i> -cyclohexane-1,2-diol (160) via Dieckmann methodology	67
Scheme 2.7: Preparation of <i>N</i> -methylmorpholine <i>N</i> -oxide (NMO) (169) from <i>N</i> -methylmorpholine (168)	70
Scheme 2.8: Synthesis of <i>meso</i> -cyclohexane-1,2-diol (170) from cyclohexane (158) via a Upjohn dihydroxylation	71
Scheme 2.9: Synthesis of <i>erythro</i> -configured aliphatic benzo[<i>b</i>][1,4]dioxepin-3-one 173 from <i>meso</i> -cyclohexane-1,2-diol (170) via Dieckmann methodology	72
Scheme 2.10: Synthesis of tetrahydropyranyl-ether protected chain (\pm)- 176 from epichlorohydrin (174)	74
Scheme 2.11: Synthesis of benzo[<i>b</i>][1,4]dioxepin-3-one (49) from catechol (177)	75
Scheme 2.12: Attempted Williamson reaction between <i>rac</i> -cyclohexane-1,2-diol (160) and <i>bis</i> -halogenated chain (\pm)- 176 , leading to dehydrohalogenation to give compound (\pm)- 181	75

Scheme 2.13: Various oxidation conditions attempted for the synthesis of 182 from (\pm)- 175	76
Scheme 2.14: Failed Williamson reaction between <i>rac</i> -cyclohexane-1,2-diol (160) and <i>bis</i> -halogenated chain 182	79
Scheme 2.15: Above: Failed Wittig reaction between <i>bis</i> -halogenated chain 182 and methyltriphenylphosphonium iodide (183); Below: Attempted ketalisation of <i>bis</i> -halogenated chain 182 with 1,2-ethanediol (185) leading to a mixed product due to halide exchange.....	80
Scheme 2.16: Synthesis of <i>bis</i> -chlorinated chain 188 from (\pm)-epichlorohydrin (174)	81
Scheme 2.17: Ketalisation of <i>bis</i> -chlorinated chain 188 to give dioxolane 189 , and the subsequent failed reaction with <i>rac</i> -cyclohexane-1,2-diol (160)	81
Scheme 2.18: Synthesis of <i>bis</i> -chlorinated chain 194 from pentaerythritol (191).....	82
Scheme 2.19: Williamson reaction of both stereoisomers of cyclohexane-1,2-diol with <i>bis</i> -chlorinated chain 194 followed by oxidation to the aliphatic benzo[<i>b</i>][1,4]dioxepin-3-one.....	83
Scheme 3.1: Failed ozonolysis of pulegone (197) to give <i>bis</i> -carbonyl intermediate 198	111
Scheme 3.2: Synthesis of <i>trans</i> - and <i>cis</i> -configured 4-methylcyclohexane-1,2-diols 201 and 202 , respectively, from pulegone (197) via reduction, ozonolysis and further reduction.....	113
Scheme 3.3: Synthesis of 7-methylhexahydrobenzo[<i>b</i>][1,4]dioxepin-3-one diastereomers 204 and 206 from <i>trans</i> - and <i>cis</i> -configured diol compounds 201 and 202 , respectively.....	115
Scheme 3.4: Synthesis of <i>rac</i> - and <i>meso</i> -cyclohex-4-ene-1,2-diols (208 and 209 , respectively) from 1,4-cyclohexadiene (207).....	117
Scheme 3.5: Synthesis of <i>rac</i> - and <i>meso</i> -5a,6,9,9a-tetrahydrobenzo[<i>b</i>][1,4]dioxepin-3-one analogues 211 and 213 from <i>trans</i> - and <i>cis</i> -configured diols 208 and 209 , respectively	118
Scheme 3.6: Enzymatic oxidation followed by selective chemical reduction to yield <i>cis</i> -diol compounds 214–216 from aromatic precursor compounds	118
Scheme 3.7: Synthesis of (5a <i>S</i> ,9a <i>R</i>)-9-methyl-5a,6,7,9a-tetrahydrobenzo[<i>b</i>][1,4]dioxepin-3-one (219) from toluene (217).....	119
Scheme 3.8: Hydrogenation and benzylation of unsaturated <i>cis</i> -diol 214 , followed by separation and hydrolysis to yield enantiopure saturated <i>cis</i> -diol compounds 222 and 223	120
Scheme 3.9: Synthesis of 6-methylhexahydrobenzo[<i>b</i>][1,4]dioxepin-3-one diastereomers 225 and 227 from <i>cis</i> -diol compounds 222 and 223 , respectively	122
Scheme 3.10: Synthesis of halogenated analogues 230 (R = Br) and 233 (R = I) from bromobenzene (228) and iodobenzene (231), respectively.....	123
Scheme 3.11: Failed hydrogenation reaction of brominated <i>cis</i> -diol compound 215	124
Scheme 3.12: Suzuki coupling between compound 233 and phenylboronic acid (235) to provide (5a <i>S</i> ,9a <i>R</i>)-9-phenyl-5a,6,7,9a-tetrahydrobenzo[<i>b</i>][1,4]dioxepin-3-one (236).....	124
Scheme 3.13: Synthesis of tricyclic analogue 240 from norbornene (237)	126
Scheme 3.14: Failed synthesis of <i>trans</i> -diol (\pm)- 242 from norbornene (237)	127
Scheme 3.15: Acid-catalysed epoxide 241 ring-opening products as reported by Willson <i>et al.</i>	128
Scheme 3.16: Synthesis of 8-membered analogue 248 from <i>cis</i> -cyclooctene (245)	129
Scheme 4.1: Synthesis of 1,4-dioxepan-6-one (269) from 1,2-ethanediol (185).....	156

Scheme 4.2: Williamson reaction methodology to give 1,4-dioxepan-6-one analogues 269 , 275–278	157
Scheme 4.3: Synthesis of racemic 4-methylpentane-1,2-diol (280) from 4-methyl-1-pentene (279)	158
Scheme 4.4: Synthesis of dioxepanone fused (+)- α -pinene analogue 283 from (+)- α -pinene (254)	160
Scheme 4.5: Synthesis of <i>para</i> -toluenesulfonylhydrazide (285) from <i>para</i> -toluenesulfonyl chloride (284)	162
Scheme 4.6: Synthesis of <i>cis</i> -diol compound 289 from (<i>R</i>)-camphor (286) and (–)-camphorquinone (290)	162
Scheme 4.7: Synthesis of dioxepanone fused (<i>R</i>)-camphor analogue 292 from <i>cis</i> -diol compound 289	164
Scheme 4.8: Synthesis of <i>trans</i> -diol 295 from (<i>S</i>)-carvone (28)	165
Scheme 4.9: Failed <i>bis</i> -etherification of <i>trans</i> -diol 295 with ethyl diazoacetate	166
Scheme 4.10: Hydrogenation of diol 295 to give saturated diol 297 , followed by failed etherification with 194	167
Scheme 4.11: Synthesis of <i>trans</i> -diol compound 302 from (+)-limonene (299)	167
Scheme 4.12: Synthesis of dioxepanone fused (+)-limonene analogue 304 from <i>trans</i> -diol 302 , with alkene isomerisation	169
Scheme 4.13: Synthesis of <i>trans</i> -diol compound 308 from (–)-menthol (305)	171
Scheme 4.14: Failed synthesis of dioxepanone fused (–)-menthol analogue 312 from <i>trans</i> -diol compound 308	173
Scheme 5.1: Synthetic pathway to <i>oxa</i> -Georgyone analogue 144 by Hicken and Corey	195
Scheme 5.2: Synthesis of (<i>S</i>)-diphenyl(pyrrolidin-2-yl)methanol (324) from L-proline (321)	196
Scheme 5.3: Synthesis of cyclic boronic acid trimer 326 from <i>ortho</i> -tolylboronic acid (325)	197
Scheme 5.4: Failed synthesis of diene compound 329 from cyclohexanone (328)	198
Scheme 5.5: Synthesis of diene compound 329 from cyclohexanone (328) via Grignard reaction and subsequent dehydration	198
Scheme 5.6: Synthesis of tributyl(vinyl)stannane (332) from tributylstannane chloride (331)	200
Scheme 5.7: Synthesis of diene compound 329 from cyclohexanone (328) via Stille coupling of enol triflate analogue 333	201
Scheme 5.8: Preparation of the (<i>S</i>)-(–)- <i>o</i> -tolyl-CBS-oxazaborolidine Diels–Alder catalyst (318) from (<i>S</i>)-diphenyl(pyrrolidin-2-yl)methanol (324) and 2,4,6-tri- <i>o</i> -tolyl-1,3,5,2,4,6-trioxatriborinane (326)	202
Scheme 5.9: Diels–Alder reaction between diene compound 329 and (<i>E</i>)-2-methyl-2-butenal (317) using 318 as a chiral catalyst	202

List of Tables

Table 1.1: Evolution of the marine/aquatic accord in modern perfumery	21
Table 1.2: Calculated relative energies of the two main conformers of compounds 50 , 98 and 101 ..	29
Table 2.1: Baldwin's favoured and disfavoured ring closing reactions	61
Table 2.2: Olfactory properties of compounds 49 , (\pm)- 167 & 173	89
Table 3.1: Experimental aliphatic benzo[<i>b</i>][1,4]dioxepin-3-one library displaying odour descriptions, and odour thresholds, where applicable	131
Table 3.2: Experimental six- and nine-substituted aliphatic benzo[<i>b</i>][1,4]dioxepin-3-one library displaying odour descriptions, and odour thresholds, where applicable	132
Table 4.1: Olfactory properties of 1,4-dioxepan-6-one analogues 269 , 275–278	175
Table 4.2: Olfactory properties of 1,4-dioxepan-6-one heterocycle fused terpenoid compounds 283 and 292	177

Chapter 1 – Introduction

1.1 – Preamble

The 2004 Nobel prize in physiology or medicine was awarded to Richard Axel and Linda Buck for their discovery of olfactory receptors and the organisation of the olfactory system.^[1-2] Their work generated high expectations for scientific advancement in the field of olfaction. This expectation was perhaps unjustified as it was also revealed that each odorant molecule triggers a combination of olfactory receptors and that any given odour perception corresponds to a highly complex neuronal activation pattern.^[3-4]

A subtle molecular alteration of an odorant may affect its binding affinities to a number of olfactory receptors. This makes correctly predicting a pattern of receptor activity far less accurate than the corresponding prediction of receptor activity involving a pharmaceutical drug. There also exists multiple layers of neurotransmission between an olfactory receptor and the cerebrum where individual signal components may be amplified, weakened or altered before being consciously perceived.^[5] An individual molecule of a complex mixture can additionally act as an agonist or antagonist to a given olfactory receptor adding further complexity.^[6] It therefore remains nearly impossible to accurately predict the olfactory properties of a molecule.^[4-5] An example that illustrates the difficulty in connecting molecular structure with olfactory properties is delineated in Figure 1.1. Compounds **1–4** all smell camphoraceous, or like camphor (**3**), despite wildly different molecular structures and functional groups.

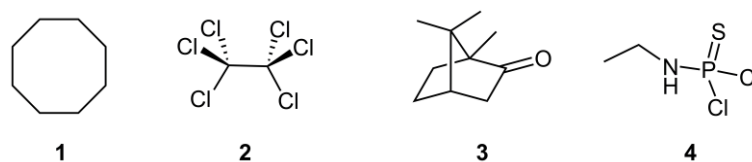


Figure 1.1: Camphoraceous odorants **1–4**, with different molecular structures.^[5]

Scientific research into the field of olfaction involves multiple disciplines including psychology, physiology, biochemistry, genetics and chemistry (Figure 1.2).^[7] The study of olfaction also involves multiple systems and organs including the olfactory cortex, olfactory bulbs and olfactory receptors. The chemical synthesis of olfactory properties is still an emerging discipline and predicting the olfactory properties of a new molecule by rational design remains challenging.^[5] In the human brain the perception of odour is strongly linked to memory and emotion.^[8] It is perhaps therefore unsurprising that despite the difficulties associated with odorant design, the production of fragrances is a multibillion dollar industry.^[9]

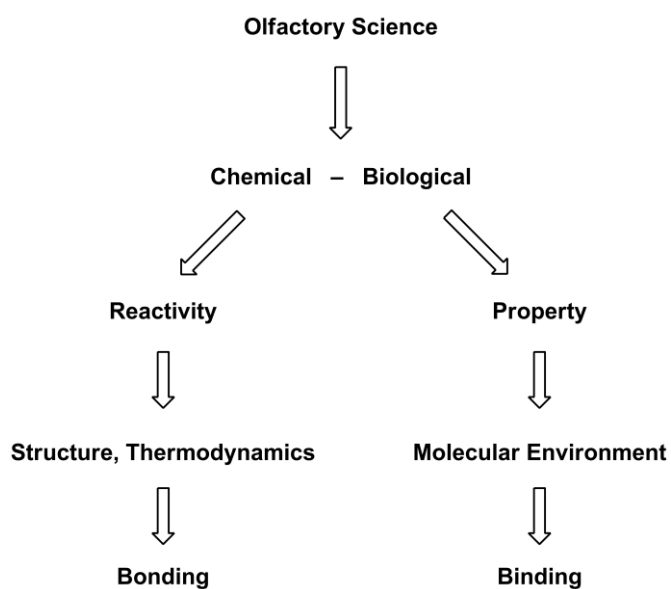


Figure 1.2: Overview of the science of olfaction.^[10]

1.2– The Chemical Senses

1.2.1 – General Physiology of Olfaction

The perception of odour and taste are a direct result of the interaction of chemical compounds with peripheral receptor systems.^[6] The physiological structure involved in odorant detection is the olfactory epithelium, a specialised tissue located inside the nasal cavity (Figure 1.3). The olfactory epithelium consists of up to 30 million primary sensor cells accompanied by a larger number of supporting and basal cells.^[6] An olfactory neuron contains cilia that point out of the olfactory epithelium and into a mucosa which is *ca.* 60 microns thick.^[11] The olfactory mucosa is a lipid-rich secretion produced by Bowman's glands which reside in the olfactory epithelium. The mucus layer is rich in odorant-binding proteins which are theorised to be involved in the transport of hydrophobic odorant molecules across the mucus layer to the olfactory receptors.^[12] The olfactory system is also responsible for the detection of chemical signals, known as pheromones, released by many animals and involved in stimulating hormonal and behavioral responses.^[3]

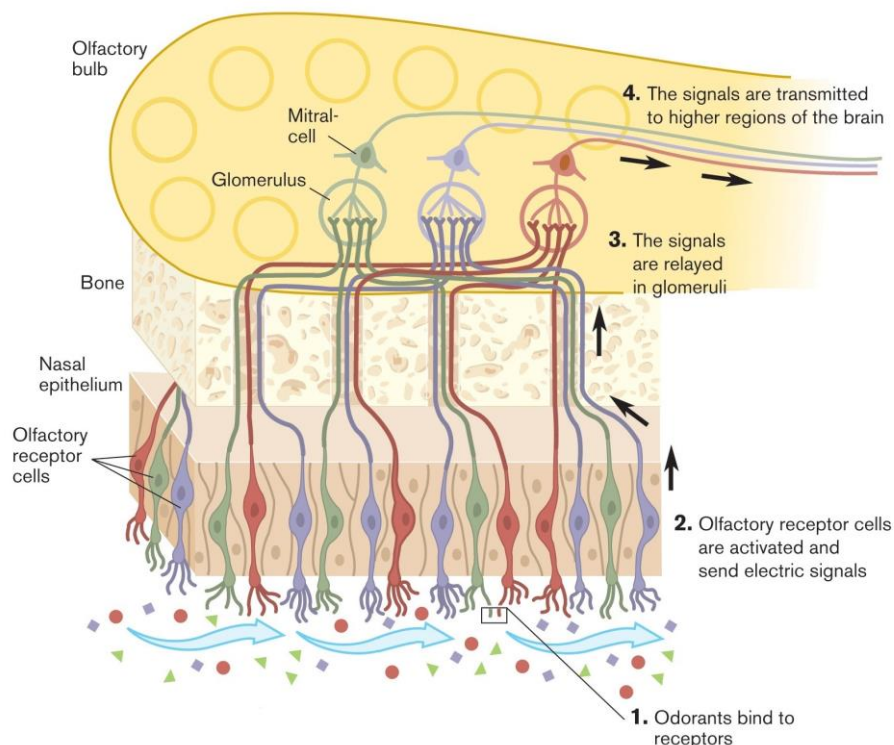


Figure 1.3: The mammalian olfactory system.^[1] Copyright The Nobel Assembly at the Karolinska Institutet, Sweden. Reproduced with permission.

Olfactory receptors are expressed in the cell membranes of olfactory receptor neurons. To maintain high sensitivity, each olfactory neuron expresses only one type of olfactory receptor.^[13] Olfactory neurons are bipolar neuron cells with dendrites pointing into the olfactory epithelium and axons passing through the ethmoid bone that separates the nasal cavity from the brain. The axons reach a structure in the brain called the olfactory bulb where they converge with post-synaptic cells to form glomeruli (Figure 1.4).^[6] All axons of a single class of olfactory receptor neuron converge on a single glomerulus.^[14] The binding of an odorant molecule to an olfactory receptor triggers depolarisation of the cell membrane. This process involves a change in electrochemical gradient across the axonal surface by an influx of positively charged cations. The resting potential of a neural cell is *ca.* -70 mV. The influx of positively charged ions lowers the electronegativity of the cytosol, and at *ca.* -40 mV, triggers the depolarisation of the membrane by a change in ion entry to produce an electrical transmission down the length of the neuron.^[6]

The human olfactory bulb appears as two halves with mirrored medial and lateral surfaces.^[7, 15] The activity patterns of glomeruli within the olfactory bulb code for odour impression, the information being transferred by mitral cells to the olfactory cortex of the brain where higher level processing takes place.^[6] The human olfactory bulb contains about 2500 glomeruli.^[15] A given odorant can activate certain glomeruli strongly whilst affecting other glomeruli weakly, or not at all.^[16] Glomeruli activation patterns within the olfactory bulb are therefore thought to represent the quantity and quality of the odorant being detected.

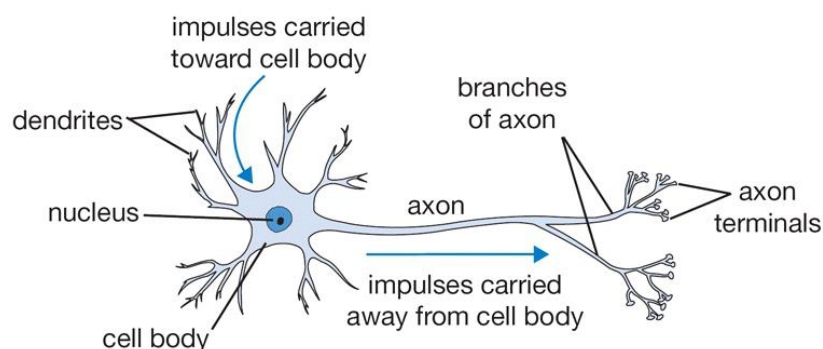


Figure 1.4: Graphical representation of a typical neuron cell.^[17]

In addition to the olfactory nerve, the trigeminal nerve also plays a role in olfactory perception.^[18] The trigeminal nerve is responsible for the sensations of heating, cooling and tingling. This nerve and its associated receptors are situated in the mucosa of the nose and tongue, and its impulses are not transmitted to the olfactory bulb, but are processed independently.^[6] Few chemosensory stimulants produce exclusively olfactory or trigeminal sensations, the vast majority of odorant molecules possessing characteristics of both odour and irritation.^[11, 19] Some notable ligands of both neural systems include menthol (mint) and allyl isothiocyanate (horseradish).^[11]

1.2.2 – Olfactory Receptors

The human olfactory receptor repertoire is comprised of over 900 genes of which more than 50% are pseudogenes deactivated by frame-shift mutations.^[6, 20-21] The genes involved in olfaction are coded on 53 different loci on 21 human chromosomes,^[22] the exceptions being chromosome 20 and the sex-determining Y chromosome.^[20] The chromosomal distribution of olfactory genes is extremely biased, with six chromosomes (1, 6, 9, 11, 14, and 19) accounting for 73% of the repertoire.^[20] Chromosome 11 alone contains 42% of the olfactory receptor genes.^[20] Genetic sequences involved in olfaction total to about three percent of the total human genome.^[23] Owing to the decreased number of functioning olfactory receptors in comparison to other primate species, it was suggested that the role of olfaction for survival and reproductive success has decreased during human evolution.^[24-25] It was shown that negative selection of olfactory receptors is still relaxed in modern humans which suggests that a plateau of minimum function has yet to be reached and that therefore future human evolution of olfactory capability may still be decreasing.^[24]

For a molecule to interact with the olfactory system it must possess certain molecular properties. Generally, odorants are small hydrophobic, non-ionic molecules that also must display a certain amphiphilic character to pass through the mucus layer that covers the receptors.^[6, 26] In addition to these characteristics, an odorant must also possess a sufficiently high vapour pressure; no known odorant possess a molecular weight greater than 294 atomic mass units.^[27] Each individual olfactory receptor class displays an affinity for a range of ligands, and conversely, a single odorant molecule may bind to a number of olfactory receptors.^[3]

The olfactory system is able to distinguish a practically infinite number of chemical compounds owing to the sheer quantity of dissimilar olfactory receptor types coupled with the combinatorial nature of ligand receptor affinity.^[11] Olfactory receptors are a member of the class A rhodopsin-like family of G protein-coupled receptors (GPCR).^[28] This class of receptor contains seven transmembrane α -helix structures that span the cell membrane and additionally feature extracellular loops.^[6] The extracellular loop structures form a cavity which is assumed to serve as a binding pocket for ligand molecules.^[6, 25] The family of G protein-coupled receptors includes receptors for many neurotransmitters including serotonin, dopamine, and histamine, as well as proteins involved in photoreception.^[7]

Different olfactory receptor proteins have different variable domains that form different binding cavities.^[6, 25] These domains bind to odorant ligands in a non-covalent manner, including van der Waals forces, Coulomb attractions and hydrogen bonding.^[6] The binding of an odorant to a receptor initiates an allosteric change in the quaternary structure of the receptor. This activates the G protein on the intracellular side of the olfactory neuron by the dissociation and phosphorylation of inactive guanosine diphosphate (GDP) to give active guanosine triphosphate (GTP) (Figure 1.5).^[6, 29]

G proteins, also known as guanine nucleotide-binding proteins, are a family of enzymes that act as a molecular switch. Once activated, the G protein in turn activates adenylate cyclase (AC) enzymes that convert adenosine triphosphate (ATP) into cyclic adenosine monophosphate (cAMP), the secondary messenger.^[30] The cAMP acts to open cyclic nucleotide-gated ion channels which allow cations such as Na^+ and Ca^{2+} to enter the cytosol, depolarising the cell and triggering an action potential which is propagated along the axon.^[6] Although there is scientific evidence for alternative secondary messengers (such as inositol trisphosphate and cyclic guanosine monophosphate), it is generally agreed that cAMP is the dominant secondary messenger involved in the process of olfaction.^[31-33]

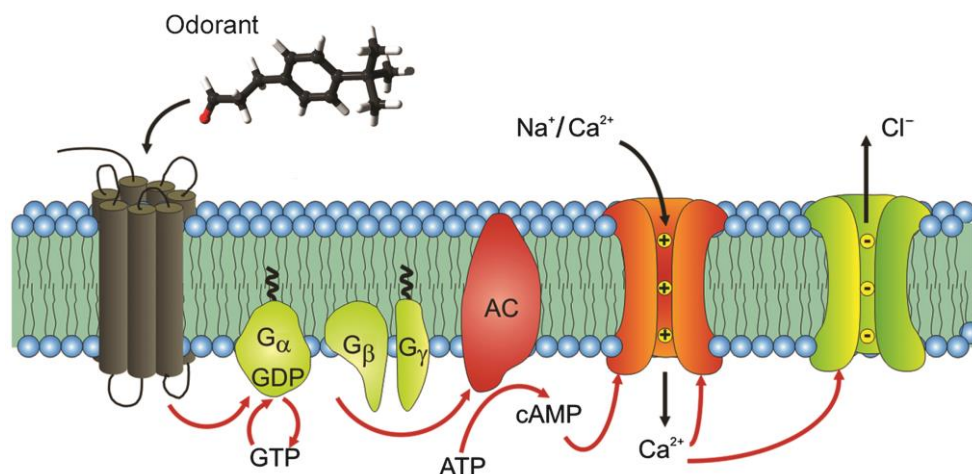


Figure 1.5: Graphical representation of the cAMP mediated transduction pathway operating in olfactory receptor neurons. GDP: guanosine diphosphate; GTP: guanosine triphosphate; ATP: adenosine triphosphate; cAMP: cyclic adenosine monophosphate; AC: adenylyl cyclase.^[6] Reproduced with permission from Professor Hanns Hatt of Ruhr University Bochum, Germany.

1.3 – Structure-Odour Relationships (SOR)

1.3.1 – Quantitative and Qualitative Olfactory Descriptions

The olfactory properties of an odorant molecule can be classified according to two parameters; potency and character. Newly synthesised molecules are generally described by perfumers as a solution of the compound absorbed onto blotter paper. Odorants are commonly evaluated at high concentration levels to reveal nuances besides just the dominant accord. The olfactory impression of a molecule is described in either a semantic way or by direct comparison to benchmark odorants.^[26, 34] Both methods of analysis give rise to a multidimensional description that relies heavily on reference to common descriptors.^[6]

A fragrance wheel is a classification chart that endeavours to demonstrate the relationship between different classes of odour. This method of classification can be applied to complex mixtures such as perfumes, or simple components such as individual molecules. The wheel displayed in Figure 1.6 includes four major families; floral, oriental, woody and fresh, each further divided into subgroups.^[35] The location of each subgroup demonstrates its olfactory relationship and ability to blend into the next subgroup.

When the human olfactory system is scientifically understood and cellular expression technology is sufficiently advanced as to be available to screen novel odorant molecules, it is conceivable that odour descriptions will be given in the form of activation patterns of olfactory receptors and glomeruli. Until that point in time, odorant descriptions must rely on inaccurate semantic or comparative methods of description.

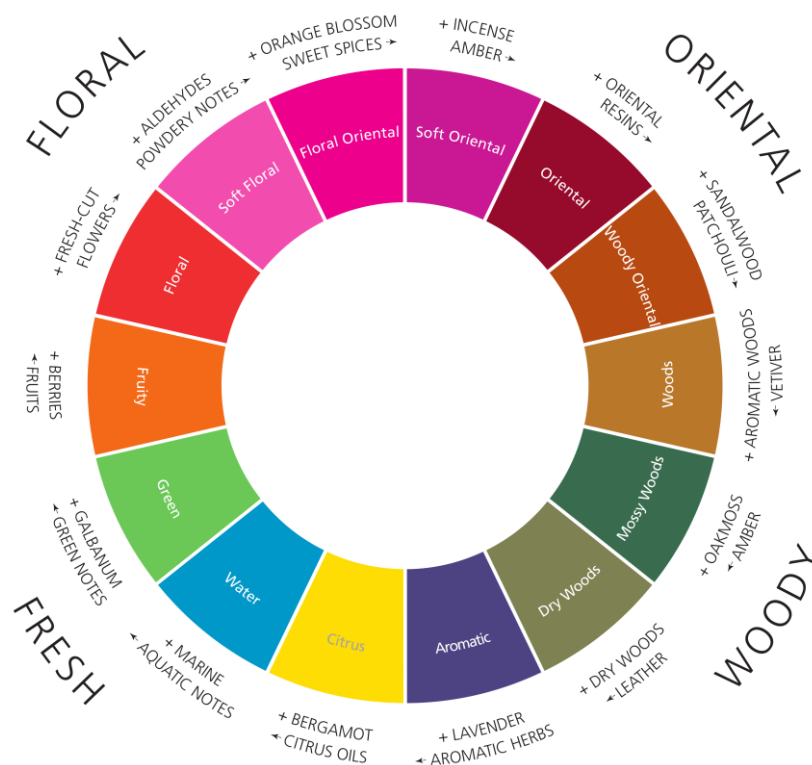


Figure 1.6: Fragrance wheel.^[35] Copyright Michael Edwards. Reproduced with permission.

The potency of an odorant is a quantitative measurement of the average minimal quantity that can be detected by the human olfactory system. This quantity is known as an odour threshold value and is generally reported in nanograms per litre (ng/L) or parts per billion (ppb). The value differs depending on the physiological and psychological condition of an individual. In general, females exhibit higher sensitivity than males, both sexes reaching their highest sensitivity immediately after puberty.^[6] A threshold value depends heavily on the method of measurement.^[36] The experimental differences between threshold values for a given compound measured in water or air can be pronounced (Figure 1.7).

Ideally, threshold values are measured in air using a technique named Gas Chromatography – Olfactometry (GC-O). This technique relies on human assessors to detect and evaluate gas-phase odorants eluting from a gas chromatograph mediated separation.^[26, 37] A threshold value for a molecule can be established by injecting dilutions of the sample substance in a descending order of concentration until the panellist fails to detect the odorant.^[38] The panellist detects in blind and if the recorded detection time matches the chromatographic retention time, the sample would be further diluted. Owing to variation in human olfactory ability, threshold values are usually established for multiple persons and an average value reported.^[37]

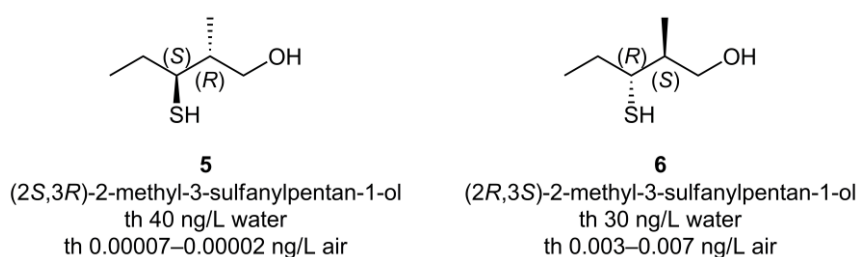


Figure 1.7: Air and water odour threshold differences of *anti*-3-mercapto-2-methylpentanol diastereomers.^[39]

1.3.2 – Structure-Odour Correlation

The Roman philosopher Lucretius proposed the first structure-odour activity theory when he stated that pleasant smelling odours were composed of particles with smooth geometries, whilst harsh smelling odours were of hooked geometries.^[6] The first scientific attempt to link olfactory properties with molecular structure was the stereochemical theory, proposed in 1951 by Amoore.^[40] The theory proposed a concept of primary odours from which all other odours are composed, analogous to the theory of primary colours within the sense of vision. Seven primary odours were proposed, each with their own hypothetical receptor binding site: ethereal, camphoraceous, musty, floral, minty, pungent and putrid.^[26, 41] Pungent and putrid odour impressions were thought to depend on the electronic nature, rather than the size or shape of the molecule.^[6] It was theorised that strongly nucleophilic molecules exhibited a putrid odour whilst strongly electrophilic molecules exhibited a pungent odour.^[42] Studies into specific anosmia, the inability to detect a particular odour, were undertaken in an attempt to offer evidence for the theory.^[26]

Another theory of olfaction is the vibrational theory, first proposed by Dyson and later extended by Wright.^[43-44] The theory states that the olfactory properties of a molecule are the direct result of vibrational frequencies in the infrared range.^[26] A further adaptation of this theory which stated that a quantum electron tunnelling mechanism could explain the link between the odorant properties and vibrational spectra of a molecule was proposed by Turin.^[45] He attempted to apply the theory in the explanation of paradoxes such as molecules with near identical molecular shapes but dissimilar odours, and molecules with similar odours but dissimilar molecular shapes.

The current scientifically accepted theory of olfaction is known as shape theory. The theory proposes that the olfactory properties of a molecule are related to molecular shape, molecular size and functional groups present.^[46] Examples of how these parameters can affect olfactory properties are delineated in Figure 1.8. The lily-of-the-valley aldehyde Lyrar[®] (**7**) and γ -bicyclohomofarnesal (**9**) both represent potent commercially available odorants. The Δ^1 isomer (**8**) of Lyrar[®] (**7**) is completely odourless owing to a different orientation of the carbonyl osmophore functionality. The β -alkene isomer (**10**) of γ -bicyclohomofarnesal (**9**) is also odourless owing to steric hindrance of the osmophore preventing interaction with olfactory receptor(s). Another noteworthy example is that the olfactory properties of the constitutional isomers β -damascone (**11**) and β -ionone (**12**) are amalgamated in the corresponding *bis*-ketone compound **13**. This phenomenon occurs because of keto-enol tautomerism; compound **13** exists as an equilibrium of the two enol forms and thus contains olfactory properties of both parent materials.^[6]

Structure-activity relationship research has generally been limited to focussing on distinct odorant groups such as ambergris, musk and sandalwood, largely owing to that fact that these odorant groups contain compounds with rigid molecular structures. Flexible molecules can adopt a larger range of energetically favourable conformations, each of which may be responsible for interacting with a different olfactory receptor.^[26] With a substantial data set, a computational model linking molecular structure and olfactory properties can be created. This type of model is a specific case of a Quantitative Structure-Activity Relationship (QSAR) model, and is referred to as an olfactophore model.^[6] These types of models correlate the activity of a ligand and a given receptor site or receptor class.

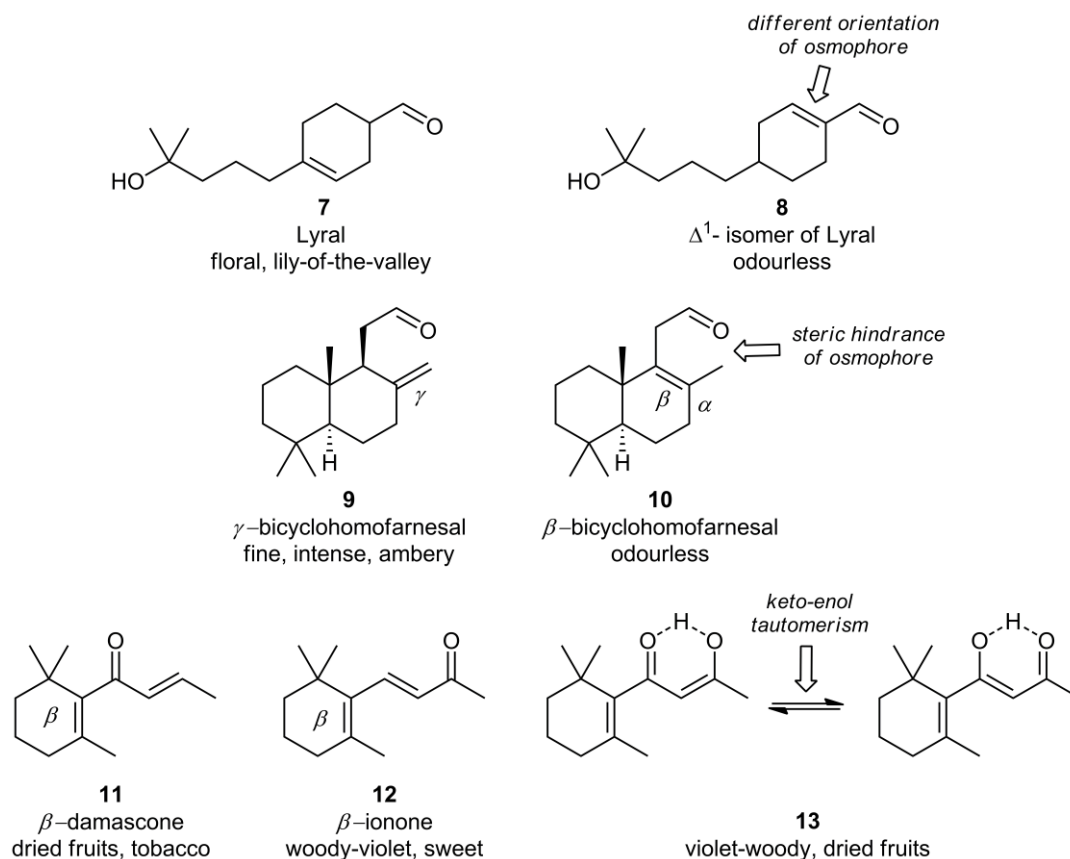


Figure 1.8: Molecular shape, molecular size and functional groups affect odorant properties.^[6]

There exist two major difficulties associated with the development of accurate structure-odour relationship models. The first arises from an incomplete understanding of the mechanism of olfaction. The second problem involves the difficulty associated with measurement; odour quality is a subjective quality dependent on concentration and organoleptic state, as opposed to chemical purity.^[26]

1.3.3 – Osmophores and Functional Groups

For a given molecule to exhibit olfactory activity it needs to interact with olfactory receptors and is therefore generally required to contain at least one H-bond acceptor or donor functionality.^[6, 47] Functional groups involved in hydrogen bonding to olfactory receptors are referred to as osmophoric groups. Such functionalities include carbonyl, hydroxyl, ester and alkoxy moieties, as well as their heterocyclic equivalents. Alkene and alkyne functionalities are also recognised to have the ability to act as osmophores.

A hydrogen-bond acceptor or donor functionality can be exchanged for a corresponding group with little alteration in the olfactory properties of the molecule.^[6] This effect is demonstrated effectively in benzaldehyde (**14**). An exchange of the H-bond acceptor functionality from an aldehyde (**14**) to a nitrile (**15**), nitro (**16**) or azide (**17**) functionality provides a compound that retains the characteristic almond fragrance of the parent material (Figure 1.9).^[6]

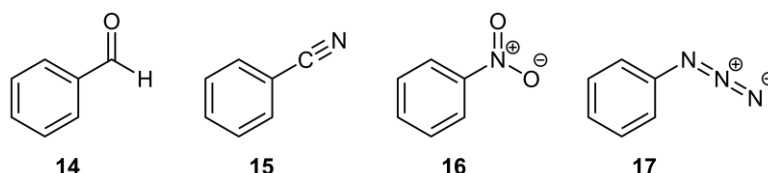


Figure 1.9: Exchanging H-bond acceptors; almond smelling analogues of benzaldehyde (**14**).^[6]

The exchange of an O-atom for an S-atom generally leads to a dramatic alteration in olfactory properties. The H-bond geometries of thioether, thioester and thioketone functionalities differ substantially to their corresponding *oxa*-analogues. Thionated compounds therefore bind to olfactory receptors in a different manner, often resulting in completely unrelated olfactory properties.^[6] An example of this effect is demonstrated during the thionation of musk odorant Exaltolide[®] (**18**). Thiolactone **21** no longer contains musk nuances, instead containing roasted and burnt notes and a much higher threshold value of 60 ng/L air, substantially weaker than the parent material (**18**). The thioketone analogue **22** is even weaker with a threshold value of 100 ng/L air, but does still possess some musk nuances. Replacement of both oxygen atoms with sulphur atoms gives near odourless compound **23** (th >300 ng/L air) (Figure 1.10).^[48]

The difference in electronegativity between sulphur and oxygen atoms, as well as the *ca.* 20% larger van der Waals radius of sulphur additionally contribute to the altered binding properties. A sulphur atom is actually a better replacement for a C=C alkene moiety.^[6] This is demonstrated in thioether compound **20** which retains the musk note and low threshold value of parent alkene **19**.^[48] Interestingly it was discovered that human sensitivity to musk odorant Exaltolide[®] (**18**) varies with hormonal conditions during the menstrual cycle.^[6] It was also found that endogenous estrogens increase sensitivity to musk odorants whilst androgens decrease sensitivity to musk odorants.^[49-50]

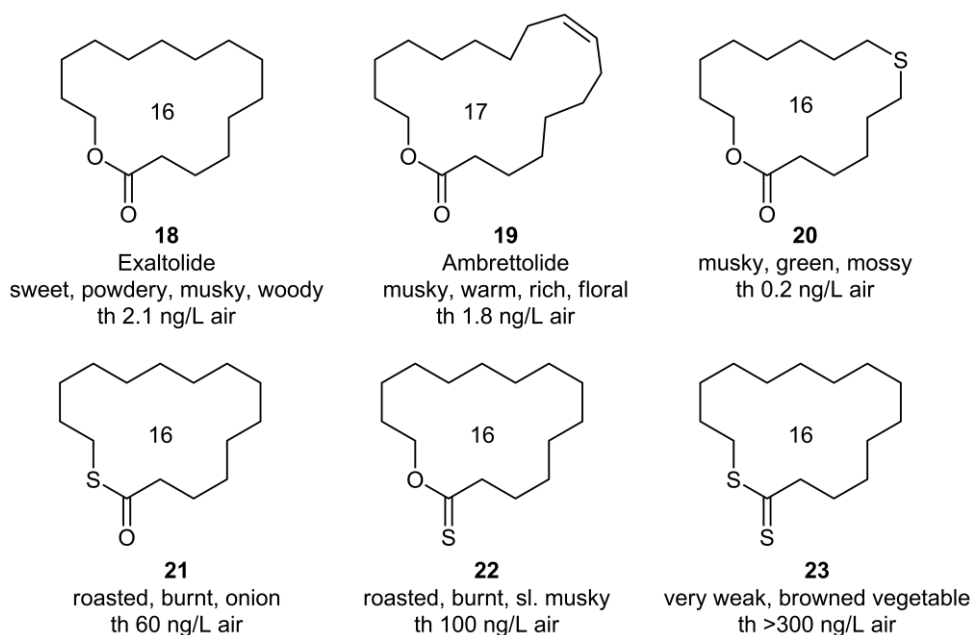


Figure 1.10: Commercially available musk odorants **18** and **19**, and thionated analogues **20–23**.^[6, 48, 51]

The strategic substitution of an oxygen atom with a sulphur atom can lead to insights into structure-odour relationships by revealing which functionalities are acting as osmophoric groups. The substitution of a carbon atom with a silicon atom is also a useful tool for the exploration of structure-odour relationships. A C–Si bond is *ca.* 20% longer than a C–C bond therefore making substitution a useful tool for exploring the molecular volume of a receptor, particularly the hydrophobic section.^[6]

Although seldom useful, it is possible to substitute a tertiary carbon atom with any Group 14 atom. A variety of tertiary carbon atom substituted analogues of benzyl(dimethyl)carbinol (**24**) are displayed in Figure 1.11. The only Group 14 analogue that retained the fresh floral note of the parent material (**24**) was the silicon substituted analogue **25**. The germanium substituted analogue dimerised immediately to provide compound **26**, for which a soapy and almond fragrance is reported, presumably due to minor quantities of the monomer entering the vapour phase. The tin substituted analogue **27** was discovered to be completely odourless, presumably too large to fit into an olfactory receptor.^[6]

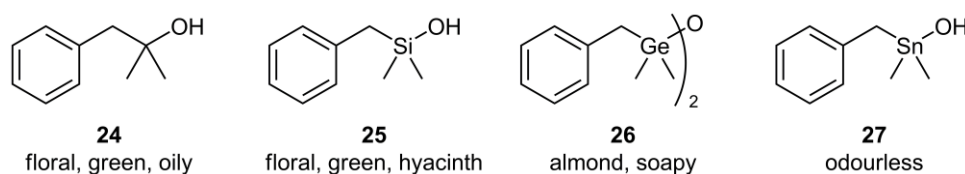


Figure 1.11: Group 14 analogues (**25–27**) of benzyl(dimethyl)carbinol (**24**).^[6]

A bioisostere for a hydrogen atom is a fluorine atom.^[6] A variety of fluorine substituted odorants were previously synthesised and it was reported that the olfactory properties of the resulting molecules were little affected. It was discovered that the same molecules were profoundly affected by the substitution of a methyl functionality at the same molecular location.^{33,34} Other halogen atoms were discovered to have a more powerful influence on the olfactory properties of the resulting molecule owing to their larger size.^[6]

1.3.4 – Stereochemistry and Odour Perception

A chiral molecule is defined as a molecule which contains geometric properties that are non-superimposable upon its mirror image.^[52] The majority of biological macromolecules are homochiral, with few exceptions. Naturally occurring protein molecules are composed of exclusively L-configured amino acid monomers, and nucleic acids, such as RNA and DNA, are composed exclusively of D-ribose and D-deoxyribose.^[53] Analogous to other protein molecules, receptors are composed of L-configured amino acids and therefore exist as chiral molecules themselves. The binding pocket of a receptor is consequently chiral and able to discriminate between enantiomers of a given molecule.^[54] This effect is important in pharmaceutical research as *ca.* 50% of all active drugs contain a stereogenic centre.^[6] The effect is also pronounced in the closely related science of gustation; for example D-asparagine having a sweet taste and L-asparagine being completely tasteless.^[53]

Previously, any olfactory differences between enantiomers were ignored or ascribed to impurities within the sample material.^[55-56] It is now scientifically recognised that enantiomers can exhibit different olfactory properties. It is also recognised that differences in the olfactory properties between enantiomers may be present only in minor nuances and thus enantiomeric purity is of utmost importance during olfactory analysis.^[6] There are four recognised relationships for enantiomers of a given odorant.^[6, 54]

- 1) *Case A: One enantiomer is odoriferous, one enantiomer is weak or odourless.*

This is the case for many highly potent odorant molecules owing to a molecular shape that is perfectly complimentary to a receptor site.

- 2) *Case B: Both enantiomers smell similar but possess different intensities.*

The most common case between odorant enantiomers. Neither enantiomer fits perfectly into the receptor but both enantiomers are interacting with the same receptor.

- 3) *Case C: Both enantiomers smell similar and possess similar intensities.*

This is the case when both enantiomers possess low receptor affinity and that therefore the chiral portion of the molecule is not differentiated by the receptor. Both enantiomers can be expected to be of low potency.

- 4) *Case D: Both enantiomers smell different.*

The rarest case between odorant enantiomers. Both enantiomers interact with different olfactory receptors leading to completely different odour descriptions and odour threshold values.

Some typical enantiomeric pairs of odorants are delineated in Figure 1.12. The enantiomers of carvone are perhaps the most striking example of enantioselectivity in odour perception. Pure samples of (+)-(S)- and (-)-(R)-carvone (**28** and **29**, respectively) had been isolated by fractional distillation of the essential oils of caraway and spearmint and were recognised to have different odour profiles.^[54, 57] It remained a possibility that the olfactory discrepancies were due to minor impurities and therefore it was not scientifically accepted that the two enantiomers could have different olfactory properties. Unequivocal evidence for olfactory enantiodiscrimination was provided in two simultaneously released publications.^[58-59] One study concentrated on enantiomeric purification and derivatisation of the parent material^[58] whilst another study concentrated on chemical interconversion between the two enantiomers,^[59] together providing undisputable evidence that enantiomeric odorant molecules can possess different olfactory properties.

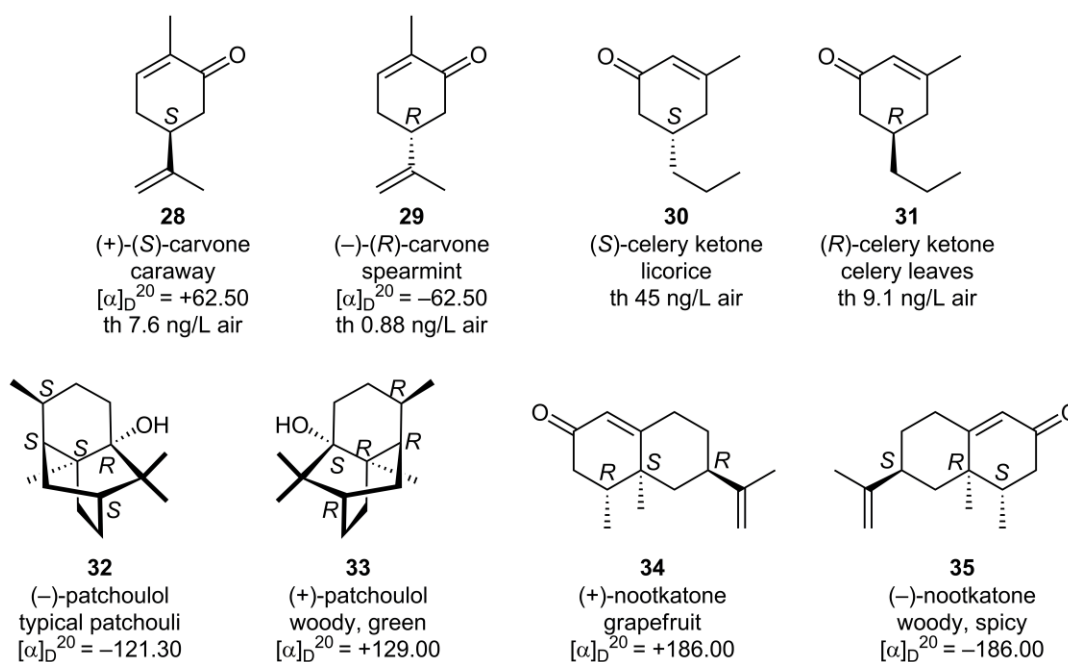
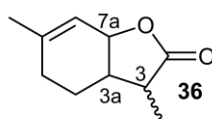


Figure 1.12: Chiral odorant pairs illustrating different odour descriptions and odour threshold (th) values.^[6]

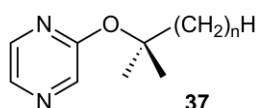
A naturally occurring odorant with strikingly dissimilar threshold values between its various enantiomers is wine lactone (**36**), an important flavour component in white wine (Figure 1.13).^[53] All eight stereoisomers were synthesised and evaluated.^[60] The variation in odour threshold was discovered to range from 0.00001–0.00004 ng/L air to a near odourless threshold value of >1000 ng/L air. The naturally occurring (3*S*,3*aS*,7*aR*)-configured stereoisomer was discovered to have the lowest odour threshold of the series, and is additionally the most potent odorant molecule known to date.^[6, 60]



configuration	odour threshold, ng/L air
(3 <i>S</i> ,3 <i>aS</i> ,7 <i>aR</i>)	0.00001 – 0.00004
(3 <i>S</i> ,3 <i>aS</i> ,7 <i>aS</i>)	0.007 – 0.014
(3 <i>S</i> ,3 <i>aR</i> ,7 <i>aR</i>)	0.05 – 0.2
(3 <i>R</i> ,3 <i>aS</i> ,7 <i>aS</i>)	8 – 16
(3 <i>R</i> ,3 <i>aR</i> ,7 <i>aR</i>)	14 – 28
(3 <i>S</i> ,3 <i>aR</i> ,7 <i>aS</i>)	80 – 160
(3 <i>R</i> ,3 <i>aR</i> ,7 <i>aS</i>)	>1000
(3 <i>R</i> ,3 <i>aS</i> ,7 <i>aR</i>)	>1000

Figure 1.13: Odour threshold values for various stereoisomers of wine lactone (**36**).^[53, 60]

Pyrazines are naturally occurring odorant molecules that have previously received attention in terms of enantiomeric olfactory variation. Some pyrazine derivatives possess a distinctive capsicum fragrance, associated with exceedingly low odour threshold values.^[61-62] A variety of synthetic alkoxy pyrazine compounds were synthesised and their olfactory properties determined (Figure 1.14).^[63] The threshold values of the prepared analogues were discovered to grow with the increasing alkyl chain length, until a length of $n = 4$, at which time the analogues became most potent. Although odour description remained identical, there was significant variation in odour threshold values between (*S*)- and (*R*)-configured enantiomers at higher chain lengths, indicating a Case B relationship between the enantiomers.



Side chain	threshold, ppb		odour description
	(<i>S</i>)-(+)	(<i>R</i>)-(-)	
n = 1	100	100	green, dusky
n = 2	100	100	fatty, metallic, green
n = 3	70	200	green, metallic, fatty, burdock
n = 4	30	90	green, fishy, amine-like, fatty

Figure 1.14: Odour comparisons of synthetic alkoxy pyrazines.^[53, 63]

1.4 – Marine Odorants

1.4.1 – Naturally Occurring Marine Odorants

Naturally occurring chemicals perceived by the human olfactory system as smelling reminiscent of the ocean appear to belong to three distinct chemical families. The primary example of a natural material which exhibits a prototypical marine olfactory character is algae. Brown algae (*Phaeophyceae*) produce multiple odoriferous C₁₁H₁₄ to C₁₁H₁₈ linear and alicyclic organic compounds that act as gamete pheromones (Figure 1.15).^[64-68] The dictyopterenes are a group of such chemical compounds that are naturally present in marine and freshwater environments. (+)-Dictyopterene A (**38**) was the first odoriferous compound to be isolated from algae and was discovered to contain the characteristic odour of seawater.^[66] A sigmatropic rearrangement of **38** gives (-)-dictyopterene C (**39**),^[69] which is reminiscent in odour to that of salmon roe.^[64] Giffordene (**40**), with a typical sea-algae odour is the principle pheromone of *Giffordia mitchellae*,^[70] whilst (-)-dictyopterene D (**41**) is more closely associated in tonality to green and tomato-leaf nuances, and is secreted by the brown algae *Ectocarpus siliculosus*.^[64, 71-72]

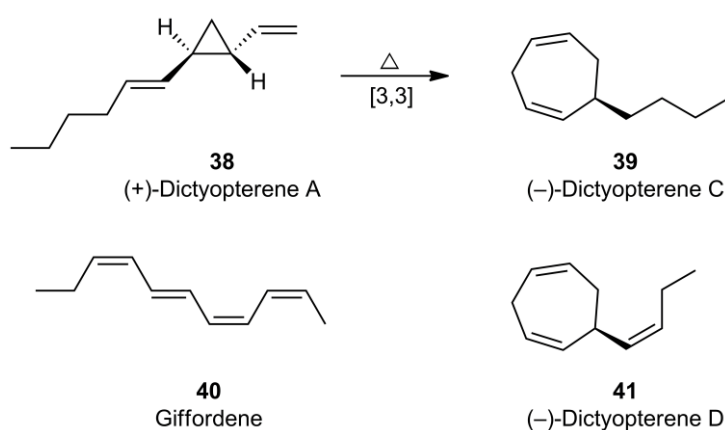


Figure 1.15: Naturally occurring odorant compounds in algae.^[64]

Another naturally occurring class of marine odorant compounds are the brominated phenol analogues (Figure 1.16).^[73] Bromophenols such as compounds **42–44** have been identified as key flavour components in seafood.^[74] It is hypothesised that bromophenol compounds make their way into the food chain by marine invertebrates feeding on phytoplankton and algae species.^[75]

A 1999 study revealed that the total bromophenol content of algae was highly varied across species, from 0.9 ng/g in the green algae *Codium fragile* to 2590 ng/g in the red algae *Pterocladia capillacea*.^[76] Multiple species of algae have been shown to contain bromoperoxidase enzymes capable of brominating organic substrates.^[77] The purpose of these compounds in algae is still yet to be determined but is hypothesised to relate to chemical defence or the reduction of peroxide toxin accumulation.^[76] Multiple odoriferous bromophenol analogues have also been isolated from various species of marine acorn worm.^[78-79]

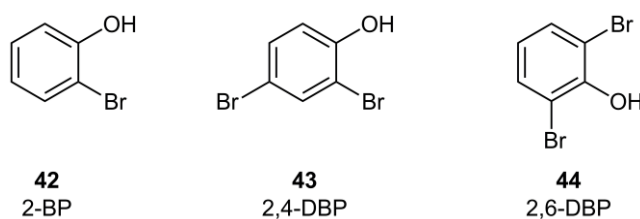


Figure 1.16: Bromophenol odorants from natural marine sources.

Unsaturated aldehyde compounds resulting from the degradation of fatty acids, such as compounds **45–47**, also contain marine tonalities (Figure 1.17).^[73] These compounds naturally occur in melon and cucumber, and are also present in algae.^[80-81] A variety of chemically related C-8 and C-9 unsaturated aldehyde, ketone and hydroxyl compounds were isolated from the terrestrial plant *Mertensia maritima*, known as oyster leaf for its unusual marine nuances.^[82]

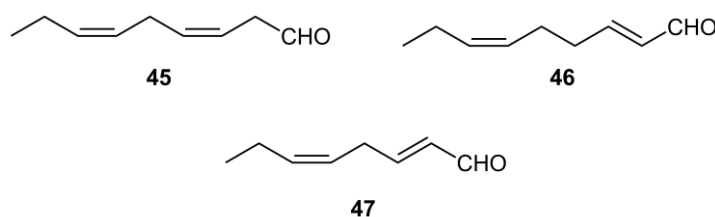


Figure 1.17: Naturally occurring unsaturated aldehyde compounds containing marine nuances.

1.4.2 – Synthetic Marine Odorants

Synthetic marine odorants have an important place in the palette of the modern perfumer (Figure 1.18). The formerly unestablished marine fragrance category is represented primarily by the synthetic odorant Calone 1951® (**50**). This material is used to convey the scent of seaside plus sea-breeze with floral overtones, and is typically present in levels below 1% in fine perfumes.^[10] Calone 1951® (**50**) is the basis of most marine fragrance accords, and although often required to be blended with aldehydic, ozonic and watermelon-like odorants, to date there is no superior perfumery material to convey the olfactory impression of a seashore.^[83]

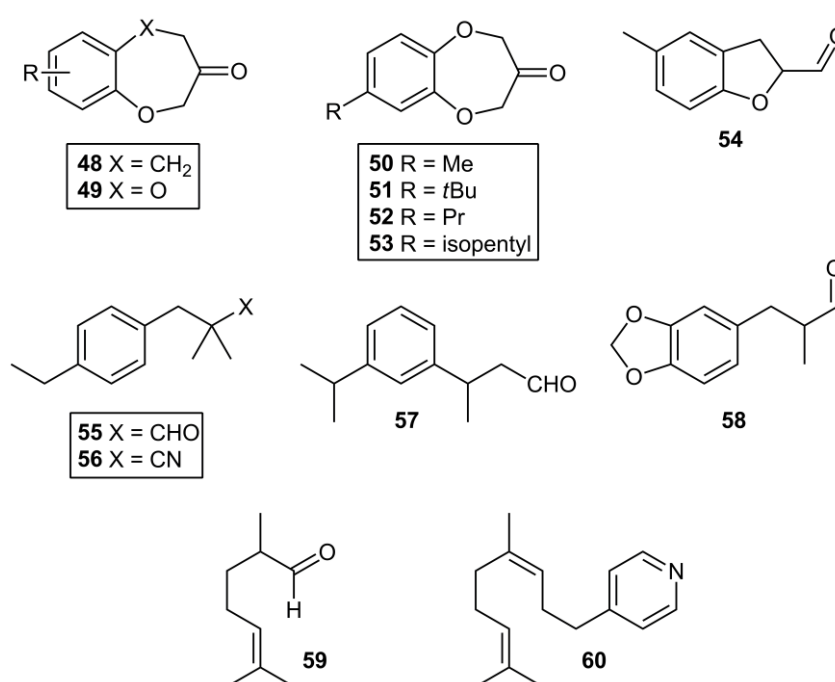


Figure 1.18: Various synthetic marine odorants.

With the launch of the perfumes “*New west for her*” (Aramis, 1990) and “*Escape for her*” (Calvin Klein, 1991), a marine trend in feminine perfumery was born.^[64] The later launch of masculine marine fragrances such as “*Kenzo pour homme*” (Kenzo, 1991) and “*L’Eau d’Issey masc*” (Issey Miyake, 1994) helped concretize the trend into modern perfumery. The original marine note incorporated just two raw materials, Calone 1951® (**50**) and Tropional® (**58**), but later evolved to include watermelon notes by the addition of the synthetic odorant Melonal® (**59**). Finally, ozonic aspects were added to the marine and watery nuances by the addition of Floralozone® (**55**) to form the typical aquatic accord found in modern

day fragrances.^[64] The evolution of the marine/aquatic accord in modern perfumery is delineated in Table 1.1.

	<i>“New west for her” (1990)</i>	<i>“Escape for her” (1991)</i>	<i>“L’Eau d’Issey” (1992)</i>	<i>“L’Eea d’Eden” (1996)</i>	<i>“Cool water fem” (1996)</i>	<i>“Polo Sport W” (1996)</i>
Calone 1951 [®] (50)	1.2%	0.8%	0.6%	0.17%	0.4%	0.45%
Tropional [®] (58)	7.5%	3.7%	2%	1.5%	4.3%	4.8%
Melonal [®] (59)	-	-	0.02%	0.03%	0.02%	0.12%
Floralozone [®] (55)	-	-	-	0.1%	0.07%	0.04%
Ratio 50 : 58	0.21	0.16	0.3	0.11	0.09	0.09

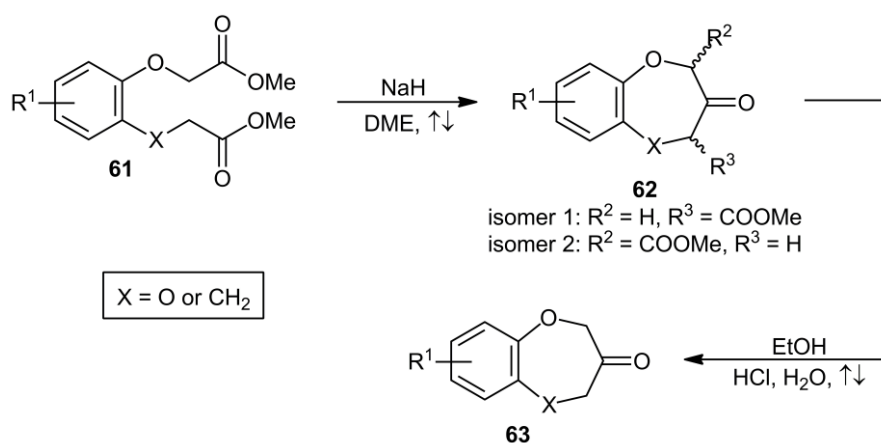
Table 1.1: Evolution of the marine/aquatic accord in modern perfumery.^[64]

The popularity of the marine fragrance trend led to the introduction of additional benzo[*b*][1,4]dioxepin-3-one marine odorant compounds including Transluzone[®] (**51**, Firmenich), Aldolone[®] (**52**, Firmenich),^[73, 84] and Azurone[®] (**53**, Givaudan).^[83] All analogues share the marine and watermelon-like olfactory characteristics of Calone 1951[®] (**50**), differing primarily in intensity and lasting power.^[38] Both the benzo[*b*][1,4]dioxepin-3-one (**49–53**) and 4,5-dihydrobenzo[*b*]oxepin-3-one (**48**) molecular scaffolds have been discovered to contain marine accords, although the latter is reported to be much weaker in olfactory impression.^[73, 85] Researchers at Firmenich recently described that the 1,4-dioxepin-6-one moiety of the marine odorant scaffold could be replaced by a 2,3-dihydrofuran-2-carbaldehyde unit leading to compound **54**, for which a powerful aldehydic-green marine odour was reported.^[86]

Unusual molecular structures to contain marine character are Fleuraniil® (**56**, IFF), a nitrile analogue of Floralozone® (**55**, IFF), and alkyl substituted pyridine analogue Maritima® (**60**, IFF). A variety of alkyl substituted pyridine compounds are patented for use as fragrances,^[87] although to be noted is that this family of odorants has a watery profile often more reminiscent of stagnant water than fresh seaside nuances.^[73]

1.4.3 – Benzo[*b*][1,4]dioxepin-3-one Discovery – Pfizer

The benzo[*b*][1,4]dioxepin-3-one synthetic marine odorant family was discovered in 1966 by serendipity at Pfizer by Beereboom, Cameron and Stephens.^[85, 88] The original synthesis involved a Dieckmann condensation reaction of various *bis*-ester compounds (type **61**) followed by decarboxylation of the resulting intermediate ester (type **62**) to furnish the completed odorant (type **63**) (Scheme 1.1). The Dieckmann condensation route of synthesis remains the commercially employed route of synthesis.^[83] The odour threshold grew for compounds claimed in the original patent as the substituted alkyl chain was increased in size from methyl (0.031 ng/L air, Calone 1951®, **50**) through to propyl (0.10 ng/L air, Aldolone®, **52**) and butyl (0.26 ng/L air), but longer chain analogues were not explored.^[6] Calone 1951® (**50**) was the only compound originally commercialised from within the series, initially only used as a nuanceur in lily-of-the-valley accords,^[83] but now produced on an estimated thirty ton annual scale.^[73]



Scheme 1.1: Original synthesis of the benzo[*b*][1,4]dioxepin-3-one and 4,5-dihydrobenzo[*b*]oxepin-3-one analogues by Beereboom, Cameron and Stephens.^[85, 88]

1.4.4 – Benzo[*b*][1,4]dioxepin-3-one Structure-Odour Relationship Studies – Givaudan

In an attempt to synthesise novel odorants containing both marine and musk characteristics, researchers at Givaudan, Switzerland discovered that more powerful benzo[*b*][1,4]dioxepin-3-one analogues could be synthesised than was previously hypothesised. A merged note is already present in the odorant Musk Alpha® (**64**) but this compound was removed from the market due to phototoxicity. To construct new odorant molecules with merged notes, the molecular structures of polycyclic musk odorant Galaxolide® (**65**) and Calone 1951® (**50**) were amalgamated (Figure 1.19). Molecular structure **66** was chosen as the target compound in order to not go beyond the previously established upper molecular weight, the *tertiary*-butyl analogue **51**.^[83]

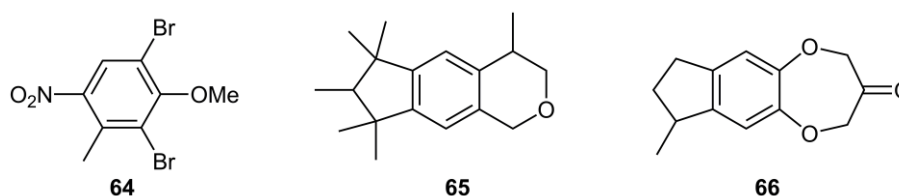
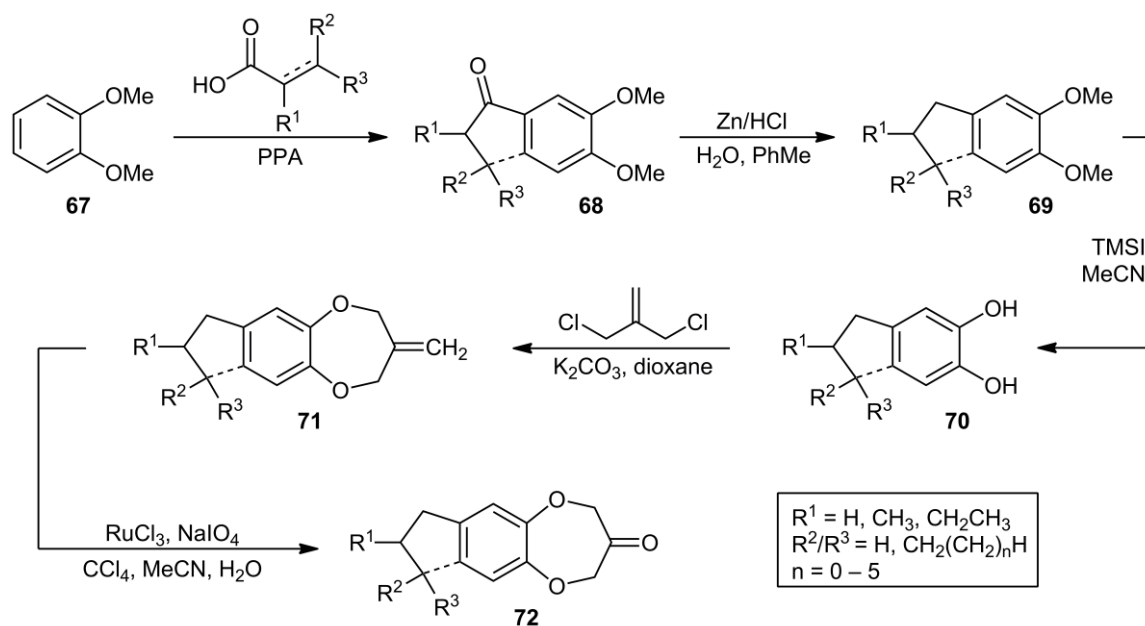


Figure 1.19: Marine nitro musk odorant **64**, polycyclic musk odorant **65** and target compound **66**.^[83]

Compound **66** was discovered to not contain the required olfactory characteristics but instead contained floral aspects that interested perfumers. To that effect a library of 7,8-annulated (**66**, **73–74**) and 7-alkyl substituted (**53**, **75–86**) analogues were synthesised beginning from veratrol (**67**). The synthetic route involved a Friedel–Crafts acylation reaction of veratrol (**67**) with various carboxylic acid analogues in the presence of polyphosphoric acid (PPA) to provide carbonyl intermediates of type **68** (Scheme 1.2). It should be noted that if the carboxylic acid analogue contained unsaturation at the C2–C3 position within the molecular structure, the intermediate compound would additionally cyclise in a Friedel–Crafts alkylation reaction to yield the corresponding annulated bicyclic structure. These unusual polyphosphoric acid catalysed Friedel–Crafts reactions of veratrol to yield substituted veratrol or indanone analogues were previously explored by Marquardt.^[89] The isolated intermediates of type **68** were subjected to Clemmensen reduction and subsequent demethylation with trimethylsilyl iodide to give substituted catechol analogues of type **70**. The catechol analogues were then cyclised in a Williamson reaction with a *bis*-halogenated alkylation agent to provide methylene compounds of type **71**, before being oxidised to yield the finished benzo[*b*][1,4]dioxepin-3-one analogues of compound type **72**.



Scheme 1.2: Synthetic route employed by Kraft *et al.*^[83] in the synthesis of 7,8-annulated and 7-alkyl substituted benzo[*b*][1,4]dioxepin-3-one analogues.

The library of analogues prepared is displayed in Figure 1.20. The most interesting compound of the series was discovered to be the 7-isopentyl substituted analogue later commercialised and named Azurone[®] (**53**).^[90] This analogue was described as possessing the intense marine aspects of Calone 1951[®] (**50**) together with floral-aldehydic nuances. Whilst it was discovered that the intensity decreased with more heavy and bulky alkyl substituents, the C₅H₁₁ group of **53** increased the intensity dramatically.

To explore this effect a variety of C–5 to C–8 analogues were synthesised, with the *n*-octyl analogue appearing to be the upper limit of marine odorant molecular dimensions. Using the odour threshold data of the prepared library, as well as data from patent literature, an olfactophore model was generated using computational software. Unsurprisingly, Azurone[®] (**53**) was discovered to be the optimum ligand. The model consisted of three hydrogen-bond acceptors, an aromatic binding site, an aliphatic hydrophobe and three excluded volumes inaccessible to the molecule (Figure 1.21).^[83]

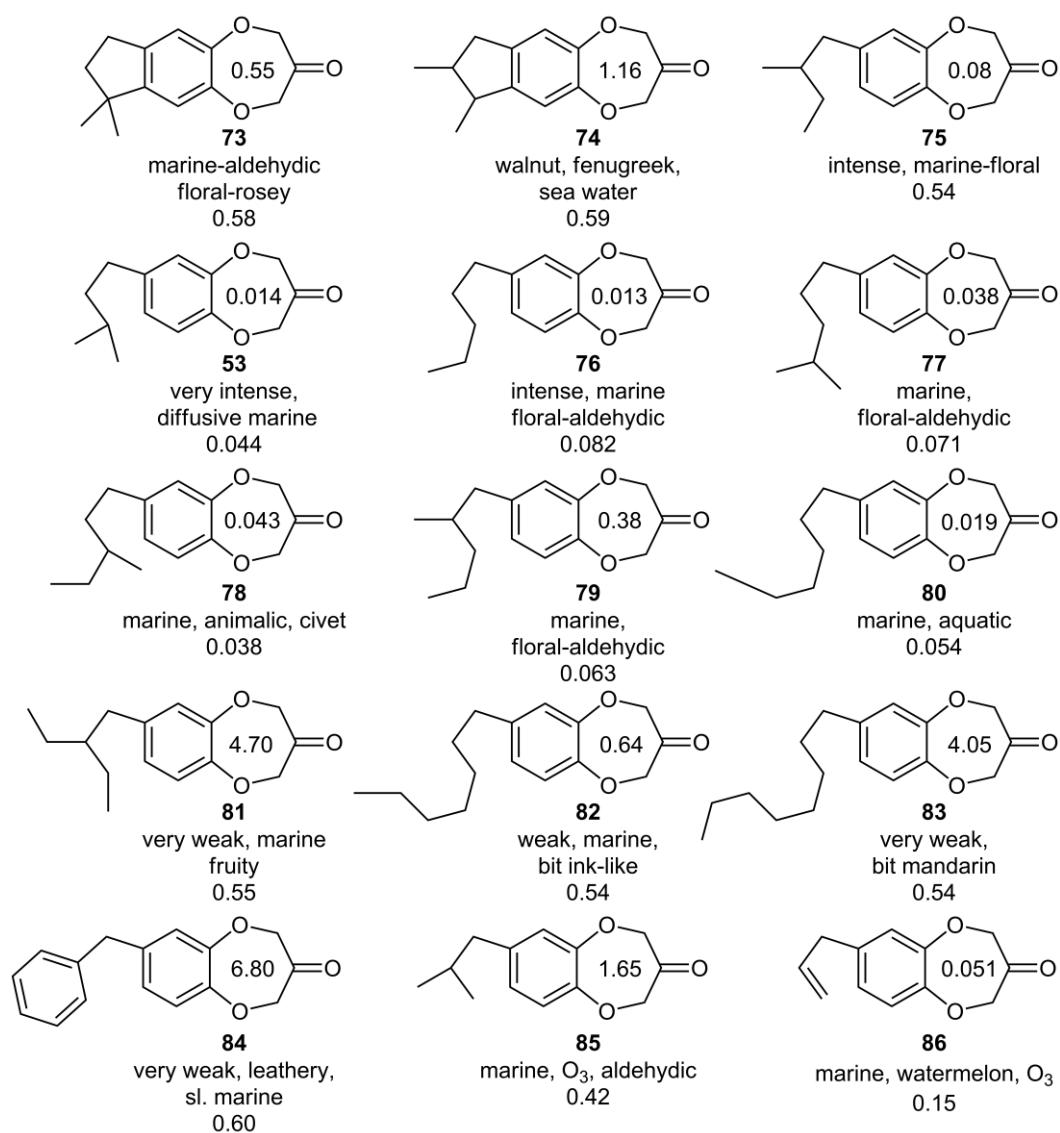


Figure 1.20: Library of 7,8-annulated and 7-alkyl substituted benzo[*b*][1,4]dioxepin-3-one analogues.^[83]

Experimental odour threshold values (ng/L air) indicated within molecular structure, calculated values outside.

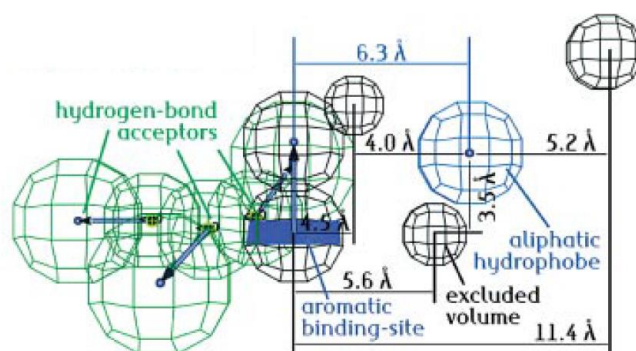
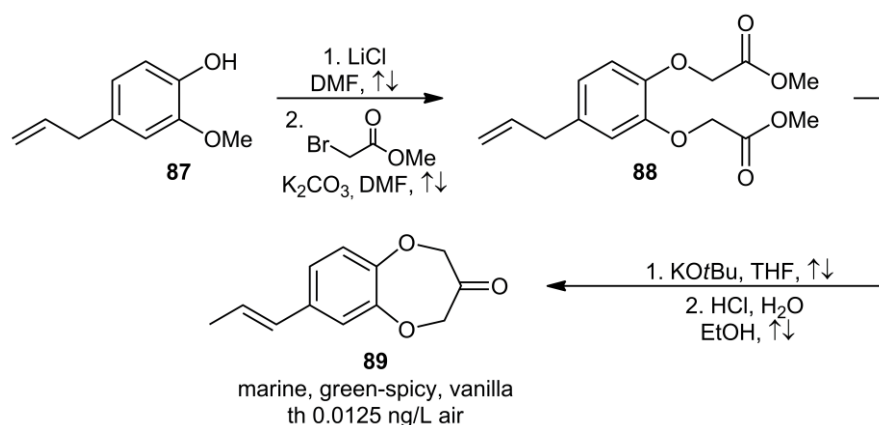


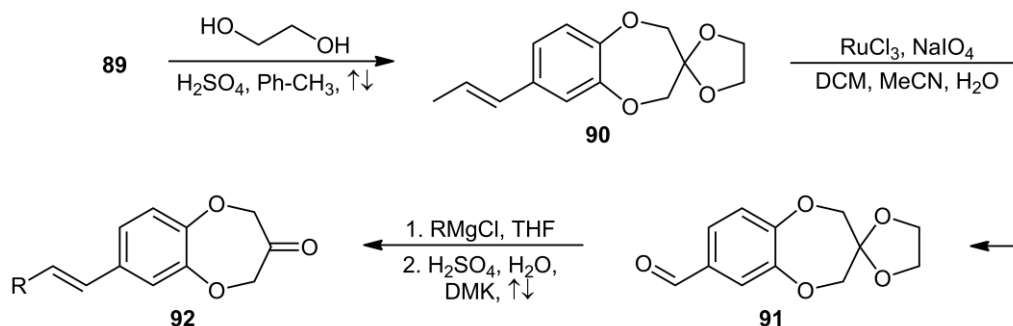
Figure 1.21: Marine odorant olfactophore model generated by Kraft *et al.*^[83] Copyright Wiley-VCH Verlag GmbH & Co. KGaA. Reproduced with permission.

During the synthesis of analogue **89** from eugenol (**87**) by Dieckmann condensation it was discovered that a change of base to potassium *tert*-butoxide, which can deprotonate irreversibly, yielded a compound with a vanilla note accompanying the typical marine fragrance (Scheme 1.3). It was revealed that an isomerisation of the alkene functionality to a benzylic position had occurred, giving a (*E*)-7-(prop-1-enyl) substituted analogue (**89**) which was discovered to be as potent as Azurone® (**53**).^[38] This discovery prompted additional research which exposed that potency, and therefore receptor binding strength, was increased with conjugated olefinic substituents.



Scheme 1.3: Synthesis of analogue **89** from eugenol (**87**), with alkene isomerisation.^[38]

A synthetic sequence beginning from compound **89** was used to construct a library of conjugated analogues. Compound **89** was protected as the 1,3-dioxolane derivative using 1,2-ethanediol and catalytic quantities of sulphuric acid to give compound **90**, followed by Katsuki-Sharpless oxidation to provide aldehyde intermediate **91** (Scheme 1.4). The aldehyde intermediate was subjected to Grignard reaction with various magnesium halide reagents, followed by an acid-catalysed dehydration and deprotection reaction to furnish the completed benzo[*b*][1,4]dioxepin-3-one analogues of type **92** for olfactory analysis.



Scheme 1.4: Synthetic route employed by Kraft *et al.*^[38] in the synthesis of conjugated seven-alkenyl substituted benzo[*b*][1,4]dioxepin-3-one analogues.

The alkenyl substituted analogues **93–96** were discovered to have extremely low odour threshold values, more potent than the most powerful steroid odorants (Figure 1.22). The extreme potency of the new experimental analogues deviated significantly from the predictions of the original marine olfactophore model. The model was revised to place the aliphatic hydrophobe in the plane of the aromatic binding site and nearly 1 Å further away, now 7.23 Å from the centre of the aromatic binding site. Two hydrogen-bond acceptors were found to be sufficient, but six excluded volumes 3.53 Å, 4.01 Å, 4.30 Å, 5.84 Å, 6.14 Å and 9.3 Å distance to the aromatic binding site were necessary for an 85% predictability of odour threshold. The revised model could bind both pseudo-twist-boat and pseudo-half-chair conformers of the heterocyclic ring system.^[38]

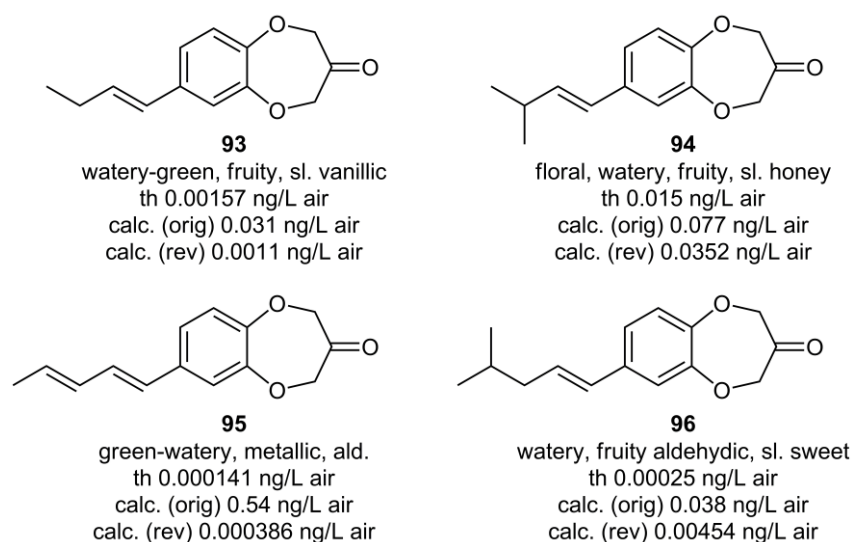


Figure 1.22: Unsaturated benzo[*b*][1,4]dioxepin-3-one analogues synthesised by Kraft *et al.*^[38] showing experimental odour thresholds and calculated odour thresholds for original and revised olfactophore models.

1.4.5 – Benzo[*b*][1,4]dioxepin-3-one Structure-Odour Relationship Studies – Firmenich

An extensive library of benzo[*b*][1,4]dioxepin-3-one analogues were synthesised and evaluated by researchers at Firmenich, Switzerland.^[73] The publication revealed important information about the marine odorant family regarding alkyl substitution, as well as the role of the O-atom(s) within the heterocyclic 1,4-dioxepin-6-one moiety (Figure 1.23). Olfactory evaluation of the prepared analogues resulted in the following conclusions; a) the presence of alkyl substitution on the aromatic ring is beneficial; b) branched alkyl substituents decrease potency; c) aromatic *bis*-substitution decreases potency; d) substitution at C-2 is unfavourable, presumably due to interference with the carbonyl osmophore; e) substitution at the C-7 position is favourable over substitution at the C-6 position. It was additionally discovered that substitution at the C-7 position was preferred for marine and watery nuances, whilst substitution at the C-6 position provided compounds with an aldehydic character.^[73]

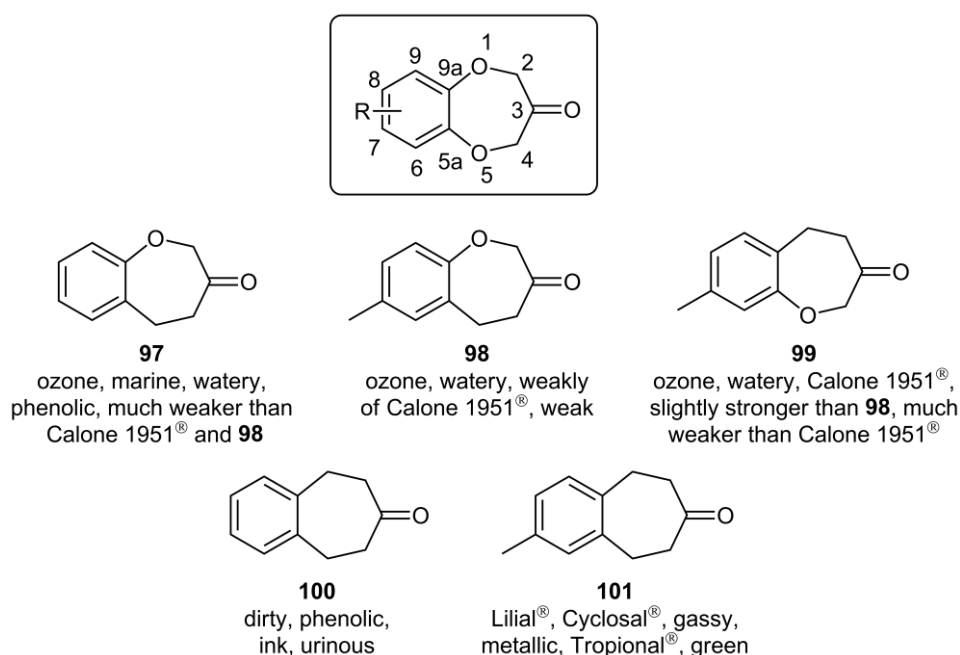


Figure 1.23: Mono- and *bis*-deoxygenated benzo[*b*][1,4]dioxepin-3-one analogues synthesised by

Gaudin *et al.*^[73]

The original patent claimed good olfactory properties for both the benzo[*b*][1,4]dioxepin-3-one and 4,5-dihydrobenzo[*b*]oxepin-3-one molecular scaffolds, but precise odour descriptions and potency were not reported.^[85] The re-synthesis of mono-deoxygenated analogues (**97–99**) revealed that both templates incorporated marine nuances but that the benzo[*b*][1,4]dioxepin-3-one template was clearly the more powerful marine odorant scaffold (Figure 1.23). A series of *bis*-deoxygenated analogues (**100–101**) were additionally synthesised and were discovered to not have marine characteristics.^[73] Discrepancies in potency between the sets of analogues led the researchers to suspect that the differences could be rationalised by the preferred conformation of the seven-membered heterocyclic ring moiety.

Computational models revealed that, whilst the potent benzo[*b*][1,4]dioxepin-3-one template (i.e. Calone 1951[®], **50**) favoured a pseudo-twist-boat conformation with the carbonyl functionality co-planar to the aromatic ring, the much weaker 8,9-dihydro-5*H*-benzo[7]annulen-7-one derivatives (i.e. **101**) favoured a pseudo-chair conformation that placed the carbonyl functionality completely out of plane. The 4,5-dihydrobenzo[*b*]oxepin-3-one analogues (i.e. **98**) showed intermittent activity between the two different conformations (Table 1.2).^[73] This contributed to the theory that co-planarity between the aromatic ring and the carbonyl functionality was linked to potent marine fragrance character.

	Pseudo-twist-boat	Pseudo-half-chair	Marine Odorant Activity
7-Methylbenzo[<i>b</i>][1,4]dioxepin-3-one (Calone 1951 [®] , 50)	0 kcal/mol	+2.7 kcal/mol	Strong
7-Methyl-4,5-dihydrobenzo[<i>b</i>]oxepin-3-one (98)	0 kcal/mol	−0.2 kcal/mol	Weak
2-Methyl-8,9-dihydro-5 <i>H</i> -benzo[7]annulen-7-one (101)	0 kcal/mol	−2.9 kcal/mol	None

Table 1.2: Calculated relative energies of the two main conformers of compounds **50**, **98** and **101**.^[73]

Additional research was later conducted by the same research group in order to address questions regarding the role of the carbonyl functionality in marine odorant perception. To that effect, a variety of analogues with alternative hydrogen-bond acceptor groups in place of the carbonyl moiety (type **102**) were synthesised and evaluated. In an effort to modify the position and spacial orientation of the carbonyl functionality by altering the molecular geometry of the original scaffold, the heterocyclic ring system was opened (type **103**) and also substituted with a five-membered ring system (type **104**) (Figure 1.24).^[86]

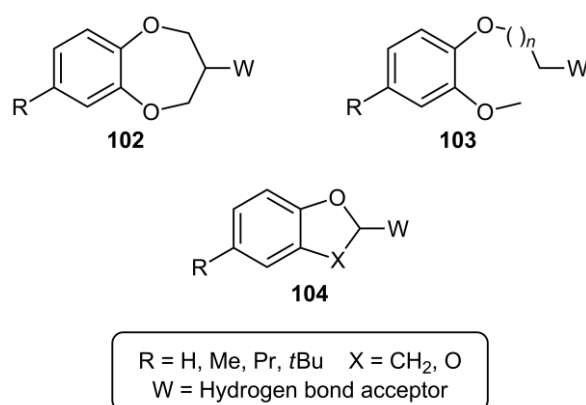


Figure 1.24: Targeted benzo[*b*][1,4]dioxepin-3-one analogue scaffolds of Gaudin *et al.*^[86]

A new more broadly-tuned olfactophore model was generated. The model contained one hydrogen-bond acceptor, an aromatic binding site and an aliphatic hydrophobe (Figure 1.25). A variety of hydroxyl, ether, acetate and epoxide substituted analogues of compound type **102** were synthesised and evaluated. The hydroxyl analogue of Calone 1951[®] (**50**) was discovered to retain marine-ozone character, but was discovered to be much weaker, presumably due to decreased volatility. The acetate and ether analogues were discovered to not contain marine nuances which was subscribed to the fact that these functionalities may lose their ability to act as hydrogen-bond acceptors. The odour of the epoxide analogue was reminiscent of the fresh marine note, but was not powerful. The results successfully confirmed that a carbonyl functionality substituted at the C-3 position is the optimal substituent for the benzo[*b*][1,4]dioxepin-3-one molecular scaffold.^[86]

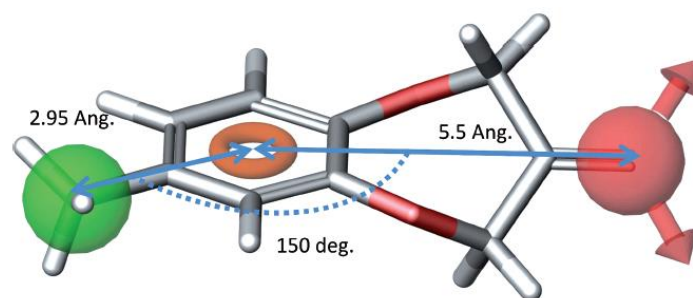


Figure 1.25: Marine-ozone olfactophore model generated by Gaudin *et al.*^[86] Copyright Wiley-VCH Verlag GmbH & Co. KGaA. Reproduced with permission.

A variety of analogues of compound type **103** were synthesised and evaluated. The motivation in opening the seven-membered heterocyclic ring system involved allowing the carbonyl osmophore to adopt an optimal conformation for receptor binding. No compounds of this class of analogues were discovered to contain ozone or marine character. This was hypothesised to be owing to a potential negative interaction of the free methoxy moiety with olfactory receptor(s). The discovery may additionally indicate that the oxygen atoms of the benzo[*b*][1,4]dioxepin-3-one template are more important for their conformation effects than for their electronic effects.^[86]

The final class of analogues synthesised and evaluated were of compound type **104** (Figure 1.26). It was discovered that compound **54** retained potent marine odour characteristics. The introduction of a methyl functionality geminal to the aldehyde (**105**) was clearly unfavourable, presumably due to interference with osmophore function. The carba analogues **106–107**,^[91-92] which have a similar molecular conformation, are in general more aldehyde, green, muguet and less ozone-marine. The authors noted that this class of molecule can fit into both the marine-ozone and lily-of-the-valley olfactophore models, and even hypothesised that these molecules could potentially interact with both olfactory receptors depending on their favoured conformation. They also suggested that the olfactory receptor for both odorant classes should be molecularly similar.^[86] Further evidence for this structural relationship arises from the fact that the *bis*-carba analogue of Calone 1951[®] (compound **101**) was described as having lily-of-the-valley-odour.^[73]

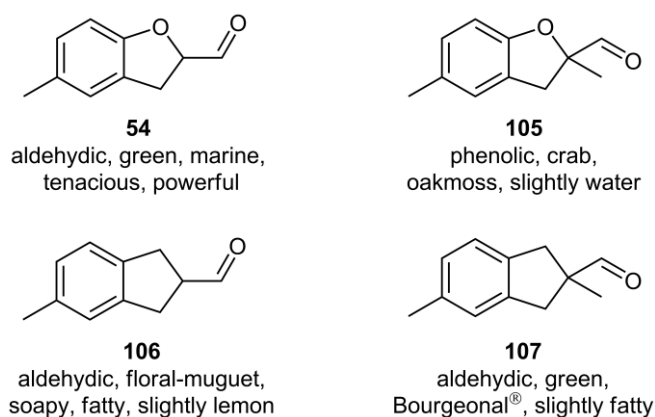
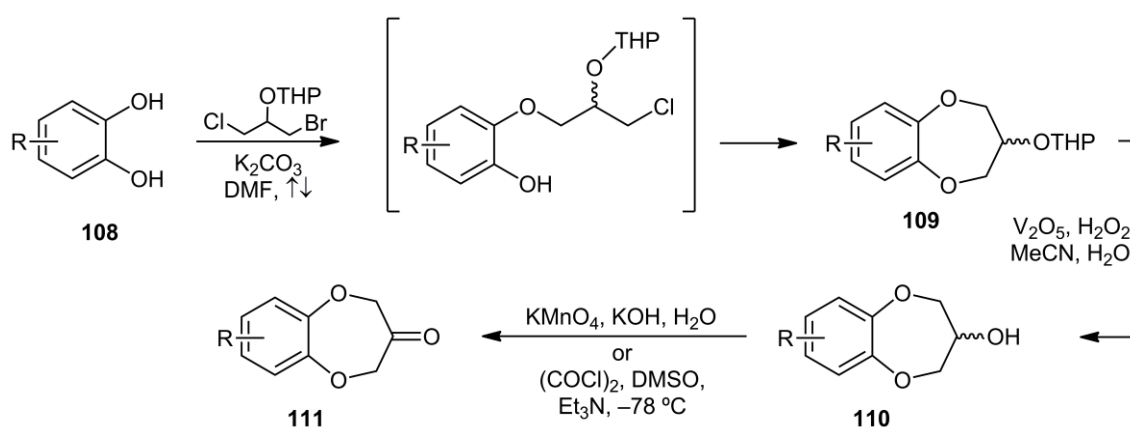


Figure 1.26: Five-membered benzo[*b*][1,4]dioxepin-3-one analogues displaying marine and lily-of-the-valley nuances.^[86]

1.4.6 – Benzo[*b*][1,4]dioxepin-3-one Structure-Odour Relationship Studies – RMIT University

A variety of substituted benzo[*b*][1,4]dioxepin-3-one analogues were synthesised and evaluated by researchers at RMIT University.^[7, 84, 93] Due to difficulties employing the patented Dieckmann condensation route in delivering new analogues, particularly those with electron withdrawing substituents, a new synthetic route was implemented (Scheme 1.5). The new synthetic route involved a Williamson reaction of various catechol analogues (type **108**) with a *bis*-halogenated alkylating agent to give an ether intermediate (type **109**) which was then deprotected and oxidised to furnish the completed odorant molecule (type **111**).



Scheme 1.5: Synthetic route to benzo[*b*][1,4]dioxepin-3-one analogues employed by Hügel *et al.*^[84]

A variety of aromatic ring substituted analogues were synthesised including nitro-, aldehyde-, bromo- and methoxy-substituted derivatives. It was discovered that the nitro- and aldehyde-substituted analogues were completely devoid of marine character, with the introduction of fruity, sweet and balsamic tonalities, indicative of an absence of any marine receptor binding interaction. Both the brominated and *tertiary*-butylated analogues were discovered to have walnut nuances, hypothesised to involve the steric bulk of the substituents. It was concluded that alkyl substitution is critical, but not essential, for marine odour characteristics, and that aromatic substitution modifies the odour perception of the benzo[*b*][1,4]dioxepin-3-one scaffold.^[84]

An additional study into the alteration of the polar osmophore functionality revealed that a carbonyl moiety is the optimal substituent, the results coinciding with those of Gaudin *et al.*^[86] It was discovered that marine tonality remains detectable upon removal of the carbonyl functionality, but that alternative dominant accords begin to arise such as aldehydic, sweet and floral-fruity (Figure 1.27). It was concluded that a complete removal of the osmophore functionality results in an absence of marine tonality.^[93]

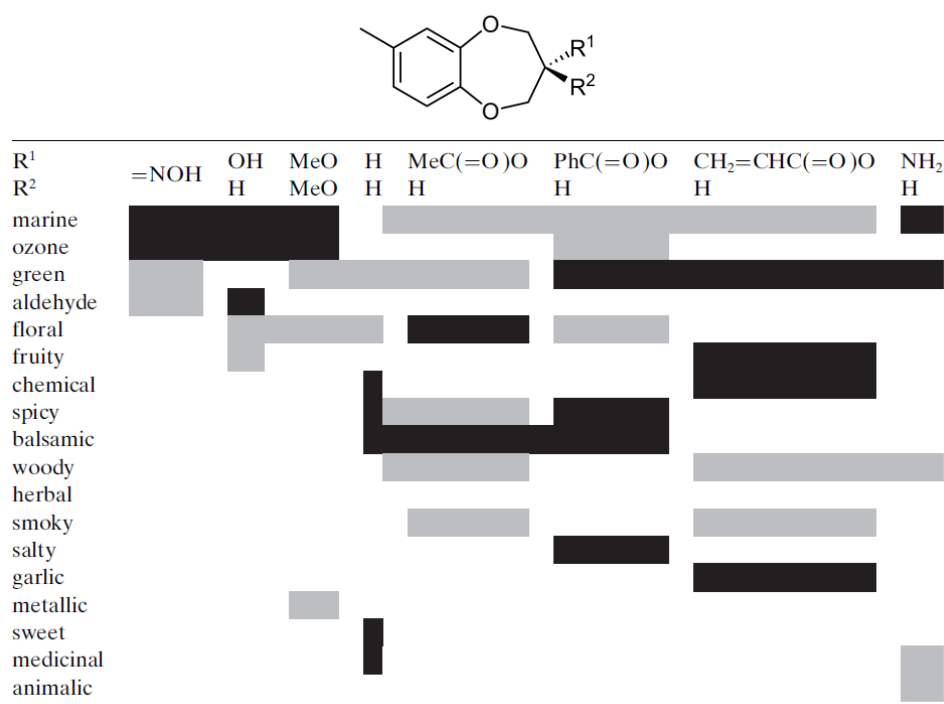
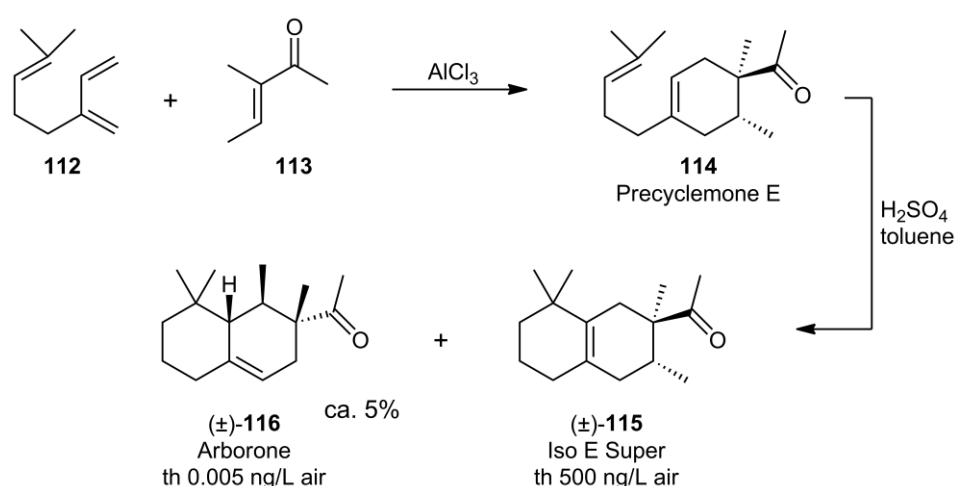


Figure 1.27: Graphical representation of the C-3 benzo[*b*][1,4]dioxepin-3-one analogues. Adapted from Hugel *et al.*^[93] Black: strong; grey: weak; white: absent.

1.5 – Isocyclemone Odorants

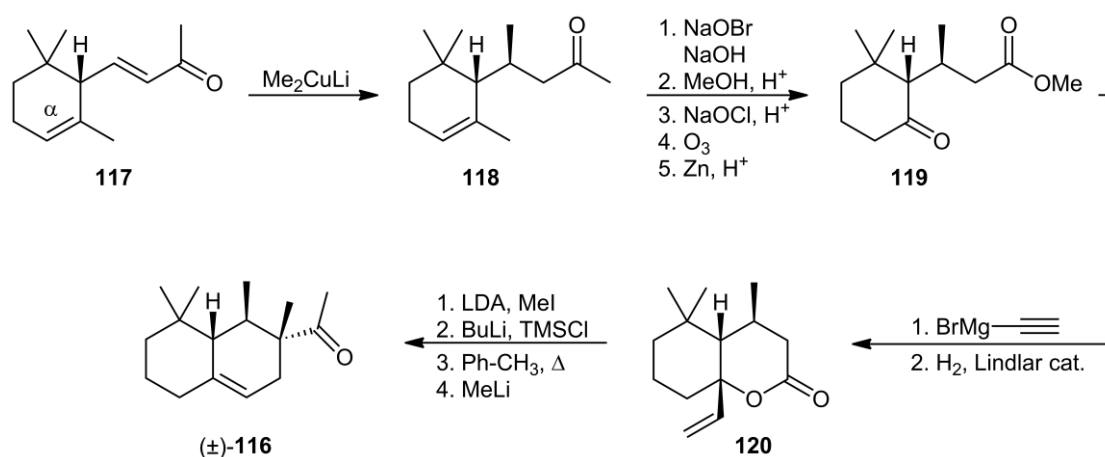
1.5.1 – Commercially Available Products

Iso E Super[®] (**115**) was discovered at International Flavors & Fragrances (IFF) in 1973^[6] and patented in 1975.^[94] Iso E Super[®] (**115**) possesses a characteristic woody-amber odour and has been one of the most influential raw materials in the fragrance industry,^[95] its application finding use from fine perfumes to detergents.^[96] The industrial synthesis commences with an aluminium chloride catalysed Diels–Alder reaction of monoterpene myrcene (**112**) with dienophile (3*E*)-3-methylpent-3-en-2-one (**113**) to give intermediate compound Precyclemone E (**114**) (Scheme 1.6). This reaction is followed by a subsequent acid-catalysed cyclisation reaction to provide the racemic target product, compound **115**.^[6, 64] The resulting product is a complex mixture of isomeric and diastereomeric compounds structurally related to the molecular structure originally proposed as Iso E Super[®] (**115**). It was later discovered that the major product of the reaction (**115**) had an odour threshold value of a mere 500 ng/L air, and that a minor constituent (**116**, ca. 5%), with an odour threshold about 100,000 times lower, was determining the overall fragrance quality of the commercial material.^[97-99] The molecular structure of compound **116** was proposed by isolation and 2D NMR experimentation, and confirmed by total synthesis, and the compound was named Arborone.^[97, 100] A raw perfumery material in which compound **116** is enriched by a factor of two is now manufactured by a different synthetic process and is commercially available under the name Iso Gamma Super[®].^[101]



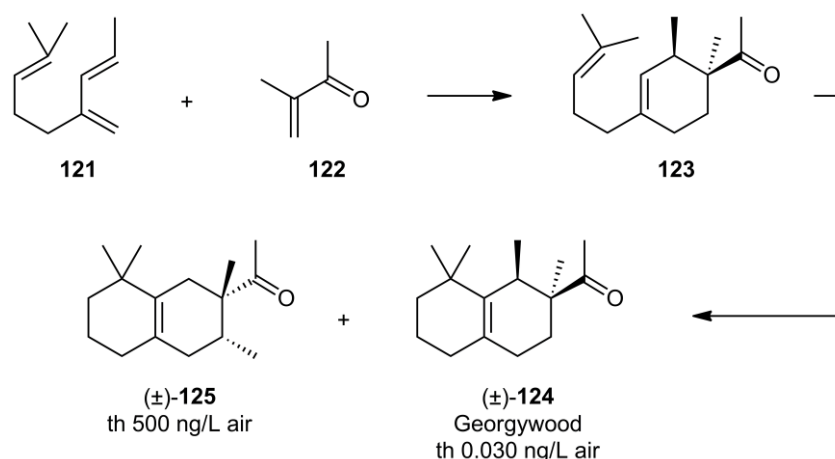
Scheme 1.6: Commercial synthesis of Iso E Super[®] (**115**) from myrcene (**112**) and (3*E*)-3-methylpent-3-en-2-one (**113**).^[6, 64]

The total synthesis of racemic Arborone (**116**) began from α -ionone (**117**) with a diastereoselective conjugate addition of lithium dimethylcuprate to give compound **118** (Scheme 1.7). Intermediate **118** was then transformed into intermediate **119** by haloform reaction, esterification and ozonolysis following isomerisation with sodium hypochlorite. A Grignard reaction of **119** with ethynylmagnesium bromide and subsequent Lindlar hydrogenation provided compound **120**. Ireland-Claisen rearrangement and methylation of the resulting carboxylic acid provided target compound (\pm)-**116** which was found to be chemically identical to the compound isolated from Iso E Super[®], thus confirming the molecular structure.^[6, 64, 97]



Scheme 1.7: Total synthesis of racemic Arborone (**116**) from α -ionone (**117**).^[97]

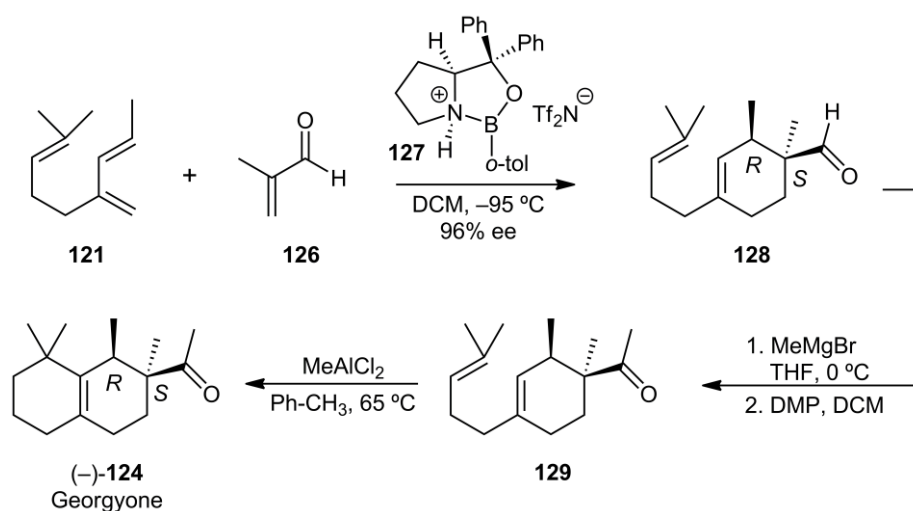
The synthesis of unadulterated Arborone (**116**) by the route delineated in Scheme 1.7 is synthetically complicated and not suitable for industrial scale. In place of a pure perfumery material composed of compound **116**, an alternative material named Georgywood[®] (**124**) was instead made commercially available.^[6, 64] Compound **124** was discovered to have an almost equal odour threshold as compound **116**, and was preferred in terms of fragrance characteristics.^[64] Compound **124** is produced industrially by the Diels–Alder reaction of homomyrcene (**121**) and 3-methylbut-3-en-2-one (**122**), followed by subsequent acid-catalysed cyclisation of the resulting intermediate (**123**) to provide target compound (\pm)-**124** (Scheme 1.8).^[6] Georgywood[®] possesses a pleasant woody odour that is distinct to the fragrances of cedar-wood or sandalwood, which exhibit additional distinctive notes.^[100] Analogous to Iso E Super[®], the commercial material contains an undesired regioisomer, (\pm)-**125**, synthesised in near equal quantity to (\pm)-**124**.^[102-103]



Scheme 1.8: Commercial synthesis of Georgywood® (**124**) from homomyrcene (**121**) and 3-methylbut-3-en-2-one (**122**).^[6]

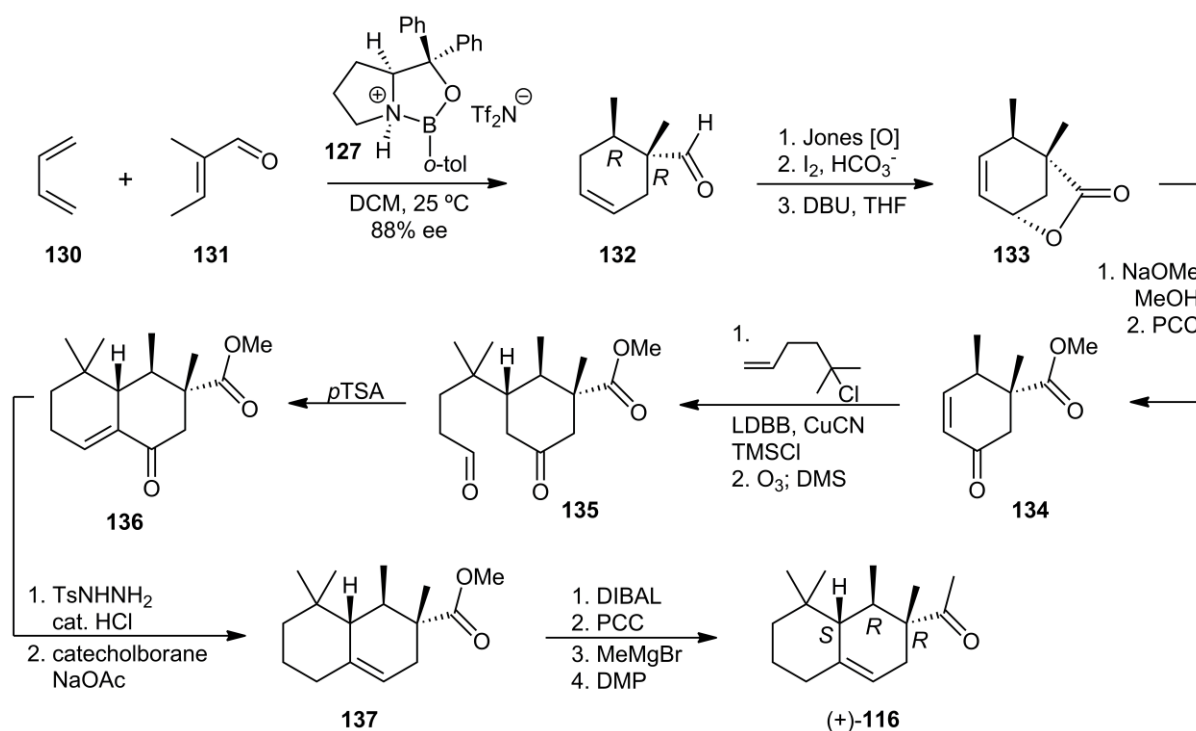
1.5.2 – Isocyclemonone Structure-Odour Relationship Studies – Harvard University

An enantioselective total synthesis of the principle odorant of the commercially available material Georgywood® was achieved by Hong and Corey, beginning from homomyrcene (**121**) and methacrylaldehyde (**126**) (Scheme 1.9).^[100] The key step in the synthetic sequence is the enantioselective Diels–Alder reaction between **121** and **126**, catalysed by (*S*)-oxazaborolidinium salt **127**, to give intermediate **128**. This compound is then reacted with methylmagnesium bromide followed by Dess-Martin periodinane oxidation of the resulting hydroxyl moiety to give compound **129**, followed by cyclisation in the presence of methylaluminium chloride to provide the enantiopure Georgywood® analogue (–)-**124**. The synthesis of the antipode of **124** using the (*R*)-configured oxazaborolidinium catalyst revealed that the odour of Georgywood® is mainly due to the (–)-(1*R*,2*S*)-configured stereoisomer (–)-**124**, later named Georgyone.^[6, 100]



Scheme 1.9: Enantioselective synthesis of (-)-Georgyone (**124**) from homomyrcene (**121**) and methacrylaldehyde (**126**).^[100]

The synthesis of an enantiopure sample of Arborone (**116**) was also achieved using the same oxazaborolidinium catalyst (**127**). The synthetic sequence began with an enantioselective Diels–Alder reaction between 1,3-butadiene (**130**) and (*E*)-2-methylbut-2-enal (**131**) to give enantiopure aldehyde **132** (Scheme 1.10). Jones oxidation followed by an iodolactonisation and a β -elimination sequence provided compound **133** which was then converted to compound **134** by sequential methanolysis and pyridinium chlorochromate oxidation. The diastereoselective reaction of **134** with a cyanocuprate reagent followed by ozonolysis of the resulting intermediate provided compound **135**, which was then cyclised by acid-catalysed aldol condensation to give compound **136**. This intermediate was then converted to compound **137** followed by diisobutylaluminium hydride reduction, oxidation, a Grignard reaction with methylmagnesium bromide and subsequent Dess-Martin periodinane oxidation to provide dextrorotatory target compound (+)-**116**. This compound was described as possessing an intense woody fragrance. The levorotatory enantiomer of this compound was also prepared by a parallel sequence and was discovered to be faint in odour.^[100]



Scheme 1.10: Enantioselective synthesis of (+)-Arborone (**116**) from 1,3-butadiene (**130**) and (*E*)-2-methylbut-2-enal (**131**).^[100]

The enantioselective syntheses of the odour active constituents of Iso E Super® (Arborone, **116**) and Georgywood® (Georgyone, **124**) revealed that the isomers differ in their configuration at the carbon atom bearing the acetyl functionality (C-2). Attention was turned to revealing the necessary structural components required for the more potent analogue (**116**) to display powerful fragrance. The synthesis of analogues **138–140** containing alteration of the geminal methyl functionalities at C-9 was undertaken to understand their role in olfactory recognition (Figure 1.28). It was discovered that only the equatorial methyl functionality at C-9 was required for strong odour perception (9*R*-configuration, **138**), and that an axial methyl functionality (9*S*-configuration, **139**) gave a compound devoid of the typical woody odour. The complete removal of both geminal methyl functionalities (compound **140**) was also discovered to abolish odour.^[100]

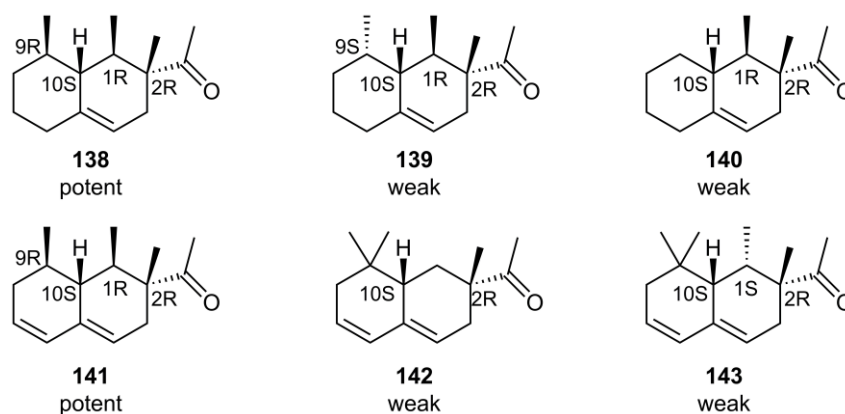


Figure 1.28: Arborone (**116**) analogues **138–143** prepared by Hong and Corey.^[100]

It was discovered that an analogue that contained only the crucial (9*R*)-configured methyl functionality, but was additionally 6,7-dehydrated (compound **141**), still retained the potent odorant characteristics of lead compound **116** (Figure 1.28). The odour of **141** was similar to **116** indicating that the addition of $\Delta^{6,7}$ unsaturation makes little difference, and thus further analogues of this scaffold were synthesised due to ease of synthetic access. Compound **142**, devoid of the (*R*)-configured methyl group at C–1 typical to both Arborone (**116**) and Georgyone (**124**) displayed little odour. The reintroduction of the methyl moiety, but a switch in stereochemistry to a (1*S*)-configuration (compound **143**), also provided a near odourless compound. The authors determined that the essential molecular features of lead compound **116** include the absolute configuration, a flat bicyclic ring system, equatorial methyl moieties at C–1 and C–2 and an acetyl functionality at C–2. The authors concluded their research by citing an amino acid sequence motif that could potentially be involved in the receptor binding of the isocyclemone molecules. Their hypothesis also provided explanation as to why compounds **116** and **124** can have different spacial orientations of the acetyl functionality but both retain potent odorant characteristics.^[100]

A study by Hicken and Corey used analogous synthetic methodology to prepare analogues of Georgyone (**124**) in which the C–6 methylene unit was replaced by an ether oxygen atom (Figure 1.29). The motive for the proposed *oxa*-analogue synthesis involved both decreasing substrate volatility and increasing water solubility and bioavailability of the resulting compounds. Analogues **144** and **145** both contained pleasant woody fragrances, not dissimilar to Arborone (**116**) or Georgyone (**124**).^[104]

The strong fragrance of compounds **144** and **145** demonstrated that the olfactory receptors responsible for woody odour can accommodate a heteroatom at C-6 and that, unexpectedly, the stereochemistry at C-1/C-2 is not as significant in Georgyone (**124**) analogues as in Arborone (**116**) analogues.^[104] The discovery offered additional support to the theory of conformational flexibility at the olfactory receptors originally proposed by Hong and Corey.^[100]

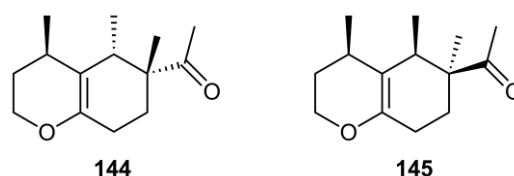


Figure 1.29: Oxa-Georgyone analogues **144** and **145** prepared by Hicken and Corey.^[104]

1.5.3 – Isocyclemone Structure-Odour Relationship Studies – Givaudan

Researchers at Givaudan performed molecular calculations that successfully linked the ionone and isocyclemone odorant families which led to the discovery of odorant **146** (Figure 1.30). This compound, as well as several chemically related analogues, were synthesised as racemic mixtures by a novel [4+2] cycloaddition reaction in the presence of Wilkinson's catalyst.^[105] A subsequent study revealed that the (9*R*,10*S*)-configured enantiomer (**146**) was 100x more powerful than its antipode, mimicking that which was discovered for Georgywood® (**124**). Additional cyclopentyl-fused analogues (i.e. **147** and **148**) were synthesised in an analogous manner. Differences in odour description between the analogues demonstrated the importance of a vicinal *bis*-methyl system displaying *trans*-configuration.^[106]

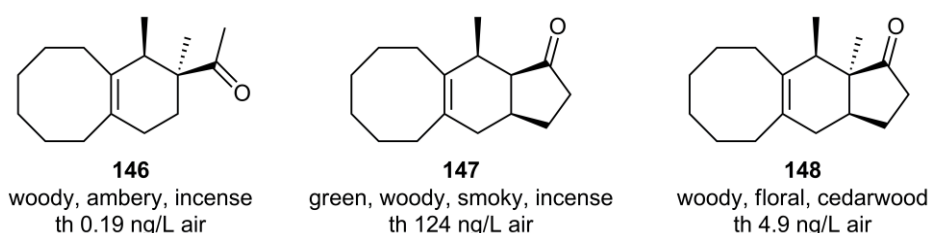


Figure 1.30: Eight-membered isocyclemone analogues **146–148** prepared by Kraft *et al.*^[105-106]

A series of spirocyclic analogues were synthesised and evaluated to study the effect of a more rigid molecular geometry on the isocyclemone molecular scaffold (Figure 1.31). The synthesis of spirocyclic analogue **149** was achieved beginning from homomyrcene (**121**). This analogue was discovered to

have a pleasant woody odour. To further explore the influence of molecular alteration, analogue **149** was deprotonated with lithium diisopropylamide followed by methylation using methyl iodide to furnish stereoisomers **150** and **151**, both potent odorants. A second methylation reaction resulted in geminal *bis*-methyl analogue **152** for which an additional unpleasant green nuance was reported. A series of cyclooctyl analogues were additionally synthesised (i.e. **153** and **154**) and it was again discovered that a *trans*-configured spatial orientation of the substituted alkyl moieties was an essential feature for potent odour character.^[99]

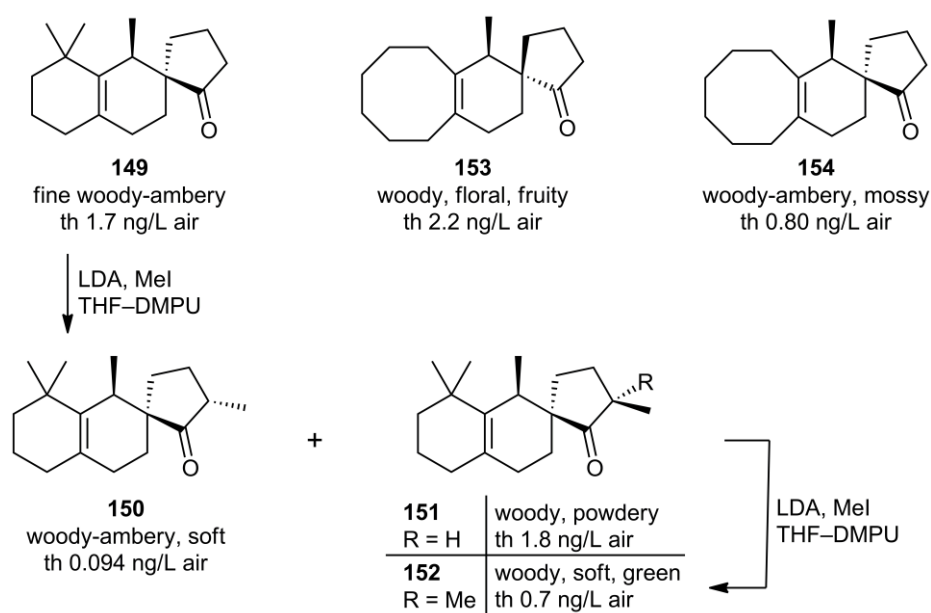


Figure 1.31: Spirocyclic isocyclemone analogues **149–154** synthesised by Kraft *et al.*^[99]

The series of new analogues synthesised provided insight that the olfactory receptor(s) can indeed discriminate between spatial orientations of the substituted alkyl moieties in the isocyclemone family. The potency of the prepared analogues also indicated that the receptor binding region is much larger than was initially hypothesised by Hong and Corey.^[100] Conclusions were also drawn that the receptor may be more complex than initially anticipated, and that the highly structure sensitive hydrophobic binding cavity may be constructed from more than one α -helix structure.^[99]

1.6 – References

1. Press Release: The 2004 Nobel Prize in Physiology or Medicine to Richard Axel and Linda B. Buck. *Nobelprize.org*. Nobel Media AB 2014. Accessed 1 Oct 2015. <http://www.nobelprize.org/nobel_prizes/medicine/laureates/2004/press.html>.
2. L. B. Buck, R. Axel, A novel multigene family may encode odorant receptors: a molecular basis for odor recognition, *Cell* **1991**, *65*, 175-187.
3. L. B. Buck, Olfactory receptors and odor coding in mammals, *Nutr Rev* **2004**, *62*, 184-188.
4. L. Doszszak, P. Kraft, H.-P. Weber, R. Bertermann, A. Triller, H. Hatt, R. Tacke, Prediction of perception: probing the hOR17-4 olfactory receptor model with silicon analogues of bourgeonal and linal, *Angew. Chem., Int. Ed.* **2007**, *46*, 3367-3371.
5. C. S. Sell, On the unpredictability of odor, *Angew. Chem., Int. Ed.* **2006**, *45*, 6254-6261.
6. G. Ohloff, W. Pickenhagen, P. Kraft, *Scent and Chemistry - The Molecular World of Odors*, Verlag Helvetica Chimica Acta, Zurich, **2012**.
7. B. Drevermann, Ph.D Thesis, RMIT University, Melbourne, Australia **2007**.
8. G. M. Shepherd, Smell images and the flavour system in the human brain, *Nature* **2006**, *444*, 316-321.
9. Flavors & Fragrances to 2012, *Freedonia*, **2009**, Study No. 2461.
10. H. M. Hugel, B. Drevermann, A. R. Lingham, P. J. Marriott, Marine fragrance chemistry, *Chem. Biodiversity* **2008**, *5*, 1034-1044.
11. J. C. Leffingwell, *Leffingwell Reports* **2002**, *2*, 1-33.
12. E. Hajjar, D. Perahia, H. Debat, C. Nespoulous, C. H. Robert, Odorant Binding and Conformational Dynamics in the Odorant-binding Protein, *J. Biol. Chem.* **2006**, *281*, 29929-29937.
13. H. Zhao, S. Firestein, Vertebrate odorant receptors, *Cell. Mol. Life Sci.* **1999**, *56*, 647-659.
14. P. Mombaerts, F. Wang, C. Dulac, S. Chao, A. Nemes, M. Mendelsohn, J. Edmondson, R. Axel, Visualizing an olfactory sensory map, *Cell* **1996**, *87*, 675-686.
15. P. Mombaerts, Targeting olfaction, *Curr. Opin. Neurobiol.* **1996**, *6*, 481-486.
16. Y. Oka, Y. Takai, K. Touhara, Nasal airflow rate affects the sensitivity and pattern of glomerular odorant responses in the mouse olfactory bulb, *J. Neurosci.* **2009**, *29*, 12070-12078.
17. Public domain image, Accessed 18 November 2015. <<http://www.wpclipart.com/medical/anatomy/cells/neuron/neuron.png.html>>.
18. H. Stone, B. Williams, E. J. Carregal, The role of the trigeminal nerve in olfaction, *Exp Neurol* **1968**, *21*, 11-19.
19. J. Frasnelli, B. Schuster, T. Hummel, Interactions between olfaction and the trigeminal system: what can be learned from olfactory loss, *Cereb Cortex* **2007**, *17*, 2268-2275.

20. G. Glusman, I. Yanai, I. Rubin, D. Lancet, The complete human olfactory subgenome, *Genome Res.* **2001**, *11*, 685-702.
21. Y. Gilad, D. Lancet, Population differences in the human functional olfactory repertoire, *Mol Biol Evol* **2003**, *20*, 307-314.
22. B. Malnic, P. A. Godfrey, L. B. Buck, The human olfactory receptor gene family, *Proc. Natl. Acad. Sci. U. S. A.* **2004**, *101*, 2584-2589.
23. C. Crasto, M. S. Singer, G. M. Shepherd, The olfactory receptor family album, *Genome Biol* **2001**, *2*.
24. D. Pierron, N. G. Cortes, T. Letellier, L. I. Grossman, Current relaxation of selection on the human genome: Tolerance of deleterious mutations on olfactory receptors, *Mol. Phylogenet. Evol.* **2013**, *66*, 558-564.
25. P. Mombaerts, Seven-transmembrane proteins as odorant and chemosensory receptors, *Science* **1999**, *286*, 707-711.
26. K. J. Rossiter, Structure-Odor Relationships, *Chem. Rev.* **1996**, *96*, 3201-3240.
27. E. Demole, H. Wuest, Stereoselective synthesis of two stereoisomeric trioxides, C₁₈H₃₀O₃₇ ambreinolide and sclareol lactone, from (+)-manool derivatives, *Helv. Chim. Acta* **1967**, *50*, 1314-1327.
28. I. Gaillard, S. Rouquier, D. Giorgi, Olfactory receptors, *Cell. Mol. Life Sci.* **2004**, *61*, 456-469.
29. A. J. Taylor, D. D. Roberts, *Flavor Perception*, Blackwell Publishing, Hoboken, **2004**.
30. T. Nakamura, G. H. Gold, A cyclic nucleotide-gated conductance in olfactory receptor cilia, *Nature* **1987**, *325*, 442-444.
31. H. Takeuchi, T. Kurahashi, Identification of second messenger mediating signal transduction in the olfactory receptor cell, *J. Gen. Physiol.* **2003**, *122*, 557-567.
32. R. Madrid, R. Delgado, J. Bacigalupo, Cyclic AMP cascade mediates the inhibitory odor response of isolated toad olfactory receptor neurons, *J. Neurophysiol.* **2005**, *94*, 1781-1788.
33. P. H. Barry, The relative contributions of cAMP and InsP₃ pathways to olfactory responses in vertebrate olfactory receptor neurons and the specificity of odorants for both pathways, *J. Gen. Physiol.* **2003**, *122*, 247-250.
34. M. Zarzo, D. T. Stanton, Understanding the underlying dimensions in perfumers' odor perception space as a basis for developing meaningful odor maps, *Attention, Perception, & Psychophysics* **2009**, *71*, 225-247.
35. Copyright M. Edwards. <<http://www.fragrancesoftheworld.com>>.
36. J. S. Jellinek, The effect of intermolecular forces on perceived odors, *Ann. N. Y. Acad. Sci.* **1964**, *116*, 725-734.
37. C. M. Delahunty, G. Eyres, J.-P. Dufour, Gas chromatography-olfactometry, *J. Sep. Sci.* **2006**, *29*, 2107-2125

38. P. Kraft, K. Popaj, P. Müller, M. Schär, 'Vanilla oceanics': synthesis and olfactory properties of (1'E)-7-(prop-1'-enyl)-2H-benzo[b][1,4]dioxepin-3(4H)-ones and homologues, *Synthesis* **2010**, 3029-3036.
39. C. S. Luntzel, S. Widder, T. Voessing, W. Pickenhagen, Enantioselective Syntheses and Sensory Properties of the 3-Mercapto-2-methylpentanols, *J. Agric. Food Chem.* **2000**, *48*, 424-427.
40. J. E. Amoore, Stereochemical specificities of human olfactory receptors, *Perfum. Essent. Oil Rec.* **1952**, *43*, 321-330.
41. P. Weyerstahl, Odor and structure, *J. Prakt. Chem.* **1994**, *336*, 95-109.
42. J. E. Amoore, The stereochemical theory of olfaction. I. Identification of the seven primary odors, *Proc. Sci. Sect. Toilet Goods Assoc. Suppl.* **1962**, *37*, 2-12.
43. G. M. Dyson, Raman effect and the concept of odor, *Perfum. Essent. Oil Rec.* **1937**, *28*, 13-19.
44. R. H. Wright, Odor and molecular vibration. I. Quantum and thermodynamic considerations, *J. Appl. Chem.* **1954**, *4*, 611-615.
45. L. Turin, A spectroscopic mechanism for primary olfactory reception, *Chem. Senses* **1996**, *21*, 773-791.
46. L. B. Vosshall, Laying a controversial smell theory to rest, *Proc. Natl. Acad. Sci. U. S. A.* **2015**, *112*, 6525-6526.
47. M. Chastrette, C. Rognon, P. Sauvegrain, R. Amouroux, On the role of chirality in structure-odor relationships, *Chem. Senses* **1992**, *17*, 555-572.
48. P. Kraft, R. Cadalbert, The thia analog of ambrettolide. Synthesis and odor of 1,8-oxathiacyclohexadecan-2-one, *Synlett* **1997**, 600-602.
49. H. S. Koelega, E. P. Koster, Some experiments on sex differences in odor perception, *Ann N Y Acad Sci* **1974**, *237*, 234-246.
50. J. E. Amoore, P. Pelosi, L. J. Forrester, Specific anosmias to 5 α -androst-16-en-3-one and ω -pentadecalactone: the urinous and musky primary odors, *Chem. Senses Flavour* **1977**, *2*, 401-425.
51. D. J. Rowe, *Chemistry and Technology of Flavors and Fragrances*, CRC Press, Boca Raton, **2005**.
52. A. D. McNaught, A. Wilkinson, *Compendium of Chemical Terminology 2nd Edition*, Blackwell, Oxford, **1997**.
53. R. Bentley, The nose as a stereochemist. Enantiomers and odor, *Chem. Rev.* **2006**, *106*, 4099-4112.
54. P. Kraft, A. Mannschreck, The Enantioselectivity of Odor Sensation: Some Examples for Undergraduate Chemistry Courses, *J. Chem. Educ.* **2010**, *87*, 598-603.
55. R. H. Wright, Odor of optical isomers, *Nature* **1963**, *198*, 782.
56. E. T. Theimer, T. Yoshida, E. M. Klaiber, Olfaction and molecular shape. Chirality as a requisite for odor, *J. Agric. Food Chem.* **1977**, *25*, 1168-1177.
57. J. C. Leffingwell, D. Leffingwell, Chiral chemistry in flavours & fragrances, *Spec. Chem. Mag.* **2011**, *31*, 30-33.

58. G. F. Russell, J. I. Hills, Odor differences between enantiomeric isomers, *Science* **1971**, *172*, 1043-1044.
59. L. Friedman, J. G. Miller, Odor incongruity and chirality, *Science* **1971**, *172*, 1044-1046.
60. H. Guth, Determination of the configuration of wine lactone, *Helv. Chim. Acta* **1996**, *79*, 1559-1571.
61. C. Rognon, M. Chastrette, Structure-odor relationships: a highly predictive tridimensional interaction model for the bell-pepper note, *Eur. J. Med. Chem.* **1994**, *29*, 595-609.
62. M. Chastrette, C. El Aidi, D. Cretin, Structure-odor relationships for bell-pepper, green and nutty notes in pyrazines and thiazoles. Comparison between neural networks and similarity searching, *SAR QSAR Environ. Res.* **1997**, *7*, 233-258.
63. H. Masuda, S. Mihara, Preparation and odor evaluation of both enantiomers of alkoxy-pyrazines, *Agric. Biol. Chem.* **1989**, *53*, 3367-3368.
64. P. Kraft, J. A. Bajgrowicz, C. Denis, G. Frater, Odds and trends: recent developments in the chemistry of odorants, *Angew. Chem., Int. Ed.* **2000**, *39*, 2980-3010.
65. R. E. Moore, Volatile compounds from marine algae, *Acc. Chem. Res.* **1977**, *10*, 40-47.
66. R. E. Moore, J. A. Pettus, Jr., J. Mistysyn, Odoriferous C₁₁ hydrocarbons from Hawaiian *Dictyopteris*, *J. Org. Chem.* **1974**, *39*, 2201-2207.
67. W. Boland, N. Schroer, C. Sieler, M. Feigel, Stereospecific syntheses and spectroscopic properties of isomeric 2,4,6,8-undecatetraenes. New hydrocarbons from the marine brown alga *Giffordia mitchellae*. Part IV, *Helv. Chim. Acta* **1987**, *70*, 1025-1040.
68. D. Wirth, I. Fischer-Lui, W. Boland, D. Icheln, T. Runge, W. A. Koenig, J. Phillips, M. Clayton, Unusual and novel C₁₁H₁₆ hydrocarbons from the Southern Australian brown alga *Dictyopteris acrostichoides* (*Phaeophyceae*), *Helv. Chim. Acta* **1992**, *75*, 734-744.
69. G. Ohloff, W. Pickenhagen, Synthesis of (±)-dictyopterene A, *Helv. Chim. Acta* **1969**, *52*, 880-886.
70. W. Boland, L. Jaenicke, D. G. Mueller, G. Gassmann, Giffordene, 2Z, 4Z, 6E, 8Z-undecatetraene, is the odoriferous principle of the marine brown alga *Giffordia mitchellae*, *Experientia* **1987**, *43*, 466-467.
71. D. G. Mueller, L. Jaenickel, M. Donike, T. Akintobi, Sex attractant in a brown alga: chemical structure, *Science* **1971**, *171*, 815-817.
72. M. P. Schneider, M. Goldbach, Facile synthesis of fucoserratene and the (±)-dictyopterenes B, D, and D' (= ectocarpene): constituents of marine brown algae, *J. Am. Chem. Soc.* **1980**, *102*, 6114-6116.
73. J.-M. Gaudin, O. Nikolaenko, J.-Y. de Saint Laumer, B. Winter, P.-A. Blanc, Structure - activity relationship in the domain of odorants having marine notes, *Helv. Chim. Acta* **2007**, *90*, 1245-1265.
74. F. B. Whitfield, J. H. Last, K. J. Shaw, C. R. Tindale, 2,6-Dibromophenol: the cause of an iodoform-like off-flavor in some Australian crustacea, *J. Sci. Food Agric.* **1988**, *46*, 29-42.
75. J. L. Boyle, R. C. Lindsay, D. A. Stuber, Occurrence and properties of flavor-related bromophenols found in the marine environment: a review, *J. Aquat. Food Prod. Technol.* **1993**, *2*, 75-112.

76. F. B. Whitfield, F. Helidoniotis, K. J. Shaw, D. Svoronos, Distribution of Bromophenols in Species of Marine Algae from Eastern Australia, *J. Agric. Food Chem.* **1999**, *47*, 2367-2373.
77. C. A. Moore, R. K. Okuda, Bromoperoxidase activity in 94 species of marine algae, *J. Nat. Toxins* **1996**, *5*, 295-305.
78. T. Higa, R. K. Okuda, R. M. Severns, P. J. Scheuer, C. H. He, C. Xu, J. Clardy, Unprecedented constituents of a new species of acorn worm, *Tetrahedron* **1987**, *43*, 1063-1070.
79. R. B. Ashworth, M. J. Cormier, Isolation of 2,6-dibromophenol from the marine hemichordate, *Balanoglossus biminiensis*, *Science* **1967**, *155*, 1558-1559.
80. N. L. J. M. Broekhof, J. G. Witteveen, A. J. A. Van der Weerd, Characteristic odoriferous compounds of brown algae. Syntheses of possible oxidation products of (6Z,9Z,12Z,15Z)-1,6,9,12,15-heneicosapentaene and (6Z,9Z,12Z,15Z,18Z)-1,6,9,12,15,18-heneicosahexaene, *Recl. Trav. Chim. Pays-Bas* **1986**, *105*, 436-442.
81. D. B. Josephson, Seafood, *Food Sci. Technol.* **1991**, *44*, 179-202.
82. E. Delort, A. Jaquier, C. Chapuis, M. Rubin, C. Starkenmann, Volatile Composition of Oyster Leaf (*Mertensia maritima* (L.) Gray), *J. Agric. Food Chem.* **2012**, *60*, 11681-11690.
83. P. Kraft, W. Eichenberger, Conception, characterization and correlation of new marine odorants, *Eur. J. Org. Chem.* **2003**, 3735-3743.
84. B. Drevermann, A. R. Lingham, H. M. Hugel, P. J. Marriott, Synthesis of benzodioxepinone analogues via a novel synthetic route with qualitative olfactory evaluation, *Helv. Chim. Acta* **2007**, *90*, 1006-1027.
85. J. J. Beereboom, D. P. Cameron, C. R. Stephens (Pfizer Inc.), **1974**, US3799892A.
86. J.-M. Gaudin, J.-Y. de Saint Laumer, Structure-Activity Relationships in the Domain of Odorants Having Marine Notes, *Eur. J. Org. Chem.* **2015**, 1437-1447.
87. H. Oertling (Symrise GmbH & Co. KG), **2009**, EP2100589A1.
88. J. J. Beereboom, D. P. Cameron, C. R. Stephens (Pfizer Inc.), **1972**, US3647479A.
89. F. H. Marquardt, FRIEDEL-CRAFTS-Reaktionen mit aromatischen äthern. 1. Mitteilung Die Herstellung von Alkoxy-indanonen-(1), *Helv. Chim. Acta.* **1965**, *48*, 1476-1485.
90. P. Kraft (Givaudan SA), **2001**, EP1136481A1.
91. S. Lamboley, C. Morel, J.-Y. d. S. Laumer, A. F. Boschung, N. G. J. Richards, B. M. Winter, Synthesis and properties of conformationally constrained analogues of floral-type odorants, *Helv. Chim. Acta* **2004**, *87*, 1767-1793.
92. B. Winter, S. Gallo-Fluckiger, Synthesis and odor properties of substituted indane-2-carboxaldehydes. Discovery of a new floral (muguet) fragrance alcohol, *Helv. Chim. Acta* **2005**, *88*, 3118-3127.
93. B. Drevermann, A. R. Lingham, H. M. Hugel, P. J. Marriott, Synthesis and qualitative olfactory evaluation of benzodioxepine analogues, *Helv. Chim. Acta* **2007**, *90*, 854-863.

-
94. J. B. Hall, J. M. Sanders (International Flavors and Fragrances Inc.), **1975**, US3907321A.
95. P. Kraft, Woody pretzels: spirocycles from Vetiver to Patchouli and Georgywood, *Chem. Biodiversity* **2008**, *5*, 970-999.
96. M. Erman, M. Williams, P. Whelan, C. Cardenas, M. Antipin, The composition of Iso E super, *Perfum. Flavor.* **2001**, *26*, 16-21.
97. C. Nussbaumer, G. Frater, P. Kraft, (\pm)-1-[(1*R**,2*R**,8*aS**)-1,2,3,5,6,7,8,8*a*-octahydro-1,2,8,8-tetramethylnaphthalen-2-yl]ethan-1-one. Isolation and stereoselective synthesis of a powerful minor constituent of the perfumery synthetic Iso E Super, *Helv. Chim. Acta* **1999**, *82*, 1016-1024.
98. M. Bella, M. Cianflone, G. Montemurro, P. Passacantilli, G. Piancatelli, Chemistry of odorants: stereoselective synthesis of octahydronaphthalene-based perfumery Georgywood, (+,-)-1-[(1*R**,2*S**)-1,2,3,4,5,6,7,8-octahydro-1,2,8,8-tetramethylnaphthalen-2-yl]ethan-1-one, *Tetrahedron* **2004**, *60*, 4821-4827.
99. P. Kraft, D. Frech, U. Muller, G. Frater, Synthesis and olfactory properties of spirocyclic Georgywood analogues, *Synthesis* **2006**, 2215-2223.
100. S. Hong, E. J. Corey, Enantioselective Syntheses of Georgyone, Arborone, and Structural Relatives. Relevance to the Molecular-Level Understanding of Olfaction, *J. Am. Chem. Soc.* **2006**, *128*, 1346-1352.
101. P. Kraft, K. Popaj, Unexpected tethering in the synthesis of methyl-substituted acetyl-1-oxaspiro[4.5]decanes: novel Woody-Ambery odorants with improved bioavailability, *Eur. J. Org. Chem.* **2008**, 261-268.
102. A. Borosy, G. Frater, U. Muller, F. Schroder, Endo-selective Diels-Alder reaction of methacrylonitrile: application to the synthesis of Georgywood, *Tetrahedron* **2009**, *65*, 10495-10505.
103. G. Frater, U. Mueller, F. Schroeder, Synthesis and olfactory properties of (-)-(1*R*,2*S*)-Georgywood, *Tetrahedron: Asymmetry* **2004**, *15*, 3967-3972.
104. E. J. Hicken, E. J. Corey, Stereoselective Synthesis of Woody Fragrances Related to Georgyone and Arborone, *Org. Lett.* **2008**, *10*, 1135-1138.
105. P. Kraft, Design and synthesis of violet odorants with bicyclo[6.4.0]dodecene and bicyclo[5.4.0]undecene skeletons, *Synthesis* **1999**, 695-703.
106. P. Kraft, S. Gallo, (-)-(9*R*,10*S*)-10-Acetyl-9,10-dimethylbicyclo[6.4.0]dodec-1(8)-ene: Optical resolution, catalyst systems, derivatives and olfactory properties, *Synthesis* **2004**, 381-388.
-

Chapter 2 – Synthesis of Hexahydrobenzo[*b*][1,4]dioxepin-3-one Stereoisomers

2.1 – Introduction

2.1.1 – Project Proposal & Rationale

Odour discrimination and perception are a combinatorial phenomenon. In the olfactory epithelium different odorant molecules are detected by varying combinations of olfactory receptors with various receptor combinations generating specific odour perceptions.^[1-3] It is well-known that the absolute configuration of a molecule is of crucial importance in determining the human perception of odour.^[4] It is also recognised that a substance evokes a sense of smell provided that the molecular shape matches a complementary space in the olfactory receptor.^[5] We can therefore define the odour of a chemical substance by the molecular shape. It is known that the benzo[*b*][1,4]dioxepin-3-one rings represent the essential structural characteristic of the synthetic marine odorant family^[6-12] and consequently we are interested in the effect of modulating the molecular shape via an aromatic/aliphatic carbocyclic ring exchange (Figure 2.1).

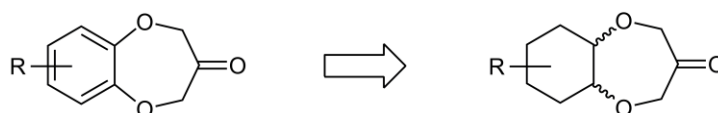


Figure 2.1: Aromatic/aliphatic ring exchange of the benzo[*b*][1,4]dioxepin-3-one molecular scaffold.

2.1.2 – Aromatic and Aliphatic Carbocyclic Rings

The benzo[*b*][1,4]dioxepin-3-one molecular scaffold consists of an aromatic cyclohexa-1,3,5-triene carbocyclic ring fused to a 1,4-dioxepan-6-one oxygenated heterocyclic ring. The organic chemistry term 'aromatic' was first proposed by August Wilhelm Hofmann in 1855 to describe his work into phenyl radicals.^[13] The modern use of the term indicates no relationship between chemical and olfactory properties. The aromatic cyclohexa-1,3,5-triene molecule, better recognised as a benzene molecule, is the simplest aromatic molecule consisting of six carbon atoms and three carbon–carbon alkene double bonds. The cyclohexa-1,3,5-triene molecular structure for benzene was first proposed by August Kekulé in 1865, and can be viewed as an amalgamation of two different resonance structures (Figure 2.2).^[14]

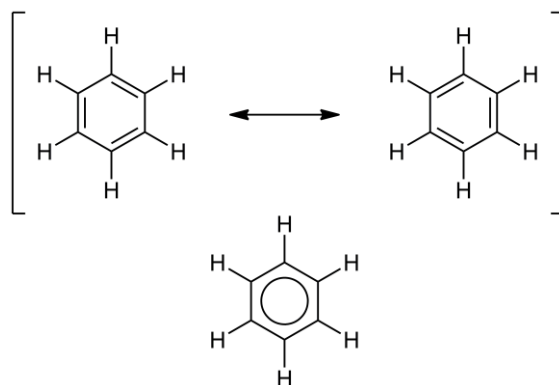


Figure 2.2: Top: Two resonance structures of a benzene molecule; Bottom: A more accurate visualisation of molecular resonance.

An aromatic benzenoid ring system is a completely planar hexagonal ring. All six carbon–carbon bonds are sp^2 hybridised and are of the same length (1.39 Å), which is intermediate between the typical length of a single bond (1.54 Å) and that of a double bond (1.34 Å).^[15] Since all atomic p orbitals overlap above and below the plane of the hexagonal ring, the six π electrons are completely delocalised and are shared equally by each carbon atom within the ring (Figure 2.3). During NMR spectroscopy, the circulation of π electrons out of the plane of the aromatic ring produces ring currents that dramatically affect the chemical shifts of the nuclei via diamagnetic anisotropy.^[15]

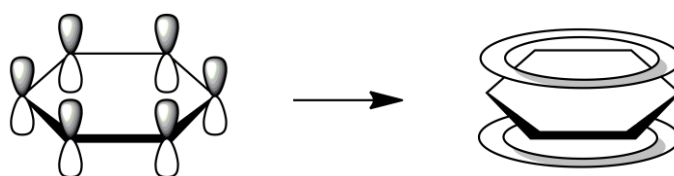


Figure 2.3: Delocalisation of π -electrons in an aromatic cyclohexa-1,3,5-triene ring.

The aliphatic analogue of a benzenoid system is known as a cyclohexyl system. Unlike benzene, in which all planar C–C–C bonds are 120° , the preferred angle between sp^3 hybridised carbons is 109.5° ; a tetrahedral angle. To minimise the resulting ring strain the carbocyclic ring adopts a non-planar conformation. The most readily identified conformations are referred to as the chair and boat conformations, although a variety of different twist-forms and half-forms are also recognised.

The chair is the lowest energy conformation and is therefore the preferred ground-state of the cyclohexyl ring system (Figure 2.4).^[16] A carbocyclic ring in any non-planar conformation has protons and/or substituents situated in two different types of environments known as axial and equatorial positions. The two possible forms of the chair conformation cyclohexane molecule rapidly interconvert at room temperature, with all axial positions becoming equatorial positions, and *vice versa*. Multi-substituted cyclohexane molecules prefer to place larger substituents in spaces occupying equatorial positions to minimise steric repulsion, and thus interconversion between forms is quenched.^[15]

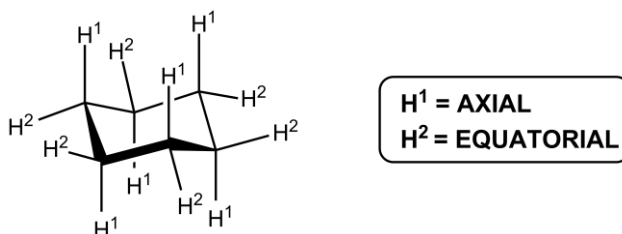
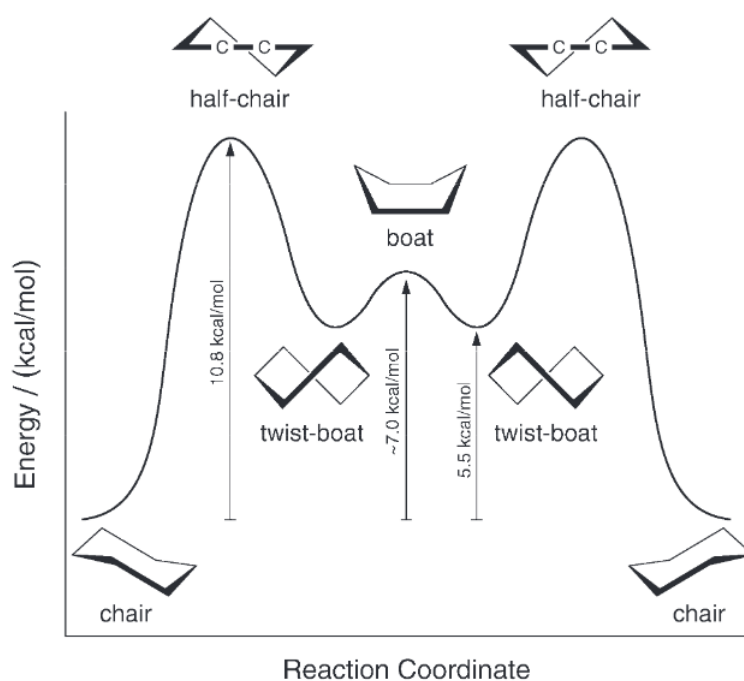


Figure 2.4: Top: Conformational changes during the inversion of cyclohexane^[16]; Bottom: Axial and equatorial positions of a chair conformation ring.

The synthetic commercial odorant Calone 1951[®] and its benzo[*b*][1,4]dioxepin-3-one scaffolded relatives contain a planar aromatic ring attached to a 7-membered oxygenated heterocyclic ring (Figure 2.5). The quantitative and qualitative olfactory analysis of previously synthesised analogues clearly indicate that chemical modification on any position of the benzo[*b*][1,4]dioxepin-3-one template has a significant effect on the resulting olfactory characteristics.^[6-7, 9-12] Accordingly we have chosen to synthesise a library of benzo[*b*][1,4]dioxepin-3-one analogues with a saturated cyclohexyl ring system in place of the usual planar benzenoid ring system.

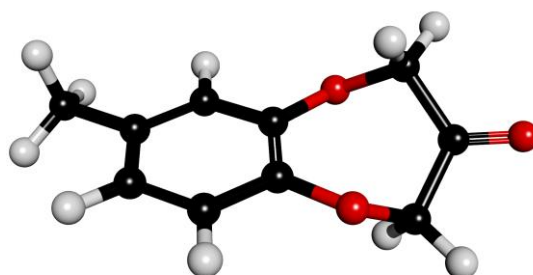


Figure 2.5: Minimum-energy conformation of 7-methylbenzo[*b*][1,4]dioxepin-3-one (Calone 1951[®]) displaying pseudo-twist-boat conformation, generated with MOE 2013.0801 software package using the Amber 12 force field with Extended Hückel Theory (EHT) parameters.^[17]

2.1.3 – Potential Synthetic Pathways to the Benzo[*b*][1,4]dioxepin-3-one Scaffold

Multiple synthetic pathways leading the aromatic benzo[*b*][1,4]dioxepin-3-one scaffold have been developed. The original Pfizer synthetic methodology involved the Williamson reaction of various catechol derivatives with methyl bromoacetate before subjection of the intermediate *bis*-ester compound to a base-catalysed Dieckmann condensation reaction.^[18-19] The resulting β -ketoester compound is then decarboxylated in a single-step acid-catalysed reaction to furnish the corresponding analogue (Figure 2.6).^[18-19]

Analogous synthetic methodology was utilised by Hgel *et al.*^[10, 20] during the synthesis of a library of benzo[*b*][1,4]dioxepin-3-one analogues for odorant evaluation, as well as during research into the comparison of yields between conventional heating and microwave irradiation. This synthetic methodology was applied by Kraft *et al.*^[7] during the synthesis of a library of conjugated olefinic chain benzo[*b*][1,4]dioxepin-3-one odorant analogues. This pathway was also employed during the synthesis

of a library of 1,5-benzodioxepin derivatives in research targeting novel muscarinic M₃ receptor antagonists.^[21] A benzo[*b*][1,4]dioxepin-3-one compound was recovered as a by-product of Dieckmann cyclisation methodologies which were being applied in an attempt to generate novel crown ether compounds.^[22]

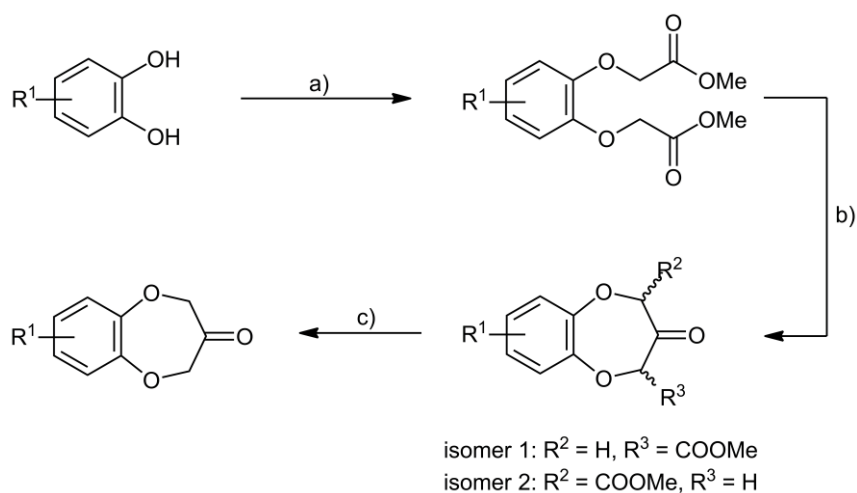


Figure 2.6: Dieckmann condensation route leading the benzo[*b*][1,4]dioxepin-3-one scaffold. General procedure:

a) methyl bromoacetate, K₂CO₃, DMF, 120 °C. b) KO^tBu, THF, ↑↓. c) HCl, EtOH, H₂O, ↑↓.

An analogous synthetic route involving a Thorpe-Ziegler reaction was developed during the synthesis of a library of 1,5-benzodioxepin analogues for use as β -adrenergic stimulants.^[23] The synthetic methodology was also assayed as a potential route to the synthesis of novel calcium channel antagonists.^[24] The synthetic pathway commences with the Williamson reaction of substituted catechol analogues with 2-chloroacetonitrile to give a *bis*-nitrile intermediate. The isolated *bis*-nitrile compound is then subjected to a base-catalysed intramolecular Thorpe-Ziegler cyclisation to yield an enamine nitrile compound which is then hydrolysed in an acidic hydrolysis at reflux temperature to yield the completed analogue (Figure 2.7).

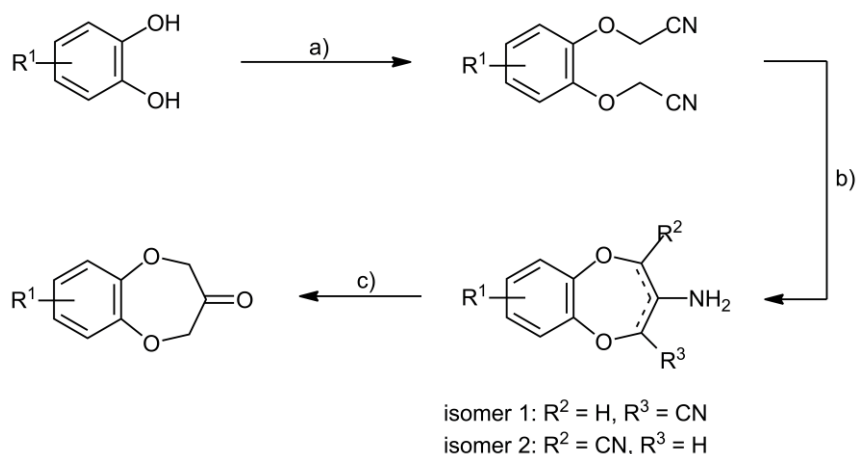


Figure 2.7: Thorpe-Ziegler route leading the benzo[*b*][1,4]dioxepin-3-one scaffold. a) 2-chloroacetonitrile, K_2CO_3 , acetone, $\uparrow\downarrow$. b) $\text{KO}t\text{Bu}$, DMSO. c) H_3PO_4 , AcOH, H_2O , $\uparrow\downarrow$.

A Williamson reaction cyclisation methodology was developed by Kraft *et al.*^[6] during the synthesis of a library of novel benzo[*b*][1,4]dioxepin-3-one analogues for olfactory evaluation (Figure 2.8, route a/c). The cyclisation methodology to give an intermediate 3-methylenebenzo[*b*][1,4]dioxepine compound was developed in 1968 by Schirmann *et al.*^[25] and involved a Williamson reaction between catechol, potassium carbonate and 3-chloro-2-(chloromethyl)prop-1-ene to yield the cyclised compound. Kraft *et al.*^[6] subsequently developed further synthetic methodologies to oxidise the methylene intermediate into the corresponding benzo[*b*][1,4]dioxepin-3-one analogue by the action of ruthenium tetroxide, generated *in situ* by the action of sodium metaperiodate on ruthenium chloride.

An alternative methodology from patent literature described a parallel reaction pathway leading to an unsubstituted analogue (Figure 2.8, route a/d/e).^[26] The synthetic pathway began with an analogous chemical reaction to Schirmann *et al.*,^[25] instead using caesium carbonate as a base. The isolated methylene compound was then oxidised to a vicinal-diol intermediate by the action of osmium tetroxide. The vicinal-diol intermediate is then oxidatively cleaved using the oxidant sodium metaperiodate to yield the corresponding benzo[*b*][1,4]dioxepin-3-one analogue. It is not clear why the vicinal-diol compound is isolated when the reaction could be performed in a one-step procedure known as the Lemieux-Johnson oxidation,^[27] but it is presumably done to minimise impurities being generated.

A simpler Williamson cyclisation protocol was developed by Gaudin *et al.*^[12] The synthetic methodology reacted substituted catechol derivatives with 1,3-dichloropropan-2-one to yield the target compound in a one-step procedure (Figure 2.8, route f). This reaction had previously been trialled by Sanchez *et al.*^[24] but was found to return only degradation products and starting material. The key difference between the two synthetic methodologies was the addition of sodium iodide to the reaction mixture. Sodium iodide is understood to undergo SN2 substitution reactions with alkyl chlorides to generate alkyl iodide intermediates, thus rendering the compound more reactive. The addition of an alkali metal halide to a primary alkyl halide for these purposes is known as a Finkelstein reaction.^[28] It should be noted that the cyclisation reagent is an extremely hazardous and lachrymatory chemical.

A palladium-catalysed cyclisation reaction between substituted catechol analogues and dimethyl (2-methylenepropane-1,3-diyl) dicarbonate to give a 3-methylenebenzo[*b*][1,4]dioxepine intermediate was reported by Sinou *et al.*^[29] (Figure 2.8, route b followed by d/e (one-pot)). The isolated methylene intermediate was oxidised to the target compound in a one-step Lemieux-Johnson oxidation. The palladium catalyst for the cyclisation reaction is pre-generated before addition to a solution of the catechol derivative alongside the dicarbonate compound. The authors noted that the cyclisation scope was limited to reactants that did not contain electron-withdrawing groups substituted on the benzene ring.

Another synthetic route was developed by Hgel *et al.*^[10] for the synthesis of a library of substituted analogues for olfactory evaluation (Figure 2.9, route a/b/d). This route involved the Williamson reaction of various catechol derivatives with 2-((1-bromo-3-chloropropan-2-yl)oxy)tetrahydro-2*H*-pyran to yield a cyclised intermediate tetrahydropyranyl-ether compound. The protecting group was then removed by the action of a vanadium complex to yield the unprotected racemic alcohol which was then oxidised with potassium permanganate to yield the corresponding target compound. An alternative procedure for the oxidation of the alcohol derivative using Dess-Martin periodinane was described within a 2008 patent.^[30]

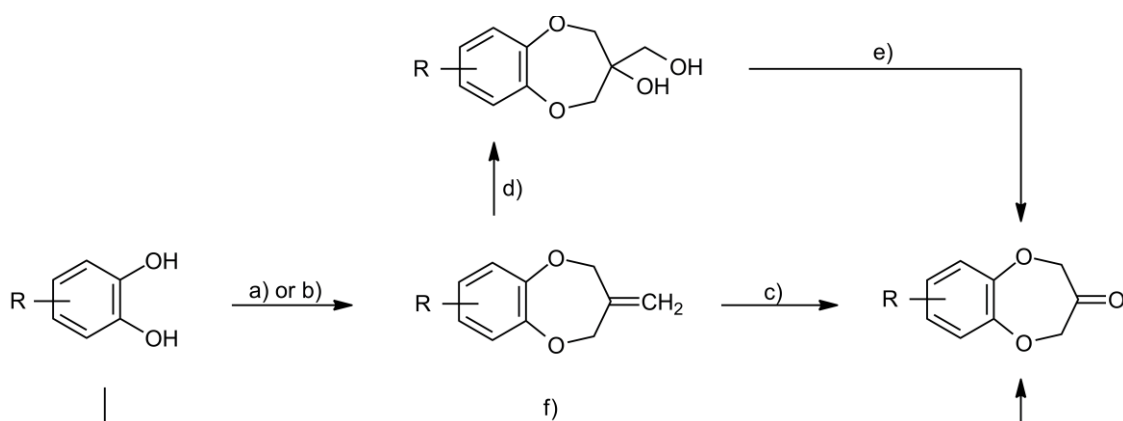


Figure 2.8: Williamson ether synthesis routes developed by Kraft *et al.* (route a/c), Curtin *et al.* (route a/d/e), Sinou *et al.* (route b followed by d/e (one-pot)) and Gaudin *et al.* (route f) leading the benzo[*b*][1,4]dioxepin-3-one scaffold. a) 3-chloro-2-(chloromethyl)prop-1-ene, K_2CO_3 , Et_2CO , dioxane, $\uparrow\downarrow$. b) dimethyl (2-methylenepropane-1,3-diyl) dicarbonate, $Pd_2(dba)_3$, dppb, THF. c) $RuCl_3$, $NaIO_4$, CCl_4 , MeCN, H_2O . d) OsO_4 , NMO, acetone, $tBuOH$, H_2O . e) $NaIO_4$, THF, H_2O . f) 1,3-dichloropropan-2-one, NaI, K_2CO_3 , acetone.

Rosnati *et al.*^[31] described the isolation of the same cyclised alcohol when a Williamson reaction was performed with 1,3-dichloropropan-2-ol (Figure 2.9, route c/d). It is noted that this compound was actually an impurity in a synthesis designed to generate a six-membered heterocyclic compound. To verify the molecular structure of the undesired alcohol, an oxidation with potassium permanganate was performed which successfully yielded the benzo[*b*][1,4]dioxepin-3-one compound, which was then further functionalised and characterised.

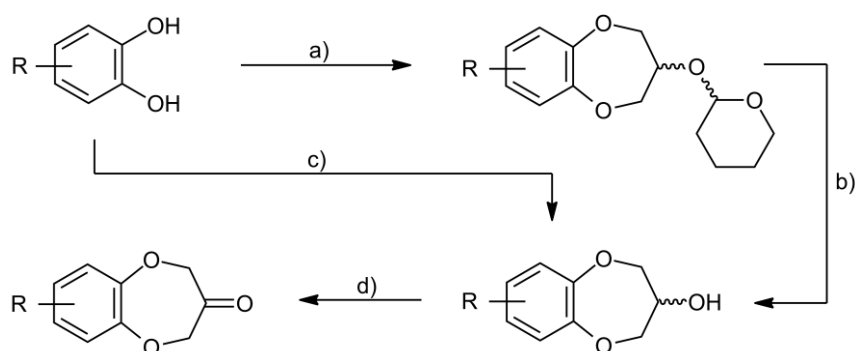


Figure 2.9: Williamson ether synthesis route developed by Hügel *et al.* (route a/b/d) and Rosnati *et al.* (route c/d) leading the benzo[*b*][1,4]dioxepin-3-one scaffold. a) 2-((1-bromo-3-chloropropan-2-yl)oxy)tetrahydro-2H-pyran, K_2CO_3 , DMF, $\uparrow\downarrow$. b) V_2O_5 , H_2O_2 , 70 °C c) 1,3-dichloropropan-2-ol, KOH, 100 °C. d) $KMnO_4$, KOH, H_2O .

A synthetic methodology leading to the heterocyclic portion of the benzo[*b*][1,4]dioxepin-3-one scaffold that involved the reaction of *bis*-hydroxyl compounds with tris- ω,ω,ω -bromomethylacetophenone to yield cyclised methylene intermediates was developed by Nerdel *et al.*^[32] (Figure 2.10). The reaction involves the *in situ* cleavage of the acetophenone derivative via the action of an alkoxide intermediate to generate 3-bromo-2-(bromomethyl)prop-1-ene. This intermediate then undergoes a standard Williamson reaction with the *bis*-hydroxyl compound to yield the cyclised target material. The authors successfully oxidised the methylene intermediate using ozone, before performing a degradation to the unsubstituted parent compound as proof of molecular structure.

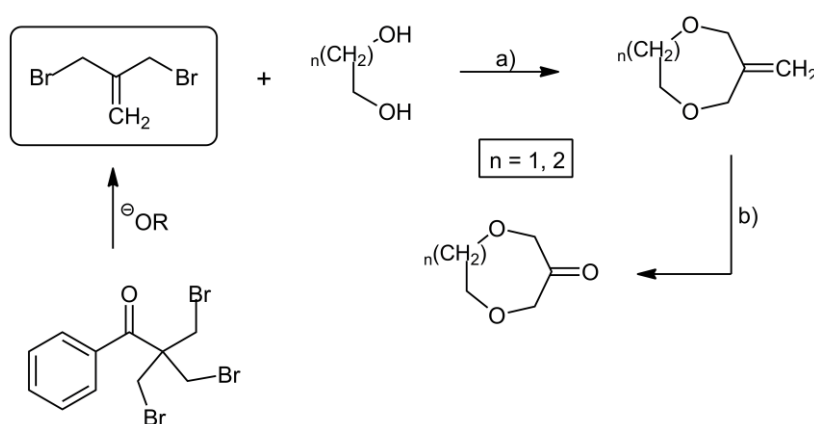


Figure 2.10: Methodology developed by Nerdel *et al.* leading to the 1,4-dioxepan-6-one scaffold ($n = 1$); a) NaH, THF. b) O₃, MeOH.

An alternative synthetic methodology, never applied to the synthesis of benzo[*b*][1,4]dioxepin-3-one analogues, but to substituted 2-dimethylbenzo[*b*][1,4]dioxepin-3-ol analogues, had been utilised in the synthesis of multiple mycotoxin compounds such as paraherquamide A & B and 9-methoxystrobilurin K.^[33-37] The synthetic methodology involves the mono-etherification of a catechol analogue with prenyl bromide, followed by epoxidation using *meta*-chloroperbenzoic acid. The isolated epoxide intermediate is then cyclised in a Lewis-acid catalysed reaction to yield the 2-dimethyl-3-hydroxyl analogue of the benzo[*b*][1,4]dioxepin-3-one template (Figure 2.11).

This synthetic methodology could presumably be modified to synthesise analogues of the benzo[*b*][1,4]dioxepin-3-one scaffold by the substitution of prenyl bromide with allyl bromide. Molecular structures bearing a 1,4-dioxepan-6-ol heterocycle were indeed isolated as impurities in two separate research studies attempting to create benzodioxane analogues using analogous methodologies, but instead using allyl bromide as the etherification reagent.^[38-39]

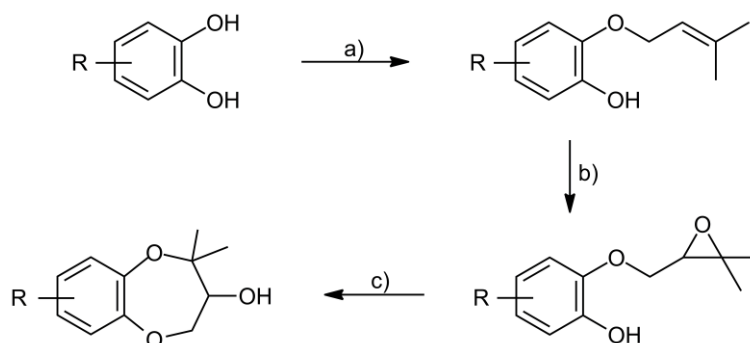


Figure 2.11: Epoxide cyclisation route to 2-dimethylbenzo[*b*][1,4]dioxepin-3-ol scaffold. a) prenyl bromide, K_2CO_3 , DMF. b) mCPBA, NaHCO_3 , CH_2Cl_2 , $0\text{ }^\circ\text{C}$. c) SnCl_4 , THF.

Another potential route to the saturated benzo[*b*][1,4]dioxepin-3-one scaffold is the direct hydrogenation of the aromatic scaffold (Figure 2.12). Aromatic hydrogenation is already employed in the fragrance industry during the synthesis of (\pm)-menthol from aromatic monoterpene compound thymol.^[40] If applied to the benzo[*b*][1,4]dioxepin-3-one molecule, this synthetic protocol may prove to be problematic owing to the target compound being produced as a racemic mixture thus making characterisation difficult. A variety of promising catalysts for aromatic ring hydrogenation under mild reaction conditions have been reported in recent literature including, but not limited to, palladium, ruthenium and gold nanoparticle catalysts absorbed onto various supporting materials.^[41-44]

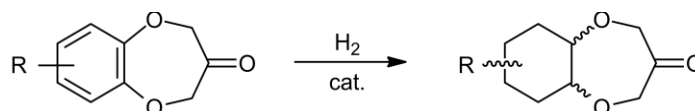


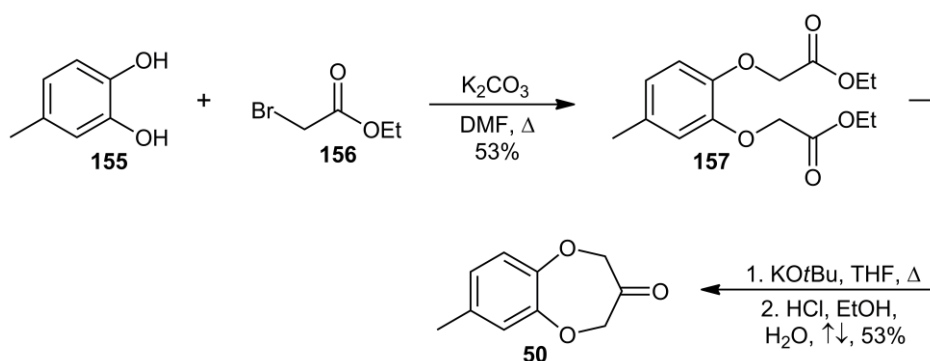
Figure 2.12: Potential hydrogenation route to the saturated benzo[*b*][1,4]dioxepin-3-one scaffold.

2.2 – Results and Discussion

2.2.1 – Synthesis of Calone 1951[®] by Dieckmann Condensation

To construct the target aliphatic benzo[*b*][1,4]dioxepin-3-one molecules it was decided to build the dioxepanone heterocycle onto the cyclohexyl carbocycle in a fashion analogous to the synthetic pathway originally described in the Pfizer patent for Calone 1951[®].^[18] To determine if the published literature methodology was accurate, the chemical synthesis of lead compound Calone 1951[®] (**50**) was performed.^[10]

The pathway first involved a Williamson reaction of 4-methylcatechol (**155**) with ethyl bromoacetate (**156**) in dimethylformamide (DMF) using anhydrous potassium carbonate (K_2CO_3) as a base (Scheme 2.1). The methodology required the reaction be heated to 120 °C for two hours followed by pouring the reaction mixture into ice-cold water followed by extraction with dichloromethane (DCM). The target compound **157** was isolated in 53% yield from the complex reaction mixture by gradient flash chromatography (15 → 20%; ethyl acetate in hexane) as a clear oil. In subsequent Williamson reactions it was discovered that superior results were obtained when the extraction solvent was changed from dichloromethane to diethylether, as the solubility of dimethylformamide is markedly lower, thereby making the extraction process more efficient.



Scheme 2.1: Synthesis of Calone 1951[®] (**50**) from 4-methylcatechol (**155**) via Dieckmann methodology.

The isolated *bis*-ester compound **157** was then cyclised by addition to a stirred solution of the strong non-nucleophilic base potassium *tert*-butoxide (KO^tBu) in tetrahydrofuran (THF) at 0 °C, followed by heating to 70 °C for one hour before quenching the reaction with the addition of an ice-cold solution of 0.2 M hydrochloric acid (HCl). This reaction gave a racemic mixture of regioisomers of the cyclic β -ketoester compound. The crude material was then decarboxylated by heating at reflux in 2 M HCl to furnish the target compound Calone 1951[®] (**50**) as a colourless crystalline solid in a 53% yield. Heteronuclear single quantum coherence spectroscopy (¹H, ¹³C, HSQC) analysis revealed that Dieckmann cyclisation and decarboxylation were successful in yielding the aromatic benzo[*b*][1,4]dioxepin-3-one molecule (Figure 2.13).

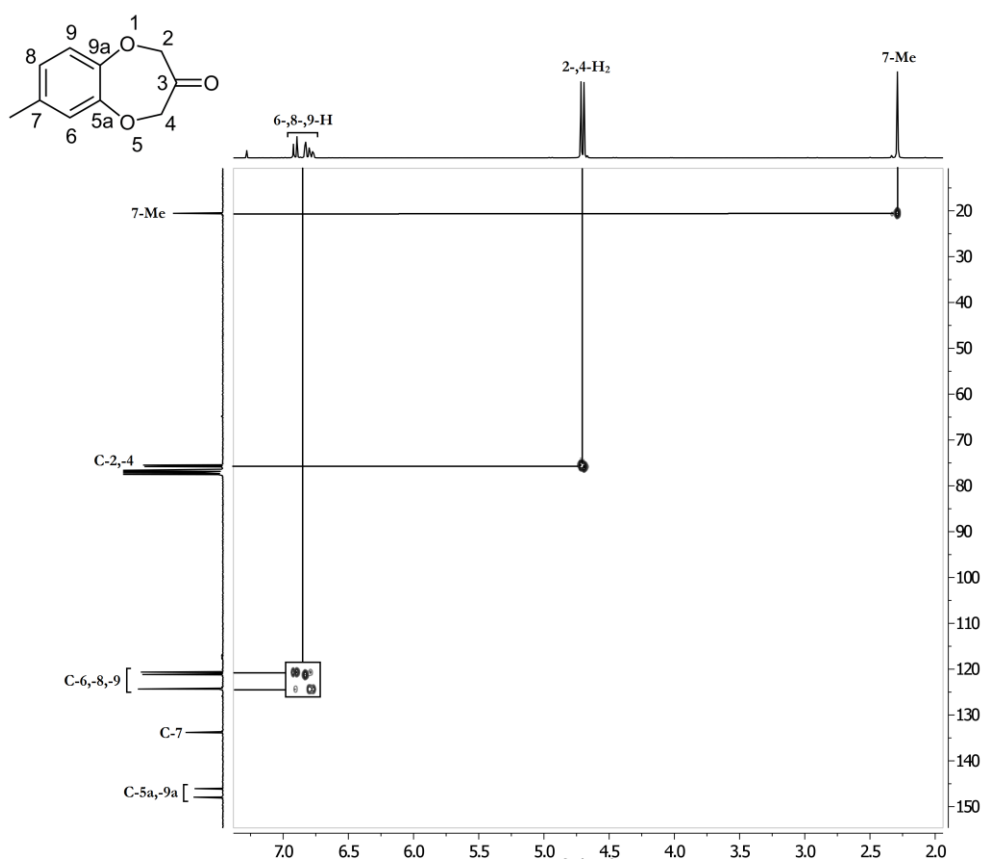


Figure 2.13: ¹H, ¹³C HSQC (CDCl₃, 300 MHz) spectrum of compound Calone 1951[®] (**50**).

The key step in the synthesis of the benzo[*b*][1,4]dioxepin-3-one molecular scaffold via this synthetic methodology is the Dieckmann condensation reaction. First published in 1894 by German chemist Walter Dieckmann, this reaction involves the intramolecular cyclisation of a *bis*-ester compound to give a β -ketoester compound, analogous to the intermolecular Claisen condensation reaction.^[45] The reaction of the *bis*-ester compound initiates with the removal of an acidic α -hydrogen resulting in the formation of an enolate anion (Figure 2.14). The enolate anion nucleophilically attacks the electropositive carbonyl carbon of the adjacent ester moiety, the corresponding alkoxide anion is released and the β -ketoester intermediate is formed. This intermediate is then further deprotonated to form an enolate from which an acidic workup is required to liberate the final β -ketoester product.

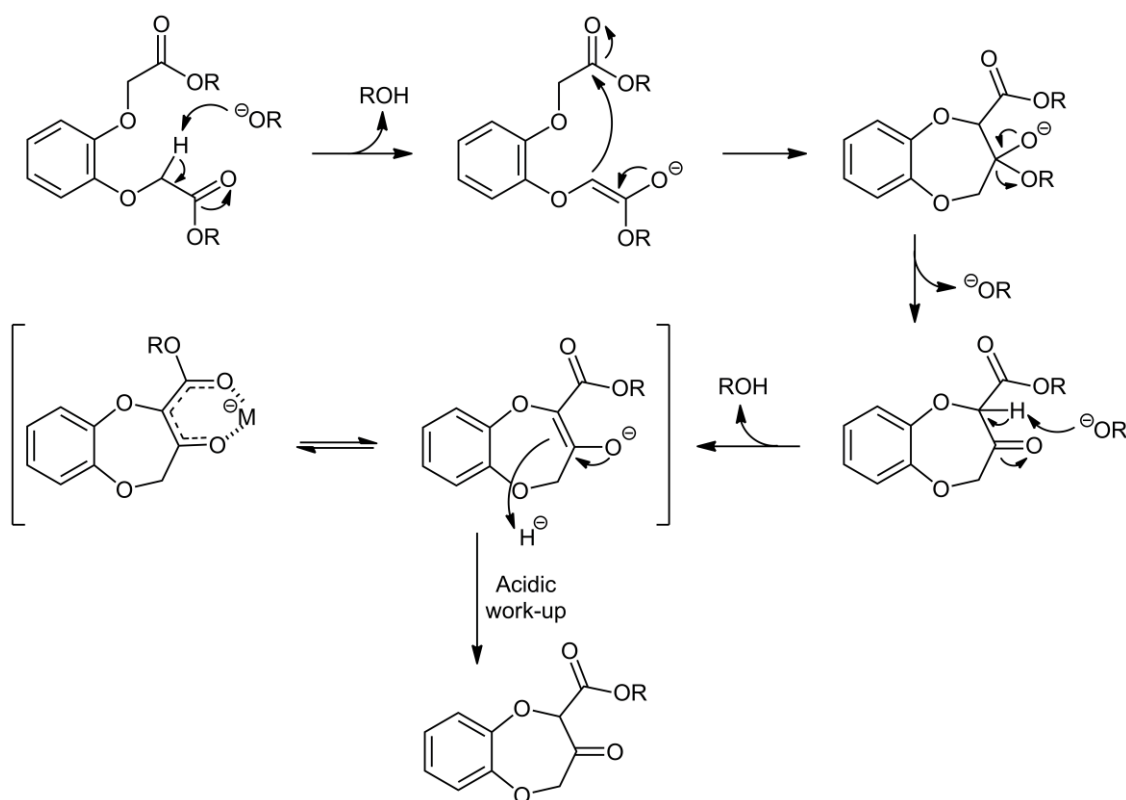


Figure 2.14: Proposed reaction mechanism for the Dieckmann condensation reaction leading to the benzo[*b*][1,4]dioxepin-3-one scaffold.

An intramolecular Dieckmann cyclisation reaction to give a seven membered ring is a 7-*exo-trig* cyclisation, indicating that it is predicted to be a favoured cyclisation reaction by Baldwin's rules (Table 2.1). First proposed in a series of papers by Jack E. Baldwin beginning in 1976, these rules predict the relative success of ring closing synthetic reactions.^[46-47]

	3		4		5		6		7	
Type	<i>exo</i>	<i>endo</i>	<i>exo</i>	<i>endo</i>	<i>exo</i>	<i>endo</i>	<i>exo</i>	<i>endo</i>	<i>exo</i>	<i>endo</i>
<i>tet</i>	✓	-	✓	-	✓	X	✓	X	✓	X
<i>trig</i>	✓	X	✓	X	✓	X	✓	✓	✓	✓
<i>dig</i>	X	✓	X	✓	✓	✓	✓	✓	✓	✓

Table 2.1: Baldwin's favoured and disfavoured ring closing reactions.

The rules follow a systematic naming convention in the form α - β - γ . α is an integer which details the ring size being formed; for a system to exist as a ring it cannot be any fewer than three atoms and the rules only remain accurate for rings containing up to seven atoms. β is a prefix of either *exo* (outside) or *endo* (inside) that refers to whether the chemical bond being broken is inside or outside of the ring being formed (Figure 2.15).

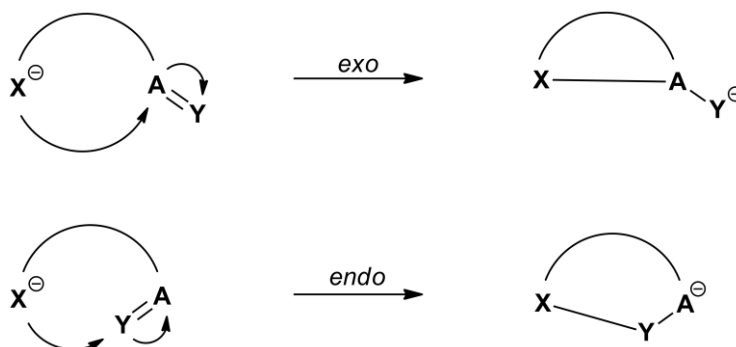


Figure 2.15: Graphical representation of *exo* (outside) and *endo* (inside) ring closing reactions.

The γ term refers to the geometry of the atom being nucleophilically attacked and can be labelled *tet*, *trig* or *dig*. The titles arise from if the electrophilic carbon is tetrahedral (sp^3 hybridised, *tet*), trigonal (sp^2 hybridised, *trig*) or digonal (sp hybridised, *dig*) (Figure 2.16). The physical basis of Baldwin's rules lie in the stereochemical requirements of the transition states for the various tetrahedral, trigonal and digonal ring closure processes.^[46] In order to achieve cyclisation a molecule must have the ability to adopt a conformation that allows overlap of the appropriate electron orbitals. The predictions actually indicate reaction speed as a reaction that is disfavoured typically does not have a rate that is able to compete efficiently with unwanted side-reactions.

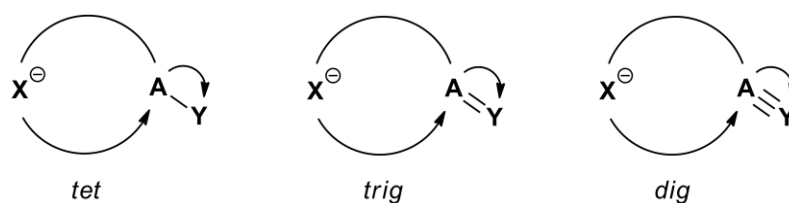


Figure 2.16: Graphical representation of *tet*, *trig* and *dig* ring closing reactions.

2.2.2 – Synthesis of *threo*-Configured Hexahydrobenzo[*b*][1,4]dioxepin-3-one

The synthetic methodology from within the published literature^[10] was shown to be effective in the synthesis of the aromatic benzo[*b*][1,4]dioxepin-3-one scaffold and so attention turned to the synthesis of the target aliphatic scaffold. The synthesis of an unsubstituted fully saturated analogue was first attempted to aid in the development of a suitable synthetic methodology that would allow access to this novel class of compounds, as well as give insight into the conformational alignments in relation to that of the original molecular template.

Examination of the planar molecular structure of cyclohexane-1,2-diol indicates that two forms and three possibly stereoisomer of the compound can exist. The two different forms arise from which face the two hydroxyl groups are oriented in reference to each other. The *trans*-diol isomer has a non-superimposable mirror image and hence is chiral and both (1*S*,2*S*) and (1*R*,2*R*) enantiomers can be successfully synthesised and isolated. The *cis*-diol isomer has a plane of symmetry and thereby its mirror images are identical; this compound is known as the *meso*-isomer.

Interestingly, the two alternative chair conformations of *cis*-cyclohexane-1,2-diol are each chiral but because they are of the same energy and interconvert rapidly, *cis*-cyclohexane-1,2-diol is effectively *meso* as predicted by analysis of the planar molecular structures (Figure 2.17).^[48] The two enantiomers of *trans*-cyclohexane-1,2-diol have identical chemical properties, although of interest to note is that the racemic material has a lower melting point than the pure enantiomeric material. The *cis*-cyclohexane-1,2-diol isomer is a completely different compound and thus has different chemical and physical properties to the *trans*-cyclohexane-1,2-diol isomers.^[49]

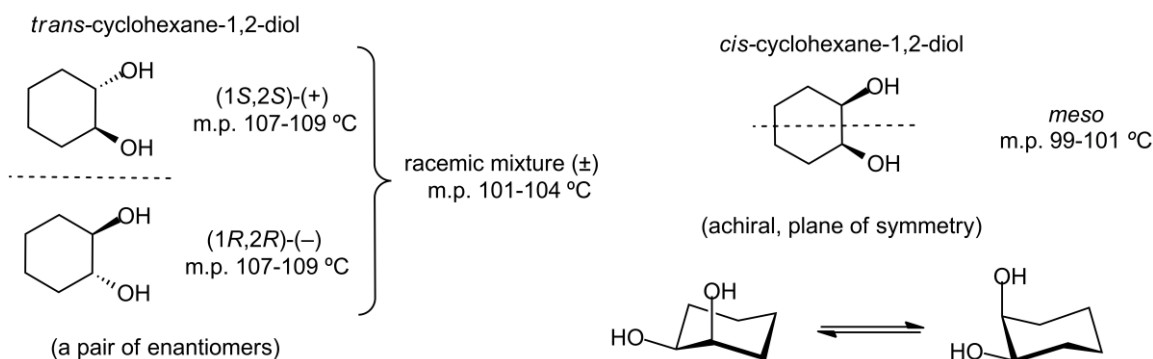
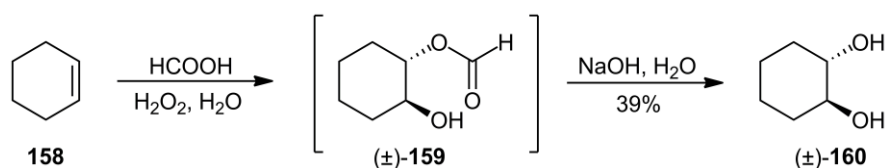


Figure 2.17: Stereochemical relationships of cyclohexane-1,2-diol. The *trans*-configured isomer exists as two enantiomers whilst the *cis*-configured isomer is a *meso* compound with different chemical properties.

It was decided that both stereoisomers of the aliphatic benzo[*b*][1,4]dioxepin-3-one scaffold would be synthesised from cyclohexane-1,2-diol, and their chemical and olfactory properties compared. Odorant molecules are commonly evaluated as a racemic mixture and are generally only synthesised as the pure enantiomeric material when the racemic compound incorporates the target odour. It was thus decided to synthesise *trans*-cyclohexane-1,2-diol as a racemic mixture of (1*S*,2*S*) and (1*R*,2*R*) enantiomers. Following the methodology of Roebuck and Adkins, cyclohexene was dihydroxylated using formic acid and hydrogen peroxide to yield an intermediate formate ester (**159**) which was then hydrolysed to the vicinal-diol compound (\pm)-**160** using sodium hydroxide (Scheme 2.2).^[50] The reaction yielded a racemic mixture of the two enantiomers of *trans*-cyclohexane-1,2-diol (**160**) as a colourless solid in a 39% yield after recrystallisation from ethyl acetate.

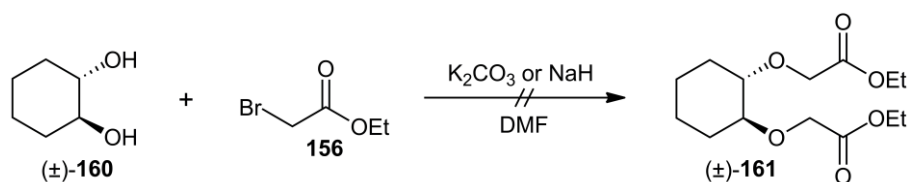


Scheme 2.2: Synthesis of *rac*-cyclohexane-1,2-diol (**160**) from cyclohexene (**158**).

An attempt was then made at following the previously successful Williamson reaction methodology by reacting *rac*-cyclohexane-1,2-diol (**160**) with ethyl bromoacetate (**156**) using potassium carbonate under refluxing conditions (Scheme 2.3). These reaction conditions were found to yield only complex mixtures of polymerised products. It was thus revealed that a stronger base would be required to deprotonate

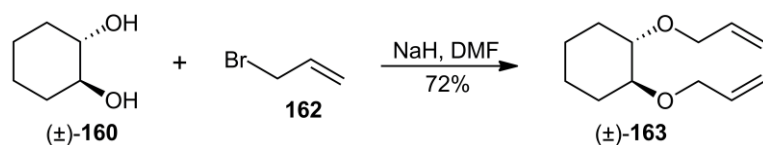
the weakly acidic hydroxyl groups. An additional literature search revealed that no heating of the reaction would be required owing to the increased nucleophilicity of the alkoxide intermediate in reference to the phenoxide intermediate.

The standard base for such aliphatic Williamson reactions is sodium hydride (NaH). The standard reaction conditions for such a system comprises of the addition of the *bis*-hydroxyl compound to a suspension of sodium hydride in dimethylformamide at 0 °C. The reaction mixture is then stirred at 0 °C for one hour to generate the *bis*-alkoxide intermediate, with the release of hydrogen gas from the solvent. This is followed by dropwise addition of the halogenated compound to the newly formed alkoxide intermediate, followed by stirring at room temperature overnight. These conditions were experimented with for a reaction between *rac*-cyclohexane-1,2-diol (**160**) and ethyl bromoacetate (**156**), but were found to yield only polymerised material (Scheme 2.3).



Scheme 2.3: Failed Williamson reactions between *rac*-cyclohexane-1,2-diol (**160**) and ethyl bromoacetate (**156**).

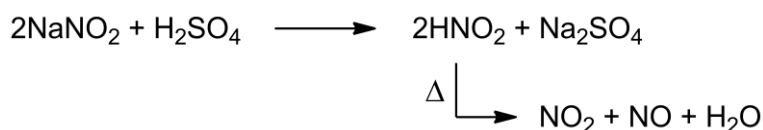
A model reaction was conducted between *rac*-cyclohexane-1,2-diol (**160**) and allyl bromide (**162**) to examine if the incompatibility of the ester functionalities of compounds **156/161** with the strongly basic *bis*-alkoxide intermediate was the origin of the problem (Scheme 2.4).^[51] The *bis*-etherified compound (**163**) was successfully isolated in a 72% yield as a clear oil providing strong evidence that functional group sensitivity was indeed the origin of the complications associated with the reaction between *rac*-cyclohexane-1,2-diol (**160**) and ethyl bromoacetate (**156**).



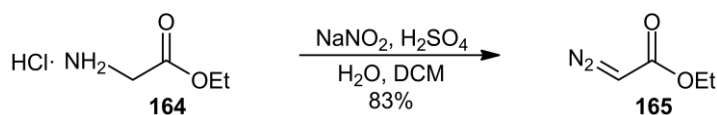
Scheme 2.4: Synthesis of *rac*-1,2-bis(allyloxy)cyclohexane (**163**) from *rac*-cyclohexane-1,2-diol (**160**), thereby providing evidence that the Williamson reaction methodology was correct, but that functional group sensitivity was the origin of the problem with the reaction displayed in Scheme 2.3.

It was assumed that any successful reaction conditions able to yield target compound (\pm)-**161** would require a mild alkylation technique which had a high degree of functional group tolerance. Fortunately, additional literature research revealed that both an enantiopure and a racemic analogue of the targeted *bis*-ester compound (\pm)-**161** had been synthesised in an alternative Lewis-acid catalysed etherification reaction, thereby circumventing the use of any strongly basic alkoxide intermediates.^[52-53] The proposed chemical reaction involved the dropwise addition of a catalytic amount of boron trifluoride diethyletherate adduct to an ice-cold dichloromethane solution of the *bis*-hydroxyl compound and ethyl diazoacetate, followed by stirring at room temperature for one hour and then at refluxing temperature for one hour.

Ethyl diazoacetate (**165**) was prepared from ethyl glycinate hydrochloride (**164**), sodium nitrite (NaNO_2) and sulphuric acid (H_2SO_4).^[54] The reaction involves the *in situ* generation of nitrous acid (HNO_2) by the action of sulphuric acid on sodium nitrite. The chemical reaction must be retained below $-5\text{ }^\circ\text{C}$ to prevent the nitrous acid from decomposing into nitrogen dioxide (NO_2), nitric oxide (NO) and water:

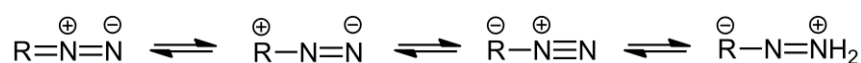


The *in situ* generated nitrous acid reacts electrophilically with the amine group of ethyl glycinate hydrochloride (**164**), followed by the elimination of two equivalents of water to yield the diazo derivative, ethyl diazoacetate (**165**), as a thin yellow oil in an 83% yield (Scheme 2.5).



Scheme 2.5: Synthesis of ethyl diazoacetate (**165**) from ethyl glycinate hydrochloride (**164**).

Under the appropriate reaction conditions, a diazo compound can behave as an acid or as a base, as a nucleophile or as an electrophile, as a 1,3-dipole or as a carbene source.^[55] Diazo compounds can be drawn as a mixture of four resonance forms:



A boron trifluoride catalysed O–H insertion reaction with ethyl diazoacetate (**165**) was first reported in 1950 by Newman and Beal during their research into the Wolff and Curtius rearrangement reactions, but has been little used in synthetic procedures to date.^[56] Other Lewis-acid catalysts such as aluminium chloride and tin(IV) chloride are also reported to be effective catalysts for the transformation.^[57]

A wide range of primary, secondary and tertiary alcohols have been transformed into alkyl ethers by the use of various diazo compounds. Yields are generally good for alkylation with diazomethane, although yields are seldom above 50% for higher diazo compounds, such as ethyl diazoacetate (**165**).^[55] The mechanism for the Lewis-acid catalysed alkylation reaction is believed to involve the boron trifluoride molecule forming a polar coordinate bond with the hydroxyl oxygen atom, drawing electrons away and thus activating it. The diazo compound then acts as a nucleophile and reacts with the activated hydroxyl group, with the elimination of a neutral nitrogen molecule. This is then followed by product dissociation and catalyst regeneration (Figure 2.18).

A more well-known adaptation for this class of alkylation reaction is the use of transition-metal catalysts such as copper or rhodium.^[58] The mechanism for this type of catalysis is believed to involve the decomposition of the diazo compound to give a metal–carbenoid intermediate, which then undergoes the O–H insertion.^[57]

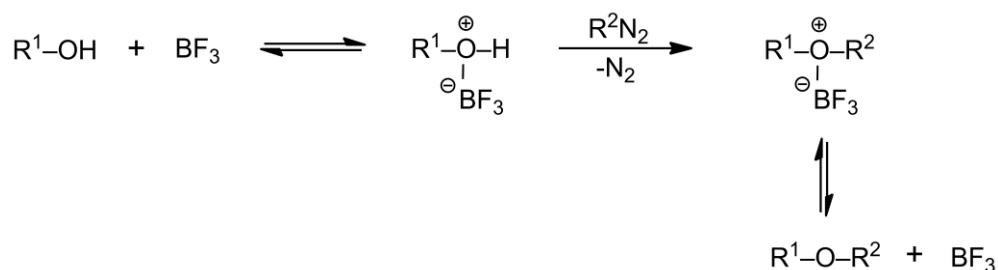
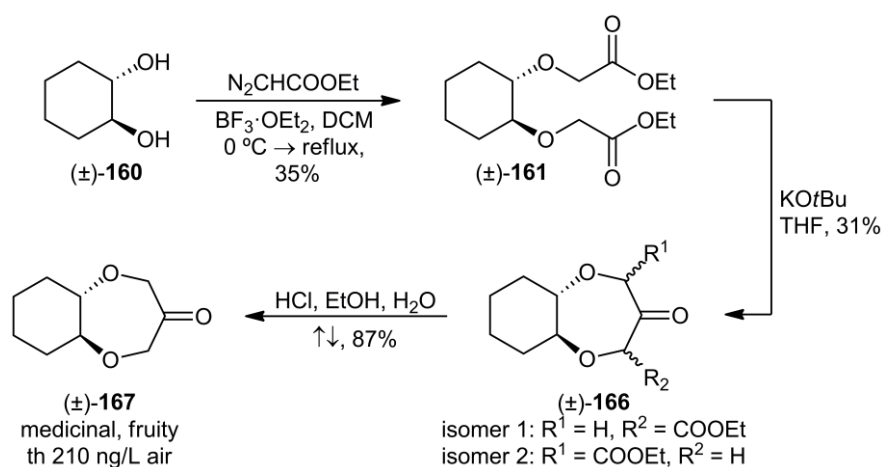


Figure 2.18: Proposed catalytic cycle for a boron trifluoride (BF₃) catalysed O–H insertion reaction with a diazo compound.^[55]

The boron trifluoride diethyletherate catalysed reaction between *rac*-cyclohexane-1,2-diol (**160**) and ethyl diazoacetate (**165**) was found to successfully yield the *bis*-ester compound (\pm)-**161** in an adequate yield of 35% as a yellow oil after flash chromatography on silica gel (Scheme 2.6, Figure 2.19). The isolated *bis*-ester compound (**161**) was then subjected to a base-catalysed Dieckmann condensation reaction using identical conditions to those used for the aromatic analogue. The reaction yielded a crude isomeric mixture of the β -ketoester compound (\pm)-**166** as a thick yellow oil that contained a readily identifiable carbonyl signal at δ 205 ppm in the ^{13}C NMR spectrum.



Scheme 2.6: Synthesis of *threo*-configured aliphatic benzo[*b*][1,4]dioxepin-3-one (\pm)-**167** from *rac*-cyclohexane-1,2-diol (**160**) via Dieckmann methodology.

Attempts at the isolation of (\pm)-**166** by flash chromatography on silica gel provided only polymerised material. It was discovered that to successfully elute the β -ketoester compound without decomposition the silica gel used within the flash chromatography column had to be deactivated by pre-elution with a 5% v/v solution of triethylamine in the regular solvent system. Silica gel contains on average 4.6 hydroxyl groups per 100 \AA^2 of particle surface and thus silica is acidic and is known to degrade sensitive organic compounds.^[59] The addition of an amine base aids in the deactivation of the active sites and thereby lowers the destructive capability of the silica adsorbent.

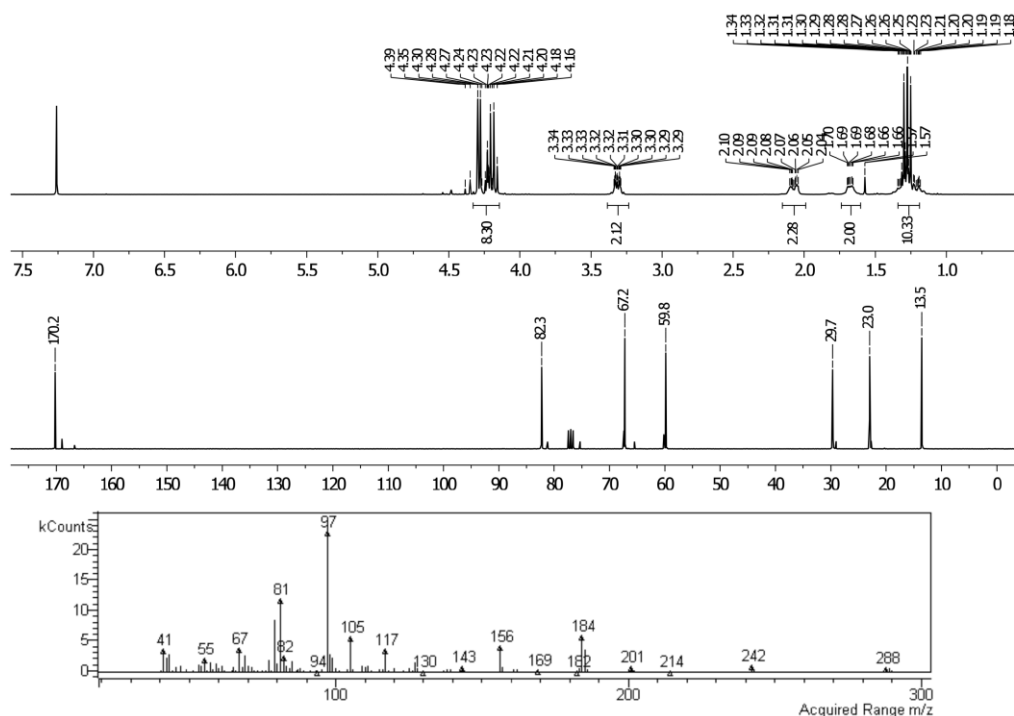


Figure 2.19: Various spectra of compound (\pm)-**161**. Top: ^1H NMR (CDCl_3 , 300 MHz) spectrum; Middle: ^{13}C NMR (CDCl_3 , 75 MHz) spectrum; Bottom: Mass spectrum (EI) showing molecular ion at m/z 288.

The target compound (\pm)-**166** was finally isolated as a mixture of stereoisomers in a 31% yield as a colourless crystalline solid. ^1H , ^{13}C HSQC analysis of compound (\pm)-**166** unequivocally proved that the cyclisation reaction was successful in yielding the first example of an aliphatic benzo[*b*][1,4]dioxpin-3-one analogue (Figure 2.20). The absence of multiple overlapping signals within the NMR spectrum indicated that the compound contained complete symmetry, an achievement considering compound (\pm)-**166** contains three chiral centers and presumably exists as an equimolar mixture of eight possible diastereomers.

The following synthetic step within the reaction sequence involved an acid-catalysed decarboxylation of the β -ketoester compound (**166**) by heating at reflux in 2 M HCl and ethanol. The reaction was found to yield a thick yellow oil that resembled polymerised resin. Flash chromatography on deactivated silica gel yielded the target saturated *threo*-configured benzo[*b*][1,4]dioxepin-3-one compound (\pm)-**167** as a colourless solid in an 87% yield.

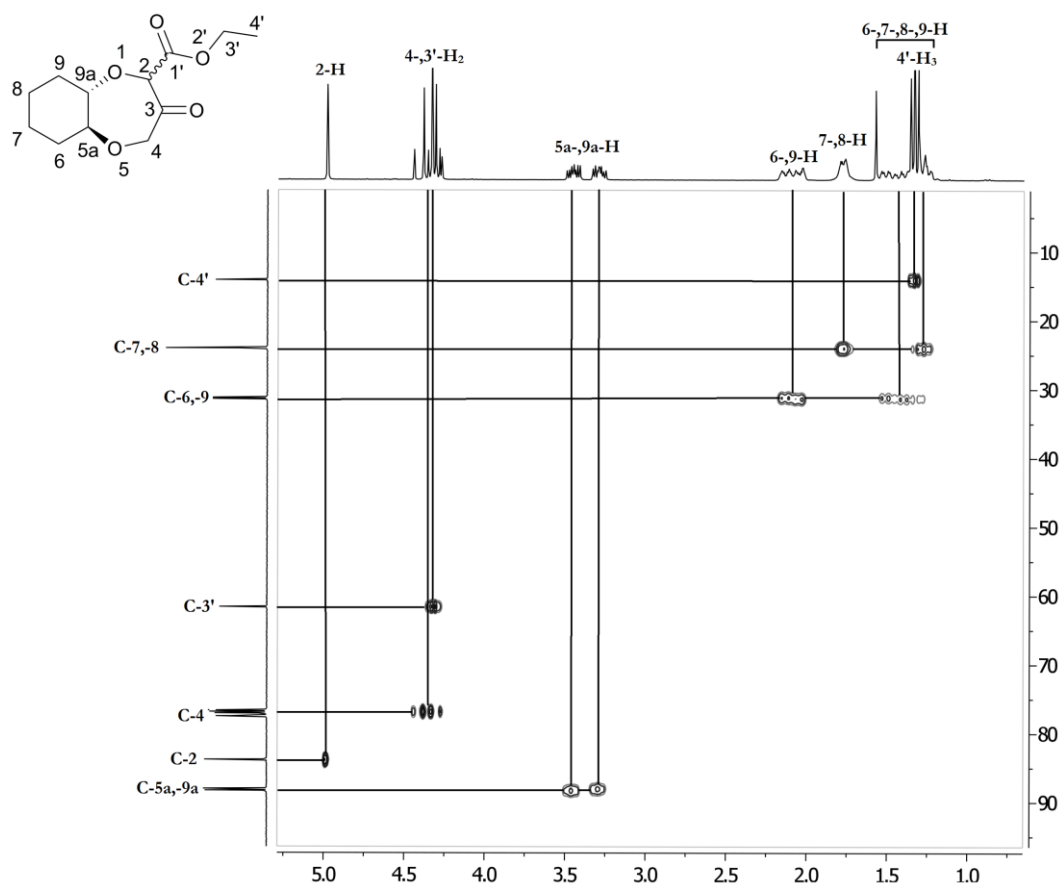


Figure 2.20: ^1H , ^{13}C HSQC (CDCl_3 , 300 MHz) spectrum of compound (\pm)-**166**.

2.2.3 – Synthesis of *erythro*-Configured Hexahydrobenzo[*b*][1,4]dioxepin-3-one

The synthesis of the alternatively configured aliphatic benzo[*b*][1,4]dioxepin-3-one molecule, the *erythro*-configured stereoisomer, was conducted. The *cis*-diol compound, *meso*-cyclohexane-1,2-diol (**170**), was synthesised from cyclohexene (**158**) by the catalytic action of osmium tetroxide. Osmium tetroxide is expensive, volatile and highly toxic, so the synthetic oxidation methodology that was settled upon was the catalytic Upjohn dihydroxylation reaction.^[60]

This synthetic methodology fortunately only requires the use of a catalytic quantity of osmium tetroxide alongside a tertiary amine *N*-oxide, such as *N*-methylmorpholine *N*-oxide (**169**), which acts as a catalyst regenerator. The catalytic cycle commences with the [3+2] cycloaddition of the osmium(VIII) oxide compound to the alkene yielding a five-membered metallacycle intermediate.^[61] This is followed by hydrolysis to liberate the vicinal-diol compound as well as a reduced osmium(VI) species which is then

reoxidised to the active osmium(VIII) oxide species by the oxidative action of the *N*-methylmorpholine *N*-oxide (Figure 2.21).

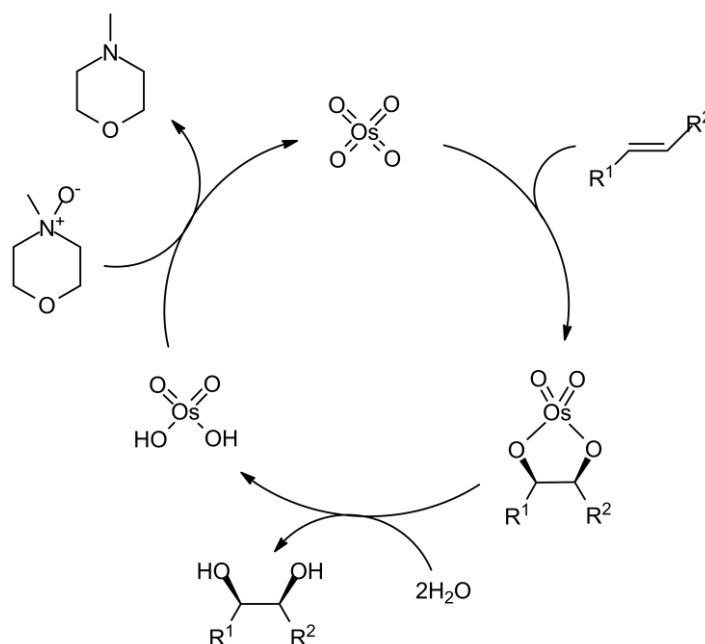
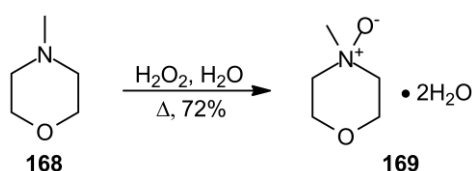


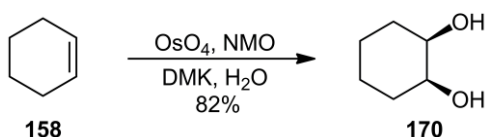
Figure 2.21: Proposed catalytic cycle of the Upjohn dihydroxylation.^[62]

The co-oxidant for this oxidation reaction, *N*-methylmorpholine *N*-oxide (**169**), was synthesised from *N*-methylmorpholine (**168**) and hydrogen peroxide (Scheme 2.7).^[62] Multiple attempts at recrystallisation of the crude material from acetone yielded a colourless crystalline solid with a melting point below that typically reported for the monohydrate (75–76 °C) which indicated that the dihydrate isomer of compound **169** had been isolated. Although not as favourable as the monohydrate due to its hygroscopic nature, this compound was used without complication, with allowances made for the larger molecular weight.



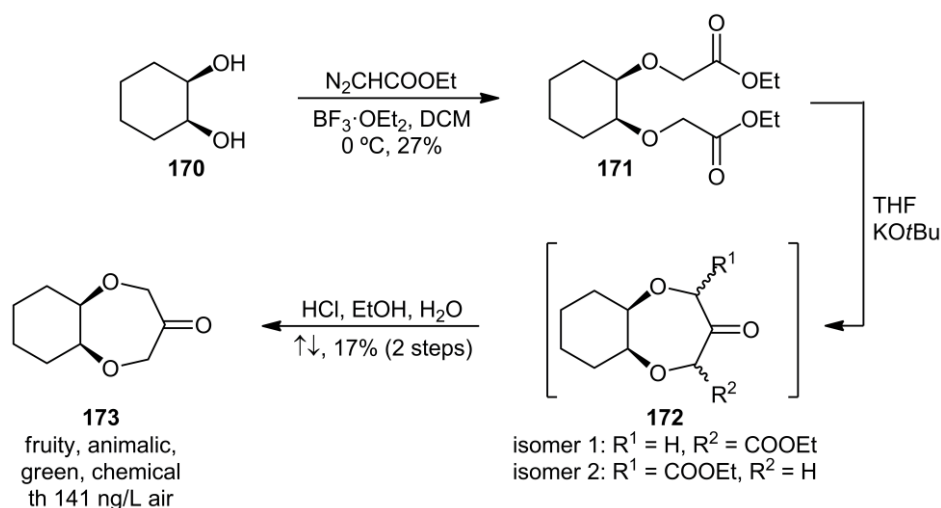
Scheme 2.7: Preparation of *N*-methylmorpholine *N*-oxide (NMO) (**169**) from *N*-methylmorpholine (**168**).

The synthesis of *meso*-cyclohexane-1,2-diol (**170**) was performed using the prepared *N*-methylmorpholine *N*-oxide (**169**) co-oxidant alongside a catalytic quantity of osmium tetroxide in a polar acetone/water (4:1) solvent system (Scheme 2.8).^[62] The reaction was performed under an inert atmosphere to limit the quantity of impurities formed by over-oxidation involving atmospheric oxygen. When reaction monitoring by thin-layer chromatography (TLC) had deemed that all cyclohexene (**158**) had reacted and thus that the catalytic cycle had ended, the dangerous osmium species was reduced by the addition of sodium hydrosulphite, followed by adsorption onto an activated magnesium silicate. The reaction mixture was filtered, followed by extraction of the filtrate using the highly polar solvent *n*-butanol. Concentration of the pooled organic extracts under reduced pressure gave a crude brown solid that was recrystallised from diisopropylether to yield the target material **170** in an 82% yield as a colourless crystalline solid.



Scheme 2.8: Synthesis of *meso*-cyclohexane-1,2-diol (**170**) from cyclohexene (**158**) via a Upjohn dihydroxylation.

The *bis*-etherification reaction of *meso*-cyclohexane-1,2-diol (**170**) with ethyl diazoacetate (**165**) proved somewhat more problematic than the analogous reaction involving the racemic *trans*-diol analogue (\pm)-**160**. Polymerised material was recovered when analogous reaction conditions were experimented with. It was discovered that the synthesis of *bis*-ester compound **171** required careful monitoring of the reaction at 0 °C to prevent polymerisation, as opposed to the 0 °C \rightarrow refluxing conditions successful in the synthesis the *trans*-configured *bis*-ester compound (\pm)-**161**. This was the first indication that the *cis*-configured (or *erythro*-configured) analogues were less stable than their *trans*-configured (or *threo*-configured) counterparts. The *bis*-ester compound **171** was finally isolated in a 27% yield as a yellow oil after flash chromatography on deactivated silica (Scheme 2.9, Figure 2.22).



Scheme 2.9: Synthesis of *erythro*-configured aliphatic benzo[*b*][1,4]dioxepin-3-one **173** from *meso*-cyclohexane-1,2-diol (**170**) via Dieckmann methodology.

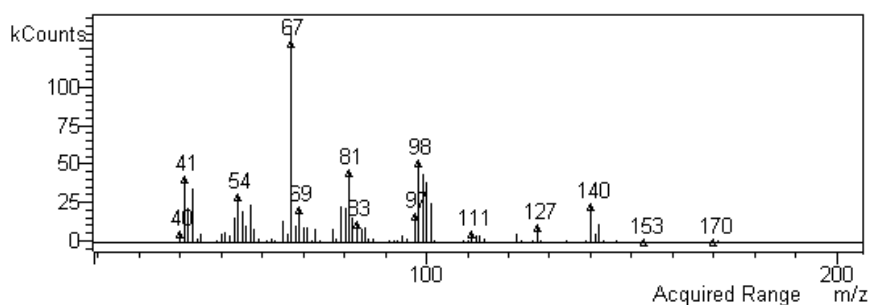


Figure 2.22: Mass spectrum (EI) of compound **173** showing molecular ion at m/z 170.

Subsequent Dieckmann cyclisation reactions of the isolated *erythro*-configured *bis*-ester **171** appeared to provide the target β -ketoester compound **172** by NMR experiments, which clearly exhibited a carbonyl signal downfield in the ^{13}C NMR spectrum. Attempts at the isolation of the β -ketoester compound **172** by flash chromatography on deactivated silica gel, analogous to the isolation and characterisation of the *threo*-configured β -ketoester analogue (\pm)-**166**, were discovered to yield only polymerised material. Attempts at the acid-catalysed decarboxylation of the crude residue were performed in optimism that the completed aliphatic benzo[*b*][1,4]dioxepin-3-one scaffold may offer additional stability relative to the 2-ethyl carboxylate intermediate. The hypothesis proved correct and the target compound **173** was isolated as a colourless crystalline solid in 17% yield after flash chromatography. The mechanism of such acid-catalysed decarboxylation reactions is delineated in Figure 2.23.

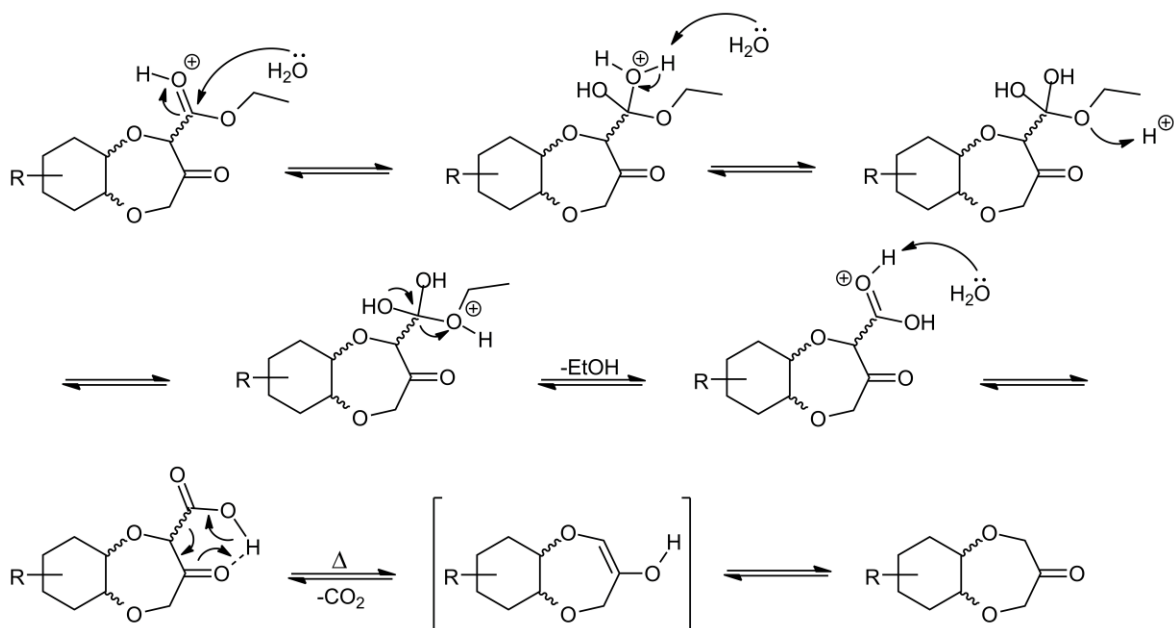


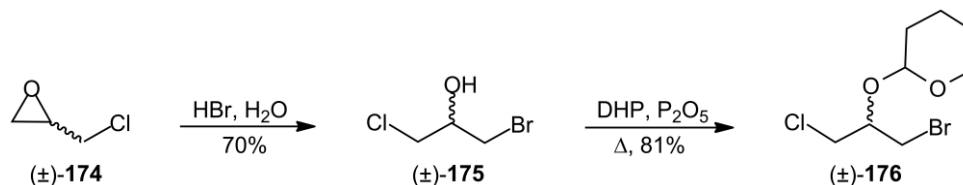
Figure 2.23: Proposed mechanism for acid-catalysed decarboxylation of a β -ketoester intermediate to yield the saturated benzo[*b*][1,4]dioxepin-3-one analogue.

2.2.4 – Attempts at Williamson Cyclisation with 2-((1-Bromo-3-chloropropan-2-yl)oxy)tetrahydro-2*H*-pyran

Alternative methodologies for the synthesis of aliphatic benzo[*b*][1,4]dioxepin-3-one analogues were also experimented with owing to differences in reaction yields and stability between the *threo*- and *erythro*-configured analogues. The synthetic methodology experimented with was a Williamson reaction cyclisation methodology developed by Hügél *et al.*^[10] in their pursuit of a library of aromatic analogues for olfactory analysis. The publication details a Williamson reaction between various catechol derivatives and a tetrahydropyranyl-ether protected analogue of 1-bromo-3-chloropropan-2-ol.^[10]

Following the methodology of Hügél *et al.*,^[10] *bis*-halogenated chain (\pm)-**176** was synthesised beginning from racemic epoxide epichlorohydrin (**174**) (Scheme 2.10). The initial reaction involved an acid-catalysed epoxide cleavage with hydrobromic acid to yield *rac*-1-bromo-3-chloropropan-2-ol (**175**) as a single isomer in a 70% yield after vacuum distillation. The reaction was found to display anti-Markovnikov type regioselectivity due to nucleophilic attack preferentially occurring at the least substituted oxirane carbon, as is generally observed for this class of chemical reactions.^[63] The free hydroxyl group was then protected in a solvent-free reaction using dihydropyran and phosphorus

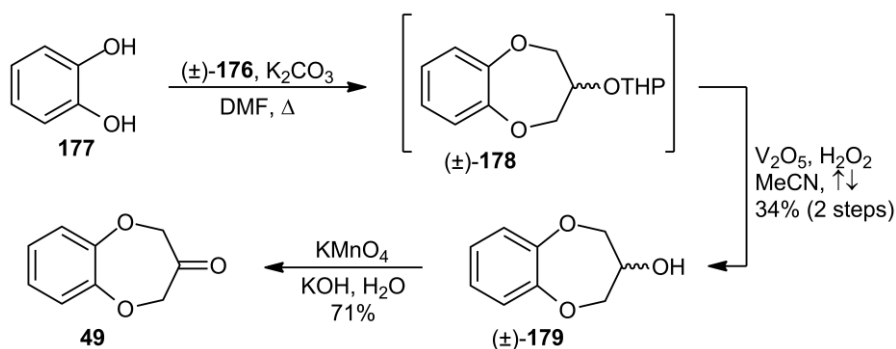
pentoxide as a catalyst to yield the tetrahydropyranyl-ether protected chain (\pm)-**176** as a clear oil in an 81% yield.



Scheme 2.10: Synthesis of tetrahydropyranyl-ether protected chain (\pm)-**176** from epichlorohydrin (**174**).

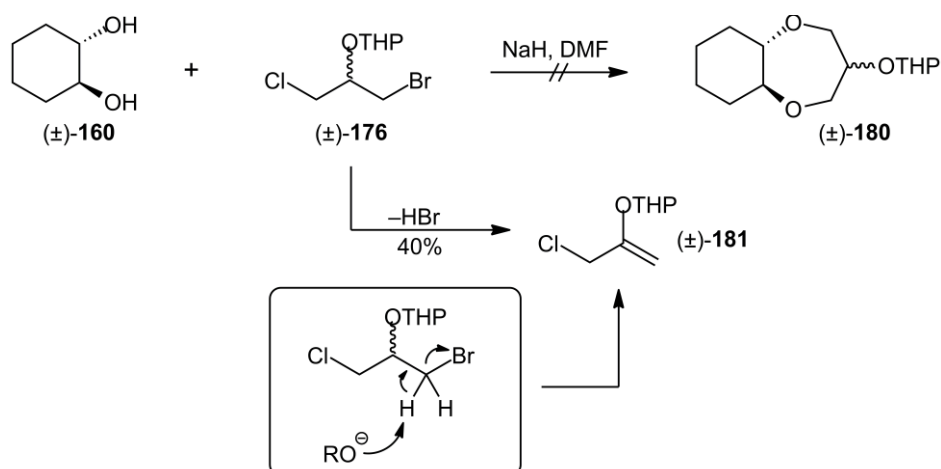
A series of model reactions on the aromatic system beginning with catechol (**177**) were then conducted to establish the reproducibility of the literature methodology. The initial step involved a Williamson reaction between catechol (**177**) and *bis*-halogenated chain (\pm)-**176** in DMF, using potassium carbonate as the base to generate the required phenoxide intermediate.^[10] This reaction was found to give a yellow oil which was partially purified by elution through a plug of silica to give a crude sample of compound (\pm)-**178** (Scheme 2.11). The deprotection of compound (\pm)-**178** was performed on the crude residue by means of a vanadium pentoxide and hydrogen peroxide system.^[64] The reaction involved the pre-generation of a peroxovanadium species before its addition to a refluxing solution of compound (\pm)-**178** in acetonitrile. This reaction successfully yielded the deprotected racemic alcohol (\pm)-**179** as a colourless solid in 34% yield after flash chromatography.

The final synthetic step in the reaction sequence involved the oxidation of the hydroxyl moiety of compound (\pm)-**179** to furnish the completed benzo[*b*][1,4]dioxepin-3-one analogue. The oxidation was achieved by the subjection of the compound to an aqueous solution of potassium permanganate and potassium hydroxide. The target analogue **49** was finally isolated as a colourless solid in 71% yield after flash chromatography. Compound **49** had olfactory characteristics similar to that of Calone 1951[®] (**50**), albeit weaker and with additional undesired nuances, as was previously reported.^[10, 12]



Scheme 2.11: Synthesis of benzo[*b*][1,4]dioxepin-3-one (**49**) from catechol (**177**).

Experimental Williamson reactions between *rac*-cyclohexane-1,2-diol (**160**) and *bis*-halogenated chain (\pm) -**176** using the previously successful reaction conditions were conducted but all that was recovered was the alkene (\pm) -**181**. Compound (\pm) -**181** is the dehydrohalogenated analogue of compound (\pm) -**176** (Scheme 2.12). The reason for the favourability of this side-reaction is presumably related to the alkoxide intermediate being too strongly basic in comparison to the phenoxide intermediate. The elimination reaction of compound (\pm) -**176** presumably occurs via an E2 mechanism.

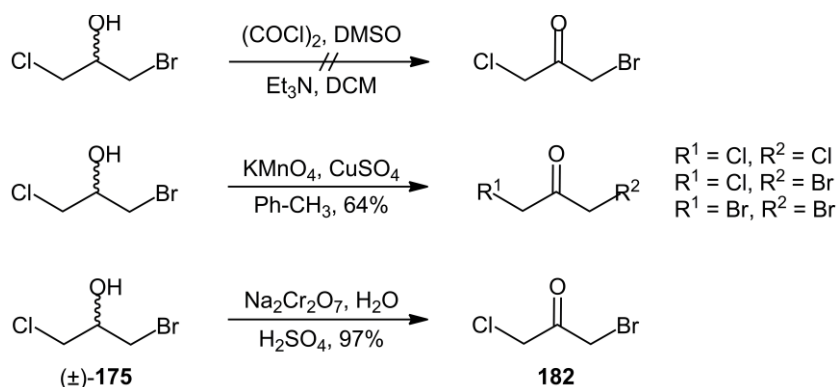


Scheme 2.12: Attempted Williamson reaction between *rac*-cyclohexane-1,2-diol (**160**) and *bis*-halogenated chain (\pm) -**176**, leading to dehydrohalogenation to give compound (\pm) -**181**.

2.2.5 – Attempts at Williamson Cyclisation with Alternative Reagents

To reduce complications associated with an elimination reaction, a *bis*-halogenated propane chain with a quaternary central carbon atom was essential. Any propane chain that fitted this requirement would still require the ability to be deprotected to reveal an oxygenated moiety. One of the simplest reagents for such a reaction would be the unprotected carbonyl compound 1-bromo-3-chloropropan-2-one (**182**). Such a synthetic methodology would be analogous to that described by Gaudin *et al.*,^[12] although their methodology instead made use of the *bis*-chlorinated analogue of compound **182**.

The oxidation conditions first chosen for testing was a Swern oxidation. This protocol was selected due to the mild nature of the reaction alongside its high tolerance for various functional groups. The reaction involves the generation of a dimethylchlorosulphonium ion by the action of oxalyl chloride on dimethylsulphoxide, followed by dropwise addition of the hydroxyl compound to this mixture.^[65] This reaction protocol was trialled but was disappointingly discovered to return only unreacted starting material (Scheme 2.13).



Scheme 2.13: Various oxidation conditions attempted for the synthesis of **182** from (±)-**175**.

The following set of reaction conditions used for experimentation was a potassium permanganate (KMnO_4) and copper sulphate pentahydrate ($\text{CuSO}_4 \cdot 5\text{H}_2\text{O}$) oxidation system.^[66] The reaction conditions suggest that a 2:1 w/w mixture of KMnO_4 and $\text{CuSO}_4 \cdot 5\text{H}_2\text{O}$, respectively, were to be ground together and added to an aromatic hydrocarbon solution of the alcohol, followed by monitoring the reaction at reflux for several hours. The role of the $\text{CuSO}_4 \cdot 5\text{H}_2\text{O}$ within the chemical reaction is not completely understood but it is hypothesised to be participating in an electron transfer process or acting as a source of water.^[67] What is understood is that in contrast to usual permanganate reactivity, this solid-support

mixture does not chemically react with alkenes, or have the same complications involving over-oxidation and therefore the $\text{CuSO}_4 \cdot 5\text{H}_2\text{O}$ can be considered to moderate the oxidation power of the permanganate ion.^{[68],[69]}

The reaction conditions were found to successfully yield an oil in a 64% crude yield (Scheme 2.13). Upon further investigation however, it was discovered that the product of the oxidation was not pure. Analysis by GC-MS revealed that the reaction product contained two impurities, one less volatile and one more volatile than the target compound **182** (Figure 2.24). It was discovered by GC-MS library match,^[70] as well as by ^{13}C NMR correlation to the Spectral Database for Organic Compounds (SDBS)^[71] that the two impurities were the *bis*-chlorinated analogue (4.042 minutes) and the *bis*-brominated analogue (6.058 minutes) of the target compound. Attempts at purification by fractional distillation under vacuum revealed that the three compounds successfully azeotrope. Repeated recrystallisations were discovered to be only moderately successful in bringing the purity of the target compound higher.

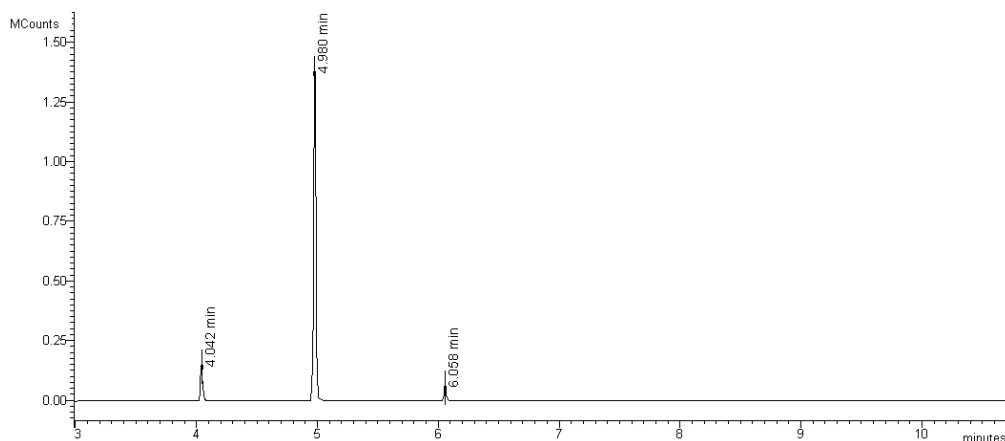
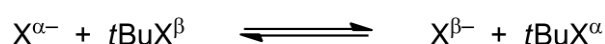


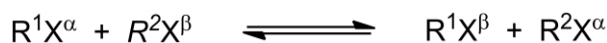
Figure 2.24: GC-MS chromatograph of the permanganate oxidation of (\pm)-**175** to **182**, showing halogen exchange. 4.042 minutes: 1,3-dichloropropan-2-one; 4.980 minutes: 1-bromo-3-chloropropan-2-one (**182**); 6.058 minutes: 1,3-dibromopropan-2-one.

The exchange of halogen atoms between alkyl halides has been previously reported in published literature and is the basis of a chemical reaction known as the Finkelstein reaction, whereby an alkyl fluoride, chloride or bromide is transformed into an alkyl iodide by treatment with sodium iodide. This reaction is an equilibrium that can be driven forward by the exploitation of halide salt solubilities or by the use of large excesses of the halide salt reagent. An adaptation of this reaction is used to substitute various aryl halide compounds to give alkyl fluoride compounds by the use of potassium fluoride in polar aprotic solvents at high temperatures.^[72]

Much research has been undertaken to understand the mechanism by which such reactions can occur.^[73-76] Initial studies into the exchange reaction between *tertiary*-butyl halides and soluble sources of an alternative halide ion hypothesised that the exchange was occurring predominantly by an SN2 mechanism.^[73] Later studies confirmed that exchange can occur by the elimination of a hydrogen halide (HX) followed by addition of a different hydrogen halide (HX) to give an exchanged halide compound; an E2 mechanism.^[74] A later study by Cook and Parker confirmed that an SN2 mechanism can also occur by experiments between halide ions and neopentyl halides, which cannot undergo an elimination reaction.^[75] Halogen exchange reactions have also been reported by the reaction of alkyl halides and the various acidic hydrogen halides such as HCl, HBr and HI.^[77] These classes of halide exchange reaction take the form of:

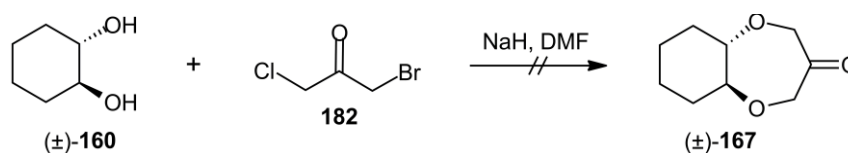


Halogen distribution reactions between alkyl halide compounds without the use of soluble alternative halides have been reported using an aluminium halide as a catalyst,^[78-79] as well as a variety of quaternary ammonium and phosphonium halide salt catalysts.^[80-81] The reaction has also been reported to occur in the gas phase by the passage of alkyl halides through a column filled with alumina coated in a phosphonium salt.^[82] This class of halide exchange reactions takes the form of:



The undesired halogen exchange reaction of compounds **175/182** could therefore be occurring by a number of different mechanisms, although an E2 mechanism is believed to be most plausible. It was hypothesised that to eliminate the undesired halogen exchange a much milder set of reaction conditions were mandatory. The reaction conditions investigated involved the use of sodium dichromate as an oxidation reagent.^[83] The reaction is a variation of the Jones oxidation and is conducted in water and the reaction held at room temperature.^[84] The mechanism involves the *in situ* generation of the strong oxidant chromic acid by the action of sulphuric acid on sodium dichromate. The oxidation conditions were discovered to successfully yield the target compound **182** in near quantitative yield, with no observable halogen exchange.

Etherification reactions performed between *rac*-cyclohexane-1,2-diol (**160**) and 1-bromo-3-chloropropan-2-one (**182**) were discovered to provide only polymerised material (Scheme 2.14). This was assumed to be due to the alkoxide intermediate having too strongly basic a character and thereby removing an acidic α -hydrogen from **182** leading to intermolecular polymerisation, presumably by an aldol-type mechanism. It is likely that the same complications were not discovered in the aromatic system owing to the decreased basicity of the phenoxide intermediate in comparison to the aliphatic alkoxide intermediate.

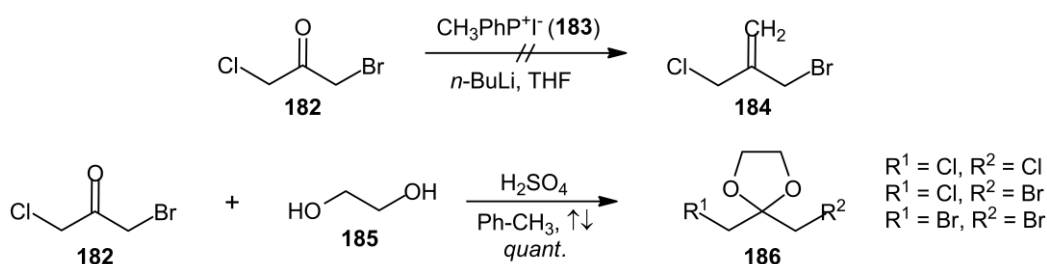


Scheme 2.14: Failed Williamson reaction between *rac*-cyclohexane-1,2-diol (**160**) and *bis*-halogenated chain **182**.

Owing to the strongly electron-withdrawing nature of the carbonyl moiety it was clear that protection would be necessary. The first option for such protection was the conversion of the carbonyl moiety to a methylene moiety. Any isolated methylene intermediate compound could be oxidised to the carbonyl analogue by the action of several different oxidants, such as O_3 , $OsO_4/NaIO_4$ or RuO_4 . This sequence would be analogous to multiple synthetic pathways previously employed in the synthesis of the aromatic benzo[*b*][1,4]dioxepin-3-one scaffold.^[6, 26, 29]

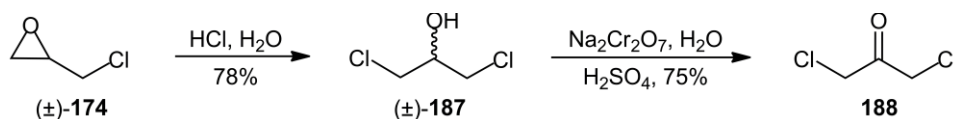
Methyltriphenylphosphonium iodide (**183**) was prepared from methyl iodide and triphenylphosphine in 86% yield according to the methodology of McGeary *et al.*^[85] A chemical reaction was then trialled between compound **182** and methylenetriphenylphosphorane, generated *in situ* by the action of *n*-butyllithium on phosphonium salt **183**, but was discovered to give only to polymerised material (Scheme 2.15).

The next protecting group experimented with was a cyclic ketal, the 1,3-dioxolane. 1,3-Dioxolanes are readily prepared from carbonyl compounds using 1,2-ethanediol (**185**) by dehydration in the presence of an acid-catalyst. The ketalisation reaction requires the use of a Dean-Stark apparatus to aid in the removal of water formed within the reaction, thus driving the equilibrium forward towards completion. The organic acid, *para*-toluenesulphonic acid, was discovered not to be a strong enough catalyst owing to starting material being recovered from the reaction. A change of catalyst to the strong mineral acid sulphuric acid yielded the desired product, although it was discovered that halogen exchange had once again occurred (Scheme 2.15).



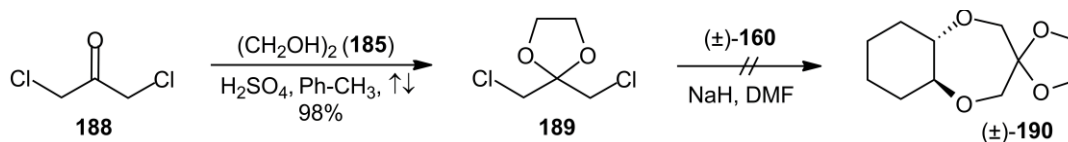
Scheme 2.15: Above: Failed Wittig reaction between *bis*-halogenated chain **182** and methyltriphenylphosphonium iodide (**183**); Below: Attempted ketalisation of *bis*-halogenated chain **182** with 1,2-ethanediol (**185**) leading to a mixed product due to halide exchange.

To eliminate any difficulties experienced with halide exchange the symmetrical *bis*-chlorinated analogue **188** was synthesised (Scheme 2.16). The synthetic pathway employed in the synthesis of compound **188** was identical to the synthetic pathway outlined for compound **182**, except that hydrochloric acid was used in place of hydrobromic acid during the initial oxirane ring-opening reaction sequence. Ketalisation of compound **188** with 1,2-ethanediol (**185**) was performed and was found to successfully yield the target cyclic ketal **189** as a clear oil in 98% yield (Scheme 2.17).



Scheme 2.16: Synthesis of *bis*-chlorinated chain **188** from (±)-epichlorohydrin (**174**).

Unreacted starting materials were recovered when Williamson reactions between *rac*-cyclohexane-1,2-diol (**160**) and dioxolane **189** were attempted (Scheme 2.17). Additional Williamson reactions were conducted at 100 °C on the assumption that any reactivity problems may be associated with steric hindrance, but no reaction was observed. It appeared that ketalisation of the carbonyl moiety had rendered the halogenated propane chain unreactive to Williamson cyclisation reactivity.

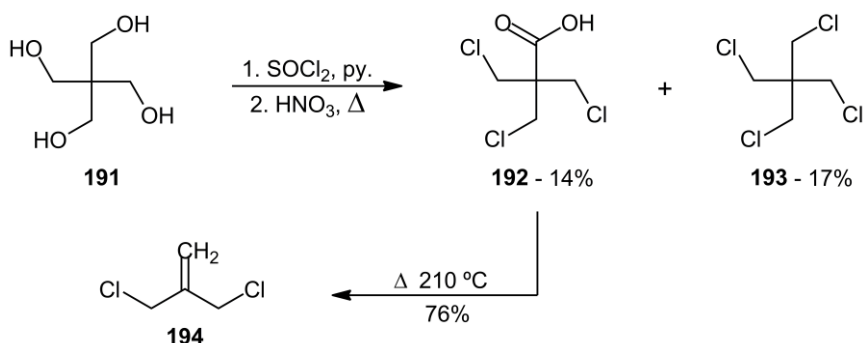


Scheme 2.17: Ketalisation of *bis*-chlorinated chain **188** to give dioxolane **189**, and the subsequent failed reaction with *rac*-cyclohexane-1,2-diol (**160**).

2.2.6 – Williamson Cyclisation with 3-Chloro-2-(chloromethyl)prop-1-ene

A publication by Kraft *et al.*^[6] detailed the synthesis of a library of benzo[*b*][1,4]dioxepin-3-one analogues for olfactory evaluation by a Williamson cyclisation reaction between various catechol derivatives and 3-chloro-2-(chloromethyl)prop-1-ene (**194**). Experimental work was first undertaken to synthesise the *bis*-chlorinated chain **194** beginning from pentaerythritol (**191**) according to the methodology of Lynch and Dailey.^[86] The synthetic sequence involved the chlorination of pentaerythritol (**191**) with thionyl chloride in pyridine to yield a mixture of trichloride and tetrachloride isomers. Without purification, the crude mixture of chlorides was oxidised in hot nitric acid to yield a mixture of 3-chloro-2,2-bis(chloromethyl)propanoic acid (**192**) and 1,3-dichloro-2,2-bis(chloromethyl)propane (**193**) (Scheme 2.18).^[86-87] Unreacted tetrachloride **193** was readily separated from carboxylic acid **192** by an acid-base extraction owing to the formation of the carboxylate salt of compound **192**, thereby making this compound water soluble.

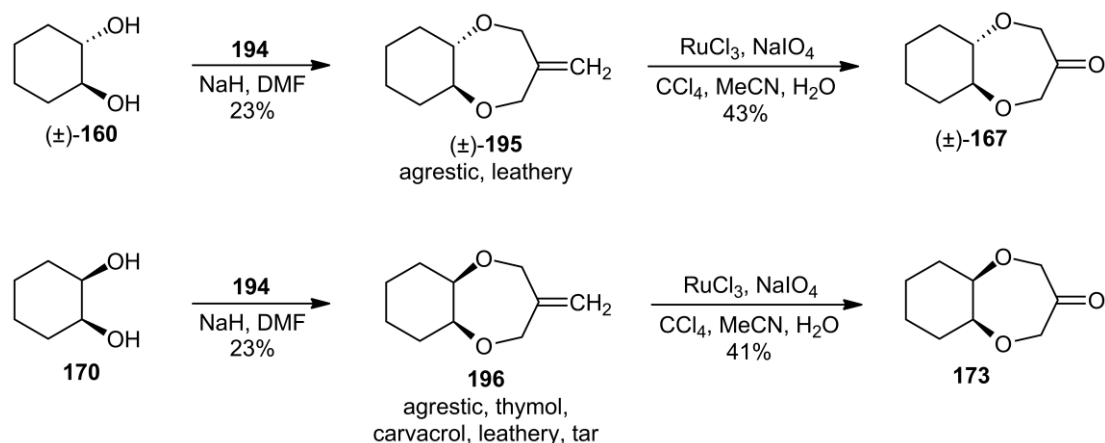
The isolated carboxylic acid compound **192** was destructively distilled by retaining a reaction vessel at 210 °C connected to a short-path distillation setup to distil 3-chloro-2-(chloromethyl)prop-1-ene (**194**) as a clear liquid. The formation of **194** occurs via the decarboxylation and elimination of compound **192**. To remove traces of hydrochloric acid it was discovered that compound **194** needed to be redistilled from calcium hydride.



Scheme 2.18: Synthesis of *bis*-chlorinated chain **194** from pentaerythritol (**191**).

Experimental Williamson reactions were conducted between *rac*-cyclohexane-1,2-diol (**160**) and 3-chloro-2-(chloromethyl)prop-1-ene (**194**) in dimethylformamide using sodium hydride as a base (Scheme 2.19). The reaction successfully yielded the cyclised methylene intermediate compound (±)-**195** in 23% yield. Additionally, the reaction was discovered to give a cleaner crude reaction mixture than etherification with ethyl diazoacetate (**165**) thereby making isolation of the target material simpler. An analogous reaction between *meso*-cyclohexane-1,2-diol (**170**) and 3-chloro-2-(chloromethyl)prop-1-ene (**194**) was then conducted and was discovered to also successfully give a cyclised intermediate (**196**) in 23% yield (Scheme 2.19).

Importantly, cyclisation reaction yields between the *threo*- and *erythro*-configured analogues were comparable. It was discovered that the two methylene intermediate compounds also displayed interesting olfactory characteristics which were described by perfumers as ‘agrestic and leathery’ and ‘agrestic, thymol, carvacrol, leathery tar’ by analysis on blotter, for the *threo*-configured isomer (±)-**195** and *erythro*-configured isomer **196**, respectively (Scheme 2.19).



Scheme 2.19: Williamson reaction of both stereoisomers of cyclohexane-1,2-diol with *bis*-chlorinated chain **194** followed by oxidation to the aliphatic benzo[*b*][1,4]dioxepin-3-one.

The reaction mechanism for the Williamson cyclisation reaction initiates when the aliphatic *bis*-hydroxyl compound reacts with sodium hydride with the release of hydrogen gas to create a *bis*-alkoxide intermediate, stabilised by sodium cations (Figure 2.25). The reaction occurs at the surface of the sodium hydride as this reagent remains non-soluble in organic solvents, consistent with the fact that the hydrogen anion remains an unknown anion in solution. The *bis*-alkoxide intermediate nucleophilically attacks a chlorinated 1° carbon of the *bis*-chlorinated chain which results in the electronegative chlorine atom leaving as an anion and ultimately forming the neutral ionic species sodium chloride. This reaction leads to an intermediate compound which is then intramolecularly cyclised by nucleophilic attack of the remaining alkoxide anion onto the remaining chlorinated 1° carbon atom, finally yielding the cyclised target compound.

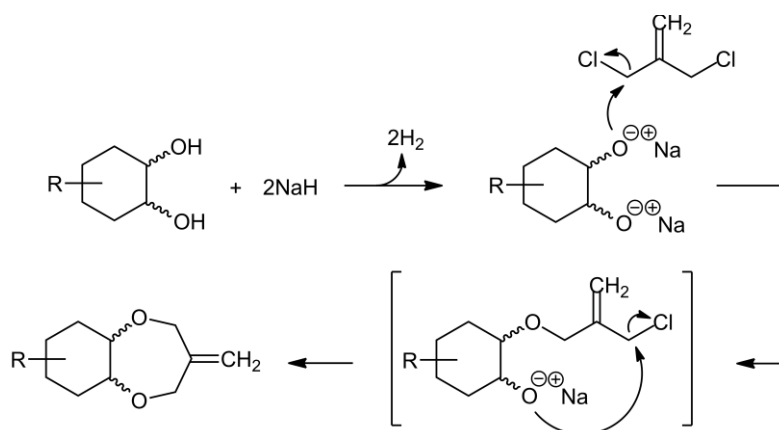


Figure 2.25: Reaction mechanism for the Williamson reaction between substituted cyclohexane-1,2-diol analogues and 3-chloro-2-(chloromethyl)prop-1-ene.

The subsequent synthetic step within the reaction sequence involved the oxidation of the isolated methylene intermediate compound to the target compound. This reaction was achieved by a ruthenium tetroxide oxidation, analogous to the methodology applied by Kraft *et al.*^[6] The catalytic reaction required *in situ* generated ruthenium tetroxide, produced by the action of oxidant sodium metaperiodate on ruthenium chloride. Experiments suggested that two additions of both the ruthenium catalyst and the oxidant spaced up to a day apart were needed for the reaction to be successful, presumably due to complications arising from catalyst deactivation. It had also been discovered that the addition of acetonitrile leads to a greatly improved oxidation system due to its ability to return deactivated ruthenium carboxylate complexes back into the catalytic cycle.^[88] The mechanism begins within the aqueous phase when RuCl_3 reacts with the oxidant to become the solvent soluble species RuO_4 . The RuO_4 migrates into the non-polar phase, oxidises an organic molecule solubilised within before returning to the aqueous phase and thereby completing the catalytic cycle (Figure 2.26).^[89]

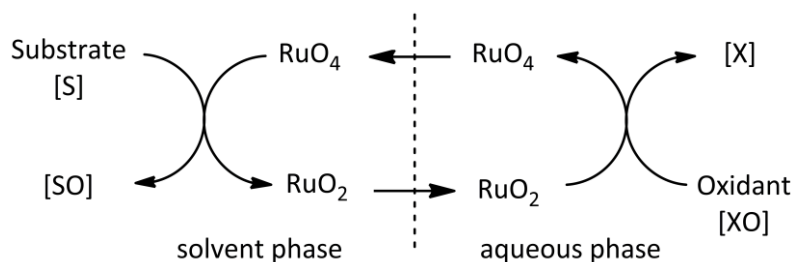


Figure 2.26: Catalytic cycle of a ruthenium tetroxide oxidation.^[89]

Ruthenium tetroxide oxidation reactions were attempted and were discovered to be successful in the oxidation of both stereoisomers of the saturated system. The reaction yields were again found to be comparable for the *threo*- and *erythro*-configured stereoisomers. The oxidation reaction was also found to be clean, yielding only the target compound and polymerised material which was readily separated by flash chromatography. NMR analysis unambiguously proved that the benzo[*b*][1,4]dioxepin-3-one compounds synthesised by both Dieckmann condensation and Williamson cyclisation methodologies were identical.

2.2.7 – Comparisons of Chemical and Olfactory Properties

Contrasts in ^1H NMR spectra between the unsubstituted aromatic benzo[*b*][1,4]dioxepin-3-one compound (**49**) and both stereoisomers of the aliphatic benzo[*b*][1,4]dioxepin-3-one molecule (compounds **167** and **173**) are delineated in Figure 2.27. Immediate dissimilarities between the aromatic and aliphatic analogue spectra include the addition of multiple proton signals from the now saturated carbocyclic ring atoms C–6, C–7, C–8 and C–9, accompanying the addition of proton signals from ring bridging atoms C–5a and C–9a. Proton signals originating from the carbocyclic ring have moved upfield from the aromatic region ($\sim \delta$ 7 ppm) to the aliphatic region ($\sim \delta$ 1–2 ppm), as was predicted owing to the addition shielding provided by the now localised electron orbitals.

Multiple dissimilarities in ^1H NMR spectra between the two stereoisomers of the aliphatic benzo[*b*][1,4]dioxepin-3-one scaffold were obvious even though both stereoisomers displayed full symmetry. Proton signals originating from ring bridging carbons C–5a and C–9a appeared further downfield for *erythro*-configured isomer **173** indicating less electron density in the ring bridging area for this stereoisomer.

The signals for the protons bonded to carbon atoms adjacent to the carbonyl moiety (C–2 and C–4) appeared as doublet signals ($J = 16.6/16.8$ Hz). This phenomenon is occurring due to the proton signals being split by the adjacent proton owing to subtle differences in chemical environment between the atoms relating to chirality, as this phenomenon was not observed for the achiral aromatic analogue **49**. Both stereoisomers gave rise to separate signals for each proton bonded to C–2 or C–4 but due to molecular symmetry only two doublet signals are revealed. It was also discovered that the two protons bonded to a single cyclohexyl ring carbon atom (C–6, C–7, C–8, C–9) gave rise to signals located in two different locations. This indicates that the axial and equatorial protons are in a different chemical environments and that conformational ring interconversion has been quenched due to a large energy barrier.

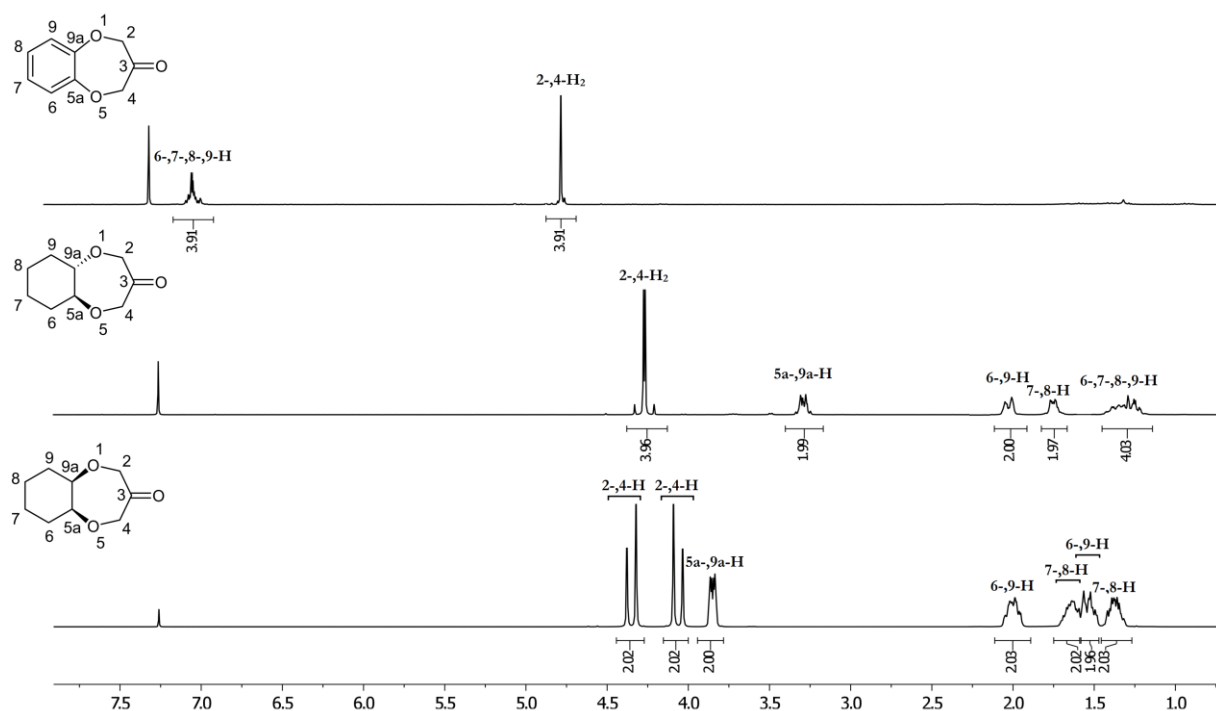


Figure 2.27: ^1H NMR (CDCl_3 , 300 MHz) spectra of the unsubstituted aromatic and aliphatic benzo[*b*][1,4]dioxepin-3-one analogues: (top) benzo[*b*][1,4]dioxepin-3-one (**49**); (middle) *rac*-hexahydrobenzo[*b*][1,4]dioxepin-3-one (**167**); (bottom) *meso*-hexahydrobenzo[*b*][1,4]dioxepin-3-one (**173**).

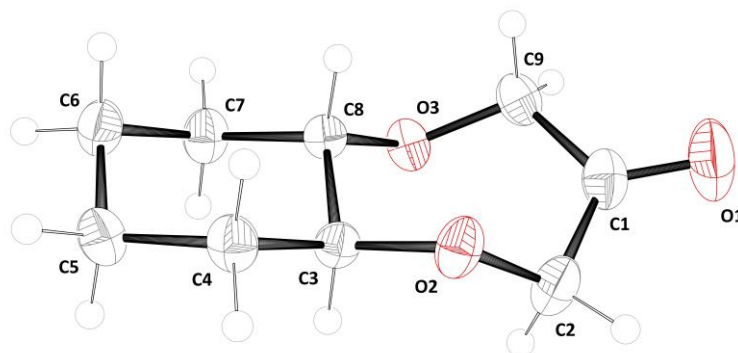


Figure 2.28: Molecular structure of *rac*-hexahydro-2*H*-benzo[*b*][1,4]dioxepin-3(4*H*)-one (**167**) showing thermal ellipsoids at a 50% probability level. Crystal data for **167**: $a = 6.7129(11)$ Å, $b = 17.188(3)$ Å, $c = 8.1744(12)$ Å, $\alpha = 90^\circ$ $\beta = 113.725(3)^\circ$ $\gamma = 90^\circ$ $V = 863.5(2)$ Å³, $Z = 4$, and space group $P\ 21/n$. Crystallographic data has been deposited with the Cambridge Crystallographic Data Centre as supplementary publication no. CCDC 968786.

An X-ray crystal structure of *threo*-configured analogue (\pm)-**167** was successfully obtained from the racemic mixture due to the compound crystallising in a space group containing a glide plane; the two enantiomers were mirrored in the unit cell and thus a structure could be successfully elucidated. The X-ray crystal structure showed that the cyclohexyl ring exists in chair conformation whilst the dioxepanone ring exists in pseudo-twist-boat conformation (Figure 2.28).

An X-ray crystal structure was also acquired for *erythro*-configured analogue **173** with considerable difficulty due to the compound having a melting point below room temperature (Figure 2.29). The crystals were chilled beforehand with liquid nitrogen to prevent melting whilst being selected and loaded into the XRD instrument. The bond lengths for C3–C8, C7–C8, O2–C3 and O3–C8 differ significantly between the two stereoisomers, with the *erythro*-configured analogue **173** having longer bond lengths in all cases. The bond angles in the region where the cyclohexyl ring intercepts the dioxepanone ring also differ significantly between the two stereoisomers.

The angle for C7–C8–O3 differs by $6.83(9)^\circ$ and the C8–O3–C9 angle by $2.84(9)^\circ$, with the *erythro*-configured analogue **173** once again having the larger value in each case. This phenomenon is probably due to repulsion between the hydrogen atoms on C7 and C9, with the shortest H–H distance being only 2.07 Å. This may indicate that the *erythro*-configured analogues are the more strained molecular structure and could also explain their instability and lower yields in comparison to the *threo*-configured analogues.

On examination of the molecular structures of the two stereoisomers it can be seen that both of the stereoisomeric dioxepanone rings are in pseudo-twist-boat conformation corresponding to that of the original benzo[*b*][1,4]dioxepin-3-one template. In place of the planar benzenoid ring the saturated derivatives possess six-membered cyclohexyl rings in chair conformation. The two rings exist in a relatively co-planar fashion in the *threo*-configured analogue (**167**), with the carbonyl group pointing only marginally out of the plane of the cyclohexyl ring. In the *erythro*-configured analogue (**173**) the carbonyl moiety is completely out of plane in relation to the six-membered ring.

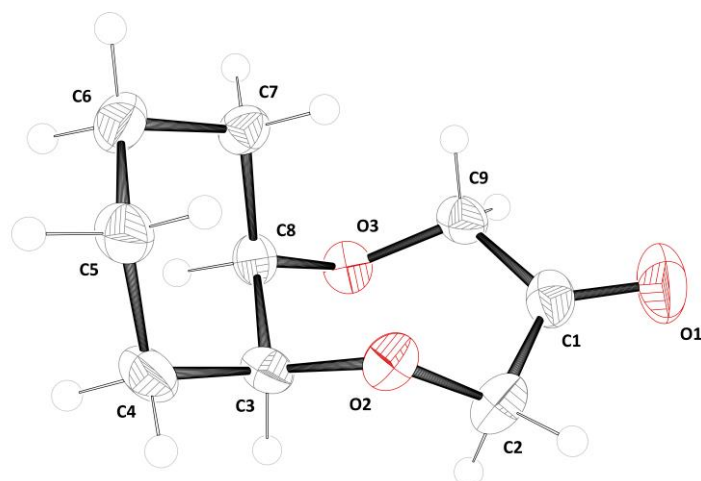


Figure 2.29: Molecular structure of *meso*-hexahydro-2*H*-benzo[*b*][1,4]dioxepin-3(4*H*)-one (**173**) showing thermal ellipsoids at a 50% probability level. Crystal data for **173**: $a = 21.883(3) \text{ \AA}$, $b = 9.2836(12) \text{ \AA}$, $c = 8.7905(14) \text{ \AA}$, $\alpha = 90^\circ$ $\beta = 104.695(11)^\circ$ $\gamma = 90^\circ$ $V = 1727.4(4) \text{ \AA}^3$, $Z = 8$, and space group $C 2/c$. Crystallographic data has been deposited with the Cambridge Crystallographic Data Centre as supplementary publication no. CCDC 968784.

Olfactory evaluations were performed by expert perfumers by blotter analysis with a 10% solution of the sample substance in dipropylene glycol (DPG). The odour threshold values were determined by GC-Olfactometry (GC-O). Any differences in olfactory properties between the two isomers can be ascribed to differences in molecular shape. It was also suspected that due to the non-planar nature of the *erythro*-configured analogue **173** there may be physical difficulty in the molecule making optimal receptor binding. The *threo*-configured analogue **167** was found to have a medicinal, fruity odour with additional sweet facets, and an odour threshold of 210 ng/L air (Table 2.2).

The *erythro*-configured analogue (**173**) was the more potent analogue of the two, having an odour threshold of 141 ng/L air and a rather different odorant profile which was best described as a fruity, animalic odour of green tonality with chemical and acidic aspects upon drying down. Neither isomer was found to contain marine odour notes (Table 2.2). Comparisons with the previously reported olfactory properties for the unsubstituted benzo[*b*][1,4]dioxepin-3-one compound (**49**) revealed strong evidence that even the aromatic scaffold fails to display potent marine fragrance notes without seven-alkyl substitution. The perfumers employed by Hgel *et al.*^[10] and Gaudin *et al.*^[12] disagreed on the exact olfactory properties of **49**, possibly due to natural variation in olfactory perception amongst a

given population, although did agree on a number of key aspects such as green notes and weak marine nuances (Table 2.2). Odour threshold data for compound **49** appears, to the best of the author's knowledge, to have never been measured and/or reported.

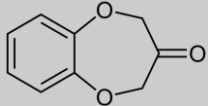
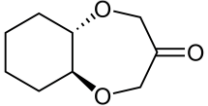
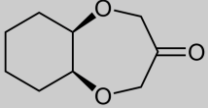
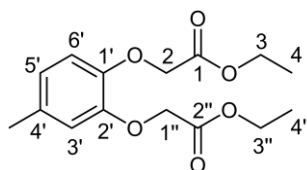
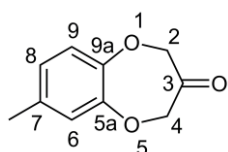
#	Molecular Structure	Description and Threshold
49		<p>Odour description: Metallic, ozone, watery, cabbage, hot iron, more metallic-phenolic, less ozony and much weaker than Calone 1951[®].^[12]</p> <p>Odour description: Green-floral, balsamic odour in the direction of Peru and Tolu balsam resinoid, slight marine salty aspect.^[10]</p>
(±)-167		<p>Odour description: Medicinal, fruity odour that is linear in the dry-down with additional sweet facets in the fond.</p> <p>Odour threshold 210 ng/L air (stan. dev. 176 ng/L air).</p>
173		<p>Odour description: Fruity, animalic odour of green tonality with chemical aspects and acidic facets in the dry-down.</p> <p>Odour threshold: 141 ng/L air (stan. dev. 99 ng/L air).</p>

Table 2.2: Olfactory properties of compounds **49**, **(±)-167** & **173**.

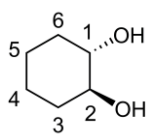
2.3 – Experimental

Diethyl 2,2'-((4-methyl-1,2-phenylene)bis(oxy))diacetate (157):^[10]

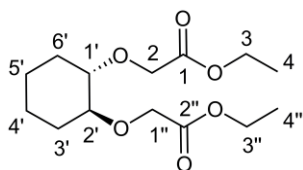
To a solution of 4-methylcatechol (3 g, 24.17 mmol) and ethyl bromoacetate (16.12 g, 96.67 mmol, 4 equiv) in DMF (150 mL) was added K_2CO_3 (13.36 g, 96.67 mmol) and the mixture heated to 120 °C for 2 h. The reaction mixture was then poured into H_2O (300 mL) and extracted with Et_2O (3 x 100 mL). The organic extracts were pooled, washed with H_2O (100 mL) and saturated $NaHCO_3$ (100 mL), dried ($MgSO_4$) and concentrated under reduced pressure. The resulting residue was then purified by flash chromatography on silica gel ($EtOAc$ /hexane; 2:8) to give diethyl 2,2'-((4-methyl-1,2-phenylene)bis(oxy))diacetate (3.76 g, 53%) as a clear oil. IR (ATR): $\tilde{\nu} = 1754/1733$ (ν ester C=O), 1509 (ν aromatic C=C), 1193 (ν C–O) cm^{-1} . 1H NMR ($CDCl_3$, 300 MHz): δ 6.83–6.70 (m, 3H, 3',-5'-6'-H), 4.70/4.68 (2s, 4H, 2,-1''-H₂), 4.31–4.21 (m, 4H, 3-,3''-H₂), 2.27 (s, 3H, 4'-Me), 1.33–1.26 (m, 6H, 4-,4''-H₃). ^{13}C NMR ($CDCl_3$, 75 MHz): δ 168.7/168.5 (2s, C-1,-2''), 147.4/145.5 (2s, C-1',-2'), 131.9 (s, C-4'), 122.3/116.1/115.5 (3s, C-3',-5',-6'), 66.6/66.2 (2t, C-2,-1''), 60.6/60.6 (2t, C-3,-3'') 20.3 (q, 4'-Me), 13.6/13.6 (2q, C-4,-4''). HRMS: m/z calculated for $C_{15}H_{20}O_6$: 296.1259 $[M]^+$; Found: 296.1259.

7-Methyl-2H-benzo[*b*][1,4]dioxepin-3(4H)-one (50):^[10]

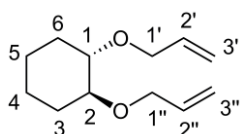
A solution of diethyl 2,2'-((4-methyl-1,2-phenylene)bis(oxy))diacetate (3.73 g, 12.59 mmol) in THF (50 mL) was added dropwise to a stirred suspension of $KOtBu$ (2.82 g, 25.18 mmol) in THF (50 mL) with cooling to 0 °C. Stirring was continued at 0 °C for 2 h before being quenched by the addition of 0.2 M HCl (300 mL) and ice (300 g). The resulting solution was then extracted with DCM (3 x 200 mL), the organic extracts pooled, dried ($MgSO_4$) and concentrated under reduced pressure. The residue was taken up in $EtOH$ (30 mL) and 2 M HCl (150 mL) and the mixture stirred at reflux for 2 h. The solution was diluted with H_2O (100 mL) and extracted with DCM (3 x 200 mL). The organic extracts were pooled, washed with H_2O (100 mL), dried ($MgSO_4$) and concentrated under reduced pressure. The resulting residue was purified by vacuum distillation (100 °C, 0.1 torr) to yield 7-methyl-2H-benzo[*b*][1,4]dioxepin-3(4H)-one (1.19 g, 53%) as a colourless solid. mp: 36–38 °C. (lit. mp: 38–39 °C (pentane)).^[10] IR (ATR): $\tilde{\nu} = 1732$ (ν C=O), 1503 (ν aromatic C=C) cm^{-1} . 1H NMR ($CDCl_3$, 300 MHz): δ 6.92–6.75 (m, 3H, 6-,8-,9-H), 4.71/4.69 (2s, 4H, 2-,4-H₂), 2.28 (s, 3H, 7-Me). ^{13}C NMR ($CDCl_3$, 75 MHz): δ 204.8 (s, C-3), 147.9/146.0 (2s, C-5a,-9a), 133.7 (s, C-7), 124.3/121.1/120.6 (3d, C-6,-8,-9), 75.7/75.4 (2t, C-2,-4), 20.5 (q, 7-Me). HRMS: m/z calculated for $C_{10}H_{10}O_3$: 178.0630 $[M]^+$; Found: 178.0628.

***rac*-Cyclohexane-1,2-diol (160):^[50]**


A 30% solution of hydrogen peroxide (50 mL, 0.5 mol) was added to an 80% solution of formic acid (238 mL, 4.89 mol). To this solution was added cyclohexene (29.28 g, 0.36 mol) dropwise over a period of 0.5 h. The reaction mixture was retained at 40 °C for 1 h and then allowed to stand at RT overnight. The mixture was then concentrated under reduced pressure before an ice-cold solution of sodium hydroxide (28.8 g, 0.72 mmol) in H₂O (55 mL) was added dropwise. The reaction mixture was then extracted with EtOAc (6 x 100 mL), the organic extracts pooled, dried (MgSO₄) and concentrated under reduced pressure. The resulting residue was recrystallised from EtOAc to give *rac*-cyclohexane-1,2-diol (16.3 g, 39%) as a colourless solid. mp: 102–104 °C. (lit. mp: 101.5–103 °C).^[50] IR (ATR): $\tilde{\nu}$ = 3357/3262 (ν O–H), 2932 (ν C–H) cm⁻¹. ¹H NMR (CDCl₃, 300 MHz): δ 3.40–3.29 (m, 2H, 1-,2-H), 3.17–3.10 (s, 2H, 1-,2-OH), 2.02–1.90 (m, 2H, 3-,6-H), 1.76–1.63 (m, 2H, 4-,5-H), 1.35–1.17 (m, 4H, 3-,4-,5-,6-H). ¹³C NMR (CDCl₃, 75 MHz): δ 75.6 (2d, C-1,-2), 32.8 (2t, C-3,-6), 24.3 (2t, C-4,-5). HRMS: *m/z* calculated for C₆H₁₂O₂: 116.0837 [M]⁺; Found: 116.0826.

***rac*-Diethyl 2,2'-(cyclohexane-1,2-diylbis(oxy))diacetate (161):^[52]**


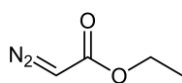
To an ice-cool solution of ethyl diazoacetate (10.91 g, 10.05 mL, 95.6 mmol) and *rac*-cyclohexane-1,2-diol (5 g, 43 mmol) in DCM (70 mL) was added dropwise BF₃·OEt₂ (0.5 mL). After addition was complete, stirring was continued at RT for 1 h followed by heating at reflux for 1 h. The reaction was allowed to cool to RT before being quenched by the addition of a saturated aqueous solution of NaHCO₃ (100 mL). The mixture was then extracted with EtOAc (3 x 100 mL), the organic extracts pooled, dried (MgSO₄) and concentrated under reduced pressure. The resulting residue was purified by flash chromatography on silica gel (EtOAc/hexane; 2:8) to yield *rac*-diethyl 2,2'-(cyclohexane-1,2-diylbis(oxy))diacetate (4.35 g, 35%) as a yellow oil. IR (ATR): $\tilde{\nu}$ = 2934 (ν C–H), 1750 (ν ester C=O), 1198 (ν ester C–O), 1120 (ν C–O) cm⁻¹. ¹H NMR (CDCl₃, 300 MHz): δ 4.33–4.16 (m, 8H, 2-,3-,1'',-3''-H₂), 3.37–3.27 (m, 2H, 1',-2'-H), 2.12–2.04 (m, 2H, 3',-6'-H), 1.72–1.65 (m, 2H, 4',-5'-H), 1.39–1.15 (m, 4H, 3',-4',-5',-6'-H), 1.28 (t, *J* = 7.1 Hz, 6H, 4-,4''-H₃). ¹³C NMR (CDCl₃, 75 MHz): δ 170.2 (2s, C-1,-2''), 82.2 (2d, C-1',-2'), 67.2 (2t, C-2,-1''), 59.8 (2t, C-3,-3''), 29.6 (2t, C-3',-6'), 22.9 (2t, C-4',-5'), 13.5 (2q, C-4,-4''). HRMS: *m/z* calculated for C₁₄H₂₄O₆: 288.1573 [M]⁺; Found: 288.1591.

***rac*-1,2-Bis(allyloxy)cyclohexane (163):^[51]**


rac-Cyclohexane-1,2-diol (500 mg, 4.3 mmol) in DMF (10 mL) was added dropwise to a solution of sodium hydride (520 mg, 12.9 mmol, 60% in mineral oil, 3 equiv) in DMF (5 mL) at 0 °C. After stirring for 1 h at 0 °C, allyl bromide (2.6 g, 21.5 mmol) was added dropwise and the resulting solution allowed to warm to RT and stirred overnight. The solution was quenched by the careful addition of H₂O (100 mL) and extracted with Et₂O (3 x 100 mL). The organic extracts were pooled and dried

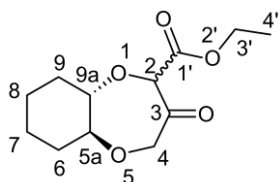
(MgSO₄) before being concentrated under reduced pressure. The resulting residue was purified by flash chromatography on silica gel (EtOAc/hexane; 3:97) to give *rac*-1,2-bis(allyloxy)cyclohexane (610 mg, 72%) as a clear oil. IR (ATR): $\tilde{\nu}$ = 2993/2860 (ν C–H), 1080 (ν C–O), 916 (ν C=C) cm⁻¹. ¹H NMR (CDCl₃, 300 MHz): δ 6.01–5.88 (m, 2H, 2',-2''-H), 5.33-5.30/5.27-5.24/5.17-5.15/5.13-5.11 (4m, 4H, 3',-3''-H₂), 4.16–4.12 (m, 4H, 1',-1''-H₂), 3.30–3.20 (m, 2H, 1-,2-H), 2.03–1.93 (m, 2H, 3-,6-H), 1.70–1.60 (m, 2H, 4-,5-H), 1.36–1.15 (m, 4H, 3-,4-,5-,6-H). ¹³C NMR (CDCl₃, 75 MHz): δ 135.4 (2d, C-2',-2''), 115.5 (2t, C-3',-3''), 80.3 (2d, C-1-,2-), 70.5 (2t, C-1',-1''), 29.9 (2t, C-3-,6-), 23.1 (2t, C-4-,5-).

Ethyl diazoacetate (165):^[54]

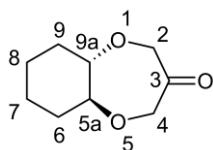


A solution of ethyl glycinate hydrochloride (140 g, 1 mol) in H₂O (250 mL) was mixed with DCM (600 mL) and cooled to –5 °C. A chilled solution of sodium nitrite (83 g) in H₂O (250 mL) was added with stirring. The temperature was lowered to –9 °C and 5% H₂SO₄ (96 g) was added by dropping funnel over a period of five minutes. The reaction mixture was then transferred to a separatory funnel and the organic layer ran into a 5% NaHCO₃ solution (1 L). The organic phase and NaHCO₃ solution was then transferred back to the separatory funnel and shaken until no trace of acid remained. The organic phase was collected, dried (MgSO₄) and concentrated under reduced pressure to give ethyl diazoacetate (96 g, 84%) as a yellow oil. IR (film): $\tilde{\nu}$ = 2985 (ν C–H), 2111 (N=N), 1693 (C=O) cm⁻¹.

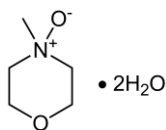
rac-Ethyl 3-oxooctahydro-2*H*-benzo[*b*][1,4]dioxepine-2-carboxylate (166):



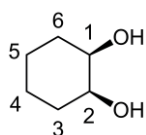
A solution of *rac*-diethyl 2,2'-(cyclohexane-1,2-diylbis(oxy))diacetate (10 g, 34.68 mmol) in THF (150 mL) was added dropwise to a stirred solution of KO^tBu (7.78 g, 69.36 mmol) in THF (150 mL) with cooling to 0 °C. Stirring was continued at 0 °C for 2 h before being quenched by the addition of 0.2 M HCl (1 L) and ice (500 g). The resulting solution was then extracted with DCM (3 x 200 mL), the organic extracts pooled, dried (MgSO₄) and concentrated under reduced pressure. The resulting residue was purified by flash chromatography on silica gel (EtOAc/hexane; 15:85) to give *rac*-ethyl 3-oxooctahydro-2*H*-benzo[*b*][1,4]dioxepine-2-carboxylate (2.6 g, 31%) as colourless crystals. mp: 78–80 °C. IR (ATR): $\tilde{\nu}$ = 2928 (ν C–H), 1748 (ν ester C=O), 1721 (ν C=O), 1100 (ν C–O) cm⁻¹. ¹H NMR (CDCl₃, 300 MHz): δ 4.98 (s, 1H, 2-H), 4.44–4.27 (m, 4H, 4-,3'-H₂), 3.49–3.41/3.33–3.25 (2m, 2H, 5a-,9a-H), 2.18–2.00 (m, 2H, 6-,9-H), 1.80–1.71 (m, 2H, 7-,8-H), 1.32 (t, *J* = 7.1 Hz, 3H, 4'-H₃) 1.55–1.21 (m, 4H, 6-,7-,8-,9-H). ¹³C NMR (CDCl₃, 75 MHz): δ 205.6 (s, C-3), 167.0 (s, C-1'), 88.2/88.0 (2d, C-5a,-9a), 83.8 (d, C-2), 76.7 (t, C-4), 61.6 (t, C-3'), 31.4/31.2 (2t, C-6,-9), 24.0/24.0 (2t, C-7,-8), 14.1 (q, C-4'). HRMS: *m/z* calculated for C₁₂H₁₈O₅: 242.1154 [M]⁺; Found: 242.1177.

***rac*-Hexahydro-2*H*-benzo[*b*][1,4]dioxepin-3(4*H*)-one (167):**


To a solution of *rac*-ethyl 3-oxooctahydro-2*H*-benzo[*b*][1,4]dioxepine-2-carboxylate (800 mg, 3.3 mmol) in EtOH (8 mL) was added 2 M HCl (40 mL) and the solution stirred at reflux for 2 h. After cooling to RT the solution was diluted with H₂O (100 mL) and extracted with DCM (3 x 50 mL). The organic extracts were pooled, washed with H₂O (50 mL), dried (MgSO₄) and concentrated under reduced pressure. The resulting residue was purified by flash chromatography on silica gel (EtOAc/hexane; 1:9) to give *rac*-hexahydro-2*H*-benzo[*b*][1,4]dioxepin-3(4*H*)-one (490 mg, 87%) as clear prisms. mp: 48–50 °C. IR (ATR): $\tilde{\nu}$ = 2939 (ν C–H), 1721 (ν C=O), 1116 (ν C–O) cm⁻¹. ¹H NMR (CDCl₃, 300 MHz): δ 4.31 (d, *J* = 16.6 Hz, 2H, 2-,4-H), 4.25 (d, *J* = 16.6 Hz, 2H, 2-,4-H), 3.34–3.22 (m, 2H, 5a-,9a-H), 2.06–1.97 (m, 2H, 6-,9-H), 1.81–1.66 (m, 2H, 7-,8-H), 1.44–1.15 (m, 4H, 6-,7-,8-,9-H). ¹³C NMR (CDCl₃, 75 MHz): δ 211.6 (s, C-3), 88.4 (2d, C-5a,-9a), 77.1 (2t, C-2,-4), 31.4 (2t, C-6,-9), 24.0 (2t, C-7,-8). HRMS: *m/z* calculated for C₉H₁₄O₃: 170.0943 [M]⁺; Found: 170.0939. Odour description: Medicinal, fruity odour that is linear in the dry-down with additional sweet facets in the fond. Odour threshold: 210 ng/L air (stan. dev. 176 ng/L air).

***N*-Methylmorpholine *N*-oxide dihydrate (169):^[62]**


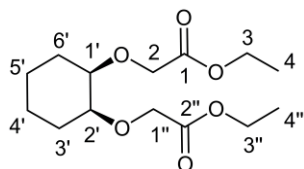
To neat *N*-methylmorpholine (32.3 g, 0.32 mol) heated to 75 °C was added dropwise a 30% aqueous solution of hydrogen peroxide (32.4 g, 0.29 mol) over a period of 2.5 h. The solution was then stirred for 20 h at 75 °C before a slurry of methanol (50 mL), charcoal (0.5 g) and celite (0.5 g) was added. After stirring for 1 h the mixture was filtered and concentrated under reduced pressure to a bath temperature of 95 °C. The resulting oil was then heated to reflux in acetone (25 mL) until a solution was formed, and then left overnight to crystallise. The crystals were filtered, washed with cold acetone and dried under vacuum to give *N*-methylmorpholine *N*-oxide dihydrate (27.17 g, 72%) as a grey solid. mp: 35 °C–onward. (lit. mp: 35–60 °C).^[62]

***meso*-Cyclohexane-1,2-diol (170):^[62]**


To a solution of *N*-methylmorpholine *N*-oxide (14.8 g, 126.3 mmol) in H₂O (20 mL) and acetone (40 mL) was added osmium tetroxide (70 mg, 0.27 mmol) and cyclohexene (8.18 g, 10.1 mL, 99.7 mmol). The solution was stirred at RT under nitrogen for 18 h before being quenched by the addition of a slurry of sodium hydrosulfite (0.5 g) and Florisil® (5 g) in H₂O (20 mL). The mixture was filtered through a pad of celite followed by the addition of 12 N H₂SO₄ (6.4 mL). The resulting solution was concentrated under reduced pressure to remove the organic solvent before being acidified to pH 2 with 12 N H₂SO₄. The resulting solution was extracted with *n*-butanol (5 x 50 mL), the organic extracts pooled and washed with aqueous NaCl (25 mL, 25% w/w solution). The organic solvent was concentrated under reduced pressure to yield a crude solid which was extracted with boiling diisopropylether (300 mL). The organic solvent was removed under reduced

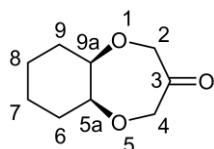
pressure and the residue recrystallised from diisopropylether to give *meso*-cyclohexane-1,2-diol (11.6 g, 82%) as a colourless solid. mp: 95–96 °C. (lit. mp: 96–97 °C).^[62] IR (ATR): $\tilde{\nu}$ = 3391/3258 (v O–H), 2929 (v C–C), 1073 (v C–O) cm^{-1} . ¹H NMR: (CDCl₃, 300 MHz): δ 3.81–3.76 (m, 2H, 1-,2-H), 1.92 (s, 2H, 1-,2-OH), 1.83–1.72 (m, 2H, 3-,6-H), 1.69–1.51 (m, 4H, 3-,4-,5-,6-H), 1.40–1.24 (m, 2H, 4-,5-H). ¹³C NMR: (CDCl₃, 75 MHz): δ 70.6 (2d, C-1,-2), 29.8 (2t, C-3,-6), 21.4 (2t, C-4,-5). HRMS: *m/z* calculated for C₆H₁₂O₂: 116.0837 [M]⁺; Found: 116.0826.

***meso*-Diethyl 2,2'-(cyclohexane-1,2-diylbis(oxy))diacetate (171):**



To an ice-cool solution of ethyl diazoacetate (10.91 g, 10.05 mL, 95.6 mmol) and *meso*-cyclohexane-1,2-diol (5 g, 43 mmol) in DCM (70 mL) was added dropwise BF₃·OEt₂ (0.5 mL). After addition was complete, stirring was continued at 0 °C for 1 h before being quenched by the addition of a saturated aqueous solution of NaHCO₃ (100 mL). The mixture was then extracted with EtOAc (3 x 100 mL), the organic extracts pooled, dried (MgSO₄) and concentrated under reduced pressure. The resulting residue was purified by flash chromatography on silica gel (EtOAc/hexane; 2:8) to give *meso*-diethyl 2,2'-(cyclohexane-1,2-diylbis(oxy))diacetate (3.41 g, 27%) as a yellow oil. IR (ATR): $\tilde{\nu}$ = 2936 (v C–H), 1750 (v ester C=O), 1194 (v ester C–O), 1114 (v C–O) cm^{-1} . ¹H NMR (CDCl₃, 300 MHz): δ 4.29–4.11 (m, 8H, 2-,3-,1'',3''-H₂), 3.69–3.64 (m, 2H, 1',2'-H), 2.00–1.87 (m, 2H, 3',6'-H), 1.74–1.60 (m, 2H, 4',5'-H), 1.59–1.47 (m, 2H, 3',6'-H), 1.35–1.20 (m, 2H, 4',5'-H), 1.28 (t, *J* = 7.1 Hz, 6H, 4-,4''-H₃). ¹³C NMR (CDCl₃, 75 MHz): δ 170.5 (2s, C-1,-2''), 77.9 (2d, C-1',-2'), 66.0 (2t, C-2,-1''), 60.0 (2t, C-3,-3''), 27.1 (2t, C-3',-6'), 21.4 (2t, C-4',-5'), 13.6 (2q, C-4,-4''). HRMS: *m/z* calculated for C₁₄H₂₄O₆: 288.1573 [M]⁺; Found: 288.1586.

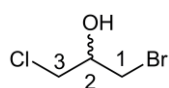
***meso*-Hexahydro-2*H*-benzo[*b*][1,4]dioxepin-3(4*H*)-one (173):**



A solution of *meso*-diethyl 2,2'-(cyclohexane-1,2-diylbis(oxy))diacetate (6.81 g, 23.61 mmol) in THF (220 mL) was added dropwise to a stirred solution of KO^tBu (5.29 g, 47.22 mmol) in THF (220 mL) with cooling to 0 °C. Stirring was continued at 0 °C for 2 h before being quenched by the addition of 0.2 M HCl (1.5 L) and ice (750 g). The resulting solution was extracted with DCM (4 x 300 mL), the organic extracts pooled, dried (MgSO₄) and concentrated under reduced pressure. The residue was taken up in EtOH (120 mL) and 2 M HCl (600 mL) and the mixture stirred at reflux for 2 h. After cooling to RT the solution was diluted with H₂O (300 mL) and extracted with DCM (3 x 300 mL). The combined organic extracts were washed with H₂O (300 mL), dried (MgSO₄) and concentrated under reduced pressure. The resulting residue was purified by flash chromatography on silica gel (EtOAc/hexane; 1:9) to give *meso*-hexahydro-2*H*-benzo[*b*][1,4]dioxepin-3(4*H*)-one (700 mg, 17%) as a clear oil. IR (ATR): $\tilde{\nu}$ = 2943 (v C–H), 1712 (v C=O), 1119 (v C–O) cm^{-1} . ¹H NMR (CDCl₃, 300 MHz): δ 4.35 (d, *J* = 16.8 Hz, 2H)/4.06 (d, *J* = 16.8 Hz, 2H) (2-,4-H₂), 3.88–3.82 (m, 2H, 5a-,9a-H), 2.06–1.94 (m, 2H, 6-,9-H), 1.71–1.59 (m, 2H, 7-,8-H), 1.58–1.47 (m, 2H,

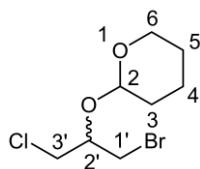
6-,9-H), 1.43–1.30 (m, 2H, 7-,8-H). ^{13}C NMR (CDCl_3 , 75 MHz): δ 212.0 (s, C-3), 80.7 (2d, C-5a,-9a), 73.6 (2t, C-2,-4), 27.5 (2t, C-6,-9), 22.1 (2t, C-7,-8). HRMS: m/z calculated for $\text{C}_9\text{H}_{14}\text{O}_3$: 170.0943 [M] $^+$; Found: 170.0921. Odour description: Fruity, animalic odour of green tonality with chemical aspects and acidic facets in the dry-down. Odour threshold: 141 ng/L air (stan. dev. 99 ng/L air).

***rac*-1-Bromo-3-chloropropan-2-ol (175):^[10]**



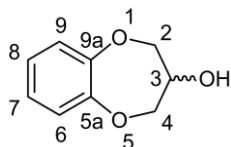
A 48% HBr solution (28.3 g) was added dropwise to neat epichlorohydrin (15 g, 162 mmol) within 2 h with vigorous stirring. The solution was stirred for an additional 0.75 h before being mixed with Et_2O (150 mL), transferred to a separatory funnel and the organic phase washed with saturated aqueous solution of NaHCO_3 (3 x 50 mL). The organic phase was dried (MgSO_4) and concentrated under reduced pressure and the resulting residue distilled under vacuum (75 °C, 5 torr) to give *rac*-1-bromo-3-chloropropan-2-ol (17.57 g, 63%) as a viscous clear oil. IR (ATR): $\tilde{\nu}$ = 3380 (ν O–H), 1037 (ν C–O) cm^{-1} . ^1H NMR (CDCl_3 , 300 MHz): δ 4.10–4.00 (m, 1H, 2-H), 3.77–3.66 (m, 2H, 3-H₂), 3.58 (d, J = 5.3 Hz, 2H, 1-H₂), 2.52 (d, J = 5.2 Hz, 1H, 2-OH). ^{13}C NMR (CDCl_3 , 75 MHz): δ 70.3 (d, C-2), 46.4 (t, C-3), 34.6 (t, C-1). HRMS: m/z calculated for $\text{C}_3\text{H}_6\text{BrClO}$: 171.9291 [M] $^+$; Found: 171.9256.

***rac*-2-((1-Bromo-3-chloropropan-2-yl)oxy)tetrahydro-2H-pyran (176):^[10]**



To 3,4-dihydro-2H-pyran (8.75 g, 104 mmol) was added *rac*-1-bromo-3-chloropropan-2-ol (16.51 g, 95.22 mmol) followed by phosphorus pentoxide (165 mg). The solution was warmed to 60 °C for 1 h and then cooled to RT and stirred for an additional 1 h. The resulting reaction mixture was dissolved in Et_2O (500 mL) and washed with a saturated aqueous solution of NaHCO_3 (3 x 300 mL). The organic phase was then dried (MgSO_4) and concentrated under reduced pressure to give a crude residue which was distilled under vacuum (80 °C, 0.8 torr) to give *rac*-2-((1-bromo-3-chloropropan-2-yl)oxy)tetrahydro-2H-pyran (19.85 g, 81%) as a clear oil. IR (ATR): $\tilde{\nu}$ = 2943 (ν C–H), 1024 (ν C–O) cm^{-1} . ^1H NMR (CDCl_3 , 300 MHz): δ 4.82–4.77 (m, 1H, 2-H), 4.09–4.00 (m, 1H, 2'-H), 3.99–3.89 (m, 1H, 6-H), 3.86–3.50 (m, 5H, 6-H, 1',-3'-H₂), 1.92–1.50 (m, 6H, 3-,4-,5-H₂). ^{13}C NMR (CDCl_3 , 75 MHz): δ 98.6 (d, C-2), 75.3 (d, C-2'), 62.5 (t, C-6), 44.1 (t, C-3'), 31.8 (t, C-1'), 30.3 (t, C-3), 25.0 (t, C-5), 19.1 (t, C-4).

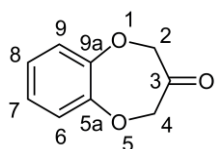
***rac*-3,4-Dihydro-2H-benzo[*b*][1,4]dioxepin-3-ol (179):^[10]**



To a solution of catechol (1.33 g, 12.08 mmol) in DMF (60 mL) was added K_2CO_3 (6.66 g, 48.18 mmol) and the mixture heated to 100 °C. To this solution was added 2-((1-bromo-3-chloropropan-2-yl)oxy)tetrahydro-2H-pyran (31 g, 12.09 mmol) in DMF (60 mL) over a period of 0.5 h and the resulting solution then stirred at 120 °C for 24 h. The reaction was quenched by the addition of H_2O (300 mL) followed by extraction with Et_2O (3 x 100 mL). The organic extracts were pooled,

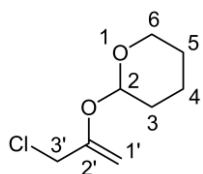
washed with H₂O (100 mL), dried (MgSO₄) and concentrated under reduced pressure. The resulting residue was purified by flash chromatography on silica gel (EtOAc/hexane; 2:8) to give a crude oil. Vanadium pentoxide (280 mg, 1.54 mmol) was added to a 30% aqueous solution of hydrogen peroxide (18 mL) and the mixture stirred at 0 °C for 10 minutes. The mixture was added to a solution of the crude oil in MeCN (80 mL) and the resulting solution heated to 70 °C for 0.5 h. The solution was then concentrated under reduced pressure, diluted with 2 M NaHCO₃ (200 mL) and extracted with DCM (3 x 100 mL). The organic extracts were pooled, dried (MgSO₄) and concentrated under reduced pressure. The resulting residue was purified by flash chromatography on silica gel (EtOAc/hexane; 25:75) to yield *rac*-3,4-dihydro-2*H*-benzo[*b*][1,4]dioxepin-3-ol (680 mg, 34%) as a colourless solid. mp: 49–50 °C. (lit. mp: 48–50 °C (pentane)).^[10] IR (ATR): $\tilde{\nu}$ = 3268 (ν O–H), 1492 (ν aromatic C=C), 1258 (ν C–O) cm⁻¹. ¹H NMR (CDCl₃, 300 MHz): δ 7.08–6.94 (m, 4H, 6-,7-,8-,9-H), 4.35–4.25 (m, 2H, 2-,4-H), 4.15–4.05 (m, 3H, 2-,3-,4-H), 2.67 (d, *J* = 8.5 Hz, 1H, 3-OH). ¹³C NMR (CDCl₃, 75 MHz): δ 150.9 (2s, C-5a,-9a), 123.8/121.4 (4d, C-6,-7,-8,-9), 74.6 (2t, C-2,-4), 69.5 (d, C-3). HRMS: *m/z* calculated for C₉H₁₀O₃: 166.0629 [M]⁺; Found: 166.0629.

2*H*-Benzo[*b*][1,4]dioxepin-3(4*H*)-one (49):^[10]



To a 4% aqueous KOH solution (8 ml) and KMnO₄ (480 mg) at 0 °C was added *rac*-3,4-dihydro-2*H*-benzo[*b*][1,4]dioxepin-3-ol (100 mg, 0.602 mmol) and the solution stirred for 2.5 h. The solution was then diluted with H₂O (50 mL) and extracted with EtOAc (3 x 50 mL). The organic extracts were pooled, dried (MgSO₄) and concentrated under reduced pressure and the resulting residue distilled under vacuum to yield 2*H*-benzo[*b*][1,4]dioxepin-3(4*H*)-one (70 mg, 71%) as a yellow oil. IR (ATR): $\tilde{\nu}$ = 1737 (ν C=O), 1490 (ν aromatic C=C), 1259 (ν C–O) cm⁻¹. ¹H NMR (CDCl₃, 300 MHz): δ 7.05–6.94 (m, 4H, 6-,7-,8-,9-H), 4.73 (s, 4H, 2-,4-H₂). ¹³C NMR (CDCl₃, 75 MHz): δ 204.5 (s, C-3), 148.3 (2s, C-5a,-9a), 123.8 (2d, C-7,-8), 120.9 (2d, C-6,-9), 75.6 (2t, C-2,-4). HRMS: *m/z* calculated for C₉H₈O₃: 164.0473 [M]⁺; Found: 164.0470.

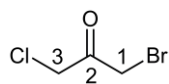
rac-2-((3-Chloroprop-1-en-2-yl)oxy)tetrahydro-2*H*-pyran (181):



rac-Cyclohexane-1,2-diol (608 mg, 5.24 mmol) in DMF (15 mL) was added dropwise to a solution of sodium hydride (315 mg, 13.1 mmol, 2.5 equiv) in DMF (25 mL) at 0 °C and the solution left to stir for 0.5 h. A solution of *rac*-2-((1-bromo-3-chloropropan-2-yl)oxy)tetrahydro-2*H*-pyran (1.215 g, 4.72 mmol, 0.9 equiv) in DMF (20 mL) was added dropwise over 1 h and the resulting solution allowed to warm to RT and stirred overnight. The reaction was quenched by the addition of H₂O (100 mL) followed by extraction with EtOAc (3 x 100 mL). The combined organic extracts were washed with H₂O (5 x 100 mL), dried (MgSO₄) and concentrated under reduced pressure. The resulting residue was purified by flash chromatography (EtOAc/hexane; 25:975) to give 2-((3-chloroprop-1-en-2-yl)oxy)tetrahydro-2*H*-pyran (330 mg, 40%) as a yellow oil. IR (ATR): $\tilde{\nu}$ = 2945 (ν C–H), 1637 (ν C=C), 992 (ν C=CH₂) cm⁻¹. ¹H NMR (CDCl₃,

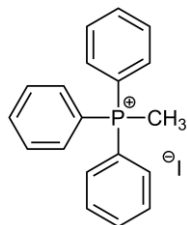
300 MHz): δ 5.25 (t, $J = 3.1$ Hz, 1H, 2-H), 4.48 (d, $J = 2.2$ Hz, 1H, 1'-H), 4.42 (d, $J = 2.2$ Hz, 1H, 1'-H), 4.00 (s, 2H, 3'-H₂), 3.93–3.85 (m, 1H, 6-H), 3.63–3.56 (m, 1H, 6-H), 2.01–1.83 (m, 1H, 4-H), 1.82–1.75 (m, 2H, 3-H₂), 1.73–1.53 (m, 3H, 4-H, 5-H₂). ¹³C NMR (CDCl₃, 75 MHz): δ 155.3 (s, C-2'), 95.5 (d, C-2), 89.5 (t, C-1'), 61.6 (t, C-6), 45.0 (t, C-3'), 29.7 (t, C-3), 24.9 (t, C-5), 18.3 (t, C-4). HRMS: m/z calculated for C₈H₁₃O₂: 141.0916 [M-Cl]⁺; Found: 141.0928.

1-Bromo-3-chloropropan-2-one (182):



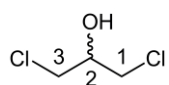
To a solution of sodium dichromate (9.38 g, 32.5 mmol) and *rac*-1-bromo-3-chloropropan-2-ol (9.98 g, 57.5 mmol) in H₂O (6 mL) was added a solution of H₂SO₄ (11.25 g) in H₂O (3 mL) over a period of 8 h with care taken to ensure the reaction did not exceed 25 °C. The solution was then diluted with H₂O (100 mL) and extracted with EtOAc (3 x 100 mL). The combined organic extracts were washed with saturated aqueous solution of NaHCO₃ (100 mL), dried (MgSO₄) and concentrated under reduced pressure to yield 1-bromo-3-chloropropan-2-one (9.6 g, 97%) as a clear oil. IR (ATR): $\tilde{\nu} = 1732$ (v C=O) cm⁻¹. ¹H NMR (CDCl₃, 300 MHz): δ 4.35 (s, 2H, 3-H₂), 4.11 (s, 2H, 1-H₂). ¹³C NMR (CDCl₃, 75 MHz): δ 194.2 (s, C-2), 45.7 (t, C-3), 31.2 (t, C-1). HRMS: m/z calculated for C₃H₄BrClO: 169.9134 [M]⁺; Found: 169.9122.

Methyltriphenylphosphonium iodide (183):^[85]



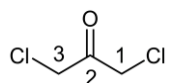
Triphenylphosphine (28 g, 106.8 mmol) and iodomethane (16.2 g, 114 mmol) in benzene (100 mL) was stirred at RT overnight. The precipitate was filtered and dried with P₂O₅ under high vacuum for 8 h to yield methyltriphenylphosphonium iodide (37.4 g, 86%) as a colourless solid. mp: 184–185 °C

rac-1,3-Dichloropropan-2-ol (187):

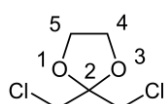


Following general procedure for compound (\pm)-**175** but instead using conc. hydrochloric acid. Clear oil, 78% yield. IR (ATR): $\tilde{\nu} = 3371$ (v O-H), 1050 (v C-H) cm⁻¹. ¹H NMR (CDCl₃, 300 MHz): δ 4.08 (p, $J = 5.3$ Hz, 1H, 2-H), 3.71 (d, $J = 5.3$ Hz, 4H, 1-,3-H₂). ¹³C NMR (CDCl₃, 75 MHz): δ 70.7 (d, C-2), 45.6 (2t, C-1,-3).

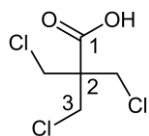
1,3-Dichloropropan-2-one (188):



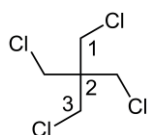
Following general procedure for compound **182** but instead using 1,3-dichloropropan-2-ol. Clear oil, 75% yield. IR (ATR): $\tilde{\nu} = 1738$ (v C=O) cm⁻¹. ¹H NMR (CDCl₃, 300 MHz): δ 4.33 (s, 4H, 1-,3-H₂). ¹³C NMR (CDCl₃, 75 MHz): δ 194.9 (s, C-2), 46.0 (2t, C-1,-3). HRMS: m/z calculated for C₃H₄Cl₂O: 125.9639 [M]⁺; Found: 125.9640.

2,2-Bis(chloromethyl)-1,3-dioxolane (189):

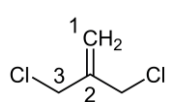
To a solution of 1,3-dichloropropan-2-one (13.6 g, 107.12 mmol) and ethylene glycol (17.42 g, 280.65 mmol) in toluene (300 mL) was added H_2SO_4 (1 mL) and the solution heated at reflux in a Dean-Stark apparatus overnight, with the removal of H_2O . The solution was then diluted with H_2O (100 mL) and extracted with EtOAc (3 x 100 mL). The organic extracts were pooled, washed with a saturated aqueous solution of NaHCO_3 (100 mL), dried (MgSO_4) and concentrated under reduced pressure to yield 2,2-bis(chloromethyl)-1,3-dioxolane (18 g, 98%) as a clear oil. IR (ATR): $\tilde{\nu} = 1015$ (ν C–O) cm^{-1} . ^1H NMR (CDCl_3 , 300 MHz): δ 4.12 (s, 4H, 4-,5- H_2), 3.68 (s, 4H, 2- $2\text{CH}_2\text{Cl}$). ^{13}C NMR (CDCl_3 , 75 MHz): δ 107.6 (s, C-2), 66.4 (2t, C-4,-5), 44.8 (2t, 2- $2\text{CH}_2\text{C}$).

3-Chloro-2,2-bis(chloromethyl)propanoic acid (192):^[86]

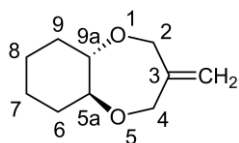
To a solution of pentaerythritol (139 g, 1.02 mmol) in pyridine (250 mL) was added thionyl chloride (378 g, 3.18 mmol) dropwise over a period of 5 h so that the temperature was maintained between 65–95 °C. The reaction was heated at 120 °C overnight before ice-cold H_2O (670 mL) was added with stirring. The reaction mixture was extracted with CHCl_3 (3 x 300 mL), the organic extracts pooled, dried (MgSO_4) and concentrated under reduced pressure. The resulting crude residue was then heated to 80 °C and conc. HNO_3 (15 mL) was added. After 15 minutes, an additional quantity of conc. HNO_3 (170 mL) was added dropwise over a period of 2 h. The reaction was then maintained at 80 °C overnight before being poured into ice-cold H_2O (500 mL) followed by extraction with DCM (4 x 300 mL). The organic extracts were pooled and washed with 1 M NaOH (3 x 300 mL), dried (MgSO_4) and concentrated under reduced pressure to yield 3-chloro-2,2-bis(chloromethyl)propanoic acid (30 g, 14%) as a colourless solid. mp: 107–109 °C. (lit. mp: 107–109 °C).^[86] IR (ATR): $\tilde{\nu} = 2863$ (ν acid OH), 1713 (ν acid C=O) cm^{-1} . ^1H NMR (CDCl_3 , 300 MHz): δ 11.47 (s, 1H, 1-COOH), 3.88 (s, 6H, 2-($2\text{CH}_2\text{Cl}$), 3- H_2). ^{13}C NMR (CDCl_3 , 75 MHz): δ 175.5 (s, C-1), 55.3 (s, C-2), 42.7 (3t, C-2($2\text{CH}_2\text{Cl}$),-3).

1,3-Dichloro-2,2-bis(chloromethyl)propane (193):^[86]

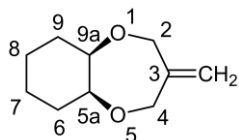
The 1 M NaOH washes from **192** were pooled, concentrated to pH 1 with conc. HCl and extracted with DCM (4 x 300 mL). The organic extracts were pooled, washed with a saturated aqueous solution of NaHCO_3 (100 mL), dried (MgSO_4) and concentrated under reduced pressure to yield 1,3-dichloro-2,2-bis(chloromethyl)propane (35 g, 17%) as a yellow solid. mp: 96–97 °C. (lit. mp: 95–96 °C (cyclohexane)).^[86] IR (ATR): $\tilde{\nu} = 696$ (ν C–Cl) cm^{-1} . ^1H NMR (CDCl_3 , 300 MHz): δ 3.69 (s, 8H, 1-,3-,2-($2\text{CH}_2\text{Cl}$)- H_2). ^{13}C NMR (CDCl_3 , 75 MHz): δ 46.6 (s, C-2), 43.9 (4t, C-1,-3,-2($2\text{CH}_2\text{Cl}$)).

3-Chloro-2-(chloromethyl)prop-1-ene (194):^[86]


A flask of neat 3-chloro-2,2-bis(chloromethyl)propanoic acid (30 g, 146 mmol) was heated to 210 °C with a short-path distillation stillhead, condenser and receiver flask. The distillate was collected and redistilled from calcium hydride to yield 3-chloro-2-(chloromethyl)prop-1-ene (14 g, 76%) as a clear liquid. IR (ATR): $\tilde{\nu}$ = 931 (ν C=CH₂), 725 (ν C–Cl) cm⁻¹. ¹H NMR (CDCl₃, 300 MHz): δ 5.34 (s, 2H, 1-H₂), 4.22 (d, J = 1.1 Hz, 4H, 3-H₂, 2-CH₂Cl). ¹³C NMR (CDCl₃, 75 MHz): δ 141.2 (s, C-2), 119.0 (t, C-1), 44.7 (2t, C-3, 2-CH₂Cl). HRMS: m/z calculated for C₄H₆Cl₂: 123.9846 [M]⁺; Found: 123.9846.

***rac*-3-Methyleneoctahydro-2*H*-benzo[*b*][1,4]dioxepine (195):**


rac-Cyclohexane-1,2-diol (608 mg, 5.24 mmol) in DMF (15 mL) was added dropwise to a solution of sodium hydride (315 mg, 13.1 mmol, 2.5 equiv) in DMF (30 mL) at 0 °C and left for 1 h. A solution of 3-chloro-2-chloromethyl-propene (655 mg, 5.24 mmol, 1 equiv) in DMF (20 mL) was added dropwise over 1 h and the solution allowed to stir at RT overnight. The reaction was quenched by the addition of H₂O (10 mL) and extracted with Et₂O (4 x 100 mL). The combined organic extracts were washed with H₂O (2 x 100 mL) before being dried (MgSO₄) and concentrated under reduced pressure. The resulting residue was then purified by flash chromatography on silica gel (EtOAc/hexane; 5:95) to give *rac*-3-methyleneoctahydro-2*H*-benzo[*b*][1,4]dioxepine (206 mg, 23%) as a yellow oil. IR (ATR): $\tilde{\nu}$ = 2933/2860 (ν C–H), 1115 (ν C–O) cm⁻¹. ¹H NMR (CDCl₃, 300 MHz): δ 4.90 (t, J = 1.3 Hz, 2H, =CH₂), 4.43 (d, J = 14.9 Hz, 2H, 2-,4-H), 4.31 (d, J = 15.1 Hz, 2H, 2-,4-H), 3.17–3.05 (m, 2H, 5a-,9a-H), 2.03–1.87 (m, 2H, 6-,9-H), 1.79–1.59 (m, 2H, 7-,8-H), 1.36–1.11 (m, 4H, 6-,7-,8-,9-H). ¹³C NMR (CDCl₃, 75 MHz): δ 148.8 (s, C-3), 109.6 (t, =CH₂), 86.1 (2d, C-5a,-9a), 73.0 (2t, C-2,-4), 31.5 (2t, C-6,-9), 24.0 (2t, C-7,-8). HRMS: m/z calculated for C₁₀H₁₆O₂: 168.1150 [M]⁺; Found: 168.1160. Odour description: Agrestic, leathery.

***meso*-3-Methyleneoctahydro-2*H*-benzo[*b*][1,4]dioxepine (196):**


Following general procedure for compound **195** but instead using *meso*-cyclohexane-1,2-diol. Yellow oil, 23% yield. IR (ATR): $\tilde{\nu}$ = 2934 (ν C–H), 1110 (ν C–O) cm⁻¹. ¹H NMR (CDCl₃, 300 MHz): δ 4.96 (t, J = 1.1 Hz, 2H, =CH₂), 4.40 (d, J = 14.4 Hz, 2H, 2-,4-H), 4.16 (d, J = 14.5 Hz, 2H, 2-,4-H), 3.76–3.70 (m, 2H, 5a-,9a-H), 2.00–1.86 (m, 2H, 6-,9-H), 1.69–1.56 (m, 2H, 7-,8-H), 1.55–1.43 (m, 2H, 6-,9-H), 1.39–1.22 (m, 2H, 7-,8-H). ¹³C NMR (CDCl₃, 75 MHz): δ 148.4 (s, C-3), 111.8 (t, =CH₂), 78.7 (2d, C-5a,-9a), 69.5 (2t, C-2,-4), 28.3 (2t, C-6,-9), 22.4 (2t, C-7,-8). HRMS: m/z calculated for C₁₀H₁₆O₂: 168.1150 [M]⁺; Found: 168.1125. Odour description: Agrestic, thymol, carvacrol, leathery tar.

General Procedure for Oxidation of 195→167 or 196→173:

Methylene compound (180 mg, 1.07 mmol) was dissolved in MeCN (5 mL), H₂O (5 mL), and CCl₄ (3 mL), and sodium metaperiodate (229 mg, 1.07 mmol) and ruthenium trichloride (22 mg, 0.107 mmol) were added. The mixture was stirred for 24 h, then further sodium metaperiodate (229 mg, 1.07 mmol) and ruthenium trichloride (22 mg, 0.107 mmol) were added. The solution was stirred for an additional 24 h. The reaction mixture was then poured into H₂O (30 mL), and the resulting mixture was extracted with DCM (3 x 20 mL). The combined organic extracts were washed with a saturated aqueous solution of NaHSO₃ (20 mL) and with H₂O (20 mL), dried (MgSO₄), and concentrated under reduced pressure. The resulting residue was purified by flash chromatography on silica gel (EtOAc/hexane; 1:9) to give the corresponding ketone.

2.4 – References

1. R. Axel, Scents and sensibility: A molecular logic of olfactory perception (nobel lecture), *Angew. Chem., Int. Ed.* **2005**, *44*, 6111-6127.
2. L. B. Buck, Information coding in the vertebrate olfactory system, *Annu. Rev. Neurosci.* **1996**, *19*, 517-544.
3. L. B. Buck, Unraveling the sense of smell (nobel lecture), *Angew. Chem., Int. Ed.* **2005**, *44*, 6128-6140.
4. E. Brenna, C. Fuganti, S. Serra, Enantioselective perception of chiral odorants, *Tetrahedron: Asymmetry* **2003**, *14*, 1-42.
5. J. E. Amoore, Specific anosmia: a clue to the olfactory code, *Nature* **1967**, *214*, 1095-1098.
6. P. Kraft, W. Eichenberger, Conception, characterization and correlation of new marine odorants, *Eur. J. Org. Chem.* **2003**, 3735-3743.
7. P. Kraft, K. Popaj, P. Müller, M. Schär, 'Vanilla oceanics': synthesis and olfactory properties of (1'*E*)-7-(prop-1'-enyl)-2*H*-benzo[*b*][1,4]dioxepin-3(4*H*)-ones and homologues, *Synthesis* **2010**, 3029-3036.
8. B. Drevermann, Ph.D Thesis, RMIT University, Melbourne, Australia **2007**.
9. B. Drevermann, A. R. Lingham, H. M. Hugel, P. J. Marriott, Synthesis and qualitative olfactory evaluation of benzodioxepine analogues, *Helv. Chim. Acta* **2007**, *90*, 854-863.
10. B. Drevermann, A. R. Lingham, H. M. Hugel, P. J. Marriott, Synthesis of benzodioxepinone analogues via a novel synthetic route with qualitative olfactory evaluation, *Helv. Chim. Acta* **2007**, *90*, 1006-1027.
11. J.-M. Gaudin, J.-Y. de Saint Laumer, Structure-Activity Relationships in the Domain of Odorants Having Marine Notes, *Eur. J. Org. Chem.* **2015**, 1437-1447.
12. J.-M. Gaudin, O. Nikolaenko, J.-Y. de Saint Laumer, B. Winter, P.-A. Blanc, Structure - activity relationship in the domain of odorants having marine notes, *Helv. Chim. Acta* **2007**, *90*, 1245-1265.
13. A. W. Hofmann, On insolinic acid, *Proceedings of the Royal Society* **1855**, *8*, 1-3.
14. A. Kekulé, Ueber einige Condensationsproducte des Aldehyds, *Justus Liebigs Ann. Chem.* **1872**, *162*, 77-124.
15. J. E. McMurry, *Organic Chemistry 7th Ed.*, Brooks Cole, Belmont, **2008**.
16. D. J. Nelson, C. N. Brammer, Toward Consistent Terminology for Cyclohexane Conformers in Introductory Organic Chemistry, *J. Chem. Educ.* **2011**, *88*, 292-294.
17. Molecular Operating Environment (MOE), release 2013.0801, Chemical Computing Group, Montreal, Quebec, Canada H3A 2R7, **2013**. For more information see <<http://www.chemcomp.com/>>.
18. J. J. Beereboom, D. P. Cameron, C. R. Stephens (Pfizer Inc.), **1972**, US3647479A.
19. J. J. Beereboom, D. P. Cameron, C. R. Stephens (Pfizer Inc.), **1974**, US3799892A.
20. B. Drevermann, A. R. Lingham, H. M. Hugel, P. J. Marriott, Microwave assisted synthesis of the fragrant compound Calone 1951, *Tetrahedron Lett.* **2005**, *46*, 39-41.

21. S. Sonda, K. Katayama, M. Fujio, H. Sakashita, K. Inaba, K. Asano, T. Akira, 1,5-Benzodioxepin derivatives as a novel class of muscarinic M₃ receptor antagonists, *Bioorg. Med. Chem. Lett.* **2007**, *17*, 925-931.
22. J. H. P. Tyman, J. Grundy, G. R. Brown, Synthesis of 7,8,9,10,11,12,20,21,22,23,24,25-dodecahydrodibenzo[*b,m*]-[1,4,12,15]tetraoxacyclodocosin, a crown ether, *J. Chem. Soc., Perkin Trans. 1* **1981**, 336-343.
23. C. S. Rooney, R. S. Stuart, B. K. Wasson, H. W. R. Williams, 3,4-Dihydro-2*H*-1,5-benzodioxepins. Novel class of β -adrenergic stimulants, *Can. J. Chem.* **1975**, *53*, 2279-2292.
24. I. Sanchez, M. D. Pujol, G. Guillaumet, R. Massingham, A. Monteil, Synthesis of dioxygenated systems. Preparation of homologs of 1,4-benzodioxin as calcium antagonists, *Sci. Pharm.* **2001**, *69*, 11-19.
25. J. P. Schirmann, A. Isard, F. Weiss, Rearrangement of diallylic-type structures. IV. α,α' -Disubstituted isobutenes: thermal rearrangements of 3-methylene-1,5-benzodioxepane, *Tetrahedron* **1968**, *24*, 6475-6483.
26. M. L. Curtin, Y. Dai, S. K. Davidsen, H. R. Heyman, J. H. Holmes, M. R. Michaelides, D. H. Steinman (Abbott Laboratories), **2000**, WO2000044739A1.
27. R. Pappo, D. S. Allen, Jr., R. U. Lemieux, W. S. Johnson, Osmium tetroxide-catalyzed periodate oxidation of olefinic bonds, *J. Org. Chem.* **1956**, *21*, 478-479.
28. H. Finkelstein, Darstellung organischer Jodide aus den entsprechenden Bromiden und Chloriden, *Ber. Dtsch. Chem. Ges.* **1910**, *43*, 1528-1532.
29. C. Damez, J.-R. Labrosse, P. Lhoste, D. Sinou, An easy palladium-catalyzed access to substituted 3-methylene-3,4-dihydro-2*H*-1,5-benzodioxepines, *Synthesis* **2001**, 1456-1458.
30. J. A. Hunt, R. F. Sweis, D. Kim, F. Kallashi, P. J. Sinclair (Merck & Co., Inc.), **2008**, WO2008156715A1.
31. V. Rosnati, F. D. Marchi, Chemical and spectroscopic properties of 2-formyl-1,4-benzodioxane and 3-oxo-3,4-dihydro-2*H*-1,5-benzodioxepin, *Tetrahedron* **1962**, *18*, 289-298.
32. F. Nerdel, M. Mamluk, P. Weyerstahl, Fragmentation reactions of carbonyl compounds with electronegative β -substituents. XVIII. Synthesis and reactions of cyclic polyethers, *Justus Liebigs Ann. Chem.* **1970**, *736*, 75-87.
33. T. D. Cushing, J. F. Sanz-Cervera, R. M. Williams, Stereocontrolled Total Synthesis of (+)-Paraherquamide B, *J. Am. Chem. Soc.* **1996**, *118*, 557-579.
34. R. M. Williams, J. Cao, H. Tsujishima, R. J. Cox, Asymmetric, Stereocontrolled Total Synthesis of Paraherquamide A, *J. Am. Chem. Soc.* **2003**, *125*, 12172-12178.
35. V. Hellwig, J. Dasenbrock, D. Klostermeyer, S. Kroiss, T. Sindlinger, P. Spitteller, B. Steffan, W. Steglich, M. Engler-Loehr, S. Semar, T. Anke, New benzodioxepin type strobilurins from basidiomycetes. Structural

- revision and determination of the absolute configuration of strobilurin D and related β -methoxyacrylate antibiotics, *Tetrahedron* **1999**, *55*, 10101-10118.
36. R. M. Williams, T. D. Cushing, Synthetic studies on paraherquamide: synthesis of the 2*H*-1,5-benzodioxepin ring system, *Tetrahedron Lett.* **1990**, *31*, 6325-6328.
 37. H. Uchiro, K. Nagasawa, Y. Aiba, T. Kotake, D. Hasegawa, S. Kobayashi, Asymmetric total synthesis of 9-methoxystrobilurin K, *Tetrahedron Lett.* **2001**, *42*, 4531-4534.
 38. E. Taniguchi, S. Yamauchi, S. Nagata, T. Ohnishi, Syntheses of 2-substituted 6/7-methoxy-1,4-benzodioxan-7/6-carbaldehydes, *Biosci., Biotechnol., Biochem.* **1992**, *56*, 630-635.
 39. B. R. McDonald, A. E. Nibbs, K. A. Scheidt, A Biomimetic Strategy to Access the Silybins: Total Synthesis of (-)-Isosilybin A, *Org. Lett.* **2015**, *17*, 98-101.
 40. G. Ohloff, W. Pickenhagen, P. Kraft, *Scent and Chemistry - The Molecular World of Odors*, Verlag Helvetica Chimica Acta, Zurich, **2012**.
 41. Y. Wang, J. Yao, H. Li, D. Su, M. Antonietti, Highly Selective Hydrogenation of Phenol and Derivatives over a Pd@Carbon Nitride Catalyst in Aqueous Media, *J. Am. Chem. Soc.* **2011**, *133*, 2362-2365.
 42. X. Yang, L. Du, S. Liao, Y. Li, H. Song, High-performance gold-promoted palladium catalyst towards the hydrogenation of phenol with mesoporous hollow spheres as support, *Catal. Commun.* **2012**, *17*, 29-33.
 43. J. Matos, A. Corma, Selective phenol hydrogenation in aqueous phase on Pd-based catalysts supported on hybrid TiO₂-carbon materials, *Appl. Catal., A* **2011**, *404*, 103-112.
 44. S. Agarwal, J. N. Ganguli, Hydrogenation by nanoscale ruthenium embedded into the nanopores of K-10 clay, *RSC Adv.* **2014**, *4*, 11893-11898.
 45. W. Dieckmann, Formation of closed chain compounds from open carbon chains, *Ber. Dtsch. Chem. Ges.* **1894**, *27*, 102-103.
 46. J. E. Baldwin, Rules for ring closure, *J. Chem. Soc., Chem. Commun.* **1976**, 734-736.
 47. J. E. Baldwin, R. C. Thomas, L. I. Kruse, L. Silberman, Rules for ring closure: ring formation by conjugate addition of oxygen nucleophiles, *J. Org. Chem.* **1977**, *42*, 3846-3852.
 48. W. H. Brown, C. S. Foote, B. L. Iverson, E. Anslyn, *Organic Chemistry 7th Ed.*, Brooks Cole, Belmont, **2014**.
 49. A. R. Lingham, Ph.D Thesis, RMIT University, Melbourne, Australia **2007**.
 50. A. Roebuck, H. Adkins, *trans*-1,2-Cyclohexanediol, *Org. Synth.* **1948**, *28*, 35-37.
 51. E. Groaz, D. Banti, M. North, Synthesis of cyclic and macrocyclic ethers using metathesis reactions of alkenes and alkynes, *Eur. J. Org. Chem.* **2007**, 3727-3745.
 52. N. Chronakis, T. Brandmuller, C. Kovacs, U. Reuther, W. Donaubaue, F. Hampel, F. Fischer, F. Diederich, A. Hirsch, Macrocyclic cyclo[*n*]malonates - synthetic aspects and observation of columnar arrangements by X-ray crystallography, *Eur. J. Org. Chem.* **2006**, 2296-2308.

53. W. O. Lin, M. C. B. V. De Souza, H. G. Alt, Synthesis, characterization, and complexation studies with K⁺ and Ca²⁺ cations of *trans*-1,2-cyclohexanedioxydiacetamides, *Z. Naturforsch., B: Chem. Sci.* **1988**, *43*, 165-170.
54. N. E. Searle, Ethyl Diazoacetate, *Org. Synth.* **1956**, *36*, 25-28.
55. G. W. Cowell, A. Ledwith, Developments in the chemistry of diazo-alkanes, *Quart. Rev., Chem. Soc.* **1970**, *24*, 119-167.
56. M. S. Newman, P. F. Beal, III, New synthesis of α -alkoxy ketones, *J. Am. Chem. Soc.* **1950**, *72*, 5161-5163.
57. D. J. Miller, C. J. Moody, Synthetic applications of the O-H insertion reactions of carbenes and carbenoids derived from diazocarbonyl and related diazo compounds, *Tetrahedron* **1995**, *51*, 10811-10843.
58. V. V. Popik, A. E. Russell, Ethyl Diazoacetate, *e-EROS Encyclopedia of Reagents for Organic Synthesis* **2007**.
59. J. B. Peri, A. L. Hensley, Jr., The surface structure of silica gel, *J. Phys. Chem.* **1968**, *72*, 2926-2933.
60. V. VanRheenen, R. C. Kelly, D. Y. Cha, An improved catalytic osmium tetroxide oxidation of olefins to *cis*-1,2-glycols using tertiary amine oxides as the oxidant, *Tetrahedron Lett.* **1976**, 1973-1976.
61. D. V. Deubel, G. Frenking, [3+2] Versus [2+2] Addition of Metal Oxides Across C:C Bonds. Reconciliation of Experiment and Theory, *Acc. Chem. Res.* **2003**, *36*, 645-651.
62. V. VanRheenen, D. Y. Cha, W. M. Hartley, Catalytic osmium tetroxide oxidation of olefins: *cis*-1,2-cyclohexanediol, *Org. Synth.* **1978**, *58*, 43-48.
63. H. Sharghi, Z. Pazirae, K. Niknam, Halogenated cleavage of epoxides into halohydrins in the presence of a series of diamine podands as catalyst with elemental iodine and bromine, *Bull. Korean Chem. Soc.* **2002**, *23*, 1611-1615.
64. R. Gopinath, A. R. Paital, B. K. Patel, V₂O₅-H₂O₂: a convenient reagent for the direct oxidation of acetals to esters, *Tetrahedron Lett.* **2002**, *43*, 5123-5126.
65. K. Omura, D. Swern, Oxidation of alcohols by "activated" dimethyl sulfoxide. A preparative steric and mechanistic study, *Tetrahedron* **1978**, *34*, 1651-1660.
66. F. A. Davis, G. V. Reddy, M. Bental, C. J. Deutsch, Synthesis of methyl 2-(fluoromethyl)-3-fluoroalanine, *Synthesis* **1994**, 701-702.
67. F. M. Menger, C. Lee, Oxidations with solid potassium permanganate, *J. Org. Chem.* **1979**, *44*, 3446-3448.
68. M. Meciarova, S. Toma, A. Heribanova, Ultrasound assisted heterogeneous permanganate oxidations, *Tetrahedron* **2000**, *56*, 8561-8566.
69. K. Pisarczyk, *Manganese compounds. Kirk-Othmer Encyclopedia of Chemical Technology 5th Edition*, John Wiley & Sons, Hoboken, **2005**.

70. The NIST Mass Spectral Search Program for the NIST/EPA/NIH Mass Spectral Library. Version 2.0 d, build December 2 2005.
71. Spectral Database for Organic Compounds (SDBS); Accessed August 13 2015. <<http://riodb01.ibase.aist.go.jp/sdbs>>.
72. G. C. Finger, C. W. Kruse, Aromatic fluorine compounds. VII. Replacement of aromatic chloro and nitro groups by fluorine, *J. Am. Chem. Soc.* **1956**, *78*, 6034-6037.
73. P. B. D. De la Mare, L. Fowden, E. D. Hughes, C. K. Ingold, J. D. H. Mackie, Mechanism of substitution at a saturated carbon atom. XLIX. Analysis of steric and polar effects of alkyl groups in bimolecular nucleophilic substitution, with special reference to halogen exchanges, *J. Chem. Soc.* **1955**, 3200-3236.
74. S. Winstein, S. G. Smith, D. Darwish, Alleged S_N2 Finkelstein substitutions of *tert*-butyl bromide, *Tetrahedron Lett.* **1959**, 24-31.
75. D. Cook, A. J. Parker, Halide exchange at a saturated carbon atom in dimethylformamide solvent. Comparison of experimental rates and Arrhenius parameters with values calculated by Ingold, *J. Chem. Soc. B* **1968**, 142-148.
76. E. D. Hughes, C. K. Ingold, J. D. H. Mackie, Mechanism of substitution at a saturated carbon atom. XLIII. Kinetics of the interaction of chloride ions with simple alkyl bromides in acetone, *J. Chem. Soc.* **1955**, 3173-3177.
77. M. Namavari, N. Satyamurthy, M. E. Phelps, J. R. Barrio, Halogen exchange reactions between alkyl halides and aqueous hydrogen halides. A new method for preparation of alkyl halides, *Tetrahedron Lett.* **1990**, *31*, 4973-4976.
78. G. Calingaert, H. Soroos, V. Hnizda, H. Shapiro, Redistribution reaction. IX. Redistribution of halides and of esters, *J. Am. Chem. Soc.* **1940**, *62*, 1545-1547.
79. P. J. Trotter, Aluminum chloride-induced halogen exchange of alkyl halides, *J. Org. Chem.* **1963**, *28*, 2093-2096.
80. D. Forster, Catalysis of halogen exchange between alkyl halides, *J. Chem. Soc., Chem. Commun.* **1975**, 917-918.
81. J. E. Lyons, Group VIII metal complexes as catalysts for halogen exchange between alkyl halides, *J. Chem. Soc., Chem. Commun.* **1975**, 418-419.
82. E. Angeletti, P. Tundo, P. Venturello, Catalytic halide exchange in hydrocarbons promoted by aluminas coated with phosphonium salts, *J. Chem. Soc., Chem. Commun.* **1980**, 1127-1128.
83. J. B. Conant, O. R. Quayle, α,γ -Dichloroacetone, *Org. Synth.* **1922**, *2*, 13-15.
84. K. Bowden, I. M. Heilbron, E. R. H. Jones, B. C. L. Weedon, Acetylenic compounds. I. Preparation of acetylenic ketones by oxidation of acetylenic carbinols and glycols, *J. Chem. Soc.* **1946**, 39-45.

85. F.-L. Wu, B. P. Ross, R. P. McGeary, New Methodology for the Conversion of Epoxides to Alkenes, *Eur. J. Org. Chem.* **2010**, 1989-1998.
86. K. M. Lynch, W. P. Dailey, Improved Preparations of 3-Chloro-2-(chloromethyl)-1-propene and 1,1-Dibromo-2,2-bis(chloromethyl)cyclopropane: Intermediates in the Synthesis of [1.1.1]Propellane, *J. Org. Chem.* **1995**, *60*, 4666-4668.
87. K. R. Mondanaro, W. P. Dailey, 3-Chloro-2-(chloromethyl)-1-propene, *Org. Synth.* **1998**, *75*, 89-97.
88. P. H. J. Carlsen, T. Katsuki, V. S. Martin, K. B. Sharpless, A greatly improved procedure for ruthenium tetroxide catalyzed oxidations of organic compounds, *J. Org. Chem.* **1981**, *46*, 3936-3938.
89. S.-I. Murahashi, N. Komiya, in *Modern Oxidation Methods*, Wiley-VCH, Weinheim, **2004**, 165-191.

Chapter 3 – Synthesis of Additional Analogues of the Aliphatic Benzo[*b*][1,4]dioxepin-3-one System

3.1 – Introduction

3.1.1 – Olfactory Receptors and Strategies for Addressing Weak Affinity

The discovery that the *threo*- and *erythro*-configured stereoisomers of the unsubstituted aliphatic benzo[*b*][1,4]dioxepin-3-one scaffold did not contain marine odorant nuances was not entirely unexpected when previous research regarding the synthetic marine odorant family was reviewed.^[1-6] The commercially produced benzo[*b*][1,4]dioxepin-3-one odorant named Azurone® (**53**) was discovered by researchers at Givaudan during the generation of an olfactophore receptor model and was the optimum ligand for the original model which consisted of three hydrogen-bond acceptors, an aromatic binding site, an aliphatic hydrophobe and three excluded volumes inaccessible to the molecule (Figure 3.1).^[1] With the later discovery that the (*E*)-7-(prop-1-enyl)-substituted analogue (**89**) was as potent an odorant as Azurone® (**53**), the initial olfactophore model was revised placing the aliphatic hydrophobe into the plane of the aromatic binding site and nearly 1 Å further away from its centre. Two hydrogen-bond acceptors were discovered to be sufficient, but six excluded volumes were necessary for an 85% predictability of odour threshold.^[2]

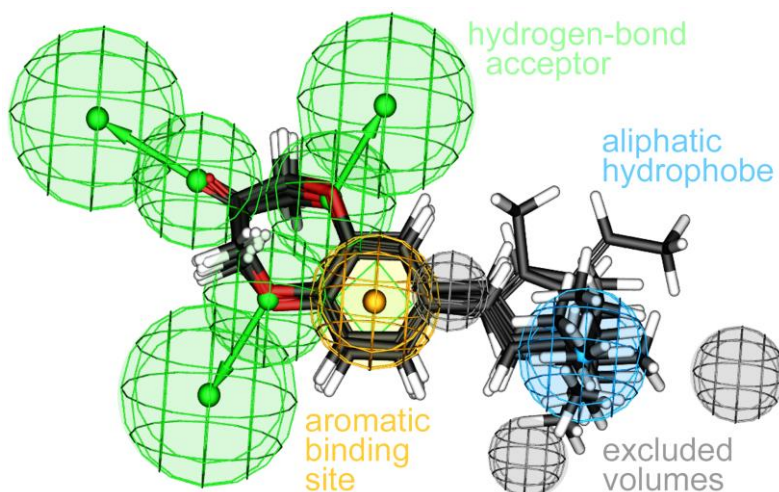


Figure 3.1: Original marine olfactophore model developed by Kraft *et al.*,^[2] with bound ligands. Copyright Georg

Thieme Verlag KG. Reproduced with permission.

Recently, researchers at Firmenich described that the heterocyclic moiety of the original benzo[*b*][1,4]dioxepin-3-one template could be replaced by a 2,3-dihydrofuran-2-carbaldehyde unit leading to compound **54**, for which a powerful aldehydic-green marine odour was reported (Figure 3.2).^[4] A library of analogues led to the proposition of an alternative qualitative olfactophore model consisting of one hydrogen-bond acceptor, an aliphatic hydrophobe and an aromatic binding site.^[4] Both the Givaudan and Firmenich receptor models agree on the requirement of at least one potent hydrogen-bond acceptor, for which a carbonyl functionality has now been independently confirmed to be optimal by both Gaudin *et al.*^[4] and Hgel *et al.*^[5]

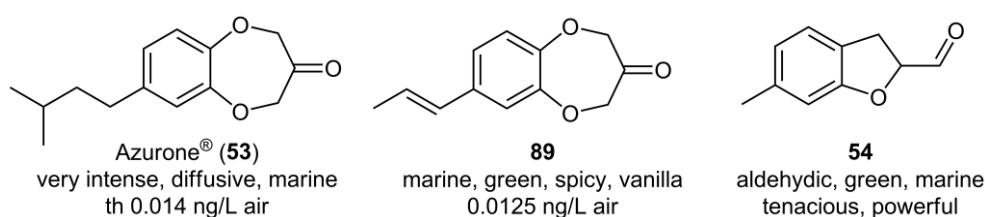


Figure 3.2: Potent synthetic marine odorant analogues and their respective odour descriptors.

It was reported by Gaudin *et al.*^[4] that the five-membered heterocyclic ring system required one ether functionality to sustain marine odorant characteristics which confirmed the requirement for a second hydrogen-bond acceptor. All receptor models feature an aromatic binding site but the question remained unanswered as to whether the binding site is an essential binding feature of the receptor or simply a molecular spacer.^[4] Strategies to increase the receptor affinity of the aliphatic scaffold included alkyl substitution as a way to address the aliphatic hydrophobe, as well as the reintroduction of unsaturation within the carbocyclic ring system in optimism that an sp^2 orbital or π electron interaction with the olfactory receptor(s) may offer additional binding capabilities.

3.1.2 – Biotransformation of Aromatic Substrates

The oxidation of aromatic substrates by the enzymes toluene dioxygenase (TDO), naphthalene dioxygenase (NDO) and biphenyl dioxygenase (BPDO) can provide uncomplicated access to enantiopure *cis*-diol compounds for chemical synthesis. In wild-type organisms this family of enzymes are involved in a process allowing aromatic compounds to be metabolised as a carbon and energy source.^[7-8] In 1968 Gibson *et al.*^[9-10] reported the first bio-oxidative degradation of simple aromatic compounds by fermentation with the bacterium *Pseudomonas putida*. In 1970 the first reported example of a mutant bacterium strain (Pp39D) lacking the enzymes responsible for the further degradation of the diene-diol metabolite was isolated (Figure 3.3).^[11] This bacterial strain was produced by treatment of the original bacterium with *N*-methyl-*N*-nitroso-*N*-nitroguanidin (MNNG), a potent mutagen.^[12]

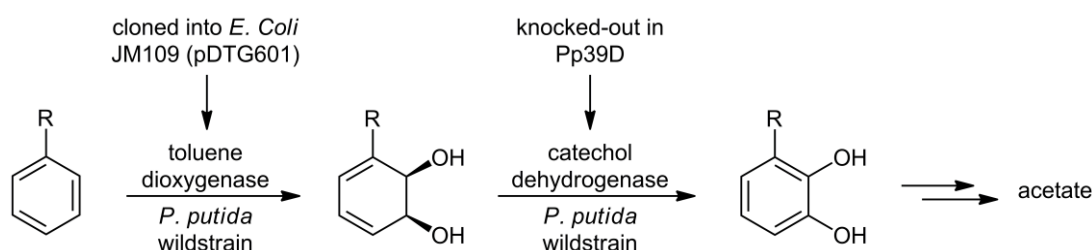


Figure 3.3: Comparison of the degradation pathway of aromatic compounds by wild type *P. putida*, the knock-out mutant (Pp39D) and the bioengineered *E. coli* strain (JM109 pDTG601).

The set of genes that encoded the enzyme toluene dioxygenase (TDO) were later cloned into a recombinant strain of *Escherichia coli* (JM109 pDTG601A).^[13] Unlike the blocked mutant strain of *P. putida*, which required the addition of a known aromatic inducer to initiate protein synthesis, the recombinant *E. coli* bacterium contained the genes for an inducer, isopropyl β -D-1-thiogalactopyranoside (IPTG), on the plasmid.^[8] A primary advantage of biocatalysis over traditional synthetic techniques is enantioselectivity.^[14] The reason for the observed selectivity involves the specific environment in which the reaction take place within the enzyme. Traditional synthetic techniques, if imparting enantioselectivity at all, do so because the control is based on electronic and steric properties of the reactant, not the actual environment in which the reaction takes place.^[15]

Toluene dioxygenase (TDO) and the related enzymatic systems are multicomponent enzymes with overlapping substrate specificities. Each enzymatic system uses an electron transport chain to transfer electrons from nicotinamide adenine dinucleotide (NADH) to the oxygenase component that consists of dissimilar subunits.^[16] The toluene dioxygenase (TDO) enzymatic system is comprised of a flavoprotein reductase component (TDO-R); a Rieske [2Fe–2S] ferredoxin component (TDO-F) and a terminal oxygenase component (TDO-O).^[17-18] The Rieske ferredoxin (TDO-F) shuttles electrons from NADH via a flavin adenine dinucleotide (FAD) cofactor contained within the reductase component (TDO-R) to the dioxygenase component (TDO-O), which catalyses the enantioselective addition of dioxygen to the aromatic substrate (Figure 3.4).^[17] The genes encoding the reductase, ferredoxin and oxygenase systems have been cloned and their respective nucleotide sequences determined.^[13]

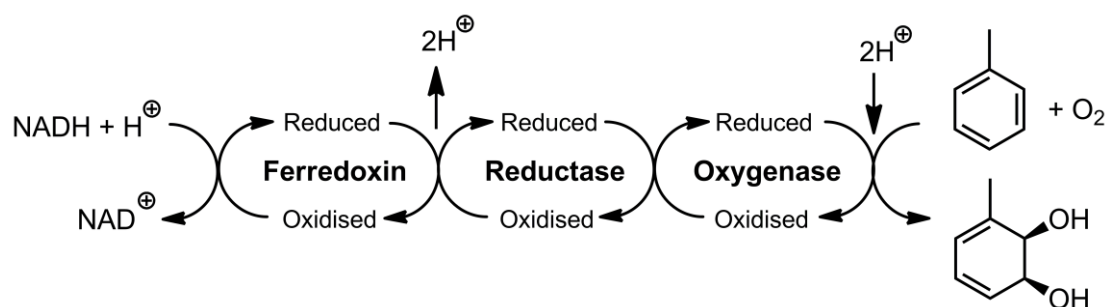


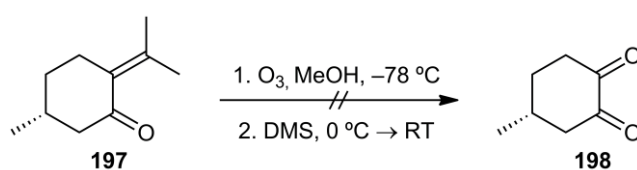
Figure 3.4: Dihydroxylation of toluene by the three-component toluene dioxygenase (TDO) enzymatic system.^[18]

3.2 – Results & Discussion

3.2.1 – Synthesis of 7-Methylhexahydrobenzo[*b*][1,4]dioxepin-3-one Analogues

The optimum choice for the reintroduction of marine fragrance characteristic into the aliphatic system was alkyl substitution at the seven-position as a means to address the proposed hydrophobic binding site of the olfactory receptor. Methylation at the seven-position would produce an aliphatic analogue of lead compound 7-methylbenzo[*b*][1,4]dioxepin-3-one (Calone 1951[®], **50**). Compound **50** is reported to contain strong marine notes relative to the unmethylated analogue (**49**).^[3, 6] Such a structural modification may assist in the docking of the molecule into the marine odorant receptor. The aliphatic binding site was predicted to be adjacent to the benzenoid ring system by Gaudin *et al.*^[4] but considered 7.23 Å distance from the benzenoid ring system by Kraft *et al.*^[2]

Synthetic access to 4-methylcyclohexane-1,2-diol beginning from chiral terpenoid compound (*R*)-(+)-pulegone (**197**) was envisioned. Conceivably compound **197** could be oxidised to give a *bis*-carbonyl intermediate followed by subsequent reduction to provide a mixture of *cis*- and *trans*-configured 4-methylcyclohexane-1,2-diol diastereomers in an unknown ratio. The reaction conditions for an oxidation using ozone were adapted from a publication by White *et al.*^[19] Reductive work-up conditions using methylthiomethane were adapted from multiple synthetic sources (Scheme 3.1).^[20-21]



Scheme 3.1: Failed ozonolysis of pulegone (**197**) to give *bis*-carbonyl intermediate **198**.

The mechanism for the synthetic reaction involving ozone (O₃) was first formulated by Rudolph Criegee in 1953.^[22] Evidence for this mechanism was later confirmed by ¹⁷O NMR spectroscopy.^[23] The reaction initiates with the 1,3-dipolar cycloaddition of ozone to an alkene to form an intermediate known as a molozonide. The unstable molozonide then reverts to the corresponding carbonyl oxide (or Criegee intermediate) and carbonyl compound in a retro-1,3-dipolar cycloaddition. This is followed by another 1,3-dipolar cycloaddition to give a relatively stable trioxolane intermediate (Figure 3.5).^[24] Varying

synthetic products can be isolated depending on the work-up conditions; reductive work-up conditions give alcohols or carbonyl compounds, whilst oxidative work-up conditions give ketones or carboxylic acids.

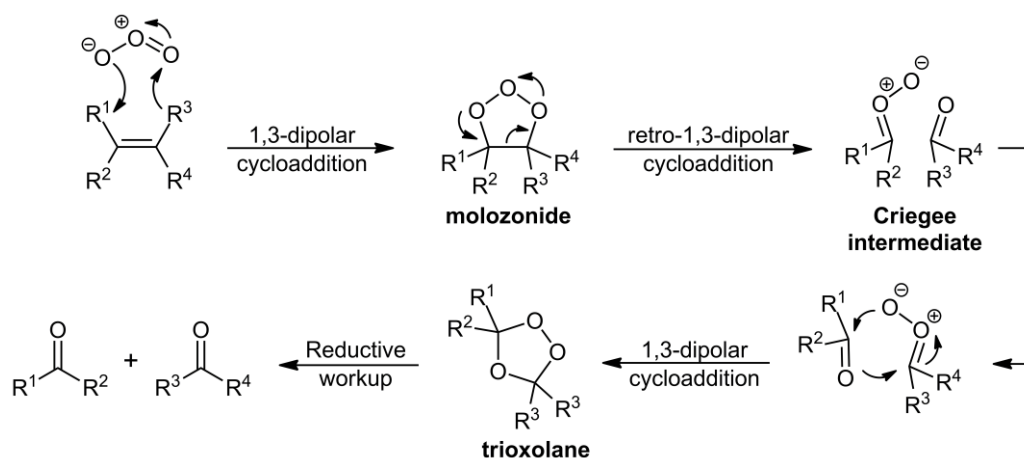


Figure 3.5: Mechanism of an ozonolysis reaction.^[22]

The ozonation reaction of compound **197** was discovered to produce a complex mixture that showed promising signs that it contained the target compound (**198**) (Figure 3.6). The ^{13}C NMR spectrum exhibited carbonyl signals located at δ 205.6/204.9 ppm which correctly matched NMR prediction software.^[25] By GC-MS analysis it appeared that the crude reaction material contained multiple unknown organics and thus the isolation of compound **198** by flash chromatography on deactivated silica was attempted. The isolated yield of the product material appeared far lower than anticipated. Further investigation by NMR revealed that the isolated material contained a number of novel signals indicating that degradation of the parent material had occurred. Attempts at additional purification by chromatography, recrystallisation and vacuum distillation were unsuccessful.

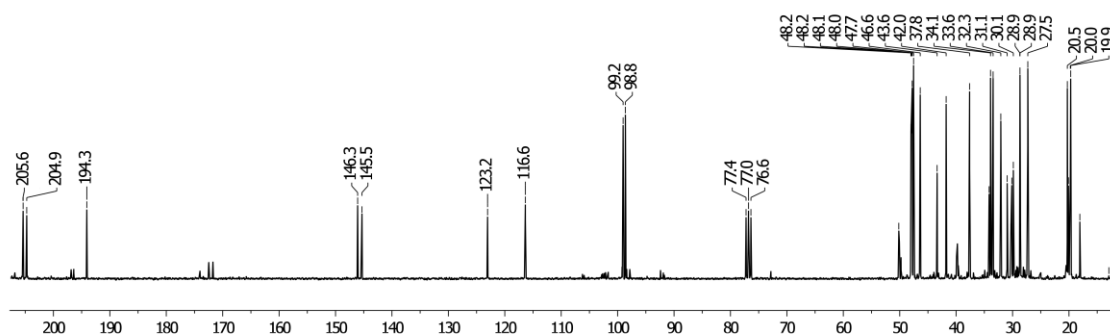
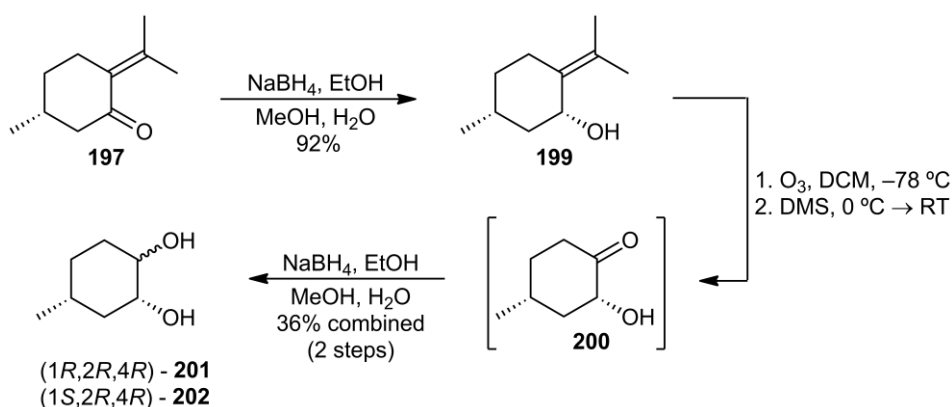


Figure 3.6: ^{13}C NMR (CDCl_3 , 75 MHz) of crude compound **198**, reaction displayed in Scheme 3.1.

An alternative synthetic route that circumvented the synthesis of an unstable *bis*-carbonyl intermediate (**198**) appeared essential. A review of the available literature revealed that a sodium borohydride reduction of (*R*)-(+)-pulegone (**197**) yielded the enantiopure hydroxyl compound *cis*-pulegol (**199**).^[26-29] The reduction reaction is stereospecific due to the high stereoselectivity of sodium borohydride in the reduction of α,β -unsaturated carbonyl compounds.^[26] The reaction was discovered to successfully provide compound **199** as a colourless solid in 92% yield and as single diastereomer (Scheme 3.2). A complication that can potentially arise during the reduction of α,β -unsaturated carbonyl compounds is the reduction of both the carbonyl and alkene moieties. The addition of cerium chloride to prevent such a problem is known as a Luche reduction.^[30] Interestingly, the addition of cerium chloride in the reduction of (*R*)-(+)-pulegone (**197**) to *cis*-pulegol (**199**) was reported to be unnecessary.^[26]



Scheme 3.2: Synthesis of *trans*- and *cis*-configured 4-methylcyclohexane-1,2-diols **201** and **202**, respectively, from pulegone (**197**) via reduction, ozonolysis and further reduction.

The enantiopure hydroxyl compound **199** was ozonated according to the synthetic methodology of Kumar *et al.*^[28] to provide acyloin intermediate **200**. Attempts at the chromatographical isolation of compound **200** proved problematic owing to instability, mirroring that of *bis*-carbonyl compound **198**. The crude reaction material was instead reduced without isolation using sodium borohydride to provide a ca. 2:1 mixture of enantiopure 4-methylcyclohexane-1,2-diol diastereomers **201** and **202**, respectively. The diastereomeric *bis*-hydroxyl compounds were readily separated by flash chromatography on silica gel owing to subtle differences in polarity. The differences in polarity arise from the increased ability of the *trans*-configured diol (**201**) to hydrogen-bond owing to less steric hindrance of the hydroxyl moieties (Figure 3.7).

Enantiomerically pure seven-methyl target compounds **204** and **206** were readily synthesised from the 4-methylcyclohexane-1,2-diol precursor compounds **201** and **202**, respectively. *Trans*-configured diol **201** was *bis*-etherified with ethyl diazoacetate in an excellent yield of 78%, followed by Dieckmann cyclisation and subsequent decarboxylation to provide *threo*-configured analogue **204** in 40% yield after flash chromatography (Scheme 3.3). It was hypothesised that the *threo*-configured seven-methyl analogue **204** would be similar in molecular conformation to lead compound Calone 1951[®] (**50**) and may therefore have high olfactory receptor affinity. Unexpectedly, compound **204** contained only minor marine character. An X-ray crystal structure was obtained for compound **204** to accurately compare the molecular resemblance of the saturated carbocyclic ring system to the aromatic carbocyclic ring system (Figure 3.8).

Dissimilarities between the molecular structures were discovered to be minor. The major difference involved the planar benzenoid ring system being replaced by a cyclohexyl ring system in chair conformation. The fact that the cyclohexyl ring system exists in a non-planar conformation also forces the substituted methyl group to be situated at an angle in reference to the plane of the molecule. In consideration of the differences, the molecular structure of compound **204** and lead compound **50** were discovered to be virtually superimposable. The molecular structure of compound **204** was also practically identical to the molecular structure of the unsubstituted *threo*-configured compound (**167**, Figure 2.28), except for the chiral methyl group (C10) situated 1.531(5) Å from C5 in an equatorial position.

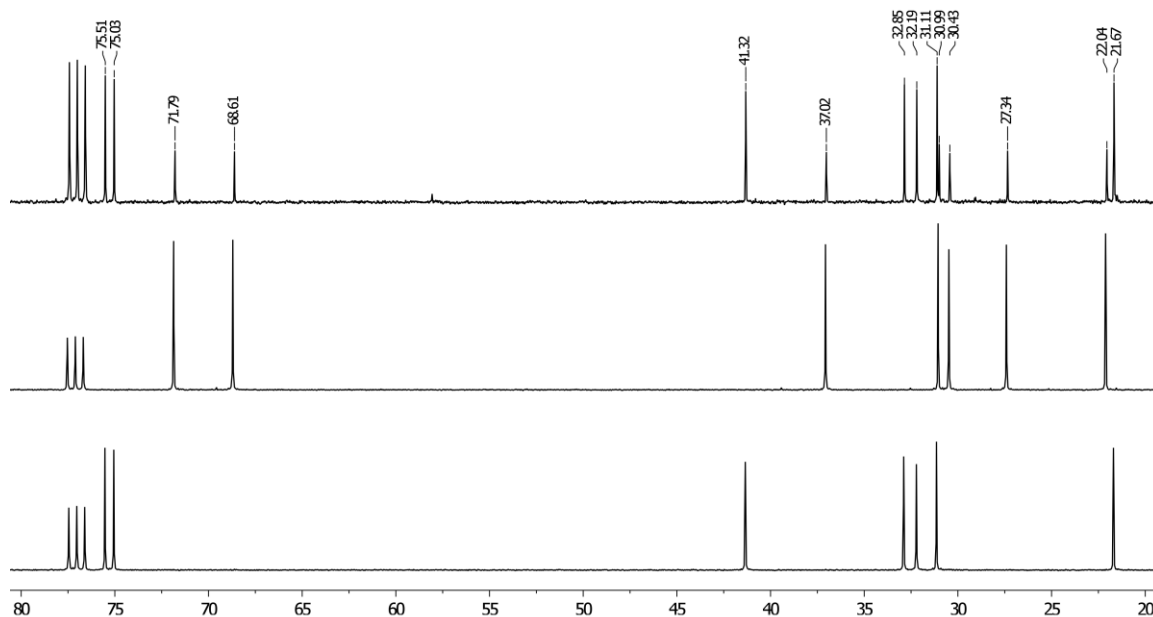
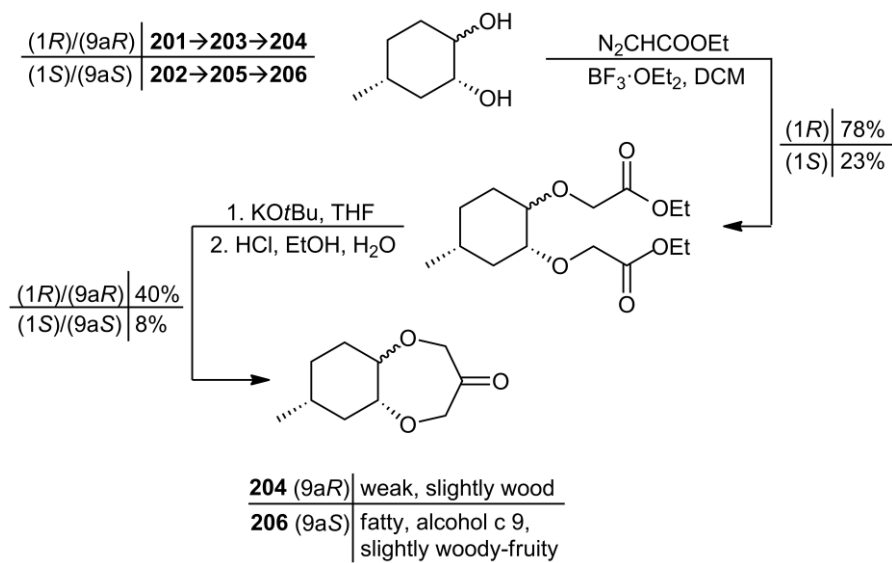


Figure 3.7: ^{13}C NMR (CDCl_3 , 75 MHz) spectra of various 4-methylcyclohexane-1,2-diol samples; Top: crude mixture of diols **201** and **202**; Middle: isolated *cis*-diol **202**; Bottom: isolated *trans*-diol **201**.



Scheme 3.3: Synthesis of 7-methylhexahydrobenzo[*b*][1,4]dioxepin-3-one diastereomers **204** and **206** from *trans*- and *cis*-configured diol compounds **201** and **202**, respectively.

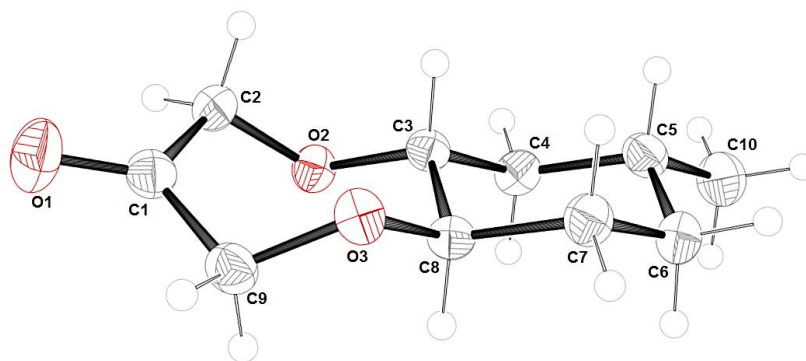


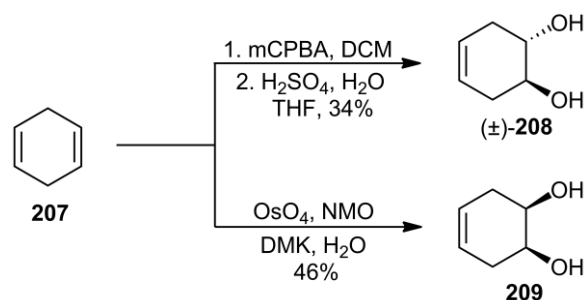
Figure 3.8: Molecular structure of (5a*R*,7*R*,9a*R*)-7-methylhexahydrobenzo[*b*][1,4]dioxepin-3-one (**204**) showing thermal ellipsoids at a 50% probability level. Crystal data for **204**: $a = 8.1940(8) \text{ \AA}$, $b = 6.1852(4) \text{ \AA}$, $c = 9.7655(11) \text{ \AA}$, $\alpha = 90^\circ$ $\beta = 96.136(9)^\circ$ $\gamma = 90^\circ$ $V = 492.10(8) \text{ \AA}^3$, $Z = 2$, and space group P 21. Crystallographic data for this structure has been deposited with the Cambridge Crystallographic Data Centre as supplementary publication no. CCDC 1020849.

The *cis*-diol diastereomer **202** was *bis*-etherified with ethyl diazoacetate to provide compound **205** as a yellow oil in 23% yield after flash chromatography. The isolated *bis*-ester compound was discovered to have a non-favourable Dieckmann cyclisation yield, yielding *erythro*-configured analogue **206** in a mere 8% yield after acid-catalysed decarboxylation (Scheme 3.3). The sample material obtained for compound **206** was discovered to be contaminated with minor quantities of compound **204** owing to impurities contained within the original *cis*-diol sample (**202**). Traces of *threo*-configured impurities were amplified to levels around four percent owing to yield differences between the alternative stereoisomeric configurations.

It was discovered that the *erythro*-configured analogue was the more potent odorant molecule, mirroring that found for the unsubstituted analogues (compounds **167** and **173**). The *erythro*-configured analogue **206** was discovered to not contain marine character which agreed with theory that the dissimilar molecular shape may lead to difficulties with the molecule entering the specific olfactory receptor. The stereochemical configuration of the 4-methylcyclohexane,1-2-diol diastereomers was confirmed by comparison of the ^1H NMR spectra of their aliphatic benzo[*b*][1,4]dioxepin-3-one derivatives. Signals associated with protons adjacent to the carbonyl moiety (C-2 and C-4) show distinct coupling patterns which are unmistakably different between the *threo*- and *erythro*-configured stereoisomers. Undisputable support for the hypothesis was provided by X-ray crystallography of compound **204**.

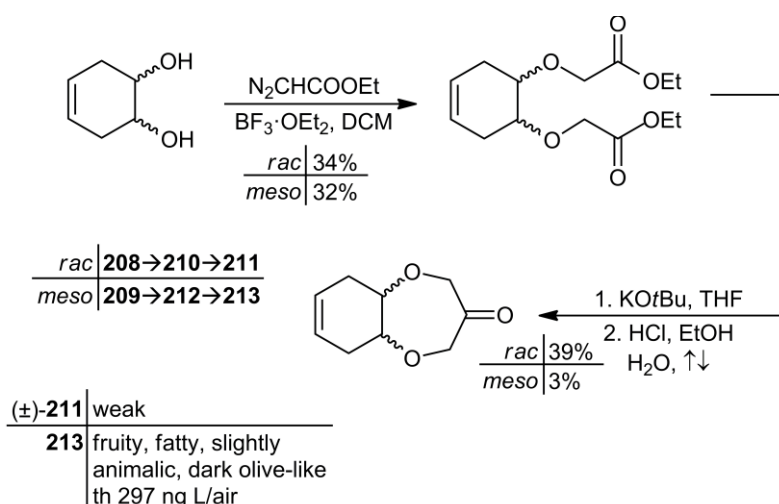
3.2.2 – Synthesis of 5a,6,9,9a-Tetrahydrobenzo[*b*][1,4]dioxepin-3-one Analogues

Both stereoisomeric configurations of the C7–C8 unsaturated hexahydrobenzo[*b*][1,4]dioxepin-3-one analogue were synthesised in order to investigate the effect of the addition of an alkene moiety/ sp^2 electron orbit. The addition may provide the analogue with marine nuances and/or lower the threshold value by aiding in receptor binding to the proposed aromatic binding site. The synthetic pathway employed to the *threo*-configured C7–C8 unsaturated analogue involved an *anti*-dihydroxylation reaction of 1,4-cyclohexadiene (**207**) using *meta*-chloroperoxybenzoic acid in dichloromethane, followed by a sulphuric acid-catalysed epoxide cleavage to yield racemic unsaturated diol (\pm)-**208** as a colourless crystalline solid in 34% yield (Scheme 3.4).^[31] The isolated *trans*-diol (**208**) was etherified using ethyl diazoacetate to give *bis*-ester compound (\pm)-**210** in a low yield of 13% yield. Dieckmann cyclisation and decarboxylation provided the unsaturated hexahydrobenzo[*b*][1,4]-dioxepin-3-one analogue (\pm)-**211** in 39% yield as a colourless crystalline solid (Scheme 3.5).



Scheme 3.4: Synthesis of *rac*- and *meso*-cyclohex-4-ene-1,2-diols (**208** and **209**, respectively) from 1,4-cyclohexadiene (**207**).

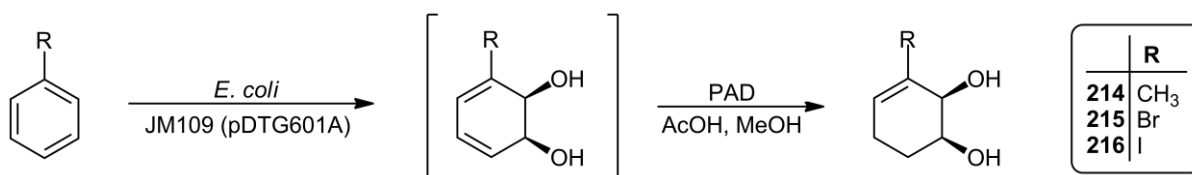
The synthetic pathway employed in the synthesis of the *erythro*-configured C7–C8 unsaturated analogue used an osmium tetroxide *syn*-dihydroxylation reaction of 1,4-cyclohexadiene (**207**) to yield unsaturated *cis*-diol compound **209** as a crystalline solid. (Scheme 3.4).^[32-33] The isolated *cis*-diol was readily *bis*-etherified with ethyl diazoacetate to yield *bis*-ester compound **212** as a yellow oil in 32% yield. Dieckmann cyclisation reactions proved problematic due to an innate tendency for the compound to undergo intermolecular reactions rather than intramolecular cyclisation. The *erythro*-configured unsaturated target compound **213** was finally isolated as a crystalline solid in a meagre 3% yield after multiple purifications by flash chromatography (Scheme 3.5).



Scheme 3.5: Synthesis of *rac*- and *meso*-5a,6,9,9a-tetrahydrobenzo[*b*][1,4]dioxepin-3-one analogues **211** and **213** from *trans*- and *cis*-configured diols **208** and **209**, respectively.

3.2.3 – Synthesis of 6/9-Substituted Aliphatic Benzo[*b*][1,4]dioxepin-3-one Analogues

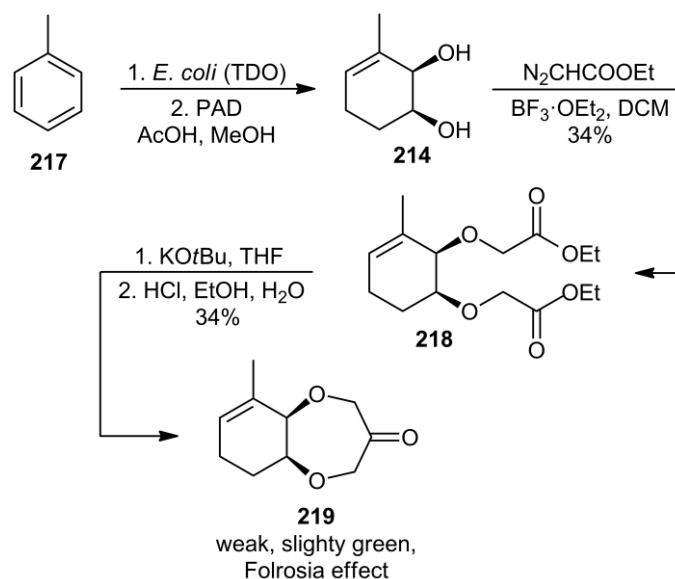
To further investigate the consequence of carbocyclic ring saturation on the benzo[*b*][1,4]dioxepin-3-one molecular template several six- and nine-substituted analogues were proposed for synthesis. Three enantiomerically pure *cis*-diol analogues were biosynthetically produced in the laboratories of collaborative researchers in preparation for the task. The *cis*-diol compounds were prepared by potassium azodicarboxylate (PAD) reduction of diene-diol metabolites produced by a recombinant strain of *Escherichia coli* (JM109 pDTG601A)^[13] which performs the *cis*-dihydroxylation of the parent aromatic material by the enzymatic action of toluene dioxygenase (TDO) (Scheme 3.6).^[7-8]



Scheme 3.6: Enzymatic oxidation followed by selective chemical reduction to yield *cis*-diol compounds **214–216** from aromatic precursor compounds. Biosynthetic and subsequent synthetic reaction performed in the laboratory of Prof. Tomáš Hudlický of Brock University, Canada.

The enantiopure 3-methyl substituted *cis*-diol compound **214**, produced by the microbial fermentation of toluene (**217**),^[34] was readily *bis*-etherified with ethyl diazoacetate to give *bis*-ester compound **218** in 34% yield as a yellow oil after flash chromatography (Scheme 3.7). Dieckmann cyclisation and

subsequent acid-catalysed decarboxylation provided nine-methyl C8–C9 unsaturated analogue **219** as a colourless crystalline solid in 34% yield (Figure 3.9).



Scheme 3.7: Synthesis of (5a*S*,9a*R*)-9-methyl-5a,6,7,9a-tetrahydrobenzo[*b*][1,4]dioxepin-3-one (**219**) from toluene (**217**).

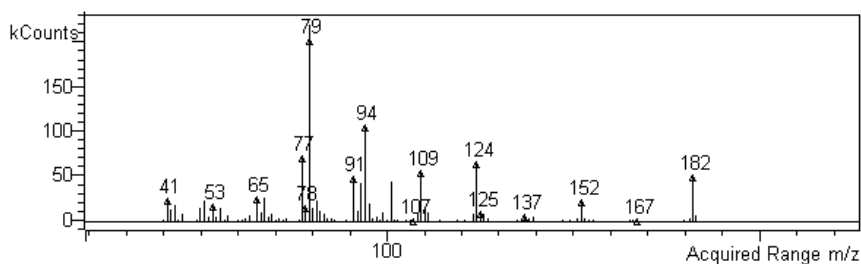
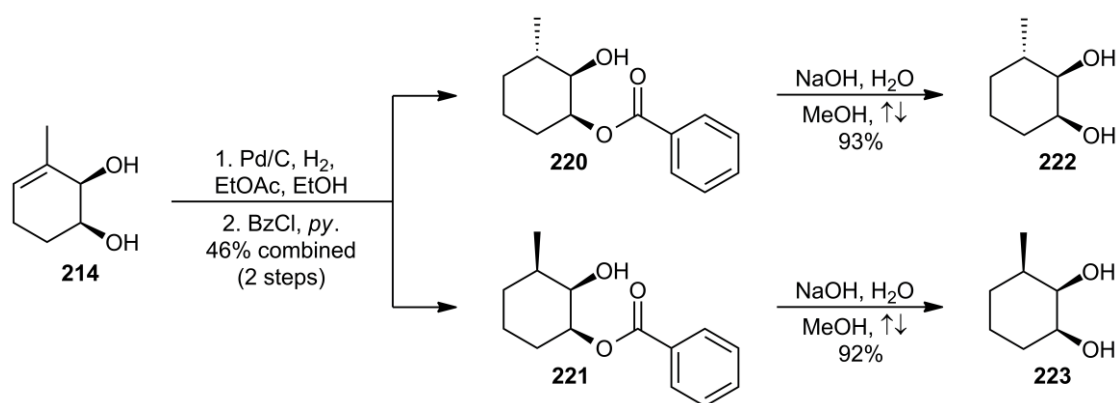


Figure 3.9: Mass spectrum (EI) of compound **219** showing molecular ion at m/z 182.

To provide synthetic access to additional enantiopure *cis*-diol analogues for chemical synthesis, the unsaturated 3-methyl *cis*-diol compound (**214**) was hydrogenated over palladium on carbon (Pd/C) under an atmosphere of hydrogen. The reaction provided a mixture of saturated *cis*-diol compounds **222** and **223** in a *ca.* 3:7 ratio, respectively.^[35] Investigations into their resolution by flash chromatography revealed that the diastereomers are unseparable owing to their analogous *cis*-configuration which results in practically identical polarity.

The separation of diastereomers by benzylation is used industrially during the resolution of (\pm)-menthol in a synthetic pathway known as the Haarmann and Reimer process.^[36] Following the methodologies of Hudlicky *et al.*^[35] the mixture of *cis*-diol compounds **222** and **223** was benzyolated using benzoyl chloride and pyridine. The two monobenzoate compounds were readily resolved by flash chromatography to provide 1-benzoyl analogues **220** and **221** in 46% combined yield as a yellow oil and colourless solid, respectively. Minor quantities of the mixed configuration *bis*-benzoyl compound were isolated and discarded. The isolated benzoate ester compounds **220** and **221** were hydrolysed in methanolic sodium hydroxide at reflux temperature to provide the enantiopure saturated *cis*-diol compounds **222** and **223** in yields of 93% and 92%, respectively (Scheme 3.8).



Scheme 3.8: Hydrogenation and benzylation of unsaturated *cis*-diol **214**, followed by separation and hydrolysis to yield enantiopure saturated *cis*-diol compounds **222** and **223**.

The relative configurations of the enantiopure material was confirmed by comparison to literature sources,^[35, 37] as well as by ¹H, ¹H NOESY NMR experiments (Figure 3.10). Only in the spectrum obtained for the (1*S*,2*R*,3*S*) configured analogue (**222**) was a Nuclear Overhauser Effect (NOE) observed between the doublet signal at δ 1.01 ($J = 6.6$ Hz) originating from the 3-Me substituent and the multiplet signal at δ 3.94–3.99 originating from the proton located at C-1. This correlation indicates that the 3-Me and 1-H substituents are on the same face of the cyclohexane ring of compound **222**. This information, alongside comparisons between known and experimental spectroscopic data, confirms the relative configuration and chirality of the 3-Me chiral center of both *cis*-diol compounds **222** and **223**.

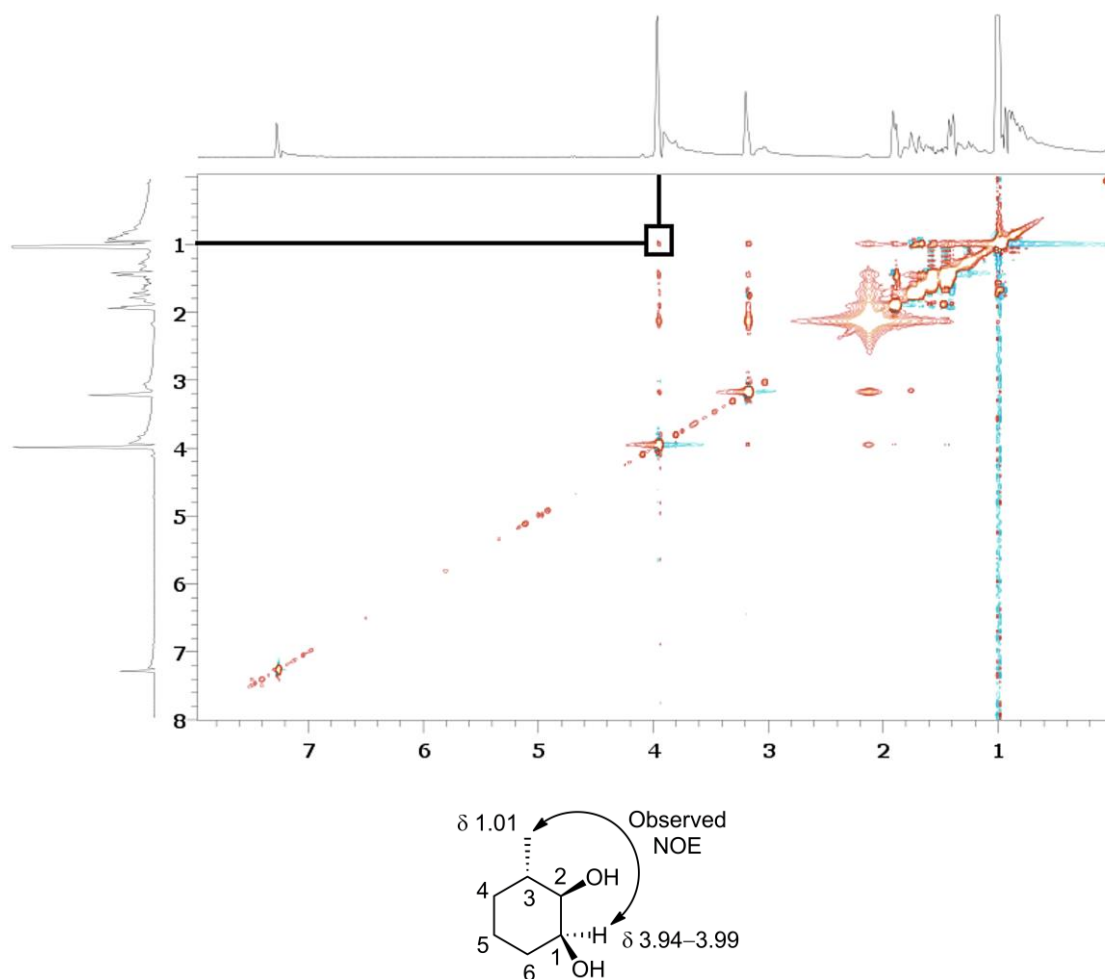
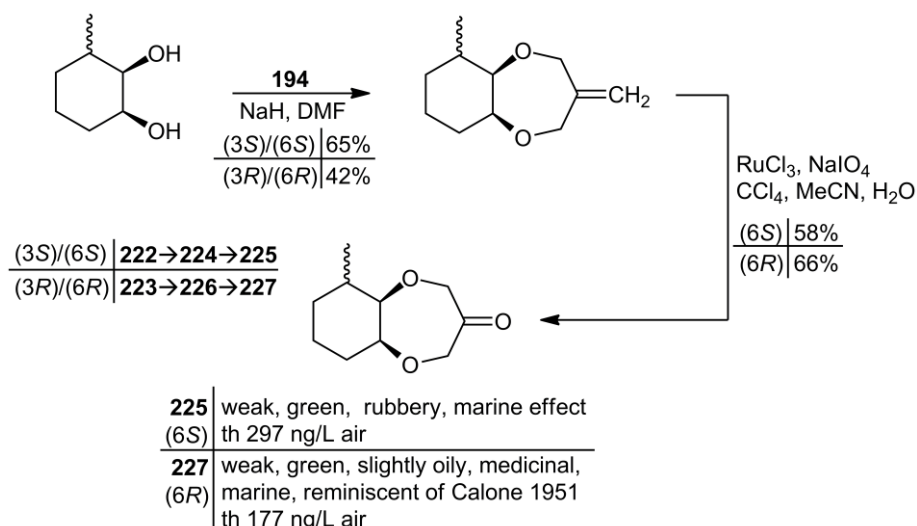


Figure 3.10: ^1H , ^1H NOESY NMR (CDCl_3 , 500 MHz) spectrum of compound **222**, showing NOE correlation between the doublet signal at δ 1.01 (originating from 3-Me) and the multiplet signal at δ 3.94–3.99 (originating from 1-H).

The (3*S*)-methyl configured *cis*-diol analogue (**222**) was readily transformed into the aliphatic benzo[*b*][1,4]dioxepin-3-one analogue by Williamson reaction. Etherification of **222** with *bis*-halogenated chain **194** provided methylene intermediate **224** in 65% yield as a yellow oil (Scheme 3.9). Katsuki-Sharpless oxidation of **224** successfully gave analogue **225** in 58% yield as a colourless crystalline solid. The (3*R*)-methyl configured *cis*-diol analogue (**223**) was similarly transformed into the benzo[*b*][1,4]dioxepin-3-one analogue. The Williamson reaction of compound **223** with *bis*-halogenated chain **194** provided methylene intermediate **226** in 42% yield as a yellow oil. A ruthenium tetroxide oxidation of compound **226** yielded analogue **227** in 66% yield as a yellow oil. Compounds **225** and **227** were both discovered to have marine odorant qualities.



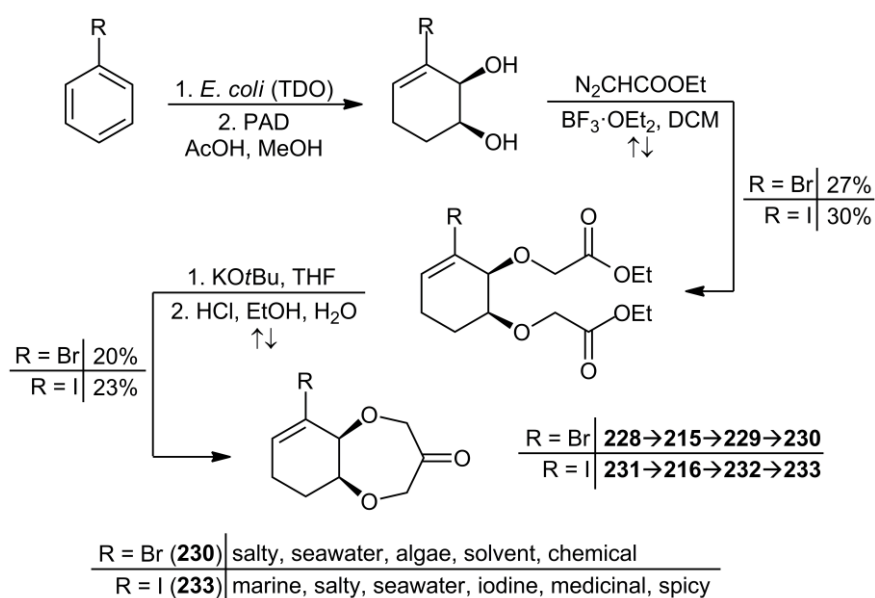
Scheme 3.9: Synthesis of 6-methylhexahydrobenzo[*b*][1,4]dioxepin-3-one diastereomers **225** and **227**

from *cis*-diol compounds **222** and **223**, respectively.

The discovery that the six-methyl substituted *erythro*-configured analogues **225** and **227** contained comparatively strong marine odorant characteristics whilst the seven-methyl substituted *threo*-configured analogue **204** contained only weak marine odorant side-notes hinted at the repulsion of the hydrophobic cyclohexyl system by the marine odorant receptor. The *erythro*-configured cyclohexyl ring system is bent at an angle to the heterocyclic ring system, as is apparent in the crystal structure of compound **173**, and may therefore be avoiding such repulsive interaction. The discovery that the seven-methyl substituted *erythro*-configured analogue **206** possessed no marine odorant qualities indicated that a positive hydrophobic interaction at the six-position was occurring between the molecules and the olfactory receptor.

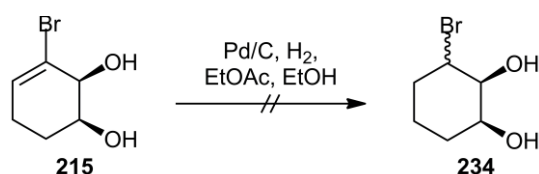
To additionally investigate the hypothetical hydrophobic binding location, attention turned to the halogen substituted *cis*-diol compounds **215** and **216**. A Dieckmann condensation route of cyclisation was nominated owing to unsaturation within the molecular structure of the carbocyclic ring system, thereby circumventing potential complications involving ring cleavage. Etherification reactions of the halogenated *cis*-diol analogues with ethyl diazoacetate under boron trifluoride catalysis required refluxing conditions to successfully furnish the *bis*-ester compounds **229** and **232**. This phenomenon was presumably due to deactivation of the electrophilic nature of the hydroxyl moieties owing to changes in electron density due to the closely situated polar haloalkene moiety.

The enantiopure three-bromo substituted analogue **215** was successfully *bis*-etherified with ethyl diazoacetate under refluxing conditions to provide compound **229** in 27% yield as a yellow oil (Scheme 3.10). Compound **229** was cyclised by Dieckmann condensation followed by subsection to an acid-catalysed decarboxylation to give analogue **230** in 20% yield as a yellow oil. The isomeric three-iodo substituted analogue **216** was *bis*-etherified with ethyl diazoacetate to give *bis*-ester compound **232** in 30% yield as a yellow oil. Dieckmann cyclisation and subsequent decarboxylation provided vinyl iodide analogue **233** in 23% yield as a yellow oil. Both halogenated analogues (**230** and **233**) were discovered to have marine odorant nuances, although more closely associated with seaweed and algae.



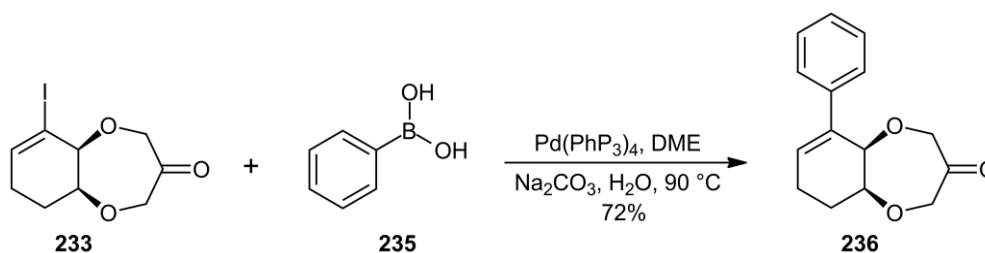
Scheme 3.10: Synthesis of halogenated analogues **230** ($\text{R} = \text{Br}$) and **233** ($\text{R} = \text{I}$) from bromobenzene (**228**) and iodobenzene (**231**), respectively.

The hydrogenation of bromo-substituted analogue **215** was attempted to provide further *cis*-diol analogues for chemical synthesis (Scheme 3.11). The reaction was discovered to provide red polymerised material which indicated that molecular bromine had been formed. Alkenyl halide hydrogenations are recognised to deliver varying quantities of the desired product alongside the hydrodehalogenated product.^[38] Multiple literature sources report successful reaction conditions to perform alkenyl halide to alkyl halide hydrogenation reactions.^[38-40] Such reactions are highly reactant specific and require metal-ligand catalysts and therefore remained outside the scope of this study.



Scheme 3.11: Failed hydrogenation reaction of brominated *cis*-diol compound **215**.

A Suzuki reaction was performed between vinyl iodide analogue **233** and boronic acid **235** to investigate if the synthesis of additional six- and nine-substituted analogues by coupling reactions were possible. Following the methodology of Bhosale *et al.*,^[41] a coupling reaction between compounds **233** and **235** was performed in dimethoxyethane at elevated temperatures using Pd(PhP₃)₄ as a catalyst and 2 M Na₂CO₃ solution as a base. Care was taken to exclude atmospheric oxygen from the reaction to prevent any disruptions to the catalytic cycle. The coupling reaction was discovered to successfully yield nine-benzyl substituted analogue **236** as a yellow oil in 72% yield (Scheme 3.12). Although successfully characterised, this compound appeared to be unstable.



Scheme 3.12: Suzuki coupling between compound **233** and phenylboronic acid (**235**) to provide (5*a**S*,9*a**R*)-9-phenyl-5*a*,6,7,9*a*-tetrahydrobenzo[*b*][1,4]dioxepin-3-one (**236**).

The Suzuki reaction, also known as the Suzuki–Miyaura reaction, was first reported in 1979.^[42] The reaction involves the coupling of an organohalide compound and a boronic acid derivative, catalysed by a palladium(0) complex and requiring base to be present. The catalytic cycle initiates with oxidative addition of the organohalide to the palladium(0) complex to produce a palladium(II) complex (Figure 3.11). This intermediate then reacts with a molecule of base, followed by transmetalation with a molecule of the base-activated boronic acid derivative. Reductive elimination yields the coupled product and regenerates the palladium(0) catalyst, thereby completing the catalytic cycle.

Oxidative addition is typically the rate-determining step in any transition metal-catalysed catalytic cycle. The relative reactivity of halides and pseudohalides decreases in order from $I > OTf > Br > Cl > F$, with organochlorides considered unreactive and organofluorides considered non-reactive in a Suzuki coupling.^[43] A wide range of palladium derived catalysts have been utilised for such cross-coupling reactions, although the palladium(0) catalyst $Pd(PPh_3)_4$ is the most commonly used catalyst for this type of transformation. Palladium(II) catalysts such as $PdCl_2(PPh_3)_2$ and $Pd(OAc)_2$, alongside triphenylphosphine or an alternative phosphine ligand, are also efficient catalysts owing to their air stability and ability to be readily reduced to an active palladium(0) complex.^[43] A variety of alternative transition metal catalysts have also been discovered to be useful for this type of transformation. Much attention has been given to nickel catalysed Suzuki–Miyaura coupling reactions due to nickel metal being more Earth abundant and also cheaper than palladium metal.^[44]

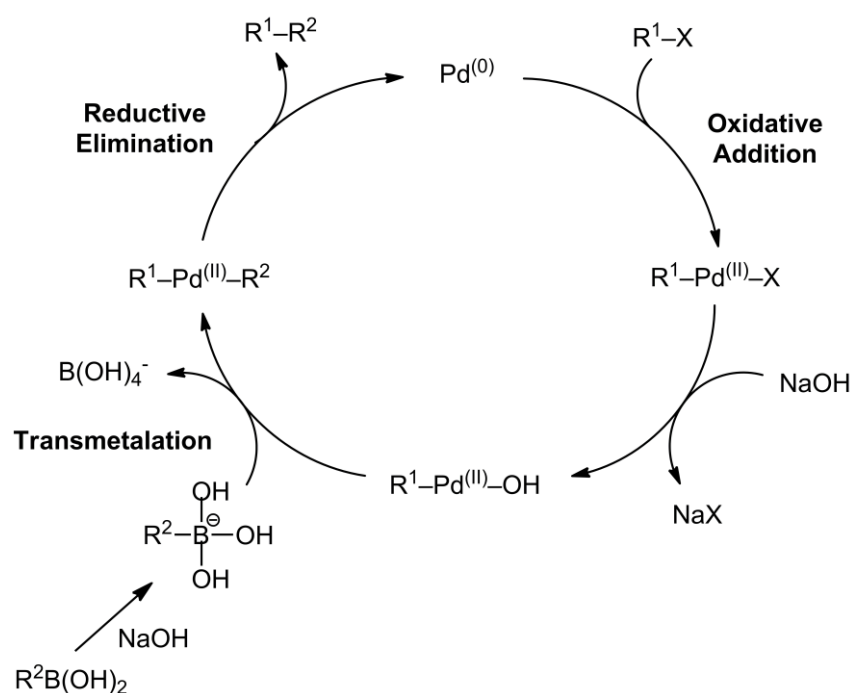
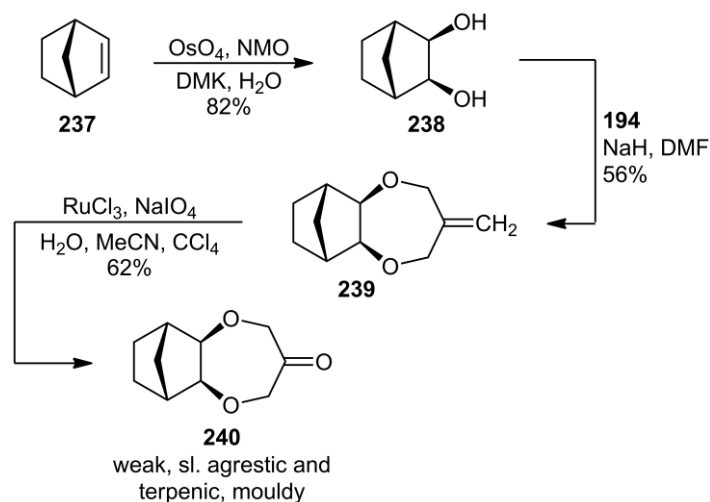


Figure 3.11: Proposed catalytic cycle for Suzuki coupling reactions.^[45]

3.2.4 – Synthesis of Alternative Ring Benzo[*b*][1,4]dioxepin-3-one Analogues

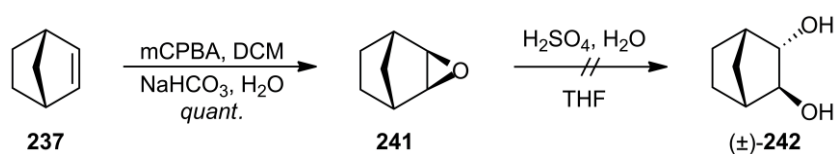
To determine the effect of bridged molecular structure on aliphatic benzo[*b*][1,4]dioxepin-3-one odorant properties, as well as the effect of substitution on both C-6 and C-9, a simple tricyclic analogue (**240**) was prepared from bicyclo[2.2.1] compound norbornene (**237**). The synthetic pathway commenced with an osmium tetroxide/*N*-methylmorpholine *N*-oxide (NMO) mediated dihydroxylation reaction of norbornene (**237**) to provide diol **238** in 82% yield as a colourless crystalline solid (Scheme 3.13). The higher steric hindrance on the *endo* face leads to a strong preference for the *exo*-configured diol stereoisomer.^[46]

Diol **238** was readily transformed into methylene intermediate **239** in 56% yield by Williamson cyclisation with *bis*-halogenated chain **194**. The intermediate methylene compound **239** was oxidised in a Katsuki-Sharpless oxidation to give bicyclo[2.2.1] saturated analogue **240** in a 62% yield as a colourless solid. Analogue **240** had no olfactory similarity to analogue **227**. This discovery indicated that the hypothetical hydrophobic binding site that provided the six- and nine-substituted analogues (compounds **225**, **227**, **230** and **233**) marine odorant characteristics was located externally to the benzo[*b*][1,4]dioxepin-3-one binding pocket, and not situated in the area above the carbocyclic ring system.



Scheme 3.13: Synthesis of tricyclic analogue **240** from norbornene (**237**).

The synthesis of an alternative bicyclo[2.2.1] *trans*-configured diol analogue commencing from norbornene was also envisioned. Norbornene (**237**) was epoxidised using *meta*-chloroperoxybenzoic acid to give *exo*-2,3-epoxynorbornane **241** as a single diastereomer in quantitative yield (Scheme 3.14). The sulphuric acid-catalysed ring-opening reaction of compound **241** provided a colourless solid that appeared to be a combination of multiple compounds by GC-MS and NMR analysis. Analysis by ^{13}C NMR revealed multiple sets of distinct signal strengths indicating that a major product was formed alongside multiple impurities (Figure 3.12). Flash chromatography was discovered to be ineffective in the isolation of the individual components of the complex reaction mixture. Repeated recrystallisations were discovered to be equally unsuccessful.



Scheme 3.14: Failed synthesis of *trans*-diol (\pm)-**242** from norbornene (**237**).

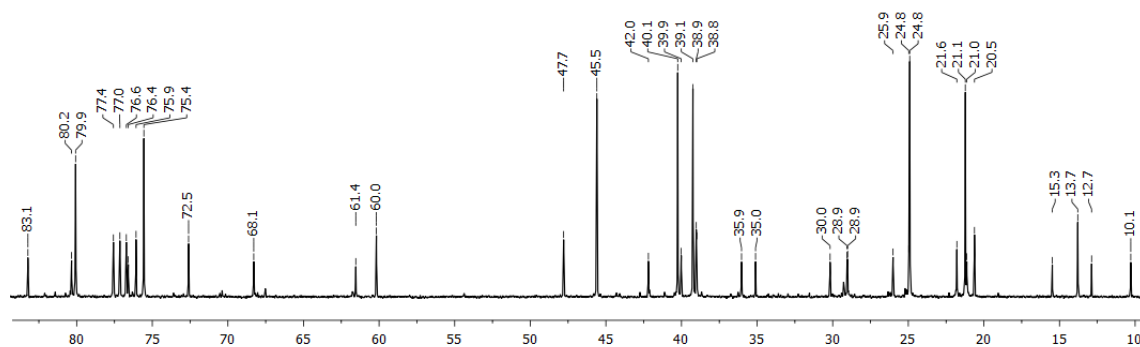
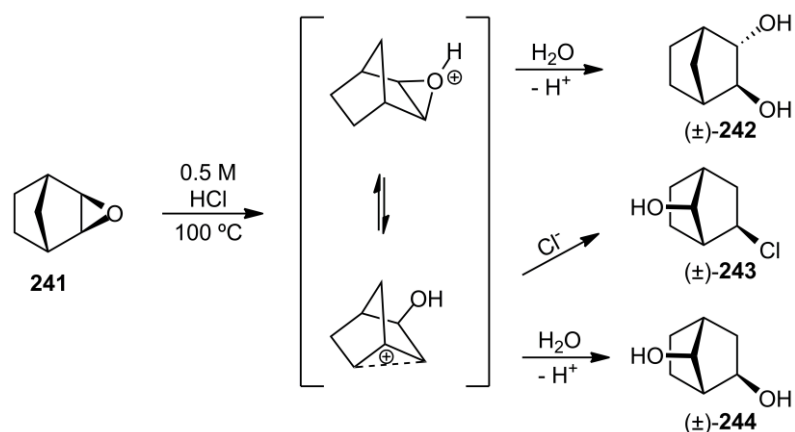


Figure 3.12: ^{13}C NMR (CDCl₃, 75 MHz) of crude material obtained for reaction of compound **241**, reaction displayed in Scheme 3.14.

An advanced literature search revealed that the ring-opening reaction of epoxide **241** under acidic conditions is recognised to yield a mixture of various *bis*-hydroxyl products owing to a norbornyl cation rearrangement reaction (Scheme 3.15).^[46-49] Research into the hydrochloric acid-catalysed reaction of epoxide **241** revealed that the reaction yielded three isomeric compounds (**242–244**), as was confirmed by X-ray crystallography of the isolated material by Willson *et al.*^[46] (Figure 3.13). The research additionally revealed that isomerisation of compound (\pm)-**242** to the thermodynamically favoured compound (\pm)-**244** was occurring.^[46] The synthesis of compound (\pm)-**242** was therefore abandoned.



Scheme 3.15: Acid-catalysed epoxide **241** ring-opening products as reported by Willson *et al.*^[46]

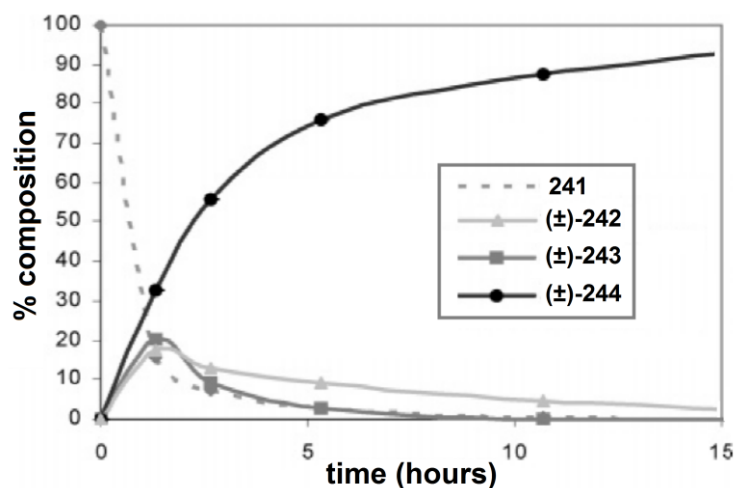
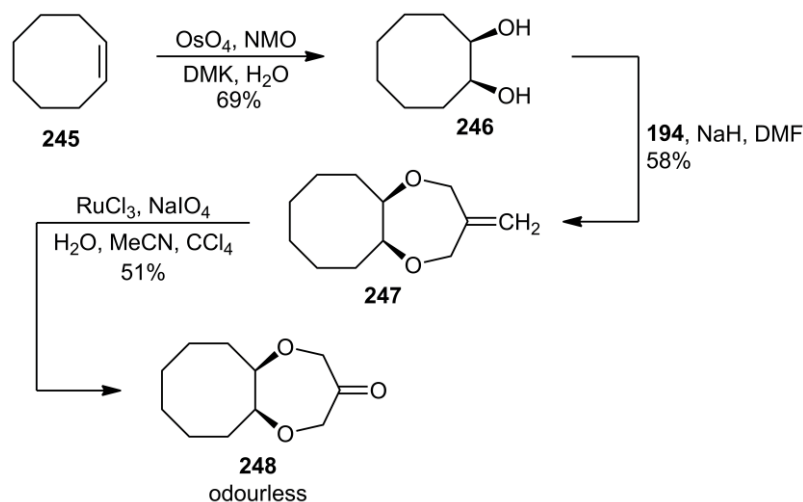


Figure 3.13: Product distribution during an acid-catalysed reaction of **241**, adapted from Willson *et al.*^[46]

To examine if perhaps an alternative sized carbocyclic ring system would have improved compatibility with the receptor binding site, the synthesis of an analogue containing an eight-membered carbocyclic ring system was performed. The *threo*-configured aliphatic analogues, which can be essentially superimposed onto the molecular structures of the aromatic lead compounds, were discovered not to have any marine odorant qualities. A number of *erythro*-configured analogues (i.e. **225**, **227**, **230** and **233**) did contain the desired characteristics, perhaps due to the carbocyclic ring system being situated outside the plane of the heterocyclic ring system and thereby avoiding repulsive interaction. The synthetic sequence commenced with an Upjohn dihydroxylation reaction of *cis*-cyclooctene (**245**) to provide *cis*-diol compound **246** in 69% yield as a colourless crystalline solid. Williamson cyclisation of compound **246** with *bis*-halogen compound **194** successfully gave methylene intermediate **247** in a 58% yield. Intermediate compound **247** was oxidised using ruthenium tetroxide to provide the

eight-membered *erythro*-configured analogue **248** which was discovered to be completely devoid of fragrance (Scheme 3.16).



Scheme 3.16: Synthesis of 8-membered analogue **248** from *cis*-cyclooctene (**245**).

3.2.5 - Structure-Odour Correlations and Conclusion

The olfactory properties of the experimental aliphatic benzo[*b*][1,4]dioxepin-3-one analogues are summarised in Table 3.1 and Table 3.2. Olfactory evaluations were performed by expert perfumers on blotter using a 10% solution of the sample substance in dipropylene glycol (DPG), odour threshold values were determined by a panel using GC–Olfactometry (GC–O). The most potent analogue synthesised was the unsubstituted *erythro*-configured analogue **173** which had an odour threshold of 141 ng/L air, a near 5000-fold decrease in potency from lead compound Calone 1951® (**50**, th 0.031 ng/L air). The saturated analogues however displayed significantly different odour profiles in comparison to their aromatic counterparts, with the exception of **225**, **227**, **230** and **233** which were discovered to have marine fragrance.

The olfactory properties of all other analogues are completely in accordance with the published marine olfactophore models^[1-2, 4] that require an aromatic binding feature to be present within the molecular structure. These compounds are therefore binding to multiple non-marine olfactory receptors, rather less specifically and with low affinity. This results in a potpourri of different odour impressions ranging from fruity, medicinal and chemical to fruity-green and fatty, and with odour thresholds above 100 ng/L air they are considered quite weak odorant molecules.

Interestingly, the unsaturation of (±)-**167**→(±)-**211** and **173**→**213** had a detrimental effect on odour strength. Unsaturation of the *threo*-configured analogue (±)-**167** caused the odour threshold to rise from 210 ng/L air to a threshold value out of the range of what can be considered useful as a perfumery ingredient. The unsaturated *erythro*-analogue **213** had its odour threshold rise by 156 ng/L air in comparison to its saturated counterpart **173**. The fruity-fatty, slightly animalic odour of **213** was found interesting in that it distinctly recalled dark olives, which is a rare and unusual fragrance character. Unfortunately, GC–O analysis revealed that compound **213** was too weak to be considered for use as commercial perfumery material.

Methyl substitution at the seven-position as a way to address the hydrophobic binding site was not effective as compounds **204** and **206** were rather weaker by blotter analysis than **167** and **173**. These analogues did somewhat address different odour receptors as they were slightly woody-fruity in odour, and in the case of **206**, more specifically recalling 1-nonanol. The published marine olfactophore models require longer alkyl chains to address the hydrophobic binding pocket and this result showed that the methyl group of Calone 1951® (**50**) does not have much affinitive receptor interaction. Longer alkyl substituents up to butyl length may conformationally hinder receptor binding as only after a pentyl length alkyl chain onwards does a positive receptor affinity result.

The halogenated 5a,6,7,9a-tetrahydrobenzo[*b*][1,4]dioxepin-3-ones compounds **230** and **233** had salty-marine odours that were more reminiscent of seawater and algae, with unpleasant medicinal and chemical aspects. The odour profile of vinyl iodide **233** had a distinct iodine connotation, potentially indicating that some degradation by nasal enzymes may have liberated iodinated compounds of lower molecular weight, or even molecular iodine. This may also explain the chemical and solvent-type malodours of vinyl bromide **230**. Further studies of halogen substituted analogues would be necessary to rule this out; however, cosmetic laws prohibit the use of such halogenated odorants in perfumery.

#	Molecular Structure	Description and Threshold
(±)-167		<p>Odour description: Medicinal, fruity odour that is linear in the dry-down with additional sweet facets in the fond.</p> <p>Odour threshold: 210 ng/L air (stan. dev. 176 ng/L air).</p>
173		<p>Odour description: Fruity, animalic odour of green tonality with chemical aspects and acidic facets in the dry-down.</p> <p>Odour threshold: 141 ng/L air (stan. dev. 99 ng/L air).</p>
(±)-211		<p>Odour description: Very weak to odourless, and uncharacteristic in smell.</p>
213		<p>Odour description: Fruity-fatty, slightly animalic odour that also recalls dark olives, and upon dry-down becomes more balsamic, fruity and cinnamate-like.</p> <p>Odour threshold: 297 ng/L air (stan. dev. 125 ng/L air).</p>
204		<p>Odour description: Weak, slightly woody odour that is linear upon dry-down and displays slightly marine, watery and salty nuances.</p>
206		<p>Odour description: Odour reminiscent of fatty alcohols, especially nonanol, with slightly woody and fruity character and green-rubbery aspects in the dry-down.</p>
240		<p>Odour description: Very weak, slightly agrestic and terpenic, slightly mouldy.</p>
248		<p>Odour description: Odourless.</p>

Table 3.1: Experimental aliphatic benzo[*b*][1,4]dioxepin-3-one library displaying odour descriptions, and odour thresholds, where applicable.

The aromatic ring system thus appears to be a prerequisite for binding to the marine odour receptor(s) and an alkene or methyl substituent had little effect on receptor affinity. The question remained as to why compounds **225**, **227**, **230** and **233** appeared to have residual affinity for the marine odourant receptor(s). The superposition analysis of the molecular structures of **167** and **227** on the minimum-energy conformer of Calone 1951[®] (**50**) may offer some explanation (Figure 3.14).

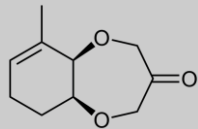
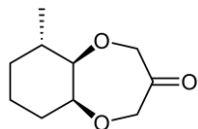
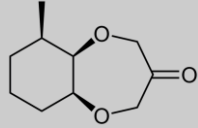
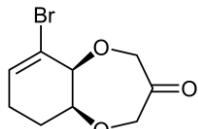
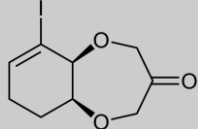
#	Molecular Structure	Description and Threshold
219		Odour description: Weak, slightly green odour with a Folrosia (4-(1-methylethyl)cyclohexan-1-ol) effect.
225		Odour description: Weak, green-rubbery odour with a marine effect. Odour threshold: 297 ng/L air (stan. dev. 188 ng/L air).
227		Odour description: Weak, green, slightly oily medicinal odour reminiscent of the medicinal aspects of Calone 1951 [®] , but also with marine facets of Calone 1951 [®] . Odour threshold: 177 ng/L air (stan. dev. 72 ng/L air).
230		Odour description: Salty, seawater, algae, solvent-like and chemical aspects.
233		Odour description: Marine, salty, seawater, iodine effect, medicinal, slightly spicy, chemical aspects.

Table 3.2: Experimental six- and nine-substituted aliphatic benzo[*b*][1,4]dioxepin-3-one library displaying odour descriptions, and odour thresholds, where applicable.

The *threo*-configured analogue **167** (blue) overlays agreeably with Calone 1951[®] (**50**, black), except that it features no methyl substitution, is non-planar and contains no aromatic binding element for the receptor. The aromatic binding pocket of the olfactory receptor appears to refuse the cyclohexyl hydrophobe: a negative interaction. In the *erythro*-configured compounds **225** and **227** the cyclohexyl ring system is at an angle to the heterocyclic ring system and hence is bent away avoiding such

repulsion. The unsaturated analogue **219** is at a shallower angle and is therefore closer to the aromatic binding feature of the marine receptor which could explain the lack of marine tonality.

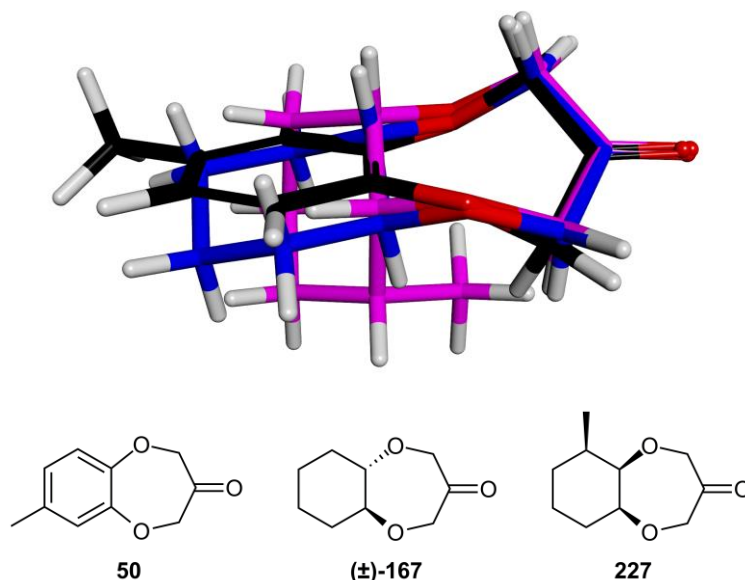


Figure 3.14: Rigid-body superposition of the X-ray structure of **167** (blue, Figure 2.28) and the structure of **227** (magenta) derived from X-ray coordinates of **173** (Figure 2.29) on the minimum-energy conformer of Calone 1951[®] (**50**, black) made with the Discovery Studio 4.1 software package using a 100% electrostatic field.^[50]

The explanation as to why the parent *erythro*-configured compounds **173** and **206** do not contain marine odour can be deduced from a positive hydrophobic interaction of the six-methyl group with the olfactory receptor(s). It was discovered that the C8–C9 unsaturation of the halogenated compounds **230** and **233** did not prevent marine odour character as was discovered for the methyl substituted analogues **219**, **225** and **227**. It is conceivable that the larger halogen substituents and their polarisability assists the molecules in binding to the hypothesised hydrophobic binding site, thereby overcoming some repulsion of the cyclohexyl ring system from the olfactory receptor.

It is known that two hydrogen-bond acceptors are sufficient for binding and that therefore a hydrophobic methyl unit is tolerated opposite to the remaining ether oxygen atom. In any case, the weak character, intensity and persistence of the aliphatic analogues is indicative that the planar aromatic ring structure is an indispensable feature of the marine odorant family and that simple modifications such as the addition of a methyl group or alkene to the basic molecular structure is not sufficient to aid in receptor binding.

3.3 – Experimental

General Procedure A:

To an ice-cool solution of diol compound (40 mmol) and ethyl diazoacetate (10 g, 88 mmol, 2.2 equiv) in DCM (80 mL) was slowly added $\text{BF}_3 \cdot \text{OEt}_2$ (0.5 mL). After addition was complete, the solution was held at 0 °C for 1 h before being quenched by the addition of a saturated aqueous solution of NaHCO_3 (100 mL). The mixture was then extracted with EtOAc (3 × 100 mL), the organic extracts pooled, dried (MgSO_4) and concentrated under reduced pressure. The resulting residue was purified by flash chromatography on silica gel (EtOAc/hexane; 2:8) to yield the corresponding *bis*-ester compound.

General Procedure B:

A solution of *bis*-ester compound (20 mmol) in THF (150 mL) was added dropwise to a stirred suspension of KO^tBu (4.5 g, 40 mmol, 2 equiv) in THF (100 mL) with cooling to 0 °C. Stirring was continued at 0 °C for 2 h before being quenched by the addition of 0.2 M HCl (800 mL) and ice (500 g). The resulting solution was then extracted with DCM (3 × 200 mL), the organic extracts pooled, dried (MgSO_4) and concentrated under reduced pressure. The resulting residue was taken up in EtOH (100 mL) and 2 M HCl (500 mL) and the mixture stirred at reflux for 2 h. The solution was diluted with H_2O (300 mL) and extracted with DCM (3 × 200 mL). The combined organic extracts were washed with H_2O (200 mL), dried (MgSO_4) and concentrated under reduced pressure. The resulting residue was purified by flash chromatography on silica gel (EtOAc/hexane; 1:9) to yield the corresponding ketone.

General Procedure C:

A solution of the diol compound (10.5 mmol) in DMF (30 mL) was added dropwise to a suspension of sodium hydride (1.05 g, 26.2 mmol, 60% dispersion in mineral oil) in DMF (60 mL) and the solution left to stir for 1 h. A solution of 3-chloro-2-(chloromethyl)-1-propene (1.31 g, 10.5 mmol) in DMF (40 mL) was then added dropwise over a period of 1 h, and the solution allowed to stir for 24 h. The reaction was then quenched by the additional of a saturated aqueous solution of NaHCO_3 (100 mL), extracted with Et_2O (4 × 100 mL), the organic extracts pooled and washed with H_2O (2 × 100 mL) before being dried (MgSO_4) and concentrated under reduced pressure. The resulting residue was then purified by flash chromatography on silica gel (EtOAc/hexane; 5:95) to yield the corresponding methylene compound.

General Procedure D:

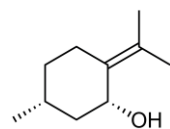
The methylene compound (5 mmol) was dissolved in MeCN (25 mL), H_2O (25 mL), and CCl_4 (15 mL), and sodium metaperiodate (1.07 g, 5 mmol) and ruthenium trichloride (0.1 g, 0.5 mmol) were added. The mixture was stirred for 24 h, then further sodium metaperiodate (1.07 g, 5 mmol) and ruthenium trichloride (0.1 g, 0.5 mmol) were

added. The solution was stirred for a further 24 h. The reaction mixture was then poured into H₂O (100 mL) and the resulting mixture was extracted with DCM (3 x 100 mL). The combined organic extracts were washed with a saturated aqueous solution of NaHSO₃ (100 mL) and with H₂O (100 mL), dried (MgSO₄), and concentrated under reduced pressure. The resulting residue was purified by flash chromatography on silica gel (EtOAc/hexane; 1:9) to give the corresponding ketone.

General Procedure E:

To a solution of alkene (20 mmol) and NMO (22 mmol) in acetone/H₂O (4:1, 50 mL) was added OsO₄ (100 mg) and the resulting solution stirred at RT for 48 h. The reaction was then quenched by the addition of Na₂SO₃ (1 g) and left for 1 h before being concentrated under reduced pressure. The residual oil was then taken up in H₂O (100 mL), extracted with EtOAc (5 x 100 mL), the organic extracts pooled and dried (MgSO₄) before being concentrated under reduced pressure. The resulting residue was then recrystallised from EtOAc/hexane to yield the corresponding *cis*-diol compound.

(1*R*,5*R*)-5-Methyl-2-(propan-2-ylidene)cyclohexan-1-ol (199):^[26]



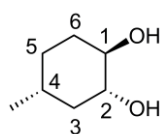
A suspension of NaBH₄ (4 g, 105.7 mmol) in EtOH (200 mL) was added dropwise to an ice-cold solution of (*R*)-pulegone (15 g, 98.5 mmol) in MeOH (180 mL) and H₂O (40 mL). Stirring was continued for 2 h at RT. The reaction was then poured into a saturated aqueous solution of NaCl (500 mL) and the mixture extracted with hexane (3 x 300 mL). The organic extracts were pooled, dried (MgSO₄) and concentrated under reduced pressure to yield (1*R*,5*R*)-5-methyl-2-(propan-2-ylidene)cyclohexan-1-ol (14.78 g, 92%) as a colourless solid. $[\alpha]_D^{23} = -167.3^\circ$ (c = 1.9, EtOH). mp: 28–39 °C. (lit. $[\alpha]_D^{25} = -105.2^\circ$ (c = 1.9, EtOH). mp: 30–31 °C).^[26] Full structural assignment could not be completed. ¹H NMR (CDCl₃, 300 MHz): δ 4.74–4.69 (m, 1H), 2.41–2.18 (m, 2H), 1.85–1.39 (m, 11H), 1.20 (d, *J* = 2.8 Hz, 1H), 1.12 (d, *J* = 6.9 Hz, 3H). ¹³C NMR (CDCl₃, 75 MHz): δ 132.4, 125.3, 67.7, 39.3, 31.7, 26.6, 22.1, 21.1, 20.0, 19.3. HRMS: *m/z* calculated for C₁₀H₁₈O: 154.1358 [M]⁺; Found: 154.1354.

Synthesis of diols 201 and 202:

A solution of (1*R*,5*R*)-5-methyl-2-(propan-2-ylidene)cyclohexan-1-ol (13.7 g, 88.8 mmol) in DCM (400 mL) was cooled to –78 °C. The cooled solution was then treated with a continuous stream of ozone and the reaction monitored for completion by the absence of starting material. Upon completion the addition of ozone was arrested and the reaction mixture purged with nitrogen for 1 h at –78 °C. Methylthiomethane (70 mL) was then added and the resulting mixture stirred at 0 °C for 1 h followed by at RT overnight. The reaction was then concentrated under reduced pressure followed by extraction with EtOAc (4 x 100 mL). The organic extracts were pooled before being dried (MgSO₄) and concentrated under reduced pressure. The residue obtained was then taken up in MeOH

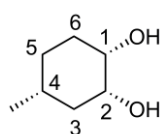
(150 mL) and H₂O (25 mL), cooled to 0 °C before NaBH₄ (3 g) in EtOH (150 mL) was added dropwise. Stirring was then continued for 2 h at RT. The reaction was poured into a saturated aqueous solution of NaCl (500 mL) and the mixture was extracted with EtOAc (3 x 300 mL). The organic extracts were pooled, dried (MgSO₄) and concentrated under reduced pressure. The resulting oil was purified by flash chromatography on silica gel (EtOAc/hexane; 55:45) to yield a 2:1 ratio of (1*R*,2*R*,4*R*)-4-methylcyclohexane-1,2-diol (2.74 g) and (1*S*,2*R*,4*R*)-4-methylcyclohexane-1,2-diol (1.42 g) in 36% combined yield.

(1*R*,2*R*,4*R*)-4-Methylcyclohexane-1,2-diol (201):



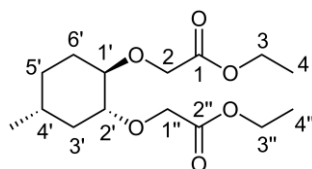
Colourless solid. $[\alpha]_D^{24} = -28.5^\circ$ ($c = 0.36$, DCM). mp: 62–63 °C. IR (ATR): $\tilde{\nu} = 3300$ (ν O–H), 2919 (ν C–H), 1055 (ν C–O) cm^{-1} . ¹H NMR (CDCl₃, 300 MHz): δ 3.46–3.30 (m, 2H, 1-,2-H), 2.15 (d, $J = 3.2$ Hz, 1H)/2.10 (d, $J = 3.5$ Hz, 1H) (1-,2-OH), 2.00–1.91 (m, 2H)/1.73–1.46 (m, 2H, 3-,4-,5-,6-H), 1.40–1.24 (m, 1H, 5-H), 1.09–0.92 (m, 2H, 3-,6-H), 0.94 (d, $J = 6.4$ Hz, 3H, 4-Me). ¹³C NMR (CDCl₃, 75 MHz): δ 75.5/75.0 (2d, C-1,-2), 41.3/32.8 (2t, C-3,-6), 32.1 (t, C-5), 31.1 (d, C-4), 21.6 (q, 4-Me). HRMS: m/z calculated for C₇H₁₄O₂: 130.0994 [M]⁺; Found: 130.1008.

(1*S*,2*R*,4*R*)-4-Methylcyclohexane-1,2-diol (202):

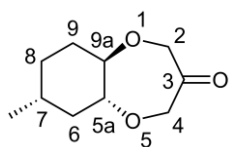


Colourless solid. $[\alpha]_D^{26} = +23.2^\circ$ ($c = 0.36$, DCM). mp: 88–89 °C. IR (ATR): $\tilde{\nu} = 3296$ (ν O–H), 2951 (ν C–H), 1033 (ν C–O) cm^{-1} . ¹H NMR (CDCl₃, 300 MHz): δ 3.94 (s, 1H, 2-H), 3.66–3.55 (m, 1H, 1-H), 2.36–2.30 (m, 1H, 2-OH), 2.23 (d, $J = 5.6$ Hz, 1H, 1-OH), 1.97–1.86 (m, 1H, 3-H) 1.69–1.61 (m, 1H, 6-H), 1.52–1.12 (m, 5H, 3-,4-,6-H, 5-H₂), 0.94 (d, $J = 6.2$, 3H, 4-Me). ¹³C NMR (CDCl₃, 75 MHz): δ 71.7 (d, C-1), 68.5 (d, C-2), 36.9 (t, C-6), 30.9 (d, C-4), 30.3 (t, C-3), 27.3 (t, C-5), 22.0 (q, 4-Me). HRMS: m/z calculated for C₇H₁₄O₂: 130.0994 [M]⁺; Found: 130.0995.

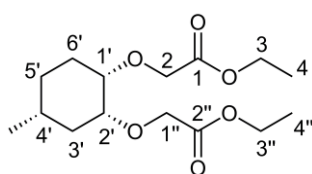
Diethyl 2,2'-(((1*R*,2*R*,4*R*)-4-methylcyclohexane-1,2-diyl)bis(oxy))diacetate (203):



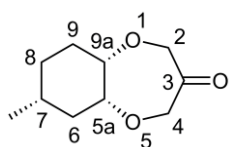
Following General Procedure A. Yellow oil, 78% yield. $[\alpha]_D^{24} = -4.2^\circ$ ($c = 1.07$, DCM). IR (ATR): $\tilde{\nu} = 1751/1732$ (ν ester C=O), 1198 (ν ester C–O), 1121 (ν C–O) cm^{-1} . Full structural assignment could not be completed. ¹H NMR (CDCl₃, 300 MHz): δ 4.07–3.80 (m, 8H), 3.06–2.90 (m, 2H), 1.82–1.72 (m, 2H), 1.38–1.28 (m, 1H), 1.20–0.90 (m, 2H), 0.96 (t, $J = 7.1$ Hz, 6H), 0.75–0.53 (m, 2H), 0.61 (d, $J = 6.6$ Hz, 3H). ¹³C NMR (CDCl₃, 75 MHz): δ 170.3, 170.2, 83.2, 82.6, 67.4, 67.4, 59.9, 38.9, 32.0, 30.3, 29.7, 21.0, 13.6. HRMS: m/z calculated for C₁₅H₂₆O₆: 302.1729 [M]⁺; Found: 302.1719.

(5a*R*,7*R*,9a*R*)-7-Methylhexahydro-2*H*-benzo[*b*][1,4]dioxepin-3(4*H*)-one (204):

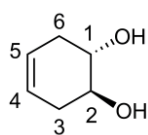
Following General Procedure B. Colourless solid, 40% yield. $[\alpha]_D^{26} = -278.1^\circ$ ($c = 1.00$, DCM). mp: 47–49 °C. IR (ATR): $\tilde{\nu} = 2945$ (ν C–H), 1722 (ν C=O), 1120 (ν C–O) cm^{-1} . $^1\text{H NMR}$ (CDCl_3 , 300 MHz): δ 4.30 (d, $J = 16.6$ Hz, 2H, 2-,4-H), 4.24 (d, $J = 16.2$ Hz, 2H, 2-,4-H), 3.39–3.25 (m, 2H, 5a-,9a-H), 2.04–1.94 (m, 2H)/1.76–1.66 (m, 1H)/1.62–1.36 (m, 2H)/1.28–0.93 (m, 2H) (7-H, 6-,8-,9-H₂), 0.97 (d, $J = 6.6$ Hz, 3H, 7-Me). $^{13}\text{C NMR}$ (CDCl_3 , 75 MHz): δ 211.6 (s, C-3), 88.3/87.8 (2d, C-5a,-9a), 77.2/77.2 (2t, C-2,-4), 39.7/32.6/30.9/30.8 (1d,3t, C-6,-7,-8,-9), 21.5 (q, 7-Me). HRMS: m/z calculated for $\text{C}_{10}\text{H}_{16}\text{O}_3$: 184.1099 $[\text{M}]^+$; Found: 184.1089. Odour description: Weak, slightly woody odour that is linear upon dry-down and displays slightly marine, watery and salty nuances.

Diethyl 2,2'-(((1*S*,2*R*,4*R*)-4-methylcyclohexane-1,2-diyl)bis(oxy))diacetate (205):

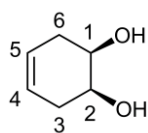
Following General Procedure A. Yellow oil, 23% yield. $[\alpha]_D^{22} = +4.1^\circ$ ($c = 1.09$, DCM). IR (ATR): $\tilde{\nu} = 2928$ (ν C–H), 1750 (ν ester C=O), 1197 (ν ester C–O), 1117 (ν C–O) cm^{-1} . Full structural assignment could not be completed. $^1\text{H NMR}$ (CDCl_3 , 300 MHz): δ 4.31–4.12 (m, 8H), 3.94–3.89 (m, 1H), 3.43–3.36 (m, 1H), 2.11–2.02 (m, 1H), 1.79–1.71 (m, 1H), 1.56–1.21 (m, 11H), 0.94 (d, $J = 5.8$ Hz, 3H). $^{13}\text{C NMR}$ (CDCl_3 , 75 MHz): δ 170.9, 170.5, 80.7, 74.8, 67.2, 65.3, 60.3, 60.2, 33.8, 31.0, 28.4, 27.7, 21.7, 13.9, 13.9. HRMS: m/z calculated for $\text{C}_{15}\text{H}_{26}\text{O}_6$: 302.1729 $[\text{M}]^+$; Found: 302.1747.

(5a*R*,7*R*,9a*S*)-7-Methylhexahydro-2*H*-benzo[*b*][1,4]dioxepin-3(4*H*)-one (206):

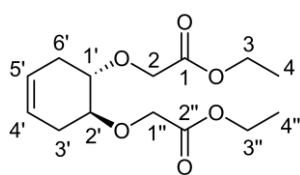
Following General Procedure B. Yellow oil, 8% yield. $[\alpha]_D^{22} = +176.6^\circ$ ($c = 1.04$, DCM). IR (ATR): $\tilde{\nu} = 2927$ (ν C–H), 1721 (ν C=O), 1123 (ν C–O) cm^{-1} . $^1\text{H NMR}$ (CDCl_3 , 300 MHz): δ 4.43 (d, $J = 17$ Hz, 1H)/4.25 (d, $J = 16.4$ Hz, 1H)/4.16 (d, $J = 16.4$ Hz, 1H)/3.95 (d, $J = 17$ Hz, 1H) (2-,4-H₂), 3.91–3.80 (m, 2H, 5a-,9a-H), 2.01–1.91 (m, 1H)/1.72 (q, $J = 17.9$ Hz, 1H)/1.60–1.36 (m, 4H)/1.26–1.07 (m, 1H) (7-H, 6-,8-,9-H₂), 0.98 (d, $J = 6.2$ Hz, 3H, 7-Me). $^{13}\text{C NMR}$ (CDCl_3 , 75 MHz): δ 212.0 (s, C-3), 81.9/78.6 (2d, C-5a,-9a), 77.2/69.9 (2t, C-2,-4), 32.1/31.4/30.5/28.3 (1d,3t, C-6,-7,-8,-9), 22.1 (q, 7-Me). HRMS: m/z calculated for $\text{C}_{10}\text{H}_{16}\text{O}_3$: 184.1099 $[\text{M}]^+$; Found: 184.1105. Odour description: Odour reminiscent of fatty alcohols, especially nonanol, with slightly woody and fruity character and green-rubbery aspects in the dry-down.

***rac*-Cyclohex-4-ene-1,2-diol (208):**^[31]


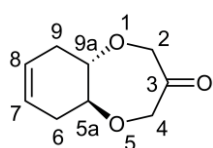
To a stirred solution of cyclohexa-1,4-diene (5 g, 62.5 mmol) in DCM (50 mL) at 0 °C was added dropwise mCPBA (14.3 g, 63.75 mmol, ≤77% purity) in DCM (300 mL) over a period of 1 h. After addition was complete a 5% aqueous solution of NaHCO₃ (175 mL) was added and stirring continued for 3 h. The organic layer was then separated and washed with saturated aqueous solutions of NaHSO₃ (100 mL) and NaHCO₃ (100 mL) before being dried (MgSO₄) and concentrated under reduced pressure. The crude residue was then taken up in THF (425 mL) and cooled to 0 °C before a 1% H₂SO₄ solution (425 mL) was added dropwise. The resulting solution was then stirred for 4 h at 0 °C followed by 1 h at RT. The mixture was then extracted with EtOAc (3 x 100 mL), the organic extracts pooled, dried (MgSO₄) and concentrated under reduced pressure. The resulting residue was then recrystallised from EtOAc/hexane to give *rac*-cyclohex-4-ene-1,2-diol (2.39 g, 34%) as a colourless solid. mp: 92–94 °C. (lit. mp: 95 °C (EtOAc/hexane)).^[31] IR (ATR): $\tilde{\nu}$ = 3318 (ν O–H), 1053 (ν C–O) cm⁻¹. ¹H NMR (d₆-DMSO, 300 MHz): δ 5.49–5.47 (m, 2H, 4-,5-H), 4.65–4.63 (m, 2H, 1-,2-OH), 3.46–3.40 (m, 2H, 1-,2-H), 2.33–2.23 (m, 2H, 3-,6-H), 1.93–1.81 (m, 2H, 3-,6-H). ¹³C NMR (d₆-DMSO, 75 MHz): δ 124.6 (2d, C-4,-5), 70.2 (2d, C-1,-2), 32.9 (2t, C-3,-6). HRMS: *m/z* calculated for C₆H₁₀O₂: 114.0681 [M]⁺; Found: 114.0681.

***meso*-Cyclohex-4-ene-1,2-diol (209):**


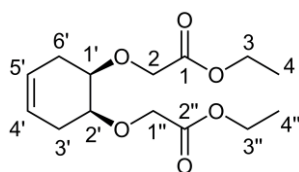
Following General Procedure E. Colourless solid, 46% yield. mp: 77–78 °C. IR (ATR): $\tilde{\nu}$ = 3244 (ν C–H), 1057 (C–O) cm⁻¹. ¹H NMR (CDCl₃, 300 MHz): δ 5.64–5.55 (m, 2H, 4-,5-H), 3.99–3.92 (m, 2H, 1-,2-H), 2.44–2.20 (m, 4H, 3-,6-H₂), 2.09 (s, 2H, 1-,2-OH). ¹³C NMR (CDCl₃, 75 MHz): δ 123.6 (2d, C-4,-5), 68.8 (2d, C-1,-2), 30.8 (2t, C-3,-6).

***rac*-Diethyl 2,2'-(cyclohex-4-ene-1,2-diylbis(oxy))diacetate (210):**


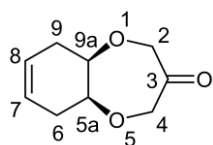
Following General Procedure A. Yellow oil, 34% yield. IR (ATR): $\tilde{\nu}$ = 1750 (ν ester C=O), 1198 (ν ester C–O), 1121 (ν C–O) cm⁻¹. ¹H NMR (CDCl₃, 300 MHz): δ 5.55–5.52 (m, 2H, 4',5'-H), 4.36 (d, *J* = 16.6 Hz, 2H)/4.29 (d, *J* = 16.4 Hz, 2H)/4.21 (q, *J* = 7 Hz, 4H) (2-,3-,1''-,3''-H₂), 3.69–3.61 (m, 2H, 1'-,2'-H), 2.64–2.53 (m, 2H, 3'-,6'-H), 2.22–2.10 (m, 2H, 3'-,6'-H), 1.29 (t, *J* = 7.1 Hz, 6H, 4-,4''-H₃). ¹³C NMR (CDCl₃, 75 MHz): δ 170.3 (2s, C-1,-2''), 123.5 (2d, C-4',-5'), 79.0 (2d, C-1',-2'), 67.6/60.1 (4t, C-2,-3,-1'',-3''), 30.6 (2t, C-3',-6'), 13.7 (2q, C-4,-4''). HRMS: *m/z* calculated for C₁₄H₂₂O₆: 286.1416 [M]⁺; Found: 286.1424.

rac-5a,6,9,9a-Tetrahydro-2H-benzo[b][1,4]dioxepin-3(4H)-one (211):

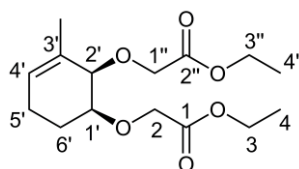
Following General Procedure B. Colourless solid, 39% yield. mp: 63–64 °C. IR (ATR): $\tilde{\nu} = 1722$ (v C=O), 1132 (v C–O) cm^{-1} . $^1\text{H NMR}$ (CDCl_3 , 300 MHz): δ 5.57–5.55 (m, 2H, 7-,8-H), 4.37 (d, $J = 16.4$ Hz, 2H, 2-,4-H), 4.26 (d, $J = 16.4$ Hz, 2H, 2-,4-H), 3.70–3.63 (m, 2H, 5a-,9a-H), 2.59–2.48 (m, 2H, 6-,9-H), 2.26–2.13 (m, 2H, 6-,9-H). $^{13}\text{C NMR}$ (CDCl_3 , 75 MHz): δ 211.1 (s, C-3), 124.0 (2d, C-7,-8), 85.0 (2d, C-5a,-9a), 76.7 (2t, C-2,-4), 32.1 (2t, C-6,-9). HRMS: m/z calculated for $\text{C}_9\text{H}_{12}\text{O}_3$: 168.0790 $[\text{M}]^+$; Found: 168.0787. Odour description: Very weak to odourless, and uncharacteristic in smell.

meso-Diethyl 2,2'-(cyclohex-4-ene-1,2-diylbis(oxy))diacetate (212):

Following General Procedure A. Yellow oil, 32% yield. IR (ATR): $\tilde{\nu} = 1749$ (v ester C=O), 1196 (v ester C–O), 1120 (v C–O) cm^{-1} . $^1\text{H NMR}$ (CDCl_3 , 300 MHz): δ 5.62–5.53 (m, 2H, 4',-5'-H), 4.33–4.15 (m, 8H, 2-,3-,1'',-3''-H₂), 3.90–3.84 (m, 2H, 1',-2'-H), 2.54–2.25 (m, 4H, 3',-6'-H₂), 1.27 (t, $J = 7$ Hz, 6H, 4-,4''-H₃). $^{13}\text{C NMR}$ (CDCl_3 , 75 MHz): δ 170.6 (2s, C-1,-2''), 123.6 (2d, C-4',-5'), 76.3 (2d, C-1',-2'), 66.7/60.4 (4q, C-2-,3-,1'',-3''), 28.8 (2t, C-3',-6'), 13.9 (2t, C-4-,4''). HRMS: Calculated for $\text{C}_{14}\text{H}_{22}\text{O}_6\text{Na}$: 309.1314 $[\text{M}+\text{Na}]^+$; Found: 309.1675.

meso-5a,6,9,9a-Tetrahydro-2H-benzo[b][1,4]dioxepin-3(4H)-one (213):

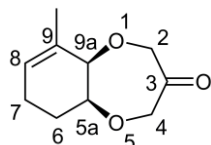
Following General Procedure B. Colourless solid, 3% yield. mp: 73–75 °C. IR (ATR): $\tilde{\nu} = 2917$ (v C–H), 1720 (v C=O), 1125 (v C–O) cm^{-1} . $^1\text{H NMR}$ (CDCl_3 , 300 MHz): δ 5.68–5.58 (m, 2H, 7-,8-H), 4.43 (d, $J = 16.9$ Hz, 2H, 2-,4-H), 4.12 (d, $J = 16.9$ Hz, 2H, 2-,4-H), 4.07 (t, $J = 6.3$ Hz, 2H, 5a-,9a-H), 2.65–2.52 (m, 2H 6-,9-H), 2.39–2.26 (m, 2H, 6-,9-H). $^{13}\text{C NMR}$ (CDCl_3 , 75 MHz): δ 211.3 (s, C-3), 123.2 (2d, C-7,-8), 78.2 (2d, C-5a,-9a), 73.9 (2t, C-2,-4), 27.5 (2t, C-6,-9). HRMS: m/z calculated for $\text{C}_9\text{H}_{12}\text{O}_3$: 168.0786 $[\text{M}]^+$; Found: 168.0770. Odour description: Fruity-fatty, slightly animalic odour that also recalls dark olives, and upon dry-down becomes more balsamic, fruity and cinnamate-like. Odour threshold: 297 ng/L air (stan. dev. 125 ng/L air).

Diethyl 2,2'-(((1S,2R)-3-methylcyclohex-3-ene-1,2-diyl)bis(oxy))diacetate (218):

Following General Procedure A. Yellow oil, 34% yield. $[\alpha]_D^{19} = -41.1^\circ$ ($c = 1.05$, DCM). IR (ATR): $\tilde{\nu} = 1750$ (v ester C=O), 1198 (v ester C–O), 1106 (v C–O) cm^{-1} . $^1\text{H NMR}$ (CDCl_3 , 300 MHz): δ 5.53 (s, 1H, 4'-H), 4.49 (d, $J = 16.8$ Hz, 1H)/4.43 (d, $J = 16.8$ Hz, 1H)/4.27–4.07 (m, 6H) (2-,3-,1'',-3''-H₂), 3.94 (d, $J = 3$ Hz, 1H)/3.62–3.55 (m, 1H) (1',-2'-H), 2.27–2.13 (m, 1H, 5'-H), 2.05–1.89 (m, 2H, 5',-6'-H), 1.86 (d, $J = 1.5$ Hz, 3H, 3'-Me), 1.82–1.70 (m, 1H, 6'-H), 1.32–1.24 (m, 6H, 4-,4''-H₃). $^{13}\text{C NMR}$ (CDCl_3 , 75 MHz): δ 170.8/170.4 (2s, C-1,-2''), 132.0 (s,

C-3'), 125.5 (d, C-4'), 79.8/77.6 (2d, C-1',-2'), 69.1/66.0/60.4/60.1 (4t, C-2,-3,-1'',-3''), 24.4 (t, C-5), 21.1 (t, C-6), 20.8 (q, 3'-Me), 13.9/13.9 (2q, C-3,-3''). HRMS: Calculated for C₁₅H₂₄O₆Na: 323.1471 [M+Na]⁺; Found: 323.1542.

(5a*S*,9a*R*)-9-Methyl-5a,6,7,9a-tetrahydro-2*H*-benzo[*b*][1,4]dioxepin-3(4*H*)-one (219):



Following General Procedure B. Colourless solid, 34% yield. $[\alpha]_D^{22} = -2.8^\circ$ ($c = 1.38$, DCM).

mp: 29–31 °C. IR (ATR): $\tilde{\nu} = 1729$ (ν C=O), 1122 (ν C–O) cm^{-1} . ¹H NMR (CDCl₃, 300 MHz):

δ 5.75–5.70 (m, 1H, 8-H), 4.43–3.95 (m, 6H, 5a-,9a-H,2-,4-H₂), 2.34–2.20 (m, 1H, 7-H),

2.09–1.93 (m, 2H, 7-,6-H), 1.76–1.73 (m, 3H, 9-Me), 1.72–1.59 (m, 1H, 6-H). ¹³C NMR (CDCl₃, 75 MHz): δ 211.8

(s, C-3), 130.8 (s, C-9), 128.3 (d, C-8), 80.7/79.6 (2d, C-5a,-9a), 73.9/73.3 (2t, C-2,-4), 24.2 (t, C-6), 22.9 (t, C-7),

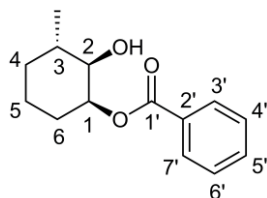
19.8 (q, 9-Me). HRMS: m/z calculated for C₁₀H₁₄O₃: 182.0943 [M]⁺; Found: 182.0948. Odour description: Weak,

slightly green odour with a Folrosia (4-(1-methylethyl)cyclohexan-1-ol) effect.

Synthesis of benzoylated diols 220 and 221:^[35]

To a solution of (1*S*,2*R*)-3-methylcyclohex-3-ene-1,2-diol (4 g) in EtOH (85 mL) and EtOAc (400 mL) was added Pd/C (700 mg) and the solution stirred under an atmosphere of H₂ for 4 h. The solution was then filtered, concentrated under reduced pressure and the resulting residue purified by flash chromatography on silica gel (EtOAc/hexane; 4:6) to yield an unseparable diastereomeric mixture. This crude residue was taken up in pyridine (65 mL), cooled to 0 °C and benzoyl chloride (6.24 mL, 53.74 mmol, 1.2 equiv) was added and the reaction left to stir overnight at RT. The reaction was then diluted with Et₂O, washed with H₂O (2 x 70 mL), washed with a saturated aqueous solution of CuSO₄ (6 x 70 mL), dried (MgSO₄) and concentrated under reduced pressure to yield a crude oil which was subsequently purified by flash chromatography on silica gel (EtOAc/hexane; 1:9) to yield (1*S*,2*R*,3*S*)-2-Hydroxy-3-methylcyclohexyl benzoate and (1*S*,2*R*,3*R*)-2-hydroxy-3-methylcyclohexyl benzoate in 46% combined yield.

(1*S*,2*R*,3*S*)-2-Hydroxy-3-methylcyclohexyl benzoate (220):^[35]



Yellow oil. $[\alpha]_D^{21} = +65.8^\circ$ ($c = 1.06$, DCM). IR (ATR): $\tilde{\nu} = 3485$ (ν O–H), 2932 (ν C–H),

1698 (ν ester C=O), 1269 (ν ester C–O) cm^{-1} . ¹H NMR (CDCl₃, 300 MHz): δ 8.08 (d,

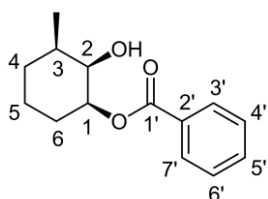
$J = 6.9$ Hz, 2H, 3'-,7'-H), 7.62–7.54 (m, 1H, 5'-H), 7.51–7.41 (m, 2H, 4'-,6'-H), 4.80 (dd,

$J = 10.3, 2.6$ Hz, 1H, 2-H), 4.20–4.15 (m, 1H, 1-H), 2.29–2.12 (m, 1H, 3-H), 1.95–1.43

(m, 5H)/1.30–1.06 (m, 2H) (2-OH, 4-,5-,6-H₂), 0.96 (d, $J = 6.6$ Hz, 3H, 3-Me). ¹³C NMR (CDCl₃, 75 MHz): δ 165.8

(s, C-1'), 132.5 (d, C-5'), 129.9 (s, C-2'), 129.2 (2d, C-3',-7'), 127.9 (2d, C-4',-6'), 80.3 (d, C-2), 67.1 (d, C-1),

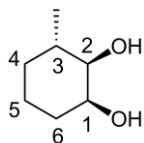
32.3/30.8/30.5/18.7 (1d,3t, C-3,-4,-5,-6), 17.7 (q, 3-Me).

(1*S*,2*R*,3*R*)-2-Hydroxy-3-methylcyclohexyl benzoate (221):^[35]

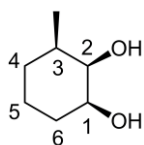
Colourless solid. $[\alpha]_D^{23} = -9.7^\circ$ ($c = 0.99$, DCM). mp: 84–85 °C. (lit. mp: 84–85 °C).^[35]
 IR (ATR): $\tilde{\nu} = 3540$ (ν C–H), 1692 (ν C=O) cm^{-1} . $^1\text{H NMR}$ (CDCl_3 , 300 MHz): δ 8.08–8.03 (m, 2H, 3',7'-H), 7.61–7.54 (m, 1H, 5'-H), 7.50–7.42 (m, 2H, 4',6'-H), 5.04–4.97 (m, 1H)/3.99 (q, $J = 2.3$ Hz, 1H) (1-,2-H), 1.95–1.64 (m, 5H)/1.50–1.35 (m, 3H) (2-OH, 3-H,4-,5-,6-H₂), 1.06 (d, $J = 6.8$ Hz, 3H, 3-Me). $^{13}\text{C NMR}$ (CDCl_3 , 75 MHz): δ 165.6 (s, C-1'), 132.6 (d, C-5'), 130.1 (s, C-2'), 129.3 (2d, C-3',-7'), 128.0 (2d, C-4',-6'), 76.2/71.3 (2d, C-1,-2), 35.3/26.3/24.3/23.1 (1d,3t, C-3,-4,-5,-6), 17.7 (q, 3-Me).

Method of debenzoylation of compounds 220 and 221:^[35]

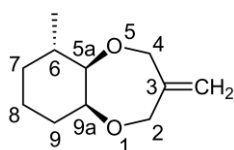
To a solution of the monobenzoate (4 g) in MeOH (40 ml) was added a 10 M solution of NaOH (4 mL) and the solution held at reflux for 1 h. The solvent was then removed under reduced pressure and the crude residue taken up in H₂O (100 mL), saturated with NaCl and extracted with EtOAc (5 x 100 mL). The organic extracts were pooled, dried (MgSO₄) and concentrated under reduced pressure to yield the corresponding *cis*-diol compound.

(1*S*,2*R*,3*S*)-3-Methylcyclohexane-1,2-diol (222):^[35]

Colourless solid. $[\alpha]_D^{22} = +54.2^\circ$ ($c = 1.06$, CHCl_3). mp: 69-70 °C. IR (ATR): $\tilde{\nu} = 3315$ (ν O–H), 2943 (ν C–H), 1059 (ν C–O) cm^{-1} . $^1\text{H NMR}$ (CDCl_3 , 300 MHz): δ 3.99–3.94 (m, 1H, 1-H), 3.22–3.15 (m, 1H, 2-H), 2.05–1.86 (m, 3H, 1-,2-OH, 4-H), 1.83–1.38 (m, 5H, 3-H,5-,6-H₂), 1.06–0.92 (m, 1H, H-4), 1.01 (d, $J = 6.6$ Hz, 3H, 3-Me). $^{13}\text{C NMR}$ (CDCl_3 , 75 MHz): δ 77.3 (d, C-2), 69.5 (d, C-1), 33.0 (d, C-3), 32.3 (t, C-4), 31.1 (t, C-6), 19.1 (t, C-5), 18.2 (q, 3-Me). HRMS: m/z calculated for C₇H₁₄O₂: 130.0994 [M]⁺; Found: 130.0988.

(1*S*,2*R*,3*R*)-3-Methylcyclohexane-1,2-diol (223):^[35]

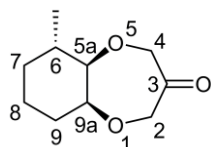
Yellow oil. $[\alpha]_D^{22} = +1.1^\circ$ ($c = 1.03$, CHCl_3). IR (ATR): $\tilde{\nu} = 3375$ (ν O–H), 2929 (ν C–H), 975 (ν C–O) cm^{-1} . $^1\text{H NMR}$ (CDCl_3 , 300 MHz): δ 3.75 (s, 1H, 2-H), 3.60–3.50 (m, 1H, 1-H), 2.36 (s, 1H)/2.21 (s, 1H) (1-,2-OH), 1.75–1.62 (m, 2H)/1.59–1.44 (m, 2H)/1.34–1.19 (m, 3H) (3-H, 4-,5-,6-H₂), 1.02 (d, $J = 6.8$ Hz, 3H, 3-Me). $^{13}\text{C NMR}$ (CDCl_3 , 75 MHz): δ 73.7 (d, C-2), 72.6 (d, C-1), 35.3 (d, C-3), 27.8 (t, C-6), 26.6/23.5 (2t, C-4,-5), 18.0 (q, 3-Me). HRMS: m/z calculated for C₇H₁₄O₂: 130.0994 [M]⁺; Found: 130.1012.

(5*aR*,6*S*,9*aS*)-6-Methyl-3-methyleneoctahydro-2*H*-benzo[*b*][1,4]dioxepine (224):

Following General Procedure C. Yellow oil, 65% yield. $[\alpha]_D^{24} = +137.4$ ($c = 1.09$, DCM).
 IR (ATR): $\tilde{\nu} = 2929$ (ν C–H), 1109 (ν C–O) cm^{-1} . $^1\text{H NMR}$ (CDCl_3 , 300 MHz): δ 5.00/4.92 (2s, 2H, =CH₂), 4.49–4.02 (m, 4H, 2-,4-H₂), 3.82–3.77 (m, 1H, 9a-H), 3.29–3.23 (m, 1H, 5a-H), 2.26–2.10 (m, 1H, 6-H), 1.95–1.84 (m, 1H, 9-H), 1.82–1.71 (m, 1H, 7-H), 1.65–1.37 (m, 3H, 9-H,8-H₂), 1.08–

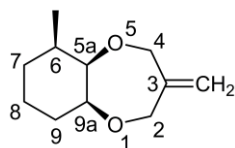
0.94 (m, 1H, 7-H), 0.97 (d, $J = 6.6$ Hz, 3H, 6-Me). ^{13}C NMR (CDCl_3 , 75 MHz): δ 148.4 (s, C-3), 111.0 (t, =CH₂), 83.5 (d, C-5a), 79.0 (d, C-9a), 72.1/65.9 (2q, C-2,-4), 33.1 (t, C-7), 31.2 (t, C-9), 29.0 (d, C-6), 19.8 (t, C-8), 17.9 (q, 6-Me). HRMS: m/z calculated for $\text{C}_{11}\text{H}_{18}\text{O}_2$: 182.1306 [M]⁺; Found: 182.1303.

(5a*R*,6*S*,9a*S*)-6-Methylhexahydro-2*H*-benzo[*b*][1,4]dioxepin-3(4*H*)-one (225):



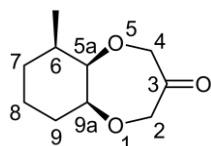
Following General Procedure D. Colourless solid, 58% yield. $[\alpha]_D^{23} = +213.1^\circ$ ($c = 1.08$, DCM). mp: 47–49 °C. IR (ATR): $\tilde{\nu} = 2937$ (v C–H), 1722 (v C=O), 1114 (v C–O) cm^{-1} . ^1H NMR (CDCl_3 , 300 MHz): δ 4.45–3.91 (m, 4H, 2,-4-H₂), 3.90–3.86 (m, 1H, 9a-H), 3.44 (dd, $J = 10.5$, 2.6 Hz, 1H, 5a-H), 2.30–2.14 (m, 1H, 6-H), 2.04–1.93 (m, 1H, 9-H), 1.87–1.77 (m, 1H, 7-H), 1.60–1.42 (m, 3H, 9-H, 8-H₂), 1.15–0.96 (m, 1H, 7-H), 0.98 (d, $J = 6.4$ Hz, 3H, 6-Me). ^{13}C NMR (CDCl_3 , 75 MHz): δ 212.0 (s, C-3), 84.4 (d, C-5a), 82.7 (d, C-9a), 76.9/69.8 (2t, C-2,-4), 32.9 (t, C-7), 31.2 (t, C-9), 28.1 (d, C-6), 19.8 (t, C-8), 17.5 (q, 6-Me). HRMS: m/z calculated for $\text{C}_{10}\text{H}_{16}\text{O}_3$: 184.1099 [M]⁺; Found: 184.1105. Odour description: Weak, green-rubbery odour with a marine effect. Odour threshold: 297 ng/L air (stan. dev. 188 ng/L air).

(5a*R*,6*R*,9a*S*)-6-Methyl-3-methyleneoctahydro-2*H*-benzo[*b*][1,4]dioxepine (226):

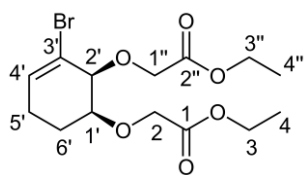


Following General Procedure C. Yellow oil, 42% yield. $[\alpha]_D^{23} = -92.9^\circ$ ($c = 1.14$, DCM). IR (ATR): $\tilde{\nu} = 2929$ (v C–H), 1116 (v C–O), 902 (v C=CH₂) cm^{-1} . ^1H NMR (CDCl_3 , 300 MHz): δ 5.03–5.00 (m, 1H)/4.96–4.93 (m, 1H) (=CH₂), 4.49–4.34 (m, 2H)/4.15–4.04 (m, 2H) (2,-4-H₂), 3.69–3.62 (m, 1H)/3.55–3.52 (m, 1H) (5a,-9a-H), 2.05–1.88 (m, 1H)/1.82–1.73 (m, 1H)/1.59–1.45 (m, 2H)/1.36–1.17 (m, 3H) (6-H, 7,-8,-9-H₂), 0.97 (d, $J = 6.8$ Hz, 3H, 6-Me). ^{13}C NMR (CDCl_3 , 75 MHz): δ 148.4 (s, C-3), 111.7 (t, =CH₂), 82.9/78.7 (2d, C-5a,-9a), 73.2/65.9 (2t, C-2,-4), 35.6 (d, C-6), 27.5/24.0/23.9 (3t, C-7,-8,-9), 17.5 (q, 6-Me). HRMS: m/z calculated for $\text{C}_{11}\text{H}_{18}\text{O}_2$: 182.1306 [M]⁺; Found: 182.1304.

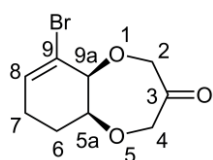
(5a*R*,6*R*,9a*S*)-6-Methylhexahydro-2*H*-benzo[*b*][1,4]dioxepin-3(4*H*)-one (227):



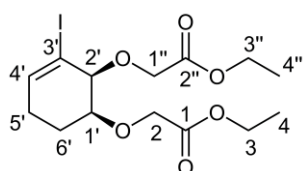
Following General Procedure D. Yellow oil, 66% yield. $[\alpha]_D^{24} = -167.2^\circ$ ($c = 1.03$, DCM). IR (ATR): $\tilde{\nu} = 2932$ (v C–H), 1722 (v C=O), 1123 (v C–O) cm^{-1} . ^1H NMR (CDCl_3 , 300 MHz): δ 4.51–3.94 (m, 4H, 2,-4-H₂), 3.88–3.81 (m, 1H, 9a-H), 3.64–3.61 (m, 1H, 5a-H), 2.06–1.92 (m, 1H, 9-H), 1.90–1.81 (m, 1H, 8-H), 1.66–1.52 (m, 2H, 6,-9-H), 1.42–1.13 (m, 3H, 8-H, 7-H₂), 1.01 (d, $J = 6.8$ Hz, 3H, 6-Me). ^{13}C NMR (CDCl_3 , 75 MHz): δ 212.1 (s, C-3), 86.7 (d, C-5a), 79.3 (d, C-9a), 77.7/69.8 (2t, C-2,-4), 35.6 (d, C-6), 27.5 (t, C-7), 23.7 (t, C-8), 22.9 (t, C-9), 17.5 (q, 6-Me). HRMS: m/z calculated for $\text{C}_{10}\text{H}_{16}\text{O}_3$: 184.1099 [M]⁺; Found: 184.1096. Odour description: Weak, green, slightly oily medicinal odour reminiscent of the medicinal aspects of Calone 1951[®], but also with marine facets of Calone 1951[®]. Odour threshold: 177 ng/L air (stan. dev. 72 ng/L air).

(1*S*,2*S*)-Diethyl 2,2'-((3-Bromocyclohex-3-ene-1,2-diyl)bis(oxy))diacetate (229):

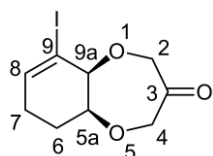
Following General Procedure A, but instead held at reflux for 1 h. Yellow oil, 27% yield. $[\alpha]_D^{23} = -25.5$ ($c = 0.91$, CH_2Cl_2). IR (ATR): $\tilde{\nu} = 2924$ (ν C–H), 1749 (ν ester C=O), 1201 (ν ester C–O), 1123 (ν C–O) cm^{-1} . $^1\text{H NMR}$ (CDCl_3 , 300 MHz): δ 6.23–6.18 (m, 1H, 4'-H), 4.53 (d, $J = 16.4$ Hz, 1H)/4.45 (d, $J = 16.4$ Hz, 1H)/4.32–4.10 (m, 7H) (2'-H, 2-,3-,1'',-3''-H₂), 3.79–3.71 (m, 1H, 1'-H), 2.36–2.23 (m, 1H, 5'-H), 2.14–1.96 (m, 2H, 5',-6'-H), 1.90–1.78 (m, 1H, 6'-H), 1.34–1.24 (m, 6H, 4-,4''-H₃). $^{13}\text{C NMR}$ (CDCl_3 , 75 MHz): δ 170.2/169.9 (2s, C-1,-2''), 133.3 (d, C-4'), 118.3 (s, C-3'), 79.3/78.9 (2d, C-1',-2'), 69.3/66.3 (2t, C-2,-1''), 60.4/60.3 (2t, C-3,-3''), 25.7 (t, C-5'), 21.2 (t, C-6'), 13.9/13.8 (2q, C-4,-4''). HRMS: m/z calculated for $\text{C}_{14}\text{H}_{22}\text{BrO}_6$: 365.0599 $[\text{M}+\text{H}]^+$; Found: 365.0569.

(5*aS*,9*aS*)-9-Bromo-5*a*,6,7,9*a*-tetrahydro-2*H*-benzo[*b*][1,4]dioxepin-3(4*H*)-one (230):

Following General Procedure B. Yellow oil, 20% yield. IR (ATR): $\tilde{\nu} = 2925$ (ν C–H), 1726 (ν C=O), 1126 (ν C–O) cm^{-1} . $^1\text{H NMR}$ (CDCl_3 , 300 MHz): δ 6.46–6.60 (m, 1H, 8-H), 4.48–4.00 (m, 6H, 5*a*,-9*a*-H, 2-,4-H₂), 2.45–2.30 (m, 1H, 7-H), 2.14–2.00 (m, 2H, 6-,7-H), 1.82–1.67 (m, 1H, 6-H). $^{13}\text{C NMR}$ (CDCl_3 , 75 MHz): δ 210.9 (s, C-3), 136.1 (d, C-8), 119.1 (s, C-9), 80.5/80.2 (2d, C-5*a*,-9*a*), 74.5/72.8 (2t, C-2,-4), 24.9/24.2 (2t, C-6,-7). HRMS: m/z calculated for $\text{C}_9\text{H}_{11}\text{BrO}_3$: 245.9892 $[\text{M}]^+$; Found: 245.9884. Odour description: Salty, seawater, algae, solvent-like and chemical aspects.

(1*S*,2*S*)-Diethyl 2,2'-((3-Iodocyclohex-3-ene-1,2-diyl)bis(oxy))diacetate (232):

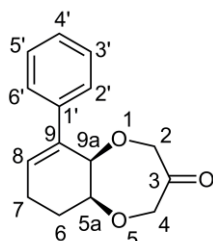
Following General Procedure A, but instead held at reflux for 1 h. Yellow oil, 30% yield. $[\alpha]_D^{23} = -64.3$ ($c = 0.56$, CH_2Cl_2). IR (ATR): $\tilde{\nu} = 2930$ (ν C–H), 1748 (ν ester C=O), 1200 (ν ester C–O), 1122 (ν C–O) cm^{-1} . $^1\text{H NMR}$ (CDCl_3 , 300 MHz): δ 6.50–6.46 (m, 1H, 4'-H), 4.52 (d, $J = 16.2$ Hz, 1H)/4.43 (d, $J = 16.2$ Hz, 1H)/4.27–4.10 (m, 7H) (2'-H, 2-,3-,1'',-3''-H₂), 3.82–3.76 (m, 1H, 1'-H), 2.37–2.24 (m, 1H, 5'-H), 2.15–1.98 (m, 2H, 5',-6'-H), 1.90–1.80 (m, 1H, 6'-H), 1.33–1.24 (m, 6H, 4-,4''-H₃). $^{13}\text{C NMR}$ (CDCl_3 , 75 MHz): δ 170.4/170.1 (2s, C-1,-2''), 141.6 (d, C-4'), 93.0 (s, C-3'), 82.0/78.9 (2d, C-1',-2'), 69.8/66.5 (2t, C-2,-1''), 60.7/60.5 (2t, C-3,-3''), 27.8 (t, C-5'), 21.3 (t, C-6'), 14.1/14.0 (2q, C-4,-4''). HRMS: m/z calculated for $\text{C}_{14}\text{H}_{22}\text{IO}_6$: 413.0461 $[\text{M}+\text{H}]^+$; Found: 413.0404.

(5*aS*,9*aS*)-9-Iodo-5*a*,6,7,9*a*-tetrahydro-2*H*-benzo[*b*][1,4]dioxepin-3(4*H*)-one (233):

Following General Procedure B. Yellow oil, 23% yield. $[\alpha]_D^{23} = +95.5$ ($c = 0.75$, CH_2Cl_2). IR (ATR): $\tilde{\nu} = 2919/2889$ (ν C–H), 1725 (ν C=O), 1122 (ν C–O) cm^{-1} . $^1\text{H NMR}$ (CDCl_3 , 300 MHz): δ 6.75–6.68 (m, 1H, 8-H), 4.44–3.97 (m, 6H, 5*a*,-9*a*-H, 2-,4-H₂), 2.45–2.31 (m, 1H, 7-H), 2.15–1.95 (m, 2H, 6-,7-H), 1.83–1.71 (m, 1H, 6-H). $^{13}\text{C NMR}$ (CDCl_3 , 75 MHz): δ 211.0 (s, C-3), 144.4

(d, C-8), 95.7 (s, C-9), 81.9/80.8 (2d, C-5a,-9a), 74.6/72.4 (2t, C-2,-4), 25.7/25.1 (2t, C-6,-7). HRMS: m/z calculated for $C_9H_{11}IO_3$: 293.9753 [M]⁺; Found: 293.9725. Odour description: Marine, salty, seawater, iodine effect, medicinal, slightly spicy, chemical aspects.

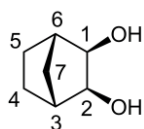
(5a*S*,9a*R*)-9-Phenyl-5a,6,7,9a-tetrahydro-2*H*-benzo[*b*][1,4]dioxepin-3(4*H*)-one (236):



Nitrogen gas was bubbled through a mixture of dimethoxyethane (15 mL) and 2 M Na_2CO_3 (5 mL) for 1 h before (5a*S*,9a*S*)-9-iodo-5a,6,7,9a-tetrahydro-2*H*-benzo[*b*][1,4]dioxepin-3(4*H*)-one (55 mg, 0.188 mmol), phenylboronic acid (27 mg, 0.226 mmol, 1.2 equiv) and $Pd(PhP_3)_4$ (50 mg) was added and the reaction mixture heated to 90 °C overnight. The reaction was then diluted with H_2O (100 mL), extracted with EtOAc (3 x 50 mL), the organic

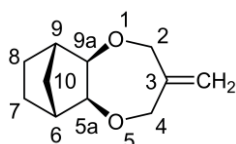
extracts pooled, dried ($MgSO_4$) and concentrated under reduced pressure. The resulting residue was purified by flash chromatography on silica gel (EtOAc/hexane; 15:85) to yield (5a*S*,9a*R*)-9-phenyl-5a,6,7,9a-tetrahydro-2*H*-benzo[*b*][1,4]dioxepin-3(4*H*)-one (33 mg, 72%) as a yellow oil. $[\alpha]_D^{23} = -30.7$ ($c = 0.23$, CH_2Cl_2). IR (ATR): $\tilde{\nu} = 2923$ (ν C–H), 1724 (ν C=O), 1126 (ν C–O). ¹H NMR ($CDCl_3$, 300 MHz): δ 7.38–7.15 (m, 5H), 6.25–6.18 (m, 1H), 4.42–4.04 (m, 4H), 2.52–2.36 (m, 1H), 2.29–2.06 (m, 2H), 1.80–1.66 (m, 1H). ¹³C NMR ($CDCl_3$, 75 MHz): δ 211.7, 139.2, 135.2, 130.9, 128.4, 127.3, 125.8, 79.6, 78.7, 74.1, 73.2, 23.8. HRMS: m/z calculated for $C_{15}H_{16}O_3$: 224.1099 [M]⁺; Found: 224.1115.

(1*R*,2*S*,3*R*,4*S*)-Bicyclo[2.2.1]heptane-2,3-diol (238):

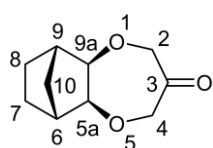


Following General Procedure E. Colourless solid, 82% yield. mp: 138–140 °C. IR (ATR): $\tilde{\nu} = 3239$ (ν O–H), 2949 (ν C–H), 1059 (ν C–O) cm^{-1} . ¹H NMR ($CDCl_3$, 300 MHz): δ 3.68 (d, $J = 1.1$ Hz, 2H, 2-,3-H), 2.99 (s, 2H, 2-,3-OH), 2.17–2.10 (m, 2H, 1-,4-H), 1.80–1.73 (m, 1H, 7-H), 1.52–1.41 (m, 2H, 5-,6-H), 1.15–1.01 (m, 3H, 5-,6-,7-H). ¹³C NMR ($CDCl_3$, 75 MHz): δ 74.3 (2d, C-2,-3), 42.6 (2d, C-1,-4), 31.4 (t, C-7), 24.3 (2t, C-5,-6). HRMS: m/z calculated for $C_7H_{12}O_2$: 128.0837 [M]⁺; Found: 128.0842.

(5a*R*,6*S*,9*R*,9a*S*)-3-Methyleneoctahydro-2*H*-6,9-methanobenzo[*b*][1,4]dioxepine (239):



Following General Procedure C. Clear oil, 56% yield. IR (ATR): $\tilde{\nu} = 2956/2872$ (ν C–H), 1107 (ν C–O) cm^{-1} . ¹H NMR ($CDCl_3$, 300 MHz): δ 5.03 (s, 2H, =CH₂), 4.50 (d, $J = 13.2$ Hz, 2H, 2-,4-H), 4.04 (d, $J = 13.0$ Hz, 2H, 2-,4-H), 3.43 (d, $J = 1.3$ Hz, 2H, 5a-,9a-H), 2.22–2.18 (m, 2H, 6-,9-H), 1.93–1.86 (m, 1H, 10-H), 1.51–1.41 (m, 2H, 7-,8-H), 1.11–1.01 (m, 3H, 7-,8-,10-H). ¹³C NMR ($CDCl_3$, 75 MHz): δ 144.7 (s, C-3), 115.1 (t, =CH₂), 85.7 (2d, C-5a,-9a), 74.9 (2t, C-2,-4), 41.9 (2d, C-6,-9), 33.0 (t, C-10), 24.3 (2t, C-7,-8). HRMS: m/z calculated for $C_{11}H_{16}O_2$: 180.1150 [M]⁺; Found: 180.1165.

(5a*R*,6*S*,9*R*,9a*S*)-Hexahydro-2*H*-6,9-methanobenzo[*b*][1,4]dioxepin-3(4*H*)-one (240):

Following General Procedure D. Colourless solid, 62% yield. mp: 82–85 °C. IR (ATR):

$\tilde{\nu}$ = 2968/2950/2876 (v C–H), 1709 (v C=O), 1157/1139 (v C–O) cm^{-1} . ^1H NMR (CDCl_3 ,

300 MHz): δ 4.61–4.53 (m, 2H, 2-,4-H), 4.19–4.11 (m, 2H, 2-,4-H), 3.56–3.53 (m, 2H,

5a-,9a-H), 2.33–2.29 (m, 2H, 6-,9-H), 2.03–1.97 (m, 1H, 10-H), 1.57–1.47 (m, 2H, 7-,8-H), 1.22–1.15 (m, 1H, 10-H),

1.14–1.05 (m, 2H, 7-,8-H). ^{13}C NMR (CDCl_3 , 75 MHz): δ 212.9 (s, C-3), 86.4 (2d, C-5a,-9a), 79.0 (2t, C-2,-4), 42.1

(2d, C-6,-9), 32.9 (t, C-10), 24.2 (2t, C-7,-8). HRMS: m/z calculated for $\text{C}_{10}\text{H}_{14}\text{O}_3$: 182.0943 $[\text{M}]^+$; Found: 182.0957.

Odour description: Very weak, slightly agrestic and terpenic, slightly mouldy.

(1*R*,2*S*,4*R*,5*S*)-3-Oxatricyclo[3.2.1.0^{2,4}]octane (241):

*m*CPBA (2.15 g, 9.56 mmol, $\leq 77\%$ purity) in DCM (50 mL) was added dropwise to a solution of

norbornene (882 mg, 9.38 mmol) in DCM (20 mL) at 0 °C over 0.5 h. After addition was complete,

a 5% aqueous solution of NaHCO_3 (30 mL) was added and stirring continued at 0 °C for 3 h. The mixture was then

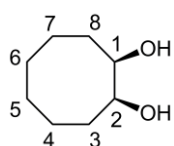
transferred to a separatory funnel, the layers separated and the organic layer washed with a saturated aqueous

solution of NaHSO_3 (15 mL), dried (MgSO_4) and concentrated under reduced pressure to yield

(1*R*,5*S*)-3-oxatricyclo[3.2.1.0^{2,4}]octane (*quant.*) as a clear oil. ^1H NMR (CDCl_3 , 300 MHz): δ 3.07 (s, 2H), 2.45

(s, 2H), 1.55–1.43 (m, 2H), 1.36–1.28 (m, 1H), 1.27–1.17 (m, 2H), 0.73–0.68 (m, 1H). ^{13}C NMR (CDCl_3 , 75 MHz):

δ 51.3, 36.5, 26.1, 25.0.

***meso*-Cyclooctane-1,2-diol (246):**

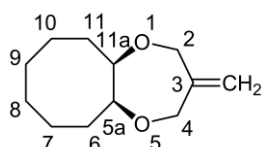
Following General Procedure E. Colourless solid, 69% yield. mp: 78–80 °C. IR (ATR): $\tilde{\nu}$ = 3268

(v O–H), 2909 (v C–H), 1032 (v C–O) cm^{-1} . ^1H NMR (CDCl_3 , 300 MHz): δ 3.96–3.86 (m, 2H,

1-,2-H), 2.10 (bs, 2H, 1-,2-OH), 1.99–1.82 (m, 2H, 3-,8-H), 1.78–1.61 (m, 4H, 3-,4-,7-,8-H),

1.61–1.43 (m, 6H, 4-,7-H,5-,6-H₂). ^{13}C NMR (CDCl_3 , 75 MHz): δ 72.8 (2d, C-1,-2), 29.8 (2t, C-3,-8), 26.1 (2t, C-5,-6),

23.5 (2t, C-4,-7). HRMS: m/z calculated for $\text{C}_8\text{H}_{16}\text{O}_2$: 144.1150 $[\text{M}]^+$; Found: 144.1151.

***meso*-3-Methylenedecahydro-2*H*-cycloocta[*b*][1,4]dioxepine (247):**

Following General Procedure C. Clear oil, 58% yield. IR (ATR): $\tilde{\nu}$ = 2917 (v C–H), 1091

(v C–O), 899 (v C=CH₂) cm^{-1} . ^1H NMR (CDCl_3 , 300 MHz): δ 4.96–4.93 (m, 2H, =CH₂),

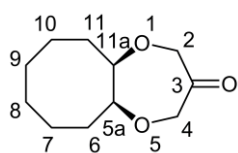
4.40 (d, J = 14.3 Hz, 2H, 2-,4-H), 4.12 (d, J = 14.3 Hz, 2H, 2-,4-H), 3.87–3.80 (m, 2H,

5a-,11a-H), 2.03–1.86 (m, 2H, 6-,11-H), 1.80–1.41 (m, 10H, 6-,11-H, 7-,8-,9-,10-H₂). ^{13}C NMR (CDCl_3 , 75 MHz):

δ 148.2 (s, C-3), 110.8 (t, =CH₂), 80.9 (2d, C-5a,-11a), 69.6 (2t, C-2,-4), 27.9 (2t, C-6,-11), 25.8/23.8 (4t,

C-7,-8,-9,-10). HRMS: m/z calculated for $\text{C}_{12}\text{H}_{21}\text{O}_2$: 197.1541 $[\text{M}+\text{H}]^+$; Found: 197.1516.

meso-Octahydro-2*H*-cycloocta[*b*][1,4]dioxepin-3(4*H*)-one (248):



Following General Procedure D. Clear oil, 51% yield. IR (ATR): $\tilde{\nu}$ = 2921 (v C–H), 1725 (v C=O), 1127 (v C–O) cm^{-1} . ^1H NMR (CDCl_3 , 300 MHz): δ 4.38 (d, J = 16.8 Hz, 2H, 2-,4-H), 4.02 (d, J = 17.1 Hz, 2H, 2-,4-H), 3.97 (d, J = 10.0 Hz, 2H, 5a-,11a-H), 2.04–1.88 (m, 2H, 6-,11-H), 1.83–1.42 (m, 10H, 7-,8-,9-,10-H₂). ^{13}C NMR (CDCl_3 , 75 MHz): δ 212.3 (s, C-3), 83.3 (2d, C-5a,-11a), 73.5 (2t, C-2,-4), 27.3 (2t, C-6,-11), 25.4/24.0 (4t, C-7,-8,-9,-10). HRMS: m/z calculated for $\text{C}_{11}\text{H}_{18}\text{O}_3$: 198.1256 $[\text{M}]^+$; Found: 198.1250. Odour description: Odourless.

3.4 – References

1. P. Kraft, W. Eichenberger, Conception, characterization and correlation of new marine odorants, *Eur. J. Org. Chem.* **2003**, 3735-3743.
2. P. Kraft, K. Popaj, P. Müller, M. Schär, 'Vanilla oceanics': synthesis and olfactory properties of (1'E)-7-(prop-1'-enyl)-2H-benzo[b][1,4]dioxepin-3(4H)-ones and homologues, *Synthesis* **2010**, 3029-3036.
3. J.-M. Gaudin, O. Nikolaenko, J.-Y. de Saint Laumer, B. Winter, P.-A. Blanc, Structure - activity relationship in the domain of odorants having marine notes, *Helv. Chim. Acta* **2007**, *90*, 1245-1265.
4. J.-M. Gaudin, J.-Y. de Saint Laumer, Structure-Activity Relationships in the Domain of Odorants Having Marine Notes, *Eur. J. Org. Chem.* **2015**, 1437-1447.
5. B. Drevermann, A. R. Lingham, H. M. Hugel, P. J. Marriott, Synthesis and qualitative olfactory evaluation of benzodioxepine analogues, *Helv. Chim. Acta* **2007**, *90*, 854-863.
6. B. Drevermann, A. R. Lingham, H. M. Hugel, P. J. Marriott, Synthesis of benzodioxepinone analogues via a novel synthetic route with qualitative olfactory evaluation, *Helv. Chim. Acta* **2007**, *90*, 1006-1027.
7. J. F. Trant, J. Froese, T. Hudlicky, Enzymatic oxidation of *para*-substituted arenes: access to new non-racemic chiral metabolites for synthesis, *Tetrahedron: Asymmetry* **2013**, *24*, 184-190.
8. J. Froese, M. A. Endoma-Arias, T. Hudlicky, Processing of *o*-Halobenzoates by Toluene Dioxygenase. The Role of the Alkoxy Functionality in the Regioselectivity of the Enzymatic Dihydroxylation Reaction, *Org. Process Res. Dev.* **2014**, *18*, 801-809.
9. D. T. Gibson, J. R. Koch, R. E. Kallio, Oxidative degradation of aromatic hydrocarbons by microorganisms. I. Enzymic formation of catechol from benzene, *Biochemistry* **1968**, *7*, 2653-2662.
10. D. T. Gibson, J. R. Koch, C. L. Schuld, R. E. Kallio, Oxidative degradation of aromatic hydrocarbons by microorganisms. II. Metabolism of halogenated aromatic hydrocarbons, *Biochemistry* **1968**, *7*, 3795-3802.
11. D. T. Gibson, M. Hensley, H. Yoshioka, T. J. Mabry, Oxidative degradation of aromatic hydrocarbons by microorganisms. III. Formation of (+)-*cis*-2,3-dihydroxy-1-methyl-4,6-cyclohexadiene from toluene by *Pseudomonas putida*, *Biochemistry* **1970**, *9*, 1626-1630.
12. R. A. Johnson, Microbial arene oxidations, *Org. React.* **2004**, *63*, 117-264.
13. G. J. Zylstra, D. T. Gibson, Toluene degradation by *Pseudomonas putida* F1. Nucleotide sequence of the *todC1C2BADE* genes and their expression in *Escherichia coli*, *J. Biol. Chem.* **1989**, *264*, 14940-14946.
14. F. Hollmann, I. W. C. E. Arends, K. Buehler, A. Schallmeyer, B. Buehler, Enzyme-mediated oxidations for the chemist, *Green Chem.* **2011**, *13*, 226-265.
15. T. Hudlicky, J. W. Reed, Applications of biotransformations and biocatalysis to complexity generation in organic synthesis, *Chem. Soc. Rev.* **2009**, *38*, 3117-3132.

16. T. Hudlický, D. Gonzalez, D. T. Gibson, Enzymatic dihydroxylation of aromatics in enantioselective synthesis: expanding asymmetric methodology, *Aldrichimica Acta* **1999**, *32*, 35-62.
17. R. Friemann, K. Lee, E. N. Brown, D. T. Gibson, H. Eklund, S. Ramaswamy, Structures of the multicomponent Rieske non-heme iron toluene 2,3-dioxygenase enzyme system, *Acta Crystallogr., Sect. D: Biol. Crystallogr.* **2009**, *65*, 24-33.
18. K. Lee, R. Friemann, J. V. Parales, D. T. Gibson, S. Ramaswamy, Purification, crystallization and preliminary x-ray diffraction studies of the three components of the toluene 2,3-dioxygenase enzyme system, *Acta Crystallogr., Sect. F: Struct. Biol. Cryst. Commun.* **2005**, *61*, 669-672.
19. J. D. White, U. M. Grether, C.-S. Lee, (*R*)-(+)-3,4-dimethylcyclohex-2-en-1-one, *Org. Synth.* **2005**, *82*, 108-114.
20. A. R. Van Dyke, K. M. Miller, T. F. Jamison, (*S*)-(+)-Neomenthylphenylphosphine in nickel-catalyzed asymmetric reductive coupling of alkynes and aldehydes: enantioselective synthesis of allylic alcohols and α -hydroxy ketones, *Org. Synth.* **2007**, *84*, 111-119.
21. L. F. Tietze, M. Bratz, Dialkyl mesoxalates by ozonolysis of dialkyl benzalmalonates: preparation of dimethyl mesoxalate, *Org. Synth.* **1993**, *71*, 214-219.
22. R. Criegee, Mechanism of Ozonolysis, *Angew. Chem. Int. Ed. Engl.* **1975**, *14*, 745-752.
23. C. Geletneky, S. Berger, The mechanism of ozonolysis revisited by ^{17}O -NMR spectroscopy, *Eur. J. Org. Chem.* **1998**, 1625-1627.
24. R. L. Kuczkowski, Formation and structure of ozonides, *Acc. Chem. Res.* **1983**, *16*, 42-47.
25. *ChemDraw Ultra 12.0*, CambridgeSoft, version 12.0.2.1076. For more information see <<http://www.cambridgesoft.com/>>
26. I. Dams, A. Bialonska, Z. Ciunik, C. Wawrzenczyk, Synthesis of terpenoid lactones with the *p*-menthane system, *Eur. J. Org. Chem.* **2004**, 2662-2668.
27. I. Dams, A. Bia-Lonska, Z. Ciunik, C. Wawrzenczyk, Lactones. 21. Synthesis and Odoriferous Properties of Lactones with the *p*-Menthane System, *J. Agric. Food Chem.* **2004**, *52*, 1630-1634.
28. R. K. Pandey, R. K. Upadhyay, S. S. Shinde, P. Kumar, Synthesis of (–)-mintlactone via intramolecular Wittig-Horner reaction, *Synth. Commun.* **2004**, *34*, 2323-2329.
29. I. Dams, A. Bialonska, Z. Ciunik, C. Wawrzenczyk, Lactones 23: Synthesis of *cis*-fused bicyclic hydroxy lactones with a *p*-menthane system, *Tetrahedron: Asymmetry* **2005**, *16*, 2087-2097.
30. J. L. Luche, Lanthanides in organic chemistry. 1. Selective 1,2 reductions of conjugated ketones, *J. Am. Chem. Soc.* **1978**, *100*, 2226-2227.
31. H. Suemune, M. Hizuka, T. Kamashita, K. Sakai, Preparation of optically active γ -hydroxyethyl α,β -unsaturated γ -lactone using an enzymic procedure, *Chem. Pharm. Bull.* **1989**, *37*, 1379-1381.

32. T. J. Donohoe, L. Mitchell, M. J. Waring, M. Helliwell, A. Bell, N. J. Newcombe, Scope of the directed dihydroxylation: application to cyclic homoallylic alcohols and trihaloacetamides, *Org. Biomol. Chem.* **2003**, *1*, 2173-2186.
33. S. Connelly, K. Line, M. N. Isupov, J. A. Littlechild, Synthesis and characterisation of a ligand that forms a stable tetrahedral intermediate in the active site of the *Aureobacterium* species (-) γ -lactamase, *Org. Biomol. Chem.* **2005**, *3*, 3260-3262.
34. T. Hudlický, C. H. Boros, E. E. Boros, A model study directed towards a practical enantioselective total synthesis of (-)-morphine, *Synthesis* **1992**, 174-178.
35. T. Hudlický, H. Luna, G. Barbieri, L. D. Kwart, Enantioselective synthesis through microbial oxidation of arenes. 1. Efficient preparation of terpene and prostanoid synthons, *J. Am. Chem. Soc.* **1988**, *110*, 4735-4741.
36. G. Ohloff, W. Pickenhagen, P. Kraft, *Scent and Chemistry - The Molecular World of Odors*, Verlag Helvetica Chimica Acta, Zurich, **2012**.
37. D. R. Boyd, N. D. Sharma, M. V. Berberian, K. S. Dunne, C. Hardacre, M. Kaik, B. Kelly, J. F. Malone, S. T. McGregor, P. J. Stevenson, Synthesis and reactions of enantiopure substituted benzene *cis*-hexahydro-1,2-diols, *Adv. Synth. Catal.* **2010**, *352*, 855-868.
38. S. M. King, X. Ma, S. B. Herzon, A Method for the Selective Hydrogenation of Alkenyl Halides to Alkyl Halides, *J. Am. Chem. Soc.* **2014**, *136*, 6884-6887.
39. M. Engman, J. S. Diesen, A. Paptchikhine, P. G. Andersson, Iridium-Catalyzed Asymmetric Hydrogenation of Fluorinated Olefins Using N,P-Ligands: A Struggle with Hydrogenolysis and Selectivity, *J. Am. Chem. Soc.* **2007**, *129*, 4536-4537.
40. G. E. Ham, W. P. Coker, Selective hydrogenation of haloalkenes to haloalkanes using rhodium catalyst, *J. Org. Chem.* **1964**, *29*, 194-198.
41. A. Rananaware, R. S. Bhosale, K. Ohkubo, H. Patil, L. A. Jones, S. L. Jackson, S. Fukuzumi, S. V. Bhosale, S. V. Bhosale, Tetraphenylethene-Based Star Shaped Porphyrins: Synthesis, Self-assembly, and Optical and Photophysical Study, *J. Org. Chem.* **2015**, *80*, 3832-3840.
42. N. Miyaura, K. Yamada, A. Suzuki, A new stereospecific cross-coupling by the palladium-catalyzed reaction of 1-alkenylboranes with 1-alkenyl or 1-alkynyl halides, *Tetrahedron Lett.* **1979**, 3437-3440.
43. N. Miyaura, A. Suzuki, Palladium-Catalyzed Cross-Coupling Reactions of Organoboron Compounds, *Chem. Rev.* **1995**, *95*, 2457-2483.
44. F.-S. Han, Transition-metal-catalyzed Suzuki-Miyaura cross-coupling reactions: a remarkable advance from palladium to nickel catalysts, *Chem. Soc. Rev.* **2013**, *42*, 5270-5298.

45. C. Amatore, A. Jutand, G. Le Duc, Kinetic Data for the Transmetalation/Reductive Elimination in Palladium-Catalyzed Suzuki-Miyaura Reactions: Unexpected Triple Role of Hydroxide Ions Used as Base, *Chem. Eur. J.* **2011**, *17*, 2492-2503.
46. S. M. Grayson, B. K. Long, S. Kusomoto, B. P. Osborn, R. P. Callahan, C. R. Chambers, C. G. Willson, Synthesis and Characterization of Norbornanediol Isomers and Their Fluorinated Analogues, *J. Org. Chem.* **2006**, *71*, 341-344.
47. J. K. Crandall, Rearrangements of norbornene oxide, *J. Org. Chem.* **1964**, *29*, 2830-2833.
48. H. M. Walborsky, D. F. Loncrini, Oxidation of bicyclo[2.2.2]oct-2-ene and bicyclo[2.2.1]hept-2-ene, *J. Am. Chem. Soc.* **1954**, *76*, 5396-5399.
49. H. Kotsuki, M. Kataoka, H. Nishizawa, High pressure-promoted uncatalyzed hydrolysis of epoxides, *Tetrahedron Lett.* **1993**, *34*, 4031-4034.
50. *Discovery Studio*, v. 4.1.0.14169, Accelrys, San Diego, CA 92121, USA, **2005–2014**. For more information see <<http://www.accelrys.com/>>.

Chapter 4 – Synthesis of 2-Substituted and 2,3-Annulated 1,4-Dioxepan-6-ones

4.1 – Introduction

4.1.1 – Terpenoids and Molecular Fusion

Terpenes, also known as isoprenoids, are a large and diverse class of organic compounds that are assembled biosynthetically from multiple units of isoprene (**249**). The monomeric isoprene unit itself does not undergo the enzyme-catalysed synthetic process, but instead activated isoprene units such as isopentenyl pyrophosphate (IPP, **250**) and dimethylallyl pyrophosphate (DMAPP, **251**) are used (Figure 4.1).^[1] These monomeric units are combined to form intermediates such as geranyl pyrophosphate (GPP, **252**) and farnesyl pyrophosphate (FPP, **253**), which are then further reacted to yield a multitude of different compounds.

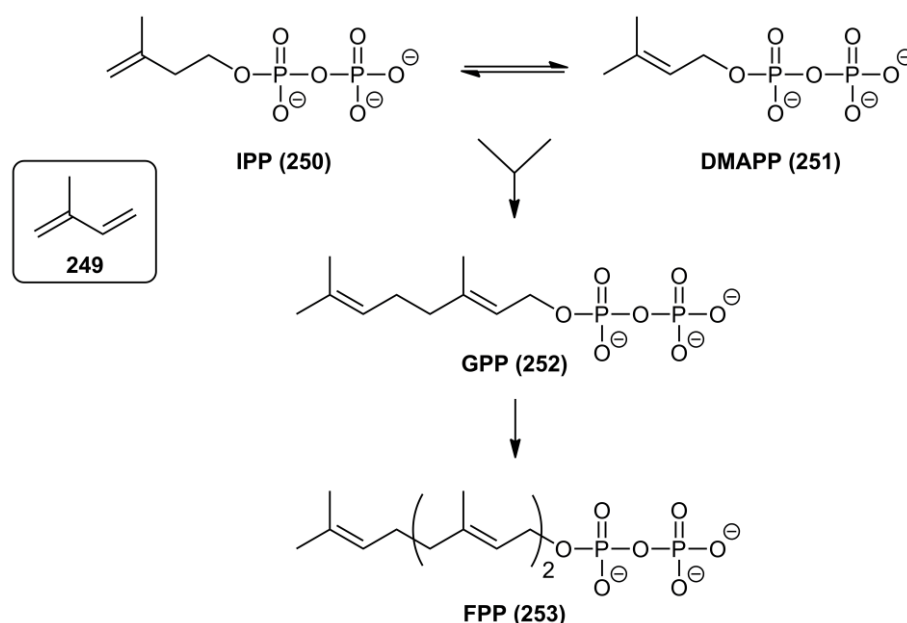


Figure 4.1: Biosynthetic intermediates leading to terpene and terpenoid compounds.

When terpene compounds are modified chemically, such as by enzyme-catalysed oxidation or rearrangement reactions, the resulting compounds are referred to as terpenoids. More than 30,000 terpene and terpenoid molecules have been isolated from plants, microorganisms and animals.^[2] Molecules that are formed from the modification of a single isoprene unit are known as

hemiterpenoids, molecules formed by the addition of two isoprene units are called monoterpenes/monoterpenoids, and molecules formed by the addition of three isoprene units are called sesquiterpenes/sesquiterpenoids.^[2] Terpenes and terpenoids are important constituents of essential oils, although higher terpene and terpenoid compounds (those made from four isoprene units or more) are generally not found in essential oils.^[2] Shown in Figure 4.2 is the structure and natural source of a variety of terpene and terpenoid odorant compounds.

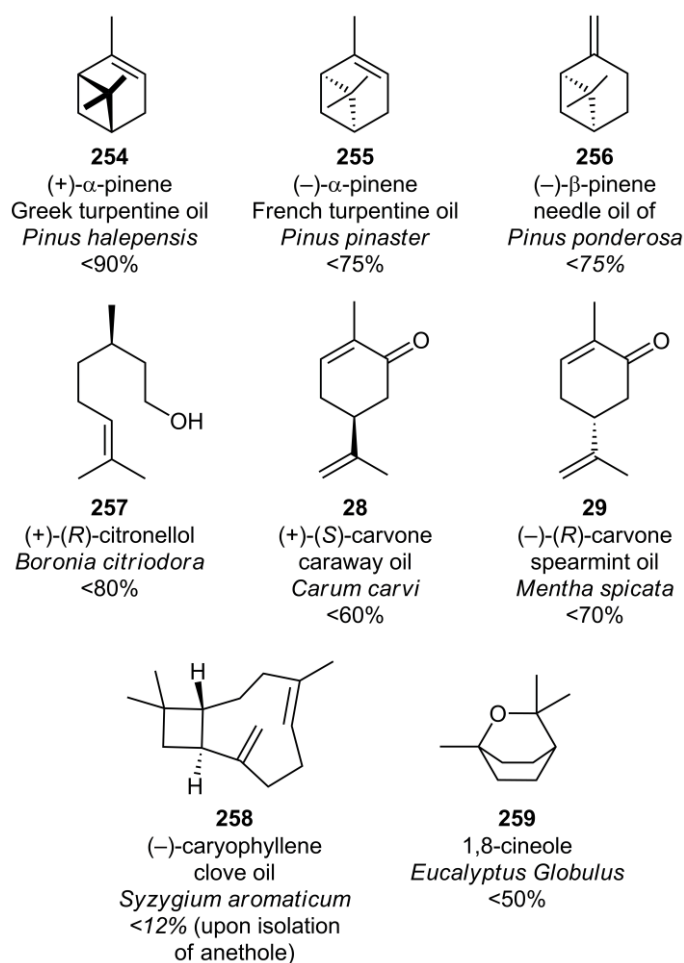


Figure 4.2: Various terpene and terpenoid odorants, and their natural source and abundance.^[3]

A recent publication by Kraft *et al.*^[4] described efforts into merging marine and musk odorant notes by the fusion of the molecular structure of Calone 1951[®] (**50**) with that of the polycyclic musk odorant Galaxolide[®] (**65**) (Figure 4.3). Disappointingly the synthetic analogues were discovered not to contain musk notes but instead incorporated marine notes with additional floral aspects.^[4] Analogous to this concept, attempts were made to synthetically merge marine notes with those of naturally occurring

odorant molecules by the fusion of 1,4-dioxepan-6-one heterocyclic ring systems onto substituted cyclohexyl terpenoid compounds such as carvone, carvotanacetone, limonene, camphor, pinene and menthol.

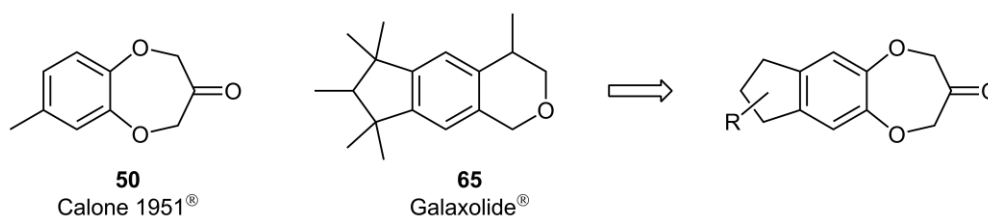


Figure 4.3: Molecular structure amalgamation of marine odorant Calone 1951[®] (50) and musk odorant Galaxolide[®] (65).^[4]

4.1.2 – The *Seco* Synthetic Technique

The organic chemistry term *seco* is defined by IUPAC as ‘the cleavage of a ring with addition of one or more hydrogen atoms at each terminal group’.^[5] The *seco* analysis of a given molecular structure can include the cleavage of chemical bonds between scaffold atoms or the complete removal of scaffold atoms from the molecular structure. Perhaps the most well-known example of a *seco* molecule is the secosteroid known as vitamin D (Figure 4.4). This compound is produced photochemically in the epidermis from the steroid molecule 7-dehydrocholesterol (260) by the cleavage of the 9,10 carbon–carbon bond of ring B. This gives a compound known as previtamin D₃ which then undergoes a 1,7-sigmatropic hydrogen transfer from C–19 to C–9 to yield vitamin D₃ (261), as shown in Figure 4.4.^[6]

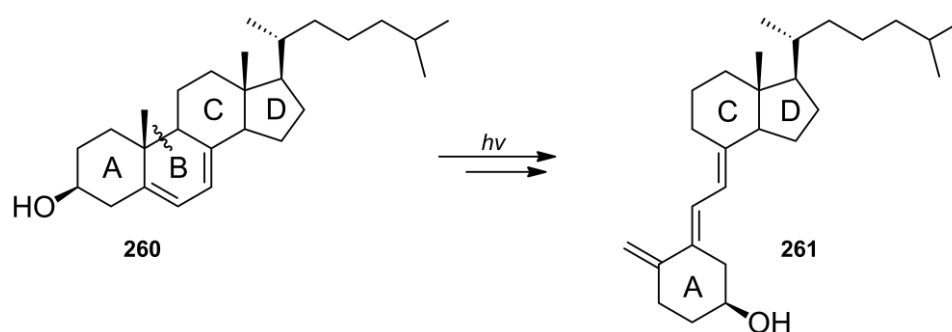


Figure 4.4: Molecular structures of 7-dehydrocholesterol (260) and cholecalciferol (vitamin D₃, 261).

The *seco* principle for targeted odorant design was first introduced into fragrance chemistry in 1962 by Sestanj.^[7] The removal of two carbon fragments from the molecular structure of β -ionone (**262**) led to acyclic fragment **263** (Figure 4.5). It was reported that the *seco* target molecule indeed contained the same violet odour notes as lead compound β -ionone (**262**).^[7] It is known that not every carbon atom of a lead compound is required to interact with a specific olfactory receptor, especially if the atoms are situated in the less specific and more voluminous hydrophobic binding pocket(s) of the receptor.^[8] The removal of carbon atoms can potentially increase receptor affinity owing to the resulting molecular structure having more conformational degrees of freedom, as well as increase the volatility of the resulting molecule. These effects can result in the target compound having a lower odour threshold value than the lead compound.^[8]

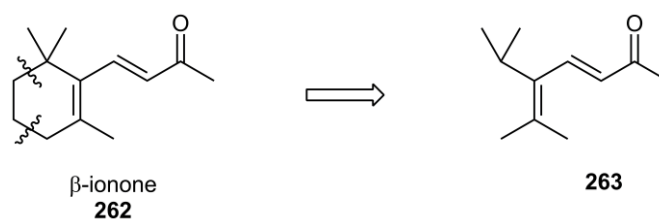


Figure 4.5: *Seco* analysis of β -ionone (**262**) to give molecular fragment **263**.

The *seco* synthetic technique has since been widely used in the production of novel captive odorant molecules. For example, the dienone musk **264** is an unusual bicyclic musk odorant that differs from other polycyclic musk compounds in that it does not contain an indane or benzenoid motif (Figure 4.6).^[9] First synthesised by Kula *et al.*^[10] from (+)-carotol, the primary sesquiterpenoid from the essential oil of carrot seed, this compound has been the target of multiple analogue studies in the search for new odorant molecules.^[9, 11-12]

Seco-derivatives of compound **264** were first synthesised by Kraft *et al.*^[11] by the removal of C-2 and C-6 atoms to give acyclic analogue **265**. This compound was discovered to contain potent musk notes, as well as ionone notes, and also had a lower odour threshold value than the parent material. The ionone notes were not surprising since this compound featured a (*E*)-hexa-3,5-dien-2-one backbone, structurally resembling the previously synthesised *seco*-ionone molecules (i.e. **263**).^[12] Due to the

positive outcome of the original research additional *seco*-analogues of compound **264**, such as compounds **266** and **267**, were synthesised and evaluated in a second study (Figure 4.6).^[12]

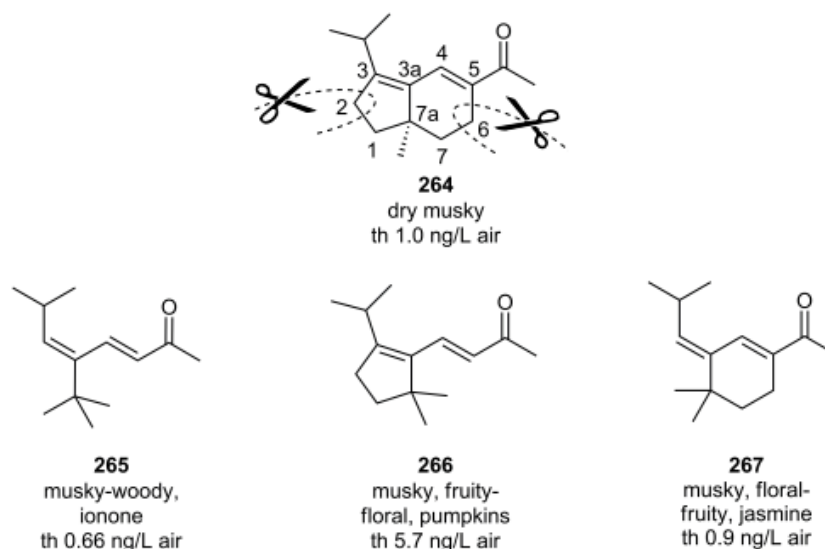


Figure 4.6: Analogues **265–267** synthesised from *seco* analysis of the molecular structure of lead compound **264**.

The synthesis of additional modified benzo[*b*][1,4]dioxepin-3-one systems seemed necessary to corroborate the lack of binding and weak odour potency of the aliphatic analogues. It was postulated that the removal of part or all of the carbocyclic ring system might help overcome the repulsion of the molecules from the olfactory receptor. In addition, owing to the fact that the previously synthesised aliphatic analogues had demonstrated a multitude of odorant descriptors, our curiosity was aroused to investigate whether other odorant families could perhaps be targeted with 1,4-dioxepan-6-one analogues. Some of the analogues can be considered *seco* derivatives of the original 7-methylbenzo[*b*][1,4]dioxepin-3-one molecular structure of Calone 1951[®] (**50**), others can be considered parent compounds or experimental derivatives (Figure 4.7).

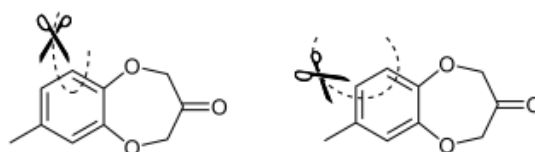


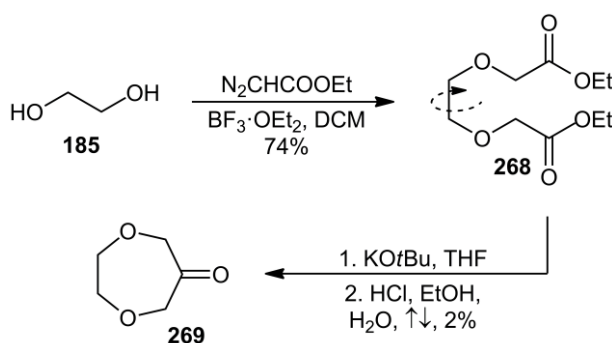
Figure 4.7: *Seco* analysis of 7-methylbenzo[*b*][1,4]dioxepin-3-one (Calone 1951[®], **50**).

4.2 – Results and Discussion

4.2.1 – Synthesis of 1,4-Dioxepan-6-one Analogues

Owing to previous conclusions that the aromatic binding region of the marine odorant receptor may be physically repelling the now hydrophobic carbocyclic ring system, the synthesis of a library of 1,4-dioxepan-6-one analogues was envisioned. The initial synthetic methodology investigated was the Dieckmann condensation conditions that were developed during the synthesis of the library of aliphatic benzo[*b*][1,4]dioxepin-3-one analogues described within Chapter 2/3. Etherification of 1,2-ethanediol (**185**) using ethyl diazoacetate and boron trifluoride diethyletherate as a Lewis-acid catalyst readily afforded *bis*-ester compound **268** in 74% yield as a yellow oil (Scheme 4.1). This was an unusually high yield for this type of *bis*-etherification reaction, perhaps attributable to free rotation and therefore less steric hindrance of the molecule.

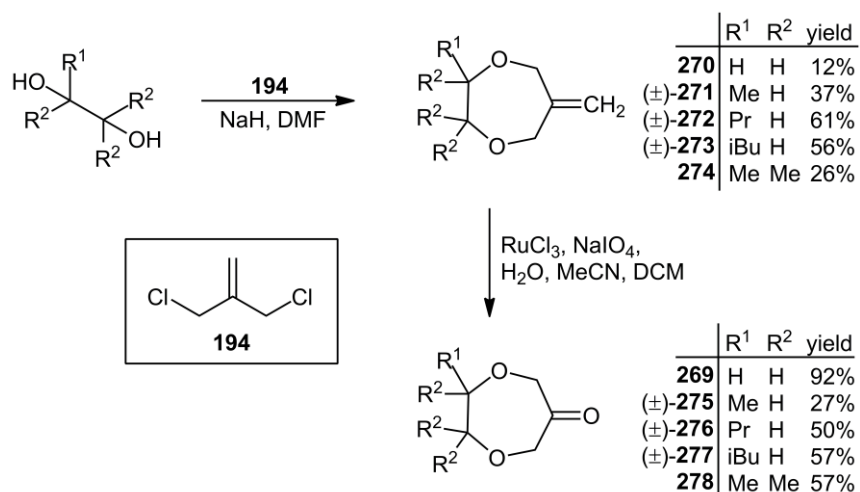
Subsequent Dieckmann condensation reactions of compound **268** were discovered to lead predominantly to polymerised materials. The target compound, 1,4-dioxepan-6-one (**269**), was eventually isolated as a clear oil in 2% yield, separated from a thick polymer matrix by flash chromatography with careful isolation due to its inherent volatility. The synthesis of compound **269** via similar Dieckmann cyclisation methodology had been previously reported in patent literature;^[13] the authors reported a superior yield of 22%, although it should be noted that the methodology made use of the weaker non-nucleophilic base sodium *tert*-butoxide.



Scheme 4.1: Synthesis of 1,4-dioxepan-6-one (**269**) from 1,2-ethanediol (**185**), showing free rotation.

In consideration of the poor yields achieved by Dieckmann condensation it was questioned if perhaps Williamson cyclisation may provide improved yields. Reactions were first trialled with 1,2-ethanediol (**185**) to give a direct comparison between the alternative cyclisation routes. The Williamson reaction between 1,2-ethanediol (**185**) and 3-chloro-2-(chloromethyl)prop-1-ene (**194**) provided methylene analogue **270** in 12% yield, lower than anticipated. Subsequent Katsuki-Sharpless oxidation provided 1,4-dioxepan-6-one (**269**) in 92% yield as a clear oil (Scheme 4.2). To be noted is that an analogous route of synthesis was developed by Nerdel *et al.*^[14] which made use of an *in situ* generated alkylating agent to give methylene compound **270**, followed by ozonolysis to yield 1,4-dioxepan-6-one (**269**) (Figure 2.10).

During the course of investigation it was discovered that a change of reaction solvent from carbon tetrachloride to dichloromethane allowed for a more simple isolation of the volatile target materials. Although the *bis*-etherification yield of 1,2-ethanediol (**185**) was poorer, the overall synthetic pathway yield was improved from 1.5% to 11% when compared to the Dieckmann condensation methodologies. Using the modified Williamson reaction procedure a variety of substituted 1,4-dioxepan-6-one analogues (**275–278**) were synthesised and their olfactory descriptions, and threshold values where applicable, were determined (Scheme 4.2, Figure 4.8).



Scheme 4.2: Williamson reaction methodology to give 1,4-dioxepan-6-one analogues **269**, **275–278**.

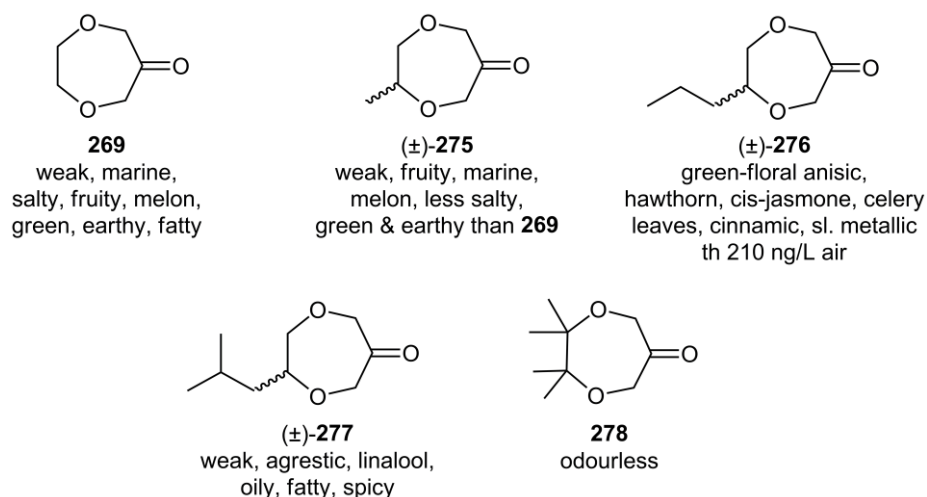
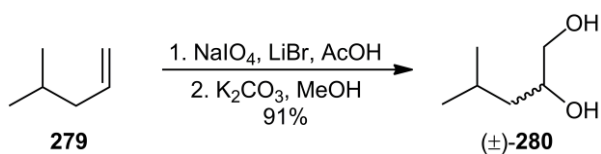


Figure 4.8: Library of 1,4-dioxepan-6-one analogues **269**, **275–278** displaying odour descriptors and odour thresholds (th) values, where applicable.

Only one *bis*-hydroxyl precursor (leading to compounds **269**, **275–278**) was not commercially available. Therefore, racemic diol precursor 4-methylpentane-1,2-diol (**280**) was synthesised from 4-methyl-1-pentene (**279**) (Scheme 4.3).^[15] The proposed synthetic mechanism involves the *in situ* generation of molecular bromine followed by bromoacetoxylation of the alkene to give a *trans*-1,2-bromoacetate intermediate which is then oxidised to a cyclic intermediate assisted anchimerically by the acetate group (Figure 4.9). The cyclic intermediate is then opened by the action of acetic acid to furnish the *cis*-hydroxyl acetate or *trans*-diacetate compound, with the liberated molecular bromine recycled back into the catalytic cycle.^[16] The final step involves a methanolic potassium carbonate hydrolysis to give racemic diol (±)-**280** as a yellow oil.



Scheme 4.3: Synthesis of racemic 4-methylpentane-1,2-diol (**280**) from 4-methyl-1-pentene (**279**).

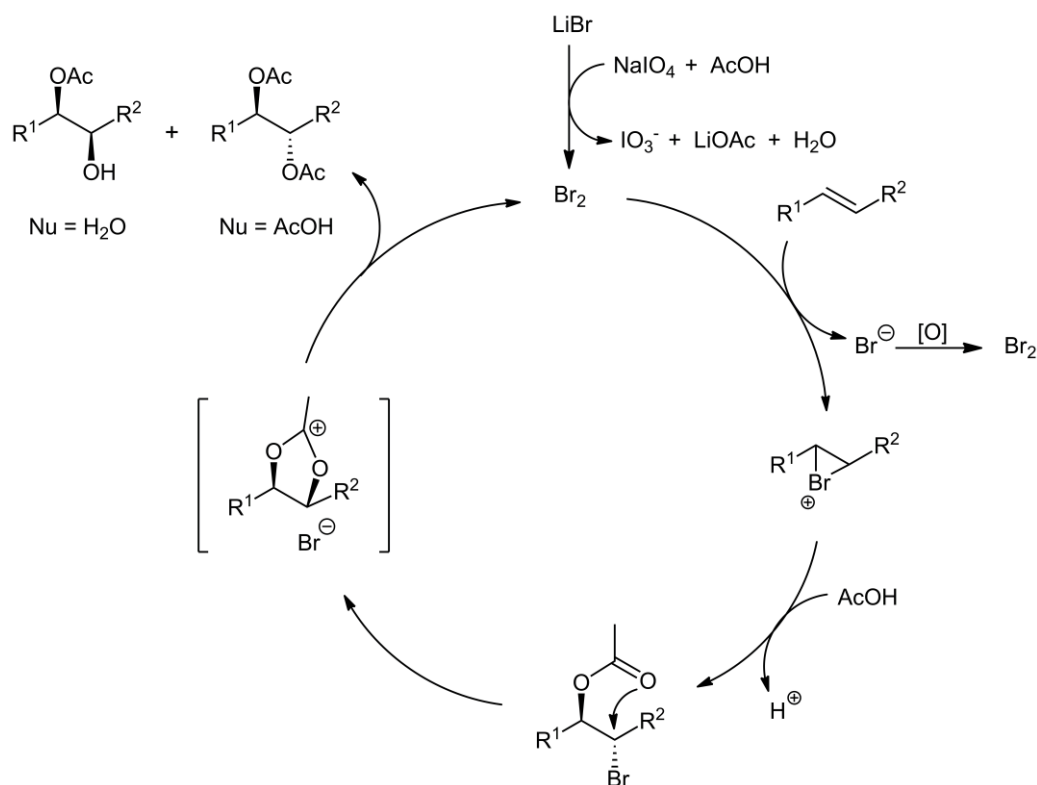


Figure 4.9: Proposed catalytic cycle for the dihydroxylation of alkenes by Sudalai *et al.*^[16]

4.2.2 – 1,4-Dioxepan-6-one/Terpenoid Odorant Fusion – (+)- α -Pinene

A dioxepanone heterocycle fused analogue of (+)- α -pinene (**254**) was prepared. Both enantiomers of α -pinene have harsh, terpene-like odour with the (+)-enantiomer (**254**) somewhat more resembling fresh mint, whilst the (–)-enantiomer (**255**) is more coniferous.^[17] The two enantiomers constitute the major component of turpentine. Dihydroxylation of (+)- α -pinene (**254**) using the standard osmium tetroxide oxidation conditions (4:1; acetone/water at room temperature) gave poor yields, leaving increasingly large amounts of starting material as the reaction was upscaled. It appeared that the reaction was sluggish, presumably due to steric hindrance, and that a catalytic quantity of osmium would not be enough to drive the reaction to completion.

Using catalytic quantities of pyridine in a refluxing solution of *tert*-butanol/water (5:1) was however found to provide *cis*-diol **281** as a colourless solid in 75% yield after flash chromatography.^[18-19] Osmium dihydroxylation reactions are accelerated by the addition of tertiary amine compounds such as pyridine and quinuclidine in a process known as ligand-accelerated catalysis (Figure 4.10).^[20] Asymmetric

osmium dihydroxylation reactions have been developed using chiral amine ligands such as derivatives of the naturally occurring alkaloids dihydroquinidine (DHQD) and dihydroquinine (DHQ).^[21]

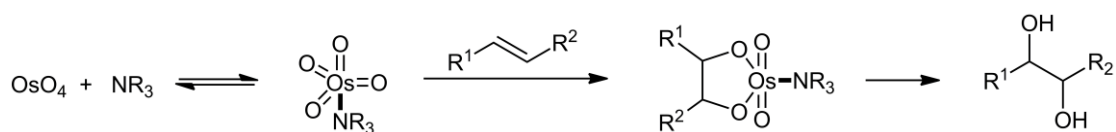
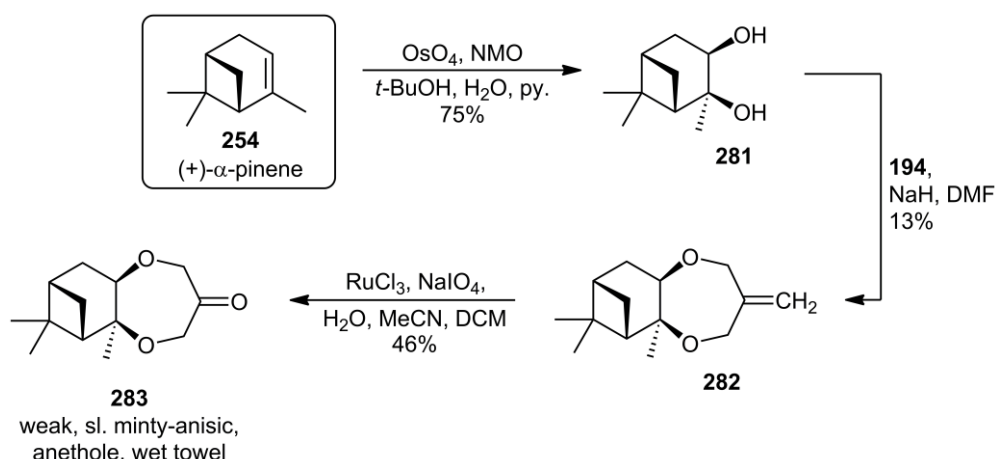


Figure 4.10: Tertiary amine ligands accelerate the reactivity of osmium tetroxide.^[20]

The absolute stereochemistry of *cis*-diol compound **281** was confirmed by comparison to literature data.^[18-19, 22] Compound **281** was subjected to Williamson cyclisation with **194** to provide compound **282** in a poor yield of 13%, presumably due to the additional steric hindrance imposed by the tertiary hydroxyl moiety. Ruthenium tetroxide oxidation of **282** furnished 2,3-annulated 1,4-dioxepan-6-one analogue **283** in 49% yield as a colourless solid (Scheme 4.4).



Scheme 4.4: Synthesis of dioxepanone fused (+)- α -pinene analogue **283** from (+)- α -pinene (**254**).

Heteronuclear single quantum coherence spectroscopy (^1H , ^{13}C HSQC) analysis of compound **283** revealed that carbon atoms C-2 and C-4 contain protons in rather different environments due to the non-symmetrical nature of the molecular structure, presumably exacerbated by the tertiary methyl moiety attached to bridging carbon C-5a. The bridging carbon atoms (C-5a/9a) could not be resolved by heteronuclear multiple bond correlation spectroscopy (^1H , ^{13}C HMBC) due to near overlapping ^{13}C signals (δ 80.7 and 80.3 ppm) (Figure 4.11). Signals from the methyl moieties attached

to C-7 (δ 27.2 and 23.8 ppm) also exist in different environments relating to the axial and equatorial positions of the cyclohexyl ring system.

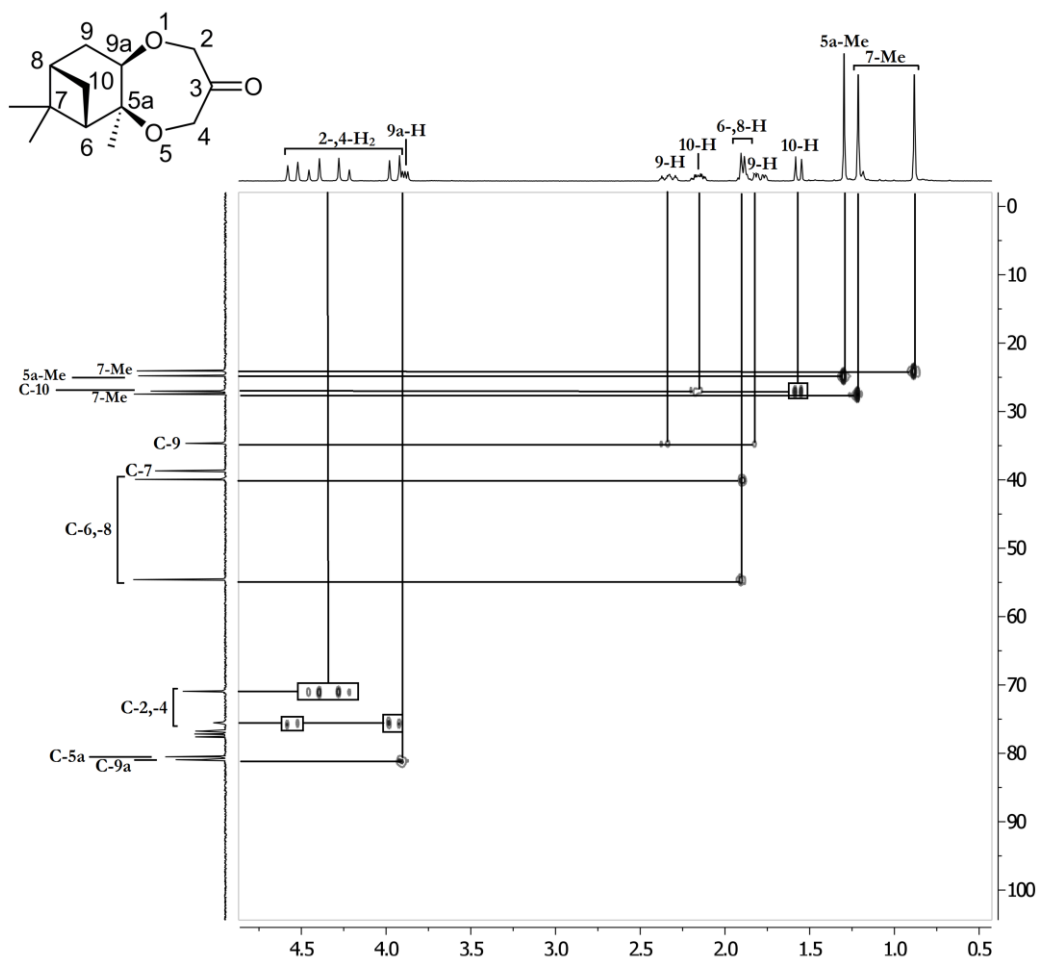
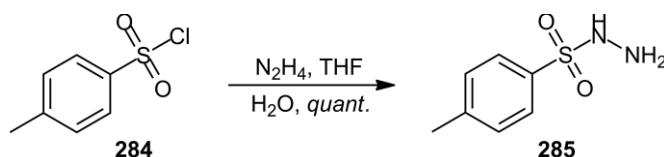


Figure 4.11: ^1H , ^{13}C HSQC (CDCl_3 , 300 MHz) spectrum of compound **283**.

4.2.3 – 1,4-Dioxepan-6-one/Terpenoid Odorant Fusion – (*R*)-Camphor

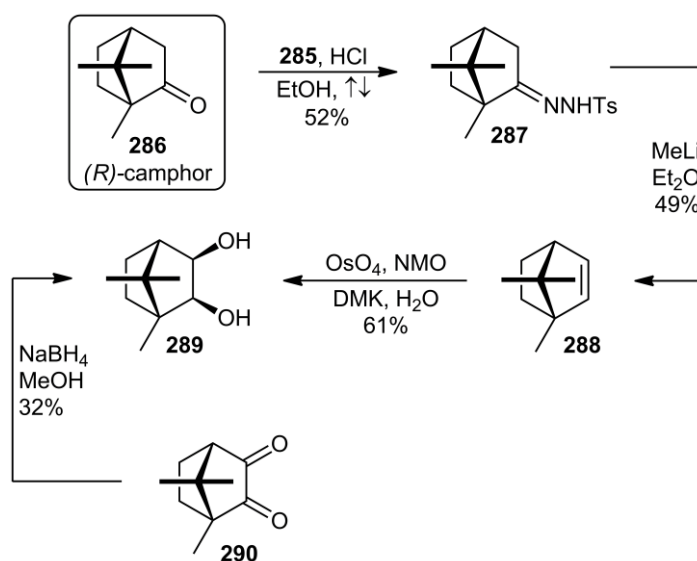
Camphor is a naturally occurring chiral bicyclic terpenoid compound. Both enantiomers give rise to the same unique odorant description of camphoraceous, meaning warm-minty, medicinal and somewhat ethereal.^[23] It should be noted that although both enantiomers are found in nature, (*R*)-camphor (**286**) is far more abundant.^[23] The synthesis of a 1,4-dioxepan-6-one heterocycle fused (*R*)-camphor analogue commenced with the synthesis of *para*-toluenesulfonylhydrazide (**285**) from *para*-toluenesulfonyl chloride (**284**) and aqueous hydrazine hydrate in quantitative yields (Scheme 4.5).^[24] The following step involved the reaction of (*R*)-camphor (**286**) and hydrazide **285** using hydrochloric acid as a catalyst to give the corresponding tosylhydrazone **287** as a colourless solid in 52% yield.^[25] This hydrazone compound was then subjected to a Shapiro reaction using two equivalents

of methyllithium to provide the volatile bicyclo[2.2.1]hept-2-ene compound **288** in 49% yield after careful isolation (Scheme 4.6).^[25]



Scheme 4.5: Synthesis of *para*-toluenesulfonylhydrazide (**285**) from *para*-toluenesulfonyl chloride (**284**).

The double bond of compound **288** was subjected to an osmium tetroxide/*N*-methylmorpholine *N*-oxide (NMO) mediated dihydroxylation reaction to provide *cis*-diol **289** in 61% yield as a colourless solid and as a single stereoisomer (Scheme 4.6). It was expected that both the *endo/endo* and *exo/exo* stereoisomers could be isolated by this methodology but it was discovered that all that was obtained was the *exo/exo* stereoisomer. The absolute configuration of compound **289** was confirmed by comparison to literature.^[26]



Scheme 4.6: Synthesis of *cis*-diol compound **289** from *(R)*-camphor (**286**) and *(-)*-camphorquinone (**290**).

The key transformation in the synthetic sequence, the Shapiro reaction,^[27] involves the addition of two equivalents of a strong organolithium base to the camphor tosylhydrazone **287**. The initiating step involves the removal of the proton from the hydrazone, followed by the removal of the proton alpha to the hydrazone carbon (Figure 4.12). The molecule then undergoes an elimination reaction to create a

carbon–carbon double bond with simultaneous expulsion of the tosyl group and formation of a diazonium anion, which eliminates as a neutral nitrogen molecule. The resulting anion is quenched by the addition of an electrophile (H_2O in the case of compound **287**) to provide the alkene. This reaction is related to the Bamford-Stevens reaction which involves the addition of a strong base as opposed to an organolithium reagent, and is also known to follow a different reaction mechanism. The advantage of the Shapiro reaction is that the resulting intermediate compounds do not have the same tendency to rearrange.^[28]

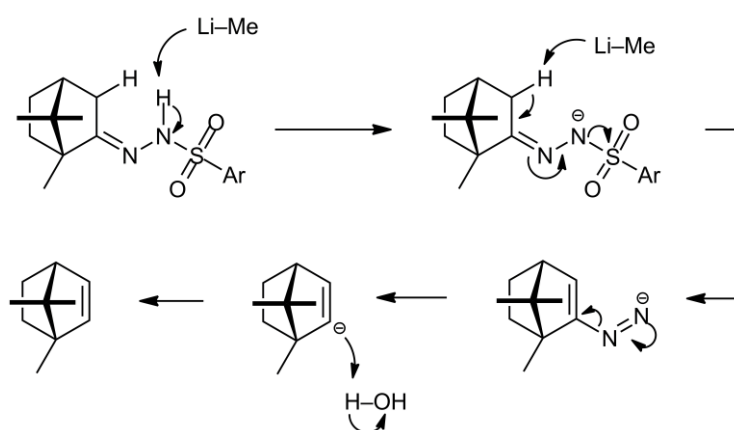
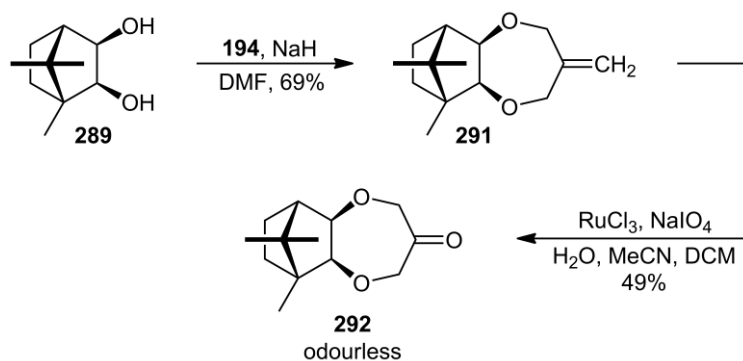


Figure 4.12: Mechanism of the Shapiro reaction of hydrazone compound **287** to give alkene **288**.

An alternative methodology to provide *cis*-diol **289** starting from (–)-camphorquinone (**290**) was also experimented with. Literature reports that a borohydride reduction of (–)-camphorquinone (**290**) gives the same *cis*-diol stereoisomer as what was discovered for the reaction sequence beginning with (*R*)-camphor (**286**).^[26] The reaction was discovered to be successful, giving compound **289** in 32% yield (Scheme 4.6). The isolated *exo,exo*-camphor-2,3-diol (**289**) was subjected to a Williamson reaction with **194** to afford methylene compound **291** in 69% yield as a clear oil after flash chromatography on silica gel. Katsuki–Sharpless oxidation provided 2,3-annulated dioxepanone **292** as a colourless solid in 48% yield (Scheme 4.7).



Scheme 4.7: Synthesis of dioxepanone fused (*R*)-camphor analogue **292** from *cis*-diol compound **289**.

An alternative literature procedure could potentially be used to synthesise all four *bis*-hydroxyl stereoisomers from (*R*)-camphor (**286**). The methodology requires the formation of an enolate intermediate using the strong base lithium diisopropylamide, followed by the addition of a molybdenum peroxide reagent (MoOPH) to perform an enolate hydroxylation.^[29] The molybdenum reagent can be synthesised from molybdenum oxide, hydrogen peroxide, hexamethylphosphoric triamide (HMPA) and pyridine in a two-step procedure.^[29] When reacted with (*R*)-camphor (**286**) the reagent provides a 5:1 *endo:exo* ratio of the α -hydroxy analogue of (*R*)-camphor (**286**). The diastereomers could be potentially separated by chromatography and reduced to a mixture of stereoisomeric *bis*-hydroxyl compounds in an unknown ratio.

4.2.4 – 1,4-Dioxepan-6-one/Terpenoid Odorant Fusion – (*S*)-Carvone and (*S*)-Carvotanacetone

The synthesis of a 1,4-dioxepan-6-one heterocycle fused terpenoid odorant beginning from (*S*)-carvone (**28**) was planned. Carvone has one chiral centre and therefore exists as two stereoisomers, both with different fragrance profiles. (*S*)-Carvone (**28**) has the odour of caraway and an odour threshold value of 7.6 ng/L air, whilst its antipode (*R*)-carvone (**29**) has the odour of spearmint and an odour threshold value of 0.88 ng/L air.^[3] These enantiomers provide good evidence that at least some human olfactory receptors are chiral. Interestingly, 8–10% of the population are not able to discern between the enantiomers; a specific type of chiral anosmia.^[30-31] The initiating step in the synthetic sequence involved an epoxidation reaction of (*S*)-carvone (**28**) using basified hydrogen peroxide at 0 °C to give a crude mixture of epoxide stereoisomers in 87% yield (Scheme 4.8).^[32-34] The mixture was discovered by GC-MS to be a 95:5 mixture of *cis*-carvone oxide (**293**) and *trans*-carvone oxide (**294**), respectively (Figure 4.13).^[35-36]

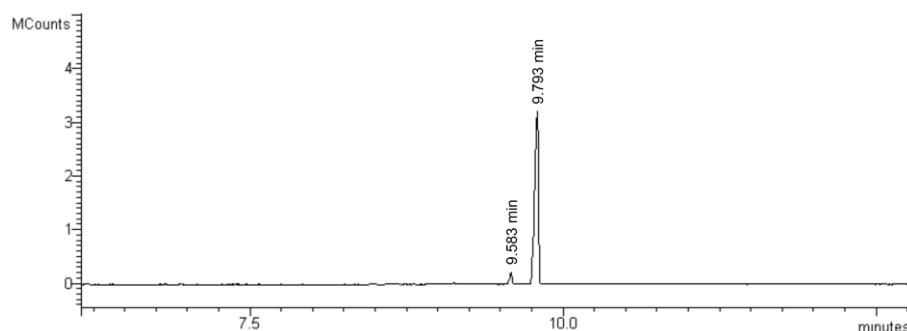
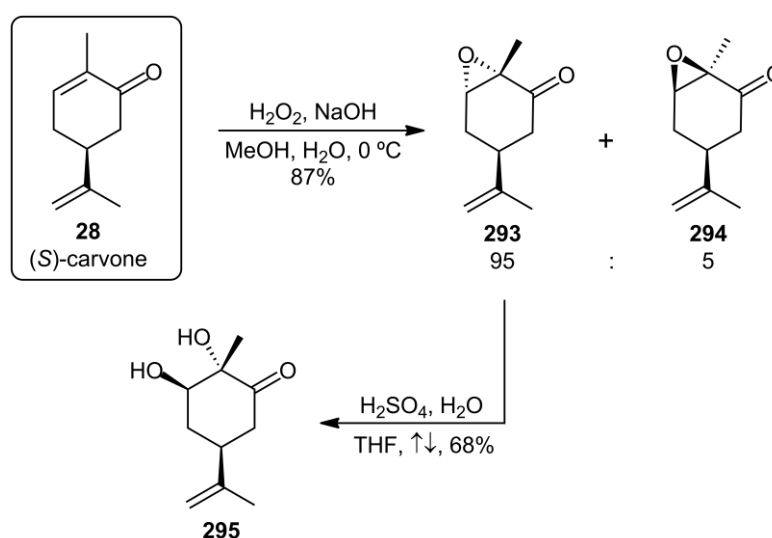


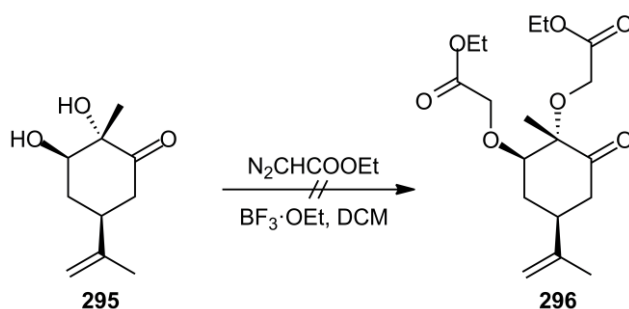
Figure 4.13: GC-MS chromatograph of the oxidation reaction of (*S*)-carvone (**28**). 9.583 minutes: *trans*-carvone oxide (**294**); 9.793 minutes: *cis*-carvone oxide (**293**).

The epoxide stereoisomers (**293** and **294**) were readily separated by flash chromatography on triethylamine deactivated silica gel. The major diastereomer (**293**) was subjected to an acid-catalysed epoxide ring-opening reaction using sulphuric acid to provide compound **295** in 68% yield.^[37] Five literature publications report the synthesis of diol **295** (or antipode) using analogous methodology. Three publications do not specify the stereochemistry of the resulting product,^[34, 37-38] one publication specifies a (*2S,3R,5S*) configured product (**295**)^[39] and one publication specifies an equimolar mixture of *cis*- and *trans*-configured diol compounds,^[40] which is improbable as *cis*-diol compounds are unlikely to arise as a major product of an acid-catalysed ring-opening reaction, this type of reaction proceeding predominantly by nucleophilic attack at the less hindered face.^[41] It is hereby assumed that the stereochemistry is (*2S,3R,5S*).



Scheme 4.8: Synthesis of *trans*-diol **295** from (*S*)-carvone (**28**).

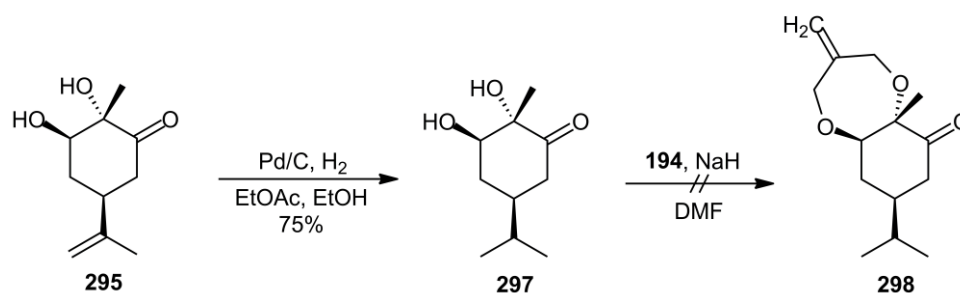
Multiple attempts at the *bis*-etherification of *trans*-diol compound **295** with ethyl diazoacetate provided only complex polymerised mixtures, presumably due to complications relating to the unprotected carbonyl moiety (Scheme 4.9). To begin the chemical reaction, more boron trifluoride diethyletherate was required than would be expected, perhaps owing to chelation with the lone-pair electrons of the carbonyl oxygen. The reaction is readily visible by the release of nitrogen gas from the dichloromethane solvent.



Scheme 4.9: Failed *bis*-etherification of *trans*-diol **295** with ethyl diazoacetate.

As the molecular structure of *trans*-diol compound **295** contained unsaturation it would be futile to attempt Williamson reaction methodologies as the subsequent Katsuki-Sharpless oxidation would be likely to oxidise both alkene functionalities. Compound **295** was therefore hydrogenated with palladium on carbon (Pd/C) in ethyl acetate under an atmosphere of hydrogen, with catalytic amounts of ethanol added to assist in catalyst activation. The reaction successfully provided saturated analogue **297** as a yellow oil in 75% yield (Scheme 4.10).

Compound **297** can be viewed as the 2,3-*bis*-hydroxyl analogue of (*S*)-carvotanacetone, a naturally occurring terpenoid with similar olfactory properties to the parent unsaturated compound (*S*)-carvone (**28**). An attempt was made at the Williamson reaction of *trans*-diol **297** with *bis*-halogen **194** but the reaction was again discovered to lead to polymer. The origin of the complications are presumably related to the removal of an acidic alpha hydrogen by the sodium hydride reagent, followed by aldol-type intermolecular polymerisation. Owing to these complications the synthesis of dioxepanone heterocycle fused analogues of (*S*)-carvone and (*S*)-carvotanacetone were abandoned.

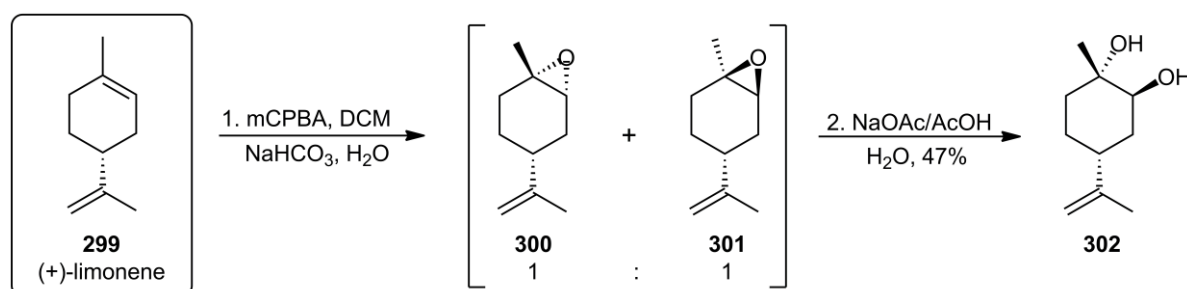


Scheme 4.10: Hydrogenation of diol **295** to give saturated diol **297**, followed by failed etherification with **194**.

4.2.5 – 1,4-Dioxepan-6-one/Terpenoid Odorant Fusion – (+)-Limonene

The following terpenoid compound to undergo experimentation was (+)-limonene (**299**), the major odorant within the citrus genus which contains considerable quantities of this terpenoid within their fruits. The odour of (+)-limonene (**299**) is described as ‘fresh citrus and orange-like’ whilst the odour of the enantiomer, (–)-limonene, is described as ‘harsh and turpentine like’.^[17]

(+)-Limonene (**299**) was epoxidised using *meta*-chloroperoxybenzoic acid to give an equimolar mixture of *trans*-limonene oxide (**300**) and *cis*-limonene oxide (**301**), with minor quantities of *bis*-epoxide impurities also identified as being present by GC-MS (Scheme 4.11, Figure 4.14).^[42-44] The racemic mixture of **300** and **301** is reported to not be separable by standard chromatographic or distillation techniques.^[45] It is reported in literature that an acidic ring-opening reaction of the diastereomeric mixture gives a single *trans*-diol product.^[46] It has been reasoned that this effect occurs due to selective axial nucleophilic attack, which can be rationalised by the Fürst-Plattner Rule.^[45, 47] A number of methods have been established to exploit this effect in the separation of the epoxide diastereomers, namely by manipulating the substantially faster reaction rate of the *cis*-diastereomer **301**.



Scheme 4.11: Synthesis of *trans*-diol compound **302** from (+)-limonene (**299**).

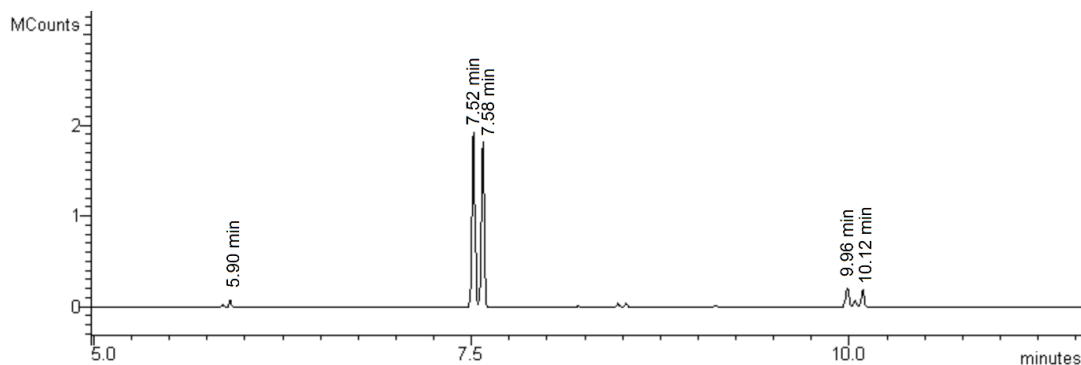


Figure 4.14: GC-MS chromatograph of the oxidation reaction of (+)-limonene (**299**). 5.90 minutes: unreacted (+)-limonene (**299**); 7.52 minutes: *cis*-limonene oxide (**301**); 7.58 minutes: *trans*-limonene oxide (**300**); 9.96–10.12: limonene *bis*-epoxide impurities.

It is reported in literature that a pH 4 buffered solution (NaOAc/AcOH) can react to give complete conversion of *cis*-limonene oxide (**301**) after 3.5 hours, thus yielding a readily separable mixture of optically pure *trans*-limonene oxide (**300**) and optically pure *trans*-diol compound **302** (Figure 4.15).^[47] It is also reported that a pH 3 buffered solution (K₂HPO₄/KH₂PO₄) reacts to give complete conversion of both diastereomers to *trans*-diol **302** after 12 hours of reaction time. Experimentation with a pH 4 buffered reagent revealed that after an extended reaction time, complete conversion of **300** and **301** to the *trans*-diol stereoisomer **302** was also possible.

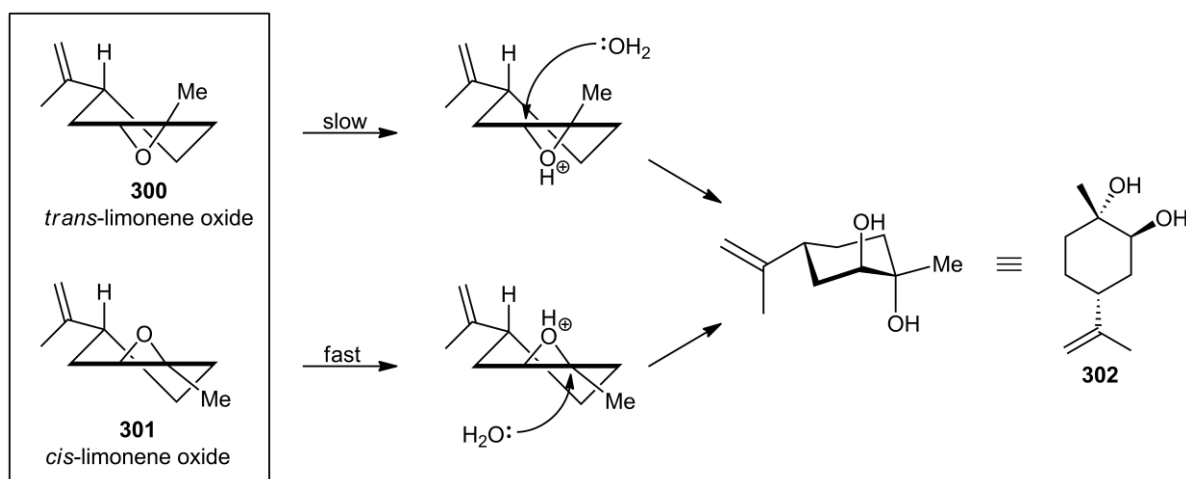
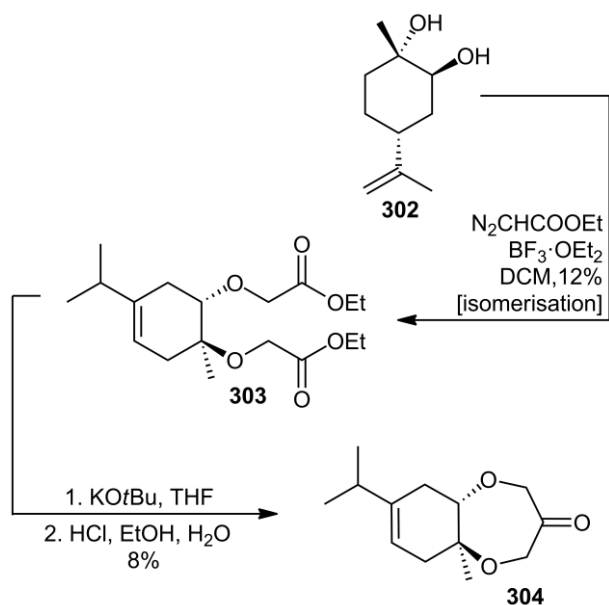


Figure 4.15: Acid-catalysed ring-opening of *cis*- and *trans*-limonene oxides to give *trans*-diol **302**.^[47]

Compound **302** was *bis*-etherified using ethyl diazoacetate and boron trifluoride as a Lewis-acid catalyst. Isomerisation was discovered to occur with the alkene moiety migrating into the cyclohexyl ring. The yield was lower than anticipated, a mere 12% of the isomerised *bis*-ester product (**303**) being isolated as a yellow oil. Alkene migration was readily confirmed by ^1H NMR integration of the alkene signal at δ 5.22 (Figure 4.16). The undesired *bis*-ester (**303**) was subjected to Dieckmann condensation, and after decarboxylation, the 2,3-annulated dioxepanone **304** was isolated in a meagre 8% yield (Scheme 4.12).



Scheme 4.12: Synthesis of dioxepanone fused (+)-limonene analogue **304** from *trans*-diol **302**, with alkene isomerisation.

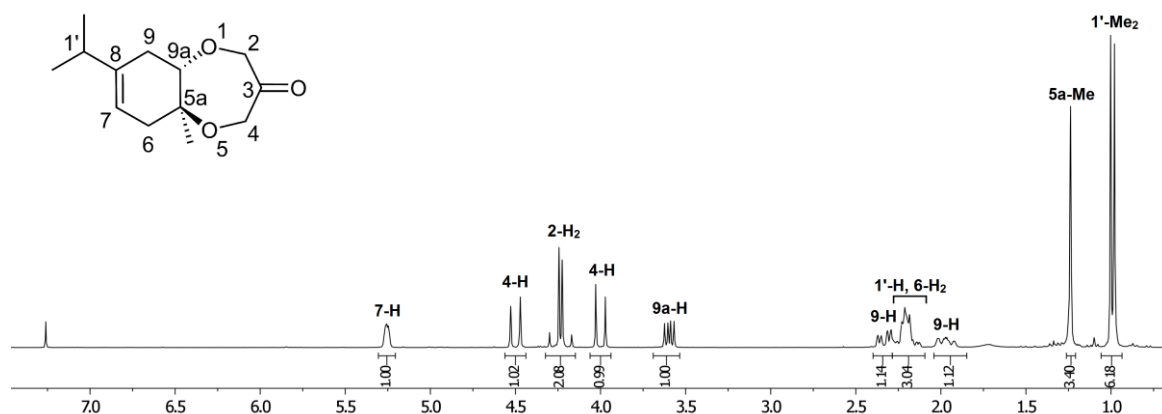


Figure 4.16: ^1H NMR (CDCl_3 , 300 MHz) spectrum of dioxepanone fused (+)-limonene analogue **304**.

The mechanism by which isomerisation occurred may be analogous to the way in which (*S*)-carvone (**28**) undergoes acid-catalysed aromatisation to give carvacrol (Figure 4.17).^[48] The sequence begins when π electrons originating from the alkene moiety nucleophilically attack a proton, giving a more stable tertiary carbocation. The intermediate then undergoes a 1,2-hydride shift followed by elimination of a proton to generate a conjugated alkene compound. Acid-catalysed enolisation then provides the highly stable aromatic compound. It can be postulated that a similar mechanism of isomerisation occurred with *trans*-diol compound **302**, stopping after carbocation rearrangement and proton elimination to give the isomerised product **303**.

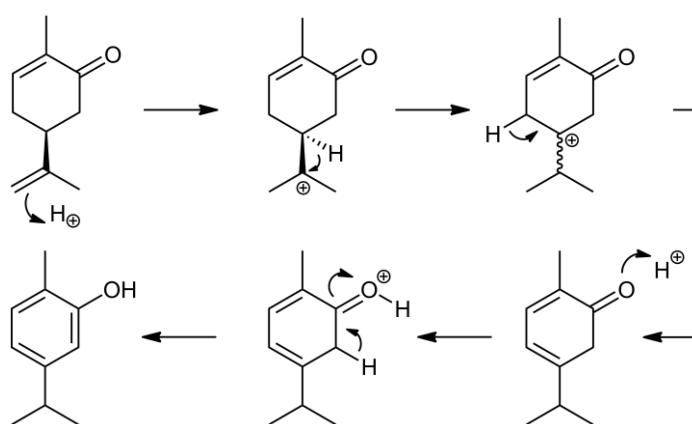
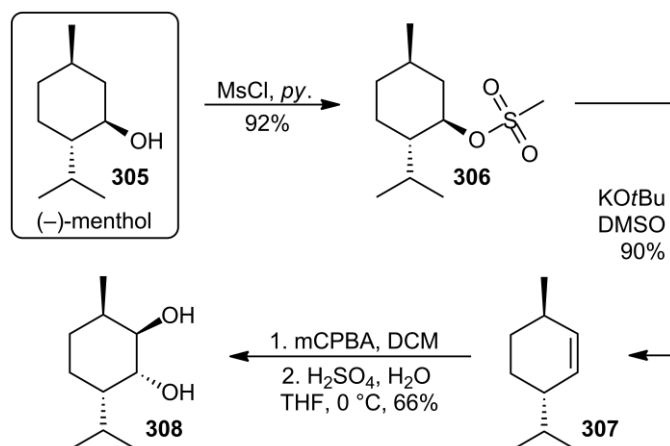


Figure 4.17: Mechanism for the acid-catalysed aromatisation of (*S*)-carvone to carvacrol.^[48]

4.2.6 – 1,4-Dioxepan-6-one/Terpenoid Odorant Fusion – (–)-Menthol

Menthol is a naturally occurring chiral terpenoid odorant isolated from the mint family. Natural menthol exists predominantly as the (1*R*,2*S*,5*R*) stereoisomer, known as (–)-menthol (**305**), and is described as being ‘sweet, fresh, minty and strongly cooling’.^[3] In an attempt to fuse a 1,4-dioxepan-6-one heterocyclic ring onto (–)-menthol (**305**) the synthesis of a *bis*-hydroxyl analogue of the starting material was required. A publication by Suemune *et al.*^[49] detailed the synthesis and characterisation of all possible stereoisomers of menthol-1,2-diol beginning from alkene (3*S*,6*R*)-3-isopropyl-6-methylcyclohex-1-ene (**307**), although reaction conditions were not provided for the synthesis of the alkene compound.



Scheme 4.13: Synthesis of *trans*-diol compound **308** from (-)-menthol (**305**).

The reaction of (-)-menthol (**305**) with methanesulfonyl chloride in pyridine gave the corresponding mesylate ester (**306**) in 92% yield as a yellow oil (Scheme 4.13).^[50, 51] Attempts at purification by vacuum bulb–bulb distillation ($>100\text{ }^\circ\text{C}$, 0.1 mm/Hg) provided an eliminated alkene product that did not match the NMR characterisation data for the required alkene compound (**307**). The isolated compound instead matched predicted ^{13}C NMR data for an alternate elimination reaction to give the higher substituted alkene compound (**309**). Another sample of the crude mesylate (**306**) was reacted with potassium *tert*-butoxide in dimethyl sulfoxide to provide the correct alkene compound (**307**) as a thin yellow liquid in 90% yield after careful isolation due to volatility (Figure 4.18).^[52]

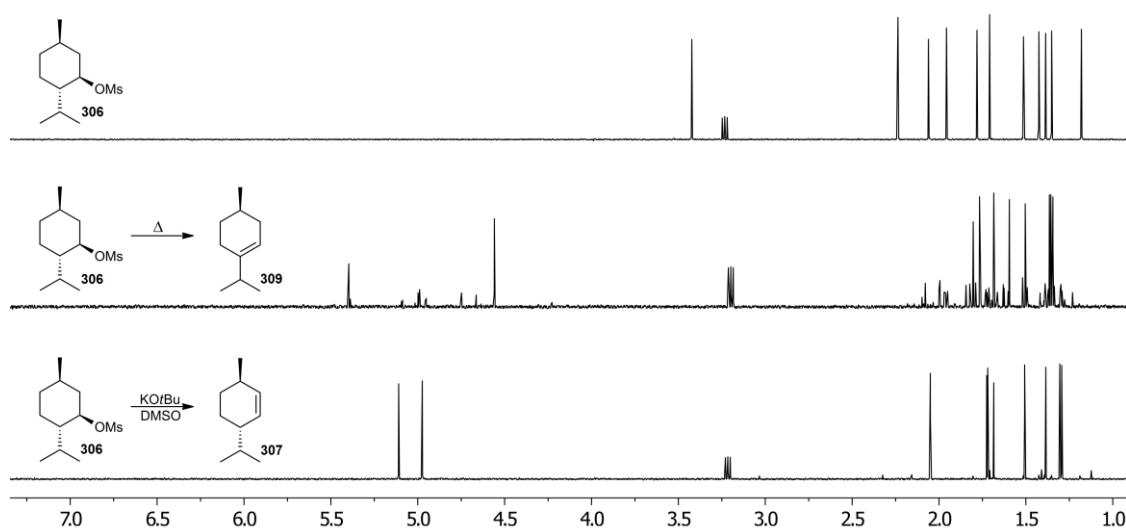


Figure 4.18: ^{13}C NMR (CDCl₃, 75 MHz) spectra showing: (top) mesylate **306**; (middle) elimination reaction of **306** with heat to give alkene **309**; (bottom) elimination of **306** with KOtBu to give alkene **307**.

The reaction of mesylate **306** with potassium *tert*-butoxide follows an E2 elimination mechanism. This infers an elimination mechanism with a single transition state and no intermediate compounds. Under standard conditions it would be expected that alkene **309** would be the major product formed owing to the greater thermodynamic stability that higher substituted alkenes offer (Zaitsev's rule). Instead, due to the steric bulk of potassium *tert*-butoxide only the removal of the less hindered proton from the secondary carbon and not the proton from the tertiary carbon can physically take place (Hofmann's rule). Additionally, the only antiperiplanar C-H atom available, in regards to the C-OMs moiety, is at C-6 owing to the configuration of (–)-menthol. This sequence provides alkene **307**, the Hofmann elimination product.

Mesylate compound **306** underwent an E1 elimination when heated during vacuum distillation. The mesylate moiety was eliminated to give a carbocation intermediate followed by the extraction of a proton to provide the alkene product. The carbocation intermediate can explain the inseparable impurities located by ^{13}C NMR analysis, as carbocation rearrangements are known to occur during this type of mechanism. The major isolated product was still alkene **309**, which followed Zaitsev's rules of alkene formation by elimination (Figure 4.19).

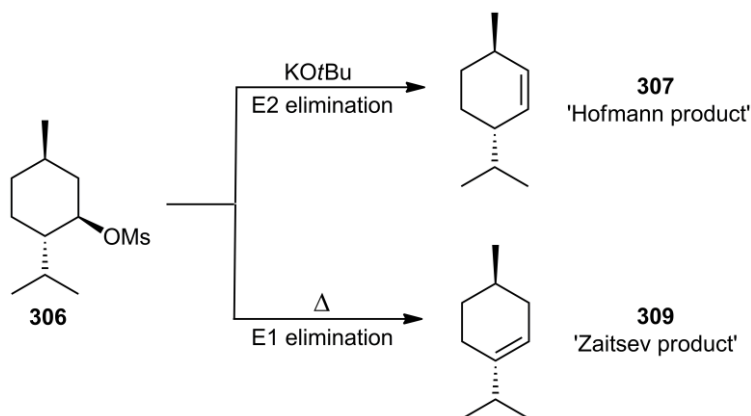
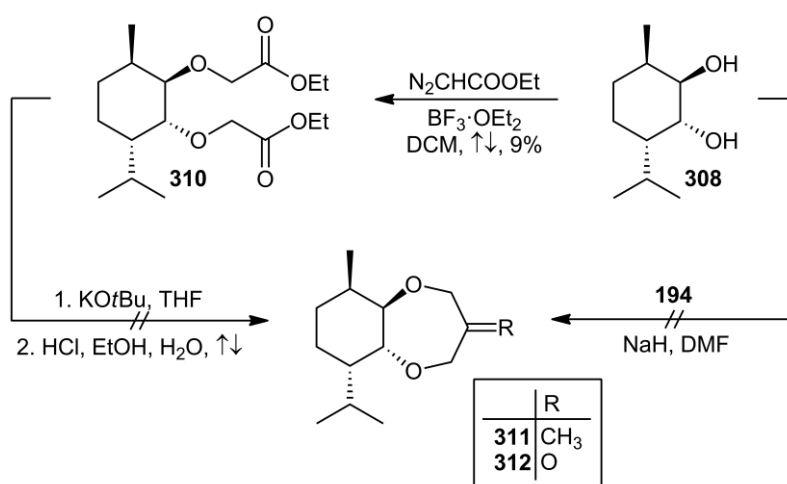


Figure 4.19: Different elimination products of mesylate compound **306**.

The isolated alkene (**307**) was epoxidised with *meta*-chloroperoxybenzoic acid to give an intermediate epoxide compound, immediately followed by an acidic ring-opening reaction with sulphuric acid to provide *trans*-diol **308** in 66% yield after flash chromatography on silica gel.^[49] It was reported that an isomeric *trans*-diol compound would be present in trace quantities,^[49] although this diastereomer was never identified or isolated.

Etherification of *trans*-diol compound **308** with ethyl diazoacetate was achieved in 9% yield only, providing *bis*-ester **310** as a yellow oil (Scheme 4.14). All attempts to subject compound **310** to Dieckmann cyclisation yielded only polymerised material. The Williamson reaction of *trans*-diol **308** with *bis*-halogen **194** also failed to provide the required product. Computational molecular modelling revealed that the isopropyl group of **308/310** is preferentially favoured when situated in an equatorial position which thereby forces the hydroxy/ether functionalities into *bis*-axial positions (Figure 4.20). This renders these moieties pointed in opposite directions out of plane and thus makes both the Dieckmann cyclisation and Williamson cyclisation reactions problematical.



Scheme 4.14: Failed synthesis of dioxepanone fused (–)-menthol analogue **312** from *trans*-diol compound **308**.

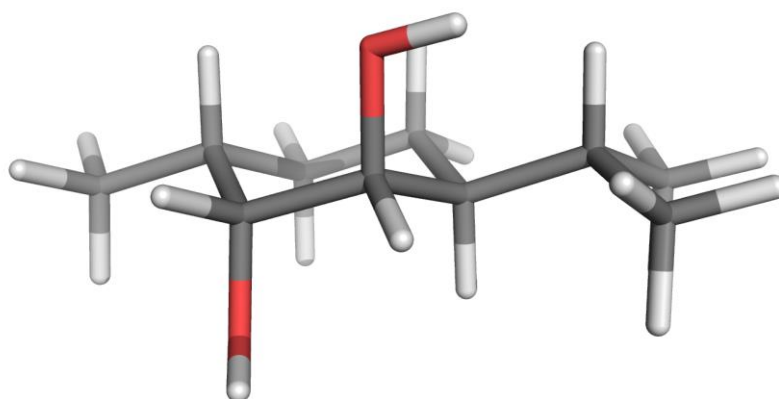


Figure 4.20: Minimum-energy conformation of (1*R*,2*R*,3*S*,6*R*)-3-isopropyl-6-methylcyclohexane-1,2-diol (**308**) generated with the HyperChem 8 scripting facility and subjected to brief molecular dynamics to take atoms and bonds out of default angles and lengths. The structure was then minimised using the *ab initio* STO-3G method.^[53]

4.2.7 - Structure-Odour Correlations and Conclusions

The olfactory properties of the substituted 1,4-dioxepan-6-one compounds are summarised in Table 4.1, and the olfactory properties of the heterocycle fused terpenoid compounds are summarised in Table 4.2. Olfactory evaluations were performed by expert perfumers on blotter using a 10% solution of the sample substance in dipropylene glycol (DPG), odour threshold values were determined by panel using GC-Olfactometry (GC-O). While the two parent 1,4-dioxepan-6-ones, **269** and (±)-**275**, did possess slight marine character, the 2-substituted 1,4-dioxepan-6-one compounds are, with the exception of (±)-**276**, too weak to be useful as perfumery material. This further corroborates the marine olfactophore models that feature the aromatic ring as an essential binding motif for marine odourant analogues.

This discovery also provided evidence that the receptor binding energy gained from a molecule binding to the aliphatic hydrophobe is lower than that gained from binding to the aromatic site. The dioxepanone analogues (±)-**276** and (±)-**277**, as well as various other analogues (i.e. **204**) can, in theory, still be interacting with the aliphatic hydrophobe adjacent to the aromatic binding site, but remain weak non-marine odourants. The results may additionally offer evidence that the receptor models developed by Kraft *et al.*,^[4, 54] which place the aliphatic hydrophobe 7.23 Å from the aromatic binding site, are more accurate than the model developed by Gaudin *et al.*^[55] which places the same binding site adjacent to the carbocyclic ring system.

Although compounds **269** and (±)-**275** contain what could be described as marine aspects, the association was unpleasant and closer to seawater and algae, not fresh marine nuances. Compounds **269** and (±)-**275** were also discovered to contain a fruity aspect in the direction of melon, but green and earthy side aspects would prevent any use of these compounds as perfumery material. Compound (±)-**275** was distinctly more melon than compound **269**, and also less salty, green and earthy. It should be noted that the original patent first described benzo[*b*][1,4]dioxepin-3-one analogues as having a watermelon-like odour.^[56] The 2-isobutyl substituted 1,4-dioxepan-6-one (±)-**277** was devoid of any fruity, watermelon or marine odour attributes, but its weak, fatty-oily agrestic odour instead recalled linalool with some additional spicy facets. The 2,2,3,3-tetramethyl-1,4-dioxepan-6-one **278** was completely odourless.

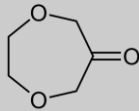
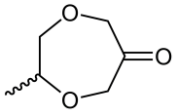
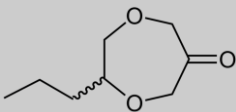
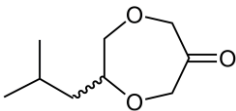
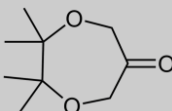
#	Molecular Structure	Odour Description
269		Odour description: Rather weak, marine, salty, fruity in direction of melon with green, earthy aspects, slightly fatty, solvent-like, slightly in the direction of petrol.
(±)-275		Odour description: Rather weak, fruity, marine, distinctly melon, more fruity than 269, more transparent while less salty, green and earthy than 269.
(±)-276		Odour description: Green-floral anisic, hawthorn-type, with aspects of <i>cis</i> -jasmone and celery leaves, as well as a cinnamic powdery inflection, and slightly metallic facets. Odour threshold: 210 ng/L air (stan. dev. 62 ng/L air).
(±)-277		Odour description: Rather weak, agrestic, linalool, slightly oily, fatty, spicy nuances.
278		Odour description: Odourless.

Table 4.1: Olfactory properties of 1,4-dioxepan-6-one analogues **269**, **275–278**.

The most potent and also most interesting odorant of the series turned out to be compound (±)-**276** which was initially described as powerful, although its odour threshold was discovered to be a mere 210 ng/L air. Yet, its rather low molecular weight coupled with an accordingly high vapour pressure makes (±)-**276** sufficiently intense as a top-note odorant. Its odour profile was however completely out of the marine range. The 2-propyl substituted 1,4-dioxepan-6-one (**276**) instead possessed a green-floral anisic, hawthorn-type odour with aspects of *cis*-jasmone and celery leaves, as well as a cinnamic powdery inflection, and slightly metallic facets.

It appeared as if the C-2 propyl substituent of (±)-**276** addressed a different odorant family related to such green-floral jasminic-anisic notes as celery ketone (3-methyl-5-propylcyclohex-2-enone, **313**) and

cis-jasmone ((2'*Z*)-3-methyl-2-pent-2'-en-1'-ylcyclopent-2-en-1-one, **314**). It was revealed during research by List *et al.*^[57] that the two enantiomers of celery ketone (**313**) have rather different fragrance profiles, of which the stronger (*R*)-enantiomer, with an odour threshold (th) value of 9.1 ng/L air, is responsible for the typical lovage and celery character of the racemate. The (*S*)-enantiomer was discovered to be roughly five times weaker and comprised predominantly of aniseed, liquorice and fennel notes. The molecular association of racemic (\pm)-**276** with that of racemic celery ketone (**313**) may give rise to the green notes, the associations being towards both jasmine and aniseed.

A biflexible alignment of the (*S*)-enantiomer of compound **276** (grey) on (*R*)-celery ketone (black, **313**) and *cis*-jasmone (white, **314**) with the Molecular Operation Environment (MOE) software package^[53] revealed that the C-3 substituent of (*S*)-**276** overlies agreeably with the (2*Z*)-pent-2-enyl substituent of *cis*-jasmone (**314**), as well as the propyl side-chain of celery ketone (**313**) (Figure 4.21). In addition, the double bonds of celery ketone (**313**) and *cis*-jasmone (**314**) come to lie in close vicinity to the O-4 ether oxygen of (*S*)-**276** indicating that the associated electron density might contribute to receptor binding besides the main docking via the carbonyl osmophore.

Since *cis*-jasmone (**314**) features no stereocenter the alignment of the (*R*)-enantiomer (*R*)-**276** on (*R*)-celery ketone (**313**) and *cis*-jasmone (**314**) is comparably good. However, with regard to the enantiodiscrimination of celery ketone (**313**), one could expect some stereodifferentiation of the enantiomers of **276**. Yet, both celery ketone (**313**) and *cis*-jasmone (**314**) are far more potent than racemic 2-propyl-1,4-dioxepan-6-one (**276**). If the green-floral jasminic-anisic notes of (\pm)-**276** are to be explored and improved, both enantiomers of **276** as well as further analogues would need to be synthesised. The insight provided by the superposition analysis delineated in Figure 4.21 could then be the starting point for a more comprehensive model on green-floral jasminic-anisic odorants.

Only two testable analogues, compounds **283** and **292**, were successfully synthesised from the six proposed terpenoid based fragrances with fused 1,4-dioxepan-6-one heterocyclic rings (Table 4.2). The analogue synthesised from (*R*)-camphor (**286**) was discovered to be completely devoid of odour whilst the analogue synthesised from (+)- α -pinene (**254**) had a minty-anisic, anethole-like smell with a wet-towel odour which is often encountered when mint and agrestic notes meet, but was rather weak

in smell and had no marine connotation at all. These results remain inconclusive regarding if the fusion of 1,4-dioxepan-6-one heterocycles onto other odorant molecules could offer additional marine nuances.

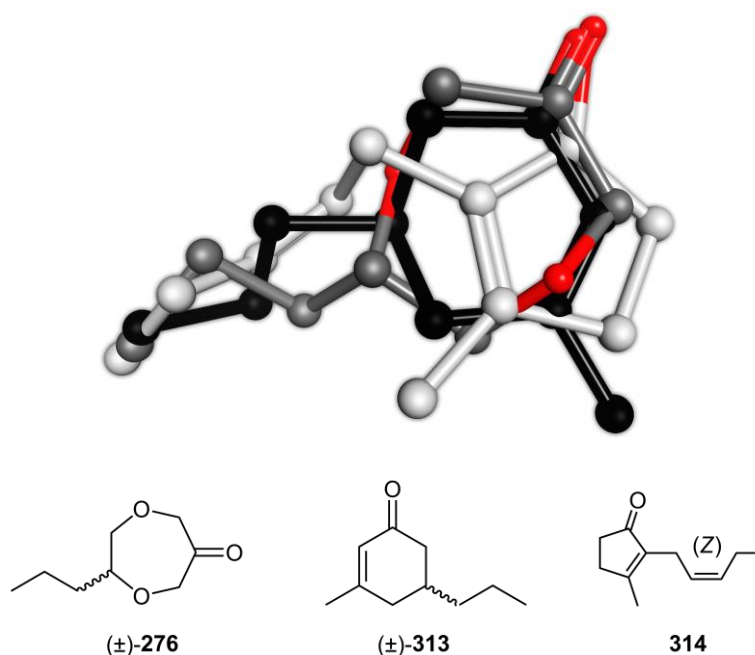


Figure 4.21. Biflexible alignment of the (*S*)-enantiomer of compound **276** (grey) on (*R*)-celery ketone (**313**), and *cis*-jasmone (white, **314**) generated with the MOE 2014.09 software package.^[53] The feature overlap (*F*), which describes the configurational similarity as the negative value of the probability density overlap function, has a value of -59.5 . The grand alignment score of the probability-density overlap is -37.5 . The grand alignment score of the (*R*)-enantiomer of compound **276** on (*R*)-celery ketone (**313**) and *cis*-jasmone (**314**) is -37.3 .

#	Molecular Structure	Description and Threshold
283		Odour description: Rather weak, slightly minty-anisic, anethole, with a wet-towel odour.
292		Odour description: Odourless.

Table 4.2: Olfactory properties of 1,4-dioxepan-6-one heterocycle fused terpenoid compounds **283** and **292**.

4.3 – Experimental Section

General Procedure A:

A solution of the diol compound (10.5 mmol) in DMF (30 mL) was added dropwise to a suspension of sodium hydride (1.05 g, 26.2 mmol, 60% dispersion in mineral oil) in DMF (60 mL) and the solution left to stir for 1 h. A solution of 3-chloro-2-(chloromethyl)-1-propene (1.31 g, 10.5 mmol) in DMF (40 mL) was then added dropwise over a period of 1 h, and the solution allowed to stir for 24 h. The reaction was then quenched by the additional of a saturated aqueous solution of NaHCO₃ (100 mL), extracted with Et₂O (4 × 100 mL), the organic extracts pooled and washed with H₂O (2 × 100 mL) before being dried (MgSO₄) and concentrated under reduced pressure. The resulting residue was then purified by flash chromatography on silica gel (EtOAc/hexane; 5:95) to yield the corresponding methylene compound.

General Procedure B:

To an ice-cool solution of the diol compound (40 mmol) and ethyl diazoacetate (10 g, 88 mmol, 2.2 equiv) in DCM (80 mL) was slowly added BF₃·OEt₂ (0.5 mL). After addition was complete the solution was held at 0 °C for 1 h before being quenched by the addition of a saturated aqueous solution of NaHCO₃ (100 mL). The mixture was then extracted with EtOAc (3 × 100 mL), the organic extracts pooled, dried (MgSO₄) and concentrated under reduced pressure. The resulting residue was purified by flash chromatography on silica gel (EtOAc/hexane; 2:8) to yield the corresponding *bis*-ester compound.

General Procedure C:

The methylene compound (5 mmol) was dissolved in MeCN (25 mL), H₂O (25 mL), and DCM (15 mL), and sodium metaperiodate (1.07 g, 5 mmol) and ruthenium trichloride (0.1 g, 0.5 mmol) were added. The mixture was stirred for 24 h, then further sodium metaperiodate (1.07 g, 5 mmol) and ruthenium trichloride (0.1 g, 0.5 mmol) were added. The solution was stirred for a further 24 h. The reaction mixture was then poured into H₂O (100 mL) and the resulting mixture was extracted with DCM (3 × 100 mL). The combined organic extracts were washed with a saturated aqueous solution of NaHSO₃ (100 mL) and with H₂O (100 mL), dried (MgSO₄), and concentrated under reduced pressure. The resulting residue was purified by flash chromatography on silica gel (EtOAc/hexane; 1:9) to give the corresponding ketone.

General Procedure D:

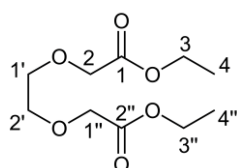
A solution of *bis*-ester compound (20 mmol) in THF (150 mL) was added dropwise to a stirred suspension of KO^tBu (4.5 g, 40 mmol, 2 equiv) in THF (100 mL) with cooling to 0 °C. Stirring was continued at 0 °C for 2 h before being quenched by the addition of 0.2 M HCl (800 mL) and ice (500 g). The resulting solution was then extracted

with DCM (3 × 200 mL), the organic extracts pooled, dried (MgSO₄) and concentrated under reduced pressure. The resulting residue was taken up in EtOH (100 mL) and 2 M HCl (500 mL) and the mixture stirred at reflux for 2 h. The solution was diluted with H₂O (300 mL) and extracted with DCM (3 × 200 mL). The combined organic extracts were washed with H₂O (200 mL), dried (MgSO₄) and concentrated under reduced pressure. The resulting residue was purified by flash chromatography on silica gel (EtOAc/hexane; 1:9) to yield the corresponding ketone.

General Procedure E:

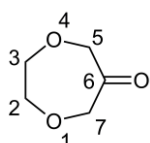
To a solution of alkene (20 mmol) and NMO (22 mmol) in acetone/H₂O (4:1, 50 mL) was added OsO₄ (100 mg) and the resulting solution stirred at RT for 48 h. The reaction was then quenched by the addition of Na₂SO₃ (1 g) and left for 1 h before being concentrated under reduced pressure. The residual oil was then taken up in H₂O (100 mL), extracted with EtOAc (5 × 100 mL), the organic extracts pooled and dried (MgSO₄) before being concentrated under reduced pressure. The resulting residue was then purified by flash chromatography on silica gel (EtOAc/hexane; 3:7) to yield the corresponding *cis*-diol compound.

Diethyl 2,2'-(ethane-1,2-diylbis(oxy))diacetate (268):



Following General Procedure B. Yellow oil, 74% yield. IR (ATR): $\tilde{\nu}$ = 1748 (v ester C=O), 1201 (v ester C–O), 1128 (v C–O) cm⁻¹. ¹H NMR (CDCl₃, 300 MHz): δ 4.21 (q, *J* = 7.1 Hz, 4H, 3-,3''-H₂), 4.15 (s, 4H, 2-,1''-H₂), 3.77 (s, 4H, 1',-2'-H₂), 1.28 (t, *J* = 7.1 Hz, 6H, 4-,4''-H₃). ¹³C NMR (CDCl₃, 75 MHz): δ 169.8 (2s, C-1,-2''), 70.4 (2t, C-1',-2'), 68.1 (2t, C-2,-1''), 60.2 (2t, C-3,-3''), 13.7 (2q, C-4,-4''). HRMS: *m/z* calculated for C₁₀H₁₈O₆: 234.1103 [M]⁺; Found: 234.1132.

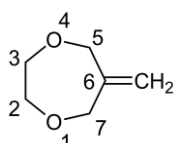
1,4-Dioxepan-6-one (269):



Following General Procedure D. Clear oil, 2% yield (92% via General Procedure C). IR (ATR): $\tilde{\nu}$ = 1720 (v C=O), 1144 (v C–O) cm⁻¹. ¹H NMR (CDCl₃, 300 MHz): δ 4.23 (s, 4H, 5-,7-H₂), 3.96 (s, 4H, 2-,3-H₂). ¹³C NMR (CDCl₃, 75 MHz): δ 211.1 (s, C-6), 78.0 (2t, C-5,-7), 75.6 (2t, C-2,-3).

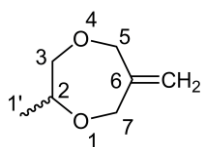
HRMS: *m/z* calculated for C₅H₈O₃: 116.0473 [M]⁺; Found: 116.0462. Odour description: Rather weak, marine, salty, fruity in direction of melon with green, earthy aspects, slightly fatty, solvent-like, slightly in the direction of petrol.

6-Methylene-1,4-dioxepane (270):

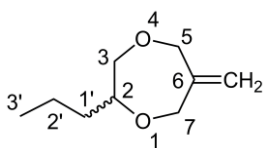


Following General Procedure A. Clear oil, 12% yield. IR (ATR): $\tilde{\nu}$ = 2925/2854 (v C–H), 1134/1092 (v C–O) cm⁻¹. ¹H NMR (CDCl₃, 300 MHz): δ 5.01–4.99 (m, 2H, =CH₂), 4.33–4.30 (m, 4H, 5-,7-H₂), 3.77–3.75 (m, 4H, 2-,3-H₂). ¹³C NMR (CDCl₃, 75 MHz): δ 148.1 (s, C-6), 111.5

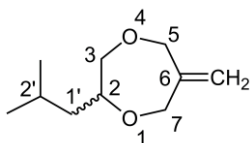
(t, =CH₂), 73.6 (2q, C-5,-7), 73.2 (2q, C-2,-3). HRMS: *m/z* calculated for C₆H₁₀O₂: 114.0681 [M]⁺; Found: 114.0674.

rac-2-Methyl-6-methylene-1,4-dioxepane (271):


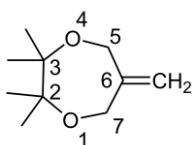
Following General Procedure A. Clear oil, 37% yield. IR (ATR): $\tilde{\nu}$ = 2937/2849 (ν C–H), 1104 (ν C–O), 884 (ν C=CH₂) cm⁻¹. ¹H NMR (CDCl₃, 300 MHz): δ 4.97–4.91 (m, 2H, =CH₂), 4.46–4.19 (m, 4H, 5-,7-H₂), 3.88 (dd, J = 12.5, 2.0 Hz, 1H, 3-H), 3.77–3.66 (m, 1H, 2-H), 3.27 (dd, J = 12.6, 9.4 Hz, 1H, 3-H), 1.10 (d, J = 6.4 Hz, 3H, 1'-H₃). ¹³C NMR (CDCl₃, 75 MHz): δ 148.6 (s, C-6), 110.5 (t, =CH₂), 78.8 (d, C-2), 78.7 (t, C-3), 73.9/72.6 (2t, C-5,-7), 16.9 (q, C-1'). HRMS: m/z calculated for C₇H₁₂O₂: 128.0837 [M]⁺; Found: 128.0842.

rac-6-Methylene-2-propyl-1,4-dioxepane (272):


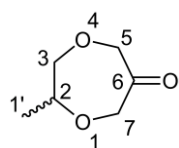
Following General Procedure A. Clear oil, 61% yield. IR (ATR): $\tilde{\nu}$ = 2958/2936 (ν C–H), 1104 (ν C–O), 897 (ν C=CH₂) cm⁻¹. ¹H NMR (CDCl₃, 300 MHz): δ 4.96–4.92 (m, 2H, =CH₂), 4.46–4.18 (m, 2H, 5-,7-H₂), 3.89 (dd, J = 12.5, 2.0 Hz, 1H, 3-H), 3.57–3.49 (m, 1H, 2-H), 3.29 (dd, J = 12.4, 9.4 Hz, 1H, 3-H), 1.54–1.24 (m, 4H, 1'-,2'-H₂), 0.96–0.88 (m, 3H, 3'-H₃). ¹³C NMR (CDCl₃, 75 MHz): δ 148.8 (s, C-6), 110.5 (t, =CH₂), 82.6 (d, C-2), 77.8 (t, C-3), 73.9/72.9 (2t, C-5,-7), 33.4 (t, C-1'), 18.7 (t, C-2'), 13.9 (q, C-3'). HRMS: m/z calculated for C₉H₁₆O₂: 156.1150 [M]⁺; Found: 156.1165.

rac-2-Isobutyl-6-methylene-1,4-dioxepane (273):


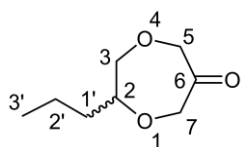
Following General Procedure A. Clear oil, 56% yield. IR (ATR): $\tilde{\nu}$ = 2954 (ν C–H), 1119 (ν C–O) cm⁻¹. ¹H NMR (CDCl₃, 300 MHz): δ 4.96–4.92 (m, 2H, =CH₂), 4.46–4.18 (m, 4H, 5-,7-H₂), 4.86 (dd, J = 12.5, 2.0 Hz, 1H, 3-H), 3.64–3.55 (m, 1H, 2-H), 3.28 (dd, J = 12.6, 9.4 Hz, 1H, 3-H), 1.84–1.73 (m, 1H, 2'-H), 1.42–1.32 (m, 1H, 1'-H), 1.10–1.00 (m, 1H, 1'-H), 0.91 (t, J = 6.4 Hz, 6H, 2'-Me₂). ¹³C NMR (CDCl₃, 75 MHz): δ 148.8 (s, C-6), 110.2 (t, =CH₂), 81.1 (d, C-2), 78.1 (t, C-3), 73.8/72.8 (2t, C-5,-7), 40.0 (t, C-1'), 24.2 (d, C-2'), 23.1/21.8 (2q, 2'-Me₂). HRMS: m/z calculated for C₁₀H₁₈O₂: 170.1307 [M]⁺; Found: 170.1284.

2,2,3,3-Tetramethyl-6-methylene-1,4-dioxepane (274):


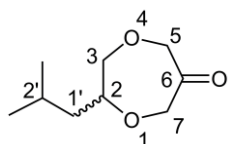
Following General Procedure A. Yellow oil, 26% yield. IR (ATR): $\tilde{\nu}$ = 2978 (ν C–H), 1152 (ν C–O) cm⁻¹. ¹H NMR (CDCl₃, 300 MHz): δ 4.90–4.87 (m, 2H, =CH₂), 4.26–4.24 (m, 4H, 5-,7-H₂), 1.22 (s, 12H, 2-,3-Me₂). ¹³C NMR (CDCl₃, 75 MHz): δ 149.3 (s, C-6), 108.9 (t, =CH₂), 80.7 (2s, C-2,-3), 66.3 (2t, C-5,-7), 22.9 (4q, 2-,3-Me₂). HRMS: m/z calculated for C₁₀H₁₈O₂Na: 193.1204 [M+Na]⁺; Found: 193.1189.

rac-2-Methyl-1,4-dioxepan-6-one (275):

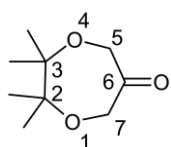
Following General Procedure C. Yellow oil, 27% yield. IR (ATR): $\tilde{\nu} = 1723$ (ν C=O), 1160/1113 (ν C–O) cm^{-1} . $^1\text{H NMR}$ (CDCl_3 , 300 MHz): δ 4.33–4.15 (m, 4H, 5-,7-H₂), 4.09 (dd, $J = 12.6$, 2.2 Hz, 1H, 3-H), 3.93–3.81 (m, 1H, 2-H), 3.40 (dd, $J = 12.6$, 9.6 Hz, 1H, 3-H), 1.17 (d, $J = 6.4$ Hz, 3H, 1'-H₃). $^{13}\text{C NMR}$ (CDCl_3 , 75 MHz): δ 211.3 (s, C-6), 81.0 (d, C-2), 80.4 (t, C-3), 77.9/76.7 (2t, C-5,-7), 16.8 (q, C-1'). HRMS: m/z calculated for $\text{C}_6\text{H}_{10}\text{O}_3$: 130.0629 [M]⁺; Found: 130.0603. Odour description: Rather weak, fruity, marine, distinctly melon, more fruity than **269**, more transparent while less salty, green and earthy than **269**.

rac-2-Propyl-1,4-dioxepan-6-one (276):

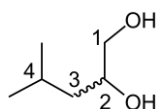
Following General Procedure C. Yellow oil, 50% yield. IR (ATR): $\tilde{\nu} = 2959/2837$ (ν C–H), 1723 (ν C=O), 1154/1111 (ν C–O) cm^{-1} . $^1\text{H NMR}$ (CDCl_3 , 300 MHz): δ 4.32–4.15 (m, 4H, 5, 7-H₂), 4.11 (dd, $J = 12.6$, 2.2 Hz, 1H, 3-H), 3.73–3.64 (m, 1H, 2-H), 3.43 (dd, $J = 12.5$, 9.7 Hz, 1H, 3-H), 1.58–1.29 (m, 4H, 1',2'-H₂), 0.94 (t, $J = 7$ Hz, 3H, 3'-H₃). $^{13}\text{C NMR}$ (CDCl_3 , 75 MHz): δ 211.2 (s, C-6), 84.7 (d, C-2), 79.3 (t, C-3), 77.7/76.8 (2t, C-5,-7), 33.0 (t, C-1'), 18.4 (t, C-2'), 13.7 (q, C-3'). HRMS: m/z calculated for $\text{C}_8\text{H}_{14}\text{O}_3$: 158.0943 [M]⁺; Found: 158.0956. Odour description: Green-floral anisic, hawthorn-type, with aspects of *cis*-jasmone and celery leaves, as well as a cinnamic powdery inflection, and slightly metallic facets. Odour threshold: 210 ng/L air (stan. dev. 62 ng/L air).

rac-2-Isobutyl-1,4-dioxepan-6-one (277):

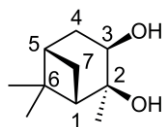
Following General Procedure C. Clear oil, 50% yield. IR (ATR): $\tilde{\nu} = 2956$ (ν C–H), 1723 (ν C=O), 1156/1127 (ν C–O) cm^{-1} . $^1\text{H NMR}$ (CDCl_3 , 300 MHz): δ 4.31–4.15 (m, 4H, 5-,7-H₂), 4.08 (dd, $J = 12.5$, 2.2 Hz, 1H, 3-H), 3.79–3.70 (m, 1H, 2-H), 3.42 (dd, $J = 12.5$, 9.7 Hz, 1H, 3-H), 1.88–1.74 (m, 1H, 2'-H), 1.48–1.38 (m, 1H, 1'-H), 1.16–1.06 (m, 1H, 1'-H), 0.93 (t, $J = 6.9$ Hz, 6H, 2'-Me₂). $^{13}\text{C NMR}$ (CDCl_3 , 75 MHz): δ 211.2 (s, C-6), 83.5 (d, C-2), 79.7 (t, C-3), 77.8/76.9 (2t, C-5,-7), 39.8 (t, C-1'), 24.2 (d, C-2'), 23.0/21.8 (2q, 2'-Me₂). HRMS: m/z calculated for $\text{C}_9\text{H}_{16}\text{O}_3$: 172.1099 [M]⁺; Found: 172.1088. Odour description: Rather weak, agrestic, linalool, slightly oily, fatty, spicy nuances.

2,2,3,3-Tetramethyl-1,4-dioxepan-6-one (278):

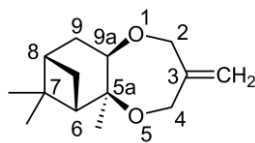
Following General Procedure C. Low-melting colourless solid, 57% yield. IR (ATR): $\tilde{\nu} = 2984$ (ν C–H), 1725 (ν C=O), 1152 (ν C–O) cm^{-1} . $^1\text{H NMR}$ (CDCl_3 , 300 MHz): δ 4.16 (s, 4H, 5-,7-H₂), 1.27 (s, 12H, 2-,3-Me₂). $^{13}\text{C NMR}$ (CDCl_3 , 75 MHz): δ 213.1 (s, C-6), 81.6 (2s, C-2,-3), 70.0 (2t, C-5,-7), 22.3 (4q, 2-,3-Me₂). HRMS: m/z calculated for $\text{C}_9\text{H}_{16}\text{O}_3$: 172.1099 [M]⁺; Found: 172.1088. Odour description: Odourless.

rac-4-Methylpentane-1,2-diol (280):^[15]


To a solution of 4-methyl-1-pentene (6 mL, 48 mmol) in acetic acid (80 mL) was added NaIO_4 (6.11 g, 28.5 mmol) and LiBr (1.65 g, 19 mmol) and the solution heated to 95 °C for 14 h. The reaction was diluted with H_2O (100 mL), washed with a saturated aqueous solution of $\text{Na}_2\text{S}_2\text{O}_3$ (30 mL) followed by washing with a saturated aqueous solution of NaHCO_3 (30 mL). The solution was extracted with EtOAc (3 × 100 mL), the organic extracts pooled, dried (MgSO_4) and concentrated under reduced pressure. The resulting residue was taken up in MeOH (120 mL), K_2CO_3 (13.1 g, 95 mmol) was added and the mixture stirred for 15 h. The reaction was then concentrated under reduced pressure, dissolved in H_2O (100 mL) followed by extraction with EtOAc (3 × 100 mL). The organic extracts were pooled, dried (MgSO_4) and concentrated under reduced pressure to yield a crude residue which was purified by flash chromatography on silica gel ($\text{EtOAc}/\text{hexane}$; 1:1) to yield 4-methylpentane-1,2-diol (5.18 g, 91%) as a yellow oil. IR (ATR): $\tilde{\nu}$ = 3338 (ν O–H), 2955/2927 (ν C–H), 1066/1026 (ν C–O) cm^{-1} . ^1H NMR (CDCl_3 , 300 MHz): δ 3.86–3.76 (m, 1H, 2-H), 3.69–3.61 (m, 1H, 1-H), 3.46–3.37 (m, 1H, 1-H), 2.15–2.04 (m, 2H, 1-,2-OH), 1.86–1.71 (m, 1H, 4-H), 1.46–1.35 (m, 1H, 3-H), 1.28–1.15 (m, 1H, 3-H), 0.96 (d, J = 6.6 Hz, 3H, 4-Me), 0.93 (d, J = 6.6 Hz, 3H, 4-Me). ^{13}C NMR (CDCl_3 , 75 MHz): δ 70.3 (d, C-2), 66.9 (t, C-1), 41.8 (t, C-3), 24.3 (d, C-4), 23.2/21.9 (2q, 4-Me₂).

(1S,2S,3R,5S)-2,6,6-Trimethylbicyclo[3.1.1]heptane-2,3-diol (281):^[18]


To a solution of (+)- α -pinene (8.83 g, 64.8 mmol) in *t*-butanol (100 mL), H_2O (20 mL) and pyridine (5 mL) was added OsO_4 (100 mg) and NMO (9.1 g, 77.76 mmol, 1.2 equiv) and the solution heated at reflux overnight. The reaction was then quenched by the addition of sodium sulphite (2 g), and left for 1 h before being concentrated under reduced pressure. The residual oil was then taken up in H_2O (100 mL), extracted with EtOAc (3 × 100 mL), the organic extracts pooled and dried (MgSO_4) before being concentrated under reduced pressure. The resulting residue was then purified by flash chromatography on silica gel ($\text{EtOAc}/\text{hexane}$; 3:7) to yield (1S,2S,3R,5S)-2,6,6-trimethylbicyclo[3.1.1]heptane-2,3-diol (8.32 g, 75%) as a colourless solid. $[\alpha]_D^{22} = +7.2$ (c = 0.37, toluene). IR (ATR): $\tilde{\nu}$ = 3349 (ν O–H), 2908 (ν C–H), 1082 (ν C–O) cm^{-1} . ^1H NMR (CDCl_3 , 300 MHz): δ 3.39 (s, 1H, 3-H), 2.92/2.61 (2s, 2H, 2-,3-OH), 2.51–2.40 (m, 1H, 4-H), 2.25–2.16 (m, 1H, 7-H), 2.05–1.99 (m, 1H, 1-H), 1.96–1.89 (m, 1H, 5-H), 1.68–1.59 (m, 1H, 4-H), 1.36 (d, J = 10.3 Hz, 1H, 7-H), 1.31 (s, 3H, 6-Me), 1.27 (s, 3H, 6-Me), 0.94 (s, 3H, 2-Me). ^{13}C NMR (CDCl_3 , 75 MHz): δ 73.3 (s, C-2), 68.5 (d, C-3), 53.5 (d, C-1), 40.1 (d, C-5), 38.4 (s, C-6), 37.5 (t, C-4), 29.4 (q, 6-Me), 27.8 (t, C-7), 27.6 (q, 6-Me), 23.9 (q, 2-Me). HRMS: m/z calculated for $\text{C}_{10}\text{H}_{18}\text{O}_2\text{Na}$: 193.1204 [$\text{M}+\text{Na}$]⁺; Found: 193.1190.

(5a*S*,6*S*,8*S*,9a*R*)-5a,7,7-Trimethyl-3-methylenooctahydro-2*H*-6,8-methanobenzo[*b*][1,4]dioxepine (282):

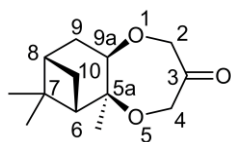
Following General Procedure A. Clear oil, 13% yield. $[\alpha]_D^{22} = +38.2$ ($c = 0.51$, CH_2Cl_2).

IR (ATR): $\tilde{\nu} = 2911$ (ν C–H), 1101 (ν C–O), 905 (ν C=CH₂) cm^{-1} . ¹H NMR (CDCl_3 , 300 MHz): δ 4.93–4.90 (m, 2H, =CH₂), 4.59–4.49 (m, 2H)/4.25 (d, $J = 14.3$ Hz, 1H)/4.06

(d, $J = 13.6$ Hz, 1H) (2-,4-H₂), 3.85–3.79 (m, 1H, 9a-H), 2.38–2.28 (m, 1H, 9-H), 2.19–2.11 (m, 1H, 10-H), 1.90–1.80 (m, 3H, 6-,8-,9-H), 1.63 (d, $J = 10.2$ Hz, 1H, 10-H), 1.39 (s, 3H, 5a-Me), 1.24 (s, 3H, 7-Me), 0.91 (s, 3H, 7-Me).

¹³C NMR (CDCl_3 , 75 MHz): δ 147.1 (s, C-3), 111.2 (t, =CH₂), 81.0 (s, C-5a), 79.8 (d, C-9a), 72.3/66.7 (2t, C-2,-4), 54.5/39.8 (2d, C-6,-8), 38.8 (s, C-7), 35.2 (t, C-9), 27.5 (q, 7-Me), 26.2 (t, C-10), 24.9 (q, 5a-Me), 24.0 (q, 7-Me).

HRMS: m/z calculated for $\text{C}_{14}\text{H}_{22}\text{O}_2$: 222.1619 [M]⁺; Found: 222.1623.

(5a*S*,6*S*,8*S*,9a*R*)-5a,7,7-Trimethylhexahydro-2*H*-6,8-methanobenzo[*b*][1,4]dioxepin-3(4*H*)-one (283):

Following General Procedure C. Colourless solid, 46% yield. $[\alpha]_D^{24} = +55.3$ ($c = 0.55$,

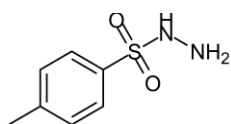
CH_2Cl_2). mp: 52–55 °C. IR (ATR): $\tilde{\nu} = 2919$ (ν C–H), 1716 (ν C=O), 1152 (ν C–O) cm^{-1} .

¹H NMR (CDCl_3 , 300 MHz): δ 4.67–4.28/4.07–3.99 (2m, 4H, 2-,4-H₂), 4.00–3.94 (m, 1H,

9a-H), 2.47–2.36 (m, 1H, 9-H), 2.29–2.19 (m, 1H, 10-H), 2.02–1.92 (m, 2H, 6-,8-H), 1.92–1.83 (m, 1H, 9-H), 1.64 (d, $J = 10.3$ Hz, 1H, 10-H), 1.38 (s, 3H, 5a-Me), 1.30 (s, 3H, 7-Me), 0.96 (s, 3H, 7-Me). ¹³C NMR (CDCl_3 , 75 MHz):

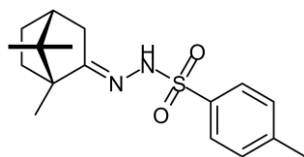
δ 213.0 (s, C-3), 80.7 (d, C-9a), 80.3 (s, C-5a), 75.3/70.7 (2t, C-2,-4), 54.4/39.7 (2d, C-6,-8), 38.5 (s, C-7), 34.4 (t, C-9), 27.2 (q, 7-Me), 26.8 (t, C-10), 24.6 (q, 5a-Me), 23.8 (q, 7-Me). HRMS: m/z calculated for $\text{C}_{13}\text{H}_{20}\text{O}_3$: 224.1412

[M]⁺; Found: 224.1418. Odour description: Rather weak, slightly minty-anisic, anethole, with a wet-towel odour.

4-Methylbenzenesulfonylhydrazide (285):^[24]

To a chilled (10–15 °C) solution of *para*-toluenesulfonyl chloride (100 g, 525 mmol) in THF (175 mL) was added a 85% aqueous hydrazine hydrate solution (68 mL) over a period of 20 minutes. Stirring was continued for a further 15 minutes before the mixture was

transferred into a separatory funnel, the aqueous layer discarded and the organic layer filtered through celite. The solution was then triturated with H₂O and the colourless precipitate filtered to give 4-methylbenzenesulfonylhydrazide (97 g, *quant.*) as a colourless solid.

4-Methyl-*N*-((1*R*,4*R*)-1,7,7-trimethylbicyclo[2.2.1]heptan-2-ylidene)benzenesulfonylhydrazide (287):^[25]

To a solution of 4-methylbenzenesulfonylhydrazide (15 g) and (*R*)-camphor (10 g, 65.69 mmol) in 95% EtOH (100 mL) was added conc. HCl (2 mL) was the solution heated at reflux for 2 h. The resulting solution was then cooled in an ice-bath and

filtered to give 4-methyl-*N*-((1*R*,4*R*)-1,7,7-trimethylbicyclo[2.2.1]heptan-2-ylidene)benzenesulfonylhydrazide

(10.9 g, 52%) as a colourless solid. $[\alpha]_D^{22} = +12.3$ ($c = 1.12$, EtOH). mp: 164–165 °C. (lit. mp: 163–164 °C).^[25]

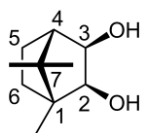
HRMS: m/z calculated for $C_{17}H_{24}N_2O_2S$: 320.1558 $[M]^+$; Found: 320.1570.

(1*S*,4*R*)-1,7,7-Trimethylbicyclo[2.2.1]hept-2-ene (288):^[25]

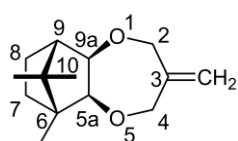


To a solution of 4-methyl-*N*-((1*R*,4*R*)-1,7,7-trimethylbicyclo[2.2.1]heptan-2-ylidene)benzenesulfonylhydrazide (26 g) in Et₂O (360 mL) was added methyllithium (1.6 N in Et₂O, 130 mL) over a period of 1 h. The solution was allowed to stir overnight before being quenched by the addition of H₂O (200 mL), followed by extraction with Et₂O (3 x 200 mL). The organic extracts were pooled, washed with H₂O (2 x 200 mL), dried (MgSO₄) and concentrated under reduced pressure to a volume of ~50 mL. Pentane (100 mL) was added and the solution was concentrated under reduced pressure to a volume of ~50 mL. The solution was then eluted through a plug of neutral alumina, followed by fractional distillation to give (1*S*,4*R*)-1,7,7-trimethylbicyclo[2.2.1]hept-2-ene (5.38 g, 49%) as a volatile colourless solid. $[\alpha]_D^{19} = -26.6$ ($c = 0.51$, CH₂Cl₂). IR (ATR): $\tilde{\nu} = 2950$ (ν C–H), 714 (ν C=C) cm⁻¹. ¹H NMR (CDCl₃, 300 MHz): δ 5.92 (dd, $J = 5.8, 3.2$ Hz, 1H, 3-H), 5.66 (d, $J = 5.6$ Hz, 1H, 2-H), 2.30–2.26 (m, 1H, 4-H), 1.85–1.76 (m, 1H, 5-H), 1.60–1.52 (m, 1H, 6-H), 1.04 (s, 3H, 1-Me), 1.02–0.87 (m, 2H, 5-,6-H), 0.83 (s, 3H, 7-Me), 0.77 (s, 3H, 7-Me). ¹³C NMR (CDCl₃, 75 MHz): δ 139.3 (d, C-2), 133.8 (d, C-3), 56.3/52.5 (2s, C-1,-7), 52.1 (d, C-4), 31.5 (t, C-6), 24.5 (t, C-5), 19.6/19.5 (2q, 7-Me₂), 13.2 (q, 1-Me). HRMS: m/z calculated for $C_{10}H_{16}$: 136.1252 $[M]^+$; Found: 136.1246.

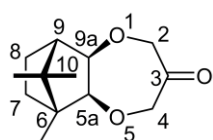
(1*R*,2*S*,3*R*,4*S*)-1,7,7-Trimethylbicyclo[2.2.1]heptane-2,3-diol (289):



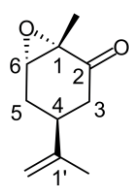
Following General Procedure E. Colourless solid, 61% yield. Alternatively synthesised from (–)-camphorquinone.^[26] To a 0 °C solution of (–)-camphorquinone (3.32 g, 20 mmol) in MeOH (100 mL) was added NaBH₄ (1.9 g, 50 mmol) over 0.5 h, and stirring continued at 25 °C for 0.5 h. The reaction mixture was then concentrated under reduced pressure, taken up in H₂O (20 mL) and extracted with EtOAc (3 x 40 mL). The combined organic extracts were pooled, dried (MgSO₄) and concentrated under reduced pressure to give (1*R*,2*S*,3*R*,4*S*)-1,7,7-trimethylbicyclo[2.2.1]heptane-2,3-diol (1.1 g, 32%) as a colourless solid. $[\alpha]_D^{23} = -14.9$ ($c = 0.37$, EtOH). mp: 255–258 °C. (lit. $[\alpha]_D^{23} = -17.3$ ($c = 0.52$, EtOH). mp: 255–257 °C).^[26] IR (ATR): $\tilde{\nu} = 3353$ (ν O–H), 2924 (ν C–H), 1049 (ν C–O) cm⁻¹. ¹H NMR (CDCl₃, 300 MHz): δ 3.88–3.83/3.65–3.59 (2m, 2H, 2-,3-H), 2.60–2.55/2.53–2.47 (2m, 2H, 2-,3-OH), 1.80–1.77 (m, 1H, 4-H), 1.72–1.60/1.54–1.40 (2m, 2H, 5-,6-H), 1.12 (s, 3H, 7-Me), 1.10–0.84 (m, 2H, 5-,6-H), 0.95 (s, 3H, 1-Me), 0.82 (s, 3H, 7-Me). ¹³C NMR (CDCl₃, 75 MHz): δ 79.7/75.9 (2d, C-2,-3), 51.3 (d, C-4), 48.6/46.3 (2s, C-1,-7), 33.1/24.0 (2t, C-5,-6), 21.8/20.9 (2q, 7-Me₂), 11.0 (q, 1-Me). HRMS: m/z calculated for $C_{10}H_{18}O_2$: 170.1307 $[M]^+$; Found: 170.0887.

(5a*S*,6*R*,9*S*,9a*R*)-6,10,10-Trimethyl-3-methyleneoctahydro-2*H*-6,9-methanobenzo[*b*][1,4]dioxepine (291):

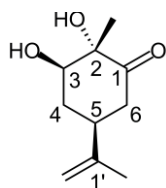
Following General Procedure A. Yellow oil, 69% yield. IR (ATR): $\tilde{\nu}$ = 2949/2872 (ν C–H), 1108 (ν C–O), 912 (ν C=CH₂) cm⁻¹. ¹H NMR (CDCl₃, 300 MHz): δ 5.01 (s, 2H, =CH₂), 4.50 (q, J = 12.7, 7.6 Hz, 2H)/3.92 (t, J = 12.6, 2H) (2-,4-H₂), 3.53 (d, J = 5.7 Hz, 1H)/3.31 (d, J = 5.8 Hz, 1H) (5a-,9a-H), 1.81–1.76 (m, 1H, 9-H), 1.75–1.64 (m, 1H, 8-H), 1.53–1.41 (m, 1H, 7-H), 1.15 (s, 3H, 10-Me), 1.08–0.95 (m, 2H, 7-,8-H), 0.90 (s, 3H, 6-Me), 0.78 (s, 3H, 10-Me). ¹³C NMR (CDCl₃, 75 MHz): δ 145.3 (s, C-3), 115.1 (t, =CH₂), 91.7/88.5 (2d, C-5a,-9a), 76.0/75.9 (2t, C-2,-4), 51.1 (d, C-9), 49.2/46.7 (2s, C-6,-10), 33.7 (t, C-7), 24.4 (t, C-8), 21.0/20.9 (2q, 10-Me), 11.4 (q, 6-Me). HRMS: m/z calculated for C₁₄H₂₂O₂: 222.1620 [M]⁺; Found: 222.1611.

(5a*S*,6*R*,9*S*,9a*R*)-6,10,10-Trimethylhexahydro-2*H*-6,9-methanobenzo[*b*][1,4]dioxepin-3(4*H*)-one (292):

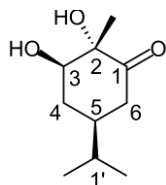
Following General Procedure C. Colourless solid, 49% yield. $[\alpha]_D^{27} = -11.1$ (c = 1.00, CH₂Cl₂). mp: 75–77 °C. IR (ATR): $\tilde{\nu}$ = 2953/2837 (ν C–H), 1708 (ν C=O), 1158 (ν C–O) cm⁻¹. ¹H NMR (CDCl₃, 300 MHz): δ 4.64–4.52/4.13–4.00 (2m, 4H, 2-,4-H₂), 3.62 (d, J = 5.8 Hz, 1H)/3.40 (d, J = 5.8 Hz, 1H) (5a-,9a-H), 1.90–1.87 (m, 1H, 9-H), 1.79–1.68 (m, 1H, 8-H), 1.55–1.45 (m, 1H, 7-H), 1.22 (s, 3H, 10-Me), 1.09–0.96 (m, 2H, 7-,8-H), 0.93 (s, 3H, 6-Me), 0.83 (s, 3H, 10-Me). ¹³C NMR (CDCl₃, 75 MHz): δ 213.3 (s, C-3), 91.4/88.0 (2d, C-5a,-9a), 79.6/79.3 (2t, C-2,-4), 51.0 (d, C-9), 49.3/46.7 (2s, C-6,-10), 33.3 (t, C-7), 24.1 (t, C-8), 20.9/20.9 (2q, 10-Me), 11.1 (q, 6-Me). HRMS: m/z calculated for C₁₃H₂₀O₃: 224.1412 [M]⁺; Found: 224.1428. Odour description: Odourless.

(1*S*,4*S*,6*S*)-1-Methyl-4-(prop-1-en-2-yl)-7-oxabicyclo[4.1.0]heptan-2-one (293):^[32]

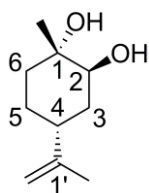
To a solution of (*S*)-carvone (5 g, 33.3 mmol) in MeOH (33 mL) was added 4 M NaOH (2.89 mL) at 0 °C. To this solution was added 30% H₂O₂ (4.13 mL, 39.95 mmol) dropwise over a period of 1 h at 0 °C. The mixture was stirred for a further 1 h before being quenched by the addition of a saturated aqueous sodium sulphite solution (80 mL) followed by extracted with EtOAc (3 x 150 mL). The combined organic extracts were pooled, dried (MgSO₄) and concentrated under reduced pressure. The resulting residue was then purified by flash chromatography on silica gel (Et₂O/hexane; 1:9) to give (1*S*,4*S*,6*S*)-1-methyl-4-(prop-1-en-2-yl)-7-oxabicyclo[4.1.0]heptan-2-one (4.81 g, 87%) as a yellow oil. IR (ATR): $\tilde{\nu}$ = 2935 (ν C–H), 1704 (ν C=O) cm⁻¹. ¹H NMR (CDCl₃, 300 MHz): δ 4.74–4.71 (m, 1H)/4.67–4.64 (m, 1H) (=CH₂), 3.40–3.37 (m, 1H, 6-H), 2.71–2.59 (m, 1H, 4-H), 2.56–2.46 (m, 1H, 3-H), 2.35–2.26 (m, 1H, 5-H), 2.02–1.80 (m, 2H, 3-,5-H), 1.66 (s, 3H, 1'-Me), 1.34 (s, 3H, 1-Me). ¹³C NMR (CDCl₃, 75 MHz): δ 204.8 (s, C-2), 146.0 (s, C-1'), 110.1 (t, =CH₂), 60.9 (d, C-6), 58.3 (s, C-1), 41.4 (t, C-3), 34.7 (d, C-4), 28.3 (t, C-5), 20.2 (q, 1'-Me), 14.9 (q, 1-Me). HRMS: m/z calculated for C₁₀H₁₄O₂: 166.0994 [M]⁺; Found: 166.0986.

(2*S*,3*R*,5*S*)-2,3-Dihydroxy-2-methyl-5-(prop-1-en-2-yl)cyclohexanone (295):^[37]


To a solution of (1*S*,4*S*,6*S*)-1-methyl-4-(prop-1-en-2-yl)-7-oxabicyclo[4.1.0]heptan-2-one (4.04 g, 24.27 mmol) in THF (32 mL) was added conc. H₂SO₄ (0.5 mL) was the solution heated at reflux for 4 h. The solution was then neutralised by the addition of a saturated aqueous solution of NaHCO₃ (50 mL) followed by extraction with EtOAc (3 x 100 mL). The combined organic extracts were pooled, dried (MgSO₄) and concentrated under reduced pressure. The resulting residue was then purified by flash chromatography on silica gel (EtOAc/hexane; 4:6) to give (2*S*,3*R*,5*S*)-2,3-dihydroxy-2-methyl-5-(prop-1-en-2-yl)cyclohexanone (3.04 g, 68%) as a yellow oil. $[\alpha]_D^{22} = -61.5$ ($c = 1.04$, DCM). IR (ATR): $\tilde{\nu} = 3460$ (ν C–H), 1714 (ν C=O), 1048 (ν C–O) cm⁻¹. ¹H NMR (CDCl₃, 300 MHz): δ 4.85–4.83 (m, 1H)/4.81–4.79 (m, 1H) (=CH₂), 4.25 (s, 1H, OH), 4.09–4.06 (m, 1H, 3-H), 2.98–2.86 (m, 2H, 5-H, OH), 2.62–2.50 (m, 2H, 6-H₂), 2.23–2.15 (m, 1H, 4-H), 1.96–1.84 (m, 1H, 4-H), 1.78 (s, 3H, 1'-Me), 1.42 (s, 3H, 2-Me). ¹³C NMR (CDCl₃, 75 MHz): δ 212.5 (s, C-1), 146.3 (s, C-1'), 109.8 (t, =CH₂), 78.1 (s, C-2), 75.6 (s, C-3), 41.4 (t, C-6), 39.5 (d, C-5), 32.9 (t, C-4), 23.1 (q, 2-Me), 20.2 (q, 1'-Me).

(2*S*,3*R*,5*S*)-2,3-Dihydroxy-5-isopropyl-2-methylcyclohexanone (297):


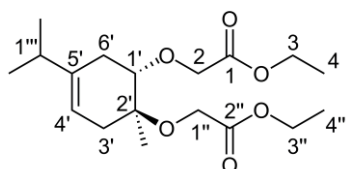
To a solution of (2*S*,3*R*,5*S*)-2,3-dihydroxy-2-methyl-5-(prop-1-en-2-yl)cyclohexanone (1.3 g) in EtOAc (90 mL) and EtOH (22 mL) was added 10% Pd/C (180 mg) and the solution stirred under an atmosphere of H₂ for 24 h. The mixture was then filtered through celite, concentrated under reduced pressure and the resulting residue purified by flash chromatography on silica gel (EtOAc/hexane; 3:7) to give (2*S*,3*R*,5*S*)-2,3-dihydroxy-5-isopropyl-2-methylcyclohexanone (0.98 g, 75%) as a yellow oil. IR (ATR): $\tilde{\nu} = 3462$ (ν C–O), 2958 (ν C–H), 1713 (ν C=O) cm⁻¹. ¹H NMR (CDCl₃, 300 MHz): δ 4.25 (s, 1H, OH), 4.08–4.04 (m, 1H, 3-H), 2.89 (d, $J = 2.0$ Hz, 1H, OH), 2.52–2.45 (m, 1H, 6-H), 2.38–2.28 (m, 1H, 6-H), 2.23–2.04 (m, 2H, 4-,5-H), 1.79–1.57 (m, 2H, 4-,1'-H), 1.39 (s, 3H, 2-Me), 0.94 (dd, $J = 6.8, 3.7$ Hz, 6H, 1'-Me₂). ¹³C NMR (CDCl₃, 75 MHz): δ 213.4 (s, C-1), 78.2 (s, C-2), 75.9 (d, C-3), 39.8 (t, C-6), 39.1 (d, C-5), 31.8 (d, C-1'), 31.2 (t, C-4), 23.0 (q, 2-Me), 19.3/18.8 (2q, 1'-Me₂). HRMS: m/z calculated for C₁₀H₁₈O₃: 186.1256 [M]⁺; Found: 186.1267.

(1*S*,2*S*,4*R*)-1-Methyl-4-(prop-1-en-2-yl)cyclohexane-1,2-diol (302):^[43, 47]


To a solution of (+)-limonene (8.52 g, 62.54 mmol) in DCM (100 mL) was added dropwise mCPBA (14.02 g, 62.54 mmol, $\leq 77\%$ pure) in DCM (400 mL) over a period of 0.5 h. A 5% aqueous solution of NaHCO₃ (160 mL) was then added and stirring continued for 2.5 h. The mixture was then transferred to a separatory funnel and the aqueous layer discarded. The organic phase was washed with a saturated aqueous solution of NaHSO₃ (100 mL), a saturated aqueous solution of NaHCO₃ (100 mL), H₂O (100 mL), dried (MgSO₄) and concentrated under reduced pressure. The resulting residue was then added to

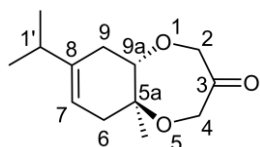
a NaOAc/AcOH buffered solution (pH 4, 200 mL) and stirring continued for 48 h. The solution was then extracted with EtOAc (3 x 200 mL) and the combined organic extracts pooled, dried (MgSO₄) and concentrated under reduced pressure. The resulting residue was purified by flash chromatography on silica gel (EtOAc/hexane; 4:6) to give (1*S*,2*S*,4*R*)-1-methyl-4-(prop-1-en-2-yl)cyclohexane-1,2-diol (5.05 g, 47%) as a colourless solid. $[\alpha]_D^{18} = +27.2$ ($c = 0.49$, CHCl₃). mp: 69–71 °C. (lit. $[\alpha]_D^{20} = +18.1$ ($c = 0.01$, CHCl₃). mp: 68–70 °C).^[47] IR (ATR): $\tilde{\nu} = 3360$ (ν O–H), 2931 (ν C–H), 1024 (ν C–O), 882 (ν C=CH₂) cm⁻¹. ¹H NMR (CDCl₃, 300 MHz): δ 4.75 (s, 2H, =CH₂), 3.67–3.63 (m, 1H, 2-H), 2.34–2.22 (m, 1H, 4-H), 2.00–1.89 (m, 1H, 3-H), 1.84–1.76 (m, 1H, 6-H), 1.74 (s, 3H, 1'-Me), 1.73–1.63 (m, 1H, 3-H), 1.62–1.50 (m, 3H, 5-H₂, 6-H), 1.42 (s, 2H, 1-,2-OH), 1.28 (s, 3H, 1-Me). ¹³C NMR (CDCl₃, 75 MHz): δ 149.2 (s, C-1'), 108.9 (t, =CH₂), 73.8 (d, C-2), 71.3 (s, C-1), 37.4 (d, C-4), 33.9/33.6 (2t, C-3,-6), 26.5 (q, 1-Me), 26.1 (t, C-5), 21.0 (q, 1'-Me). HRMS: m/z calculated for C₁₀H₁₈O₂Na: 193.1204 [M+Na]⁺; Found: 193.1184.

(1*S*,2*S*)-Diethyl 2,2'-((5-isopropyl-2a-methylcyclohex-4-ene-1,2-diyl)bis(oxy))diacetate (303):

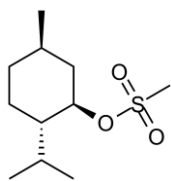


Following General Procedure B. Yellow oil, 12% yield. IR (ATR): $\tilde{\nu} = 2962$ (ν C–H), 1753 (ν ester C=O), 1119 (ν ester C–O), 1121 (ν C–O) cm⁻¹. ¹H NMR (CDCl₃, 300 MHz): δ 5.22 (s, 1H, 4'-H), 4.40–4.06 (m, 8H, 2-,3-,1''-,3''-H₂), 3.66 (dd, $J = 8.8, 6.0$ Hz, 1H, 1'-H), 2.54–2.45 (m, 1H, 6'-H), 2.26–2.13 (m, 3H, 3'-H₂, 1'''-H), 2.11–1.99 (m, 1H, 6'-H), 1.29 (t, $J = 7.1$ Hz, 6H, 4-,4''-H₃), 1.21 (s, 3H, 2'-Me), 0.99 (d, $J = 6.8$ Hz, 6H, 1'''-Me₂). ¹³C NMR (CDCl₃, 75 MHz): δ 171.0/170.9 (2s, C-1,-2''), 140.8 (s, C-5'), 115.0 (d, C-4'), 81.2 (d, C-1'), 78.0 (s, C-2'), 68.1/60.6/60.4/60.3 (4t, C-2,-3,-1'',-3''), 36.0 (t, C-3'), 34.1 (d, C-1'''), 30.9 (t, C-6'), 21.2/20.8 (2q, 1'''-Me₂), 15.6 (q, 2'-Me), 14.0/13.9 (2q, C-4,-4''). HRMS: m/z calculated for C₁₈H₃₀O₆Na: 365.1940 [M+Na]⁺; Found: 365.1947.

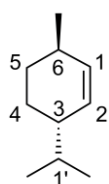
(5a*S*,9a*S*)-8-Isopropyl-5a-methyl-5a,6,9,9a-tetrahydro-2*H*-benzo[*b*][1,4]dioxepin-3(4*H*)-one (304):



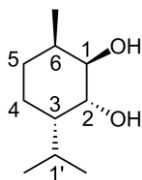
Following General Procedure D. Yellow oil, 8% yield. $[\alpha]_D^{22} = +218.6$ ($c = 0.76$, CH₂Cl₂). IR (ATR): $\tilde{\nu} = 2962/2902$ (ν C–H), 1725 (ν C=O), 1122 (ν C–O) cm⁻¹. ¹H NMR (CDCl₃, 300 MHz): δ 5.29–5.24 (m, 1H, 7-H), 4.51 (d, $J = 17$ Hz, 1H, 4-H), 4.28 (d, $J = 16.6$ Hz, 1H, 2-H), 4.21 (d, $J = 16.6$ Hz, 1H, 2-H), 4.01 (d, $J = 17$ Hz, 1H, 4-H), 3.60 (dd, $J = 10.7, 6$ Hz, 1H, 9a-H), 2.39–2.28 (m, 1H, 9-H), 2.27–2.12 (m, 3H, 1'-H, 6-H₂), 2.05–1.91 (m, 1H, 9-H), 1.25 (s, 3H, 5a-Me), 1.00 (d, $J = 6.9$ Hz, 6H, 1'-Me₂). ¹³C NMR (CDCl₃, 75 MHz): δ 212.1 (s, C-3), 141.1 (s, C-8), 116.5 (d, C-7), 87.5 (d, C-9a), 78.7 (s, C-5a), 77.7 (t, C-2), 70.1 (t, C-4), 39.5 (t, C-6), 34.2 (d, C-1'), 32.3 (t, C-9), 21.5/21.0 (2q, 1'-Me₂), 14.2 (q, 5a-Me). HRMS: m/z calculated for C₁₃H₂₀O₃: 224.1412 [M]⁺; Found: 224.1403.

(1*R*,2*S*,5*R*)-2-Isopropyl-5-methylcyclohexyl methanesulfonate (306):^[50, 51]


To a solution of mesyl chloride (1.39 mL, 17.88 mmol) in pyridine (3 mL) at 0 °C was added (-)-menthol (2 g, 12.79 mmol) in pyridine (3 mL). Stirring was continued for 0.5 h at 0 °C followed by RT overnight. The reaction was then poured into ice-cold 10% HCl (100 mL) and extracted with Et₂O (3 x 100 mL). The organic extracts were pooled, dried (MgSO₄) and concentrated under reduced pressure to yield (1*R*,2*S*,5*R*)-2-isopropyl-5-methylcyclohexyl methanesulfonate (2.76 g, 92%) as a yellow oil. IR (ATR): $\tilde{\nu}$ = 2955/2931 (ν C–H), 1171 (ν C–O) cm⁻¹. Full structural assignment could not be completed. ¹H NMR (CDCl₃, 300 MHz): δ 4.60–4.50 (m, 1H), 3.01 (s, 3H), 2.30–2.22 (m, 1H), 2.13–2.02 (m, 1H), 1.77–1.64 (m, 2H), 1.56–1.37 (m, 2H), 1.34–1.21 (m, 1H), 1.13–0.98 (m, 1H), 0.97–0.80 (m, 10H). ¹³C NMR (CDCl₃, 75 MHz): δ 82.7, 47.0, 41.7, 38.6, 33.3, 31.1, 25.3, 22.6, 21.4, 20.4, 15.2.

(3*S*,6*R*)-3-Isopropyl-6-methylcyclohex-1-ene (307):^[51, 52]


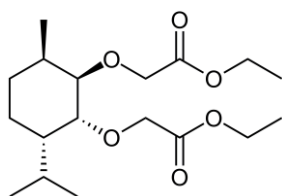
A solution of (1*R*,2*S*,5*R*)-2-isopropyl-5-methylcyclohexyl methanesulfonate (4.00 g, 17.1 mmol) in DMSO (15 mL) was added dropwise to a solution of KO^tBu (4.78 g, 42.6 mmol, 2.5 equiv) in DMSO (15 mL) at RT and the solution then stirred for 1 h at 70 °C. The residual gum was then taken up in H₂O (100 mL), extracted with hexane (3 x 100 mL), the organic extracts pooled and dried (MgSO₄) before being concentrated under reduced pressure to give (3*S*,6*R*)-3-Isopropyl-6-methylcyclohex-1-ene (2.12 g, 90%) as a yellow oil. $[\alpha]_D^{19}$ = +107.0 (c = 1.07, CH₂Cl₂). IR (ATR): $\tilde{\nu}$ = 2955/2925 (ν C–H), 724 (ν C=C) cm⁻¹. ¹H NMR (CDCl₃, 300 MHz): δ 5.54 (s, 2H, 1-,2-H), 2.19–2.06 (m, 1H, 6-H), 1.98–1.90 (m, 1H, 3-H), 1.89–1.79 (m, 1H, 5-H), 1.76–1.66 (m, 1H, 4-H), 1.63–1.51 (m, 1H, 1'-H), 1.33–1.19 (m, 1H, 4-H), 1.19–1.05 (m, 1H, 5-H), 0.96 (d, *J* = 6.9 Hz, 3H, 6-Me), 0.89 (t, *J* = 6.9 Hz, 6H, 1'-Me₂). ¹³C NMR (CDCl₃, 75 MHz): δ 133.9/129.8 (2d, C-1,-2), 41.9 (d, C-3), 32.2 (d, C-1'), 32.0 (t, C-5), 30.9 (d, C-6), 25.6 (t, C-4), 21.9 (q, 6-Me), 19.5/19.2 (2q, 1'-Me₂). HRMS: *m/z* calculated for C₁₀H₁₈: 138.1408 [M]⁺; Found: 138.1389.

(1*R*,2*R*,3*S*,6*R*)-3-Isopropyl-6-methylcyclohexane-1,2-diol (308):^[49]


To a solution of (3*S*,6*R*)-3-isopropyl-6-methylcyclohex-1-ene (2 g, 14.47 mmol) in DCM (80 mL) at 0 °C was added dropwise a solution of mCPBA (4.6 g, 20.53 mmol, ≤77% pure) in DCM (30 mL) over a period of 0.5 h. The solution was stirred for 8 h at 0 °C before being transferred to a separatory funnel. The organic phase was washed with a saturated aqueous solution of NaHSO₃ (100 mL), a saturated aqueous solution of NaHCO₃ (100 mL), H₂O (100 mL), dried (MgSO₄) and concentrated under reduced pressure. The resulting residue was then taken up in THF (10 mL), cooled to 0 °C and an ice-cool 3% aqueous solution of H₂SO₄ (60 mL) was added. The solution was then stirred at 0 °C for 7 h before being quenched by the addition of a saturated aqueous solution of NaHCO₃ (100 mL). The mixture was extracted

with EtOAc (3 x 100 mL), the organic extracts pooled, dried (MgSO₄) and concentrated under reduced pressure. The resulting residue was then purified by flash chromatography on silica gel (EtOAc/hexane; 3:7) to give (1*R*,2*R*,3*S*,6*R*)-3-isopropyl-6-methylcyclohexane-1,2-diol (0.85 g, 66%) as a yellow oil. $[\alpha]_D^{26} = +37.9$ ($c = 1.02$, CHCl₃). (lit. $[\alpha]_D^{26} = +38.6$ ($c = 1.01$, CHCl₃).^[49] IR (ATR): $\tilde{\nu} = 3412$ (v O–H), 2956/2923 (v C–H) cm⁻¹. ¹H NMR (CDCl₃, 300 MHz): δ 4.01–3.98 (m, 1H, 2-H), 3.71–3.67 (m, 1H, 1-H), 1.94–1.83 (m, 1H, 6-H), 1.69–1.60 (m, 1H, 5-H), 1.59–1.51 (m, 1H, 1'-H), 1.48–1.32 (m, 3H, 4-H, 1-,2-OH), 1.32–1.19 (m, 3H, 3-,4-,5-H), 1.00–0.93 (m, 9H, 1'-Me₂, 6-Me). ¹³C NMR (CDCl₃, 75 MHz): δ 74.4 (d, C-1), 71.1 (d, C-2), 41.7 (d, C-3), 30.1 (d, C-6), 28.6 (d, C-1'), 27.6 (t, C-4), 23.6 (t, C-5), 21.2/20.6 (2q, 1'-Me₂), 17.5 (q, 6-Me). HRMS: m/z calculated for C₁₀H₂₀O₂: 172.1463 [M]⁺; Found: 172.1450.

(1*R*,2*R*,3*S*,6*R*)-Diethyl 2,2'-(3-Isopropyl-6-methylcyclohexane-1,2-diyl)bis(oxy)diacetate (310):



Following General Procedure B. Yellow oil, 9% yield. $[\alpha]_D^{22} = -0.9$ ($c = 1.16$, CH₂Cl₂). IR (ATR): $\tilde{\nu} = 2956/2929$ (v C–H), 1754 (v ester C=O), 1197 (v ester C–O), 1119 (v C–O) cm⁻¹. Full structural assignment could not be completed. ¹H NMR (CDCl₃, 300 MHz): δ 4.26–4.04 (m, 8H), 3.85–3.81 (m, 1H), 3.49–3.44 (m, 1H), 1.98–1.85 (m, 1H), 1.79–1.65 (m, 1H), 1.63–1.53 (m, 1H), 1.43–1.15 (m, 4H), 1.30 (t, $J = 7.1$ Hz, 3H), 1.29 (t, $J = 7.1$ Hz, 3H), 1.02–0.89 (m, 9H). ¹³C NMR (CDCl₃, 75 MHz): δ 170.4, 170.2, 80.3, 78.3, 68.6, 67.9, 60.2, 60.2, 41.9, 30.4, 28.0, 27.9, 23.3., 20.8, 20.5, 17.5, 13.8, 13.7. HRMS: m/z calculated for C₁₈H₃₂O₄Na: 367.2096 [M+Na]⁺; Found: 367.2054.

4.4 – References

1. J. W. Cornforth, Terpenoid biosynthesis, *Chem. Brit.* **1968**, *4*, 102-106.
2. R. G. Berger, *Flavours and Fragrances: Chemistry, Bioprocessing and Sustainability*, Springer GmbH, Berlin, **2007**.
3. G. Ohloff, W. Pickenhagen, P. Kraft, *Scent and Chemistry - The Molecular World of Odors*, Verlag Helvetica Chimica Acta, Zurich, **2012**.
4. P. Kraft, W. Eichenberger, Conception, characterization and correlation of new marine odorants, *Eur. J. Org. Chem.* **2003**, 3735-3743.
5. A. D. McNaught, A. Wilkinson, *Compendium of Chemical Terminology 2nd Edition*, Blackwell, Oxford, **1997**.
6. A. W. Norman, Sunlight, season, skin pigmentation, vitamin D, and 25-hydroxyvitamin D: integral components of the vitamin D endocrine system, *Am. J. Clin. Nutr.* **1998**, *67*, 1108-1110.
7. K. Sestanj, Synthesis of an acyclic analog of ionone, *Croat. Chem. Acta* **1962**, *34*, 211-217.
8. P. Kraft, V. Di Cristofaro, S. Jordi, From Cassyrane to Cashmeran - The Molecular Parameters of Odorants, *Chem. Biodiversity* **2014**, *11*, 1567-1596.
9. P. Kraft, S. Jordi, N. Denizot, I. Felker, On the Dienone Motif of Musks: Synthesis and Olfactory Properties of Partially and Fully Hydrogenated Dienone Musks, *Eur. J. Org. Chem.* **2014**, *2014*, 554-563.
10. J. Kula, R. Bonikowski, M. Staniszewska, A. Krakowiak, M. W. Wieczorek, W. R. Majzner, G. D. Bujacz, Transformation of carotol into the hydroindane-derived musk odorant, *Eur. J. Org. Chem.* **2002**, 1826-1829.
11. P. Kraft, K. Popaj, Musk or violet? Design, synthesis and odor of *seco*-derivates of a musky carotol lead, *Tetrahedron* **2006**, *62*, 12211-12219.
12. P. Kraft, K. Popaj, New musk odorants: (3*E*)-4-(2'-alkyl-5',5'-dimethylcyclopent-1'-enyl)but-3-en-2-ones and (3*E*)-1-acetyl-3-alkylidene-4,4-dimethylcyclohexenes, *Eur. J. Org. Chem.* **2008**, 4806-4814.
13. A. Dreyer, H. Doods, K. Gerlach, D. Gottschling, A. Heimann, S. G. Mueller, K. Rudolf, G. Schaezle (Boehringer Ingelheim International GmbH), **2010**, WO2010139717A1.
14. F. Nerdel, M. Mamluk, P. Weyerstahl, Fragmentation reactions of carbonyl compounds with electronegative β -substituents. XVIII. Synthesis and reactions of cyclic polyethers, *Justus Liebigs Ann. Chem.* **1970**, *736*, 75-87.
15. A. D. Worthy, X. Sun, K. L. Tan, Site-selective catalysis: toward a regiodivergent resolution of 1,2-diols, *J. Am. Chem. Soc.* **2012**, *134*, 7321-7324.
16. A. Sudalai, A. Khenkin, R. Neumann, Sodium periodate mediated oxidative transformations in organic synthesis, *Org. Biomol. Chem.* **2015**, *13*, 4374-4394.

17. M. H. Boelens, L. J. van Gemert, Sensory properties of optical isomers, *Perfum. Flavor.* **1993**, *18*, 1-16.
18. M. Gomes, Jr., O. A. C. Antunes, Upjohn catalytic osmium tetroxide oxidation process: diastereoselective dihydroxylation of monoterpenes, *Catal. Commun.* **2001**, *2*, 225-227.
19. O. V. Gozhina, J. S. Svendsen, T. Lejon, Synthesis and antimicrobial activity of α -aminoboronic-containing peptidomimetics, *J. Pept. Sci.* **2014**, *20*, 20-24.
20. Y. Gao, T. J. Donohoe, R. M. Harris, M. J. Chughtai, J. W. Yang, S. M. Kim, J. S. Oh, C. E. Song, Osmium Tetroxide, *e-EROS Encyclopedia of Reagents for Organic Synthesis* **2001**.
21. D. J. Berrisford, C. Bolm, K. B. Sharpless, Ligand-accelerated catalysis, *Angew. Chem., Int. Ed. Engl.* **1995**, *34*, 1059-1070.
22. Y. Zhu, X. Zhao, X. Zhu, G. Wu, Y. Li, Y. Ma, Y. Yuan, J. Yang, Y. Hu, L. Ai, Q. Gao, Design, Synthesis, Biological Evaluation, and Structure-Activity Relationship (SAR) Discussion of Dipeptidyl Boronate Proteasome Inhibitors, Part I: Comprehensive Understanding of the SAR of α -Amino Acid Boronates, *J. Med. Chem.* **2009**, *52*, 4192-4199.
23. P. Kraft, A. Mannschreck, The Enantioselectivity of Odor Sensation: Some Examples for Undergraduate Chemistry Courses, *J. Chem. Educ.* **2010**, *87*, 598-603.
24. L. Friedman, R. L. Little, W. R. Reichle, *p*-Toluenesulfonylhydrazide, *Org. Synth.* **1960**, *40*, 93-95.
25. R. H. Shapiro, J. H. Duncan, 2-Bornene, *Org. Syn.* **1971**, *51*, 66-69.
26. M. Periasamy, N. Sanjeevakumar, P. O. Reddy, Convenient methods to access chiral camphanyl amine derivatives by sodium borohydride reduction of D-(–)-camphorquinone imines, *Synthesis* **2012**, *44*, 3185-3190.
27. R. H. Shapiro, M. F. Lipton, K. J. Kolonko, R. L. Buswell, L. A. Capuano, Tolylsulfonyl hydrazones and alkyllithium reagents. Regiospecificity of the reaction and the trapping of three intermediates, *Tetrahedron Lett.* **1975**, 1811-1814.
28. G. Raj, *Organic Name Reactions and Molecular Rearrangements*, Krishna Prakashan Media, Meerut, **2013**.
29. E. Vedejs, S. Larsen, Hydroxylation of Enolates with Oxodiperoxymolybdenum (Pyridine)(Hexamethylphosphoric Triamide), $\text{MoO}_5\cdot\text{Py}\cdot\text{HMPA}(\text{MoOPH})$: 3-Hydroxy-1,7,7-Trimethylbicyclo[2.2.1]Heptan-2-one, *Organic Syntheses* **1986**, *64*, 127.
30. L. Friedman, J. G. Miller, Odor incongruity and chirality, *Science* **1971**, *172*, 1044-1046.
31. P. Pelosi, R. Viti, Specific anosmia to L-carvone: the minty primary odor, *Chem. Senses Flavour* **1978**, *3*, 331-337.
32. S. Takita, S. Yokoshima, T. Fukuyama, A Practical Synthesis of (–)-Kainic Acid, *Org. Lett.* **2011**, *13*, 2068-2070.

33. M. Isobe, S. Niyomchon, C.-Y. Cheng, A. Hasakunpaisarn, Synthesis of bicyclo[4.2.0]octan-2-ol, a substructure of solanoeclipin A, *Tetrahedron Lett.* **2011**, *52*, 1847-1850.
34. K. Mori, K. Fukamatsu, A new synthesis of (+)-grandisol, *Liebigs Ann. Chem.* **1992**, 489-493.
35. J. D. McChesney, T. N. Thompson, Stereochemistry of the reductive alkylation of α,β -epoxy ketones, *J. Org. Chem.* **1985**, *50*, 3473-3481.
36. N. Lindquist, M. A. Battiste, W. M. Whitten, N. H. Williams, L. Strekowski, *trans*-Carvone oxide, a monoterpene epoxide from the fragrance of *Catasetum*, *Phytochemistry* **1985**, *24*, 863-865.
37. H. Weinstabl, T. Gaich, J. Mulzer, Application of the Rodriguez-Pattenden Photo-Ring Contraction: Total Synthesis and Configurational Reassignment of 11-Gorgiacerol and 11-Epigorgiacerol, *Org. Lett.* **2012**, *14*, 2834-2837.
38. R. Mizutani, T. Morimitsu, K. Nakashima, M. Tori, Synthesis of a hydrindenone in rings C and D of YW3699, *Nat. Prod. Commun.* **2013**, *8*, 949-953.
39. W. Roelofs, M. Gieselmann, A. Carde, H. Tashiro, D. S. Moreno, C. A. Henrick, R. J. Anderson, Identification of the California red scale (*Aonidiella aurantii*) sex pheromone, *J. Chem. Ecol.* **1978**, *4*, 211-224.
40. J. F. Lavalley, C. Spino, R. Ruel, K. T. Hogan, P. Deslongchamps, Stereoselective synthesis of *cis*-decalins via Diels-Alder and double Michael addition of substituted Nazarov reagents, *Can. J. Chem.* **1992**, *70*, 1406-1426.
41. J. E. McMurry, *Organic Chemistry 7th Ed.*, Brooks Cole, Belmont, California, **2008**.
42. E. Paruch, Z. Ciunik, C. Wawrzencyk, Synthesis of spirolactones from the limonene system, *Eur. J. Org. Chem.* **1998**, 2677-2682.
43. K. Geoghegan, P. Evans, Synthesis of (+)-perillyl alcohol from (+)-limonene, *Tetrahedron Lett.* **2014**, *55*, 1431-1433.
44. R. Rodriguez, C. Ollivier, M. Santelli, Vitamin D: a concise synthesis of the C₁₉ hydroxylated enyne A-ring, an interesting precursor for the preparation of C₁₉ substituted vitamin D analogues, *Tetrahedron Lett.* **2004**, *45*, 2289-2292.
45. Z.-B. Xu, J. Qu, Water-promoted kinetic separation of *trans*- and *cis*-limonene oxides, *Chin. J. Chem.* **2012**, *30*, 1133-1136.
46. E. E. Royals, J. C. Leffingwell, Reactions of the limonene 1,2-oxides. I. The stereospecific reactions of the (+)-*cis*- and (+)-*trans*-limonene 1,2-oxides, *J. Org. Chem.* **1966**, *31*, 1937-1944.
47. M. Blair, P. C. Andrews, B. H. Fraser, C. M. Forsyth, P. C. Junk, M. Massi, K. L. Tuck, Facile methods for the separation of the *cis*- and *trans*-diastereomers of limonene 1,2-oxide and convenient routes to diequatorial and diaxial 1,2-diols, *Synthesis* **2007**, 1523-1527.

48. R. A. Kjonaas, S. P. Mattingly, Acid-catalyzed isomerization of carvone to carvacrol, *J. Chem. Educ.* **2005**, *82*, 1813-1814.
49. T. Kiguchi, Y. Tsurusaki, S. Yamada, M. Aso, M. Tanaka, K. Sakai, H. Suemune, Insight into acid-mediated asymmetric spirocyclization in the presence of a chiral diol, *Chem. Pharm. Bull.* **2000**, *48*, 1536-1540.
50. A. Gansaeuer, S. Narayan, N. Schiffer-Ndene, H. Bluhm, J. E. Oltra, J. M. Cuerva, A. Rosales, M. Nieger, An improved synthesis of Kagan's menthyl substituted titanocene and zirconocene dichloride, comparison of their crystal structures, and preliminary catalyst evaluation, *J. Organomet. Chem.* **2006**, *691*, 2327-2331.
51. S. Antoniotti, N. Alezra, X. Fernandez, E. Dunach, Catalytic epoxide oxidation: a novel access to flavouring and odorant α -diketones, *Flavour Fragrance J.* **2004**, *19*, 373-381.
52. C. H. Snyder, A. R. Soto, Reaction of primary and secondary alkylaryl and alkyl sulfonates with potassium *tert*-butoxide in dimethyl sulfoxide, *J. Org. Chem.* **1964**, *29*, 742-745.
53. Molecular Operating Environment (MOE), release 2014.09, Chemical Computing Group, Montreal, Quebec, Canada H3A 2R7, **2014**. For more information see <<http://www.chemcomp.com/>>.
54. P. Kraft, K. Popaj, P. Müller, M. Schär, 'Vanilla oceanics': synthesis and olfactory properties of (1'*E*)-7-(prop-1'-enyl)-2*H*-benzo[*b*][1,4]dioxepin-3(4*H*)-ones and homologues, *Synthesis* **2010**, 3029-3036.
55. J.-M. Gaudin, J.-Y. de Saint Laumer, Structure-Activity Relationships in the Domain of Odorants Having Marine Notes, *Eur. J. Org. Chem.* **2015**, 1437-1447.
56. J. J. Beereboom, D. P. Cameron, C. R. Stephens (Pfizer Inc.), **1974**, US3799892A.
57. J. Zhou, V. Wakchaure, P. Kraft, B. List, Primary-amine-catalyzed enantioselective intramolecular aldolizations, *Angew. Chem., Int. Ed.* **2008**, *47*, 7656-7658.

Chapter 5 – Studies Towards the Synthesis of Isocyclemone Analogues

5.1 – Introduction

Iso E Super[®], produced on an estimated 2500–3000 tonne annual scale, is a commercially available odorant mixture used to convey a woody–ambery fragrance.^[1] This mixture is composed primarily of compound (±)-**115** but is also recognised to contain a number of isomeric compounds, with a single enantiomer of the minor constituent (±)-**116** essentially determining the overall olfactory value of the material (Figure 5.1).^[2-4] A higher quality material in which the quantity of (±)-**116** is enriched is commercially available under the name Iso Gamma Super[®] since it contains ca. 18% of the γ -isomer (±)-**315**.^[5] An alternative high-grade material named Georgywood[®] has additionally been introduced to the market, consisting primarily of compound (±)-**124**.

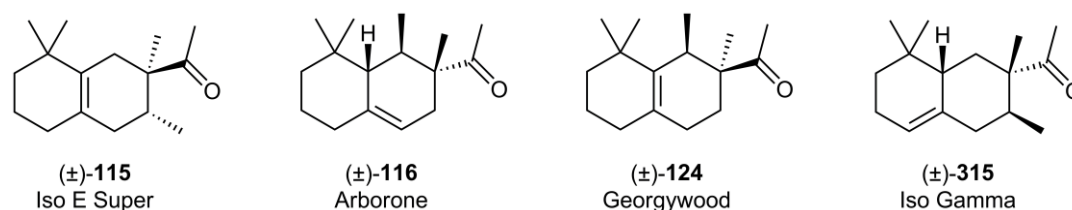
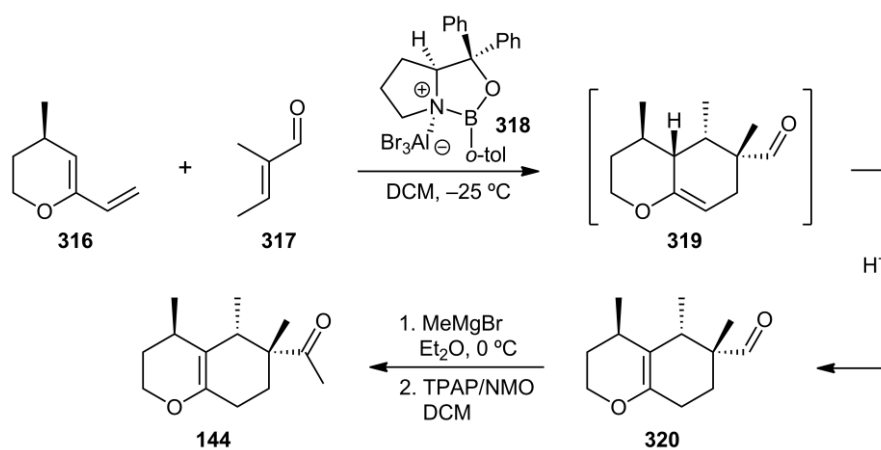


Figure 5.1: Commercially available isocyclemone odorants.

A major concern regarding Iso E Super[®] is its poor biodegradation and high octanol/water partition coefficient, ultimately leading to an accumulation of isocyclemone analogues within the natural environment.^[4] An environmental study of the Rohr River in Germany reported concentrations of compound (±)-**115** in the range of 30 to 100 ng/L water.^[6] The discovery of biodegradable analogues of the isocyclemone scaffold is essential. To achieve this goal, the water solubility and polarity of these compounds must be improved.^[4] Hicken and Corey recently described that the olfactory receptor(s) responsible for binding to isocyclemone odorants can accommodate an oxygen atom at the C-6 position.^[7] A series of enantiopure *oxa*-analogues were synthesised in Diels–Alder reactions catalysed by a chiral oxazaborolidine catalyst, followed by Grignard reaction and subsequent oxidation to furnish the completed isocyclemone analogue (Scheme 5.1).

The Lewis-acid catalyst which the Diels–Alder reaction relies upon is known as the CBS catalyst (Corey-Bakshi-Shibata catalyst).^[8-9] This catalyst is derived from the naturally occurring amino acid L-proline and finds use in many asymmetric transformations; particularly reduction and cycloaddition reactions.^[10] The active catalyst (**318**) is generated from an oxazaborolidine precursor by the *in situ* addition of the strong Lewis-acid aluminium bromide.^[11-12] Alternative active forms of the Diels–Alder catalyst involve its coordination to strong protic acids such as triflic acid or trifluoromethanesulfonimide, aromatic methyl substitution as well as its condensation with alternative boron reagents.^[10, 13-16]



Scheme 5.1: Synthetic pathway to oxa-Georgyone analogue **144** by Hicken and Corey.^[7]

In an effort to improve the polarity of the isocyclemone scaffold the synthesis of a library of oxygenated analogues for olfactory analysis was proposed following the synthetic methodology outlined in Scheme 5.1 (Figure 5.2). Potential molecular modifications include alternative ring size and substituents, as well as analogues differing at the acetyl functionality. As limited Structure-Odour Relationship (SOR) research has been conducted on the isocyclemone odorant family, the synthesis of experimental analogues can aid in understanding their molecular interactions with olfactory receptors.

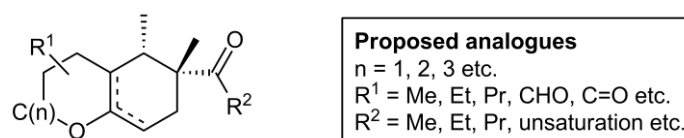


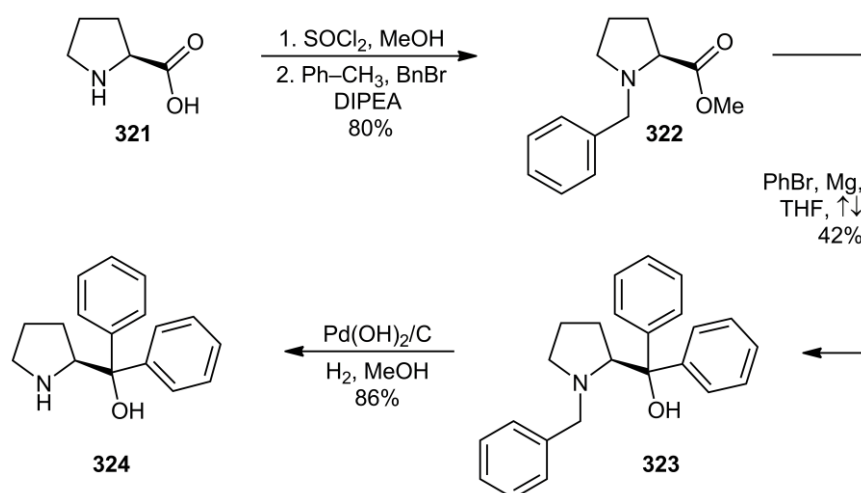
Figure 5.2: Proposed oxa-isocyclemone analogues.

5.2 – Results and Discussion

5.2.1 – Synthesis of Oxazaborolidine Catalyst Precursors

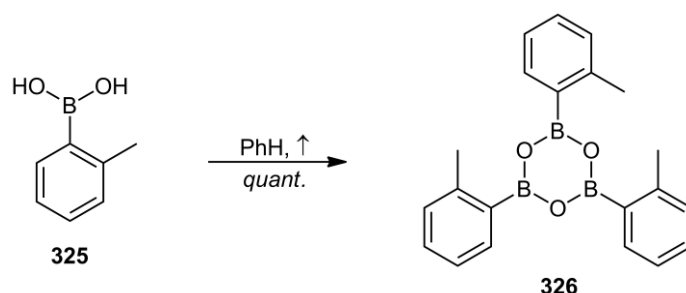
The synthesis of the major component of the active oxazaborolidine Diels–Alder catalyst was achieved beginning from chiral amino acid L-proline (**321**).^[17-19] The initial reaction involved *bis*-protection of the carboxylic acid and amine functionalities. The carboxylic acid moiety of L-proline (**321**) was protected using thionyl chloride to generate an acyl chloride intermediate which was then reacted with methanol to give the methylated ester analogue. The crude material obtained from this reaction was taken up in toluene and reacted with benzyl bromide using diisopropylethylamine (Hünig's base) to provide the *bis*-protected analogue **322** in 80% yield after vacuum distillation (Scheme 5.2).^[19]

The subsequent step involved a Grignard reaction of compound **322** with phenylmagnesium bromide, generated *in situ* from magnesium and bromobenzene. The formation of this reagent was shown to require the addition of a catalytic quantity of iodine to aid in removing the passivating layer of magnesium oxide. The reaction successfully provided compound **323** as a colourless solid in 42% yield after recrystallisation from ethanol.^[17, 19] Compound **323** was then debenzylated by hydrogenation over Pearlman's catalyst ($\text{Pd}(\text{OH})_2/\text{C}$) to yield target compound **324** as a colourless solid in 86% yield after recrystallisation from hexane.^[18]



Scheme 5.2: Synthesis of (S)-diphenyl(pyrrolidin-2-yl)methanol (**324**) from L-proline (**321**).

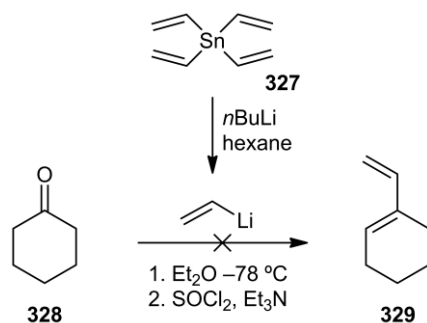
Attention turned to the preparation of the boronated section of the oxazaborolidine catalyst. The synthesis of cyclic boronic acid trimer **326** by the dehydration of *ortho*-tolylboronic acid (**325**) was achieved by multiple distillations of a sample of this compound solubilised within benzene.^[13] This distillation exploits the phenomenon that benzene and water azeotrope together, thus driving the equilibrium towards the trimerised compound. The recovered material was recrystallised from benzene to provide a sample of **326** which was stored under anhydrous conditions (Scheme 5.3).



Scheme 5.3: Synthesis of cyclic boronic acid trimer **326** from *ortho*-tolylboronic acid (**325**).

5.2.2 – Synthesis of Diene Precursors – Organolithium Route

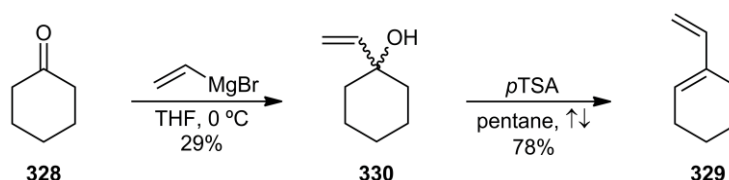
Owing to the perceived difficulty of the synthetic chemistry, coupled with the volatility of the substrate compounds, model reactions with cyclohexanone (**328**) were proposed. The synthetic route first explored for the synthesis of the corresponding Diels–Alder reagent 1-vinylcyclohex-1-ene (**329**) was the reaction of cyclohexanone (**328**) with an organolithium reagent analogous to the synthetic methodology of Hicken and Corey.^[7] The production of a *ca.* 1 M vinyl lithium in diethylether solution was achieved by the action of *n*-butyllithium on tetravinylstannane (**327**) (Scheme 5.4).^[20] This pre-generated reagent was then added to cyclohexanone (**328**) at -78 °C, followed by the subsequent addition of thionyl chloride and triethylamine.^[7] The mechanism for this reaction is hypothesised to involve the nucleophilic attack of vinyl lithium onto the carbonyl functionality to provide a hydroxyl intermediate which is then substituted by a chlorine atom, followed by elimination to furnish the diene compound. This reaction was discovered to be unsuccessful in the synthesis of compound **329**, presumably due to the loss of the minute quantity of volatile product synthesised. Additional synthetic pathways that could be performed economically on a larger scale were researched.



Scheme 5.4: Failed synthesis of diene compound **329** from cyclohexanone (**328**).

5.2.3 – Synthesis of Diene Precursors – Grignard Reaction Route

The subsequent synthetic pathway explored involved a Grignard reaction followed by an elimination reaction to provide the diene compound. The reaction between Grignard reagent vinylmagnesium bromide and cyclohexanone (**328**) at 0 °C was discovered to successfully provide analogue **330** as a yellow oil in 29% yield after vacuum distillation (Scheme 5.5).^[21-23] Multiple attempts at optimising the yield of the Grignard reaction, including using alternative reaction conditions, were unsuccessful. An isolated sample of compound **330** was dehydrated using acidic catalyst *para*-toluenesulphonic acid in pentane at reflux temperature to provide target diene compound **329** in 78% yield as a volatile clear liquid (Figure 5.3).^[23-25]



Scheme 5.5: Synthesis of diene compound **329** from cyclohexanone (**328**) via Grignard reaction and subsequent dehydration.

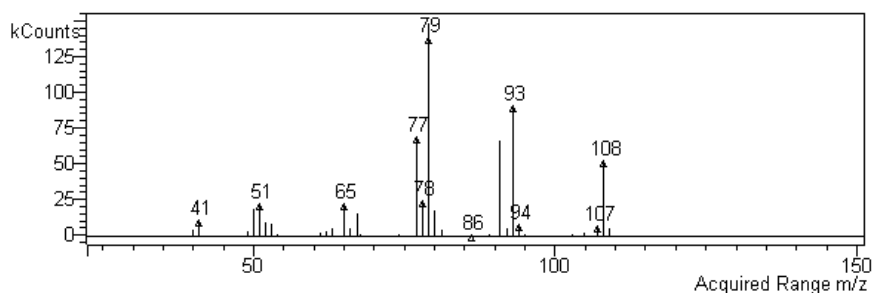
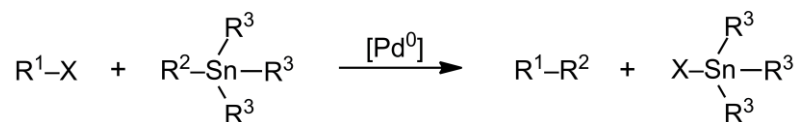


Figure 5.3: Mass spectrum (EI) of compound **329** showing molecular ion at *m/z* 108. Spectrum indicates that isomerisation has occurred during fragmentation.

5.2.4 – Synthesis of Diene Precursors – Stille Coupling Route

An alternative synthetic route was additionally explored owing to the unfavourable yields associated with the Grignard reaction in the synthetic sequence delineated in Scheme 5.5. The Stille reaction (or Migita-Kosugi-Stille coupling) involves a palladium catalysed coupling reaction of an organostannane compound and an electrophile.



The R^2 functionality bonded to the stannane moiety is usually sp^2 hybridised and typically consists of an allyl or aryl group whilst the R^3 functionalities are typically alkyl groups. A tetraorganostannane compound readily transfers its first group to an electrophile, the second group transferring about 100 times slower from the subsequent $XSnR^3$ species, and thus with stoichiometric quantities only the most reactive group is transferred.^[26] Examples of coupling reactions between organostannanes and electrophiles were first published during 1976–1977 by the research groups of Eaborn^[27] and Kosugi.^[28-30] Extensive mechanistic research later published by Stille *et al.*^[31-32] developed the reaction to become a standard methodology for chemical synthesis.^[33]

The catalytic cycle begins with the oxidative addition of a halide or pseudohalide electrophile to the palladium catalyst. This is followed by transmetalation with the stannane compound, followed by reductive elimination to yield the coupled product and regenerate the active palladium catalyst (Figure 5.4).^[26, 33-34] The rigorous anhydrous and air-free conditions required for other palladium catalysed reactions can usually be relaxed for the Stille coupling. In some cases water has actually been found to promote coupling.^[35] Whilst oxygen can also play a beneficial role, it can be involved in side reactions and is therefore best excluded unless otherwise specified.^[35]

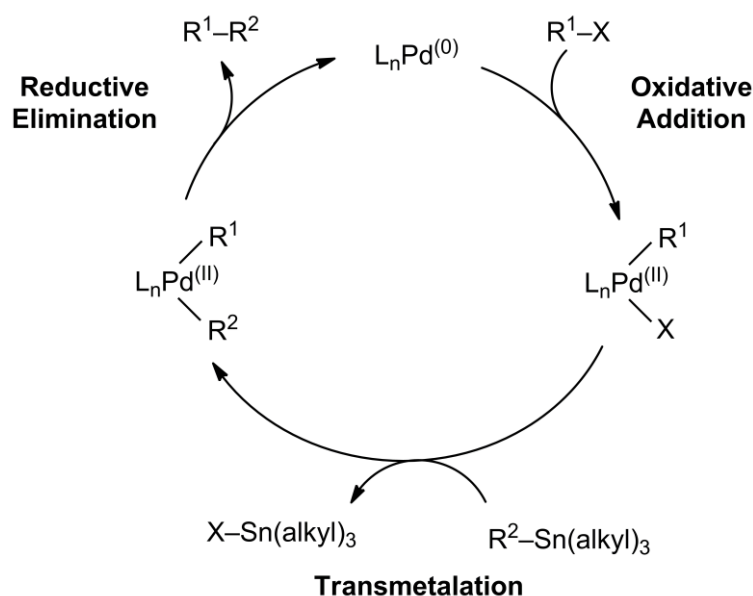
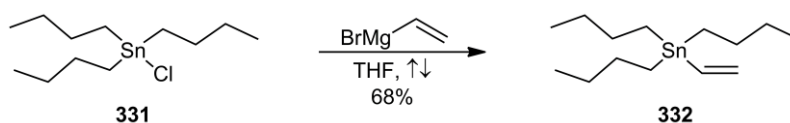


Figure 5.4: Simplified catalytic cycle of a Stille coupling reaction.^[34]

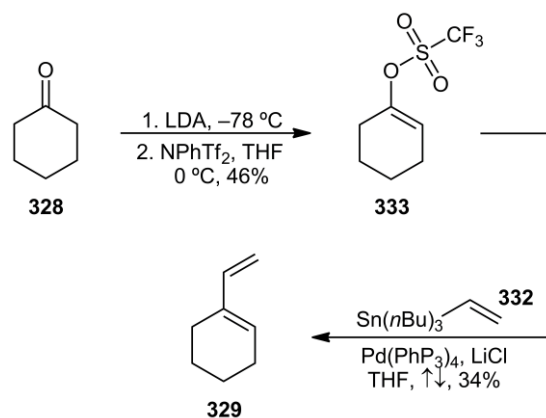
The newly devised synthetic route involved the enol triflation of the carbonyl functionality followed by a coupling reaction with an organostannane compound to provide the required diene. The tributylstannane analogue was chosen owing to its reduced toxicity in comparison to smaller alkyl substituted analogues such as the trimethylstannanes.^[34] The synthesis of tributyl(vinyl)stannane (**332**) from tributylstannane chloride (**331**) was achieved by heating to reflux with a solution of vinylmagnesium bromide in tetrahydrofuran. The reaction successfully provided compound **332** in 68% yield as a clear oil after vacuum distillation (Scheme 5.6).^[36-37]



Scheme 5.6: Synthesis of tributyl(vinyl)stannane (**332**) from tributylstannane chloride (**331**).

The synthetic sequence to produce the enol triflate analogue involved the reaction of cyclohexanone (**328**) with the non-nucleophilic base lithium diisopropylamide (LDA) at $-78\text{ }^{\circ}\text{C}$, pre-generated *in situ* by the action of *n*-butyllithium on diisopropylamine. This reaction yields an intermediate enolate which is trapped by the addition of *N*-phenyl-bis(trifluoromethanesulfonimide) to provide enol triflate analogue **333** in 46% yield as a yellow oil (Scheme 5.7).^[23] The subsequent Stille coupling of compound **333** with tributyl(vinyl)stannane (**332**) in tetrahydrofuran using $\text{Pd}(\text{PhP}_3)_4$ as a

catalyst and lithium chloride as a rate accelerator successfully provided compound **329** in 34% yield.^[23, 38-39] Thus, the Grignard reaction synthetic pathway remained the more efficient synthetic route with an overall yield of 22.6%, opposed to 15.6% for the Stille coupling synthetic route.



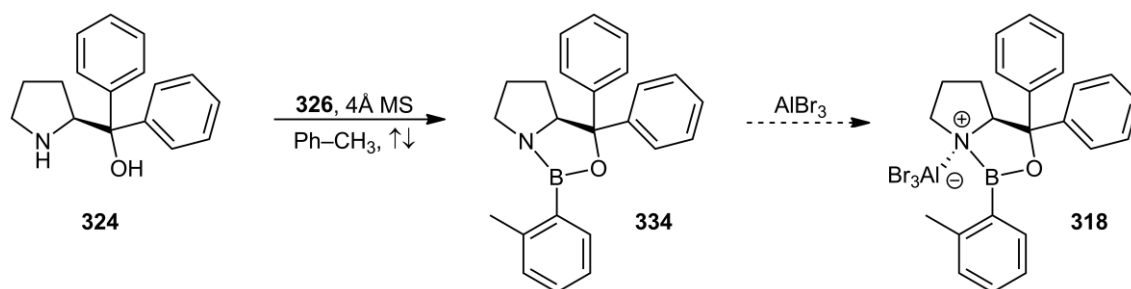
Scheme 5.7: Synthesis of diene compound **329** from cyclohexanone (**328**) via Stille coupling of enol triflate analogue **333**.

5.2.5 – Catalyst Generation and Diels–Alder Experiment

The synthesis of oxazaborolidine compound **334** was achieved by refluxing a solution of (*S*)-diphenyl(pyrrolidine-2-yl)methanol (**324**) and 2,4,6-tri-*o*-tolyl-1,3,5,2,4,6-trioxatriborinane (**326**) in anhydrous toluene in a flask attached to a pressure-equalising dropping funnel filled with activated 4Å molecular sieves and functioning as a Soxhlet extractor, followed by azeotropic distillation of multiple additions of anhydrous toluene (Scheme 5.8).^[7] The active oxazaborolidine catalyst (**318**) was then prepared from a dichloromethane solution of compound **334** by the addition of a solution of aluminium bromide in dibromomethane (ratio of **334** to AlBr₃; 2:1).^[12] Once activated, the oxazaborolidine catalyst is reported to be stable in solution between a temperature range of -20 to -78 °C.^[10]

A single Diels–Alder reaction between diene compound **329** and (*E*)-2-methyl-2-butenal (**317**) was attempted (Scheme 5.9). The reaction appeared to proceed smoothly, but owing to the reaction having to be manually chilled at -25 °C, the temperature is believed to have fluctuated beyond the stability range of the active oxazaborolidine catalyst thereby aborting the reaction before completion. ¹³C NMR analysis of the recovered material revealed that a new aldehyde peak was present at δ 206.4 ppm, but also that a substantial quantity of (*E*)-2-methyl-2-butenal (**317**) remained unreacted (Figure 5.5). Owing

to time constraints, further experimentation was not attempted. This reaction is expected to proceed to completion with optimisation and the use of a mechanical chiller.



Scheme 5.8: Preparation of the (S)-(-)-*o*-tolyl-CBS-oxazaborolidine Diels–Alder catalyst (**318**) from (S)-diphenyl(pyrrolidin-2-yl)methanol (**324**) and 2,4,6-tri-*o*-tolyl-1,3,5,2,4,6-trioxatriborinane (**326**).

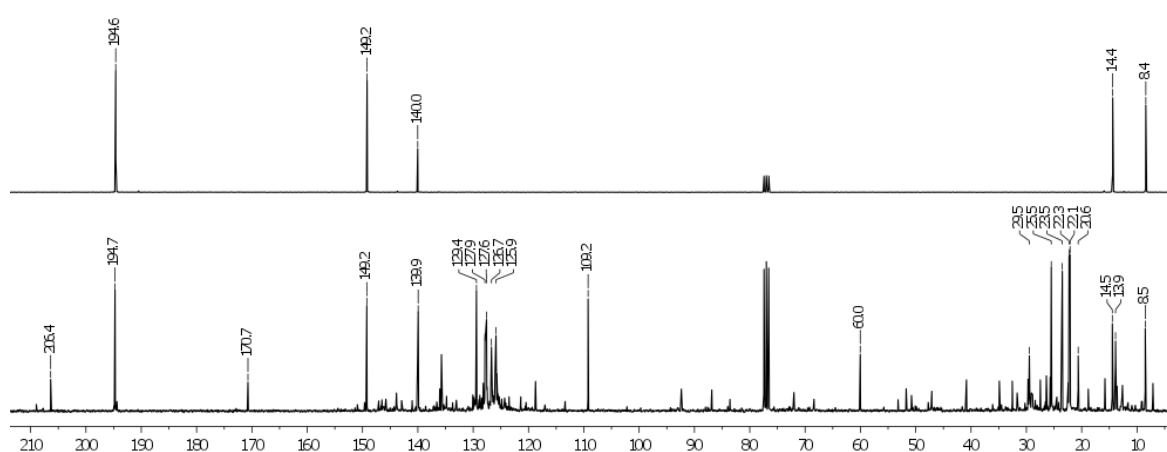
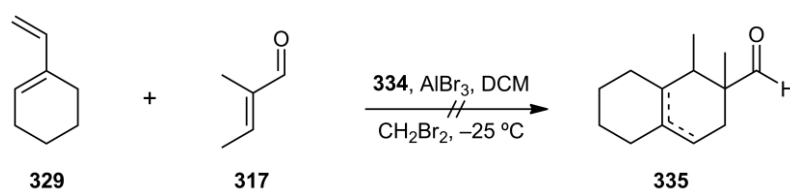


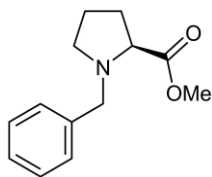
Figure 5.5: ^{13}C NMR (CDCl_3 , 75 MHz) spectra of (E)-2-methyl-2-butenal (**317**, top) and the crude material obtained from reaction displayed in Scheme 5.9 (bottom), displaying a new aldehyde peak at δ 206.4 ppm.



Scheme 5.9: Diels–Alder reaction between diene compound **329** and (E)-2-methyl-2-butenal (**317**) using **318** as a chiral catalyst.

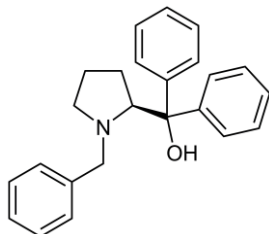
5.3 – Experimental

(S)-Methyl 1-benzylpyrrolidine-2-carboxylate (322):^[19]

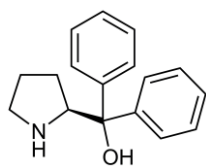


A solution of L-proline (23.04 g, 200 mmol) and MeOH (400 mL) was cooled to 0 °C and thionyl chloride (17.5 mL, 240 mmol) was added dropwise over 0.25 h. The solution was warmed to RT before being held at reflux for 2 h. The solution was then concentrated under reduced pressure followed by co-evaporation with toluene (3 x 80 mL). The resulting residue was dissolved in toluene (200 mL) and diisopropylethylamine (170.8 mL) was added at RT. The solution was cooled to 0 °C and benzyl bromide (26.16 mL) was added over 0.25 h and the mixture then heated at reflux for 24 h. The reaction was quenched by the addition of a saturated solution of NaHCO₃ (400 mL) followed by extraction with EtOAc (3 x 300 mL). The combined organic extracts were pooled, dried (MgSO₄) and concentrated under reduced pressure to give a yellow oil which was purified by vacuum distillation (100 °C, 0.5 torr) to give (S)-methyl 1-benzylpyrrolidine-2-carboxylate (35 g, 80%) as a viscous clear oil. ¹H NMR (CDCl₃, 300 MHz): δ 7.35–7.22 (m, 5H), 3.89 (d, *J* = 12.8 Hz, 1H), 3.58 (d, *J* = 12.8 Hz, 1H), 3.66 (s, 2H), 3.26 (dd, *J* = 8.7, 6.3 Hz, 1H), 3.09–3.03 (m, 1H), 2.44–2.36 (m, 1H), 2.20–2.07 (m, 1H), 2.03–1.88 (m, 1H), 1.86–1.75 (m, 1H). ¹³C NMR (CDCl₃, 75 MHz): δ 173.7, 137.8, 128.5, 127.5, 126.4, 64.5, 58.0, 52.5, 50.9, 28.7, 22.4.

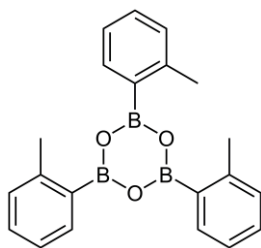
(S)-(1-Benzylpyrrolidin-2-yl)diphenylmethanol (323):^[19]



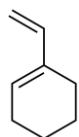
To a mixture of magnesium filings (9.76 g, 400 mmol), iodine (32 mg) and THF (160 mL) was added bromobenzene (13.47 mL, 128 mmol) and the mixture warmed until a reaction had initiated. A further amount of bromobenzene (28.64 mL, 272 mmol) was then added over 0.5 h and the reaction heated at reflux for 0.5 h. The mixture was cooled to 5–10 °C and a solution of (S)-methyl 1-benzylpyrrolidine-2-carboxylate (35 g, 160 mmol) in THF (64 mL) was added dropwise over 0.25 h. The mixture was stirred at RT for 16 h, cooled to 0 °C and quenched by the addition of conc. HCl (320 mL). The mixture was then stirred for an additional 2 h before being concentrated under reduced pressure. The residual solid was taken up in a mixture of EtOAc (500 mL) and 4 M NaOH (1 L) and the phases separated. The aqueous phase was extracted with EtOAc (3 x 500 mL). The organic extracts were pooled, dried (MgSO₄) and concentrated under reduced pressure to give a tan solid that was recrystallised from EtOH to give (S)-(1-benzylpyrrolidin-2-yl)diphenylmethanol (23 g, 42%) as a colourless solid. mp: 121–122 °C. (lit. mp: 118.8–119.6 °C (EtOH)).^[19] IR (ATR): $\tilde{\nu}$ = 3250 (ν O–H) cm⁻¹. ¹H NMR (CDCl₃, 300 MHz): δ 7.77–7.70 (m, 2H), 7.62–7.56 (m, 2H), 7.34–7.02 (m, 11H), 4.94 (s, 1H), 4.02–3.95 (m, 1H), 3.24 (d, *J* = 12.6 Hz, 1H), 3.03 (d, *J* = 12.6 Hz, 1H), 2.97–2.89 (m, 1H), 2.41–2.31 (m, 1H), 2.05–1.90 (m, 1H), 1.83–1.51 (m, 3H). ¹³C NMR (CDCl₃, 75 MHz): δ 148.0, 146.6, 139.6, 128.5, 128.1, 128.1, 128.0, 126.8, 126.3, 126.2, 125.6, 125.5, 77.9, 70.6, 60.5, 55.5, 29.8, 24.1.

(S)-Diphenyl(pyrrolidin-2-yl)methanol (324):^[18]

A solution of (S)-(1-benzylpyrrolidin-2-yl)diphenylmethanol (6.92 g, 20 mmol) in MeOH (120 mL) was hydrogenated under an atmosphere of H₂ over 20% Pd(OH)₂/C (1.4 g) for 24 h. The reaction mixture was filtered through a pad of celite before taken up in EtOAc (80 mL) and 1 M NaOH (80 mL). The phases were separated and the aqueous phase extracted with EtOAc (3 x 80 mL). The organic extracts were pooled, dried (MgSO₄) and concentrated under reduced pressure to yield a crude solid which was recrystallised from hexane to give (S)-diphenyl(pyrrolidin-2-yl)methanol (4.35 g, 86%) as a colourless solid. mp: 78–79 °C. (lit. mp: 75.5–76.5 °C (CHCl₃/hexane)).^[18] IR (ATR): $\tilde{\nu}$ = 3369 (ν O–H), 2959/2887/2835 (ν C–H) cm⁻¹. ¹H NMR (CDCl₃, 75 MHz): δ 7.65–7.59 (m, 2H), 7.58–7.52 (m, 2H), 7.37–7.27 (m, 4H), 7.25–7.17 (m, 2H), 4.29 (t, *J* = 7.4 Hz, 1H), 3.10–2.91 (m, 2H), 1.85–1.53 (m, 4H). ¹³C NMR (CDCl₃, 75 MHz): δ 148.1, 145.3, 128.1, 127.8, 126.3, 126.2, 125.7, 125.4, 77.0, 64.3, 46.6, 26.2, 25.4.

2,4,6-Tri-*o*-tolyl-1,3,5,2,4,6-trioxatriborinane (326):^[13]

o-Tolylboronic acid (0.75 g, 0.55 mmol) was dehydrated by azeotropic distillation with benzene (3 x 20 mL). The residual solid was then recrystallised from benzene to give 2,4,6-tri-*o*-tolyl-1,3,5,2,4,6-trioxatriborinane (*quant.*) as a colourless solid.

1-Vinylcyclohex-1-ene (329):

¹H NMR (CDCl₃, 300 MHz): δ 6.35 (dd, *J* = 17.5, 10.7 Hz, 1H), 5.80–5.74 (m, 1H), 5.07 (d, *J* = 17.3 Hz, 1H), 4.89 (d, *J* = 10.5 Hz, 1H), 2.19–2.09 (m, 4H), 1.75–1.56 (m, 4H). ¹³C NMR (CDCl₃, 75 MHz): δ 140.2, 136.0, 129.8, 109.5, 25.7, 23.7, 22.5, 22.3.

Via vinylolithium and elimination reaction:^[7]

To tetravinylstannane (0.3 mL, 1.65 mmol) was slowly added *n*-butyllithium (3.6 mL, 5.77 mmol, 1.6 M in hexane). The mixture was stirred at RT for 3.5 h, concentrated under reduced pressure and the residual solid washed with pentane (3 x 1.5 mL). The residual solid was then dissolved in Et₂O (3 mL) to give a ca. 1 M solution of vinylolithium. γ -Butyrolactone (259 mg, 3 mmol) was cooled to –78 °C before a 1 M vinylolithium in Et₂O solution (3 mL) was added and the mixture stirred at –78 °C for 0.5 h. To this mixture was then added thionyl chloride (0.22 mL, 3 mmol) followed by triethylamine (0.88 mL, 6.33 mmol). The mixture was then warmed to 0 °C over 1 h and then stirred at 0 °C for 0.5 h. The reaction was quenched with a saturated solution of NaHCO₃ (3.5 mL) and H₂O (3.5 mL), the phases separated and the aqueous phase extracted with Et₂O (3 x 5 mL). The organic extracts were pooled, dried

(MgSO₄) and concentrated under reduced pressure. The reaction methodology failed to yield 1-vinylcyclohex-1-ene.

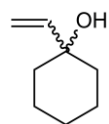
Via dehydration of 1-vinylcyclohexanol:^[23-25]

To a solution of 1-vinylcyclohexanol (300 mg, 2.37 mmol) in pentane (1.5 mL) was added *para*-toluenesulfonic acid (67 mg) and the mixture held at reflux for 5 h. The organic solution was washed with H₂O (50 mL), dried (MgSO₄) and concentrated under reduced pressure to yield 1-vinylcyclohex-1-ene (200 mg, 78%) as a clear oil.

Via Stille coupling of cyclohex-1-en-1-yl trifluoromethanesulfonate:^[23]

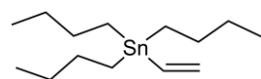
To a solution of lithium chloride (2.05 g, 40.5 mmol) in THF (60 mL) was added Pd(PPh₃)₄ (192 mg, 0.168 mmol) and the mixture stirred for 0.25 h. A solution of cyclohex-1-en-1-yl trifluoromethanesulfonate (1.86 g, 8.1 mmol) and tributyl(vinyl)stannane (2.58 g, 8.1 mmol) in THF (45 mL) was added and the mixture heated at reflux for 48 h. The mixture was extracted with hexane (150 mL), the organic extracts pooled, washed with a saturated solution of NaHCO₃ (100 mL), dried (MgSO₄) and concentrated under reduced pressure. The resulting residue was distilled under vacuum (50 °C, 0.2 torr) to yield 1-vinylcyclohex-1-ene (301 mg, 34%) as a clear oil.

***rac*-1-Vinylcyclohexanol (330):**^[21-23]



To a solution of cyclohexanone (4.9 g, 50 mmol) in THF (60 mL) was added vinylmagnesium bromide (100 mL, 1 M in THF, 2 equiv) over 0.5 h at 35 °C. The reaction mixture was then held at reflux for 2 h before being quenched by the addition of a 50% saturated solution of ammonium chloride (160 mL) and left for 0.5 h followed by concentration under reduced pressure. The resulting residue was taken up in H₂O (300 mL) and extracted with Et₂O (3 x 200 mL). The organic extracts were pooled, dried (MgSO₄) and concentrated under reduced pressure to give a crude oil which was vacuum distilled to yield 1-vinylcyclohexanol (1.8 g, 29%) as a yellow oil. IR (ATR): $\tilde{\nu}$ = 3367 (ν O–H), 2929 (ν C–H), 959 (ν C=CH₂) cm⁻¹. ¹H NMR (CDCl₃, 300 MHz): δ 5.99 (dd, *J* = 17.3, 10.7 Hz, 1H), 5.25 (dd, *J* = 17.3, 1.3 Hz, 1H), 5.05 (dd, *J* = 10.7, 1.3 Hz, 1H), 1.77–1.19 (m, 10H). ¹³C NMR (CDCl₃, 75 MHz): δ 145.8, 111.0, 71.3, 37.1, 25.2, 21.6. HRMS: *m/z* calculated for C₈H₁₄O: 126.1045 [M]⁺; Found: 126.1049.

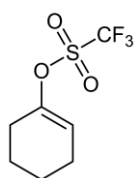
Tributyl(vinyl)stannane (332):^[36]



To vinylmagnesium bromide (61 mL, 1 M in THF, 61 mmol) was added tributylstannane chloride (10.75 g, 33 mmol) dissolved in THF (9 mL) at a rate that a gentle reflux was maintained. The reaction was then held at reflux for 19 h, cooled to RT and quenched by the addition of a saturated solution of NH₄Cl (20 mL). The aqueous layer was extracted with Et₂O (3 x 100 mL) and the residual oil fractionally

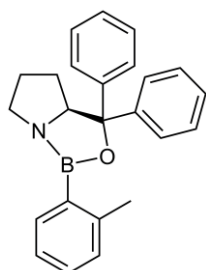
distilled under vacuum (80 °C, 0.5 torr) to give tributyl(vinyl)stannane (7.16 g, 68%) as a clear oil. IR (ATR): $\tilde{\nu} = 2956/2925$ (ν C–H) cm^{-1} . ^1H NMR: (CDCl_3 , 300MHz): δ 6.54–6.42 (m, 1H), 6.20–6.13 (m, 1H), 5.72–5.63 (m, 1H), 1.66–1.44 (m, 6H), 1.39–1.26 (m, 6H), 1.02–1.79 (m, 15H). ^{13}C NMR (CDCl_3 , 75 MHz): δ 139.2, 133.6, 29.1, 27.2, 13.6, 9.3.

Cyclohex-1-en-1-yl trifluoromethanesulfonate (333):^[23]



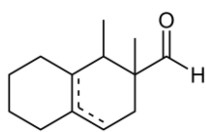
n-Butyllithium (29.6 mL, 47.29 mmol, 1.6 M in hexanes) was added to a solution of diisopropylamine (4.6 g, 45.48 mmol) in THF (50 mL) at 0 °C. After ten minutes the solution was cooled to –78 °C and cyclohexanone (3.3 g, 33.66 mmol) in THF (50 mL) was added dropwise. The reaction was stirred at –78 °C for 2 h at which point *N*-phenyl-bis(trifluoromethanesulfonimide) (15.62 g, 43.76 mmol, 1.3 equiv) in THF (40 mL) was added. The solution was then stirred at 0 °C for 3 h and then at RT overnight. The reaction was quenched by the addition of H_2O (200 mL) and extracted with EtOAc (4 x 200 mL). The organic extracts were pooled, dried (MgSO_4) and concentrated under reduced pressure to yield a viscous orange oil that was purified by vacuum distillation at (80 °C, 0.5 torr) to give cyclohex-1-en-1-yl trifluoromethanesulfonate (3.57 g, 46%) as a viscous clear oil. IR (ATR): $\tilde{\nu} = 2943$ (ν C–H), 1200/1139 (ν C–F₃) cm^{-1} . ^1H NMR (CDCl_3 , 300 MHz): δ 5.79–5.74 (m, 1H), 2.36–2.29 (m, 2H), 2.23–2.15 (m, 2H), 1.84–1.74 (m, 2H), 1.66–1.57 (m, 2H). ^{13}C NMR (CDCl_3 , 75 MHz): δ 149.3, 118.5 (q, $J = 320.2$ Hz), 118.3, 27.5, 23.7, 22.5, 20.9. HRMS: m/z calculated for $\text{C}_7\text{H}_9\text{F}_3\text{O}_3\text{S}$: 230.0225 [M]⁺; Found: 230.0231.

(S)-3,3-Diphenyl-1-(*o*-tolyl)hexahydropyrrolo[1,2-*c*][1,3,2]oxazaborole (334):^[7]



To flask fitted with a pressure-equalising dropped funnel filled with 4Å molecular sieves (functioning as a soxhlet extractor) was added (*S*)-diphenyl(pyrrolidin-2-yl)methanol (159 mg, 0.625 mmol), 2,4,6-tri-*o*-tolyl-1,3,5,2,4,6-trioxatriborinane (73 mg, 0.209 mmol) and toluene (20 mL). The resulting solution was held at reflux for 3 h. The pressure-equalising dropping funnel was replaced with a distillation device and the reaction was distilled to a volume of ca. 5 mL. The distillation was repeated three times with the addition of toluene (3 x 5 mL). The reaction was then cooled to RT and concentrated under high vacuum (0.1 torr) for 1 h. The resulting residue was then dissolved in DCM (2.4 mL) to provide a ca. 0.25 M solution of (*S*)-3,3-diphenyl-1-(*o*-tolyl)hexahydropyrrolo[1,2-*c*][1,3,2]oxazaborole.

1,2-Dimethyl-1,2,3,5,6,7,8,8a-octahydronaphthalene-2-carbaldehyde (335):



A solution of (*S*)-3,3-diphenyl-1-(*o*-tolyl)hexahydropyrrolo[1,2-*c*][1,3,2]oxazaborole (1.8 mL, ca. 0.25 M in DCM, 0.45 mmol) was cooled to $-25\text{ }^{\circ}\text{C}$ before a solution of aluminium bromide (0.225 mL, 1 M in CH_2Br_2 , 0.225 mmol) was added. The resulting solution was stirred at $-25\text{ }^{\circ}\text{C}$ for 0.5 h and (*E*)-2-methyl-2-butenal (0.217 mL, 2.25 mmol) was added. A solution of 1-vinylcyclohex-1-ene (230 mg, 2.13 mmol) in DCM (2 mL) was then added over a period of 3 h. The reaction was stirred overnight at $-25\text{ }^{\circ}\text{C}$ and quenched by the addition of triethylamine (0.15 mL). The reaction was taken up in H_2O (30 mL) and extracted with EtOAc (3 x 30 mL). The organic extracts were pooled, dried (MgSO_4) and concentrated under reduced pressure. This reaction failed to yield 1,2-dimethyl-1,2,3,5,6,7,8,8a-octahydronaphthalene-2-carbaldehyde.

5.4 – References

1. M. Gautschi, J. A. Bajgrowicz, P. Kraft, Fragrance chemistry - milestones and perspectives, *Chimia* **2001**, *55*, 379-387.
2. M. Bella, M. Cianflone, G. Montemurro, P. Passacantilli, G. Piancatelli, Chemistry of odorants: stereoselective synthesis of octahydronaphthalene-based perfumery Geogywood, (+,-)-1-[(1*R**,2*S**)-1,2,3,4,5,6,7,8-octahydro-1,2,8,8-tetramethylnaphthalen-2-yl]ethan-1-one, *Tetrahedron* **2004**, *60*, 4821-4827.
3. C. Nussbaumer, G. Frater, P. Kraft, (±)-1-[(1*R**,2*R**,8*aS**)-1,2,3,5,6,7,8,8*a*-octahydro-1,2,8,8-tetramethylnaphthalen-2-yl]ethan-1-one. Isolation and stereoselective synthesis of a powerful minor constituent of the perfumery synthetic Iso E Super, *Helv. Chim. Acta* **1999**, *82*, 1016-1024.
4. G. Ohloff, W. Pickenhagen, P. Kraft, *Scent and Chemistry - The Molecular World of Odors*, Verlag Helvetica Chimica Acta, Zurich, **2012**.
5. P. Kraft, K. Popaj, Unexpected tethering in the synthesis of methyl-substituted acetyl-1-oxaspiro[4.5]decanes: novel Woody-Ambery odorants with improved bioavailability, *Eur. J. Org. Chem.* **2008**, 261-268.
6. K. Bester, N. Hueffmeyer, E. Schaub, J. Klasmeier, Surface water concentrations of the fragrance compound OTNE in Germany - A comparison between data from measurements and models, *Chemosphere* **2008**, *73*, 1366-1372.
7. E. J. Hicken, E. J. Corey, Stereoselective Synthesis of Woody Fragrances Related to Geogyone and Arborone, *Org. Lett.* **2008**, *10*, 1135-1138.
8. E. J. Corey, R. K. Bakshi, S. Shibata, Highly enantioselective borane reduction of ketones catalyzed by chiral oxazaborolidines. Mechanism and synthetic implications, *J. Am. Chem. Soc.* **1987**, *109*, 5551-5553.
9. E. J. Corey, R. K. Bakshi, S. Shibata, C. P. Chen, V. K. Singh, A stable and easily prepared catalyst for the enantioselective reduction of ketones. Applications to multistep syntheses, *J. Am. Chem. Soc.* **1987**, *109*, 7925-7926.
10. S. Mukherjee, E. J. Corey, Enantioselective synthesis based on catalysis by chiral oxazaborolidinium cations, *Aldrichimica Acta* **2010**, *43*, 49-58.
11. D. Liu, E. Canales, E. J. Corey, Chiral Oxazaborolidine-Aluminum Bromide Complexes Are Unusually Powerful and Effective Catalysts for Enantioselective Diels-Alder Reactions, *J. Am. Chem. Soc.* **2007**, *129*, 1498-1499.
12. E. Canales, E. J. Corey, Highly Enantioselective [2+2]-Cycloaddition Reactions Catalyzed by a Chiral Aluminum Bromide Complex, *J. Am. Chem. Soc.* **2007**, *129*, 12686-12687.

13. E. J. Corey, T. Shibata, T. W. Lee, Asymmetric Diels-Alder Reactions Catalyzed by a Triflic Acid Activated Chiral Oxazaborolidine, *J. Am. Chem. Soc.* **2002**, *124*, 3808-3809.
14. D. H. Ryu, T. W. Lee, E. J. Corey, Broad-Spectrum Enantioselective Diels-Alder Catalysis by Chiral, Cationic Oxazaborolidines, *J. Am. Chem. Soc.* **2002**, *124*, 9992-9993.
15. D. H. Ryu, E. J. Corey, Triflimide Activation of a Chiral Oxazaborolidine Leads to a More General Catalytic System for Enantioselective Diels-Alder Addition, *J. Am. Chem. Soc.* **2003**, *125*, 6388-6390.
16. E. J. Corey, C. J. Helal, Reduction of carbonyl compounds with chiral oxazaborolidine catalysts: A new paradigm for enantioselective catalysis and a powerful new synthetic method, *Angew. Chem., Int. Ed.* **1998**, *37*, 1986-2012.
17. Y.-M. Zhang, P. Liu, H.-L. Zhang, Synthesis and crystal structure of the chiral β -amino alcohol (S)- α,α -diphenyl-2-pyrrolidinemethanol, *J. Chem. Res.* **2010**, *34*, 610-612.
18. P.-A. Wang, W.-M. Liu, X.-L. Sun, A simple synthesis of (S)- α,α -diaryl-2-pyrrolidinemethanols, *Org. Prep. Proced. Int.* **2011**, *43*, 477-483.
19. C. Sparr, E.-M. Tanzer, J. Bachmann, R. Gilmour, A concise synthesis of (S)-2-(fluorodiphenylmethyl)pyrrolidine: a novel organocatalyst for the stereoselective epoxidation of α,β -unsaturated aldehydes, *Synthesis* **2010**, 1394-1397.
20. D. Seyferth, M. A. Weiner, Preparation of organolithium compounds by the transmetalation reaction. I. Vinylolithium, *J. Am. Chem. Soc.* **1961**, *83*, 3583-3586.
21. A. Zhang, T. V. RajanBabu, Hydrovinylation of 1,3-Dienes: A New Protocol, an Asymmetric Variation, and a Potential Solution to the Exocyclic Side Chain Stereochemistry Problem, *J. Am. Chem. Soc.* **2006**, *128*, 54-55.
22. W. Herz, R. R. Juo, Photooxygenation of 1-vinylcycloalkenes. The competition between ene reaction and cycloaddition of singlet oxygen, *J. Org. Chem.* **1985**, *50*, 618-627.
23. W. Liu, J. Zhou, G. Geng, Q. Shi, F. Sauriol, J. H. Wu, Antiandrogenic, Maspin Induction, and Antiprostata Cancer Activities of Tanshinone IIA and Its Novel Derivatives with Modification in Ring A, *J. Med. Chem.* **2012**, *55*, 971-975.
24. J. Zhang, W. Duan, J. Cai, Asymmetric synthesis of 3(S),17-dihydroxytanshinone, *Tetrahedron* **2004**, *60*, 1665-1669.
25. J. Rodriguez, P. Brun, B. Waegell, Isomerization of functionalized 1,5-dienes with pentacarbonyliron, *J. Organomet. Chem.* **1989**, *359*, 343-369.
26. J. K. Stille, Palladium-catalyzed coupling reactions of organic electrophiles with organic tin compounds, *Angew. Chem.* **1986**, *98*, 504-519.

27. D. Azarian, S. S. Dua, C. Eaborn, D. R. M. Walton, Reactions of organic halides with R_3MMR_3 compounds (M = silicon, germanium, tin) in the presence of tetrakis(triarylphosphine)palladium, *J. Organomet. Chem.* **1976**, *117*, 55-57.
28. M. Kosugi, K. Sasazawa, Y. Shimizu, T. Migita, Reactions of allyltin compounds. III. Allylation of aromatic halides with allyltributyltin in the presence of tetrakis(triphenylphosphine)palladium(0), *Chem. Lett.* **1977**, 301-302.
29. M. Kosugi, Y. Shimizu, T. Migita, Alkylation, arylation, and vinylation of acyl chlorides by means of organotin compounds in the presence of catalytic amounts of tetrakis(triphenylphosphine)palladium(0), *Chem. Lett.* **1977**, 1423-1424.
30. M. Kosugi, Y. Shimizu, T. Migita, Reaction of allyltin compounds. II. Facile preparation of allyl ketones via allyltins, *J. Organomet. Chem.* **1977**, *129*, 36-38.
31. D. Milstein, J. K. Stille, A general, selective, and facile method for ketone synthesis from acid chlorides and organotin compounds catalyzed by palladium, *J. Am. Chem. Soc.* **1978**, *100*, 3636-3638.
32. D. Milstein, J. K. Stille, Palladium-catalyzed coupling of tetraorganotin compounds with aryl and benzyl halides. Synthetic utility and mechanism, *J. Am. Chem. Soc.* **1979**, *101*, 4992-4998.
33. P. Espinet, A. M. Echavarren, C-C coupling: The mechanisms of the Stille reaction, *Angew. Chem., Int. Ed.* **2004**, *43*, 4704-4734.
34. C. Cordovilla, C. Bartolome, J. M. Martinez-Ilarduya, P. Espinet, The Stille Reaction, 38 Years Later, *ACS Catal.* **2015**, *5*, 3040-3053.
35. V. Farina, G. P. Roth, Recent advances in the Stille reaction, *Adv. Met.-Org. Chem.* **1996**, *5*, 1-53.
36. D. Seyferth, F. G. A. Stone, Vinyl derivatives of the metals. I. Synthesis of vinyltin compounds, *J. Am. Chem. Soc.* **1957**, *79*, 515-517.
37. A. K. Flatt, S. M. Dirk, J. C. Henderson, D. E. Shen, J. Su, M. A. Reed, J. M. Tour, Synthesis and testing of new end-functionalized oligomers for molecular electronics, *Tetrahedron* **2003**, *59*, 8555-8570.
38. W. J. Scott, G. T. Crisp, J. K. Stille, Palladium-catalyzed coupling of vinyl triflates with organostannanes: 4-tert-butyl-1-vinylcyclohexene and 1-(4-tert-butylcyclohexen-1-yl)-2-propen-1-one, *Org. Synth.* **1990**, *68*, 116-129.
39. W. J. Scott, J. K. Stille, Palladium-catalyzed coupling of vinyl triflates with organostannanes. Synthetic and mechanistic studies, *J. Am. Chem. Soc.* **1986**, *108*, 3033-3340.

Chapter 6 – Conclusions and Recommendation for Future Research

6.1 – Conclusions

The benzo[*b*][1,4]dioxepin-3-one analogues displayed in Figure 6.1 are powerful marine fragrances. The marine odorant family remains small and narrowly defined in chemical structure, and is therefore amenable for studies into structure-odour correlations. Kraft *et al.*^[1] revealed that more potent odorants could be synthesised than had been previously hypothesised, and a computational olfactophore model was generated. In a second study it was discovered that potency, and therefore receptor binding strength, was increased when the seven-substituted alkyl groups were replaced with conjugated olefinic substituents.^[2] A revised receptor model was produced which placed the aliphatic hydrophobe in the plane of the aromatic binding site and 7.23 Å from its centre. The modified olfactophore model consisted of two hydrogen-bond acceptors that anchor the molecule into the receptor, aromatic and aliphatic binding sites and six excluded volumes inaccessible to the ligand. The revised model could bind both pseudo-twist-boat and pseudo-half-chair conformers of the heterocyclic ring system.^[2]

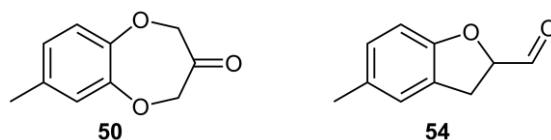


Figure 6.1: Selected benzo[*b*][1,4]dioxepin-3-one analogues.

Researchers at Firmenich recently targeted the role of the carbonyl functionality in marine odorant perception. A qualitative marine-ozone olfactophore model consisting of only one hydrogen-bond acceptor, one aliphatic hydrophobe and one aromatic binding site was proposed.^[3] Both receptor models agreed on the requirement of at least one potent hydrogen-bond acceptor, for which a carbonyl functionality has now been independently confirmed to be optimal in two studies.^[3-4] It was also described that the 5*H*-1,4-dioxepin-6(7*H*)-one moiety of the original molecular template could be replaced by a 2,3-dihydrofuran-2-carbaldehyde unit leading to compound **54**, for which potent marine notes were reported (Figure 6.1).^[3] The five-membered ring system of compound **54** required one ether linkage to sustain marine characteristics, thereby supporting the requirement for a second hydrogen-bond acceptor within the receptor model.

The strongest aromatic benzo[*b*][1,4]dioxepin-3-one odorants feature substitution at the seven-position. Unexpectedly it was discovered that the aliphatic benzo[*b*][1,4]dioxepin-3-one analogues that displayed marine notes were those that were substituted at the six- and nine-positions. The *threo*-configured analogue **204**, which superimposes favourably onto the molecular structure of Calone 1951[®] (**50**), was virtually devoid of marine fragrance (Figure 6.2). This indicated a repulsion of the hydrophobic cyclohexyl ring system from the marine odorant receptor. The *erythro*-configured analogues **225** and **227**, but not their Δ^{8-9} unsaturated counterpart (**219**), were found to contain marine notes. Molecular modelling revealed that the carbocyclic ring system of compound **219** is bent at a shallower angle than that of the saturated compounds (**225** and **227**) and therefore does not avoid the same amount of repulsive interaction. The fact that analogue **206** is devoid of marine fragrance is likely due to a positive hydrophobic interaction at the position adjacent to the ether oxygen atoms (positions six and nine), which was more correctly targeted by (*R*)-configured methyl substitution.

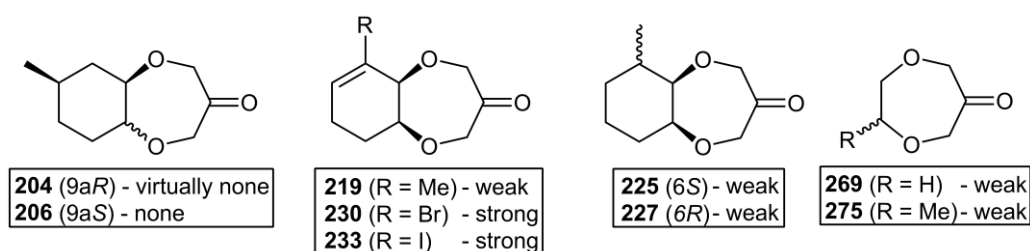


Figure 6.2: Aliphatic benzo[*b*][1,4]dioxepin-3-one and 1,4-dioxepan-6-one analogues.

Description following compound name describes marine odour character.

To offer additional evidence of an aliphatic hydrophobe at this spacial position, two Δ^{8-9} unsaturated analogues bearing halogen substitution were synthesised and evaluated (compounds **230** and **233**, Figure 6.2). Whilst these analogues both contained unsaturation within their carbocyclic ring systems, it was revealed that the larger size and increased polarisability of the halogen substituents was sufficient to resist repulsion from the olfactory receptor. This could presumably be due to increased molecular bonding to the putative hydrophobic binding pocket of the olfactory receptor.

Owing to the postulate that the cyclohexyl ring system was being repelled from the aromatic binding site of the olfactory receptor, a series of 1,4-dioxepan-6-one analogues were synthesised and evaluated (Figure 6.2). The two parent compounds, **269** and **275**, both contained marine notes, albeit weak in comparison to compounds **230** and **233**, possibly due to a lack of effective hydrophobic interaction.

Importantly, all marine odorant receptor models feature an aromatic binding site. Our research into the effects of the dearomatisation of the benzo[*b*][1,4]dioxepin-3-one template has successfully revealed that the models were correct in assuming that the aromatic binding site is not just a molecular spacer, but an essential binding feature. The aromatic binding site of the G protein-coupled receptor may rely on CH- π interactions for ligand binding,^[5-7] albeit with limited insight into G protein-coupled odorant receptors it remains somewhat speculative at this time to further discuss any specific interaction with a hypothetical marine odorant receptor.

6.2 – Recommendation for Future Research

Should the synthesis of aliphatic benzo[*b*][1,4]dioxepin-3-one analogues be further explored, the most obvious route for increasing marine receptor binding strength would be the synthesis of *erythro*-configured analogues containing alkyl substitution at the six-position (type **336**, Figure 6.3). A bulky *tertiary*-butyl group may offer increased binding capabilities, as may ethyl or propyl groups, depending on the size and location of the hydrophobic binding pocket. Synthetic access to a range of such compounds could be via the Suzuki reaction of a halogenated precursor compound, as shown to be viable in Scheme 3.12. Targeted enantioselective synthesis would be required to effectively probe any residual binding to the receptor(s) owing to threshold differences discovered between the stereoisomeric configurations. With regard to the instability, functional group sensitivity and all-round impotency of the aliphatic benzo[*b*][1,4]dioxepin-3-one scaffold it is unlikely that further research would be fruitful.

Other potential aromatic benzo[*b*][1,4]dioxepin-3-one analogues to investigate include the proposed scaffolds **337–340** (Figure 6.3). Scaffold **337** would comprise of sulphur atom substitution at the ether oxygen atoms located within the heterocyclic ring system. As the analysis of previously synthesised analogues clearly indicates that chemical modification at any position of the molecule has a significant effect on odorant characteristics, the decreased electronegativity, larger atom size and reduced ability to hydrogen-bond may render the thionated derivatives interesting analogues to study. An unsuccessful synthesis of an analogue of type **337** was attempted in an S_N2 sulphonation of a *bis*-lithiated benzene intermediate by the addition of elemental sulphur, followed the addition of an alkylating agent.^[8-9] Unsuccessfully attempts were also made at the sulphonation of the carbonyl functionality using Lawesson's reagent, as the resulting thioketone oligomerised.^[9]

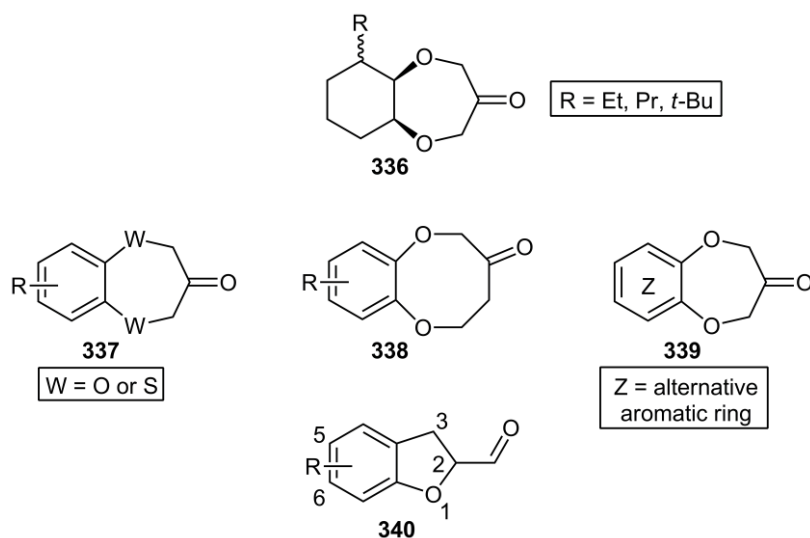


Figure 6.3: Proposed scaffolds for new marine odorants.

An additional class of derivatives for potential exploration are those of type **338**, a ring-expanded analogue of the marine odorant template (Figure 6.3). An analogue of compound **338** that was devoid of the carbonyl osmophore was synthesised and found to contain minor marine nuances.^[4] Potential modifications of the scaffold include the synthesis of vicinal *bis*-carbonyl analogues. It should be noted that six-membered analogues of the benzo[*b*][1,4]dioxepin-3-one template have been previously isolated as synthetic impurities and are reported to be odourless.^[10]

Analogues containing alternative aromatic ring systems to the standard benzenoid system may offer an opportunity to further probe the aromatic binding site of the olfactory receptor, as well as lead to interesting new odorant molecules (type **339**, Figure 6.3). The most obvious choice for an aromatic ring exchange would be with a pyridine heterocycle, as the unusual marine odorant Maritima® (**60**, Figure 1.18) features such a system.

The most viable choice for the synthesis of potent new marine odorants would be compounds related to type **340**, the scaffold recently developed by Gaudin *et al.*^[3] (Figure 6.3). To date, only limited analogues of this scaffold have been synthesised and evaluated. It was reported that methyl substitution at the two-position hindered binding to the marine receptor, hypothesised to be due to interference with the carbonyl osmophore.^[3] Analogues bearing substitution at the three-position may potentially offer additional binding capabilities to the hydrophobic binding pocket that offered the six- and nine-substituted aliphatic benzo[*b*][1,4]dioxepin-3-one analogues (**225**, **227**, **230**, **233**) marine nuances. The synthesis of analogues of type **340** bearing alkenyl substitution at the five- and six-positions may also lead to potent new marine odorants with additional nuances.

6.3 – References

1. P. Kraft, W. Eichenberger, Conception, characterization and correlation of new marine odorants, *Eur. J. Org. Chem.* **2003**, 3735-3743.
2. P. Kraft, K. Popaj, P. Müller, M. Schär, 'Vanilla oceanics': synthesis and olfactory properties of (1'E)-7-(prop-1'-enyl)-2H-benzo[b][1,4]dioxepin-3(4H)-ones and homologues, *Synthesis* **2010**, 3029-3036.
3. J.-M. Gaudin, J.-Y. de Saint Laumer, Structure-Activity Relationships in the Domain of Odorants Having Marine Notes, *Eur. J. Org. Chem.* **2015**, 1437-1447.
4. B. Drevermann, A. R. Lingham, H. M. Hugel, P. J. Marriott, Synthesis and qualitative olfactory evaluation of benzodioxepine analogues, *Helv. Chim. Acta* **2007**, *90*, 854-863.
5. M. Nishio, CH/ π hydrogen bonds in crystals, *CrystEngComm* **2004**, *6*, 130-158.
6. M. Nishio, The CH/ π hydrogen bond in chemistry. Conformation, supramolecules, optical resolution and interactions involving carbohydrates, *Phys. Chem. Chem. Phys.* **2011**, *13*, 13873-13900.
7. M. Nishio, Y. Umezawa, J. Fantini, M. S. Weiss, P. Chakrabarti, CH- π hydrogen bonds in biological macromolecules, *Phys. Chem. Chem. Phys.* **2014**, *16*, 12648-12683.
8. J. Ham, I. Yang, H. Kang, A facile one-pot synthesis of alkyl aryl sulfides from aryl bromides, *J. Org. Chem.* **2004**, *69*, 3236-3239.
9. B. Drevermann, Ph.D Thesis, RMIT University, Melbourne, Australia **2007**.
10. B. Drevermann, A. R. Lingham, H. M. Hugel, P. J. Marriott, Synthesis of benzodioxepinone analogues via a novel synthetic route with qualitative olfactory evaluation, *Helv. Chim. Acta* **2007**, *90*, 1006-1027.

Table of Appendixes

General Experimental Conditions.....	220
Crystal Structure Data for Compounds 167 , 173 and 204	221
NMR Spectra	
¹ H and ¹³ C spectra for compound 49	230
¹ H and ¹³ C spectra for compound 50	231
¹ H and ¹³ C spectra for compound 157	232
¹ H and ¹³ C spectra for compound (±)- 160	233
¹ H and ¹³ C spectra for compound (±)- 161	234
¹ H and ¹³ C spectra for compound (±)- 163	235
¹ H and ¹³ C spectra for compound (±)- 166	236
¹ H and ¹³ C spectra for compound (±)- 167	237
¹ H and ¹³ C spectra for compound 170	238
¹ H and ¹³ C spectra for compound 171	239
¹ H and ¹³ C spectra for compound 173	240
¹ H and ¹³ C spectra for compound (±)- 175	241
¹ H and ¹³ C spectra for compound (±)- 176	242
¹ H and ¹³ C spectra for compound (±)- 179	243
¹ H and ¹³ C spectra for compound (±)- 181	244
¹ H and ¹³ C spectra for compound 182	245
¹ H and ¹³ C spectra for compound (±)- 187	246
¹ H and ¹³ C spectra for compound 188	247
¹ H and ¹³ C spectra for compound 189	248
¹ H and ¹³ C spectra for compound 192	249
¹ H and ¹³ C spectra for compound 193	250
¹ H and ¹³ C spectra for compound 194	251
¹ H and ¹³ C spectra for compound (±)- 195	252
¹ H and ¹³ C spectra for compound 196	253
¹ H and ¹³ C spectra for compound 199	254
¹ H and ¹³ C spectra for compound 201	255
¹ H and ¹³ C spectra for compound 202	256
¹ H and ¹³ C spectra for compound 203	257
¹ H and ¹³ C spectra for compound 204	258
¹ H and ¹³ C spectra for compound 205	259
¹ H and ¹³ C spectra for compound 206	260
¹ H and ¹³ C spectra for compound (±)- 208	261
¹ H and ¹³ C spectra for compound 209	262
¹ H and ¹³ C spectra for compound (±)- 210	263
¹ H and ¹³ C spectra for compound (±)- 211	264
¹ H and ¹³ C spectra for compound 212	265
¹ H and ¹³ C spectra for compound 213	266
¹ H and ¹³ C spectra for compound 218	267
¹ H and ¹³ C spectra for compound 219	268
¹ H and ¹³ C spectra for compound 220	269

¹ H and ¹³ C spectra for compound 221	270
¹ H and ¹³ C spectra for compound 222	271
¹ H and ¹³ C spectra for compound 223	272
¹ H and ¹³ C spectra for compound 224	273
¹ H and ¹³ C spectra for compound 225	274
¹ H and ¹³ C spectra for compound 226	275
¹ H and ¹³ C spectra for compound 227	276
¹ H and ¹³ C spectra for compound 229	277
¹ H and ¹³ C spectra for compound 230	278
¹ H and ¹³ C spectra for compound 232	279
¹ H and ¹³ C spectra for compound 233	280
¹ H and ¹³ C spectra for compound 236	281
¹ H and ¹³ C spectra for compound 238	282
¹ H and ¹³ C spectra for compound 239	283
¹ H and ¹³ C spectra for compound 240	284
¹ H and ¹³ C spectra for compound 241	285
¹ H and ¹³ C spectra for compound 246	286
¹ H and ¹³ C spectra for compound 247	287
¹ H and ¹³ C spectra for compound 248	288
¹ H and ¹³ C spectra for compound 268	289
¹ H and ¹³ C spectra for compound 269	290
¹ H and ¹³ C spectra for compound 270	291
¹ H and ¹³ C spectra for compound (±)- 271	292
¹ H and ¹³ C spectra for compound (±)- 272	293
¹ H and ¹³ C spectra for compound (±)- 273	294
¹ H and ¹³ C spectra for compound 274	295
¹ H and ¹³ C spectra for compound (±)- 275	296
¹ H and ¹³ C spectra for compound (±)- 276	297
¹ H and ¹³ C spectra for compound (±)- 277	298
¹ H and ¹³ C spectra for compound 278	299
¹ H and ¹³ C spectra for compound (±)- 280	300
¹ H and ¹³ C spectra for compound 281	301
¹ H and ¹³ C spectra for compound 282	302
¹ H and ¹³ C spectra for compound 283	303
¹ H and ¹³ C spectra for compound 288	304
¹ H and ¹³ C spectra for compound 289	305
¹ H and ¹³ C spectra for compound 291	306
¹ H and ¹³ C spectra for compound 292	307
¹ H and ¹³ C spectra for compound 293	308
¹ H and ¹³ C spectra for compound 295	309
¹ H and ¹³ C spectra for compound 297	310
¹ H and ¹³ C spectra for compound 302	311
¹ H and ¹³ C spectra for compound 303	312
¹ H and ¹³ C spectra for compound 304	313
¹ H and ¹³ C spectra for compound 306	314

¹ H and ¹³ C spectra for compound 307	315
¹ H and ¹³ C spectra for compound 308	316
¹ H and ¹³ C spectra for compound 310	317
¹ H and ¹³ C spectra for compound 322	318
¹ H and ¹³ C spectra for compound 323	319
¹ H and ¹³ C spectra for compound 324	320
¹ H and ¹³ C spectra for compound 329	321
¹ H and ¹³ C spectra for compound (±)- 330	322
¹ H and ¹³ C spectra for compound 332	323
¹ H and ¹³ C spectra for compound 333	324

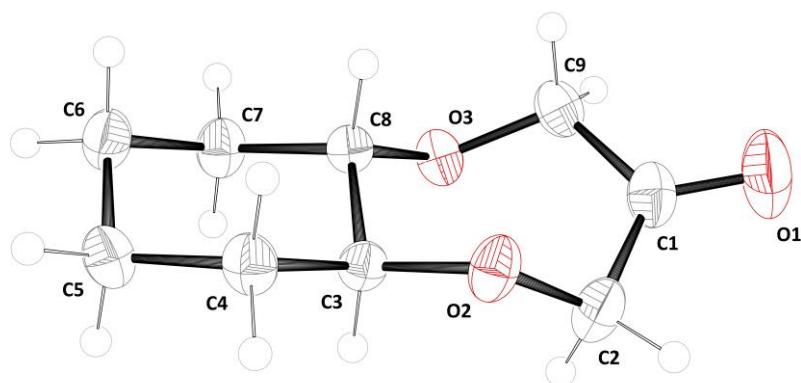
General Experimental Conditions

Unless otherwise noted, all materials obtained from commercial suppliers were used as received. All reactions were carried out under an atmosphere of nitrogen unless otherwise noted. Dichloromethane (DCM) was dried and distilled from CaH₂; tetrahydrofuran (THF) was dried and distilled from sodium/benzophenone ketyl. *N,N*-dimethylformamide (DMF) was dried and distilled under reduced pressure from CaH₂. Thin layer chromatography was carried out on aluminium-backed SiO₂ gel TLC plates (60 F₂₅₄), which were visualised with either KMnO₄ dip (KMnO₄, K₂CO₃, NaOH, H₂O) or iodine stain. Flash column chromatography was carried out with Davisil LC35a SiO₂ (40–63 μm). Silica was deactivated by flushing with a triethylamine solution (5% v/v) prior to flash chromatography. NMR spectra were obtained with a Bruker Avance III 300 MHz spectrometer or Agilent DD2 500 MHz spectrometer, and the residual solvent peaks from the deuterated solvents (CDCl₃: ¹H δ = 7.27 ppm, ¹³C δ = 77.0 ppm; *d*₆-DMSO: ¹H δ = 2.5 ppm, ¹³C δ = 128 ppm) were used as a reference. EI-HRMS spectra were recorded with a Waters GCT Premier (HR-TOFMS) instrument equipped with an Agilent 7890 GC. CI-HRMS spectra were recorded with a Bruker autoflex speed (MALDI-TOF) instrument or AB Sciex Qstar Elite (QTOF). FT-IR spectra were obtained with a Perkin–Elmer Spectrum 100 spectrometer. Melting points were recorded with a Stuart SMP10 melting-point apparatus.

Crystals suitable for single-crystal X-ray diffraction were obtained by recrystallisation from methanol (compound **167**) or from EtOAc/hexane (compound **173** and **204**). Using a drop of Nujol (inert oil), crystals were mounted onto a nylon loop, and then they were transferred into a stream of cold nitrogen. For the mounting of compound **173**, the crystals had been previously cooled with nitrogen to prevent their melting. The reflections were collected with a D8 Bruker diffractometer (compounds **167** and **173**) equipped with an APEX-II area detector and a 1 μS microsource; or with a STOE IPDS-2(T) diffractometer (compound **204**) equipped with an image plate detector and a fine-focus sealed tube source. In all three cases, a graphite-monochromator and Mo-*K*_α radiation (λ = 0.71073 Å) were used. For compounds **167** and **173**, data collection was carried out in φ- and ω-scan modes using SMART software, SAINT was used to process the data, and the absorption corrections were done with SADABS. For compound **204**, data collection was carried out in ω-scan mode, and the data was processed with X-Area. The structures were solved with direct methods, and were refined with full-matrix least-squares methods on *F*² using the SHELX-TL package. Thermal ellipsoid plots were created with ORTEP-3 v2.02.

Olfactory evaluations were performed by expert perfumers on blotter using a 10% solution of the sample substance in dipropylene glycol (DPG). The odour thresholds were determined by GC-Olfactometry: Different dilutions of the sample substance were injected into a gas chromatograph in descending order of concentration until the panellist failed to detect the respective substance at the sniffing port. The panellist smelled in blind and pressed a button on perceiving an odour. If the recorded time matched the retention time, the sample was further diluted. The last concentration detected at the correct retention time was the individual odour threshold. The reported threshold values are the geometrical mean values of the individual odour thresholds of the different panellists.

Crystal Structure Data for Compounds 167, 173 and 204



Crystals from methanol.

Table 1. Crystal data and structure refinement for compound **167**.

Empirical formula	$C_9H_{14}O_3$	
Formula weight	170.20	
Temperature	200(2) K	
Wavelength	0.71073 Å	
Crystal system	Monoclinic	
Space group	P 21/n	
Unit cell dimensions	$a = 6.7129(11)$ Å	$a = 90^\circ$
	$b = 17.188(3)$ Å	$b = 113.725(3)^\circ$
	$c = 8.1744(12)$ Å	$g = 90^\circ$
Volume	$863.5(2)$ Å ³	
Z	4	
Density (calculated)	1.309 Mg/m ³	
Absorption coefficient	0.097 mm ⁻¹	
F(000)	368	
Crystal size	0.149 x 0.143 x 0.101 mm ³	
Theta range for data collection	2.370 to 35.081°	
Index ranges	$-10 \leq h \leq 10$, $-27 \leq k \leq 27$, $-13 \leq l \leq 13$	
Reflections collected	27340	
Independent reflections	3805 [R(int) = 0.0450]	
Completeness to theta = 35.081°	99.4 %	
Absorption correction	Semi-empirical from equivalents	
Max. and min. transmission	0.7469 and 0.6698	
Refinement method	Full-matrix least-squares on F ²	
Data / restraints / parameters	3805 / 0 / 109	
Goodness-of-fit on F ²	1.068	
Final R indices [$I > 2\sigma(I)$]	R1 = 0.0416, wR2 = 0.1219	
R indices (all data)	R1 = 0.0546, wR2 = 0.1290	
Largest diff. peak and hole	0.281 and -0.264 e.Å ⁻³	

Table 2. Atomic coordinates ($\times 10^4$) and equivalent isotropic displacement parameters ($\text{\AA}^2 \times 10^3$) for **167**. $U(\text{eq})$ is defined as one third of the trace of the orthogonalized U^{ij} tensor.

	x	y	z	$U(\text{eq})$
O(1)	11294(2)	3707(1)	6331(2)	64(1)
O(2)	11682(1)	1744(1)	6803(1)	33(1)
O(3)	7283(1)	2288(1)	5976(1)	29(1)
C(1)	10447(2)	3076(1)	6179(1)	36(1)
C(2)	11329(2)	2372(1)	5586(1)	39(1)
C(3)	9870(1)	1235(1)	6433(1)	25(1)
C(4)	10741(1)	484(1)	7454(1)	31(1)
C(5)	8904(1)	-89(1)	7186(1)	34(1)
C(6)	7166(1)	275(1)	7691(1)	35(1)
C(7)	6321(1)	1030(1)	6663(1)	32(1)
C(8)	8173(1)	1595(1)	6983(1)	24(1)
C(9)	8513(1)	2970(1)	6653(1)	33(1)

Table 3. Bond lengths [\AA] and angles [$^\circ$] for **167**.

O(1)-C(1)	1.2080(11)	C(3)-C(8)	1.5152(10)
O(2)-C(2)	1.4207(11)	C(3)-C(4)	1.5189(10)
O(2)-C(3)	1.4294(9)	C(4)-C(5)	1.5242(12)
O(3)-C(9)	1.4125(10)	C(5)-C(6)	1.5202(13)
O(3)-C(8)	1.4348(8)	C(6)-C(7)	1.5265(12)
C(1)-C(9)	1.5081(13)	C(7)-C(8)	1.5148(11)
C(1)-C(2)	1.5102(14)		
C(2)-O(2)-C(3)	115.42(6)	C(3)-C(4)-C(5)	111.11(6)
C(9)-O(3)-C(8)	114.91(6)	C(6)-C(5)-C(4)	111.06(7)
O(1)-C(1)-C(9)	119.96(9)	C(5)-C(6)-C(7)	110.88(7)
O(1)-C(1)-C(2)	121.58(10)	C(8)-C(7)-C(6)	110.67(6)
C(9)-C(1)-C(2)	118.41(7)	O(3)-C(8)-C(7)	108.07(6)
O(2)-C(2)-C(1)	111.11(8)	O(3)-C(8)-C(3)	111.03(6)
O(2)-C(3)-C(8)	111.36(6)	C(7)-C(8)-C(3)	110.42(6)
O(2)-C(3)-C(4)	107.29(6)	O(3)-C(9)-C(1)	115.25(7)
C(8)-C(3)-C(4)	110.72(6)		

Table 4. Anisotropic displacement parameters ($\text{\AA}^2 \times 10^3$) for **167**. The anisotropic displacement factor exponent takes the form: $-2p^2[h^2a^*2U^{11} + \dots + 2hk a^* b^* U^{12}]$

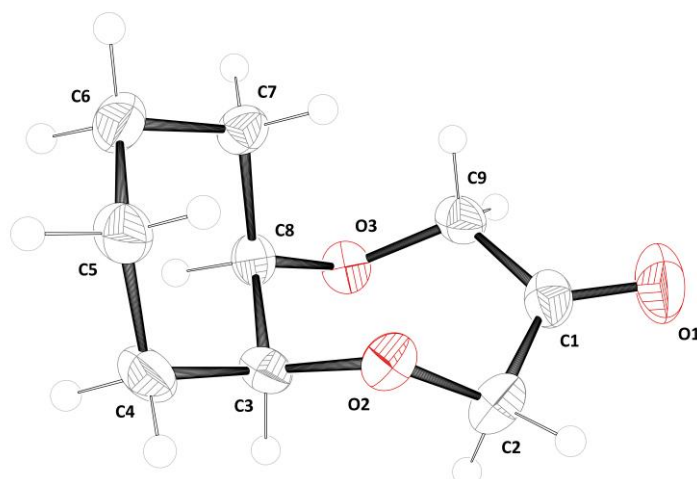
	U ¹¹	U ²²	U ³³	U ²³	U ¹³	U ¹²
O(1)	61(1)	36(1)	98(1)	-1(1)	35(1)	-16(1)
O(2)	23(1)	33(1)	44(1)	8(1)	15(1)	2(1)
O(3)	23(1)	24(1)	34(1)	3(1)	5(1)	3(1)
C(1)	33(1)	31(1)	39(1)	6(1)	9(1)	-3(1)
C(2)	38(1)	37(1)	47(1)	10(1)	24(1)	-1(1)
C(3)	23(1)	26(1)	29(1)	1(1)	11(1)	2(1)
C(4)	27(1)	26(1)	39(1)	3(1)	13(1)	5(1)
C(5)	36(1)	25(1)	41(1)	0(1)	14(1)	1(1)
C(6)	34(1)	30(1)	43(1)	4(1)	19(1)	-2(1)
C(7)	22(1)	32(1)	44(1)	3(1)	14(1)	0(1)
C(8)	20(1)	24(1)	26(1)	1(1)	8(1)	3(1)
C(9)	33(1)	24(1)	38(1)	0(1)	10(1)	2(1)

Table 5. Hydrogen coordinates ($\times 10^4$) and isotropic displacement parameters ($\text{\AA}^2 \times 10^3$) for **167**.

	x	y	z	U(eq)
H(2A)	10286	2209	4384	46
H(2B)	12718	2509	5504	46
H(3)	9195	1119	5124	30
H(4A)	11515	602	8742	37
H(4B)	11795	246	7036	37
H(5A)	8243	-255	5920	41
H(5B)	9502	-557	7931	41
H(6A)	7783	383	8990	41
H(6B)	5945	-95	7423	41
H(7A)	5585	916	5370	39
H(7B)	5242	1269	7052	39
H(8)	8862	1729	8283	28
H(9A)	9035	2967	7972	39
H(9B)	7541	3426	6204	39

Table 6. Torsion angles [$^\circ$] for **167**.

C(3)-O(2)-C(2)-C(1)	89.58(9)	C(9)-O(3)-C(8)-C(3)	-84.17(8)
O(1)-C(1)-C(2)-O(2)	127.32(10)	C(6)-C(7)-C(8)-O(3)	179.58(6)
C(9)-C(1)-C(2)-O(2)	-50.29(11)	C(6)-C(7)-C(8)-C(3)	57.96(9)
C(2)-O(2)-C(3)-C(8)	-76.75(8)	O(2)-C(3)-C(8)-O(3)	62.91(7)
C(2)-O(2)-C(3)-C(4)	161.94(7)	C(4)-C(3)-C(8)-O(3)	-177.80(6)
O(2)-C(3)-C(4)-C(5)	178.23(6)	O(2)-C(3)-C(8)-C(7)	-177.24(6)
C(8)-C(3)-C(4)-C(5)	56.52(9)	C(4)-C(3)-C(8)-C(7)	-57.95(8)
C(3)-C(4)-C(5)-C(6)	-55.13(10)	C(8)-O(3)-C(9)-C(1)	80.51(9)
C(4)-C(5)-C(6)-C(7)	55.04(10)	O(1)-C(1)-C(9)-O(3)	163.07(9)
C(5)-C(6)-C(7)-C(8)	-56.62(10)	C(2)-C(1)-C(9)-O(3)	-19.28(11)
C(9)-O(3)-C(8)-C(7)	154.59(7)		



Crystals from ethyl acetate/hexane.

Table 1. Crystal data and structure refinement for compound **173**.

Empirical formula	$C_9H_{14}O_3$	
Formula weight	170.20	
Temperature	200(2) K	
Wavelength	0.71073 Å	
Crystal system	Monoclinic	
Space group	C 2/c	
Unit cell dimensions	$a = 21.883(3)$ Å	$a = 90^\circ$
	$b = 9.2836(12)$ Å	$b = 104.695(11)^\circ$
	$c = 8.7905(14)$ Å	$c = 90^\circ$
Volume	$1727.4(4)$ Å ³	
Z	8	
Density (calculated)	1.309 Mg/m ³	
Absorption coefficient	0.097 mm ⁻¹	
F(000)	736	
Crystal size	0.215 x 0.154 x 0.117 mm ³	
Theta range for data collection	1.924 to 32.549°	
Index ranges	$-32 \leq h \leq 32$, $-14 \leq k \leq 14$, $-13 \leq l \leq 13$	
Reflections collected	19527	
Independent reflections	3110 [R(int) = 0.0309]	
Completeness to theta = 35.549°	99.0 %	
Absorption correction	Semi-empirical from equivalents	
Max. and min. transmission	0.7464 and 0.6631	
Refinement method	Full-matrix least-squares on F ²	
Data / restraints / parameters	3110 / 0 / 110	
Goodness-of-fit on F ²	1.078	
Final R indices [$I > 2\sigma(I)$]	R1 = 0.0422, wR2 = 0.1241	
R indices (all data)	R1 = 0.0502, wR2 = 0.1282	
Extinction coefficient	0.0044(10)	
Largest diff. peak and hole	0.348 and -0.219 e.Å ⁻³	

Appendix

Table 2. Atomic coordinates ($\times 10^4$) and equivalent isotropic displacement parameters ($\text{\AA}^2 \times 10^3$) for **173**. $U(\text{eq})$ is defined as one third of the trace of the orthogonalized U^{ij} tensor.

	x	y	z	$U(\text{eq})$
O(1)	1388(1)	2429(1)	483(1)	60(1)
O(2)	672(1)	5776(1)	-119(1)	30(1)
O(3)	1940(1)	5775(1)	-633(1)	31(1)
C(1)	1366(1)	3676(1)	65(1)	34(1)
C(2)	742(1)	4383(1)	-729(1)	36(1)
C(3)	919(1)	6934(1)	-872(1)	28(1)
C(4)	596(1)	8317(1)	-565(1)	36(1)
C(5)	789(1)	8782(1)	1161(1)	35(1)
C(6)	1507(1)	8871(1)	1759(1)	37(1)
C(7)	1814(1)	7438(1)	1508(1)	29(1)
C(8)	1634(1)	7046(1)	-235(1)	27(1)
C(9)	1970(1)	4547(1)	338(1)	32(1)

Table 3. Bond lengths [\AA] and angles [$^\circ$] for **173**.

O(1)-C(1)	1.2119(13)	C(3)-C(4)	1.5236(13)
O(2)-C(2)	1.4230(12)	C(3)-C(8)	1.5259(13)
O(2)-C(3)	1.4376(12)	C(4)-C(5)	1.5297(15)
O(3)-C(9)	1.4159(12)	C(5)-C(6)	1.5283(15)
O(3)-C(8)	1.4431(11)	C(6)-C(7)	1.5314(13)
C(1)-C(2)	1.5155(15)	C(7)-C(8)	1.5257(13)
C(1)-C(9)	1.5156(15)		
C(2)-O(2)-C(3)	114.67(7)	C(3)-C(4)-C(5)	112.91(8)
C(9)-O(3)-C(8)	117.75(7)	C(6)-C(5)-C(4)	110.97(9)
O(1)-C(1)-C(2)	121.06(11)	C(5)-C(6)-C(7)	110.73(8)
O(1)-C(1)-C(9)	119.68(11)	C(8)-C(7)-C(6)	109.93(8)
C(2)-C(1)-C(9)	119.26(8)	O(3)-C(8)-C(7)	114.90(7)
O(2)-C(2)-C(1)	112.97(8)	O(3)-C(8)-C(3)	110.52(7)
O(2)-C(3)-C(4)	107.64(8)	C(7)-C(8)-C(3)	111.33(7)
O(2)-C(3)-C(8)	110.65(7)	O(3)-C(9)-C(1)	115.43(8)
C(4)-C(3)-C(8)	110.93(8)		

Table 4. Anisotropic displacement parameters ($\text{\AA}^2 \times 10^3$) for **173**. The anisotropic displacement factor exponent takes the form: $-2p^2[h^2a^*2U^{11} + \dots + 2hk a^* b^* U^{12}]$

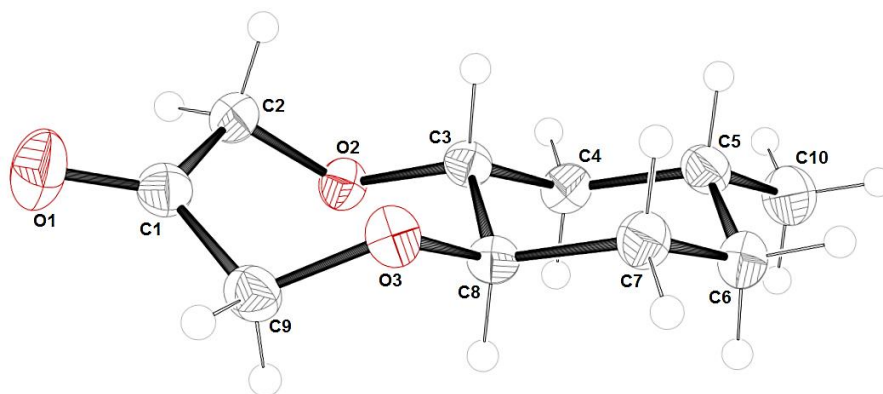
	U ¹¹	U ²²	U ³³	U ²³	U ¹³	U ¹²
O(1)	83(1)	30(1)	70(1)	10(1)	24(1)	0(1)
O(2)	26(1)	31(1)	36(1)	-5(1)	12(1)	-2(1)
O(3)	30(1)	32(1)	34(1)	0(1)	15(1)	3(1)
C(1)	46(1)	27(1)	32(1)	-1(1)	16(1)	1(1)
C(2)	31(1)	33(1)	47(1)	-11(1)	14(1)	-6(1)
C(3)	29(1)	32(1)	23(1)	2(1)	5(1)	5(1)
C(4)	40(1)	35(1)	30(1)	5(1)	3(1)	14(1)
C(5)	38(1)	32(1)	35(1)	-2(1)	7(1)	11(1)
C(6)	39(1)	27(1)	41(1)	-7(1)	7(1)	-1(1)
C(7)	24(1)	29(1)	32(1)	-3(1)	5(1)	-1(1)
C(8)	28(1)	26(1)	30(1)	3(1)	12(1)	0(1)
C(9)	33(1)	31(1)	32(1)	0(1)	6(1)	9(1)

Table 5. Hydrogen coordinates ($\times 10^4$) and isotropic displacement parameters ($\text{\AA}^2 \times 10^3$) for **173**.

	x	y	z	U(eq)
H(9A)	709	4464	-1870	44
H(9B)	392	3760	-596	44
H(8)	817	6752	-2030	34
H(7A)	132	8175	-885	43
H(7B)	701	9098	-1222	43
H(6A)	602	9735	1272	42
H(6B)	623	8081	1805	42
H(5A)	1622	9112	2893	44
H(5B)	1669	9647	1193	44
H(4A)	2279	7519	1886	35
H(4B)	1671	6670	2119	35
H(3)	1774	7868	-801	32
H(2A)	2089	4864	1450	39
H(2B)	2310	3909	177	39

Table 6. Torsion angles [$^\circ$] for **173**.

C(3)-O(2)-C(2)-C(1)	88.19(10)	C(9)-O(3)-C(8)-C(3)	-82.28(9)
O(1)-C(1)-C(2)-O(2)	134.45(11)	C(6)-C(7)-C(8)-O(3)	174.96(7)
C(9)-C(1)-C(2)-O(2)	-45.54(13)	C(6)-C(7)-C(8)-C(3)	-58.45(10)
C(2)-O(2)-C(3)-C(4)	158.47(8)	O(2)-C(3)-C(8)-O(3)	64.84(9)
C(2)-O(2)-C(3)-C(8)	-80.18(9)	C(4)-C(3)-C(8)-O(3)	-175.76(7)
O(2)-C(3)-C(4)-C(5)	68.52(11)	O(2)-C(3)-C(8)-C(7)	-64.11(9)
C(8)-C(3)-C(4)-C(5)	-52.66(12)	C(4)-C(3)-C(8)-C(7)	55.29(10)
C(3)-C(4)-C(5)-C(6)	53.05(12)	C(8)-O(3)-C(9)-C(1)	78.15(10)
C(4)-C(5)-C(6)-C(7)	-55.58(12)	O(1)-C(1)-C(9)-O(3)	158.82(10)
C(5)-C(6)-C(7)-C(8)	58.48(11)	C(2)-C(1)-C(9)-O(3)	-21.19(13)
C(9)-O(3)-C(8)-C(7)	44.72(11)		



Crystals from ethyl acetate/hexane.

The crystal is a twin (Twin law for transforming hkl(1) to hkl(2): -0.52870 0.00011 -0.76224 0.00195 -0.99917 -0.00088 -0.94190 -0.00454 0.53014).

Table 1. Crystal data and structure refinement for compound **204**.

Empirical formula	$C_{10}H_{16}O_3$	
Formula weight	184.23	
Temperature	150(2) K	
Wavelength	0.71073 Å	
Crystal system	Monoclinic	
Space group	P 21	
Unit cell dimensions	$a = 8.1940(8)$ Å	$a = 90^\circ$
	$b = 6.1852(4)$ Å	$b = 96.136(9)^\circ$
	$c = 9.7655(11)$ Å	$g = 90^\circ$
Volume	$492.10(8)$ Å ³	
Z	2	
Density (calculated)	1.243 Mg/m ³	
Absorption coefficient	0.090 mm ⁻¹	
F(000)	200	
Crystal size	0.600 x 0.150 x 0.080 mm ³	
Theta range for data collection	2.500 to 27.997°	
Index ranges	$-10 \leq h \leq 10$, $-8 \leq k \leq 8$, $-12 \leq l \leq 12$	
Reflections collected	8618	
Independent reflections	8618	
Completeness to theta = 27.997°	99.9 %	
Absorption correction	None	
Refinement method	Full-matrix least-squares on F ²	
Data / restraints / parameters	8618 / 1 / 120	
Goodness-of-fit on F ²	1.123	
Final R indices [$I > 2\sigma(I)$]	$R1 = 0.0482$, $wR2 = 0.1245$	
R indices (all data)	$R1 = 0.0596$, $wR2 = 0.1307$	
Absolute structure parameter	0.3(8)	
Largest diff. peak and hole	0.184 and -0.194 e.Å ⁻³	

Table 2. Atomic coordinates ($\times 10^4$) and equivalent isotropic displacement parameters ($\text{\AA}^2 \times 10^3$) for **204**. $U(\text{eq})$ is defined as one third of the trace of the orthogonalized U^{ij} tensor.

	x	y	z	U(eq)
O(1)	7830(4)	10705(6)	2221(3)	47(1)
O(2)	6468(3)	7342(4)	4818(2)	27(1)
O(3)	8748(3)	10819(4)	5767(2)	28(1)
C(1)	7661(4)	10097(6)	3377(4)	29(1)
C(2)	7313(5)	7729(6)	3645(3)	29(1)
C(3)	7492(4)	7290(6)	6109(3)	24(1)
C(4)	6617(4)	5984(6)	7129(3)	29(1)
C(5)	7617(4)	5828(6)	8541(4)	30(1)
C(6)	8030(5)	8096(6)	9093(4)	33(1)
C(7)	8881(4)	9447(6)	8066(3)	30(1)
C(8)	7854(4)	9562(5)	6673(3)	24(1)
C(9)	7788(5)	11657(6)	4580(4)	30(1)
C(10)	6686(5)	4523(8)	9540(4)	41(1)

Table 3. Bond lengths [\AA] and angles [$^\circ$] for **204**.

O(1)-C(1)	1.212(4)	C(3)-C(4)	1.520(4)
O(2)-C(2)	1.421(4)	C(3)-C(8)	1.526(5)
O(2)-C(3)	1.438(4)	C(4)-C(5)	1.530(5)
O(3)-C(9)	1.426(4)	C(5)-C(6)	1.527(6)
O(3)-C(8)	1.437(4)	C(5)-C(10)	1.531(5)
C(1)-C(9)	1.516(5)	C(6)-C(7)	1.529(5)
C(1)-C(2)	1.520(5)	C(7)-C(8)	1.523(4)
C(2)-O(2)-C(3)	114.9(2)	C(6)-C(5)-C(4)	109.7(3)
C(9)-O(3)-C(8)	115.1(3)	C(6)-C(5)-C(10)	111.5(3)
O(1)-C(1)-C(9)	121.3(4)	C(4)-C(5)-C(10)	110.6(3)
O(1)-C(1)-C(2)	120.1(3)	C(5)-C(6)-C(7)	111.7(3)
C(9)-C(1)-C(2)	118.6(3)	C(8)-C(7)-C(6)	111.3(3)
O(2)-C(2)-C(1)	114.7(3)	O(3)-C(8)-C(7)	107.8(3)
O(2)-C(3)-C(4)	108.3(3)	O(3)-C(8)-C(3)	111.6(3)
O(2)-C(3)-C(8)	111.6(3)	C(7)-C(8)-C(3)	110.3(3)
C(4)-C(3)-C(8)	109.9(3)	O(3)-C(9)-C(1)	112.6(3)
C(3)-C(4)-C(5)	112.3(3)		

Symmetry transformations used to generate equivalent atoms:

Appendix

Table 4. Anisotropic displacement parameters ($\text{\AA}^2 \times 10^3$) for **204**. The anisotropic displacement factor exponent takes the form: $-2p^2 [h^2 a^* 2U^{11} + \dots + 2hka^* b^* U^{12}]$

	U ¹¹	U ²²	U ³³	U ²³	U ¹³	U ¹²
O(1)	64(2)	47(2)	31(1)	5(1)	12(1)	-10(2)
O(2)	26(1)	30(1)	25(1)	-1(1)	1(1)	-4(1)
O(3)	26(1)	28(1)	30(1)	3(1)	1(1)	-5(1)
C(1)	23(2)	34(2)	31(2)	2(2)	3(1)	1(1)
C(2)	34(2)	30(2)	25(2)	-3(1)	4(1)	2(2)
C(3)	21(1)	25(2)	26(2)	0(1)	1(1)	0(1)
C(4)	31(2)	25(2)	30(2)	-2(1)	5(1)	-4(2)
C(5)	31(2)	29(2)	31(2)	5(2)	3(1)	5(2)
C(6)	37(2)	36(2)	25(2)	-1(2)	1(1)	2(2)
C(7)	30(2)	30(2)	28(2)	-4(2)	-1(1)	-2(2)
C(8)	22(1)	23(2)	27(2)	0(1)	4(1)	-1(1)
C(9)	33(2)	24(2)	33(2)	3(1)	4(1)	1(1)
C(10)	49(2)	39(2)	36(2)	9(2)	8(2)	2(2)

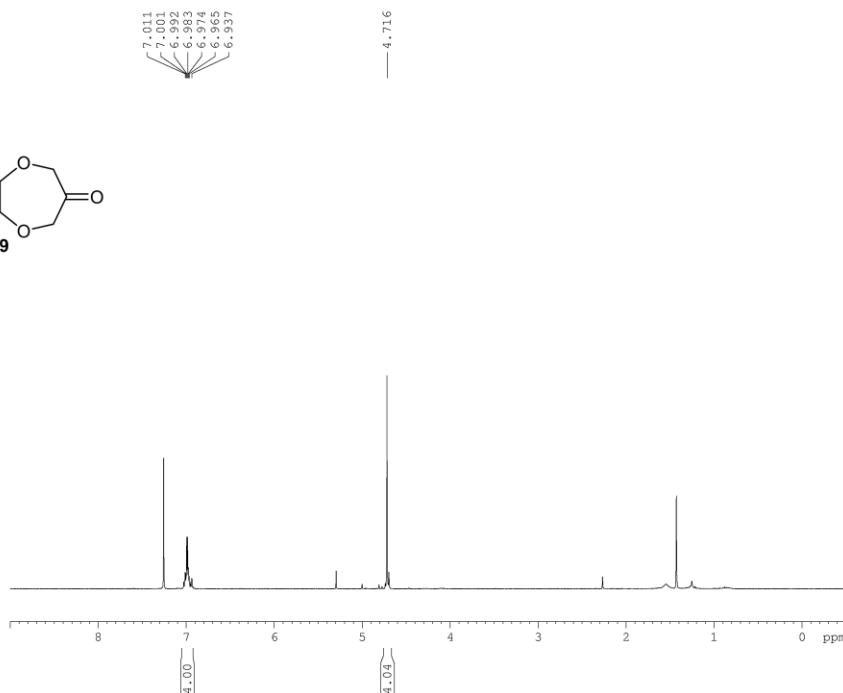
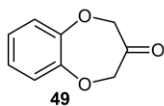
Table 5. Hydrogen coordinates ($\times 10^4$) and isotropic displacement parameters ($\text{\AA}^2 \times 10^3$) for **204**.

	x	y	z	U(eq)
H(2A)	6653	7128	2824	35
H(2B)	8368	6938	3762	35
H(3)	8552	6561	5971	29
H(4A)	6403	4509	6759	34
H(4B)	5545	6667	7236	34
H(5)	8669	5061	8427	36
H(6A)	8755	7984	9968	40
H(6B)	7007	8832	9288	40
H(7A)	9069	10928	8435	36
H(7B)	9962	8800	7949	36
H(8)	6793	10305	6786	29
H(9A)	8286	13025	4301	36
H(9B)	6672	11990	4820	36
H(10A)	5647	5246	9659	62
H(10B)	7353	4418	10432	62
H(10C)	6464	3069	9167	62

Table 6. Torsion angles [$^\circ$] for **204**.

C(3)-O(2)-C(2)-C(1)	-82.6(4)	C(9)-O(3)-C(8)-C(7)	-161.3(3)
O(1)-C(1)-C(2)-O(2)	-154.2(3)	C(9)-O(3)-C(8)-C(3)	77.4(3)
C(9)-C(1)-C(2)-O(2)	25.7(5)	C(6)-C(7)-C(8)-O(3)	-179.0(3)
C(2)-O(2)-C(3)-C(4)	-156.6(3)	C(6)-C(7)-C(8)-C(3)	-56.9(4)
C(2)-O(2)-C(3)-C(8)	82.4(3)	O(2)-C(3)-C(8)-O(3)	-62.5(3)
O(2)-C(3)-C(4)-C(5)	179.8(3)	C(4)-C(3)-C(8)-O(3)	177.4(3)
C(8)-C(3)-C(4)-C(5)	-58.1(4)	O(2)-C(3)-C(8)-C(7)	177.7(3)
C(3)-C(4)-C(5)-C(6)	56.1(4)	C(4)-C(3)-C(8)-C(7)	57.5(3)
C(3)-C(4)-C(5)-C(10)	179.4(3)	C(8)-O(3)-C(9)-C(1)	-88.1(4)
C(4)-C(5)-C(6)-C(7)	-54.2(4)	O(1)-C(1)-C(9)-O(3)	-135.4(4)
C(10)-C(5)-C(6)-C(7)	-177.0(3)	C(2)-C(1)-C(9)-O(3)	44.6(4)
C(5)-C(6)-C(7)-C(8)	55.7(4)		

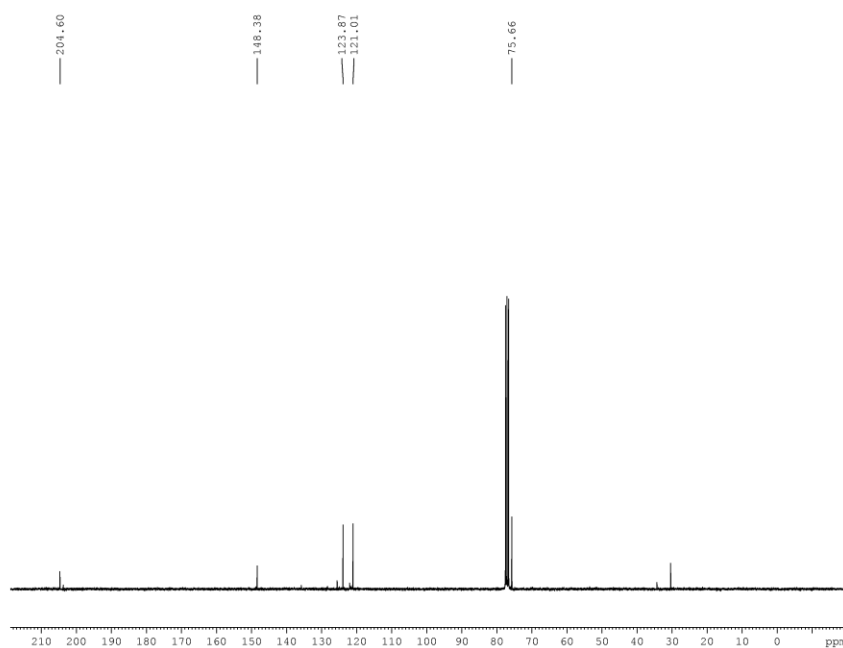
Symmetry transformations used to generate equivalent atoms:



```

EXPNO 1
PROCNO 1
Date_ 20150227
Time 15.51
INSTRUM spect
PROBHD 5 mm PABBO BB-
PULPROG zg30
TD 65536
SOLVENT CDCl3
NS 16
DS 2
SWH 6188.119 Hz
FIDRES 0.094423 Hz
AQ 5.2953587 sec
RG 203
DM 80.800 usec
DE 6.50 usec
TE 298.0 K
D1 1.0000000 sec
TDO 1

===== CHANNEL f1 =====
NUC1 1H
P1 13.70 usec
PL1 1.90 dB
PL1W 8.36853981 W
SF01 300.1418535 MHz
SI 32768
SF 300.1400076 MHz
WDW EM
SSB 0
LB 0.30 Hz
GB 0
PC 1.00
    
```

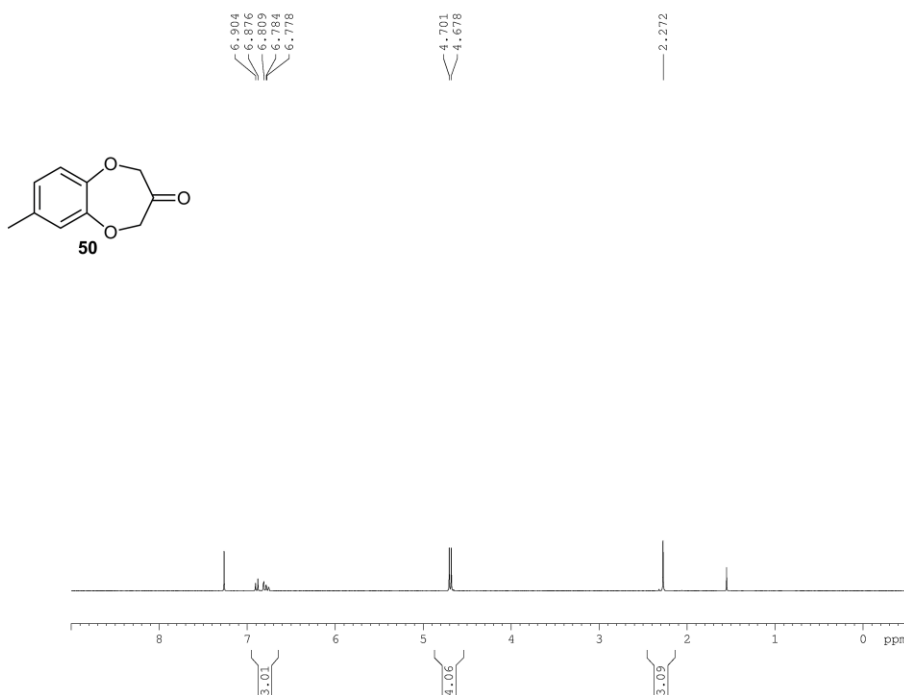


```

EXPNO 1
PROCNO 1
Date_ 20150227
Time 15.03
INSTRUM spect
PROBHD 5 mm PABBO BB-
PULPROG zgpg30
TD 65536
SOLVENT CDCl3
NS 1650
DS 4
SWH 18028.846 Hz
FIDRES 0.275098 Hz
AQ 1.8175818 sec
RG 203
DM 27.733 usec
DE 6.50 usec
TE 298.0 K
D1 2.0000000 sec
D11 0.0300000 sec
TDO 1

===== CHANNEL f1 =====
NUC1 13C
P1 10.82 usec
PL1 0.00 dB
PL1W 30.14263725 W
SF01 75.4778101 MHz

===== CHANNEL f2 =====
CPDPRG2 waltz16
NUC2 1H
PCPD2 100.00 usec
PL2 1.90 dB
PL12 19.17 dB
PL13 23.94 dB
PL2W 8.36853981 W
PL12W 0.15690966 W
PL13W 0.05231782 W
SF02 300.1412006 MHz
SI 32768
SF 75.4702648 MHz
WDW EM
SSB 0
LB 1.00 Hz
GB 0
PC 1.40
    
```

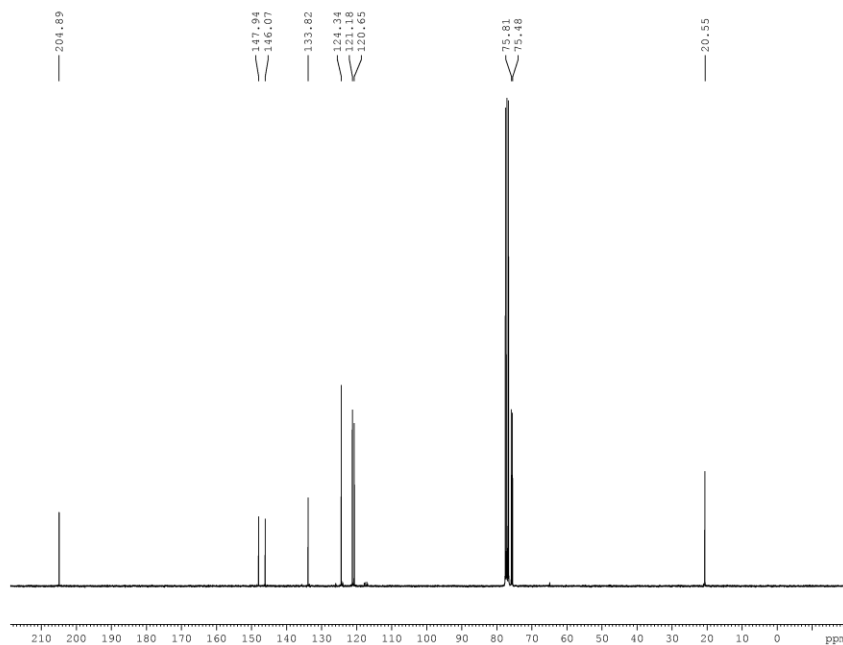


```

EXPNO          4
PROCNO         1
Date_          20140515
Time          13.51
INSTRUM        spect
PROBHD         5 mm PABBO BB-
PULPROG        zg30
TD             65536
SOLVENT        CDC13
NS             16
DS             2
SWH            6188.119 Hz
FIDRES         0.094423 Hz
AQ            5.2953587 sec
RG            203
DW            80.800 usec
DE            6.50 usec
TE            673.2 K
D1            1.0000000 sec
TD0           1
    
```

```

===== CHANNEL f1 =====
NUC1           1H
P1            13.70 usec
PL1           1.90 dB
PL1W          8.36853981 W
SFO1          300.1418535 MHz
SI            32768
SF            300.1400056 MHz
WDW           EM
SSB           0
LB            0.30 Hz
GB            0
PC            1.00
    
```



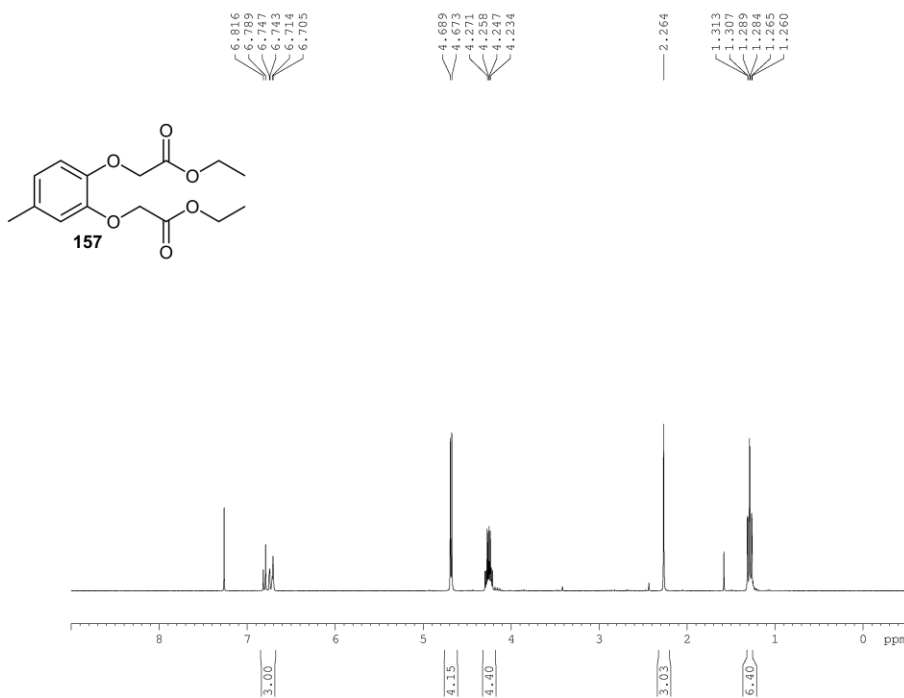
```

EXPNO          2
PROCNO         1
Date_          20140514
Time          17.19
INSTRUM        spect
PROBHD         5 mm PABBO BB-
PULPROG        zgpg30
TD             65536
SOLVENT        CDC13
NS            10000
DS             4
SWH           18028.846 Hz
FIDRES         0.275098 Hz
AQ            1.8175818 sec
RG            203
DW            27.733 usec
DE            6.50 usec
TE            673.2 K
D1            2.0000000 sec
D11           0.0300000 sec
TD0           1
    
```

```

===== CHANNEL f1 =====
NUC1           13C
P1            10.82 usec
PL1           0.00 dB
PL1W          30.14263725 W
SFO1          75.4778101 MHz

===== CHANNEL f2 =====
CPDPRG2        waltz16
NUC2           1H
PCPD2         100.00 usec
PL2           1.90 dB
PL12          19.17 dB
PL13          23.94 dB
PL2W          8.36853981 W
PL12W         0.15690966 W
PL13W         0.05231782 W
SFO2          300.1412006 MHz
SI            32768
SF            75.4702630 MHz
WDW           EM
SSB           0
LB            1.00 Hz
GB            0
PC            1.40
    
```

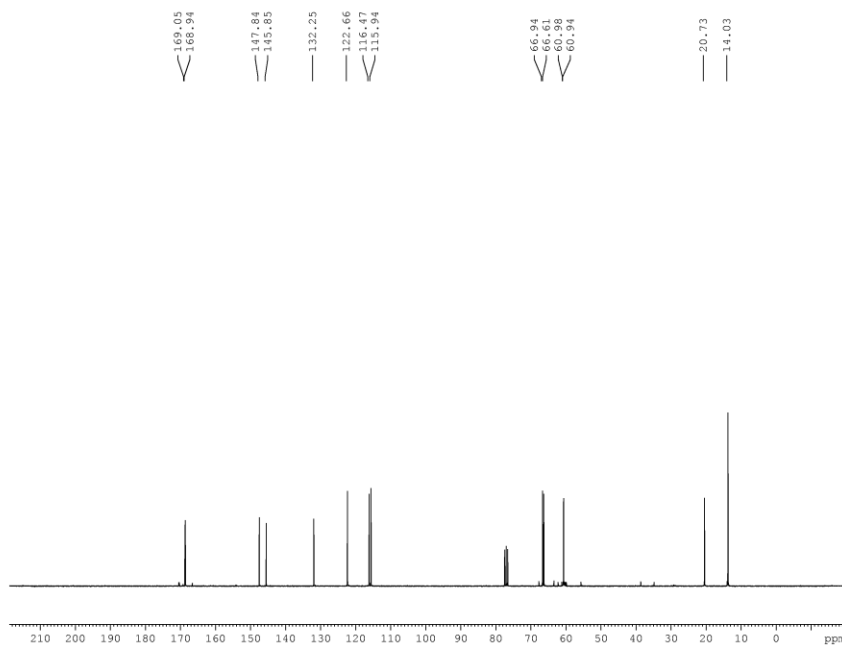


```

EXPNO 1
PROCNO 1
Date_ 20140506
Time 14.48
INSTRUM spect
PROBHD 5 mm PABBO BB-
PULPROG zg30
TD 65536
SOLVENT CDC13
NS 16
DS 2
SWH 6188.119 Hz
FIDRES 0.094423 Hz
AQ 5.2953587 sec
RG 203
DW 80.800 usec
DE 6.50 usec
TE 298.0 K
D1 1.0000000 sec
TDO 1
    
```

```

===== CHANNEL f1 =====
NUC1 1H
P1 13.70 usec
PL1 1.90 dB
PL1W 8.36853981 W
SFO1 300.1418535 MHz
SI 32768
SF 300.1400056 MHz
WDW EM
SSB 0
LB 0.30 Hz
GB 0
PC 1.00
    
```



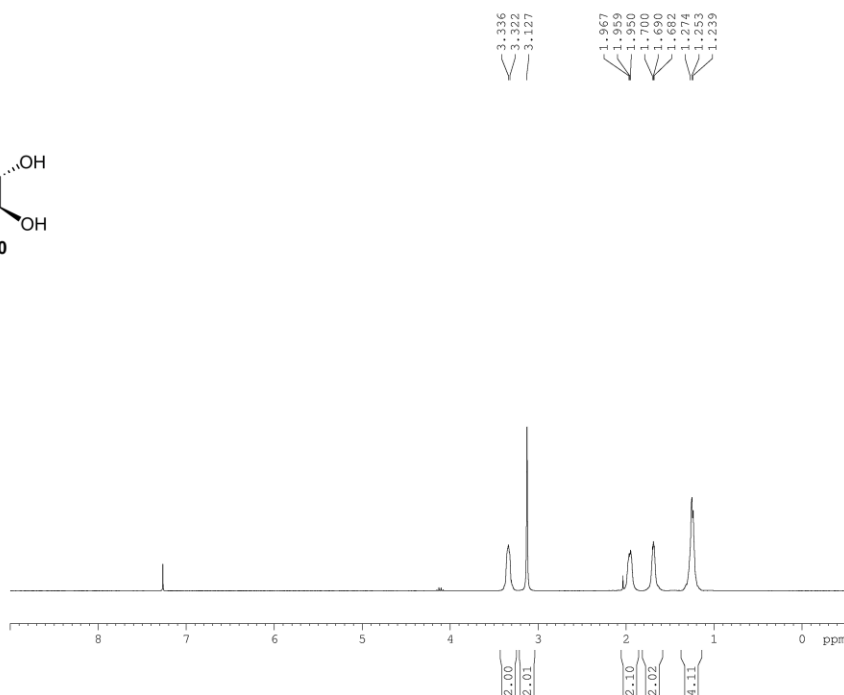
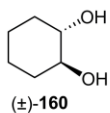
```

EXPNO 1
PROCNO 1
Date_ 20140505
Time 15.43
INSTRUM spect
PROBHD 5 mm PABBO BB-
PULPROG zgpg30
TD 65536
SOLVENT CDC13
NS 485
DS 4
SWH 18028.846 Hz
FIDRES 0.275098 Hz
AQ 1.8175818 sec
RG 203
DW 27.733 usec
DE 6.50 usec
TE 298.1 K
D1 2.0000000 sec
D11 0.0300000 sec
TDO 1
    
```

```

===== CHANNEL f1 =====
NUC1 13C
P1 10.82 usec
PL1 0.00 dB
PL1W 30.14263725 W
SFO1 75.4778101 MHz

===== CHANNEL f2 =====
CPDPRG2 waltz16
NUC2 1H
PCPD2 100.00 usec
PL2 1.90 dB
PL12 19.17 dB
PL13 23.94 dB
PL2W 8.36853981 W
PL12W 0.15690966 W
PL13W 0.05231782 W
SFO2 300.1412006 MHz
SI 32768
SF 75.4702900 MHz
WDW EM
SSB 0
LB 1.00 Hz
GB 0
PC 1.40
    
```

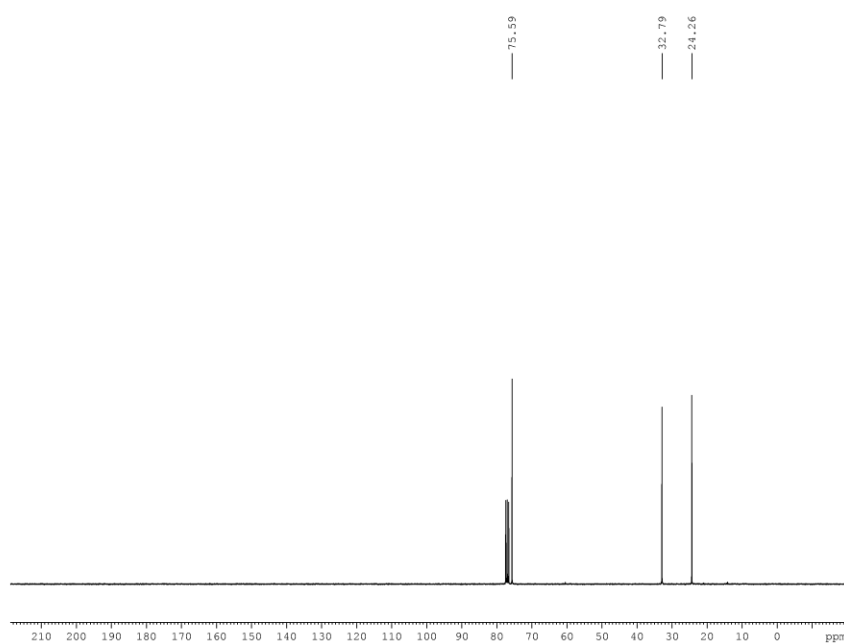



```

EXPNO 1
PROCNO 1
Date_ 20120831
Time 14.05
INSTRUM spect
PROBHD 5 mm PABBO BB-
PULPROG zg30
TD 65536
SOLVENT CDCl3
NS 16
DS 2
SWH 6188.119 Hz
FIDRES 0.094423 Hz
AQ 5.2953587 sec
RG 71.8
DW 80.800 usec
DE 6.50 usec
TE 298.0 K
D1 1.0000000 sec
TDO 1
    
```

```

===== CHANNEL f1 =====
NUC1 1H
P1 13.70 usec
PL1 1.90 dB
PL1W 8.36853981 W
SF01 300.1418535 MHz
SI 32768
SF 300.1400044 MHz
WDW EM
SSB 0
LB 0.30 Hz
GB 0
PC 1.00
    
```



```

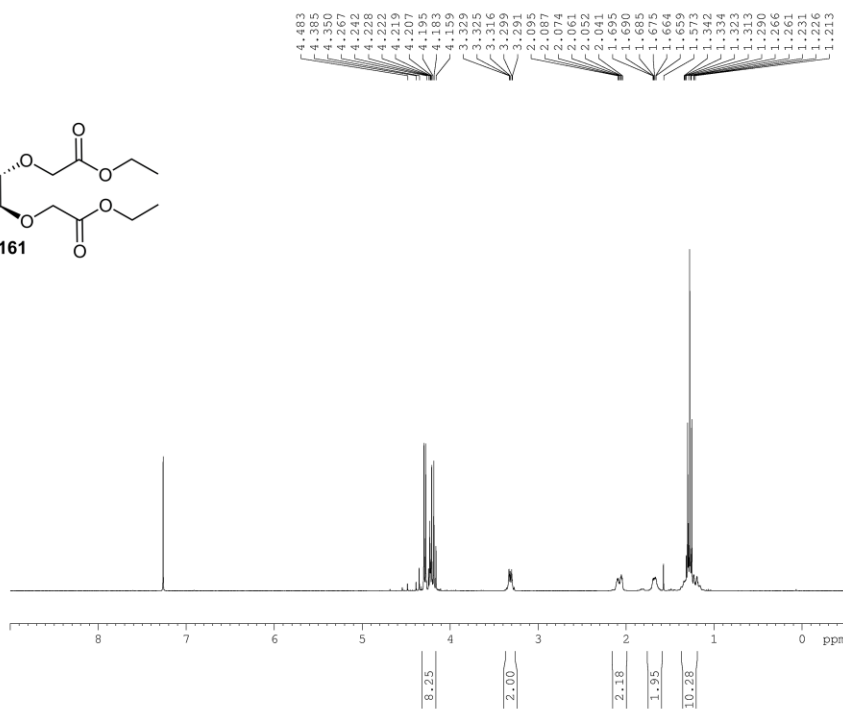
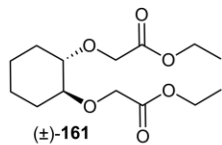
EXPNO 2
PROCNO 1
Date_ 20120831
Time 15.04
INSTRUM spect
PROBHD 5 mm PABBO BB-
PULPROG zgpg30
TD 65536
SOLVENT CDCl3
NS 1024
DS 4
SWH 18028.846 Hz
FIDRES 0.275098 Hz
AQ 1.8175818 sec
RG 203
DW 27.733 usec
DE 6.50 usec
TE 298.0 K
D1 2.0000000 sec
D11 0.0300000 sec
TDO 1
    
```

```

===== CHANNEL f1 =====
NUC1 13C
P1 10.82 usec
PL1 0.00 dB
PL1W 30.14263725 W
SF01 75.4778101 MHz
    
```

```

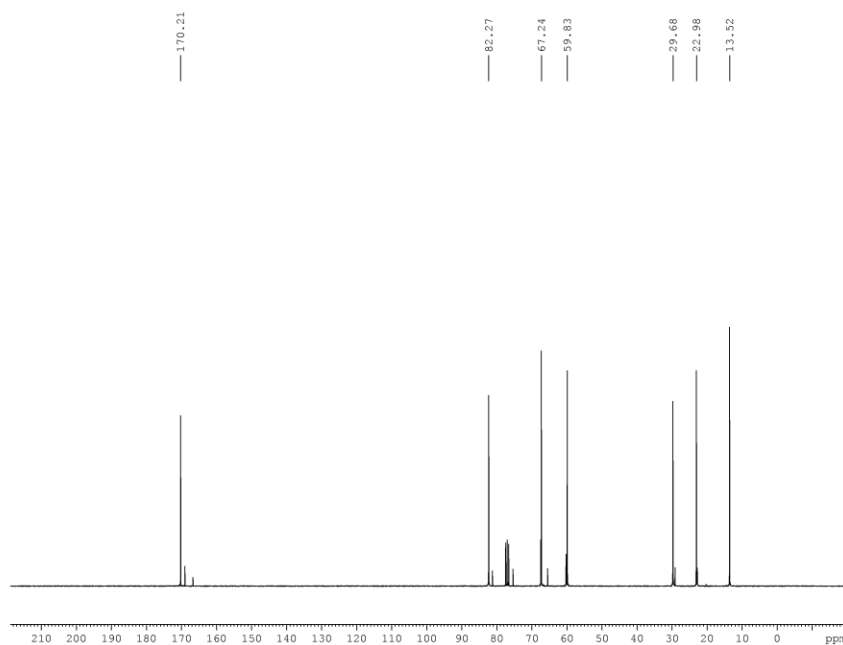
===== CHANNEL f2 =====
CPDPRG2 waltz16
NUC2 1H
PCPD2 100.00 usec
PL2 1.90 dB
PL12 19.17 dB
PL13 23.94 dB
PL1W 8.36853981 W
PL12W 0.15690966 W
PL13W 0.05231782 W
SF02 300.1412006 MHz
SI 32768
SF 75.4702703 MHz
WDW EM
SSB 0
LB 1.00 Hz
GB 0
PC 1.40
    
```



```

EXPNO 1
PROCNO 1
Date_ 20121113
Time 10.29
INSTRUM spect
PROBHD 5 mm PABBO BB-
PULPROG zg30
TD 65536
SOLVENT CDC13
NS 32
DS 2
SWH 6188.119 Hz
FIDRES 0.094423 Hz
AQ 5.2953587 sec
RG 203
DW 80.800 usec
DE 6.50 usec
TE 298.0 K
D1 1.0000000 sec
TDO 1

===== CHANNEL f1 =====
NUC1 1H
P1 13.70 usec
PL1 1.90 dB
PL1W 8.36853981 W
SFO1 300.1418535 MHz
SI 32768
SF 300.1400056 MHz
WDW EM
SSB 0
LB 0.30 Hz
GB 0
PC 1.00
    
```

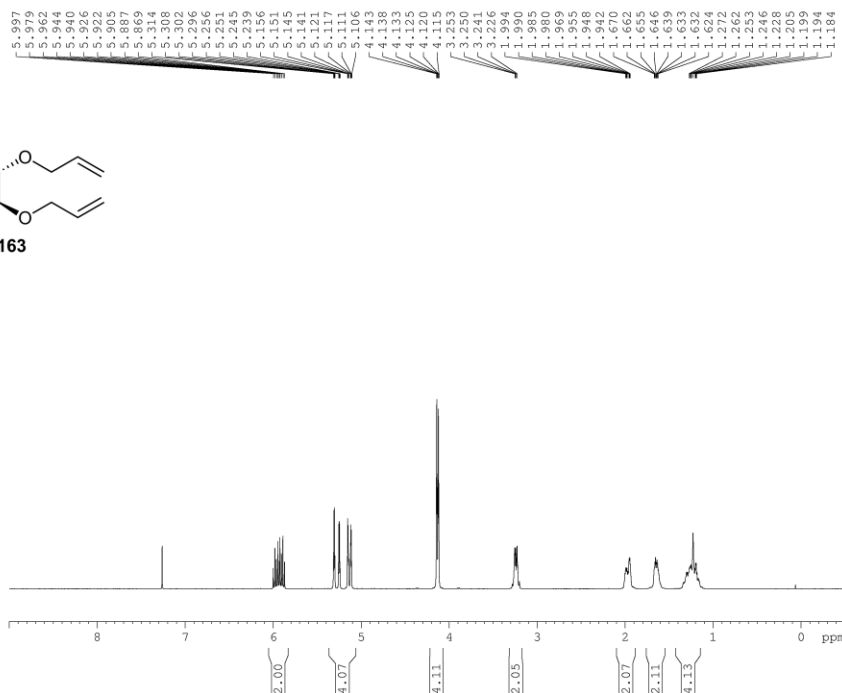
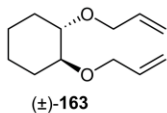


```

EXPNO 1
PROCNO 1
Date_ 20121113
Time 11.42
INSTRUM spect
PROBHD 5 mm PABBO BB-
PULPROG zgpg30
TD 65536
SOLVENT CDC13
NS 1024
DS 4
SWH 18028.846 Hz
FIDRES 0.275098 Hz
AQ 1.8175818 sec
RG 203
DW 27.733 usec
DE 6.50 usec
TE 298.0 K
D1 2.0000000 sec
D11 0.0300000 sec
TDO 1

===== CHANNEL f1 =====
NUC1 13C
P1 10.82 usec
PL1 0.00 dB
PL1W 30.14263725 W
SFO1 75.4778101 MHz

===== CHANNEL f2 =====
CPDPRG2 waltz16
NUC2 1H
PCPD2 100.00 usec
PL2 1.90 dB
PL12 19.17 dB
PL13 23.94 dB
PL1W 8.36853981 W
PL12W 0.15690966 W
PL13W 0.05231782 W
SFO2 300.1412006 MHz
SI 32768
SF 75.4702929 MHz
WDW EM
SSB 0
LB 1.00 Hz
GB 0
PC 1.40
    
```

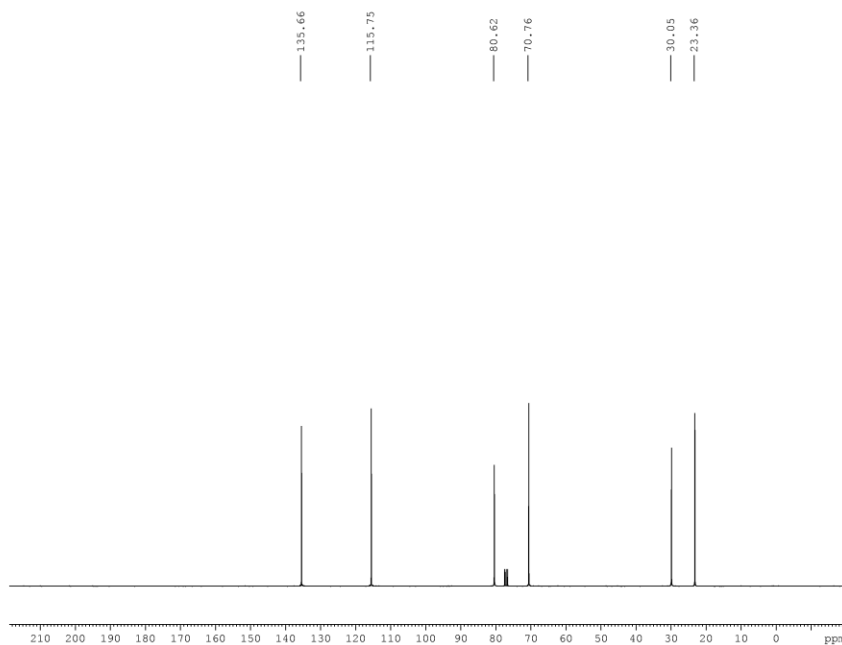


```

EXPNO 1
PROCNO 1
Date_ 20121015
Time 11.26
INSTRUM spect
PROBHD 5 mm PABBO BB-
PULPROG zg30
TD 65536
SOLVENT CDC13
NS 32
DS 2
SWH 6188.119 Hz
FIDRES 0.094423 Hz
AQ 5.2953587 sec
RG 71.8
DW 80.800 usec
DE 6.50 usec
TE 298.0 K
D1 1.0000000 sec
TDO 1
    
```

```

===== CHANNEL f1 =====
NUC1 1H
P1 13.70 usec
PL1 1.90 dB
PL1W 8.36853981 W
SF01 300.1418535 MHz
SI 32768
SF 300.1400055 MHz
WDW EM
SSB 0
LB 0.30 Hz
GB 0
PC 1.00
    
```



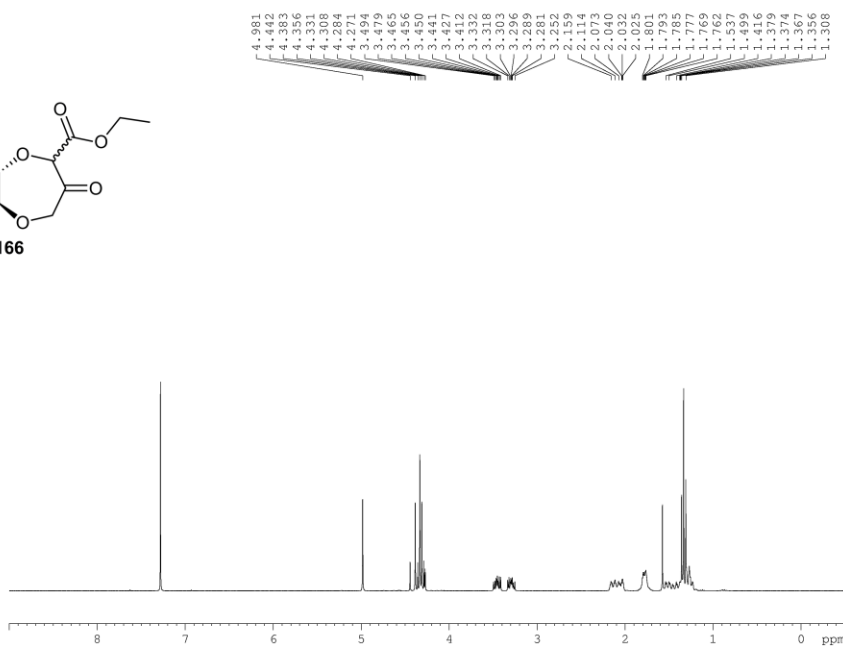
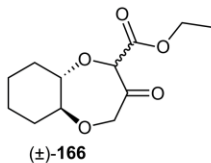
```

EXPNO 1
PROCNO 1
Date_ 20121015
Time 12.39
INSTRUM spect
PROBHD 5 mm PABBO BB-
PULPROG zgpg30
TD 65536
SOLVENT CDC13
NS 1024
DS 4
SWH 18028.846 Hz
FIDRES 0.275098 Hz
AQ 1.8175818 sec
RG 203
DW 27.733 usec
DE 6.50 usec
TE 298.0 K
D1 2.0000000 sec
D11 0.0300000 sec
TDO 1
    
```

```

===== CHANNEL f1 =====
NUC1 13C
P1 10.82 usec
PL1 0.00 dB
PL1W 30.14263725 W
SF01 75.4778101 MHz

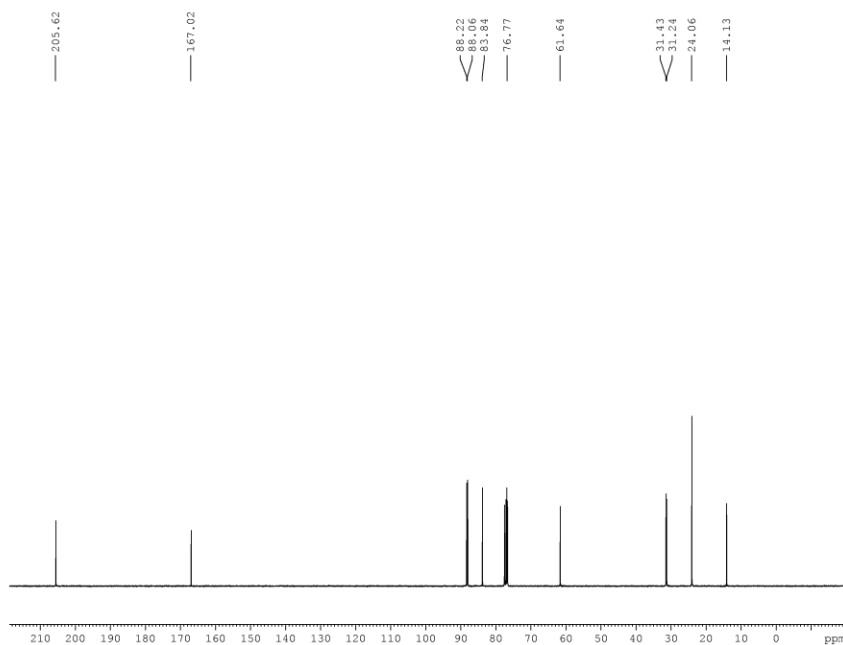
===== CHANNEL f2 =====
CPDPRG2 waltz16
NUC2 1H
PCPD2 100.00 usec
PL2 1.90 dB
PL12 19.17 dB
PL13 23.94 dB
PL2W 8.36853981 W
PL12W 0.15690966 W
PL13W 0.05231782 W
SF02 300.1412006 MHz
SI 32768
SF 75.4702812 MHz
WDW EM
SSB 0
LB 1.00 Hz
GB 0
PC 1.40
    
```



```

EXPNO 1
PROCNO 1
Date_ 20130205
Time 13.14
INSTRUM spect
PROBHD 5 mm PABBO BB-
PULPROG zg30
TD 65536
SOLVENT CDC13
NS 32
DS 2
SWH 6188.119 Hz
FIDRES 0.094423 Hz
AQ 5.2953587 sec
RG 203
DW 80.800 usec
DE 6.50 usec
TE 294.6 K
D1 1.00000000 sec
TDO 1

===== CHANNEL f1 =====
NUC1 1H
P1 13.70 usec
PL1 1.90 dB
PL1W 8.36853981 W
SF01 300.1418535 MHz
SI 32768
SF 300.1400000 MHz
WDW EM
SSB 0
LB 0.30 Hz
GB 0
PC 1.00
    
```

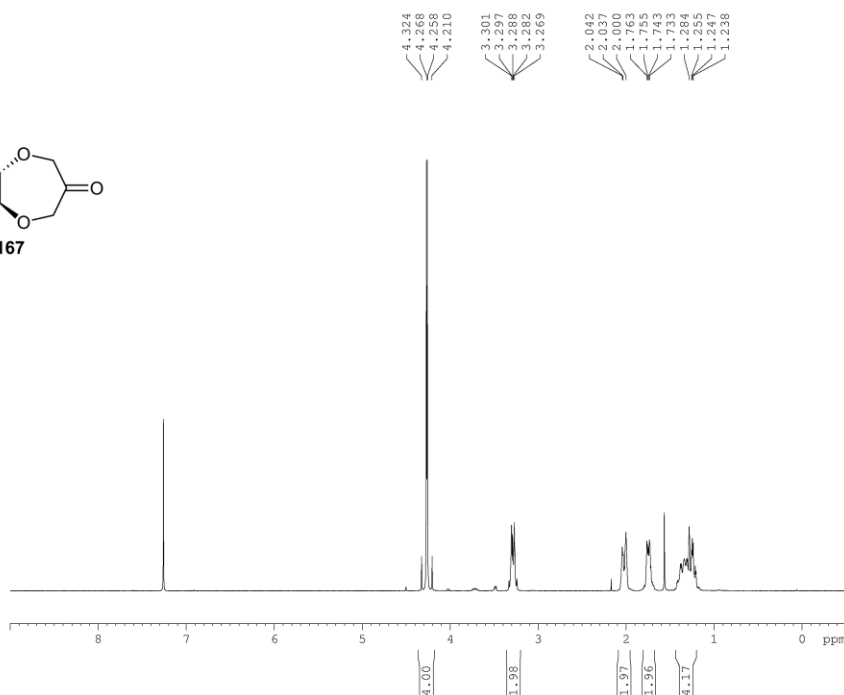
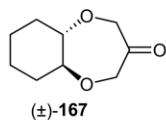


```

EXPNO 1
PROCNO 1
Date_ 20130205
Time 13.59
INSTRUM spect
PROBHD 5 mm PABBO BB-
PULPROG zgpg30
TD 65536
SOLVENT CDC13
NS 1024
DS 4
SWH 18028.846 Hz
FIDRES 0.275098 Hz
AQ 1.8175818 sec
RG 203
DW 27.713 usec
DE 6.50 usec
TE 294.8 K
D1 2.00000000 sec
D11 0.03000000 sec
TDO 1

===== CHANNEL f1 =====
NUC1 13C
P1 10.82 usec
PL1 0.00 dB
PL1W 30.14263725 W
SF01 75.4778101 MHz

===== CHANNEL f2 =====
CPDPRG2 waltz16
NUC2 1H
PCPD2 100.00 usec
PL2 1.90 dB
PL12 19.17 dB
PL13 23.94 dB
PL1W 8.36853981 W
PL12W 0.15690966 W
PL13W 0.05231782 W
SF02 300.1412006 MHz
SI 32768
SF 75.4702718 MHz
WDW EM
SSB 0
LB 1.00 Hz
GB 0
PC 1.40
    
```

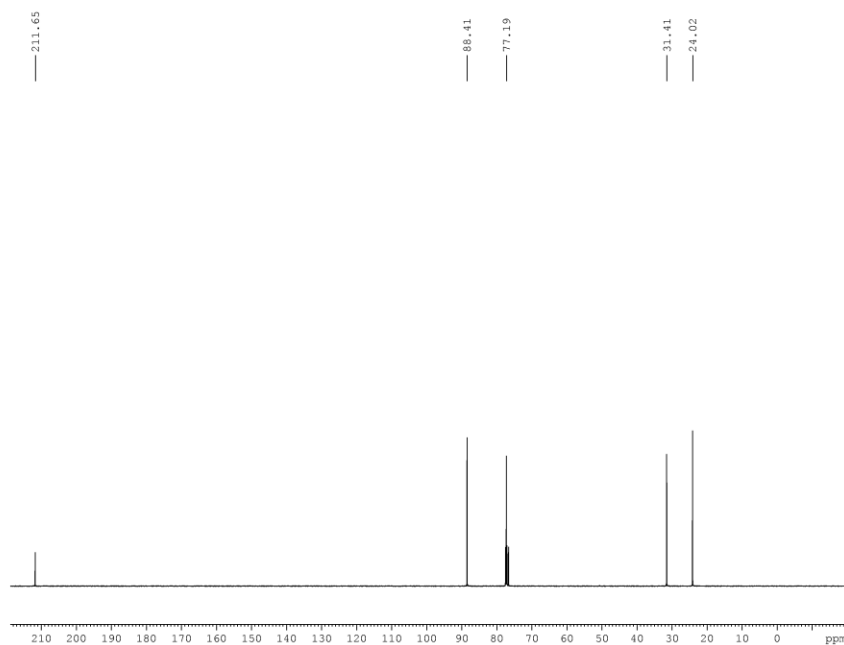


```

EXPNO 1
PROCNO 1
Date_ 20130207
Time 11.38
INSTRUM spect
PROBHD 5 mm PABBO BB-
PULPROG zg30
TD 65536
SOLVENT CDC13
NS 32
DS 2
SWH 6188.119 Hz
FIDRES 0.094423 Hz
AQ 5.2953587 sec
RG 203
DW 80.800 usec
DE 6.50 usec
TE 294.3 K
D1 1.0000000 sec
TDO 1
    
```

```

===== CHANNEL f1 =====
NUC1 1H
P1 13.70 usec
PL1 1.90 dB
PL1W 8.36853981 W
SFO1 300.1418535 MHz
SI 32768
SF 300.1400067 MHz
WDW EM
SSB 0
LB 0.30 Hz
GB 0
PC 1.00
    
```



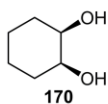
```

EXPNO 1
PROCNO 1
Date_ 20130207
Time 14.22
INSTRUM spect
PROBHD 5 mm PABBO BB-
PULPROG zgpg30
TD 65536
SOLVENT CDC13
NS 865
DS 4
SWH 18028.846 Hz
FIDRES 0.275098 Hz
AQ 1.8175818 sec
RG 203
DW 27.733 usec
DE 6.50 usec
TE 294.6 K
D1 2.0000000 sec
D11 0.0300000 sec
TDO 1
    
```

```

===== CHANNEL f1 =====
NUC1 13C
P1 10.82 usec
PL1 0.00 dB
PL1W 30.14263725 W
SFO1 75.4778101 MHz

===== CHANNEL f2 =====
CPDPRG2 waltz16
NUC2 1H
PCPD2 100.00 usec
PL2 1.90 dB
PL12 19.17 dB
PL13 23.94 dB
PL2W 8.36853981 W
PL12W 0.15690966 W
PL13W 0.05231782 W
SFO2 300.1412006 MHz
SI 32768
SF 75.4702710 MHz
WDW EM
SSB 0
LB 1.00 Hz
GB 0
PC 1.40
    
```

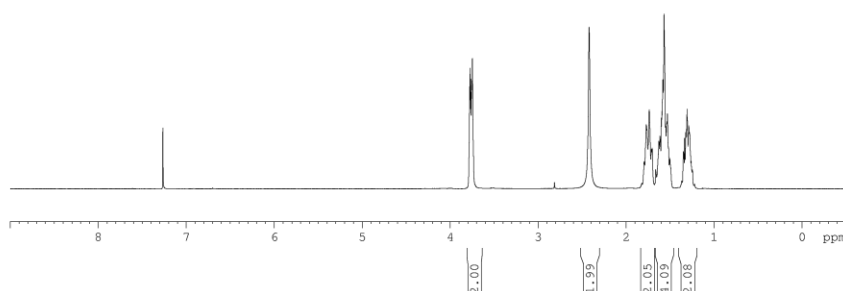


3.760
3.750
3.740
3.732
2.405
1.778
1.756
1.788
1.697
1.699
1.613
1.601
1.597
1.585
1.580
1.573
1.567
1.553
1.536
1.524
1.510
1.498
1.488
1.334
1.330
1.319
1.307
1.299
1.289
1.289



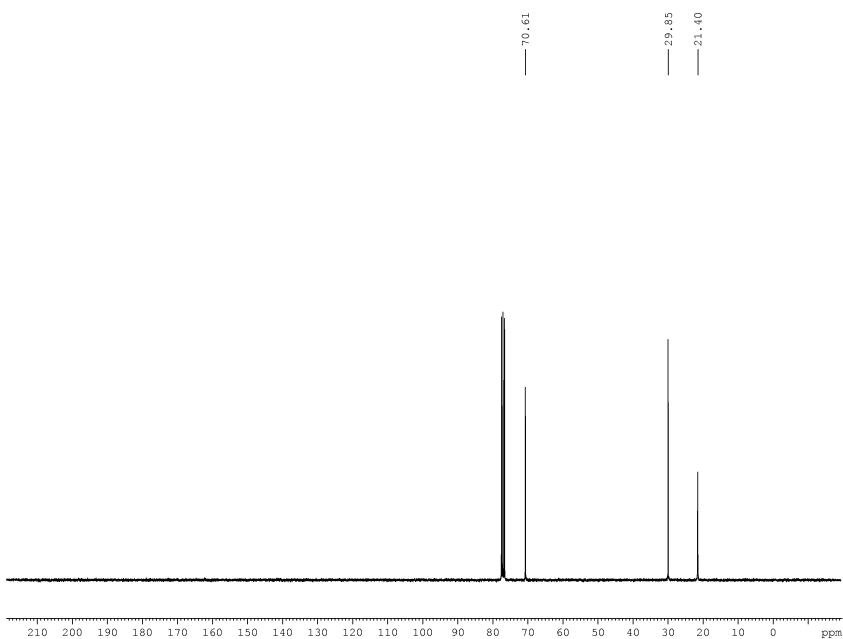
```

EXPNO 1
PROCNO 1
Date_ 20130403
Time 13.37
INSTRUM spect
PROBHD 5 mm PABBO BB-
PULPROG zg30
TD 65536
SOLVENT CDCl3
NS 16
DS 2
SWH 6188.119 Hz
FIDRES 0.094423 Hz
AQ 5.2953587 sec
RG 71.8
DW 80.800 usec
DE 6.50 usec
TE 298.0 K
D1 1.00000000 sec
TDO 1
    
```



```

----- CHANNEL f1 -----
NUC1 1H
P1 13.70 usec
PL1 1.90 dB
PL1W 8.36853981 W
SFO1 300.1418535 MHz
SI 32768
SF 300.1400048 MHz
WDW EM
SSB 0
LB 0.30 Hz
GB 0
PC 1.00
    
```



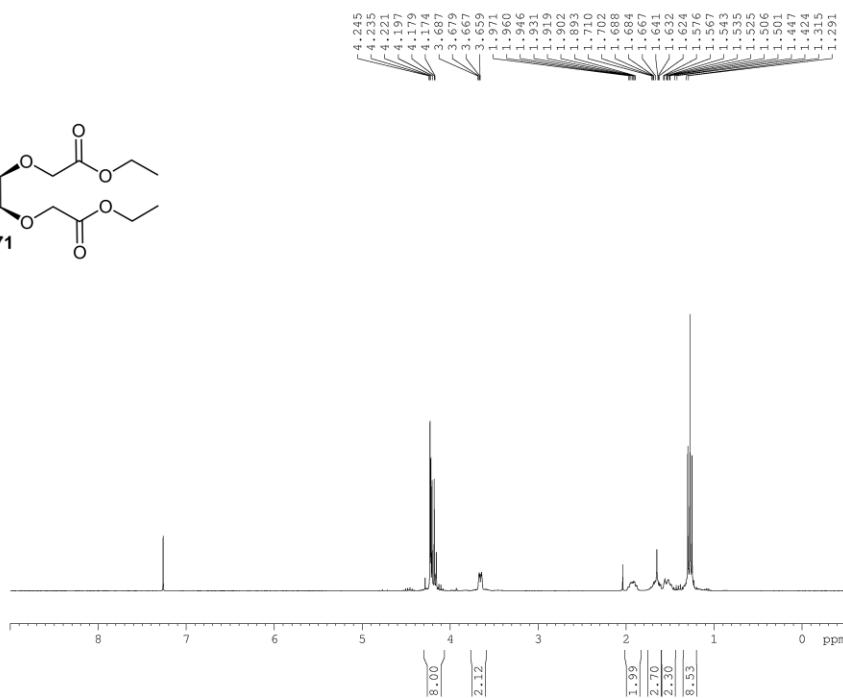
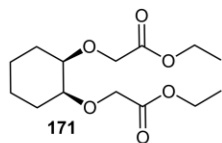
```

EXPNO 1
PROCNO 1
Date_ 20130403
Time 13.35
INSTRUM spect
PROBHD 5 mm PABBO BB-
PULPROG zgpg30
TD 65536
SOLVENT CDCl3
NS 1394
DS 4
SWH 18028.846 Hz
FIDRES 0.275098 Hz
AQ 1.8175818 sec
RG 203
DW 27.733 usec
DE 6.50 usec
TE 298.0 K
D1 2.00000000 sec
D11 0.03000000 sec
TDO 1
    
```

```

----- CHANNEL f1 -----
NUC1 13C
P1 10.82 usec
PL1 0.00 dB
PL1W 30.14263725 W
SFO1 75.4778101 MHz

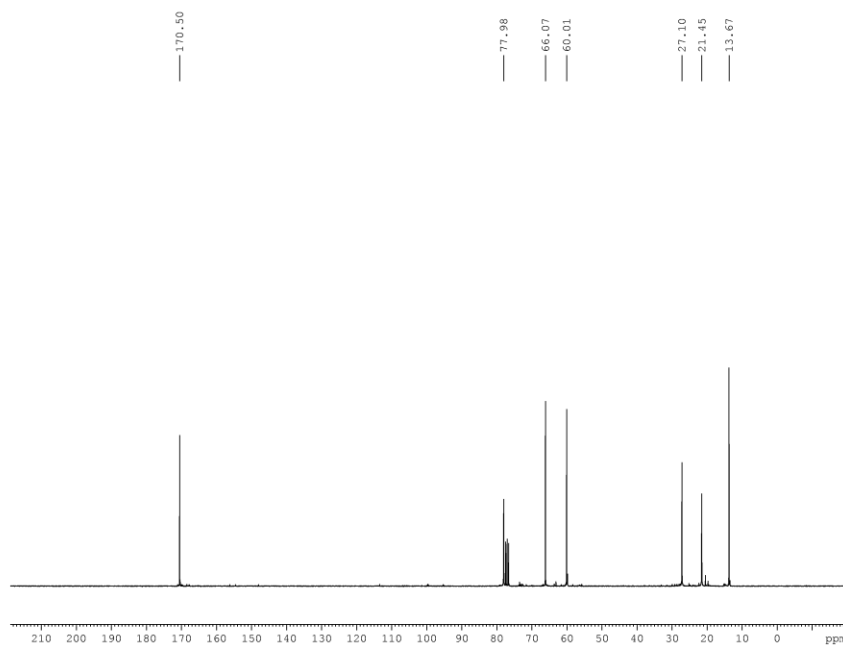
----- CHANNEL f2 -----
CPDPRG2 waltz16
NUC2 1H
FCPD2 100.00 usec
PL2 1.90 dB
PL12 19.17 dB
PL13 23.94 dB
PL2W 8.36853981 W
PL12W 0.15690966 W
PL13W 0.05231782 W
SFO2 300.1412006 MHz
SI 32768
SF 75.4702661 MHz
WDW EM
SSB 0
LB 1.00 Hz
GB 0
PC 1.40
    
```



```

EXPNO          5
PROCNO         1
Date_          20130613
Time          9.24
INSTRUM       spect
PROBHD        5 mm PABBO BB-
PULPROG       zg30
TD            65536
SOLVENT       CDC13
NS            32
DS            2
SWH           6188.119 Hz
FIDRES        0.094423 Hz
AQ           5.2953587 sec
RG            90.5
DW           80.800 usec
DE            6.50 usec
TE            298.0 K
D1            1.0000000 sec
TD0           1

===== CHANNEL f1 =====
NUC1          1H
P1            13.70 usec
PL1           1.90 dB
PL1W         8.36853981 W
SFO1         300.1418535 MHz
SI            32768
SF           300.1400055 MHz
WDW           EM
SSB           0
LB            0.30 Hz
GB            0
PC            1.00
    
```

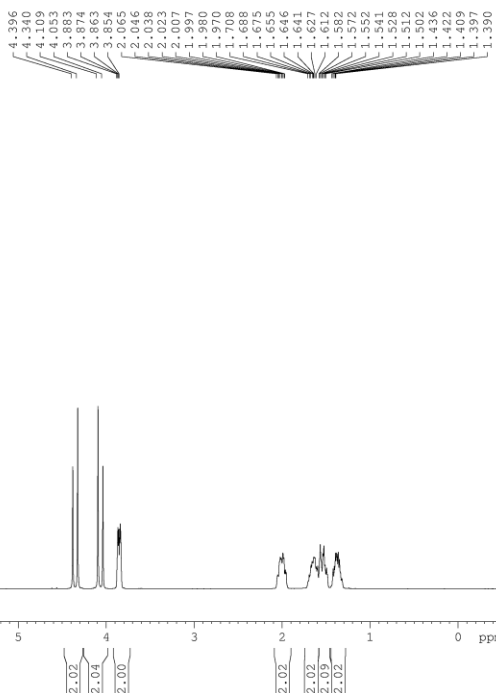
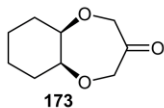


```

EXPNO          1
PROCNO         1
Date_          20130612
Time          17.29
INSTRUM       spect
PROBHD        5 mm PABBO BB-
PULPROG       zgpg30
TD            65536
SOLVENT       CDC13
NS            1024
DS            4
SWH           18028.846 Hz
FIDRES        0.275098 Hz
AQ           1.8175818 sec
RG            203
DW           27.733 usec
DE            6.50 usec
TE            298.0 K
D1            2.0000000 sec
D11           0.0300000 sec
TD0           1

===== CHANNEL f1 =====
NUC1          13C
P1            10.82 usec
PL1           0.00 dB
PL1W         30.14263725 W
SFO1         75.4778101 MHz

===== CHANNEL f2 =====
CPDPRG2       waltz16
NUC2          1H
PCPD2        100.00 usec
PL2           1.90 dB
PL12         19.17 dB
PL13         23.94 dB
PL1W         8.36853981 W
PL12W        0.15690966 W
PL13W        0.05231782 W
SFO2         300.1412006 MHz
SI            32768
SF           75.4702857 MHz
WDW           EM
SSB           0
LB            1.00 Hz
GB            0
PC            1.40
    
```

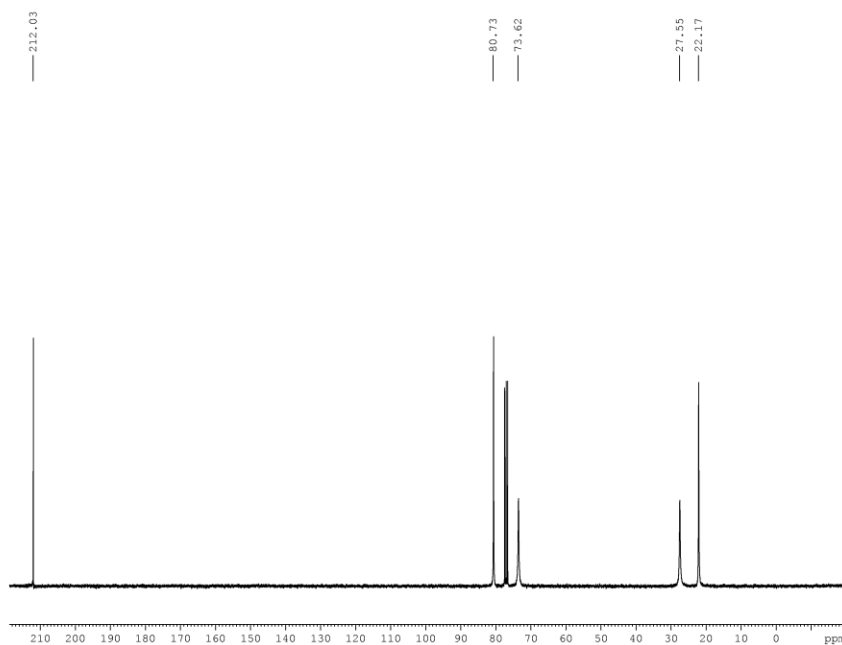


```

EXPNO 1
PROCNO 1
Date_ 20130801
Time 16.57
INSTRUM spect
PROBHD 5 mm PABBO BB-
PULPROG zg30
TD 65536
SOLVENT CDC13
NS 32
DS 2
SWH 6188.119 Hz
FIDRES 0.094423 Hz
AQ 5.2953587 sec
RG 57
DW 80.800 usec
DE 6.50 usec
TE 294.7 K
D1 1.0000000 sec
TDO 1
    
```

```

===== CHANNEL f1 =====
NUC1 1H
P1 13.70 usec
PL1 1.90 dB
PL1W 8.36853981 W
SF01 300.1418535 MHz
SI 32768
SF 300.1400055 MHz
WDW EM
SSB 0
LB 0.30 Hz
GB 0
PC 1.00
    
```



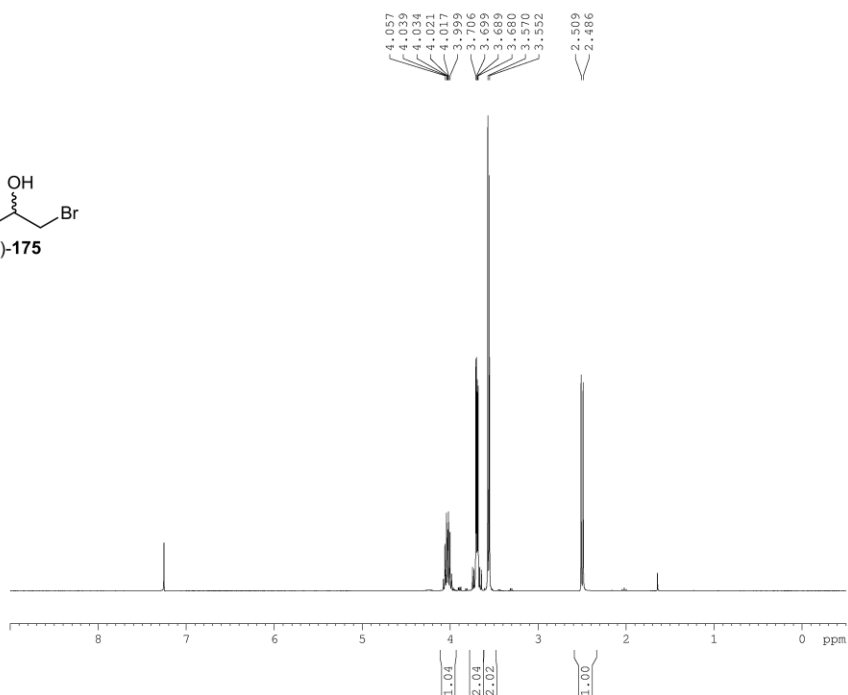
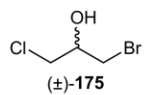
```

EXPNO 1
PROCNO 1
Date_ 20130801
Time 16.04
INSTRUM spect
PROBHD 5 mm PABBO BB-
PULPROG zgpg30
TD 65536
SOLVENT CDC13
NS 674
DS 4
SWH 18028.846 Hz
FIDRES 0.275098 Hz
AQ 1.8175818 sec
RG 203
DW 27.733 usec
DE 6.50 usec
TE 294.9 K
D1 2.0000000 sec
D11 0.0300000 sec
TDO 1
    
```

```

===== CHANNEL f1 =====
NUC1 13C
P1 10.82 usec
PL1 0.00 dB
PL1W 30.14263725 W
SF01 75.4778101 MHz

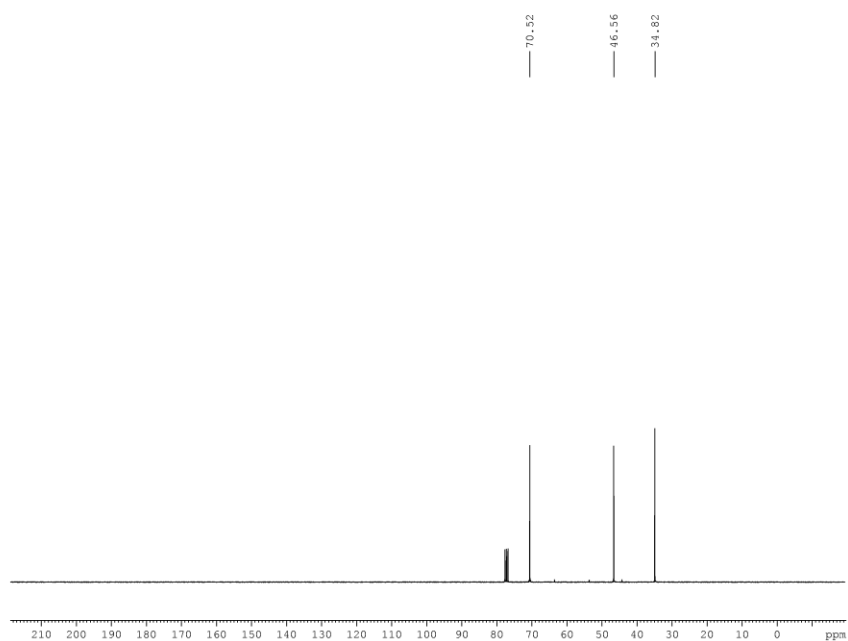
===== CHANNEL f2 =====
CPDPRG2 waltz16
NUC2 1H
PCPD2 100.00 usec
PL2 1.90 dB
PL12 19.17 dB
PL13 23.94 dB
PL2W 8.36853981 W
PL12W 0.15690966 W
PL13W 0.05231782 W
SF02 300.1412006 MHz
SI 32768
SF 75.4702742 MHz
WDW EM
SSB 0
LB 1.00 Hz
GB 0
PC 1.40
    
```

```

EXPNO 1
PROCNO 1
Date_ 20120806
Time 15.05
INSTRUM spect
PROBHD 5 mm PABBO BB-
PULPROG zg30
TD 65536
SOLVENT CDCl3
NS 32
DS 2
SWH 6188.119 Hz
FIDRES 0.094423 Hz
AQ 5.2953587 sec
RG 90.5
DM 80.800 usec
DE 6.50 usec
TE 298.0 K
D1 1.0000000 sec
TDO 1

===== CHANNEL f1 =====
NUC1 1H
P1 13.70 usec
PL1 1.90 dB
PL1W 8.36853981 W
SF01 300.1418535 MHz
SI 32768
SF 300.1400081 MHz
WDW EM
SSB 0
LB 0.30 Hz
GB 0
PC 1.00
  
```

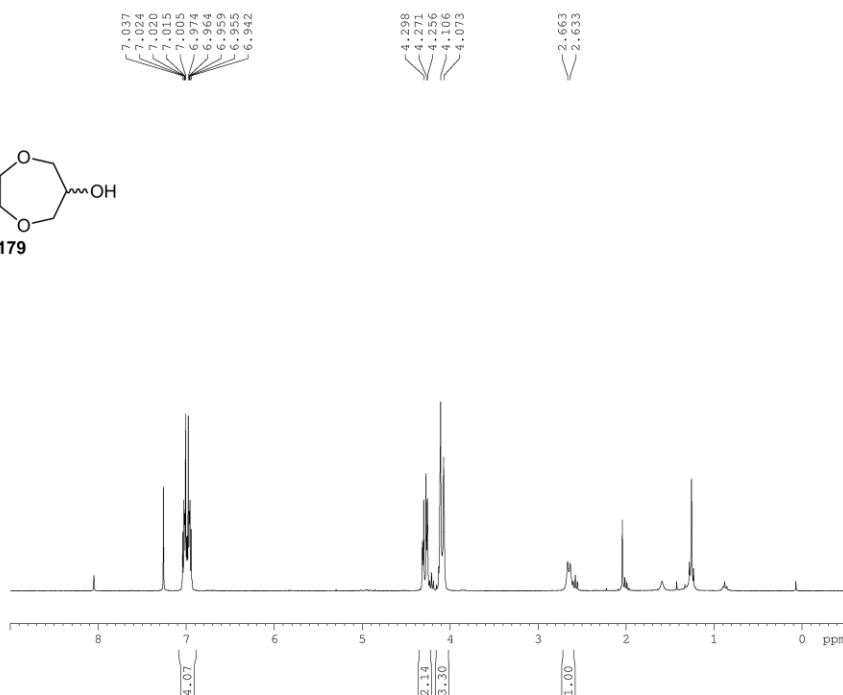
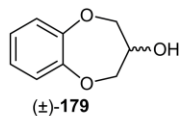


```

EXPNO 1
PROCNO 1
Date_ 20120803
Time 15.50
INSTRUM spect
PROBHD 5 mm PABBO BB-
PULPROG zgpg30
TD 65536
SOLVENT CDCl3
NS 872
DS 4
SWH 18028.846 Hz
FIDRES 0.275098 Hz
AQ 1.8175818 sec
RG 203
DM 27.733 usec
DE 6.50 usec
TE 298.0 K
D1 2.0000000 sec
D11 0.0300000 sec
TDO 1

===== CHANNEL f1 =====
NUC1 13C
P1 10.82 usec
PL1 0.00 dB
PL1W 30.14263725 W
SF01 75.4778101 MHz

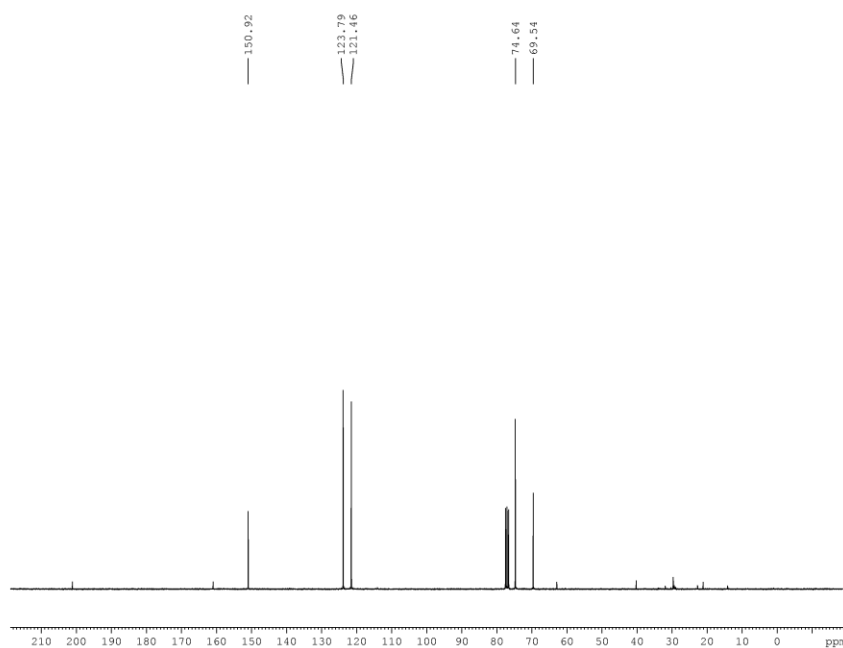
===== CHANNEL f2 =====
CPDPRG2 waltz16
NUC2 1H
PCPD2 100.00 usec
PL2 1.90 dB
PL12 19.17 dB
PL13 23.94 dB
PL1W 8.36853981 W
PL12W 0.15690966 W
PL13W 0.05231782 W
SF02 300.1412006 MHz
SI 32768
SF 75.4702630 MHz
WDW EM
SSB 0
LB 1.00 Hz
GB 0
PC 1.40
  
```

```

EXPNO 1
PROCNO 1
Date_ 20150225
Time 14.10
INSTRUM spect
PROBHD 5 mm PABBO BB-
PULPROG zg30
TD 65536
SOLVENT CDCl3
NS 16
DS 2
SWH 6188.119 Hz
FIDRES 0.094423 Hz
AQ 5.2953587 sec
RG 203
DM 80.800 usec
DE 6.50 usec
TE 298.0 K
D1 1.0000000 sec
TDO 1

===== CHANNEL f1 =====
NUC1 1H
P1 13.70 usec
PL1 1.90 dB
PL1W 8.36853981 W
SF01 300.1418535 MHz
SI 32768
SF 300.1400068 MHz
WDW EM
SSB 0
LB 0.30 Hz
GB 0
PC 1.00
    
```

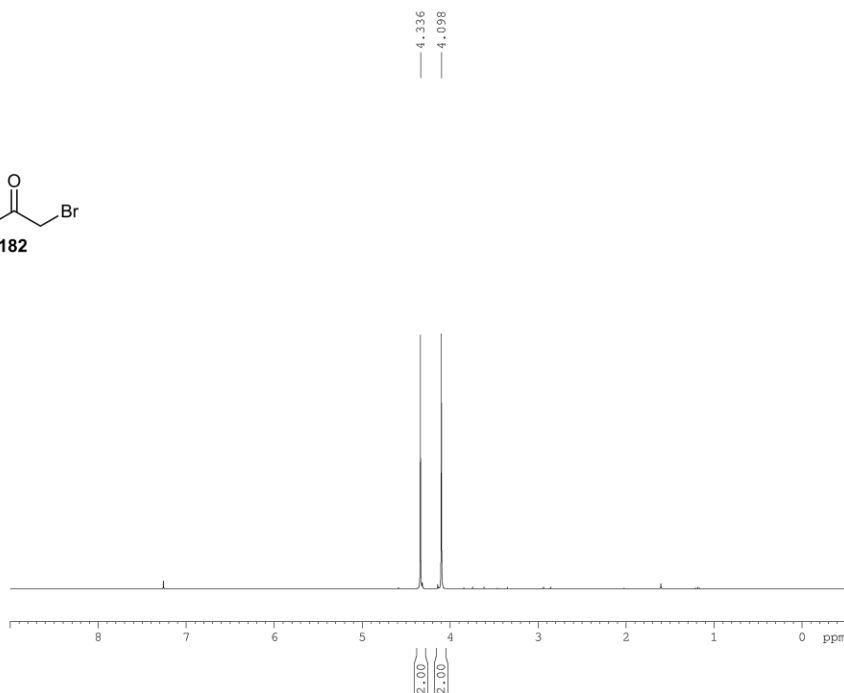
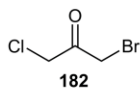


```

EXPNO 3
PROCNO 1
Date_ 20150225
Time 13.44
INSTRUM spect
PROBHD 5 mm PABBO BB-
PULPROG zgpg30
TD 65536
SOLVENT CDCl3
NS 1024
DS 4
SWH 18028.846 Hz
FIDRES 0.275098 Hz
AQ 1.8175818 sec
RG 203
DM 27.733 usec
DE 6.50 usec
TE 298.0 K
D1 2.0000000 sec
D11 0.0300000 sec
TDO 1

===== CHANNEL f1 =====
NUC1 13C
P1 10.82 usec
PL1 0.00 dB
PL1W 30.14263725 W
SF01 75.4778101 MHz

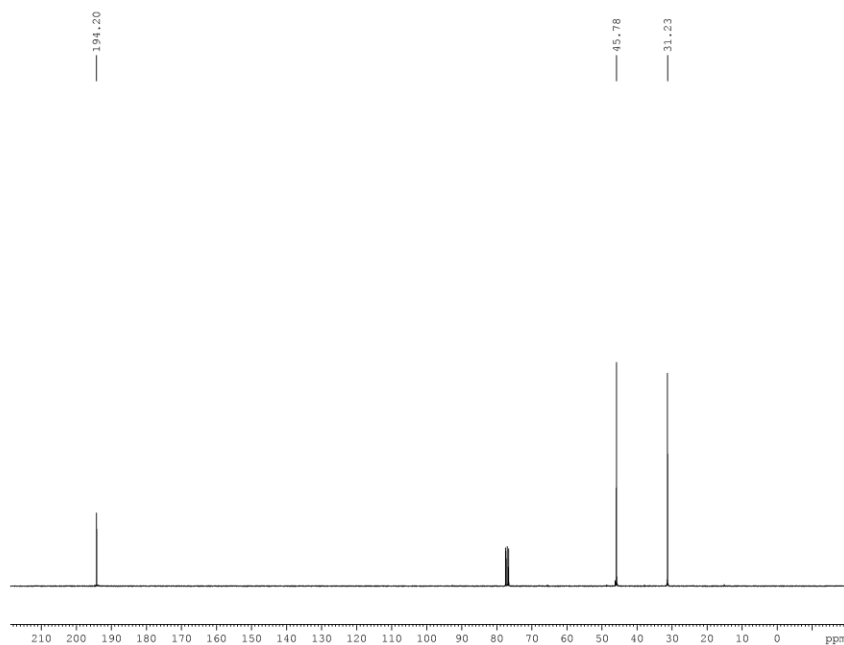
===== CHANNEL f2 =====
CPDPRG2 waltz16
NUC2 1H
PCPD2 100.00 usec
PL2 1.90 dB
PL12 19.17 dB
PL13 23.94 dB
PL2W 8.36853981 W
PL12W 0.15690966 W
PL13W 0.05231782 W
SF02 300.1412006 MHz
SI 32768
SF 75.4702714 MHz
WDW EM
SSB 0
LB 1.00 Hz
GB 0
PC 1.40
    
```

```

EXPNO      1
PROCNO     1
Date_      20130116
Time       13.56
INSTRUM    spect
PROBHD     5 mm PABBO BB-
PULPROG    zg30
TD         65536
SOLVENT    CDCl3
NS         32
DS         2
SWH        6188.119 Hz
FIDRES     0.094423 Hz
AQ         5.2953587 sec
RG         80.6
DW         80.800 usec
DE         6.50 usec
TE         298.0 K
D1         1.0000000 sec
TDO        1

===== CHANNEL f1 =====
NUC1       1H
P1         13.70 usec
PL1        1.90 dB
PL1W       8.36853981 W
SF01       300.1418535 MHz
SI         32768
SF         300.1400065 MHz
WDW        EM
SSB        0
LB         0.30 Hz
GB         0
PC         1.00
    
```

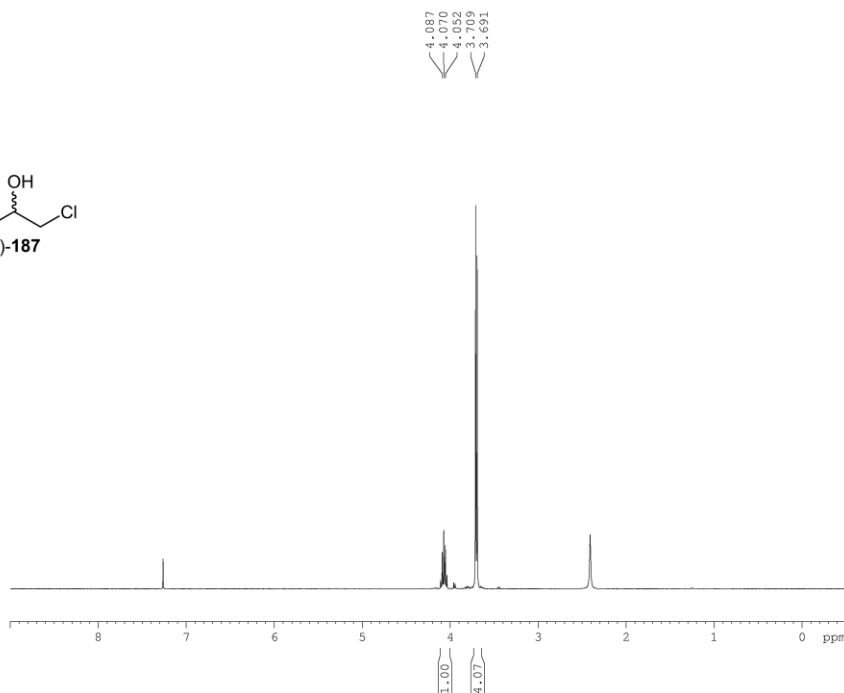
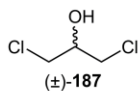


```

EXPNO      1
PROCNO     1
Date_      20130116
Time       15.16
INSTRUM    spect
PROBHD     5 mm PABBO BB-
PULPROG    zgpg30
TD         65536
SOLVENT    CDCl3
NS         1024
DS         4
SWH        18028.846 Hz
FIDRES     0.275098 Hz
AQ         1.8175818 sec
RG         203
DW         27.733 usec
DE         6.50 usec
TE         298.0 K
D1         2.0000000 sec
D11        0.0300000 sec
TDO        1

===== CHANNEL f1 =====
NUC1       13C
P1         10.82 usec
PL1        0.00 dB
PL1W       30.14263725 W
SF01       75.4778101 MHz

===== CHANNEL f2 =====
CPDPRG2    waltz16
NUC2       1H
PCPD2     100.00 usec
PL2        1.90 dB
PL12       19.17 dB
PL13       23.94 dB
PL1W       8.36853981 W
PL12W      0.15690966 W
PL13W      0.05231782 W
SF02       300.1412006 MHz
SI         32768
SF         75.4702830 MHz
WDW        EM
SSB        0
LB         1.00 Hz
GB         0
PC         1.40
    
```

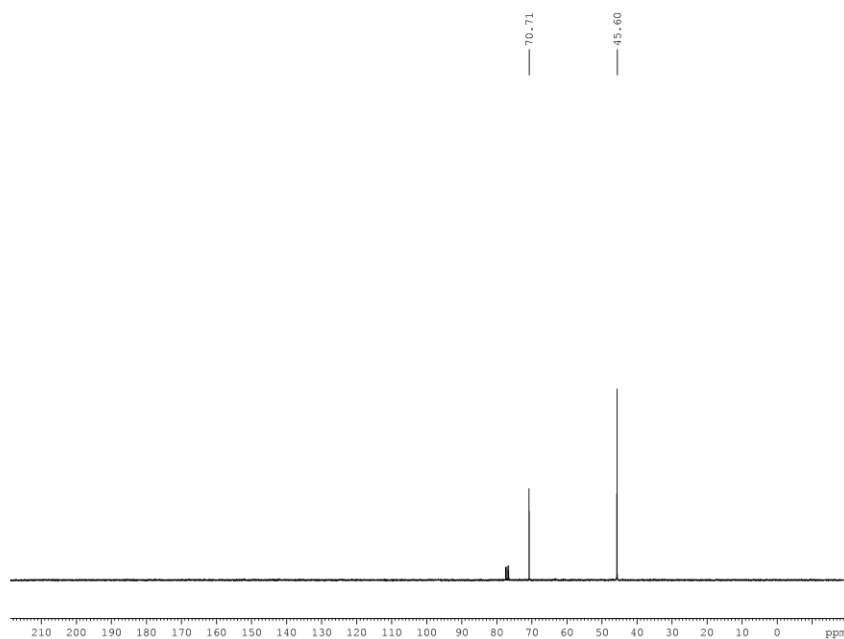


```

EXPNO 1
PROCNO 1
Date_ 20141127
Time 9.55
INSTRUM spect
PROBHD 5 mm PABBO BB-
PULPROG zg30
TD 65536
SOLVENT CDCl3
NS 16
DS 2
SWH 6188.119 Hz
FIDRES 0.094423 Hz
AQ 5.2953587 sec
RG 181
DW 80.800 usec
DE 6.50 usec
TE 298.0 K
D1 1.00000000 sec
TDO 1
  
```

```

----- CHANNEL f1 -----
NUC1 1H
P1 13.70 usec
PL1 1.90 dB
PL1W 8.36853981 W
SF01 300.1418535 MHz
SI 32768
SF 300.1400054 MHz
WDW EM
SSB 0
LB 0.30 Hz
GB 0
PC 1.00
  
```



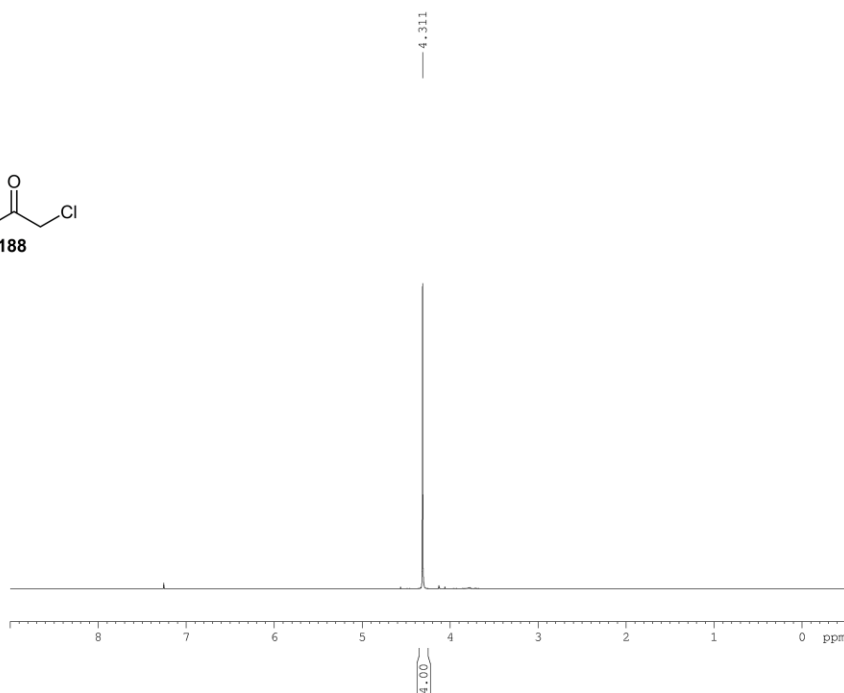
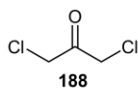
```

EXPNO 1
PROCNO 1
Date_ 20141127
Time 9.25
INSTRUM spect
PROBHD 5 mm PABBO BB-
PULPROG zgpg30
TD 65536
SOLVENT CDCl3
NS 37
DS 4
SWH 18028.046 Hz
FIDRES 0.275098 Hz
AQ 1.8175818 sec
RG 203
DW 27.733 usec
DE 6.50 usec
TE 298.1 K
D1 2.00000000 sec
D11 0.03000000 sec
TDO 1
  
```

```

----- CHANNEL f1 -----
NUC1 13C
P1 10.82 usec
PL1 0.00 dB
PL1W 30.14263725 W
SF01 75.4778101 MHz

----- CHANNEL f2 -----
CPDPRG2 waltz16
NUC2 1H
PCPD2 100.00 usec
PL2 1.90 dB
PL12 19.17 dB
PL13 23.94 dB
PLW 8.36853981 W
PL12W 0.15590966 W
PL13W 0.05231782 W
SF02 300.1412006 MHz
SI 32768
SF 75.4702761 MHz
WDW EM
SSB 0
LB 1.00 Hz
GB 0
PC 1.40
  
```

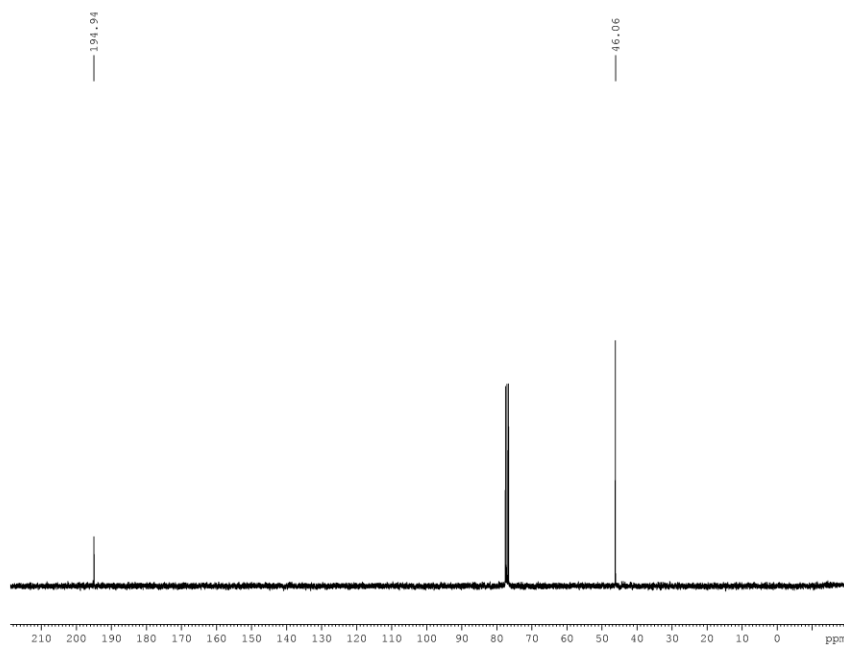


```

EXPNO      1
PROCNO     1
Date_      20141204
Time       11.31
INSTRUM    spect
PROBHD     5 mm PABBO BB-
PULPROG    zg30
TD         65536
SOLVENT    CDCl3
NS         16
DS         2
SWH        6188.119 Hz
FIDRES     0.094423 Hz
AQ         5.2953587 sec
RG         161
DW         80.800 usec
DE         6.50 usec
TE         298.0 K
D1         1.00000000 sec
TDO        1
    
```

```

===== CHANNEL f1 =====
NUC1       1H
P1         13.70 usec
PL1        1.90 dB
PL1W       8.36853981 W
SF01       300.1418535 MHz
SI         32768
SF         300.1400080 MHz
WDW        EM
SSB        0
LB         0.30 Hz
GB         0
PC         1.00
    
```



```

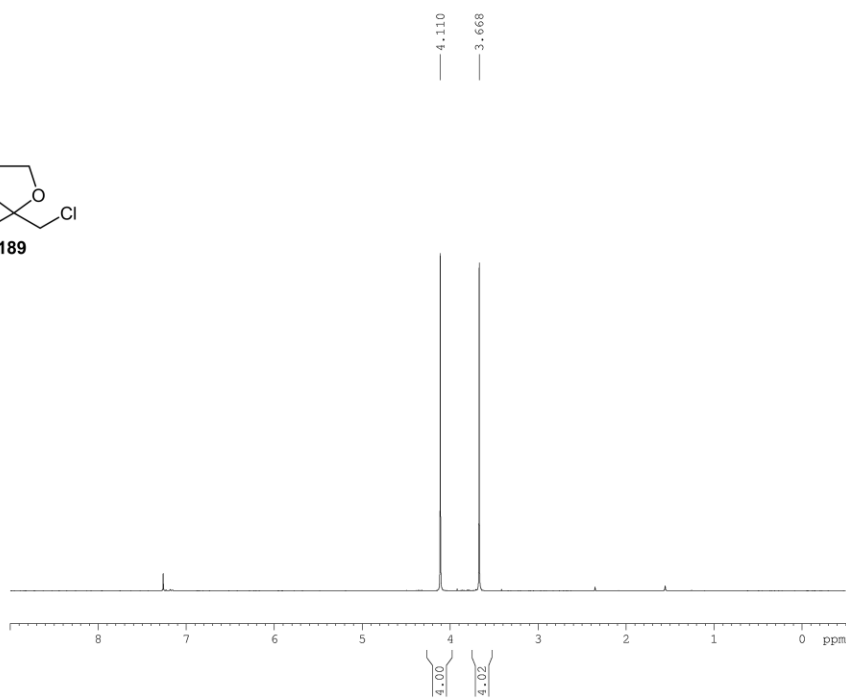
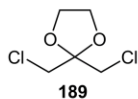
EXPNO      1
PROCNO     1
Date_      20141204
Time       12.06
INSTRUM    spect
PROBHD     5 mm PABBO BB-
PULPROG    zgpg30
TD         65536
SOLVENT    CDCl3
NS         140
DS         4
SWH        18028.846 Hz
FIDRES     0.275098 Hz
AQ         1.8175818 sec
RG         203
DW         27.733 usec
DE         6.50 usec
TE         298.0 K
D1         2.00000000 sec
D11        0.03000000 sec
TDO        1
    
```

```

===== CHANNEL f1 =====
NUC1       13C
P1         10.82 usec
PL1        0.00 dB
PL1W       30.14263725 W
SF01       75.4778101 MHz
    
```

```

===== CHANNEL f2 =====
CPDPRG2    waltz16
NUC2       1H
PCPD2     100.00 usec
PL2        1.90 dB
PL12       19.17 dB
PL13       23.94 dB
PL1W       8.36853981 W
PL12W      0.15690966 W
PL13W      0.05231782 W
SF02       300.1412006 MHz
SI         32768
SF         75.4702661 MHz
WDW        EM
SSB        0
LB         1.00 Hz
GB         0
PC         1.40
    
```



```

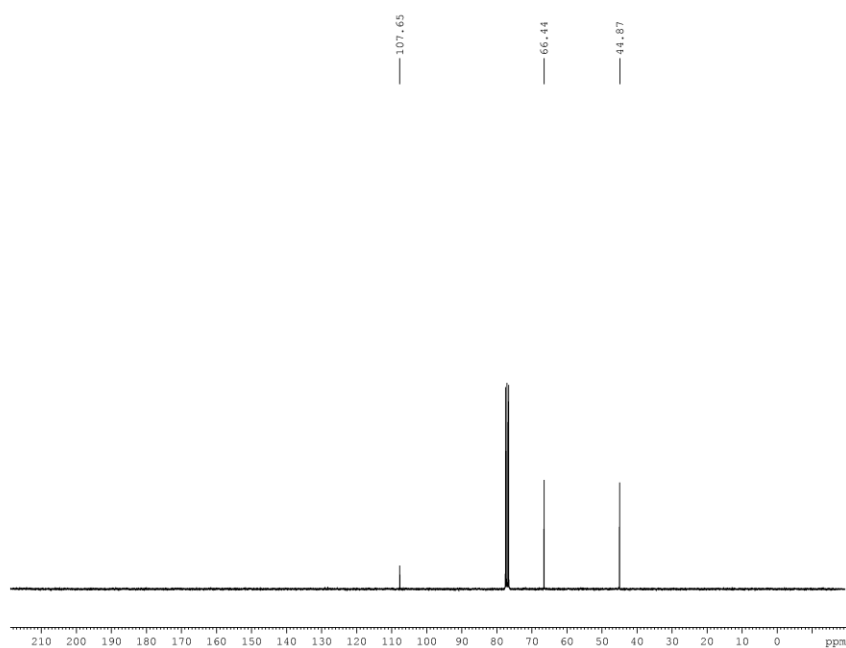
EXPNO          1
PROCNO         1
Date_          20141203
Time          16.24
INSTRUM       spect
PROBHD        5 mm PABBO BB-
PULPROG       zg30
TD            65536
SOLVENT       CDCl3
NS            16
DS            2
SWH           6188.119 Hz
FIDRES        0.094423 Hz
AQ            5.2953587 sec
RG            203
DW            80.800 usec
DE            6.50 usec
TE            298.0 K
D1            1.00000000 sec
TDO           1

```

```

===== CHANNEL f1 =====
NUC1           1H
P1            13.70 usec
PL1           1.90 dB
PL1W          8.36853981 W
SF01          300.1418535 MHz
SI            32768
SF            300.1400060 MHz
WDW           EM
SSB           0
LB            0.30 Hz
GB            0
PC            1.00

```



```

EXPNO          1
PROCNO         1
Date_          20141204
Time          10.56
INSTRUM       spect
PROBHD        5 mm PABBO BB-
PULPROG       zgpg30
TD            65536
SOLVENT       CDCl3
NS            1024
DS            4
SWH           18028.846 Hz
FIDRES        0.275098 Hz
AQ            1.8175818 sec
RG            203
DW            27.733 usec
DE            6.50 usec
TE            298.0 K
D1            2.00000000 sec
D11           0.03000000 sec
TDO           1

```

```

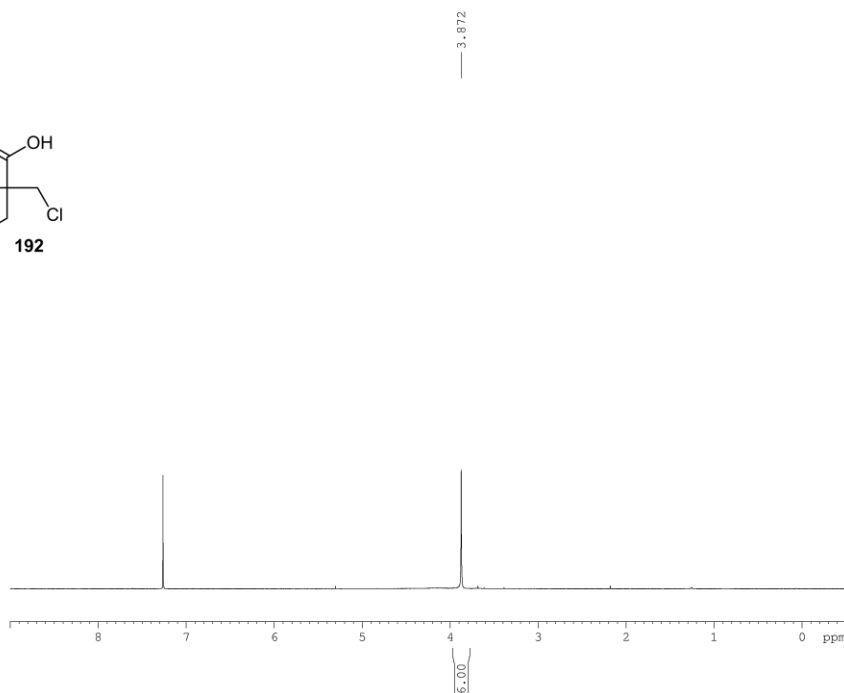
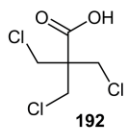
===== CHANNEL f1 =====
NUC1           13C
P1            10.82 usec
PL1           0.00 dB
PL1W          30.14263725 W
SF01          75.4778101 MHz

```

```

===== CHANNEL f2 =====
CPDPRG2       waltz16
NUC2           1H
PCPD2         100.00 usec
PL2           1.90 dB
PL12          19.17 dB
PL13          23.94 dB
PL1W          8.36853981 W
PL12W         0.15690966 W
PL13W         0.05231782 W
SF02          300.1412006 MHz
SI            32768
SF            75.4702653 MHz
WDW           EM
SSB           0
LB            1.00 Hz
GB            0
PC            1.40

```

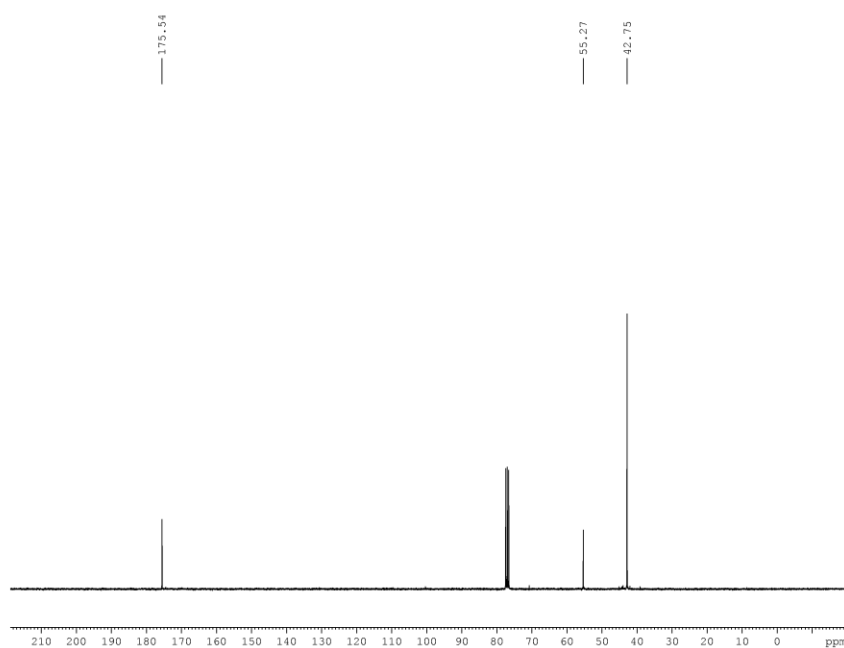



```

EXPNO      1
PROCNO     1
Date_      20140221
Time       8.52
INSTRUM    spect
PROBHD     5 mm PABBO BB-
PULPROG    zg30
TD          65536
SOLVENT    CDCl3
NS          16
DS          2
SWH         6188.119 Hz
FIDRES     0.094423 Hz
AQ          5.2953587 sec
RG          203
DW          80.800 usec
DE          6.50 usec
TE          298.0 K
D1          1.0000000 sec
TDO        1
    
```

```

===== CHANNEL f1 =====
NUC1       1H
P1         13.70 usec
PL1        1.90 dB
PL1W       8.36853981 W
SF01       300.1418535 MHz
SI         32768
SF         300.1400052 MHz
WDW        EM
SSB        0
LB         0.30 Hz
GB         0
PC         1.00
    
```



```

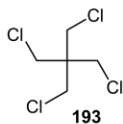
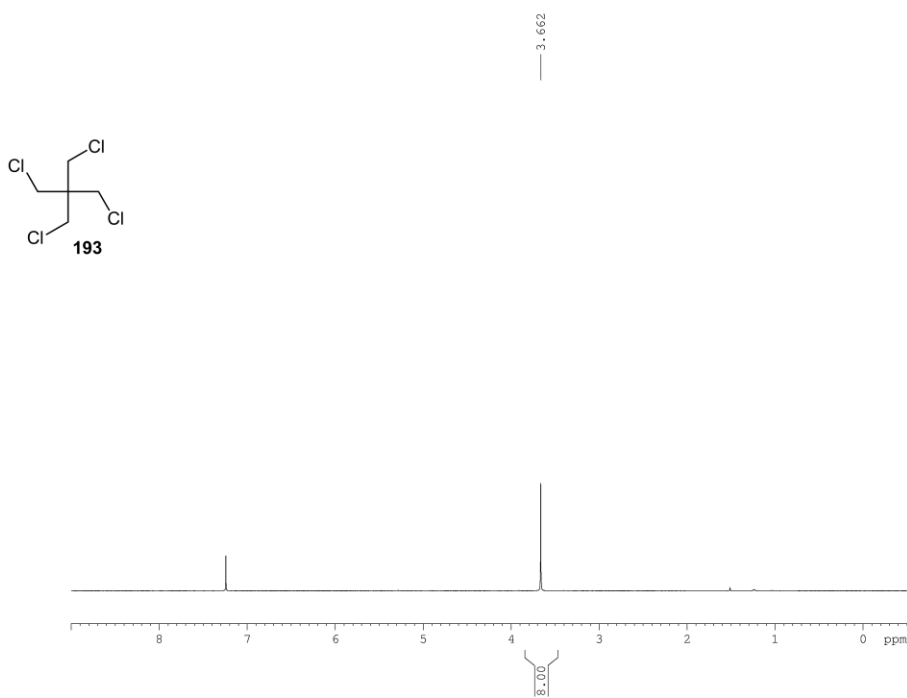
EXPNO      2
PROCNO     1
Date_      20140220
Time       15.19
INSTRUM    spect
PROBHD     5 mm PABBO BB-
PULPROG    zgpg30
TD          65536
SOLVENT    CDCl3
NS          765
DS          4
SWH        18028.846 Hz
FIDRES     0.275098 Hz
AQ         1.8175818 sec
RG          203
DW         27.733 usec
DE          6.50 usec
TE          298.1 K
D1          2.0000000 sec
D11         0.0300000 sec
TDO        1
    
```

```

===== CHANNEL f1 =====
NUC1       13C
P1         10.82 usec
PL1        0.00 dB
PL1W       30.14263725 W
SF01       75.4778101 MHz
    
```

```

===== CHANNEL f2 =====
CPDPRG2    waltz16
NUC2       1H
PCPD2     100.00 usec
PL2        1.90 dB
PL12       19.17 dB
PL13       23.94 dB
PL1W       8.36853981 W
PL12W      0.15690966 W
PL13W      0.05231782 W
SF02       300.1412006 MHz
SI         32768
SF         75.4702675 MHz
WDW        EM
SSB        0
LB         1.00 Hz
GB         0
PC         1.40
    
```



```

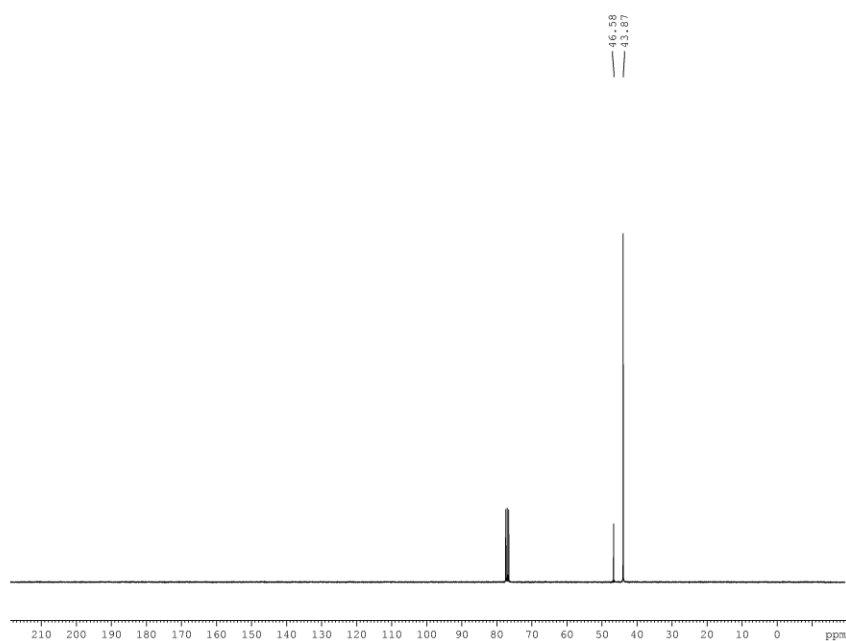
EXPNO          1
PROCNO         1
Date_          20140228
Time           11.12
INSTRUM       spect
PROBHD        5 mm PABBO BB-
PULPROG       zg30
TD             65536
SOLVENT       CDCl3
NS             16
DS             2
SWH           6188.119 Hz
FIDRES        0.094423 Hz
AQ            5.2953587 sec
RG            203
DW            80.800 usec
DE            6.50 usec
TE            298.0 K
D1            1.0000000 sec
TDO           1

```

```

===== CHANNEL f1 =====
NUC1           1H
P1            13.70 usec
PL1           1.90 dB
PL1W          8.36853981 W
SF01          300.1418535 MHz
SI            32768
SF            300.1400113 MHz
WDW           EM
SSB           0
LB            0.30 Hz
GB            0
PC            1.00

```



```

EXPNO          2
PROCNO         1
Date_          20140227
Time           11.40
INSTRUM       spect
PROBHD        5 mm PABBO BB-
PULPROG       zgpg30
TD             65536
SOLVENT       CDCl3
NS            1024
DS             4
SWH           18028.846 Hz
FIDRES        0.275098 Hz
AQ            1.8175818 sec
RG            203
DW            27.733 usec
DE            6.50 usec
TE            298.0 K
D1            2.0000000 sec
D11           0.0300000 sec
TDO           1

```

```

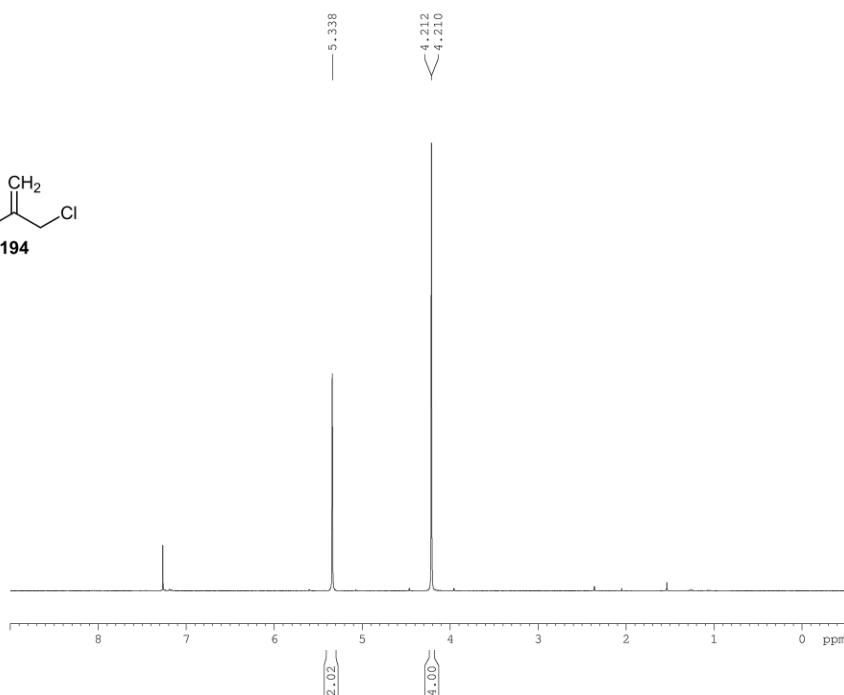
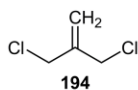
===== CHANNEL f1 =====
NUC1           13C
P1            10.82 usec
PL1           0.00 dB
PL1W          30.14263725 W
SF01          75.4778101 MHz

```

```

===== CHANNEL f2 =====
CPDPRG2       waltz16
NUC2           1H
PCPD2         100.00 usec
PL2           1.90 dB
PL12          19.17 dB
PL13          23.94 dB
PL1W          8.36853981 W
PL12W         0.15690966 W
PL13W         0.05231782 W
SF02          300.1412006 MHz
SI            32768
SF            75.4702696 MHz
WDW           EM
SSB           0
LB            1.00 Hz
GB            0
PC            1.40

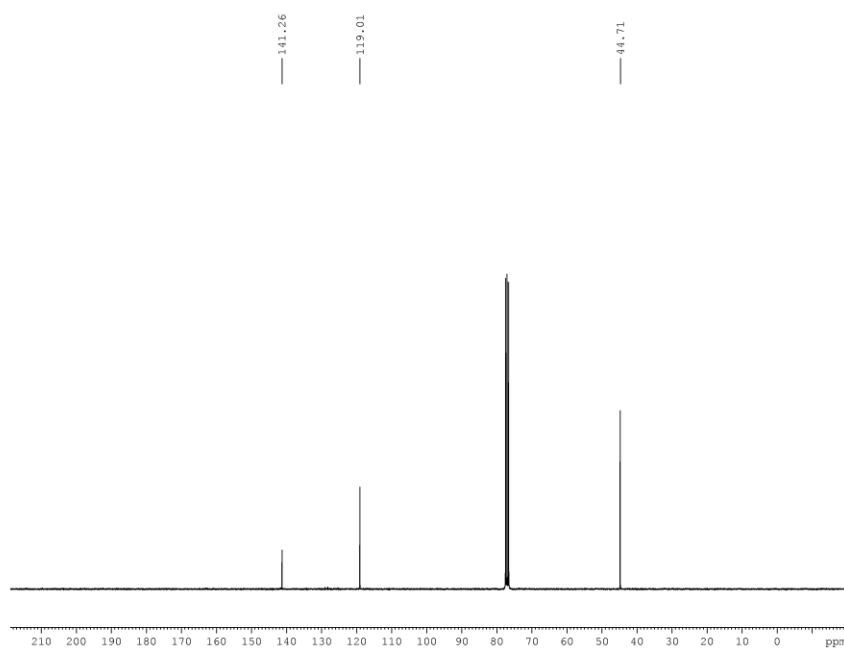
```



```

EXPNO 1
PROCNO 1
Date_ 20140222
Time 17.49
INSTRUM spect
PROBHD 5 mm PABBO BB-
PULPROG zg30
TD 65536
SOLVENT CDCl3
NS 16
DS 2
SWH 6188.119 Hz
FIDRES 0.094423 Hz
AQ 5.2953587 sec
RG 203
DW 80.800 usec
DE 6.50 usec
TE 298.0 K
D1 1.0000000 sec
TDO 1

===== CHANNEL f1 =====
NUC1 1H
P1 13.70 usec
PL1 1.90 dB
PL1W 8.36853981 W
SF01 300.1418535 MHz
SI 32768
SF 300.1400046 MHz
WDW EM
SSB 0
LB 0.30 Hz
GB 0
PC 1.00
    
```

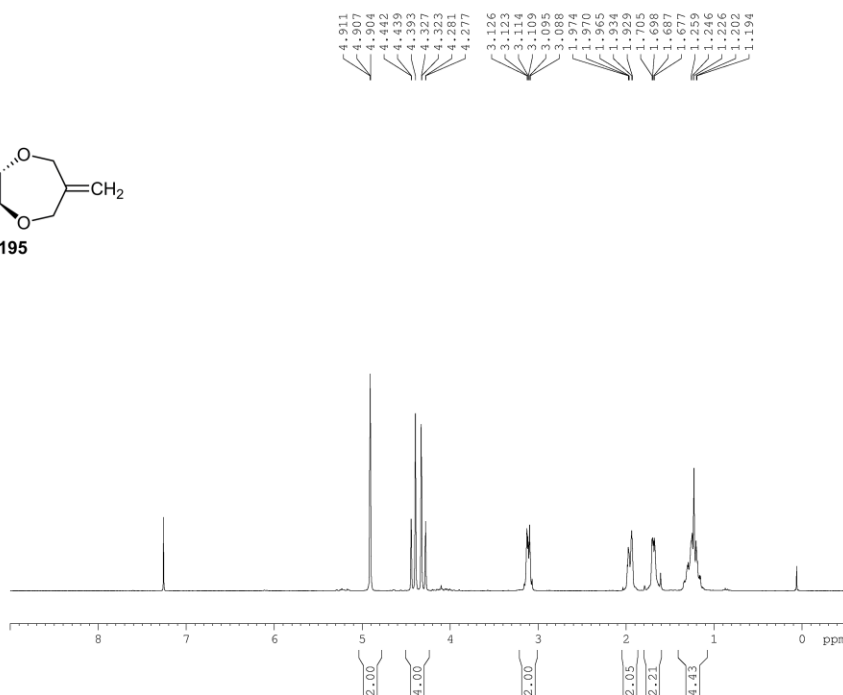
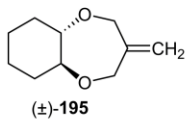


```

EXPNO 2
PROCNO 1
Date_ 20140223
Time 2.28
INSTRUM spect
PROBHD 5 mm PABBO BB-
PULPROG zgpg30
TD 65536
SOLVENT CDCl3
NS 8000
DS 4
SWH 18028.846 Hz
FIDRES 0.275098 Hz
AQ 1.8175818 sec
RG 203
DW 27.733 usec
DE 6.50 usec
TE 298.0 K
D1 2.0000000 sec
D11 0.0300000 sec
TDO 1

===== CHANNEL f1 =====
NUC1 13C
P1 10.82 usec
PL1 0.00 dB
PL1W 30.14263725 W
SF01 75.4778101 MHz

===== CHANNEL f2 =====
CPDPRG2 waltz16
NUC2 1H
PCPD2 100.00 usec
PL2 1.90 dB
PL12 19.17 dB
PL13 23.94 dB
PL2W 8.36853981 W
PL12W 0.15690966 W
PL13W 0.05231782 W
SF02 300.1412006 MHz
SI 32768
SF 75.4702655 MHz
WDW EM
SSB 0
LB 1.00 Hz
GB 0
PC 1.40
    
```

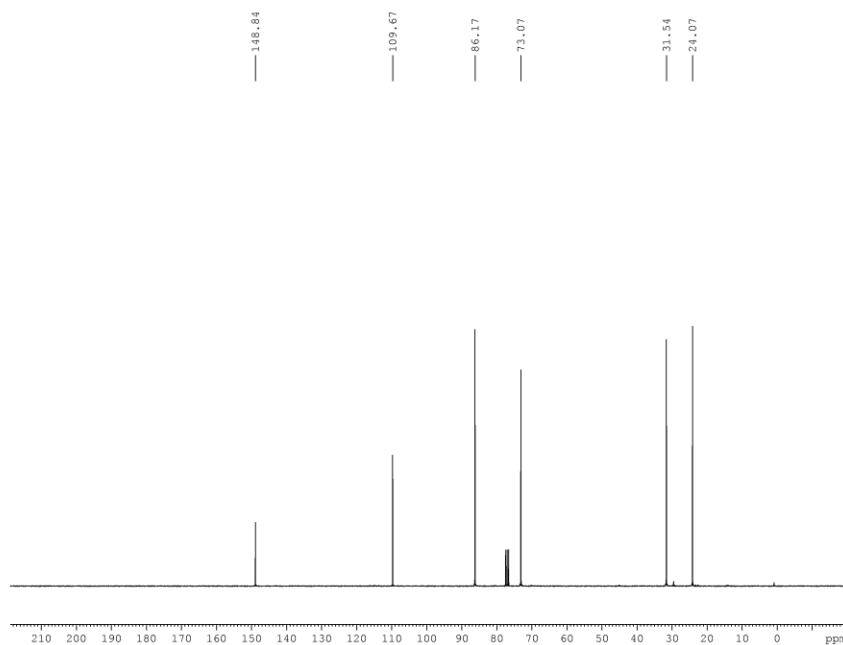


```

EXPNO 1
PROCNO 1
Date_ 20130319
Time 15.53
INSTRUM spect
PROBHD 5 mm PABBO BH-
PULPROG zg30
TD 65536
SOLVENT CDCl3
NS 32
DS 2
SWH 6188.119 Hz
FIDRES 0.094423 Hz
AQ 5.2953587 sec
RG 90.5
DW 80.800 usec
DE 6.50 usec
TE 298.0 K
D1 1.0000000 sec
TDO 1
    
```

```

===== CHANNEL f1 =====
NUC1 1H
P1 13.70 usec
PL1 1.90 dB
PL1W 8.36853981 W
SF01 300.1418535 MHz
SI 32768
SF 300.1400068 MHz
WDW EM
SSB 0
LB 0.30 Hz
GB 0
PC 1.00
    
```



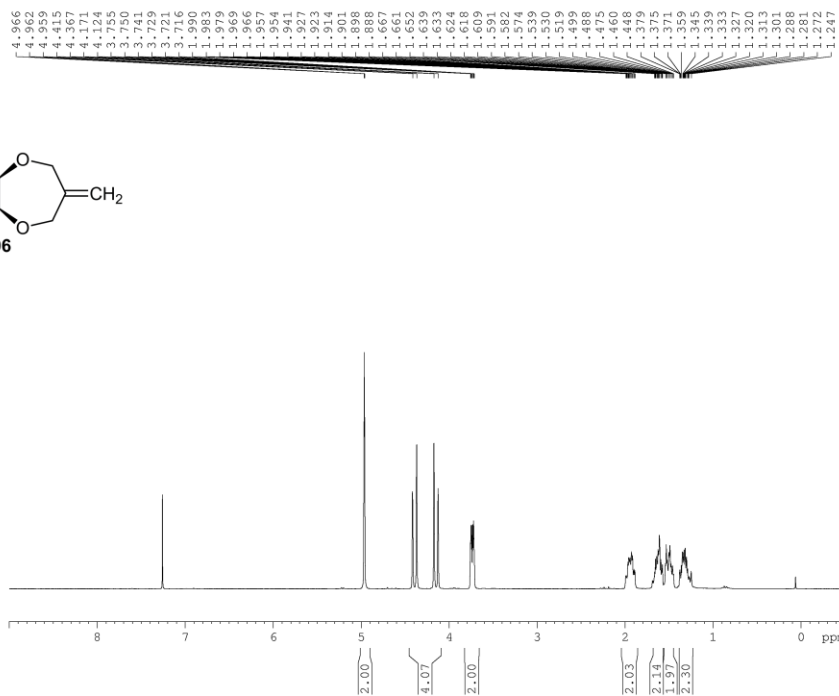
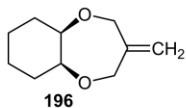
```

EXPNO 1
PROCNO 1
Date_ 20130319
Time 16.20
INSTRUM spect
PROBHD 5 mm PABBO BH-
PULPROG zgpg30
TD 65536
SOLVENT CDCl3
NS 815
DS 4
SWH 18028.846 Hz
FIDRES 0.275098 Hz
AQ 1.8175818 sec
RG 203
DW 27.733 usec
DE 6.50 usec
TE 298.0 K
D1 2.0000000 sec
D11 0.0300000 sec
TDO 1
    
```

```

===== CHANNEL f1 =====
NUC1 13C
P1 10.82 usec
PL1 0.00 dB
PL1W 30.14263725 W
SF01 75.4778101 MHz

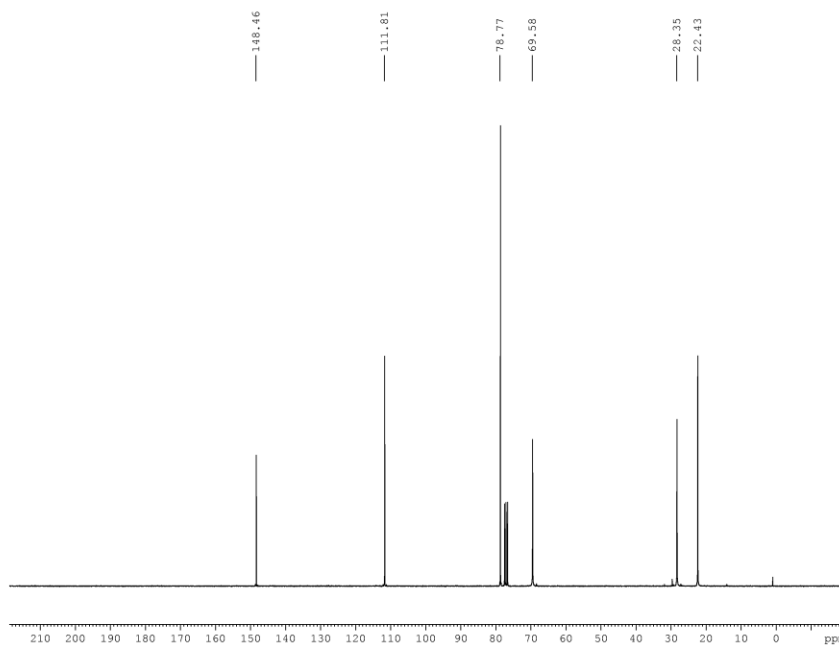
===== CHANNEL f2 =====
CPDPRG2 waltz16
NUC2 1H
PCPD2 100.00 usec
PL2 1.90 dB
PL12 19.17 dB
PL13 23.94 dB
PL1W 8.36853981 W
PL12W 0.15690966 W
PL13W 0.05231782 W
SF02 300.1412006 MHz
SI 32768
SF 75.4702742 MHz
WDW EM
SSB 0
LB 1.00 Hz
GB 0
PC 1.40
    
```



```

EXPNO 1
PROCNO 1
Date_ 20130417
Time 15.53
INSTRUM spect
PROBHD 5 mm PABBO BB-
PULPROG zg30
TD 65536
SOLVENT CDC13
NS 32
DS 2
SWH 6188.119 Hz
FIDRES 0.094423 Hz
AQ 5.2953587 sec
RG 90.5
DW 80.800 usec
DE 6.50 usec
TE 298.0 K
D1 1.0000000 sec
TDO 1

===== CHANNEL f1 =====
NUC1 1H
P1 13.70 usec
PL1 1.90 dB
PL1W 8.36853981 W
SF01 300.1418535 MHz
SI 32768
SF 300.1400067 MHz
WDW EM
SSB 0
LB 0.30 Hz
GB 0
PC 1.00
    
```

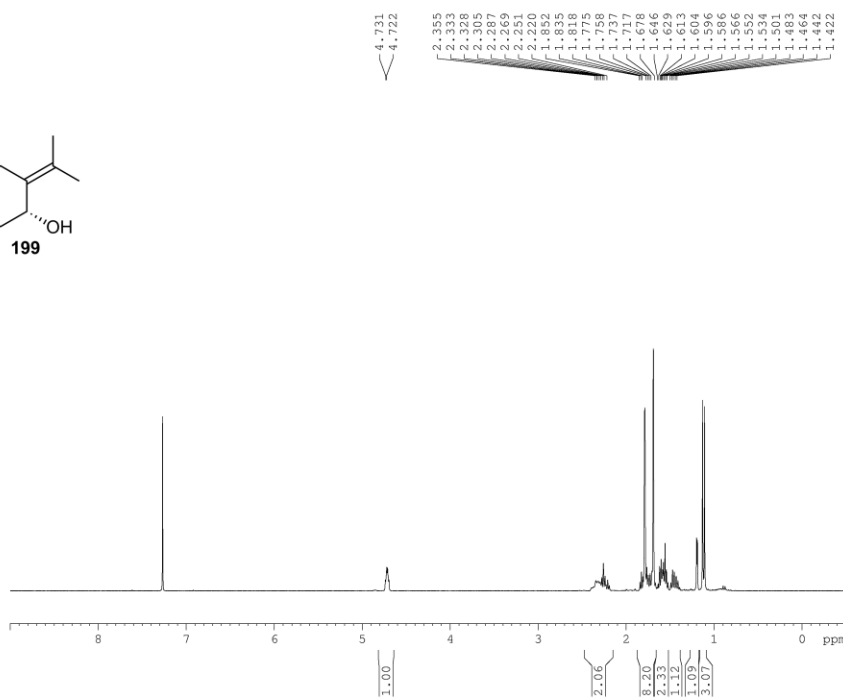
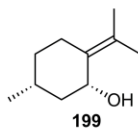


```

EXPNO 2
PROCNO 1
Date_ 20130418
Time 19.16
INSTRUM spect
PROBHD 5 mm PABBO BB-
PULPROG zgpg30
TD 65536
SOLVENT CDC13
NS 2048
DS 4
SWH 18028.846 Hz
FIDRES 0.275098 Hz
AQ 1.8175818 sec
RG 203
DW 27.733 usec
DE 6.50 usec
TE 298.0 K
D1 2.0000000 sec
D11 0.0300000 sec
TDO 1

===== CHANNEL f1 =====
NUC1 13C
P1 10.82 usec
PL1 0.00 dB
PL1W 30.14263725 W
SF01 75.4778101 MHz

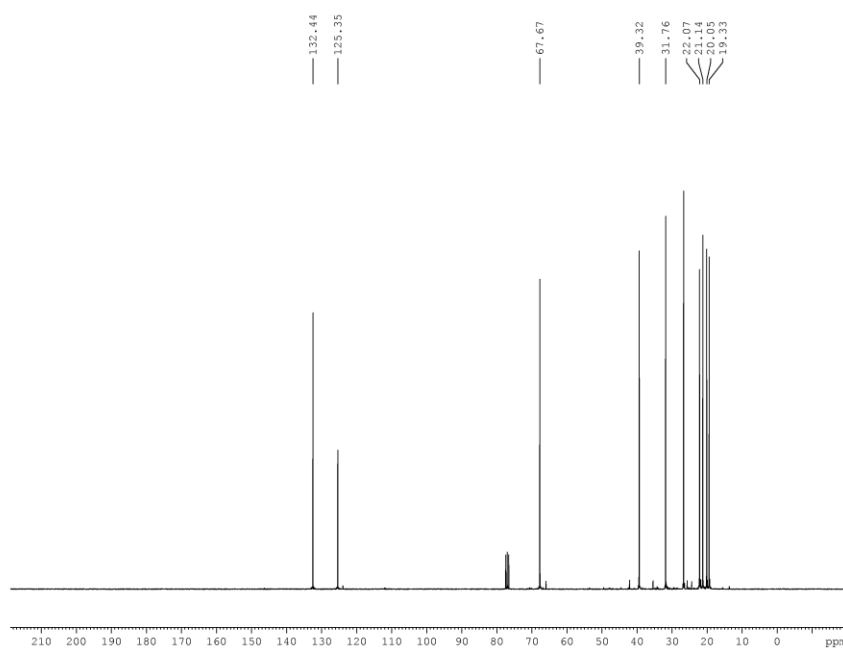
===== CHANNEL f2 =====
CPDPRG2 waltz16
NUC2 1H
PCPD2 100.00 usec
PL2 1.90 dB
PL12 19.17 dB
PL13 23.94 dB
PL1W 8.36853981 W
PL12W 0.15690966 W
PL13W 0.05231782 W
SF02 300.1412006 MHz
SI 32768
SF 75.4702704 MHz
WDW EM
SSB 0
LB 1.00 Hz
GB 0
PC 1.40
    
```



```

EXPNO 1
PROCNO 1
Date_ 20130430
Time 10.50
INSTRUM spect
PROBHD 5 mm PABBO BB-
PULPROG zg30
TD 65536
SOLVENT CDC13
NS 16
DS 2
SWH 6188.119 Hz
FIDRES 0.094423 Hz
AQ 5.2953587 sec
RG 203
DW 80.800 usec
DE 6.50 usec
TE 298.0 K
D1 1.0000000 sec
TDO 1

===== CHANNEL f1 =====
NUC1 1H
P1 13.70 usec
PL1 1.90 dB
PL1W 8.36853981 W
SFO1 300.1418535 MHz
SI 32768
SF 300.1400037 MHz
WDW EM
SSB 0
LB 0.30 Hz
GB 0
PC 1.00
    
```

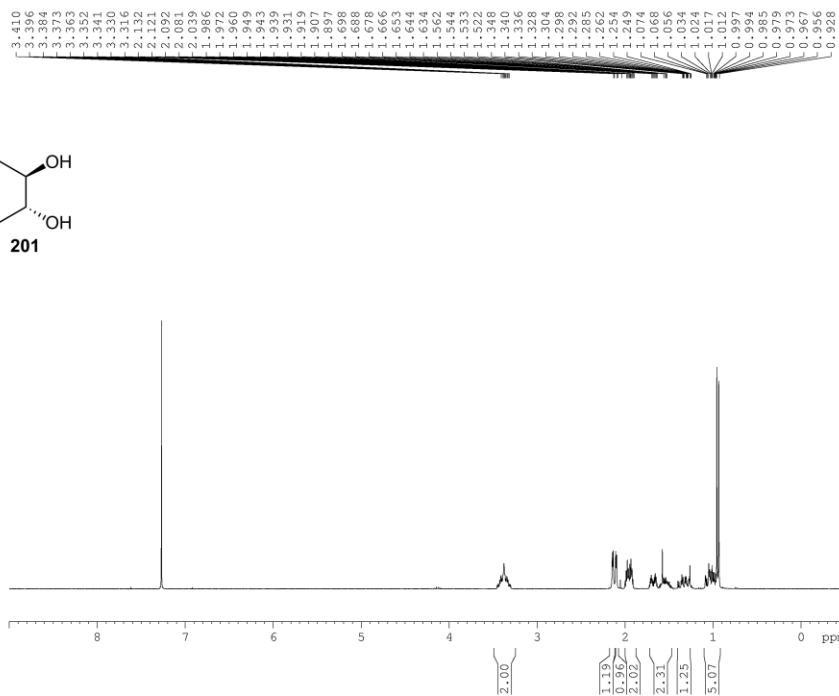
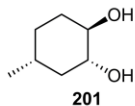


```

EXPNO 1
PROCNO 1
Date_ 20130430
Time 12.07
INSTRUM spect
PROBHD 5 mm PABBO BB-
PULPROG zgpg30
TD 65536
SOLVENT CDC13
NS 1024
DS 4
SWH 18028.846 Hz
FIDRES 0.275098 Hz
AQ 1.8175818 sec
RG 203
DW 27.733 usec
DE 6.50 usec
TE 298.0 K
D1 2.0000000 sec
D11 0.0300000 sec
TDO 1

===== CHANNEL f1 =====
NUC1 13C
P1 10.82 usec
PL1 0.00 dB
PL1W 30.14263725 W
SFO1 75.4778101 MHz

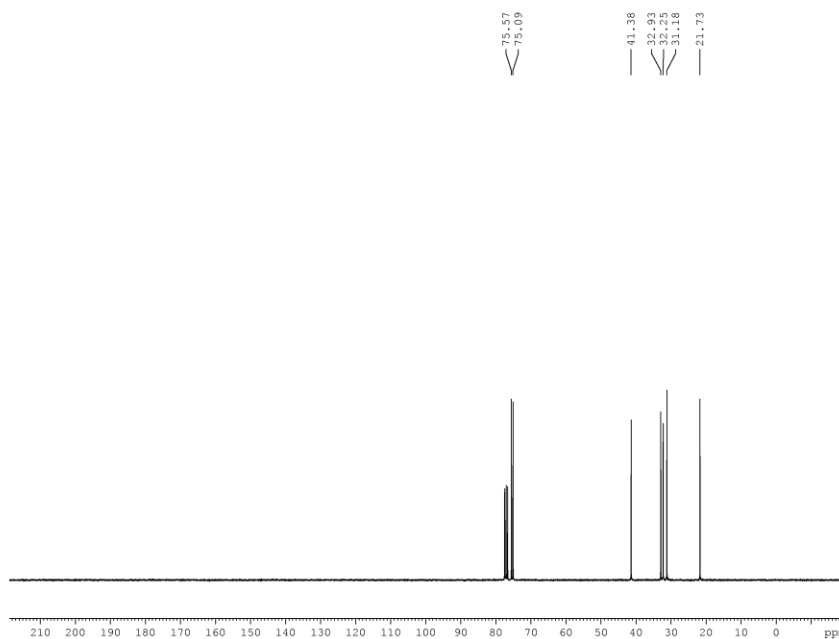
===== CHANNEL f2 =====
CPDPRG2 waltz16
NUC2 1H
PCPD2 100.00 usec
PL2 1.90 dB
PL12 19.17 dB
PL13 23.94 dB
PL1W 8.36853981 W
PL12W 0.15690966 W
PL13W 0.05231782 W
SFO2 300.1412006 MHz
SI 32768
SF 75.4702870 MHz
WDW EM
SSB 0
LB 1.00 Hz
GB 0
PC 1.40
    
```



```

EXPNO 6
PROCNO 1
Date_ 20130625
Time 9.30
INSTRUM spect
PROBHD 5 mm PABBO BB-
PULPROG zg30
TD 65536
SOLVENT CDCl3
NS 16
DS 2
SWH 6188.119 Hz
FIDRES 0.094423 Hz
AQ 5.2953587 sec
RG 203
DM 80.800 usec
DE 6.50 usec
TE 298.0 K
D1 1.0000000 sec
TDO 1

===== CHANNEL f1 =====
NUC1 1H
P1 13.70 usec
PL1 1.90 dB
PL1W 8.36853981 W
SF01 300.1418535 MHz
SI 32768
SF 300.1400030 MHz
WDW EM
SSB 0
LB 0.30 Hz
GB 0
PC 1.00
    
```

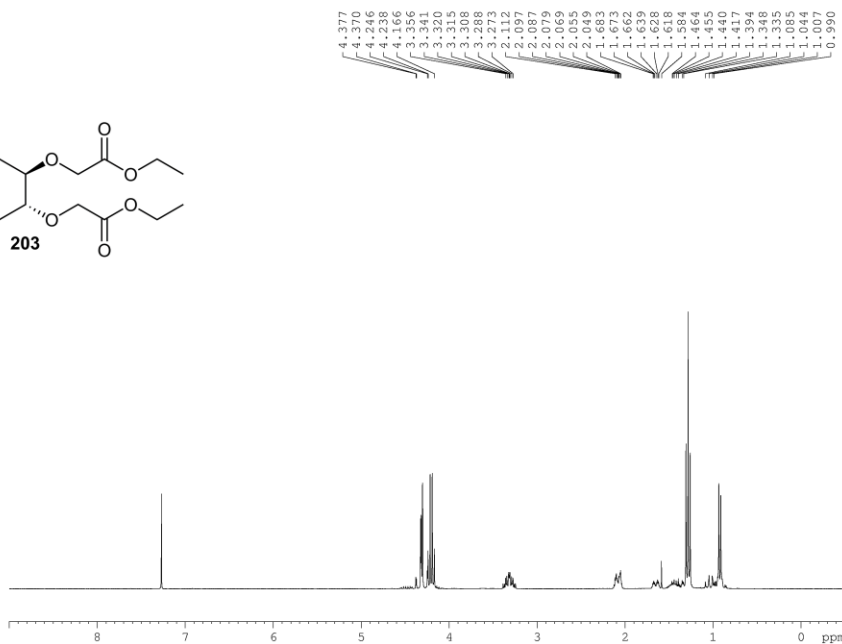
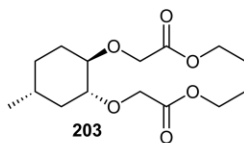


```

EXPNO 2
PROCNO 1
Date_ 20130623
Time 11.38
INSTRUM spect
PROBHD 5 mm PABBO BB-
PULPROG zgpg30
TD 65536
SOLVENT CDCl3
NS 586
DS 4
SWH 18028.846 Hz
FIDRES 0.275098 Hz
AQ 1.8175818 sec
RG 203
DM 27.733 usec
DE 6.50 usec
TE 298.0 K
D1 2.0000000 sec
D11 0.0300000 sec
TDO 1

===== CHANNEL f1 =====
NUC1 13C
P1 10.82 usec
PL1 0.00 dB
PL1W 30.14263725 W
SF01 75.4778101 MHz

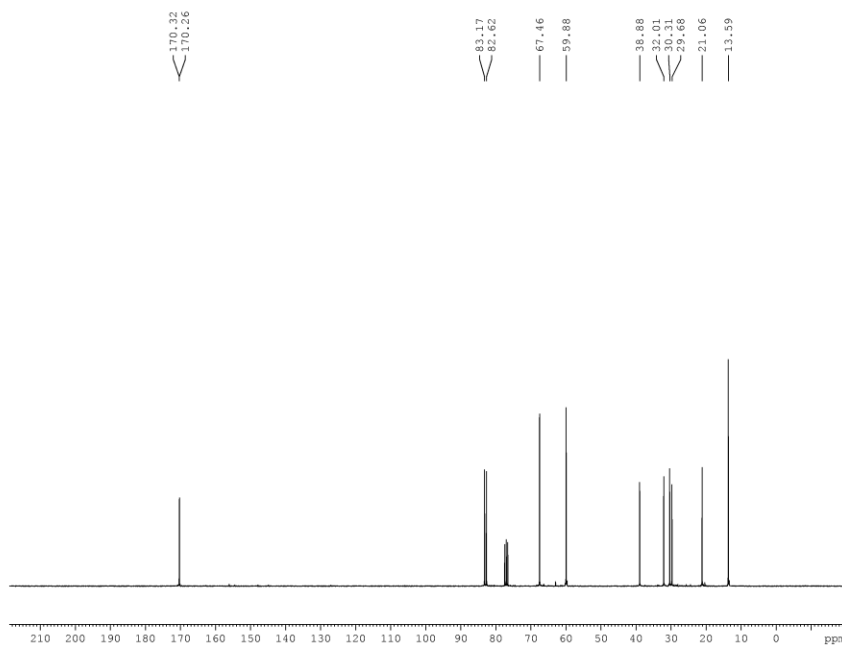
===== CHANNEL f2 =====
CPDPRG2 waltz16
NUC2 1H
PCPD2 100.00 usec
PL2 1.90 dB
PL12 19.17 dB
PL13 23.94 dB
PL1W 8.36853981 W
PL12W 0.15690966 W
PL13W 0.05231782 W
SF02 300.1412006 MHz
SI 32768
SF 75.4702704 MHz
WDW EM
SSB 0
LB 1.00 Hz
GB 0
PC 1.40
    
```

```

EXPNO 1
PROCNO 1
Date_ 20131107
Time 10.08
INSTRUM spect
PROBHD 5 mm PABBO BB-
PULPROG zg30
TD 65536
SOLVENT CDC13
NS 16
DS 2
SWH 6188.119 Hz
FIDRES 0.094423 Hz
AQ 5.2953587 sec
RG 203
DW 80.800 usec
DE 6.50 usec
TE 298.0 K
D1 1.0000000 sec
TDO 1

===== CHANNEL f1 =====
NUC1 1H
P1 13.70 usec
PL1 1.90 dB
PL1W 8.36853981 W
SFO1 300.1418535 MHz
SI 32768
SF 300.1400031 MHz
WDW EM
SSB 0
LB 0.30 Hz
GB 0
PC 1.00
    
```

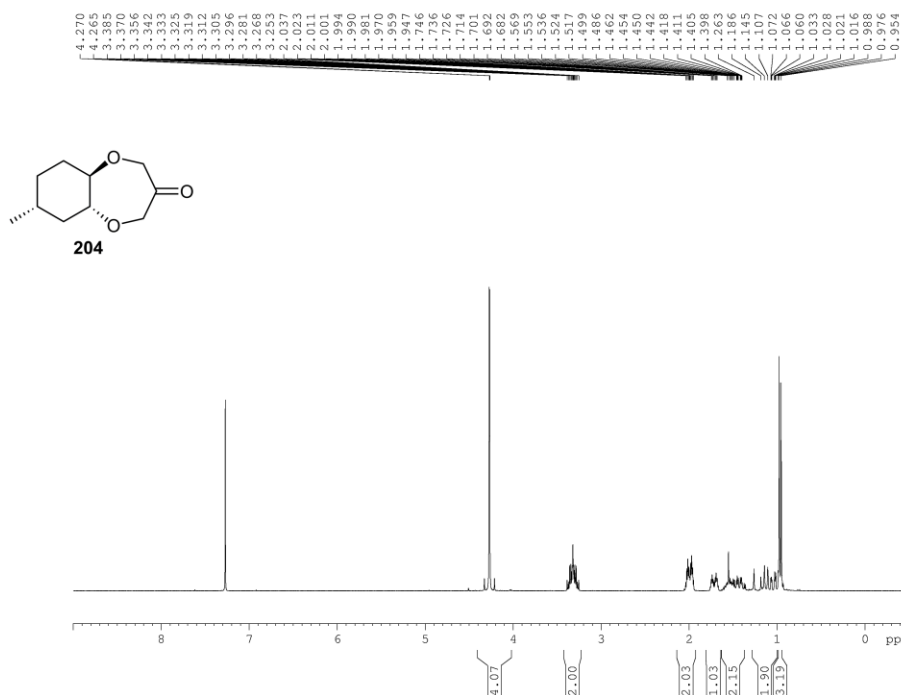


```

EXPNO 2
PROCNO 1
Date_ 20131107
Time 12.07
INSTRUM spect
PROBHD 5 mm PABBO BB-
PULPROG zgpg30
TD 65536
SOLVENT CDC13
NS 1024
DS 4
SWH 18028.846 Hz
FIDRES 0.275098 Hz
AQ 1.8175818 sec
RG 203
DW 27.733 usec
DE 6.50 usec
TE 298.0 K
D1 2.0000000 sec
D11 0.0300000 sec
TDO 1

===== CHANNEL f1 =====
NUC1 13C
P1 10.82 usec
PL1 0.00 dB
PL1W 30.14263725 W
SFO1 75.4778101 MHz

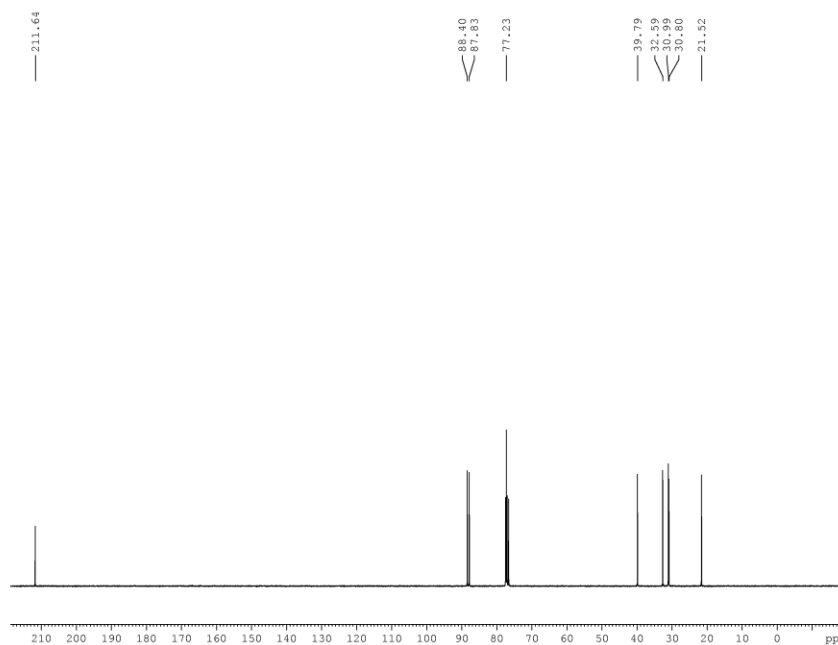
===== CHANNEL f2 =====
CPDPRG2 waltz16
NUC2 1H
PCPD2 100.00 usec
PL2 1.90 dB
PL12 19.17 dB
PL13 23.94 dB
PL2W 8.36853981 W
PL12W 0.15690966 W
PL13W 0.05231782 W
SFO2 300.1412006 MHz
SI 32768
SF 75.4702907 MHz
WDW EM
SSB 0
LB 1.00 Hz
GB 0
PC 1.40
    
```



```

EXPNO 1
PROCNO 1
Date_ 20131119
Time 13.25
INSTRUM spect
PROBHD 5 mm PABBO BB-
PULPROG zg30
TD 65536
SOLVENT CDC13
NS 16
DS 2
SWH 6188.119 Hz
FIDRES 0.094423 Hz
AQ 5.2953587 sec
RG 203
DW 80.800 usec
DE 6.50 usec
TE 298.0 K
D1 1.0000000 sec
TDO 1

===== CHANNEL f1 =====
NUC1 1H
P1 13.70 usec
PL1 1.90 dB
PL1W 8.36853981 W
SF01 300.1418535 MHz
SI 32768
SF 300.1400027 MHz
WDW EM
SSB 0
LB 0.30 Hz
GB 0
PC 1.00
    
```

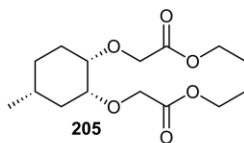


```

EXPNO 1
PROCNO 1
Date_ 20131119
Time 15.29
INSTRUM spect
PROBHD 5 mm PABBO BB-
PULPROG zgpg30
TD 65536
SOLVENT CDC13
NS 1024
DS 4
SWH 18028.846 Hz
FIDRES 0.275098 Hz
AQ 1.8175818 sec
RG 203
DW 27.733 usec
DE 6.50 usec
TE 298.0 K
D1 2.0000000 sec
D11 0.0300000 sec
TDO 1

===== CHANNEL f1 =====
NUC1 13C
P1 10.82 usec
PL1 0.00 dB
PL1W 30.14263725 W
SF01 75.4778101 MHz

===== CHANNEL f2 =====
CPDPRG2 waltz16
NUC2 1H
PCPD2 100.00 usec
PL2 1.90 dB
PL12 19.17 dB
PL13 23.94 dB
PL1W 8.36853981 W
PL12W 0.15690966 W
PL13W 0.05231782 W
SF02 300.1412006 MHz
SI 32768
SF 75.4702675 MHz
WDW EM
SSB 0
LB 1.00 Hz
GB 0
PC 1.40
    
```



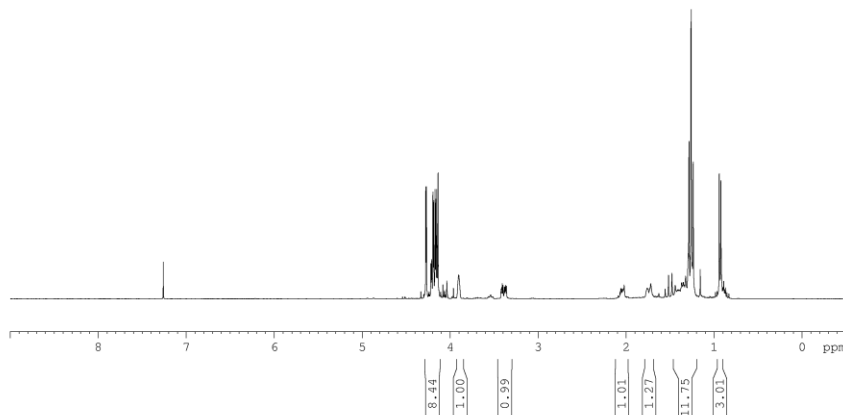
4.217
4.208
4.146
4.080
4.036
3.961
3.910
3.410
3.405
3.397
3.381
3.372
3.366
3.366
2.037
2.034
2.021
1.799
1.796
1.756
1.716
1.516
1.477
1.439
1.376
1.367
1.357
1.337
1.321
1.292
1.268
1.245
1.245
1.245
1.245
0.899



```

EXPNO      1
PROCNO     1
Date_      20131029
Time       8.54
INSTRUM    spect
PROBHD     5 mm PABBO BB-
PULPROG    zg30
TD         65536
SOLVENT    CDCl3
NS         16
DS         2
SWH        6188.119 Hz
FIDRES     0.094423 Hz
AQ         5.2953587 sec
RG         64
DW         80.800 usec
DE         6.50 usec
TE         298.0 K
D1         1.00000000 sec
TDO        1

===== CHANNEL f1 =====
NUC1       1H
P1         13.70 usec
PL1        1.90 dB
PL1W       8.36853981 W
SFO1       300.1418535 MHz
SI         32768
SF         300.1400059 MHz
WDW        EM
SSB        0
LB         0.30 Hz
GB         0
PC         1.00
    
```



170.97
170.54

80.69
74.78
67.21
65.32
60.34
60.17

33.79
30.98
28.45
27.74
21.75
13.89
13.87

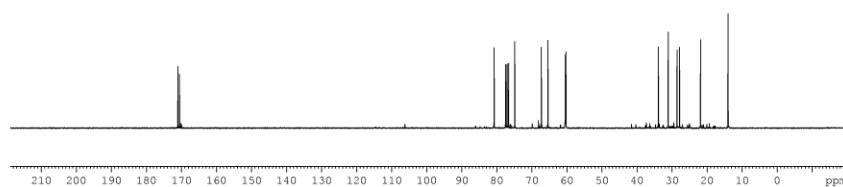


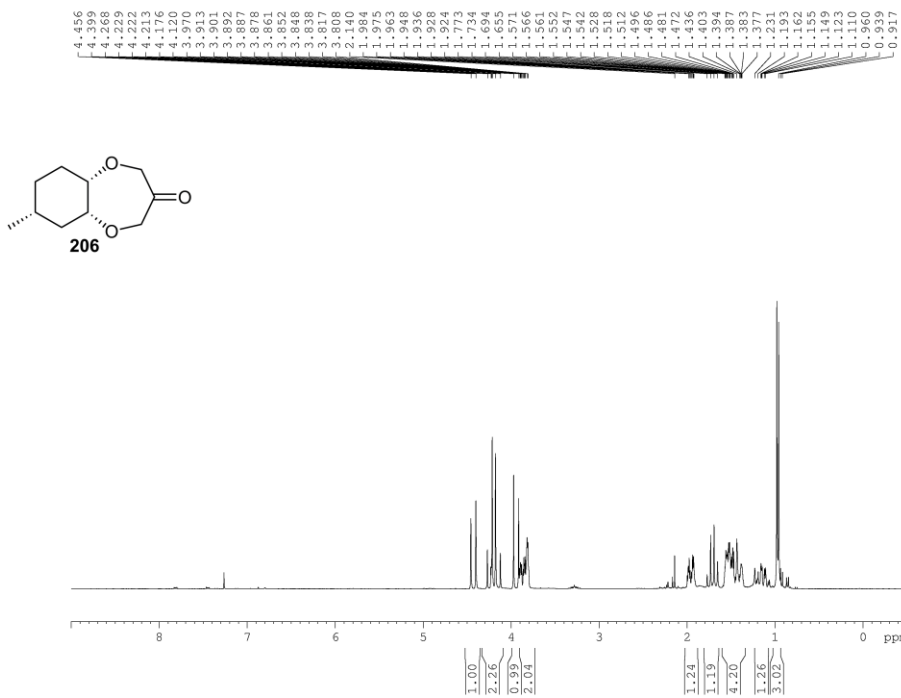
```

EXPNO      1
PROCNO     1
Date_      20131028
Time       16.03
INSTRUM    spect
PROBHD     5 mm PABBO BB-
PULPROG    zgpg30
TD         65536
SOLVENT    CDCl3
NS         723
DS         4
SWH        18028.846 Hz
FIDRES     0.275098 Hz
AQ         1.8175818 sec
RG         203
DW         27.733 usec
DE         6.50 usec
TE         298.0 K
D1         2.00000000 sec
D11        0.03000000 sec
TDO        1

===== CHANNEL f1 =====
NUC1       13C
P1         10.82 usec
PL1        0.00 dB
PL1W       30.14263725 W
SFO1       75.4778101 MHz

===== CHANNEL f2 =====
CPDPRG2    waltz16
NUC2       1H
PCPD2     100.00 usec
PL2        1.90 dB
PL12       19.17 dB
PL13       23.94 dB
PL1W       8.36853981 W
PL12W      0.15690966 W
PL13W      0.05231782 W
SFO2       300.1412006 MHz
SI         32768
SF         75.4702785 MHz
WDW        EM
SSB        0
LB         1.00 Hz
GB         0
PC         1.40
    
```

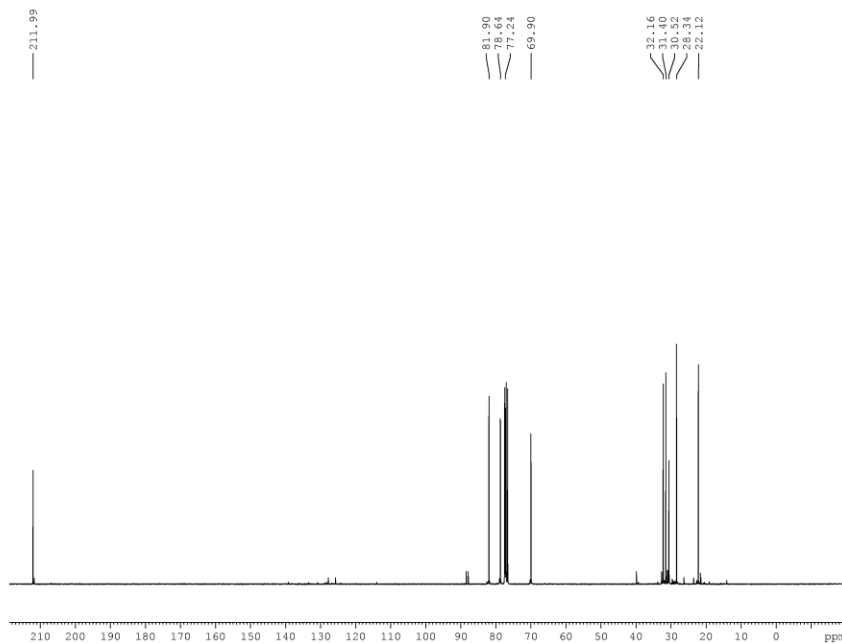




```

EXPNO 1
PROCNO 1
Date_ 20131104
Time 17.48
INSTRUM spect
PROBHD 5 mm PABBO BB-
PULPROG zg30
TD 65536
SOLVENT CDC13
NS 16
DS 2
SWH 6188.119 Hz
FIDRES 0.094423 Hz
AQ 5.2953587 sec
RG 40.3
DW 80.800 usec
DE 6.50 usec
TE 298.0 K
D1 1.0000000 sec
TDO 1

===== CHANNEL f1 =====
NUC1 1H
P1 13.70 usec
PL1 1.90 dB
PL1W 8.36853981 W
SF01 300.1418535 MHz
SI 32768
SF 300.1400050 MHz
WDW EM
SSB 0
LB 0.30 Hz
GB 0
PC 1.00
    
```

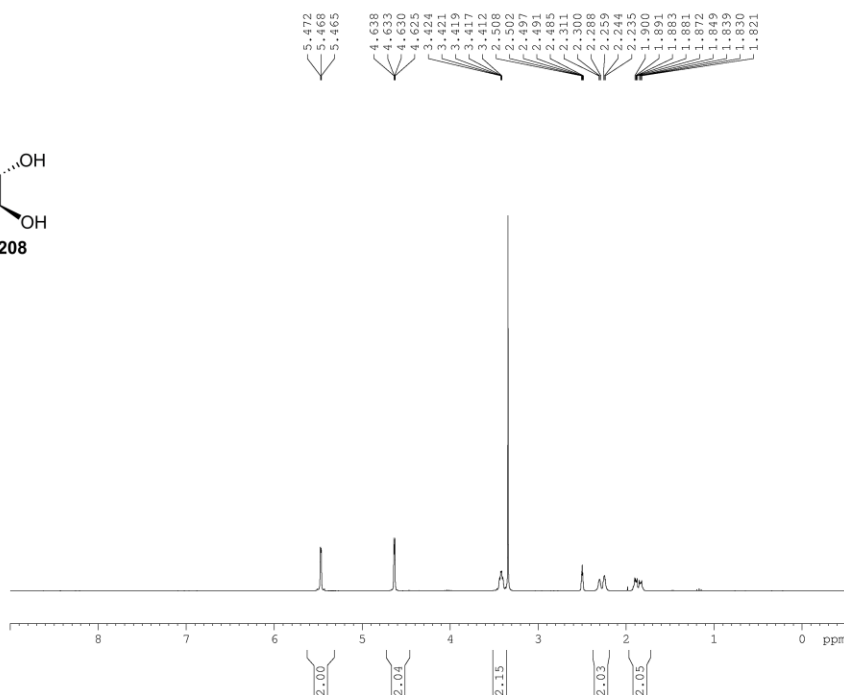
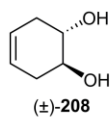


```

EXPNO 1
PROCNO 1
Date_ 20131105
Time 5.58
INSTRUM spect
PROBHD 5 mm PABBO BB-
PULPROG zgpg30
TD 65536
SOLVENT CDC13
NS 10000
DS 4
SWH 18028.846 Hz
FIDRES 0.275098 Hz
AQ 1.8175818 sec
RG 203
DW 27.733 usec
DE 6.50 usec
TE 298.0 K
D1 2.0000000 sec
D11 0.0300000 sec
TDO 1

===== CHANNEL f1 =====
NUC1 13C
P1 10.82 usec
PL1 0.00 dB
PL1W 30.14263725 W
SF01 75.4778101 MHz

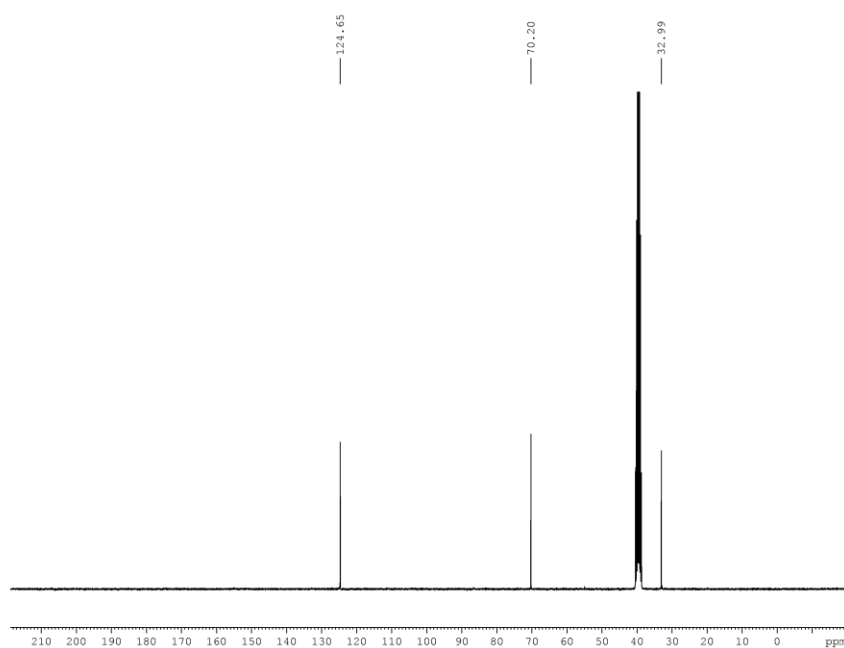
===== CHANNEL f2 =====
CPDPRG2 waltz16
NUC2 1H
PCPD2 100.00 usec
PL2 1.90 dB
PL12 19.17 dB
PL13 23.94 dB
PL2W 8.36853981 W
PL12W 0.15690966 W
PL13W 0.05231782 W
SF02 300.1412006 MHz
SI 32768
SF 75.4702687 MHz
WDW EM
SSB 0
LB 1.00 Hz
GB 0
PC 1.40
    
```



```

EXPNO          2
PROCNO         1
Date_          20131009
Time           18.33
INSTRUM       spect
PROBHD        5 mm PABBO BB-
PULPROG       zg30
TD             65536
SOLVENT       DMSO
NS             16
DS             2
SWH           6188.119 Hz
FIDRES       0.094423 Hz
AQ           5.2953587 sec
RG            80.6
DW            80.800 usec
DE            6.50 usec
TE            298.0 K
D1            1.00000000 sec
TDO           1

===== CHANNEL f1 =====
NUC1           1H
P1             13.70 usec
PL1            1.90 dB
PL1W           8.36853981 W
SF01          300.1418535 MHz
SI             32768
SF            300.1400019 MHz
WDW            EM
SSB            0
LB             0.30 Hz
GB             0
PC             1.00
    
```

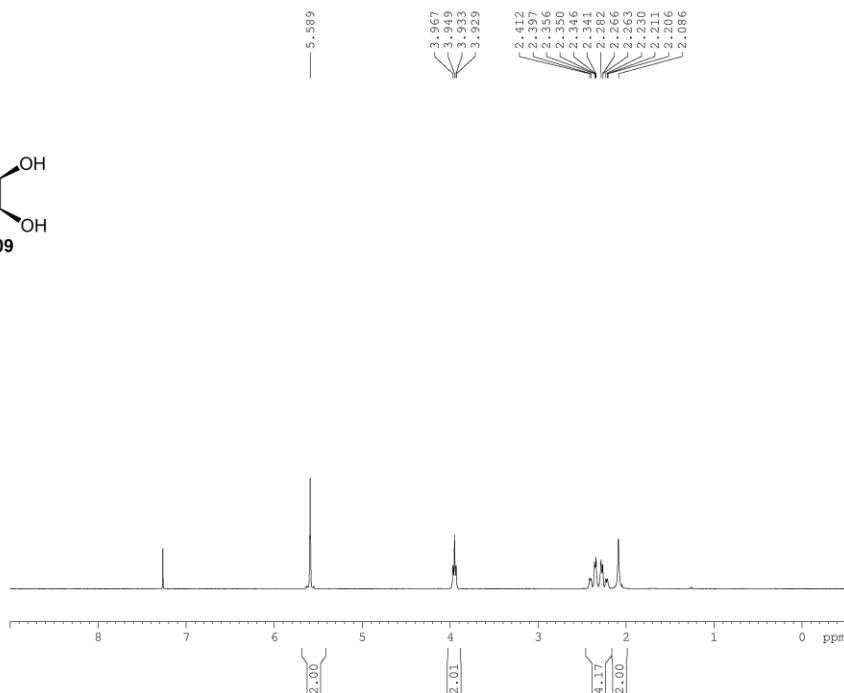
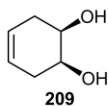


```

EXPNO          7
PROCNO         1
Date_          20131023
Time           5.45
INSTRUM       spect
PROBHD        5 mm PABBO BB-
PULPROG       zgpg30
TD             65536
SOLVENT       DMSO
NS             12000
DS             4
SWH           18028.846 Hz
FIDRES       0.275098 Hz
AQ           1.8175818 sec
RG            203
DW            27.733 usec
DE            6.50 usec
TE            298.0 K
D1            2.00000000 sec
D11           0.03000000 sec
TDO           1

===== CHANNEL f1 =====
NUC1           13C
P1             10.82 usec
PL1            0.00 dB
PL1W           30.14263725 W
SF01          75.4778101 MHz

===== CHANNEL f2 =====
CPDPRG2       waltz16
NUC2           1H
PCPD2         100.00 usec
PL2            1.90 dB
PL12           19.17 dB
PL13           23.94 dB
PL1W           8.36853981 W
PL12W         0.15690966 W
PL13W         0.05231782 W
SF02          300.1412006 MHz
SI             32768
SF            75.4702981 MHz
WDW            EM
SSB            0
LB             1.00 Hz
GB             0
PC             1.40
    
```

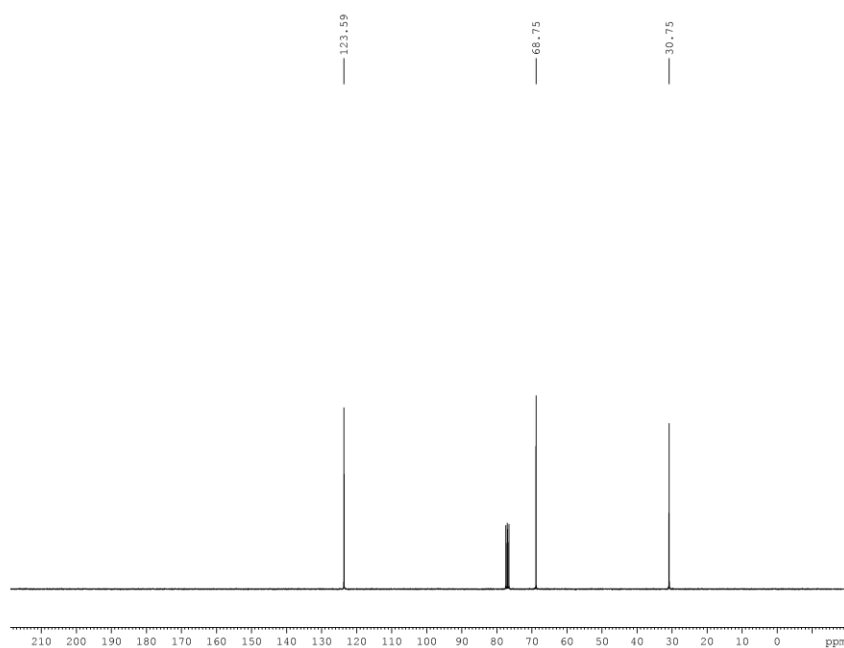


```

EXPNO 1
PROCNO 1
Date_ 20140108
Time 15.47
INSTRUM spect
PROBHD 5 mm PABBO BB-
PULPROG zg30
TD 65536
SOLVENT CDCl3
NS 16
DS 2
SWH 6188.119 Hz
FIDRES 0.094423 Hz
AQ 5.2953587 sec
RG 203
DM 80.800 usec
DE 6.50 usec
TE 298.0 K
D1 1.0000000 sec
TDO 1
    
```

```

===== CHANNEL f1 =====
NUC1 1H
P1 13.70 usec
PL1 1.90 dB
PL1W 8.36853981 W
SF01 300.1418535 MHz
SI 32768
SF 300.1400047 MHz
WDW EM
SSB 0
LB 0.30 Hz
GB 0
PC 1.00
    
```



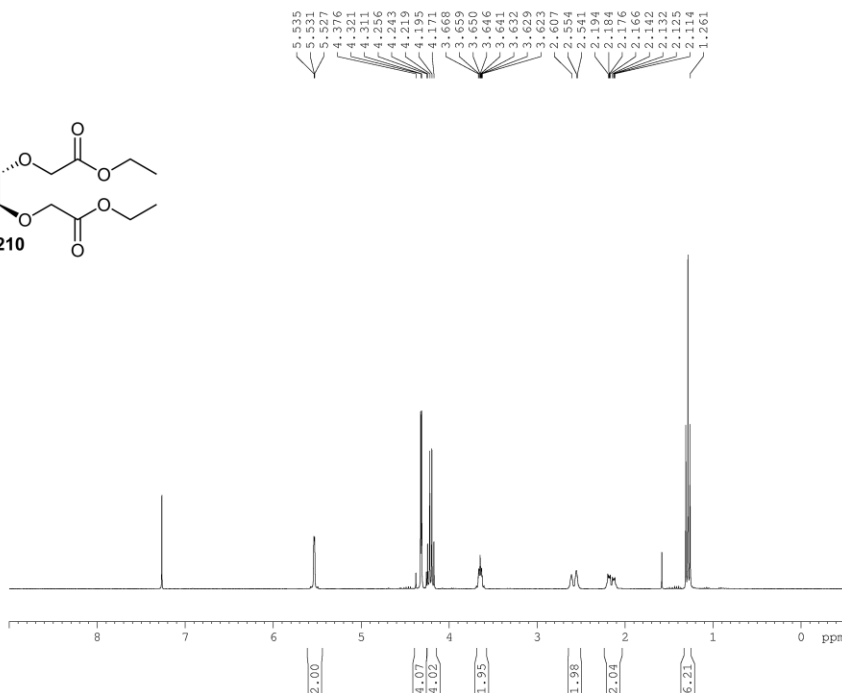
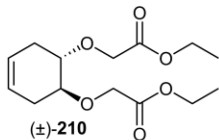
```

EXPNO 1
PROCNO 1
Date_ 20140108
Time 14.50
INSTRUM spect
PROBHD 5 mm PABBO BB-
PULPROG zgpg30
TD 65536
SOLVENT CDCl3
NS 782
DS 4
SWH 18028.846 Hz
FIDRES 0.275098 Hz
AQ 1.8175818 sec
RG 203
DM 27.733 usec
DE 6.50 usec
TE 298.0 K
D1 2.0000000 sec
D11 0.0300000 sec
TDO 1
    
```

```

===== CHANNEL f1 =====
NUC1 13C
P1 10.82 usec
PL1 0.00 dB
PL1W 30.14263725 W
SF01 75.4778101 MHz

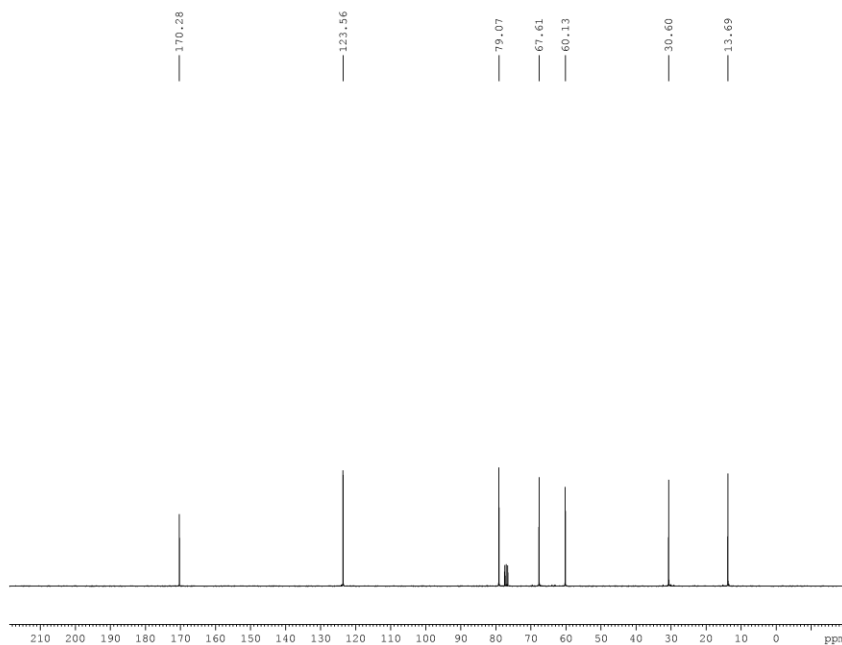
===== CHANNEL f2 =====
CPDPRG2 waltz16
NUC2 1H
PCPD2 100.00 usec
PL2 1.90 dB
PL12 19.17 dB
PL13 23.94 dB
PL1W 8.36853981 W
PL12W 0.15690966 W
PL13W 0.05231782 W
SF02 300.1412006 MHz
SI 32768
SF 75.4702744 MHz
WDW EM
SSB 0
LB 1.00 Hz
GB 0
PC 1.40
    
```



```

EXPNO 1
PROCNO 1
Date_ 20131113
Time 18.25
INSTRUM spect
PROBHD 5 mm PABBO BB-
PULPROG zg30
TD 65536
SOLVENT CDC13
NS 16
DS 2
SWH 6188.119 Hz
FIDRES 0.094423 Hz
AQ 5.2953587 sec
RG 203
DW 80.800 usec
DE 6.50 usec
TE 298.0 K
D1 1.0000000 sec
TDO 1

===== CHANNEL f1 =====
NUC1 1H
P1 13.70 usec
PL1 1.90 dB
PL1W 8.36853981 W
SFO1 300.1418535 MHz
SI 32768
SF 300.1400045 MHz
WDW EM
SSB 0
LB 0.30 Hz
GB 0
PC 1.00
    
```

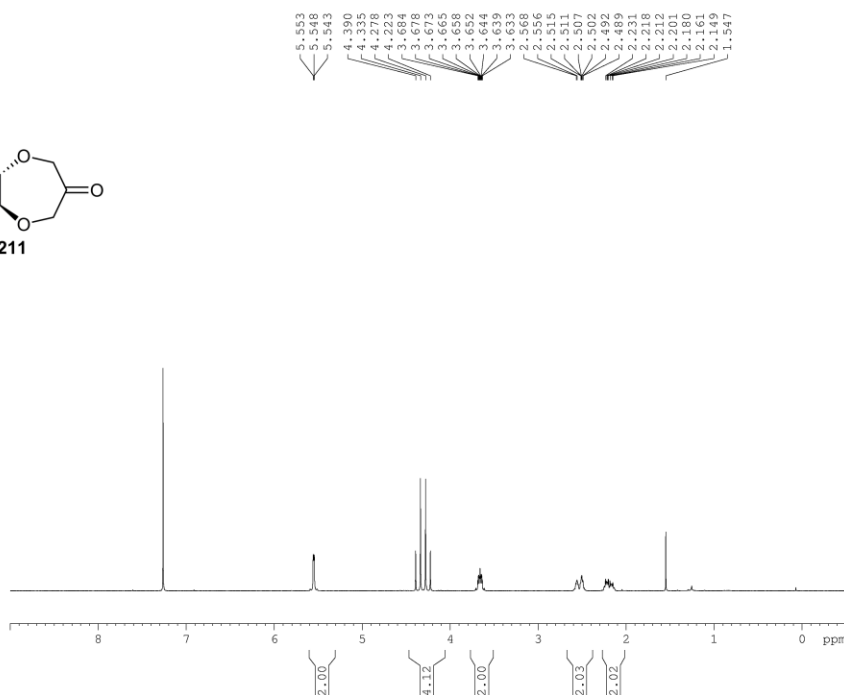
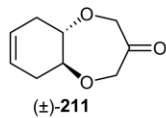


```

EXPNO 2
PROCNO 1
Date_ 20131113
Time 15.52
INSTRUM spect
PROBHD 5 mm PABBO BB-
PULPROG zgpg30
TD 65536
SOLVENT CDC13
NS 500
DS 4
SWH 18028.846 Hz
FIDRES 0.275098 Hz
AQ 1.8175818 sec
RG 203
DW 27.733 usec
DE 6.50 usec
TE 298.1 K
D1 2.0000000 sec
D11 0.0300000 sec
TDO 1

===== CHANNEL f1 =====
NUC1 13C
P1 10.82 usec
PL1 0.00 dB
PL1W 30.14263725 W
SFO1 75.4778101 MHz

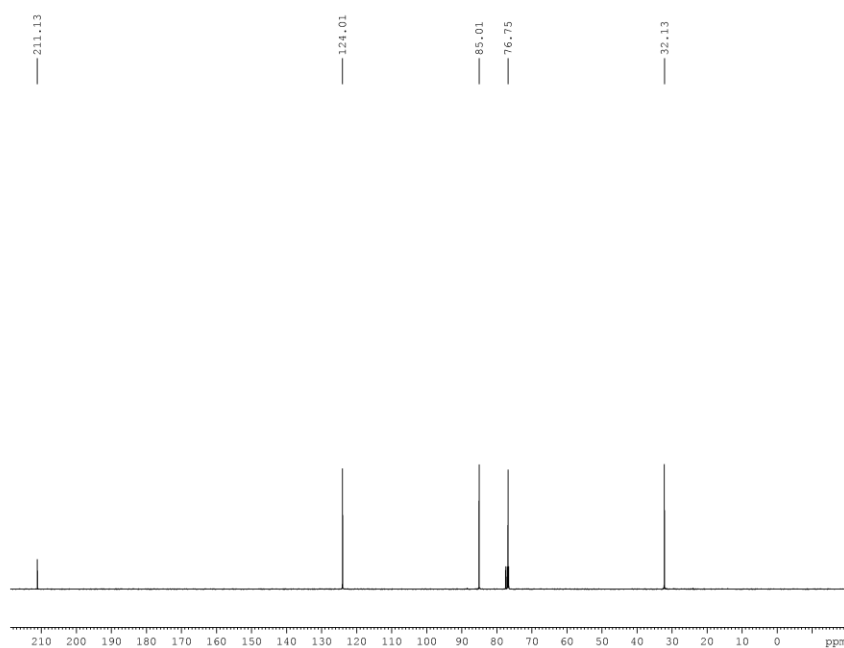
===== CHANNEL f2 =====
CPDPRG2 waltz16
NUC2 1H
PCPD2 100.00 usec
PL2 1.90 dB
PL12 19.17 dB
PL13 23.94 dB
PL1W 8.36853981 W
PL12W 0.15690966 W
PL13W 0.05231782 W
SFO2 300.1412006 MHz
SI 32768
SF 75.4702868 MHz
WDW EM
SSB 0
LB 1.00 Hz
GB 0
PC 1.40
    
```



```

EXPNO 1
PROCNO 1
Date_ 20131126
Time 13.05
INSTRUM spect
PROBHD 5 mm PABBO BB-
PULPROG zg30
TD 65536
SOLVENT CDC13
NS 16
DS 2
SWH 6188.119 Hz
FIDRES 0.094423 Hz
AQ 5.2953587 sec
RG 203
DW 80.800 usec
DE 6.50 usec
TE 294.7 K
D1 1.00000000 sec
TDO 1

===== CHANNEL f1 =====
NUC1 1H
P1 13.70 usec
PL1 1.90 dB
PL1W 8.36853981 W
SF01 300.1418535 MHz
SI 32768
SF 300.1400055 MHz
WDW EM
SSB 0
LB 0.30 Hz
GB 0
PC 1.00
    
```

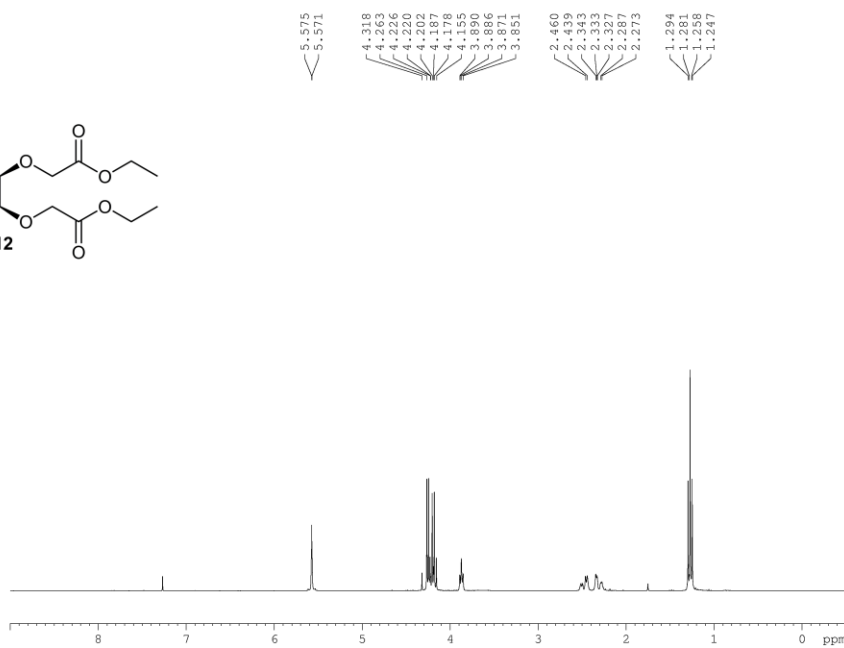
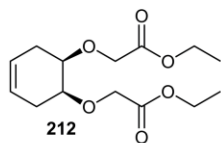


```

EXPNO 1
PROCNO 1
Date_ 20131125
Time 15.44
INSTRUM spect
PROBHD 5 mm PABBO BB-
PULPROG zgpg30
TD 65536
SOLVENT CDC13
NS 570
DS 4
SWH 18028.846 Hz
FIDRES 0.275098 Hz
AQ 1.8175818 sec
RG 203
DW 27.733 usec
DE 6.50 usec
TE 294.9 K
D1 2.00000000 sec
D11 0.03000000 sec
TDO 1

===== CHANNEL f1 =====
NUC1 13C
P1 10.82 usec
PL1 0.00 dB
PL1W 30.14263725 W
SF01 75.4778101 MHz

===== CHANNEL f2 =====
CPDPRG2 waltz16
NUC2 1H
PCPD2 100.00 usec
PL2 1.90 dB
PL12 19.17 dB
PL13 23.94 dB
PL2W 8.36853981 W
PL12W 0.15690966 W
PL13W 0.05231782 W
SF02 300.1412006 MHz
SI 32768
SF 75.4702734 MHz
WDW EM
SSB 0
LB 1.00 Hz
GB 0
PC 1.40
    
```

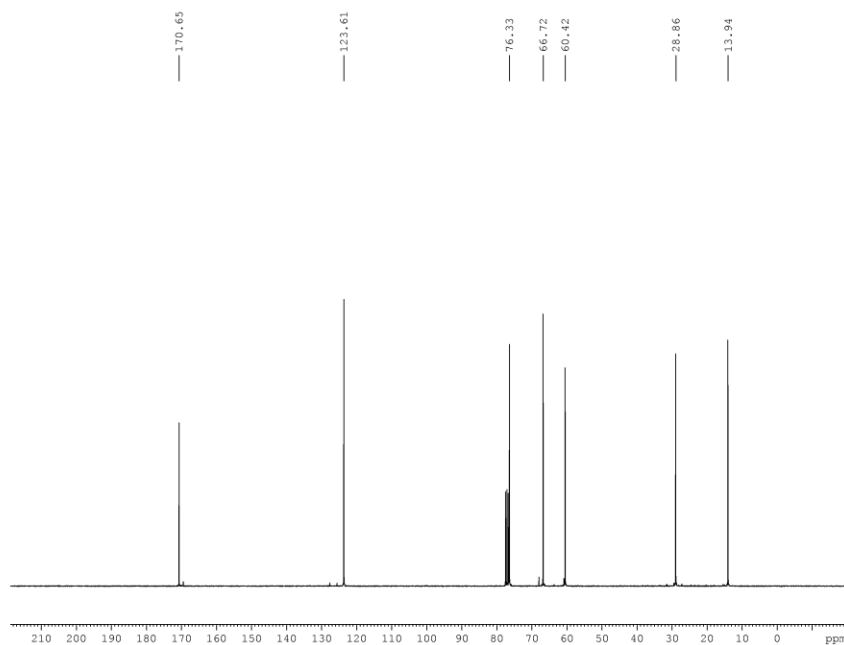



```

EXPNO 1
PROCNO 1
Date_ 20140117
Time 9.18
INSTRUM spect
PROBHD 5 mm PABBO BB-
PULPROG zg30
TD 65536
SOLVENT CDC13
NS 16
DS 2
SWH 6188.119 Hz
FIDRES 0.094423 Hz
AQ 5.2953587 sec
RG 71.8
DW 80.800 usec
DE 6.50 usec
TE 298.0 K
D1 1.0000000 sec
TDO 1
    
```

```

===== CHANNEL f1 =====
NUC1 1H
P1 13.70 usec
PL1 1.90 dB
PL1W 8.36853981 W
SFO1 300.1418535 MHz
SI 32768
SF 300.1400037 MHz
WDW EM
SSB 0
LB 0.30 Hz
GB 0
PC 1.00
    
```



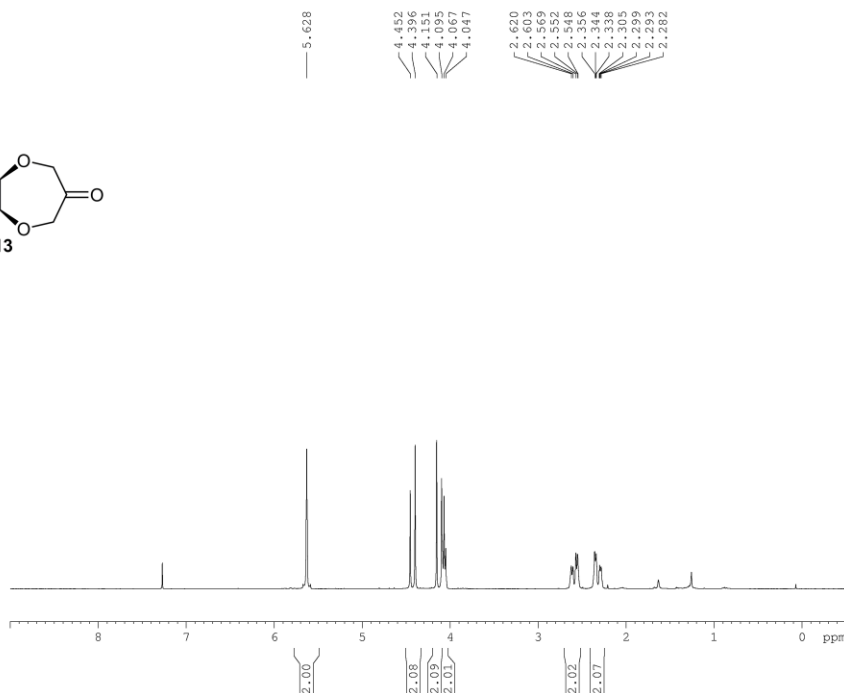
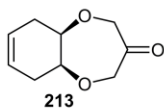
```

EXPNO 1
PROCNO 1
Date_ 20140114
Time 23.04
INSTRUM spect
PROBHD 5 mm PABBO BB-
PULPROG zgpg30
TD 65536
SOLVENT CDC13
NS 5000
DS 4
SWH 18028.846 Hz
FIDRES 0.275098 Hz
AQ 1.8175818 sec
RG 203
DW 27.733 usec
DE 6.50 usec
TE 298.0 K
D1 2.0000000 sec
D11 0.0300000 sec
TDO 1
    
```

```

===== CHANNEL f1 =====
NUC1 13C
P1 10.82 usec
PL1 0.00 dB
PL1W 30.14263725 W
SFO1 75.4778101 MHz

===== CHANNEL f2 =====
CPDPRG2 waltz16
NUC2 1H
PCPD2 100.00 usec
PL2 1.90 dB
PL12 19.17 dB
PL13 23.94 dB
PL2W 8.36853981 W
PL12W 0.15690966 W
PL13W 0.05231782 W
SFO2 300.1412006 MHz
SI 32768
SF 75.4702765 MHz
WDW EM
SSB 0
LB 1.00 Hz
GB 0
PC 1.40
    
```

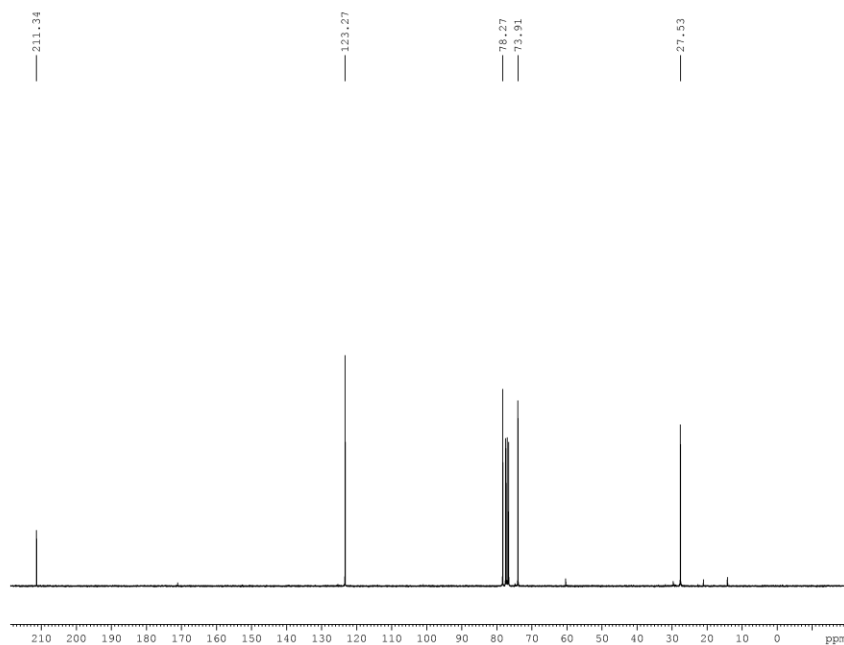


```

EXPNO          2
PROCNO         1
Date_          20140130
Time           14.35
INSTRUM       spect
PROBHD        5 mm PABBO BB-
PULPROG       zg30
TD            65536
SOLVENT       CDC13
NS            16
DS            2
SWH           6188.119 Hz
FIDRES        0.094423 Hz
AQ            5.2953587 sec
RG            80.6
DW            80.800 usec
DE            6.50 usec
TE            298.0 K
D1            1.0000000 sec
TD0           1
    
```

```

===== CHANNEL f1 =====
NUC1           1H
P1            13.70 usec
PL1           1.90 dB
PL1W          8.36853981 W
SFO1          300.1418535 MHz
SI            32768
SF           300.1400028 MHz
WDW           EM
SSB           0
LB            0.30 Hz
GB            0
PC            1.00
    
```



```

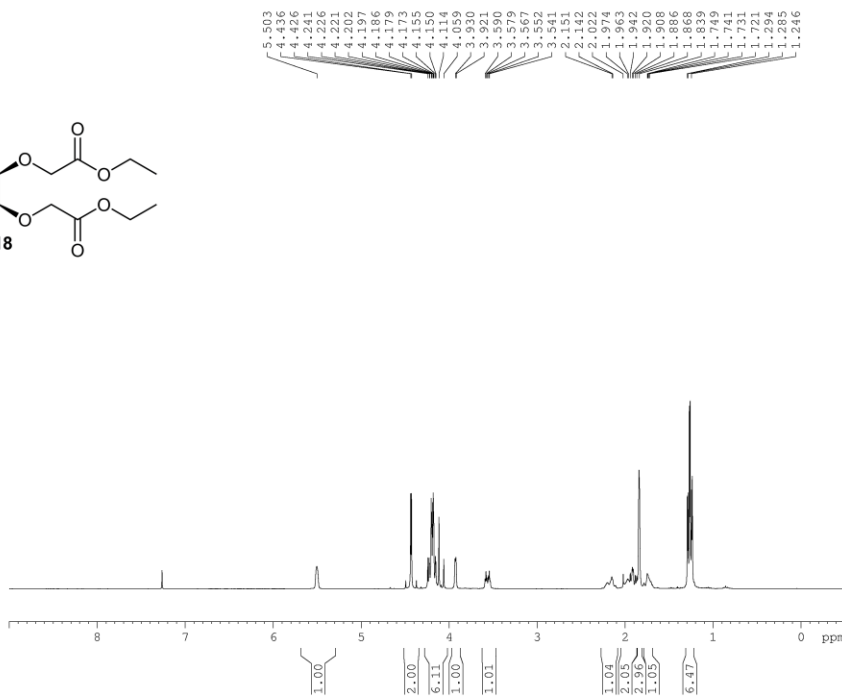
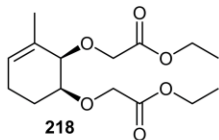
EXPNO          2
PROCNO         1
Date_          20140130
Time           9.05
INSTRUM       spect
PROBHD        5 mm PABBO BB-
PULPROG       zgpg30
TD            65536
SOLVENT       CDC13
NS            1800
DS            4
SWH           18028.846 Hz
FIDRES        0.275098 Hz
AQ            1.8175818 sec
RG            203
DW            27.733 usec
DE            6.50 usec
TE            298.0 K
D1            2.0000000 sec
D11           0.0300000 sec
TD0           1
    
```

```

===== CHANNEL f1 =====
NUC1           13C
P1            10.82 usec
PL1           0.00 dB
PL1W          30.14263725 W
SFO1          75.4778101 MHz
    
```

```

===== CHANNEL f2 =====
CPDPRG2       waltz16
NUC2           1H
PCPD2         100.00 usec
PL2           1.90 dB
PL12          19.17 dB
PL13          23.94 dB
PL1W          8.36853981 W
PL12W         0.15690966 W
PL13W         0.05231782 W
SFO2          300.1412006 MHz
SI            32768
SF           75.4702675 MHz
WDW           EM
SSB           0
LB            1.00 Hz
GB            0
PC            1.40
    
```

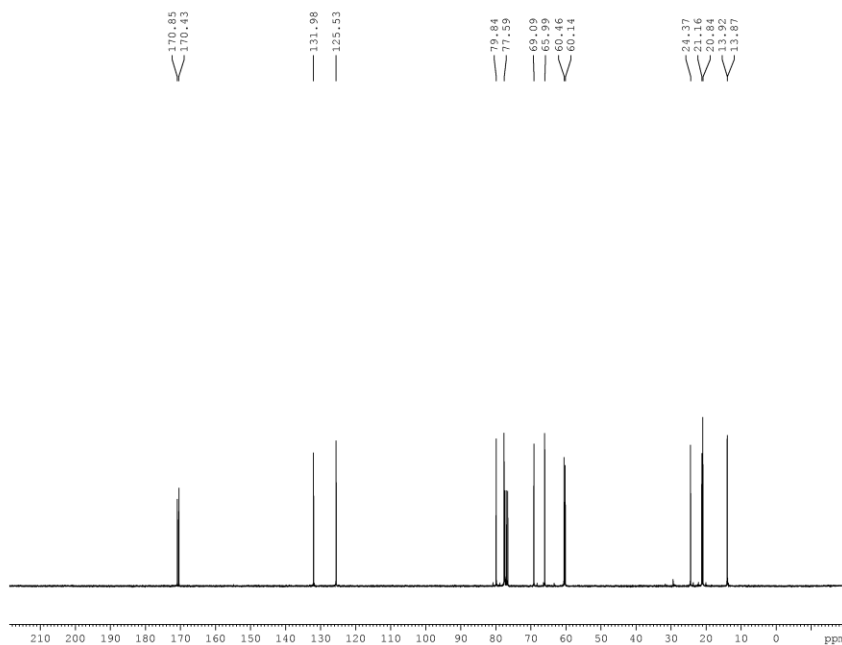


```

EXPNO 1
PROCNO 1
Date_ 20130628
Time 9.54
INSTRUM spect
PROBHD 5 mm PABBO BB-
PULPROG zg30
TD 65536
SOLVENT CDC13
NS 32
DS 2
SWH 6188.119 Hz
FIDRES 0.094423 Hz
AQ 5.2953587 sec
RG 50.8
DW 80.800 usec
DE 6.50 usec
TE 298.0 K
D1 1.0000000 sec
TDO 1
    
```

```

===== CHANNEL f1 =====
NUC1 1H
P1 13.70 usec
PL1 1.90 dB
PL1W 8.36853981 W
SF01 300.1418535 MHz
SI 32768
SF 300.1400052 MHz
WDW EM
SSB 0
LB 0.30 Hz
GB 0
PC 1.00
    
```



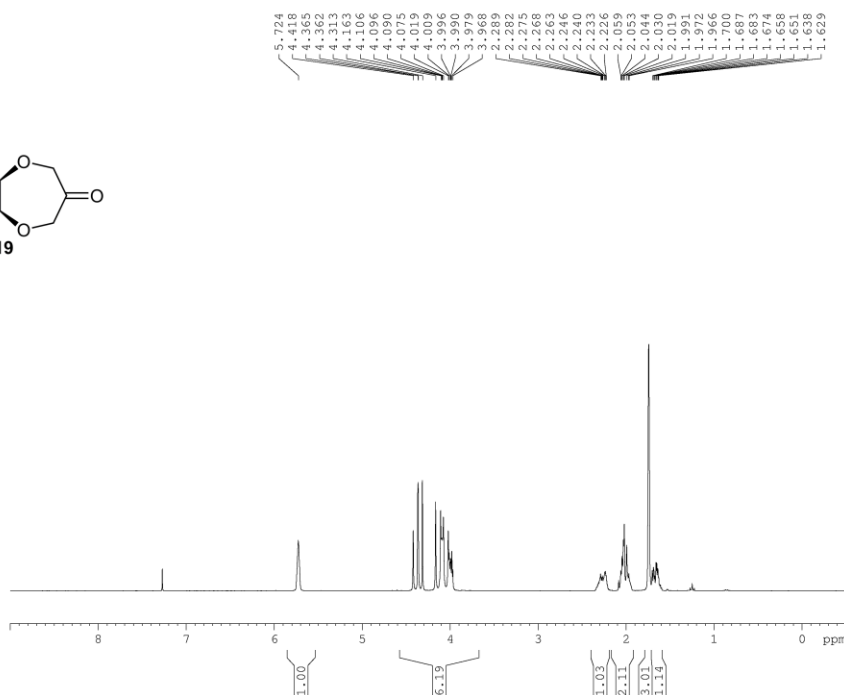
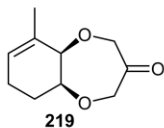
```

EXPNO 1
PROCNO 1
Date_ 20130628
Time 15.41
INSTRUM spect
PROBHD 5 mm PABBO BB-
PULPROG zgpg30
TD 65536
SOLVENT CDC13
NS 599
DS 4
SWH 18028.846 Hz
FIDRES 0.275098 Hz
AQ 1.8175818 sec
RG 203
DW 27.733 usec
DE 6.50 usec
TE 298.0 K
D1 2.0000000 sec
D11 0.0300000 sec
TDO 1
    
```

```

===== CHANNEL f1 =====
NUC1 13C
P1 10.82 usec
PL1 0.00 dB
PL1W 30.14263725 W
SF01 75.4778101 MHz

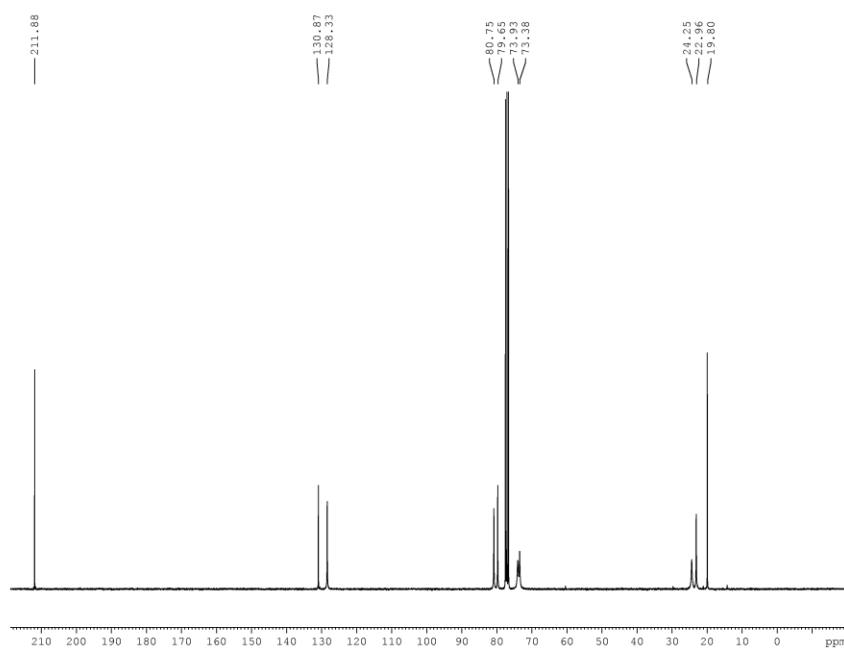
===== CHANNEL f2 =====
CPDPRG2 waltz16
NUC2 1H
PCPD2 100.00 usec
PL2 1.90 dB
PL12 19.17 dB
PL13 23.94 dB
PL2W 8.36853981 W
PL12W 0.15690966 W
PL13W 0.05231782 W
SF02 300.1412006 MHz
SI 32768
SF 75.4702797 MHz
WDW EM
SSB 0
LB 1.00 Hz
GB 0
PC 1.40
    
```



```

EXPNO 1
PROCNO 1
Date_ 20130704
Time 16.54
INSTRUM spect
PROBHD 5 mm PABBO BB-
PULPROG zg30
TD 65536
SOLVENT CDC13
NS 32
DS 2
SWH 6188.119 Hz
FIDRES 0.094423 Hz
AQ 5.2953587 sec
RG 57
DW 80.800 usec
DE 6.50 usec
TE 298.5 K
D1 1.0000000 sec
TDO 1

===== CHANNEL f1 =====
NUC1 1H
P1 13.70 usec
PL1 1.90 dB
PL1W 8.36853981 W
SFO1 300.1418535 MHz
SI 32768
SF 300.1400027 MHz
WDW EM
SSB 0
LB 0.30 Hz
GB 0
PC 1.00
    
```

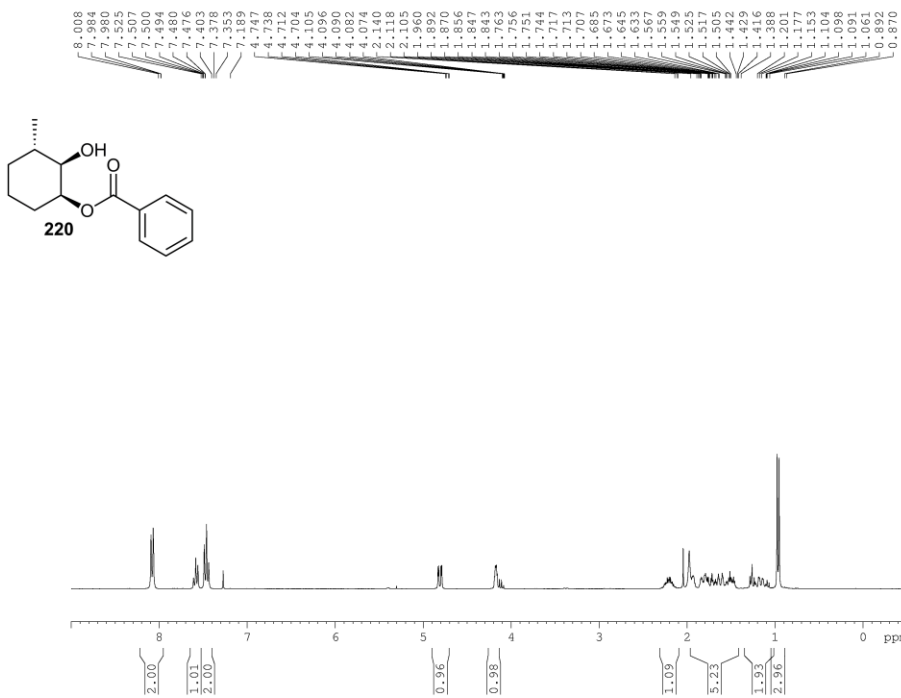


```

EXPNO 2
PROCNO 1
Date_ 20130705
Time 5.54
INSTRUM spect
PROBHD 5 mm PABBO BB-
PULPROG zgpg30
TD 65536
SOLVENT CDC13
NS 12000
DS 4
SWH 18028.846 Hz
FIDRES 0.275098 Hz
AQ 1.8175818 sec
RG 203
DW 27.733 usec
DE 6.50 usec
TE 298.9 K
D1 2.0000000 sec
D11 0.0300000 sec
TDO 1

===== CHANNEL f1 =====
NUC1 13C
P1 10.82 usec
PL1 0.00 dB
PL1W 30.14263725 W
SFO1 75.4778101 MHz

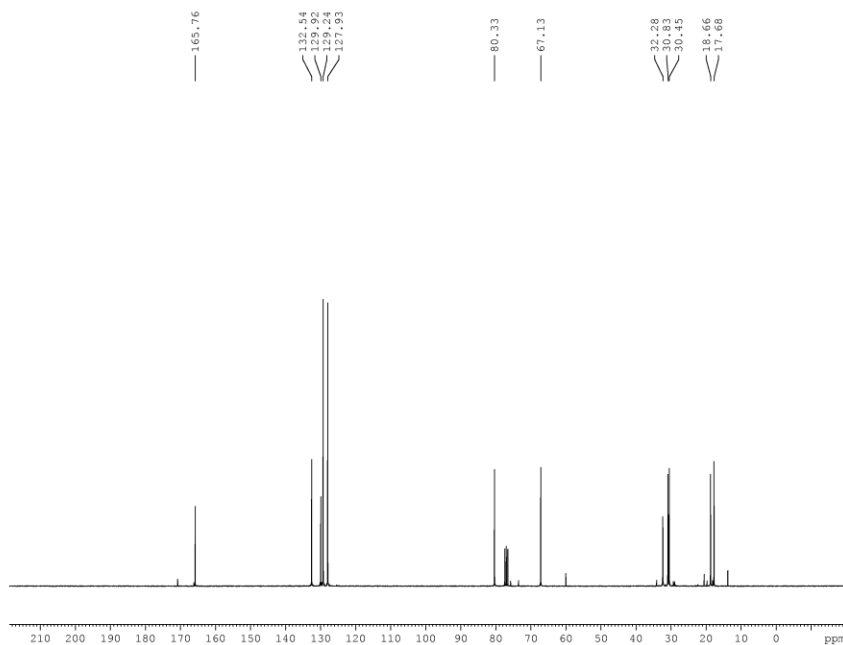
===== CHANNEL f2 =====
CPDPRG2 waltz16
NUC2 1H
PCPD2 100.00 usec
PL2 1.90 dB
PL12 19.17 dB
PL13 23.94 dB
PL2W 8.36853981 W
PL12W 0.15690966 W
PL13W 0.05231782 W
SFO2 300.1412006 MHz
SI 32768
SF 75.4702668 MHz
WDW EM
SSB 0
LB 1.00 Hz
GB 0
PC 1.40
    
```



```

EXPNO 1
PROCNO 1
Date_ 20140228
Time 10.44
INSTRUM spect
PROBHD 5 mm PABBO BB-
PULPROG zg30
TD 65536
SOLVENT CDCl3
NS 16
DS 2
SWH 6188.119 Hz
FIDRES 0.094423 Hz
AQ 5.2953587 sec
RG 64
DM 80.800 usec
DE 6.50 usec
TE 298.0 K
D1 1.0000000 sec
TDO 1

===== CHANNEL f1 =====
NUC1 1H
P1 13.70 usec
PL1 1.90 dB
PL1W 8.36853981 W
SF01 300.1418535 MHz
SI 32768
SF 300.1400022 MHz
WDW EM
SSB 0
LB 0.30 Hz
GB 0
PC 1.00
    
```

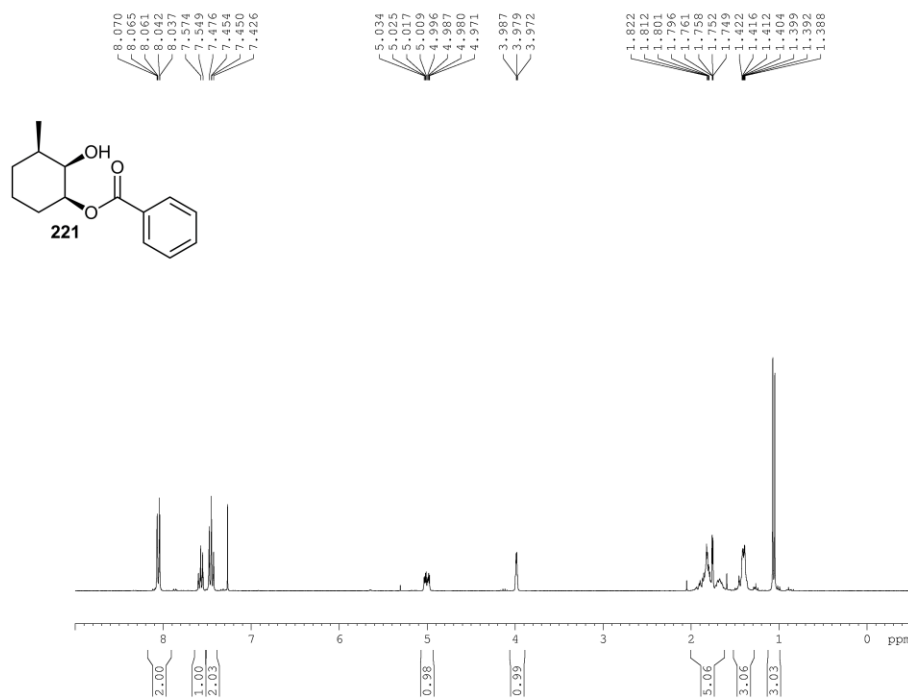


```

EXPNO 1
PROCNO 1
Date_ 20140227
Time 16.49
INSTRUM spect
PROBHD 5 mm PABBO BB-
PULPROG zgpg30
TD 65536
SOLVENT CDCl3
NS 1024
DS 4
SWH 18028.846 Hz
FIDRES 0.275098 Hz
AQ 1.8175818 sec
RG 203
DM 27.733 usec
DE 6.50 usec
TE 298.0 K
D1 2.0000000 sec
D11 0.0300000 sec
TDO 1

===== CHANNEL f1 =====
NUC1 13C
P1 10.82 usec
PL1 0.00 dB
PL1W 30.14263725 W
SF01 75.4778101 MHz

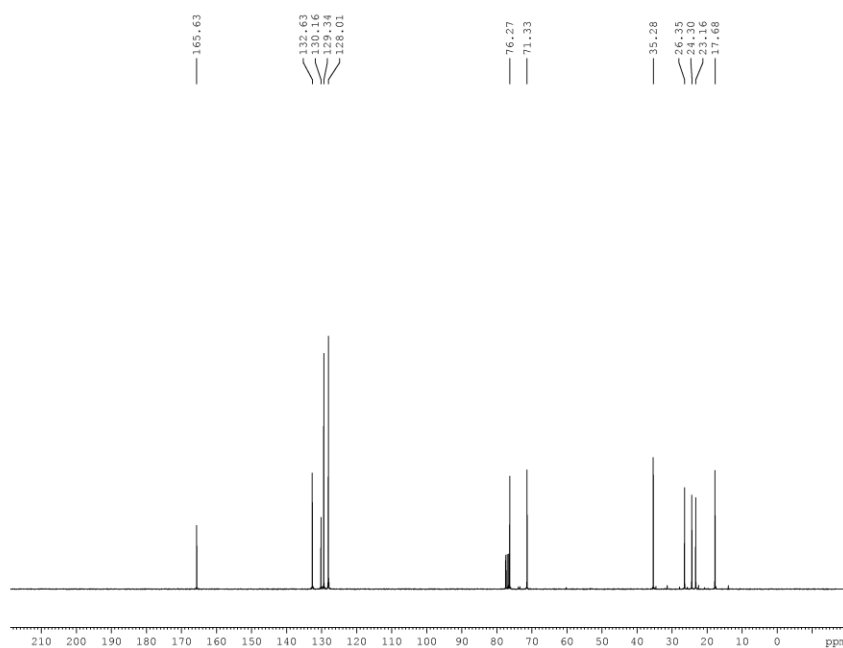
===== CHANNEL f2 =====
CPDPRG2 waltz16
NUC2 1H
PCPD2 100.00 usec
PL2 1.90 dB
PL12 19.17 dB
PL13 23.94 dB
PL1W 8.36853981 W
PL12W 0.15690966 W
PL13W 0.05231782 W
SF02 300.1412006 MHz
SI 32768
SF 75.4702894 MHz
WDW EM
SSB 0
LB 1.00 Hz
GB 0
PC 1.40
    
```



```

EXPNO 1
PROCNO 1
Date_ 20140204
Time 14.01
INSTRUM spect
PROBHD 5 mm PABBO BB-
PULPROG zg30
TD 65536
SOLVENT CDCl3
NS 16
DS 2
SWH 6188.119 Hz
FIDRES 0.094423 Hz
AQ 5.2953587 sec
RG 161
DM 80.800 usec
DE 6.50 usec
TE 298.0 K
D1 1.00000000 sec
TDO 1

===== CHANNEL f1 =====
NUC1 1H
P1 13.70 usec
PL1 1.90 dB
PL1W 8.36853981 W
SF01 300.1418535 MHz
SI 32768
SF 300.1400035 MHz
WDW EM
SSB 0
LB 0.30 Hz
GB 0
PC 1.00
    
```

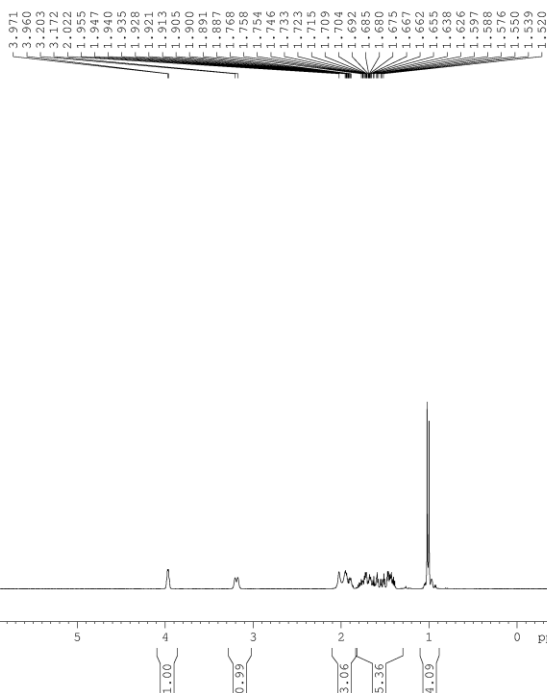
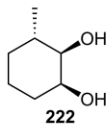


```

EXPNO 3
PROCNO 1
Date_ 20140204
Time 12.55
INSTRUM spect
PROBHD 5 mm PABBO BB-
PULPROG zgpg30
TD 65536
SOLVENT CDCl3
NS 874
DS 4
SWH 18028.846 Hz
FIDRES 0.275098 Hz
AQ 1.8175818 sec
RG 203
DM 27.733 usec
DE 6.50 usec
TE 298.0 K
D1 2.00000000 sec
D11 0.03000000 sec
TDO 1

===== CHANNEL f1 =====
NUC1 13C
P1 10.82 usec
PL1 0.00 dB
PL1W 30.14263725 W
SF01 75.4778101 MHz

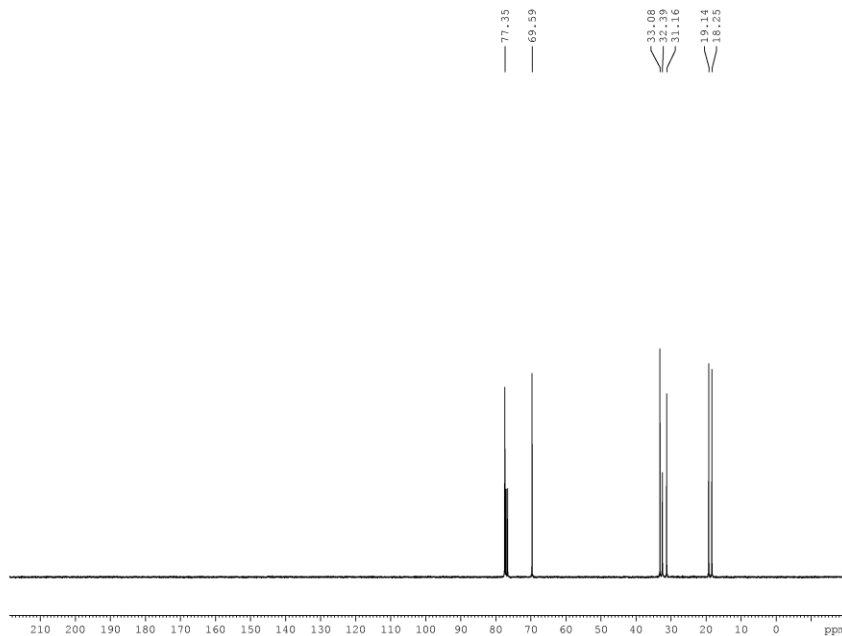
===== CHANNEL f2 =====
CPDPRG2 waltz16
NUC2 1H
PCPD2 100.00 usec
PL2 1.90 dB
PL12 19.17 dB
PL13 23.94 dB
PL1W 8.36853981 W
PL12W 0.15690966 W
PL13W 0.05231782 W
SF02 300.1412006 MHz
SI 32768
SF 75.4702828 MHz
WDW EM
SSB 0
LB 1.00 Hz
GB 0
PC 1.40
    
```



```

EXPNO 1
PROCNO 1
Date_ 20140211
Time 10.20
INSTRUM spect
PROBHD 5 mm PABBO BB-
PULPROG zg30
TD 65536
SOLVENT CDCl3
NS 16
DS 2
SWH 6188.119 Hz
FIDRES 0.094423 Hz
AQ 5.2953587 sec
RG 203
DW 80.800 usec
DE 6.50 usec
TE 298.0 K
D1 1.00000000 sec
TDO 1

===== CHANNEL f1 =====
NUC1 1H
P1 13.70 usec
PL1 1.90 dB
PL1W 8.36853981 W
SFO1 300.1418535 MHz
SI 32768
SF 300.1400028 MHz
WDW EM
SSB 0
LB 0.30 Hz
GB 0
PC 1.00
    
```

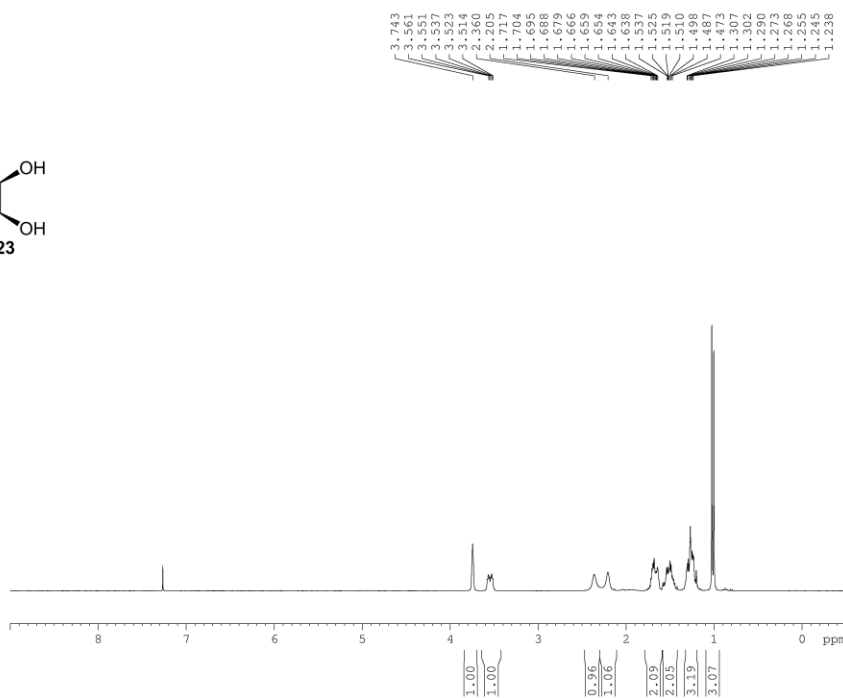
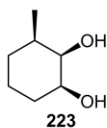


```

EXPNO 1
PROCNO 1
Date_ 20140211
Time 11.57
INSTRUM spect
PROBHD 5 mm PABBO BB-
PULPROG zgpg30
TD 65536
SOLVENT CDCl3
NS 4
DS 4
SWH 18028.846 Hz
FIDRES 0.275098 Hz
AQ 1.8175818 sec
RG 203
DW 27.733 usec
DE 6.50 usec
TE 298.0 K
D1 2.00000000 sec
D11 0.03000000 sec
TDO 1

===== CHANNEL f1 =====
NUC1 13C
P1 10.82 usec
PL1 0.00 dB
PL1W 30.14263725 W
SFO1 75.4778101 MHz

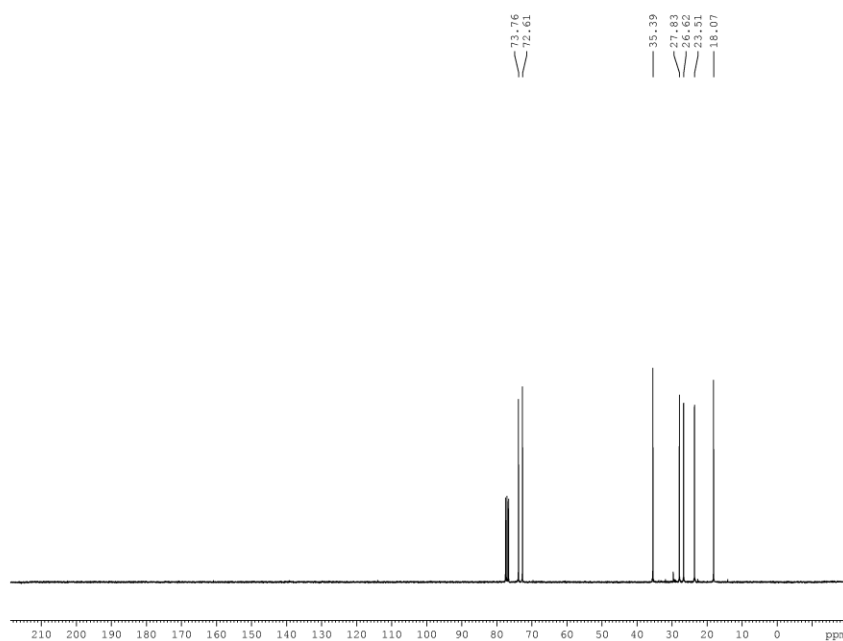
===== CHANNEL f2 =====
CPDPRG2 waltz16
NUC2 1H
PCPD2 100.00 usec
PL2 1.90 dB
PL12 19.17 dB
PL13 23.94 dB
PL2W 8.36853981 W
PL12W 0.15690966 W
PL13W 0.05231782 W
SFO2 300.1412006 MHz
SI 32768
SF 75.4702692 MHz
WDW EM
SSB 0
LB 1.00 Hz
GB 0
PC 1.40
    
```



```

EXPNO 1
PROCNO 1
Date_ 20140211
Time 14.38
INSTRUM spect
PROBHD 5 mm PABBO BB-
PULPROG zg30
TD 65536
SOLVENT CDC13
NS 16
DS 2
SWH 6188.119 Hz
FIDRES 0.094423 Hz
AQ 5.2953587 sec
RG 64
DW 80.800 usec
DE 6.50 usec
TE 298.0 K
D1 1.00000000 sec
TDO 1

===== CHANNEL f1 =====
NUC1 1H
P1 13.70 usec
PL1 1.90 dB
PL1W 8.36853981 W
SFO1 300.1418535 MHz
SI 32768
SF 300.1400043 MHz
WDW EM
SSB 0
LB 0.30 Hz
GB 0
PC 1.00
    
```

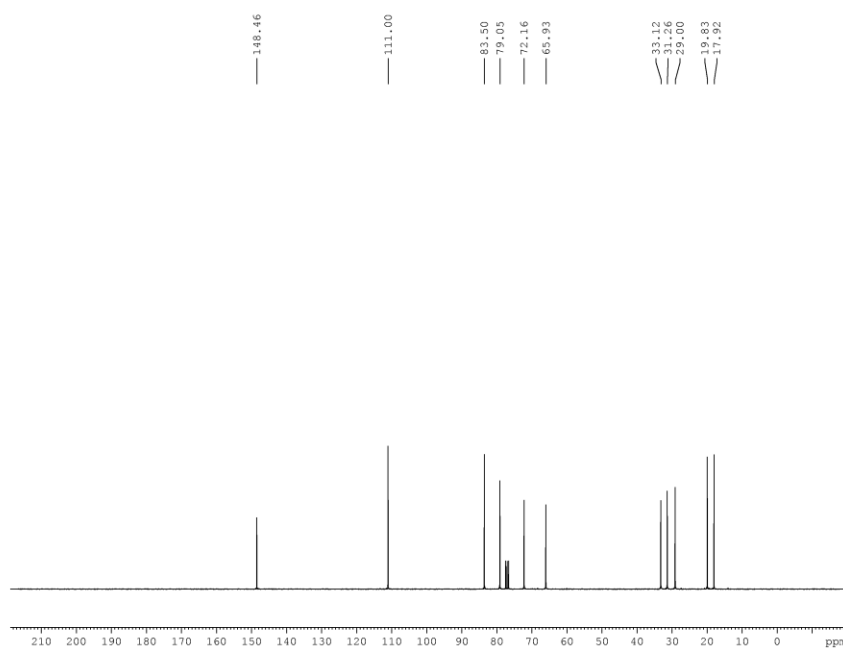
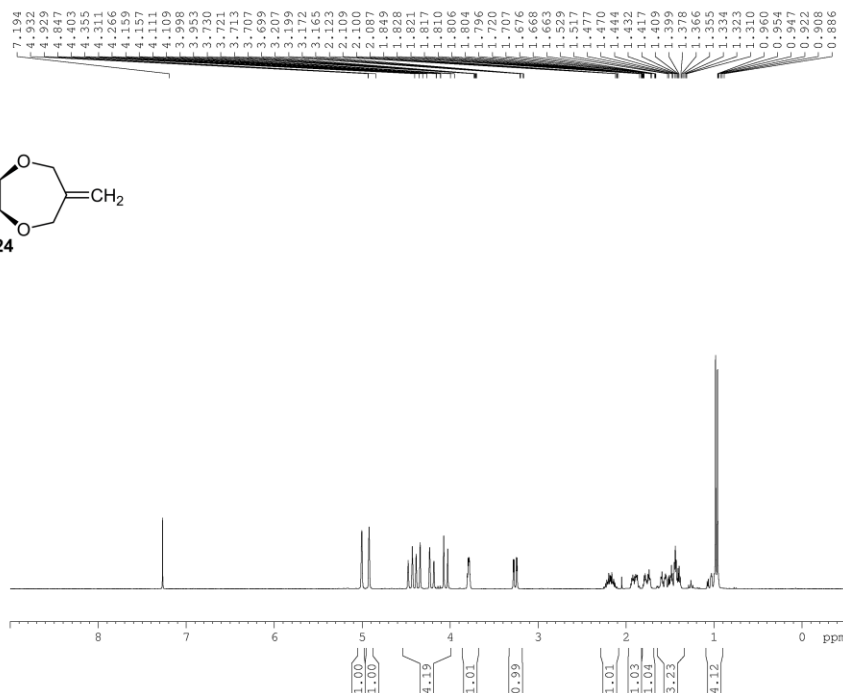
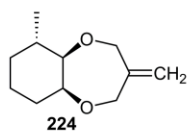


```

EXPNO 1
PROCNO 1
Date_ 20140211
Time 15.49
INSTRUM spect
PROBHD 5 mm PABBO BB-
PULPROG zgpg30
TD 65536
SOLVENT CDC13
NS 578
DS 4
SWH 18028.846 Hz
FIDRES 0.275098 Hz
AQ 1.8175818 sec
RG 203
DW 27.733 usec
DE 6.50 usec
TE 298.0 K
D1 2.00000000 sec
D11 0.03000000 sec
TDO 1

===== CHANNEL f1 =====
NUC1 13C
P1 10.82 usec
PL1 0.00 dB
PL1W 30.14263725 W
SFO1 75.4778101 MHz

===== CHANNEL f2 =====
CPDPRG2 waltz16
NUC2 1H
PCPD2 100.00 usec
PL2 1.90 dB
PL12 19.17 dB
PL13 23.94 dB
PL2W 8.36853981 W
PL12W 0.15690966 W
PL13W 0.05231782 W
SFO2 300.1412006 MHz
SI 32768
SF 75.4702685 MHz
WDW EM
SSB 0
LB 1.00 Hz
GB 0
PC 1.40
    
```

```

EXPNO 1
PROCNO 1
Date_ 20140307
Time 14.13
INSTRUM spect
PROBHD 5 mm PABBO BB-
PULPROG zg30
TD 65536
SOLVENT CDC13
NS 16
DS 2
SWH 6188.119 Hz
FIDRES 0.094423 Hz
AQ 5.2953587 sec
RG 161
DW 80.800 usec
DE 6.50 usec
TE 298.0 K
D1 1.0000000 sec
TDO 1

===== CHANNEL f1 =====
NUC1 1H
P1 13.70 usec
PL1 1.90 dB
PL1W 8.36853981 W
SFO1 300.1418535 MHz
SI 32768
SF 300.1400036 MHz
WDW EM
SSB 0
LB 0.30 Hz
GB 0
PC 1.00
    
```

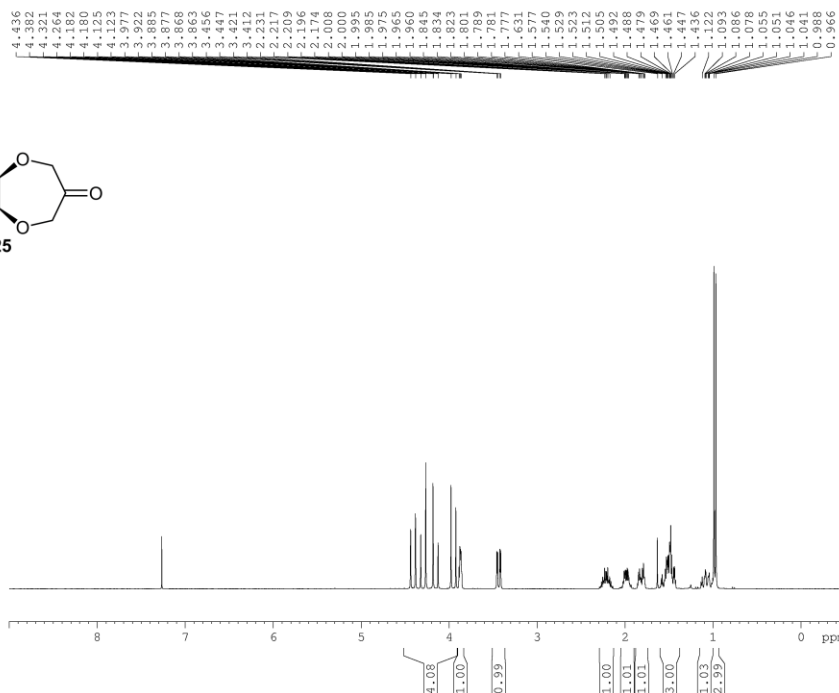
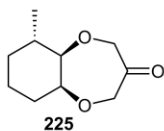


```

EXPNO 1
PROCNO 1
Date_ 20140307
Time 15.25
INSTRUM spect
PROBHD 5 mm PABBO BB-
PULPROG zgpg30
TD 65536
SOLVENT CDC13
NS 688
DS 4
SWH 18028.846 Hz
FIDRES 0.275098 Hz
AQ 1.8175818 sec
RG 203
DW 27.733 usec
DE 6.50 usec
TE 298.0 K
D1 2.0000000 sec
D11 0.0300000 sec
TDO 1

===== CHANNEL f1 =====
NUC1 13C
P1 10.82 usec
PL1 0.00 dB
PL1W 30.14263725 W
SFO1 75.4778101 MHz

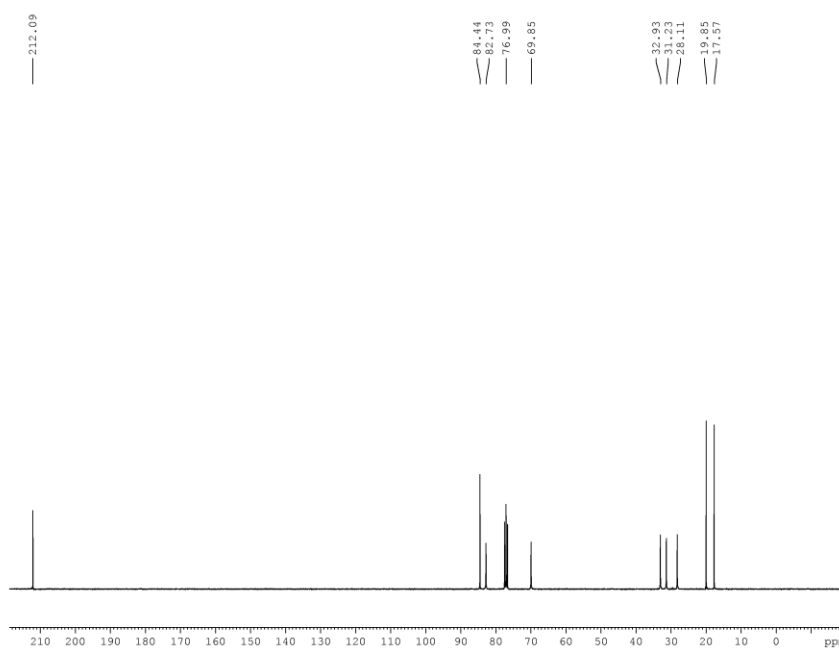
===== CHANNEL f2 =====
CPDPRG2 waltz16
NUC2 1H
PCPD2 100.00 usec
PL2 1.90 dB
PL12 19.17 dB
PL13 23.94 dB
PL2W 8.36853981 W
PL12W 0.15690966 W
PL13W 0.05231782 W
SFO2 300.1412006 MHz
SI 32768
SF 75.4702769 MHz
WDW EM
SSB 0
LB 1.00 Hz
GB 0
PC 1.40
    
```



```

EXPNO          2
PROCNO         1
Date_          20140319
Time           12.46
INSTRUM       spect
PROBHD        5 mm PABBO BB-
PULPROG       zg30
TD             65536
SOLVENT       CDC13
NS            16
DS            2
SWH           6188.119 Hz
FIDRES       0.094423 Hz
AQ           5.2953587 sec
RG            80.6
DW           80.800 usec
DE            6.50 usec
TE            298.0 K
D1            1.0000000 sec
TD0           1

===== CHANNEL f1 =====
NUC1          1H
P1            13.70 usec
PL1          1.90 dB
PL1W         8.36853981 W
SFO1         300.1418535 MHz
SI            32768
SF           300.1400044 MHz
WDW           EM
SSB           0
LB            0.30 Hz
GB            0
PC            1.00
    
```

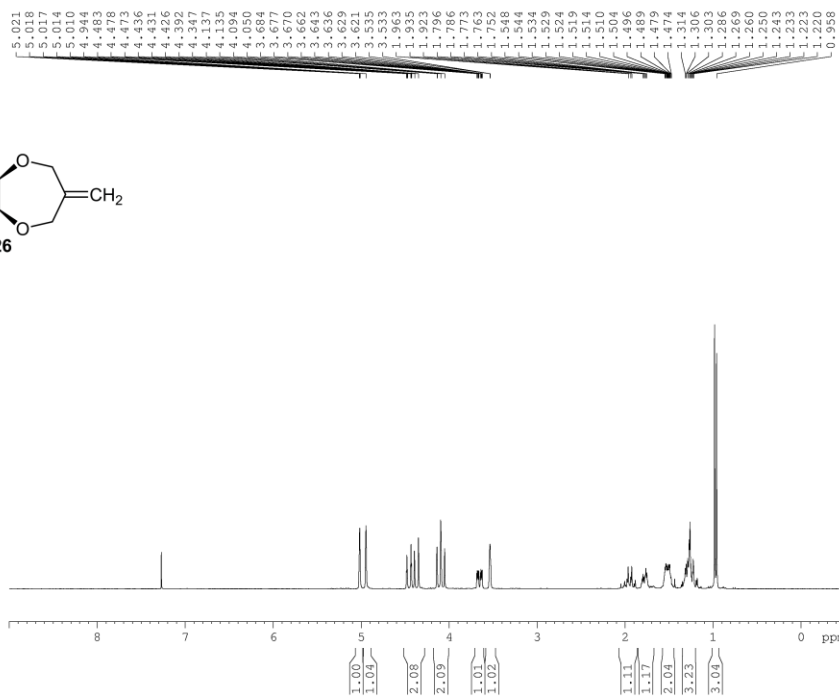
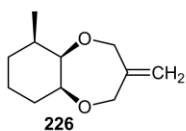


```

EXPNO          2
PROCNO         1
Date_          20140320
Time           15.54
INSTRUM       spect
PROBHD        5 mm PABBO BB-
PULPROG       zgpg30
TD             65536
SOLVENT       CDC13
NS            811
DS            4
SWH           18028.846 Hz
FIDRES       0.275098 Hz
AQ           1.8175818 sec
RG            203
DW           27.733 usec
DE            6.50 usec
TE            298.0 K
D1            2.0000000 sec
D11           0.0300000 sec
TD0           1

===== CHANNEL f1 =====
NUC1          13C
P1            10.82 usec
PL1           0.00 dB
PL1W        30.14263725 W
SFO1         75.4778101 MHz

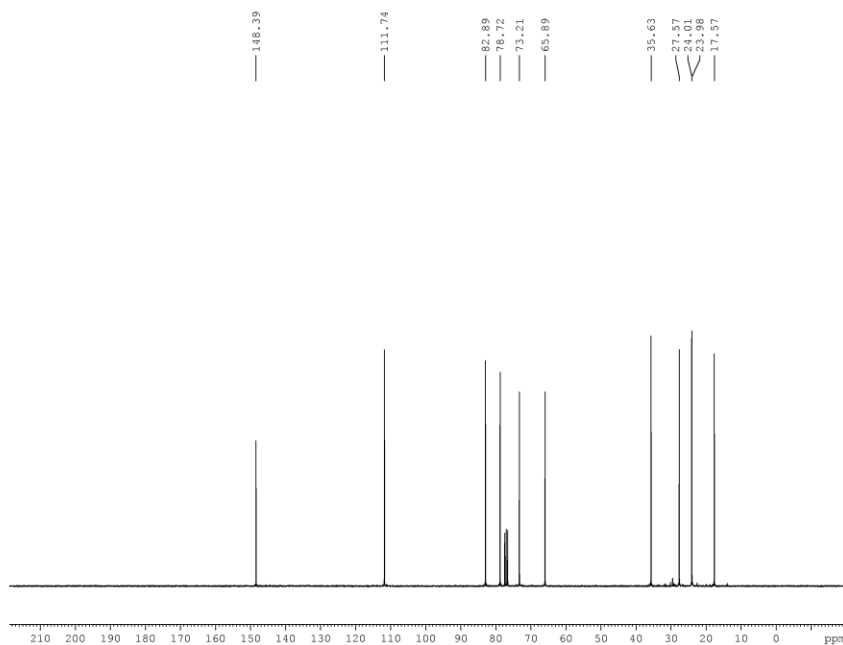
===== CHANNEL f2 =====
CPDPRG2       waltz16
NUC2          1H
PCPD2        100.00 usec
PL2           1.90 dB
PL12         19.17 dB
PL13         23.94 dB
PL1W         8.36853981 W
PL12W        0.15690966 W
PL13W        0.05231782 W
SFO2         300.1412006 MHz
SI            32768
SF           75.4702717 MHz
WDW           EM
SSB           0
LB            1.00 Hz
GB            0
PC            1.40
    
```



```

EXPNO          2
PROCNO         1
Date_          20140226
Time           15.21
INSTRUM       spect
PROBHD        5 mm PABBO BB-
PULPROG       zg30
TD             65536
SOLVENT       CDC13
NS             16
DS             2
SWH           6188.119 Hz
FIDRES       0.094423 Hz
AQ           5.2953587 sec
RG            71.8
DW           80.800 usec
DE            6.50 usec
TE           298.0 K
D1           1.0000000 sec
TD0          1

===== CHANNEL f1 =====
NUC1          1H
P1           13.70 usec
PL1          1.90 dB
PL1W         8.36853981 W
SF01         300.1418535 MHz
SI           32768
SF           300.1400029 MHz
WDW          EM
SSB          0
LB           0.30 Hz
GB           0
PC           1.00
    
```

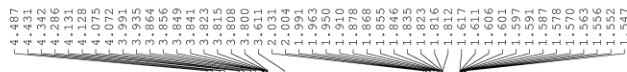
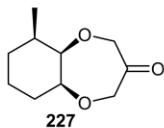


```

EXPNO          2
PROCNO         1
Date_          20140226
Time           13.27
INSTRUM       spect
PROBHD        5 mm PABBO BB-
PULPROG       zgpg30
TD             65536
SOLVENT       CDC13
NS             364
DS             4
SWH           18028.846 Hz
FIDRES       0.275098 Hz
AQ           1.8175818 sec
RG            203
DW           27.733 usec
DE            6.50 usec
TE           298.0 K
D1           2.0000000 sec
D11          0.0300000 sec
TD0          1

===== CHANNEL f1 =====
NUC1          13C
P1           10.82 usec
PL1          0.00 dB
PL1W        30.14263725 W
SF01         75.4778101 MHz

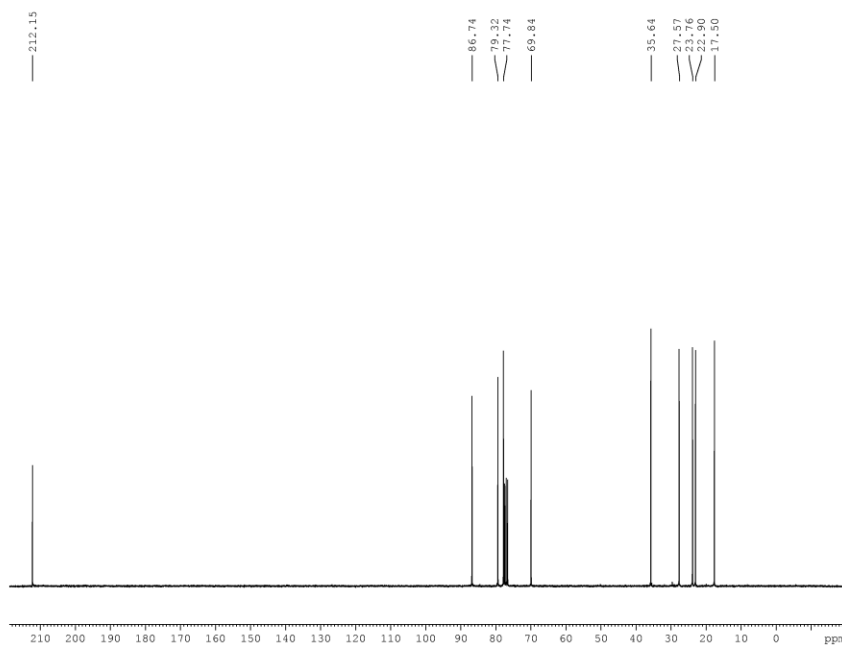
===== CHANNEL f2 =====
CPDPRG2       waltz16
NUC2          1H
PCPD2        100.00 usec
PL2          1.90 dB
PL12         19.17 dB
PL13         23.94 dB
PL1W         8.36853981 W
PL12W        0.15690966 W
PL13W        0.05231782 W
SF02         300.1412006 MHz
SI           32768
SF           75.4702744 MHz
WDW          EM
SSB          0
LB           1.00 Hz
GB           0
PC           1.40
    
```



```

EXPNO          2
PROCNO         1
Date_          20140304
Time           14.40
INSTRUM        spect
PROBHD         5 mm PABBO BB-
PULPROG        zg30
TD             65536
SOLVENT        CDC13
NS             16
DS             2
SWH            6188.119 Hz
FIDRES         0.094423 Hz
AQ            5.2953587 sec
RG            203
DW            80.800 usec
DE            6.50 usec
TE            298.0 K
D1            1.0000000 sec
TD0           1

===== CHANNEL f1 =====
NUC1           1H
P1            13.70 usec
PL1           1.90 dB
PL1W          8.36853981 W
SFO1          300.1418535 MHz
SI            32768
SF            300.1400057 MHz
WDW           EM
SSB           0
LB            0.30 Hz
GB            0
PC            1.00
    
```

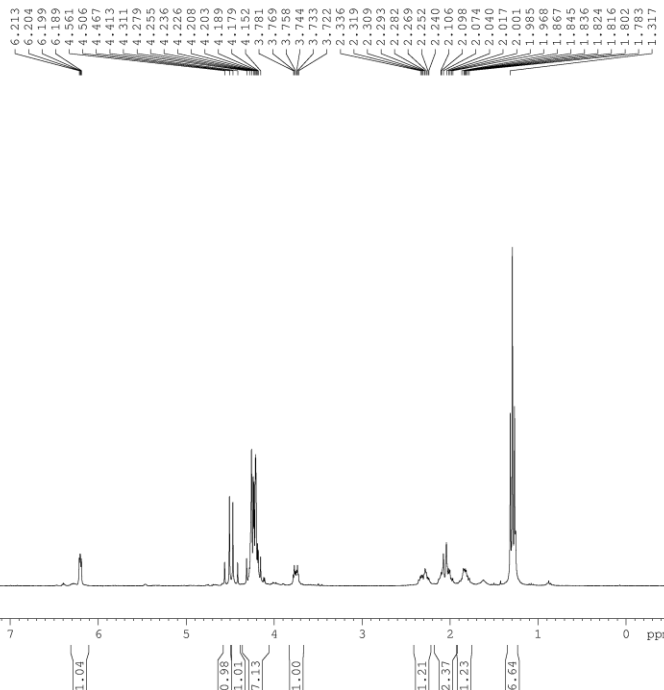
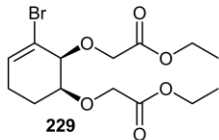


```

EXPNO          2
PROCNO         1
Date_          20140304
Time           12.56
INSTRUM        spect
PROBHD         5 mm PABBO BB-
PULPROG        zgpg30
TD             65536
SOLVENT        CDC13
NS             698
DS             4
SWH            18028.846 Hz
FIDRES         0.275098 Hz
AQ            1.8175818 sec
RG            203
DW            27.733 usec
DE            6.50 usec
TE            298.0 K
D1            2.0000000 sec
D11           0.0300000 sec
TD0           1

===== CHANNEL f1 =====
NUC1           13C
P1            10.82 usec
PL1           0.00 dB
PL1W          30.14263725 W
SFO1          75.4778101 MHz

===== CHANNEL f2 =====
CPDPRG2        waltz16
NUC2           1H
PCPD2         100.00 usec
PL2           1.90 dB
PL12          19.17 dB
PL13          23.94 dB
PL1W          8.36853981 W
PL12W         0.15690966 W
PL13W         0.05231782 W
SFO2          300.1412006 MHz
SI            32768
SF            75.4702720 MHz
WDW           EM
SSB           0
LB            1.00 Hz
GB            0
PC            1.40
    
```

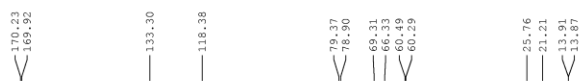


```

EXPNO 1
PROCNO 1
Date_ 20140903
Time 15.32
INSTRUM spect
PROBHD 5 mm PABBO BB-
PULPROG zg30
TD 65536
SOLVENT CDC13
NS 16
DS 2
SWH 6188.119 Hz
FIDRES 0.094423 Hz
AQ 5.2953587 sec
RG 203
DW 80.800 usec
DE 6.50 usec
TE 293.7 K
D1 1.0000000 sec
TDO 1
    
```

```

===== CHANNEL f1 =====
NUC1 1H
P1 13.70 usec
PL1 1.90 dB
PL1W 8.36853981 W
SF01 300.1418535 MHz
SI 32768
SF 300.1400036 MHz
WDW EM
SSB 0
LB 0.30 Hz
GB 0
PC 1.00
    
```



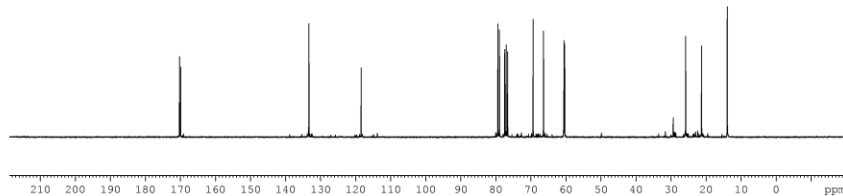
```

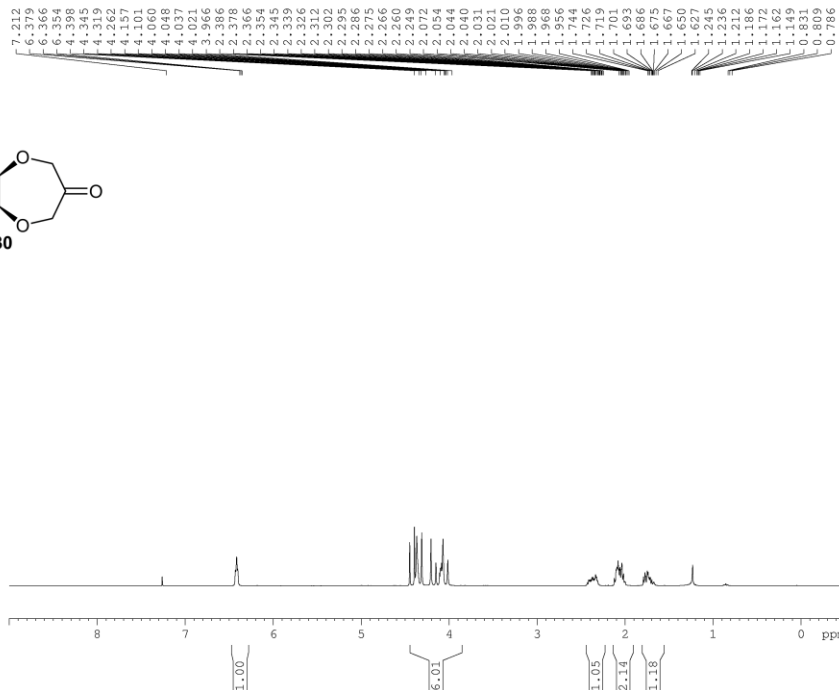
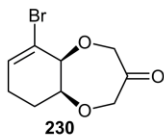
EXPNO 1
PROCNO 1
Date_ 20140903
Time 17.33
INSTRUM spect
PROBHD 5 mm PABBO BB-
PULPROG zgpg30
TD 65536
SOLVENT CDC13
NS 1024
DS 4
SWH 18028.846 Hz
FIDRES 0.275098 Hz
AQ 1.8175818 sec
RG 203
DW 27.733 usec
DE 6.50 usec
TE 300.0 K
D1 2.0000000 sec
D11 0.0300000 sec
TDO 1
    
```

```

===== CHANNEL f1 =====
NUC1 13C
P1 10.82 usec
PL1 0.00 dB
PL1W 30.14263725 W
SF01 75.4778101 MHz

===== CHANNEL f2 =====
CPDPRG2 waltz16
NUC2 1H
PCPD2 100.00 usec
PL2 1.90 dB
PL12 19.17 dB
PL13 23.94 dB
PL2W 8.36853981 W
PL12W 0.15690966 W
PL13W 0.05231782 W
SF02 300.1412006 MHz
SI 32768
SF 75.4702820 MHz
WDW EM
SSB 0
LB 1.00 Hz
GB 0
PC 1.40
    
```



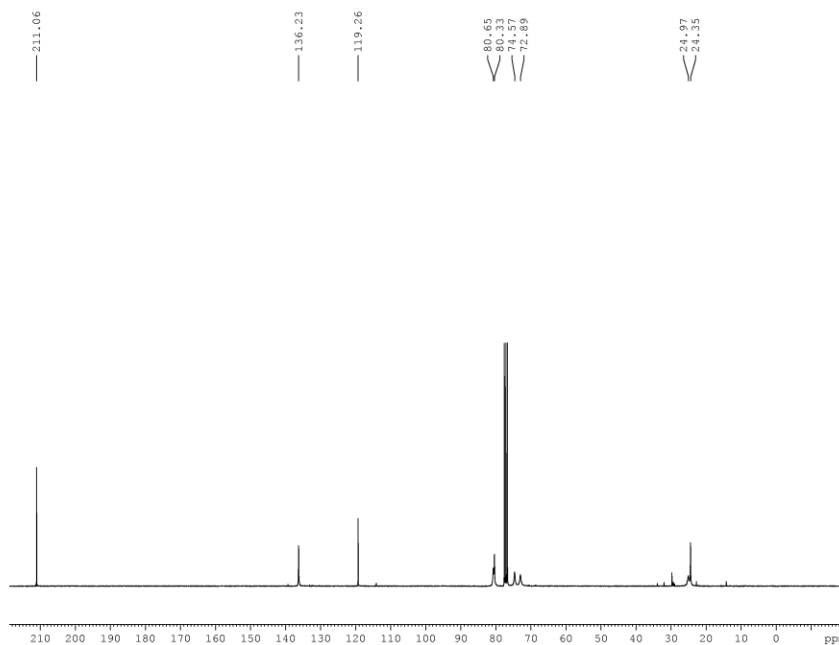


```

EXPNO 1
PROCNO 1
Date_ 20141018
Time 17.50
INSTRUM spect
PROBHD 5 mm PABBO BB-
PULPROG zg30
TD 65536
SOLVENT CDCl3
NS 16
DS 2
SWH 6188.119 Hz
FIDRES 0.094423 Hz
AQ 5.2953587 sec
RG 57
DN 80.800 usec
DE 6.50 usec
TE 298.0 K
D1 1.00000000 sec
TDO 1
    
```

```

----- CHANNEL f1 -----
NUC1 1H
P1 13.70 usec
PL1 1.90 dB
PL1W 8.36853981 W
SF01 300.1418535 MHz
SI 32768
SF 300.1400059 MHz
WDW EM
SSB 0
LB 0.30 Hz
GB 0
PC 1.00
    
```



```

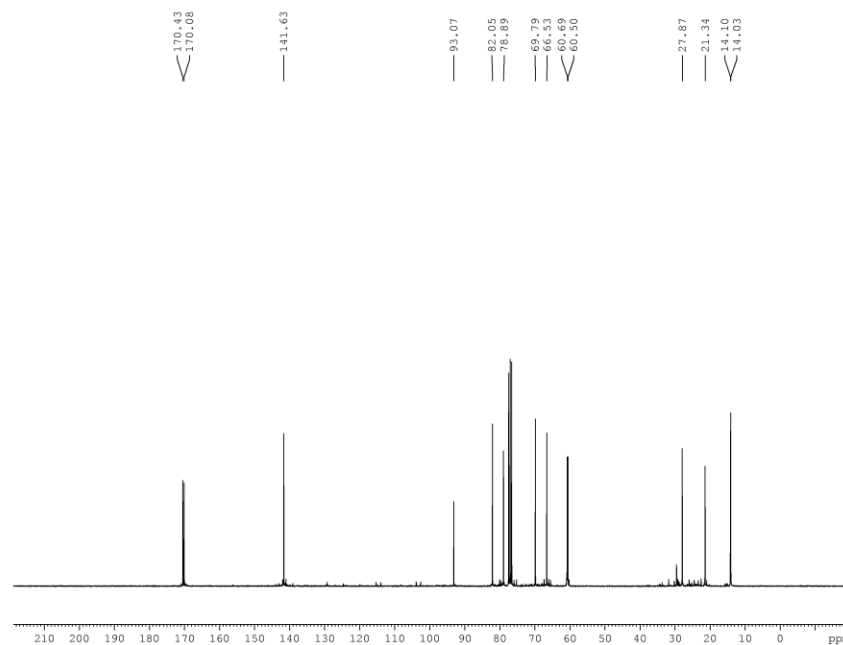
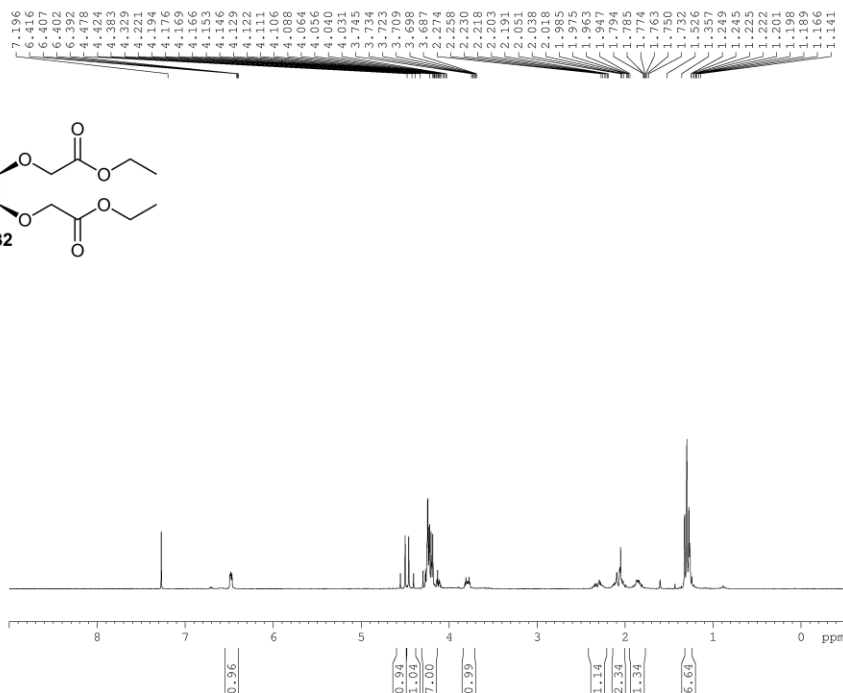
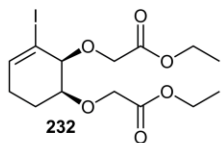
EXPNO 1
PROCNO 1
Date_ 20141019
Time 17.54
INSTRUM spect
PROBHD 5 mm PABBO BB-
PULPROG zgpg30
TD 65536
SOLVENT CDCl3
NS 22000
DS 4
SWH 18028.046 Hz
FIDRES 0.275098 Hz
AQ 1.8175818 sec
RG 203
DN 27.733 usec
DE 6.50 usec
TE 298.0 K
D1 2.00000000 sec
D11 0.03000000 sec
TDO 1
    
```

```

----- CHANNEL f1 -----
NUC1 13C
P1 10.82 usec
PL1 0.00 dB
PL1W 30.14263725 W
SF01 75.4778101 MHz
    
```

```

----- CHANNEL f2 -----
CPDPRG2 waltz16
NUC2 1H
PCPD2 100.00 usec
PL2 1.90 dB
PL12 13.17 dB
PL13 23.94 dB
PL2W 8.36853981 W
PL12W 0.15590966 W
PL13W 0.05231782 W
SF02 300.1412006 MHz
SI 32768
SF 75.4702630 MHz
WDW EM
SSB 0
LB 1.00 Hz
GB 0
PC 1.40
    
```



```

EXPNO 1
PROCNO 1
Date_ 20140930
Time 15.03
INSTRUM spect
PROBHD 5 mm PABBO BB-
PULPROG zg30
TD 65536
SOLVENT CDCl3
NS 16
DS 2
SWH 6188.119 Hz
FIDRES 0.094423 Hz
AQ 5.2953587 sec
RG 161
DW 80.800 usec
DE 6.50 usec
TE 298.0 K
D1 1.00000000 sec
TDO 1
    
```

```

===== CHANNEL f1 =====
NUC1 1H
P1 13.70 usec
PLL 1.90 dB
PLLW 8.36853981 W
SF01 300.141835 MHz
SI 32768
SF 300.1400027 MHz
WDW EM
SSB 0
LB 0.30 Hz
GB 0
PC 1.00
    
```



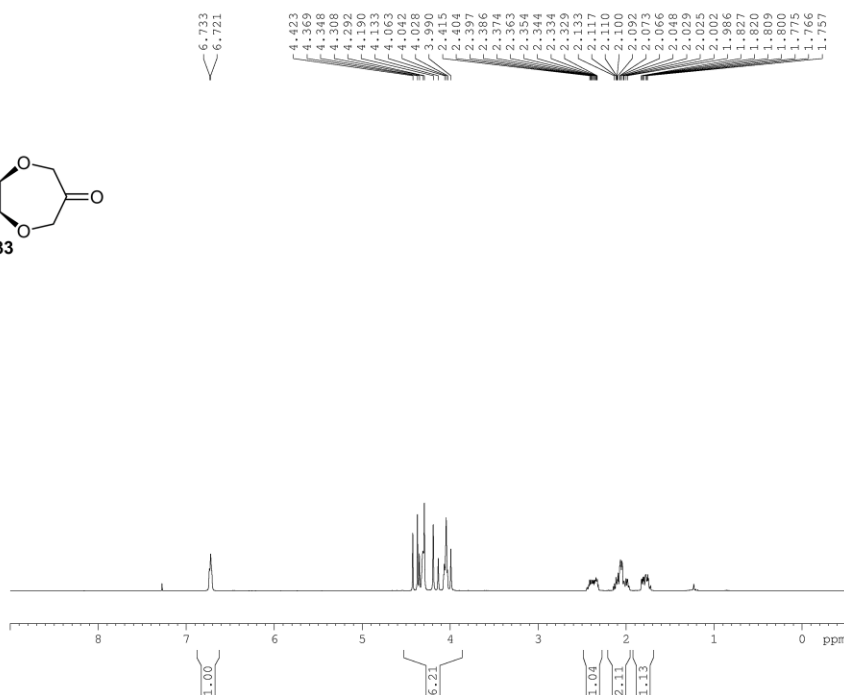
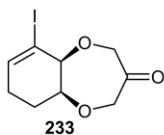
```

EXPNO 1
PROCNO 1
Date_ 20141001
Time 4.18
INSTRUM spect
PROBHD 5 mm PABBO BB-
PULPROG zgpg30
TD 65536
SOLVENT CDCl3
NS 10000
DS 4
SWH 18028.846 Hz
FIDRES 0.275098 Hz
AQ 1.8175818 sec
RG 203
DW 27.733 usec
DE 6.50 usec
TE 298.0 K
D1 2.00000000 sec
D11 0.03000000 sec
TDO 1
    
```

```

===== CHANNEL f1 =====
NUC1 13C
P1 10.82 usec
PLL 0.00 dB
PLLW 30.14263725 W
SF01 75.4778101 MHz

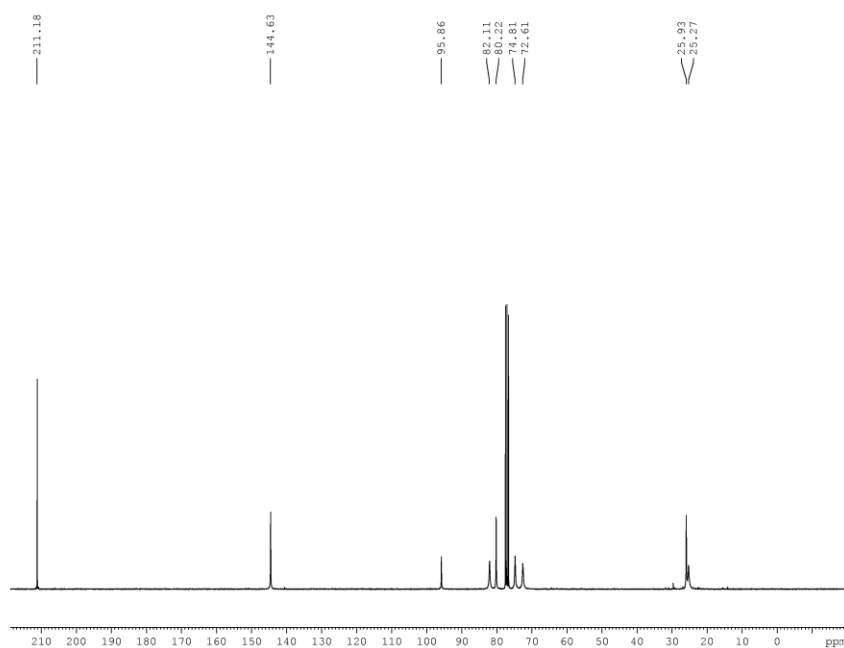
===== CHANNEL f2 =====
CPDPRG2 waltz16
NUC2 1H
PCPD2 100.00 usec
PL2 1.90 dB
PL12 19.17 dB
PL13 23.94 dB
PL2W 8.36853981 W
PL12W 0.15690966 W
PL13W 0.05231782 W
SF02 300.1412006 MHz
SI 32768
SF 75.4702742 MHz
WDW EM
SSB 0
LB 1.00 Hz
GB 0
PC 1.40
    
```



```

EXPNO 1
PROCNO 1
Date_ 20141013
Time 17.09
INSTRUM spect
PROBHD 5 mm PABBO BB-
PULPROG zg30
TD 65536
SOLVENT CDCl3
NS 8
DS 0
SWH 6188.119 Hz
FIDRES 0.094423 Hz
AQ 5.2953587 sec
RG 45.2
DM 80.800 usec
DE 6.50 usec
TE 298.0 K
D1 1.00000000 sec
TDO 1

===== CHANNEL f1 =====
NUC1 1H
P1 13.70 usec
PL1 1.90 dB
PL1W 8.36853981 W
SF01 300.1418535 MHz
SI 32768
SF 300.1400018 MHz
WDW EM
SSB 0
LB 0.30 Hz
GB 0
PC 1.00
    
```

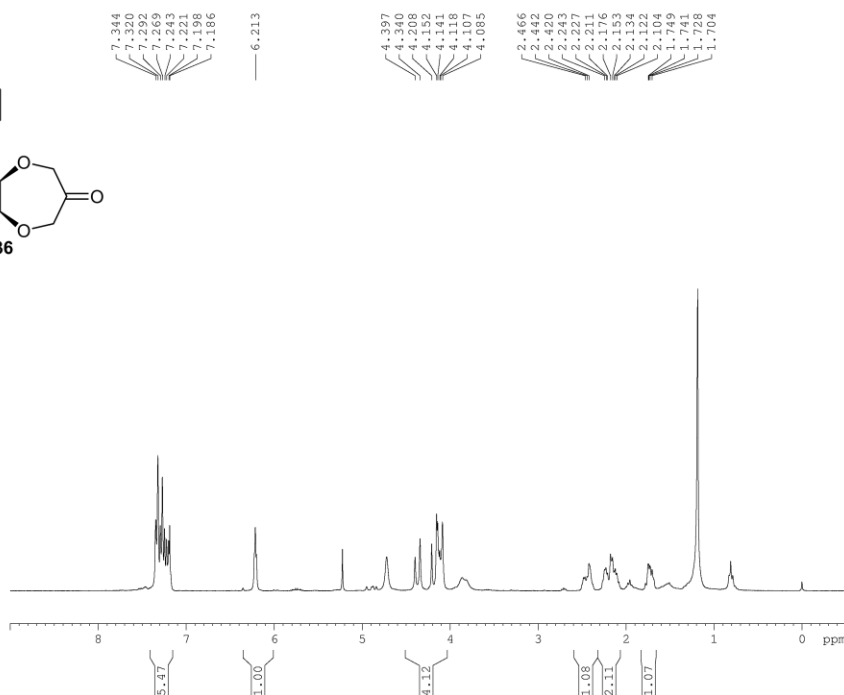
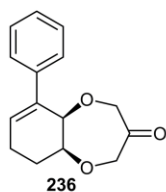


```

EXPNO 1
PROCNO 1
Date_ 20141014
Time 6.06
INSTRUM spect
PROBHD 5 mm PABBO BB-
PULPROG zgpg30
TD 65536
SOLVENT CDCl3
NS 12000
DS 4
SWH 18028.046 Hz
FIDRES 0.275098 Hz
AQ 1.8175818 sec
RG 203
DM 27.753 usec
DE 6.50 usec
TE 298.0 K
D1 2.00000000 sec
D11 0.03000000 sec
TDO 1

===== CHANNEL f1 =====
NUC1 13C
P1 10.82 usec
PL1 0.00 dB
PL1W 30.14263725 W
SF01 75.4778101 MHz

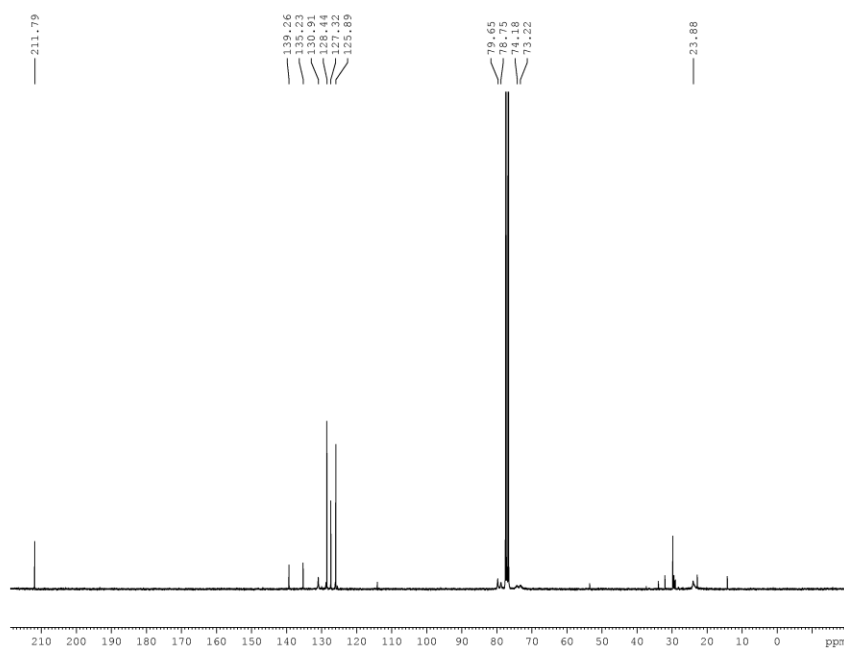
===== CHANNEL f2 =====
CPDPRG2 waltz16
NUC2 1H
PCPD2 100.00 usec
PL2 1.90 dB
PL12 13.17 dB
PL13 23.94 dB
PL2W 8.36853981 W
PL12W 0.15590966 W
PL13W 0.05231782 W
SF02 300.1412006 MHz
SI 32768
SF 75.4702728 MHz
WDW EM
SSB 0
LB 1.00 Hz
GB 0
PC 1.40
    
```

```

EXPNO 1
PROCNO 1
Date_ 20150316
Time 16.50
INSTRUM spect
PROBHD 5 mm PABBO BB-
PULPROG zg30
TD 65536
SOLVENT CDCl3
NS 16
DS 2
SWH 6188.119 Hz
FIDRES 0.094423 Hz
AQ 5.2953587 sec
RG 90.5
DM 80.800 usec
DE 6.50 usec
TE 298.0 K
D1 1.00000000 sec
TDO 1

===== CHANNEL f1 =====
NUC1 1H
P1 13.70 usec
PL1 1.90 dB
PL1W 8.36853981 W
SF01 300.1418535 MHz
SI 32768
SF 300.1400281 MHz
WDW EM
SSB 0
LB 0.30 Hz
GB 0
PC 1.00
    
```

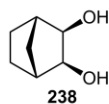


```

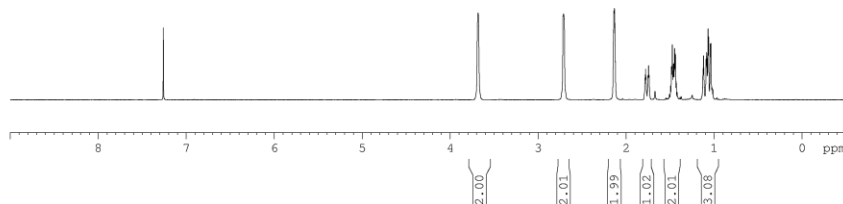
EXPNO 1
PROCNO 1
Date_ 20150316
Time 16.53
INSTRUM spect
PROBHD 5 mm PABBO BB-
PULPROG zgpg30
TD 65536
SOLVENT CDCl3
NS 14000
DS 4
SWH 18028.846 Hz
FIDRES 0.275098 Hz
AQ 1.8175818 sec
RG 203
DM 27.733 usec
DE 6.50 usec
TE 298.0 K
D1 2.00000000 sec
D11 0.03000000 sec
TDO 1

===== CHANNEL f1 =====
NUC1 13C
P1 10.82 usec
PL1 0.00 dB
PL1W 30.14263725 W
SF01 75.4778101 MHz

===== CHANNEL f2 =====
CPDPRG2 waltz16
NUC2 1H
PCPD2 100.00 usec
PL2 1.90 dB
PL12 19.17 dB
PL13 23.94 dB
PL1W 8.36853981 W
PL12W 0.15690966 W
PL13W 0.05231782 W
SF02 300.1412006 MHz
SI 32768
SF 75.4702654 MHz
WDW EM
SSB 0
LB 1.00 Hz
GB 0
PC 1.40
    
```



3.681
2.714
2.710
2.701
2.146
2.136
2.131
2.125
2.120
1.783
1.777
1.748
1.742
1.737
1.493
1.482
1.473
1.466
1.448
1.445
1.438
1.438
1.428
1.419
1.414
1.414
1.089
1.084
1.079

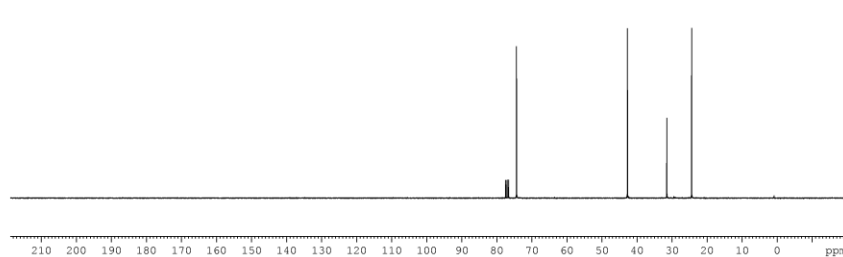


```

EXPNO      2
PROCNO     1
Date_      20140522
Time       9.20
INSTRUM    spect
PROBHD     5 mm PABBO BB-
PULPROG    zg30
TD          65536
SOLVENT    CDCl3
NS          16
DS          2
SWH         6188.119 Hz
FIDRES     0.094423 Hz
AQ          5.2953587 sec
RG          181
DW          80.800 usec
DE          6.50 usec
TE          298.0 K
D1          1.0000000 sec
TDO         1

===== CHANNEL f1 =====
NUC1       1H
P1         13.70 usec
PL1        1.90 dB
PL1W       8.36853981 W
SF01       300.1418535 MHz
SI         32768
SF         300.1400063 MHz
WDW        EM
SSB        0
LB         0.30 Hz
GB         0
PC         1.00
    
```

74.31
42.63
31.39
24.31

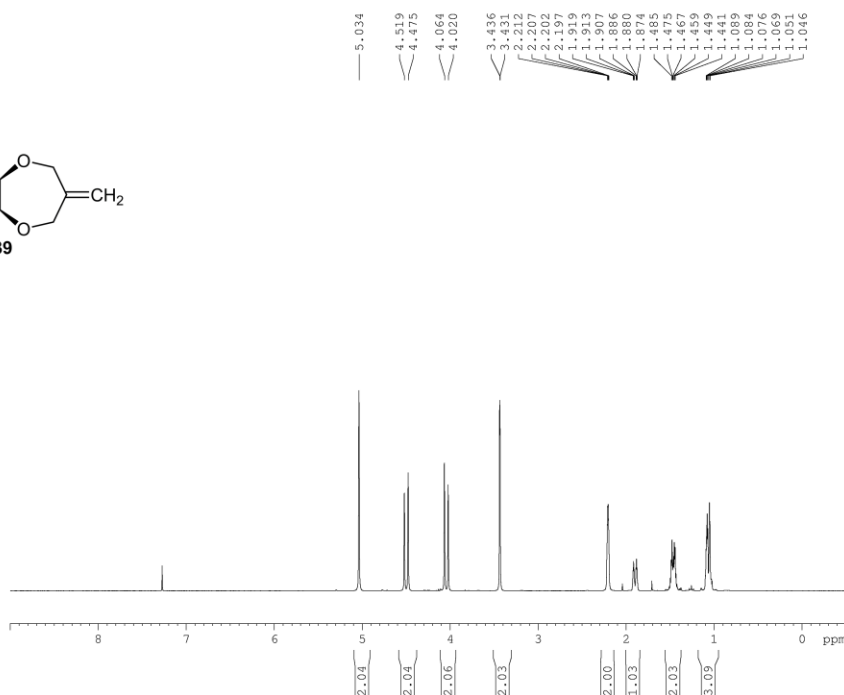
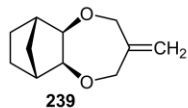


```

EXPNO      1
PROCNO     1
Date_      20140414
Time       15.37
INSTRUM    spect
PROBHD     5 mm PABBO BB-
PULPROG    zgpg30
TD          65536
SOLVENT    CDCl3
NS          4
DS          4
SWH         18028.846 Hz
FIDRES     0.275098 Hz
AQ          1.8175818 sec
RG          203
DW          27.733 usec
DE          6.50 usec
TE          298.0 K
D1          2.0000000 sec
D11        0.0300000 sec
TDO         1

===== CHANNEL f1 =====
NUC1       13C
P1         10.82 usec
PL1        0.00 dB
PL1W       30.14263725 W
SF01       75.4778101 MHz

===== CHANNEL f2 =====
CPDPRG2    waltz16
NUC2       1H
PCPD2     100.00 usec
PL2        1.90 dB
PL12       19.17 dB
PL13       23.94 dB
PL1W       8.36853981 W
PL12W     0.15690966 W
PL13W     0.05231782 W
SF02       300.1412006 MHz
SI         32768
SF         75.4702760 MHz
WDW        EM
SSB        0
LB         1.00 Hz
GB         0
PC         1.40
    
```

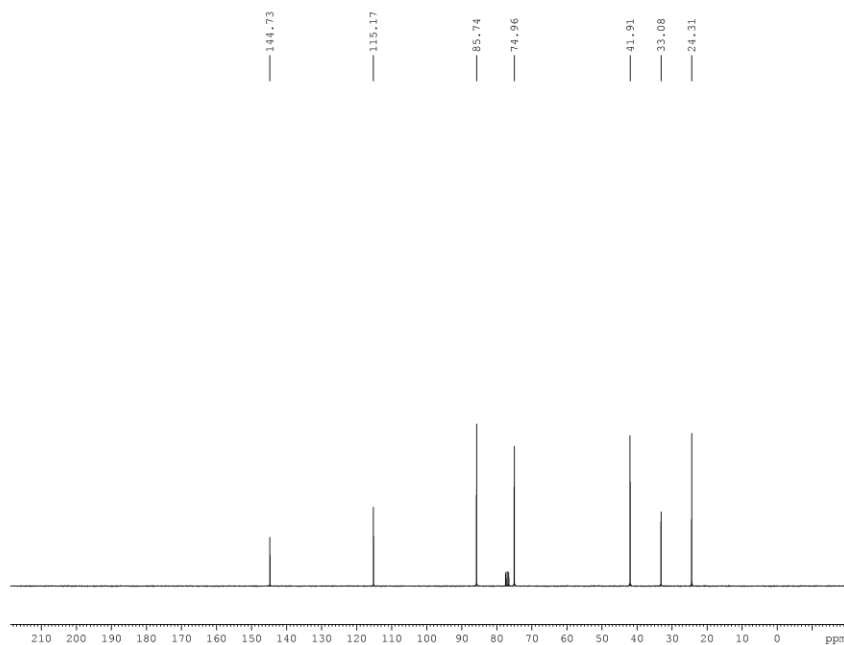


```

EXPNO 1
PROCNO 1
Date_ 20140502
Time 9.51
INSTRUM spect
PROBHD 5 mm PABBO BB-
PULPROG zg30
TD 65536
SOLVENT CDC13
NS 16
DS 2
SWH 6188.119 Hz
FIDRES 0.094423 Hz
AQ 5.2953587 sec
RG 64
DW 80.800 usec
DE 6.50 usec
TE 298.0 K
D1 1.0000000 sec
TDO 1
    
```

```

===== CHANNEL f1 =====
NUC1 1H
P1 13.70 usec
PL1 1.90 dB
PL1W 8.36853981 W
SFO1 300.1418535 MHz
SI 32768
SF 300.1400022 MHz
WDW EM
SSB 0
LB 0.30 Hz
GB 0
PC 1.00
    
```



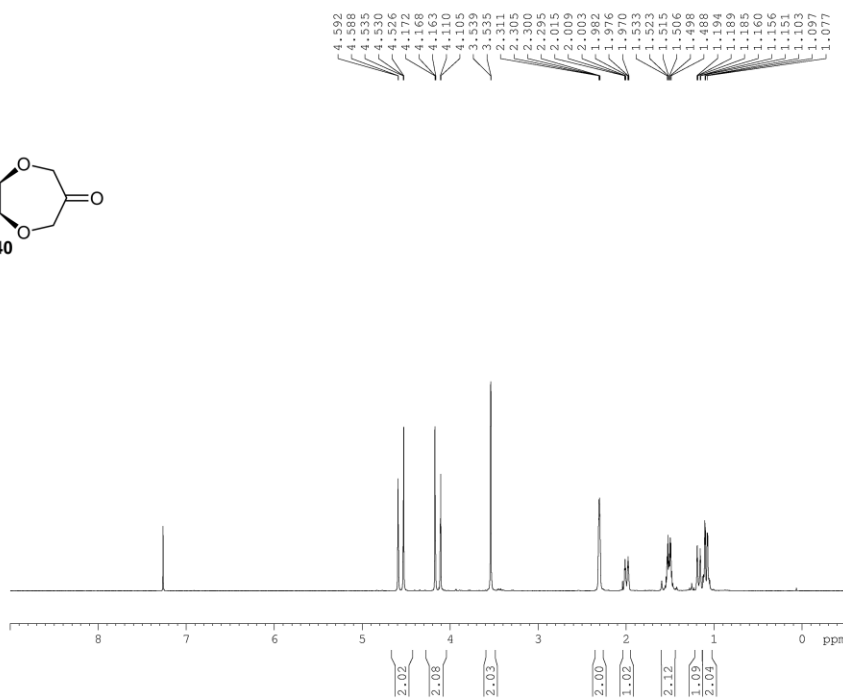
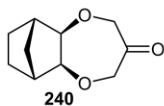
```

EXPNO 1
PROCNO 1
Date_ 20140429
Time 16.48
INSTRUM spect
PROBHD 5 mm PABBO BB-
PULPROG zgpg30
TD 65536
SOLVENT CDC13
NS 162
DS 4
SWH 18028.846 Hz
FIDRES 0.275098 Hz
AQ 1.8175818 sec
RG 203
DW 27.733 usec
DE 6.50 usec
TE 298.0 K
D1 2.0000000 sec
D11 0.0300000 sec
TDO 1
    
```

```

===== CHANNEL f1 =====
NUC1 13C
P1 10.82 usec
PL1 0.00 dB
PL1W 30.14263725 W
SFO1 75.4778101 MHz

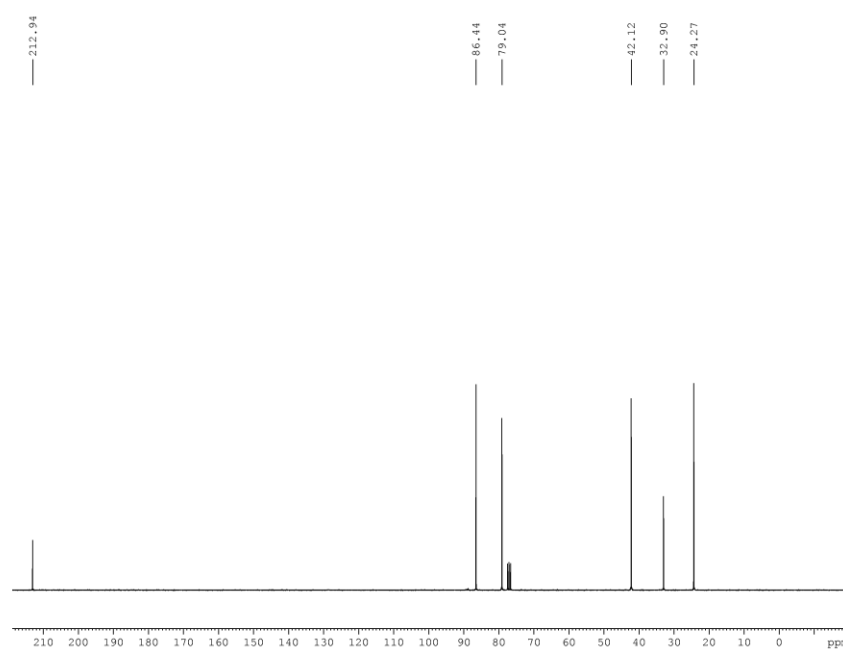
===== CHANNEL f2 =====
CPDPRG2 waltz16
NUC2 1H
PCPD2 100.00 usec
PL2 1.90 dB
PL12 19.17 dB
PL13 23.94 dB
PL2W 8.36853981 W
PL12W 0.15690966 W
PL13W 0.05231782 W
SFO2 300.1412006 MHz
SI 32768
SF 75.4702853 MHz
WDW EM
SSB 0
LB 1.00 Hz
GB 0
PC 1.40
    
```



```

EXPNO 1
PROCNO 1
Date_ 20140507
Time 4.20
INSTRUM spect
PROBHD 5 mm PABBO BB-
PULPROG zg30
TD 65536
SOLVENT CDC13
NS 16
DS 2
SWH 6188.119 Hz
FIDRES 0.094423 Hz
AQ 5.2953587 sec
RG 144
DW 80.800 usec
DE 6.50 usec
TE 298.0 K
D1 1.0000000 sec
TDO 1

===== CHANNEL f1 =====
NUC1 1H
P1 13.70 usec
PL1 1.90 dB
PL1W 8.36853981 W
SFO1 300.1418535 MHz
SI 32768
SF 300.1400052 MHz
WDW EM
SSB 0
LB 0.30 Hz
GB 0
PC 1.00
    
```

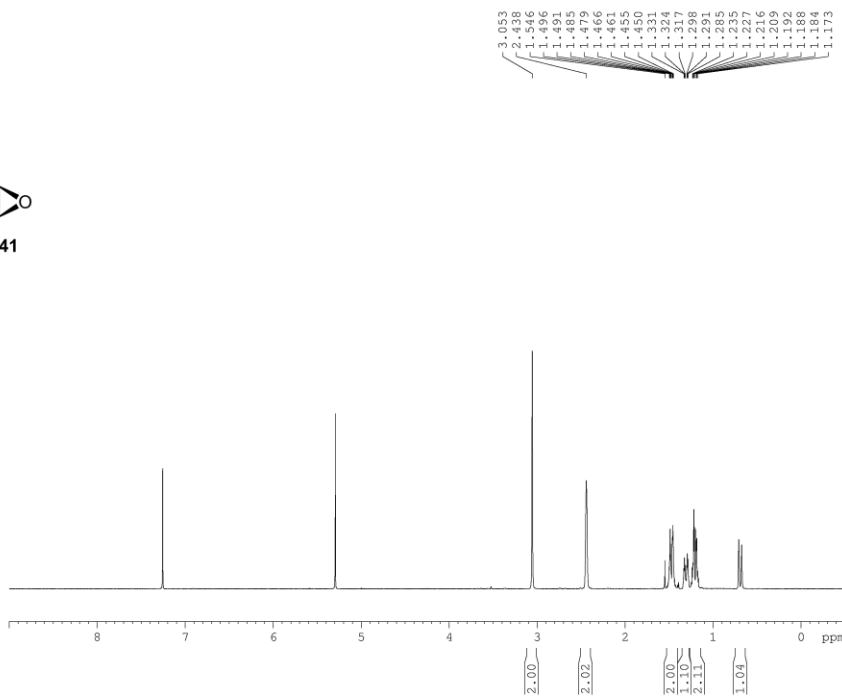


```

EXPNO 1
PROCNO 1
Date_ 20140507
Time 5.23
INSTRUM spect
PROBHD 5 mm PABBO BB-
PULPROG zgpg30
TD 65536
SOLVENT CDC13
NS 313
DS 4
SWH 18028.846 Hz
FIDRES 0.275098 Hz
AQ 1.8175818 sec
RG 203
DW 27.733 usec
DE 6.50 usec
TE 298.0 K
D1 2.0000000 sec
D11 0.0300000 sec
TDO 1

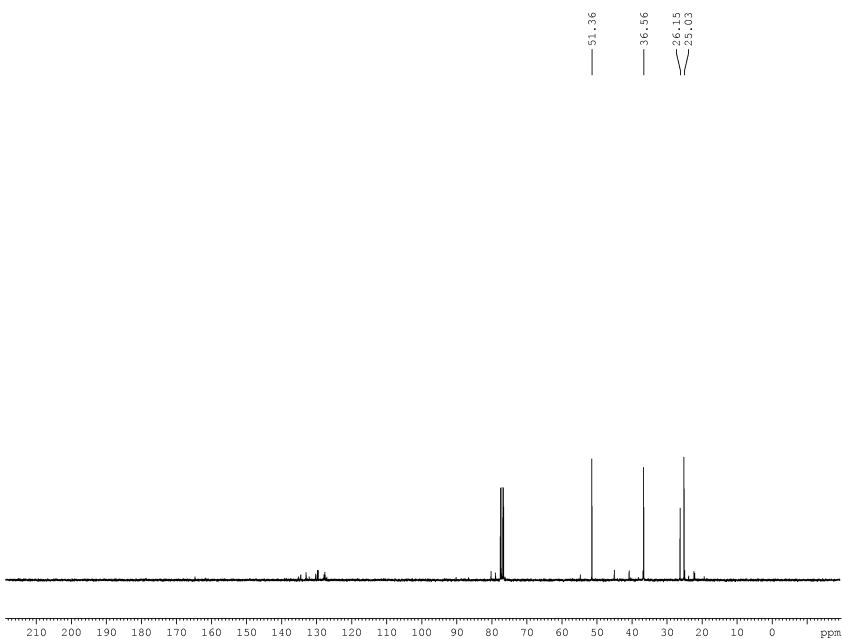
===== CHANNEL f1 =====
NUC1 13C
P1 10.82 usec
PL1 0.00 dB
PL1W 30.14263725 W
SFO1 75.4778101 MHz

===== CHANNEL f2 =====
CPDPRG2 waltz16
NUC2 1H
PCPD2 100.00 usec
PL2 1.90 dB
PL12 19.17 dB
PL13 23.94 dB
PL2W 8.36853981 W
PL12W 0.15690966 W
PL13W 0.05231782 W
SFO2 300.1412006 MHz
SI 32768
SF 75.4702760 MHz
WDW EM
SSB 0
LB 1.00 Hz
GB 0
PC 1.40
    
```



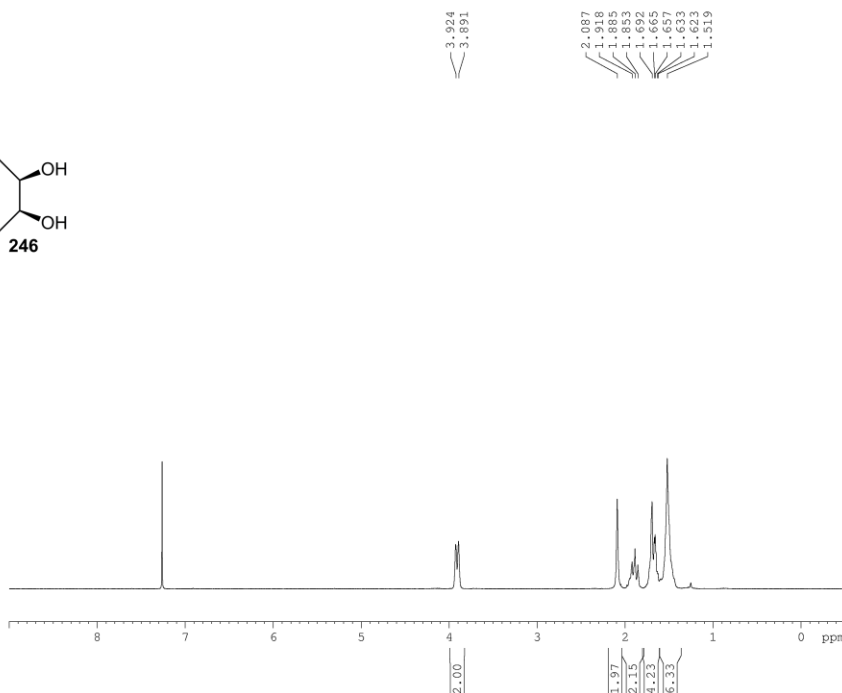
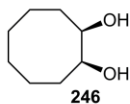
```

EXPNO          3
PROCNO         1
Date_          20131120
Time           15.59
INSTRUM        spect
PROBHD         5 mm PABBO BB-
PULPROG        zg30
TD             65536
SOLVENT        CDC13
NS             10
DS            2
SWH            6188.119 Hz
FIDRES         0.094423 Hz
AQ            5.2953587 sec
RG            203
DW            80.800 usec
DE            6.50 usec
TE            298.0 K
D1            1.00000000 sec
D11           1
D12           1
D13           1
D14           1
D15           1
D16           1
D17           1
D18           1
D19           1
D20           1
D21           1
D22           1
D23           1
D24           1
D25           1
D26           1
D27           1
D28           1
D29           1
D30           1
D31           1
D32           1
D33           1
D34           1
D35           1
D36           1
D37           1
D38           1
D39           1
D40           1
D41           1
D42           1
D43           1
D44           1
D45           1
D46           1
D47           1
D48           1
D49           1
D50           1
D51           1
D52           1
D53           1
D54           1
D55           1
D56           1
D57           1
D58           1
D59           1
D60           1
D61           1
D62           1
D63           1
D64           1
D65           1
D66           1
D67           1
D68           1
D69           1
D70           1
D71           1
D72           1
D73           1
D74           1
D75           1
D76           1
D77           1
D78           1
D79           1
D80           1
D81           1
D82           1
D83           1
D84           1
D85           1
D86           1
D87           1
D88           1
D89           1
D90           1
D91           1
D92           1
D93           1
D94           1
D95           1
D96           1
D97           1
D98           1
D99           1
D100          1
===== CHANNEL f1 =====
NUC1           1H
P1            13.70 usec
PL1           1.90 dB
PL1W          8.36853981 W
SFO1          300.1418535 MHz
SI            32768
SF            300.1400074 MHz
WDW           EM
SSB           0
LB            0.30 Hz
GB            0
PC            1.00
    
```



```

EXPNO          2
PROCNO         1
Date_          20131120
Time           14.43
INSTRUM        spect
PROBHD         5 mm PABBO BB-
PULPROG        zgpg30
TD             65536
SOLVENT        CDCl3
NS            268
DS            4
SWH            18028.846 Hz
FIDRES         0.275098 Hz
AQ            1.8175818 sec
RG            203
DW            27.733 usec
DE            6.80 usec
TE            298.0 K
D1            2.00000000 sec
D11           0.03000000 sec
D12           1
D13           1
D14           1
D15           1
D16           1
D17           1
D18           1
D19           1
D20           1
D21           1
D22           1
D23           1
D24           1
D25           1
D26           1
D27           1
D28           1
D29           1
D30           1
D31           1
D32           1
D33           1
D34           1
D35           1
D36           1
D37           1
D38           1
D39           1
D40           1
D41           1
D42           1
D43           1
D44           1
D45           1
D46           1
D47           1
D48           1
D49           1
D50           1
D51           1
D52           1
D53           1
D54           1
D55           1
D56           1
D57           1
D58           1
D59           1
D60           1
D61           1
D62           1
D63           1
D64           1
D65           1
D66           1
D67           1
D68           1
D69           1
D70           1
D71           1
D72           1
D73           1
D74           1
D75           1
D76           1
D77           1
D78           1
D79           1
D80           1
D81           1
D82           1
D83           1
D84           1
D85           1
D86           1
D87           1
D88           1
D89           1
D90           1
D91           1
D92           1
D93           1
D94           1
D95           1
D96           1
D97           1
D98           1
D99           1
D100          1
===== CHANNEL f1 =====
NUC1           13C
P1            10.82 usec
PL1           0.00 dB
PL1W          30.14263725 W
SFO1          75.4778101 MHz
===== CHANNEL f2 =====
CPDPRG2        waltz16
NUC2           1H
PCPD2         100.00 usec
PL2           1.90 dB
PL12          19.17 dB
PL13          23.94 dB
PL2W          8.36853981 W
PL12W         0.15690966 W
PL13W         0.05231782 W
SFO2          300.1412006 MHz
SI            32768
SF            75.4702670 MHz
WDW           EM
SSB           0
LB            1.00 Hz
GB            0
PC            1.40
    
```

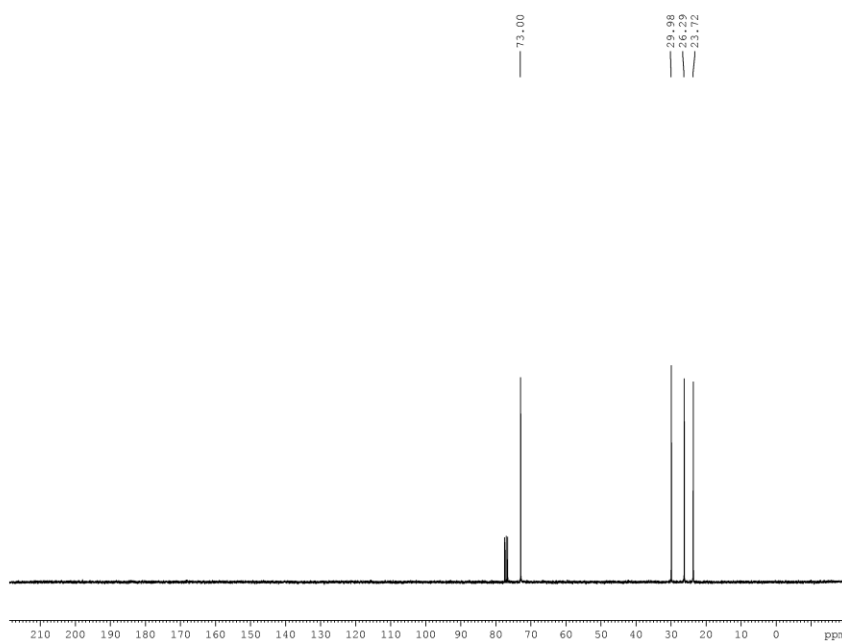


```

EXPNO 1
PROCNO 1
Date_ 20150121
Time 15.28
INSTRUM spect
PROBHD 5 mm PABBO BB-
PULPROG zg30
TD 65536
SOLVENT CDC13
NS 16
DS 2
SWH 6188.119 Hz
FIDRES 0.094423 Hz
AQ 5.2953587 sec
RG 203
DW 80.800 usec
DE 6.50 usec
TE 294.7 K
D1 1.00000000 sec
TDO 1
    
```

```

===== CHANNEL f1 =====
NUC1 1H
P1 13.70 usec
PL1 1.90 dB
PL1W 8.36853981 W
SFO1 300.1418535 MHz
SI 32768
SF 300.1400057 MHz
WDW EM
SSB 0
LB 0.30 Hz
GB 0
PC 1.00
    
```



```

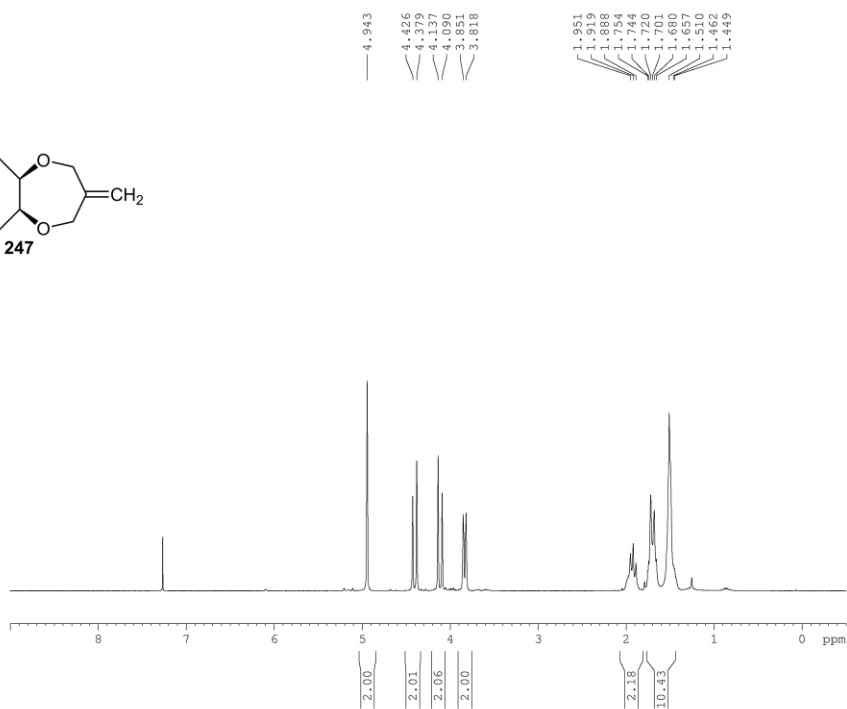
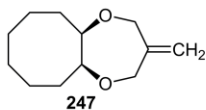
EXPNO 1
PROCNO 1
Date_ 20150121
Time 13.23
INSTRUM spect
PROBHD 5 mm PABBO BB-
PULPROG zgpg30
TD 65536
SOLVENT CDC13
NS 30
DS 4
SWH 18028.846 Hz
FIDRES 0.275098 Hz
AQ 1.8175818 sec
RG 203
DW 27.733 usec
DE 6.50 usec
TE 294.3 K
D1 2.00000000 sec
D11 0.03000000 sec
TDO 1
    
```

```

===== CHANNEL f1 =====
NUC1 13C
P1 10.82 usec
PL1 0.00 dB
PL1W 30.14263725 W
SFO1 75.4778101 MHz
    
```

```

===== CHANNEL f2 =====
CPDPRG2 waltz16
NUC2 1H
PCPD2 100.00 usec
PL2 1.90 dB
PL12 19.17 dB
PL13 23.94 dB
PL2W 8.36853981 W
PL12W 0.15690966 W
PL13W 0.05231782 W
SFO2 300.1412006 MHz
SI 32768
SF 75.4702751 MHz
WDW EM
SSB 0
LB 1.00 Hz
GB 0
PC 1.40
    
```

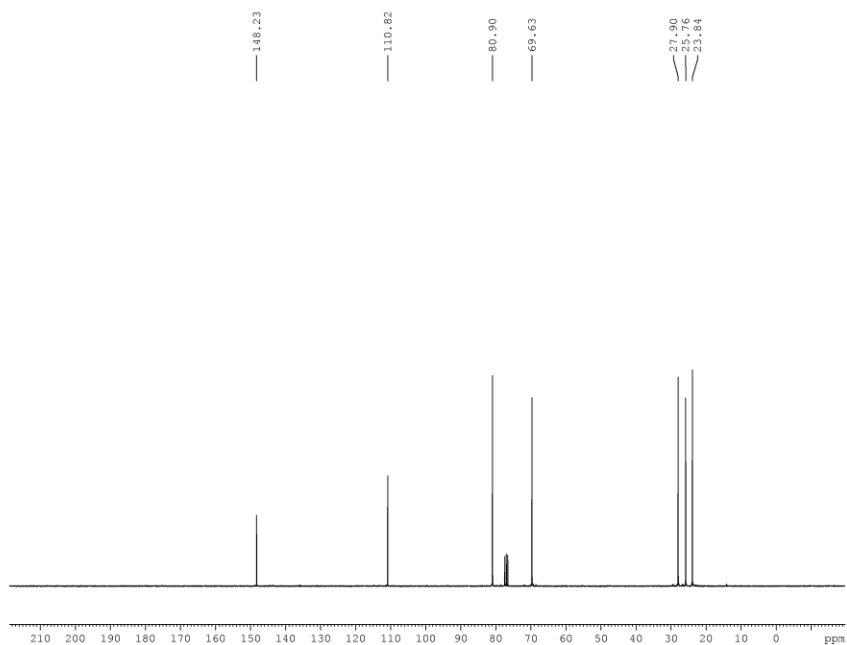


```

EXPNO 1
PROCNO 1
Date_ 20150130
Time 14.59
INSTRUM spect
PROBHD 5 mm PABBO BB-
PULPROG zg30
TD 65536
SOLVENT CDC13
NS 16
DS 2
SWH 6188.119 Hz
FIDRES 0.094423 Hz
AQ 5.2953587 sec
RG 80.6
DW 80.800 usec
DE 6.50 usec
TE 294.3 K
D1 1.0000000 sec
TDO 1
    
```

```

===== CHANNEL f1 =====
NUC1 1H
P1 13.70 usec
PL1 1.90 dB
PL1W 8.36853981 W
SFO1 300.1418535 MHz
SI 32768
SF 300.1400039 MHz
WDW EM
SSB 0
LB 0.30 Hz
GB 0
PC 1.00
    
```



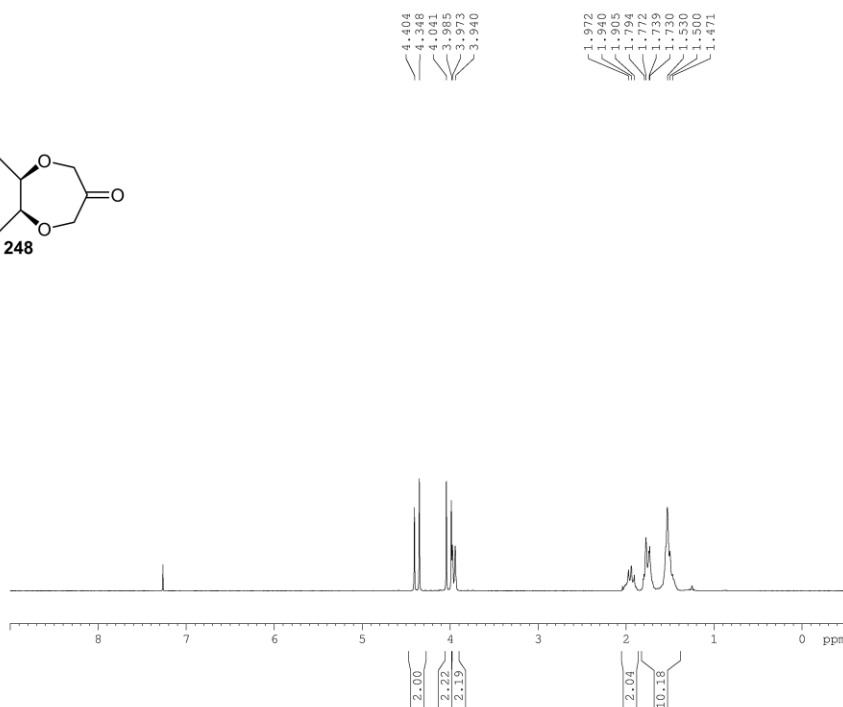
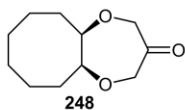
```

EXPNO 1
PROCNO 1
Date_ 20150130
Time 16.39
INSTRUM spect
PROBHD 5 mm PABBO BB-
PULPROG zgpg30
TD 65536
SOLVENT CDC13
NS 200
DS 4
SWH 18028.846 Hz
FIDRES 0.275098 Hz
AQ 1.8175818 sec
RG 203
DW 27.733 usec
DE 6.50 usec
TE 294.6 K
D1 2.0000000 sec
D11 0.0300000 sec
TDO 1
    
```

```

===== CHANNEL f1 =====
NUC1 13C
P1 10.82 usec
PL1 0.00 dB
PL1W 30.14263725 W
SFO1 75.4778101 MHz

===== CHANNEL f2 =====
CPDPRG2 waltz16
NUC2 1H
PCPD2 100.00 usec
PL2 1.90 dB
PL12 19.17 dB
PL13 23.94 dB
PL2W 8.36853981 W
PL12W 0.15690966 W
PL13W 0.05231782 W
SFO2 300.1412006 MHz
SI 32768
SF 75.4702819 MHz
WDW EM
SSB 0
LB 1.00 Hz
GB 0
PC 1.40
    
```

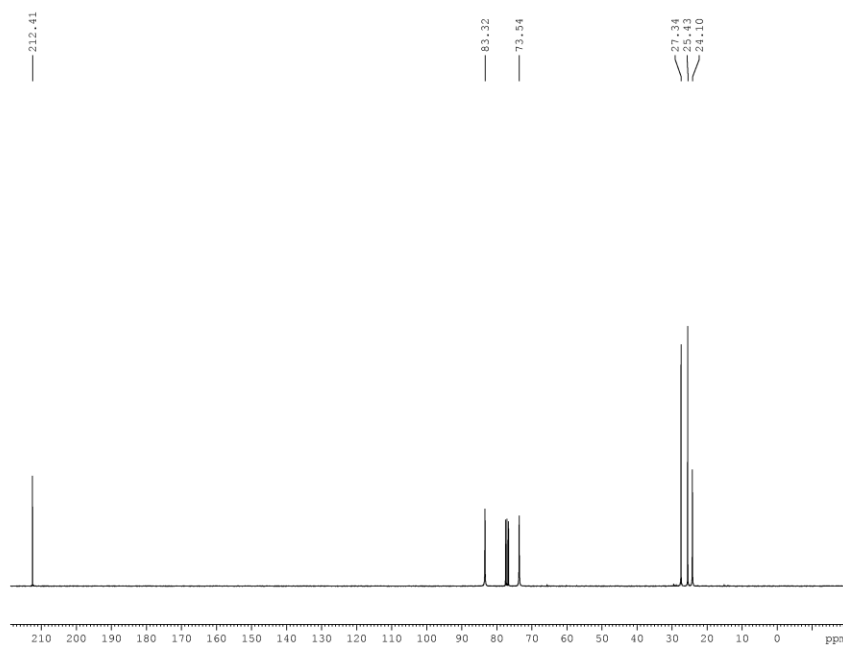


```

EXPNO 1
PROCNO 1
Date_ 20150208
Time 15.22
INSTRUM spect
PROBHD 5 mm PABBO BB-
PULPROG zg30
TD 65536
SOLVENT CDC13
NS 16
DS 2
SWH 6188.119 Hz
FIDRES 0.094423 Hz
AQ 5.2953587 sec
RG 71.8
DW 80.800 usec
DE 6.50 usec
TE 295.0 K
D1 1.0000000 sec
TDO 1
    
```

```

===== CHANNEL f1 =====
NUC1 1H
P1 13.70 usec
PL1 1.90 dB
PL1W 8.36853981 W
SFO1 300.1418535 MHz
SI 32768
SF 300.1400051 MHz
WDW EM
SSB 0
LB 0.30 Hz
GB 0
PC 1.00
    
```



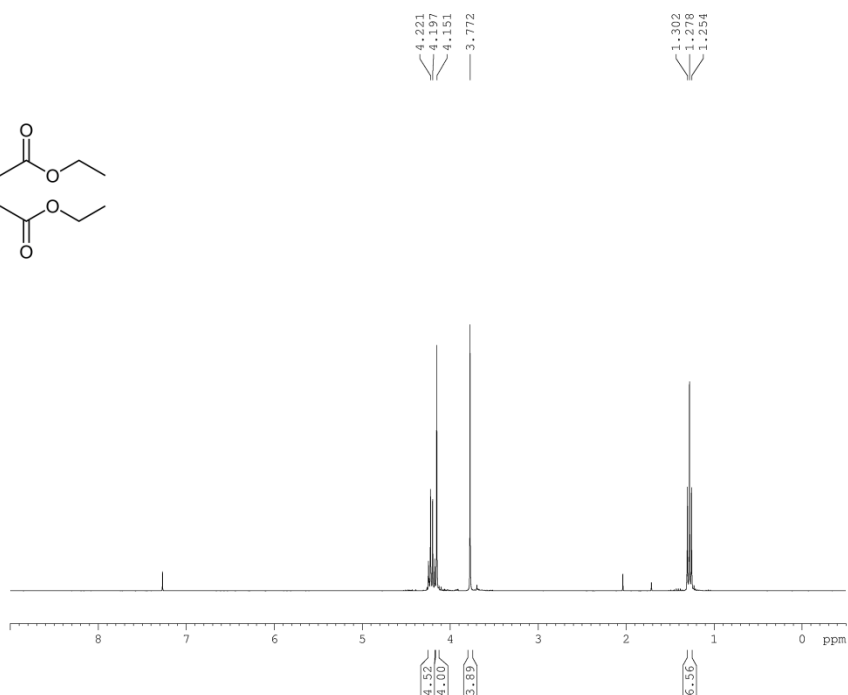
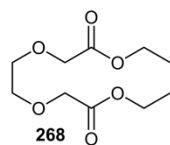
```

EXPNO 1
PROCNO 1
Date_ 20150208
Time 22.40
INSTRUM spect
PROBHD 5 mm PABBO BB-
PULPROG zgpg30
TD 65536
SOLVENT CDC13
NS 3000
DS 4
SWH 18028.846 Hz
FIDRES 0.275098 Hz
AQ 1.8175818 sec
RG 203
DW 27.733 usec
DE 6.50 usec
TE 295.1 K
D1 2.0000000 sec
D11 0.0300000 sec
TDO 1
    
```

```

===== CHANNEL f1 =====
NUC1 13C
P1 10.82 usec
PL1 0.00 dB
PL1W 30.14263725 W
SFO1 75.4778101 MHz

===== CHANNEL f2 =====
CPDPRG2 waltz16
NUC2 1H
PCPD2 100.00 usec
PL2 1.90 dB
PL12 19.17 dB
PL13 23.94 dB
PL2W 8.36853981 W
PL12W 0.15690966 W
PL13W 0.05231782 W
SFO2 300.1412006 MHz
SI 32768
SF 75.4702755 MHz
WDW EM
SSB 0
LB 1.00 Hz
GB 0
PC 1.40
    
```

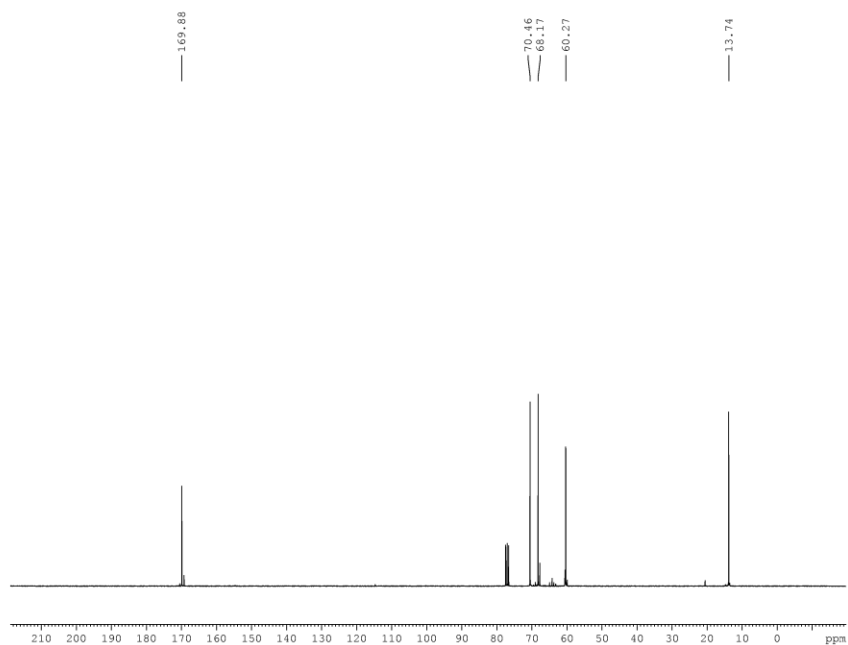



```

EXPNO 1
PROCNO 1
Date_ 20131217
Time 9.08
INSTRUM spect
PROBHD 5 mm PABBO BB-
PULPROG zg30
TD 65536
SOLVENT CDC13
NS 16
DS 2
SWH 6188.119 Hz
FIDRES 0.094423 Hz
AQ 5.2953587 sec
RG 90.5
DW 80.800 usec
DE 6.50 usec
TE 298.0 K
D1 1.0000000 sec
TDO 1
    
```

```

===== CHANNEL f1 =====
NUC1 1H
P1 13.70 usec
PL1 1.90 dB
PL1W 8.36853981 W
SFO1 300.1418535 MHz
SI 32768
SF 300.1400032 MHz
WDW EM
SSB 0
LB 0.30 Hz
GB 0
PC 1.00
    
```



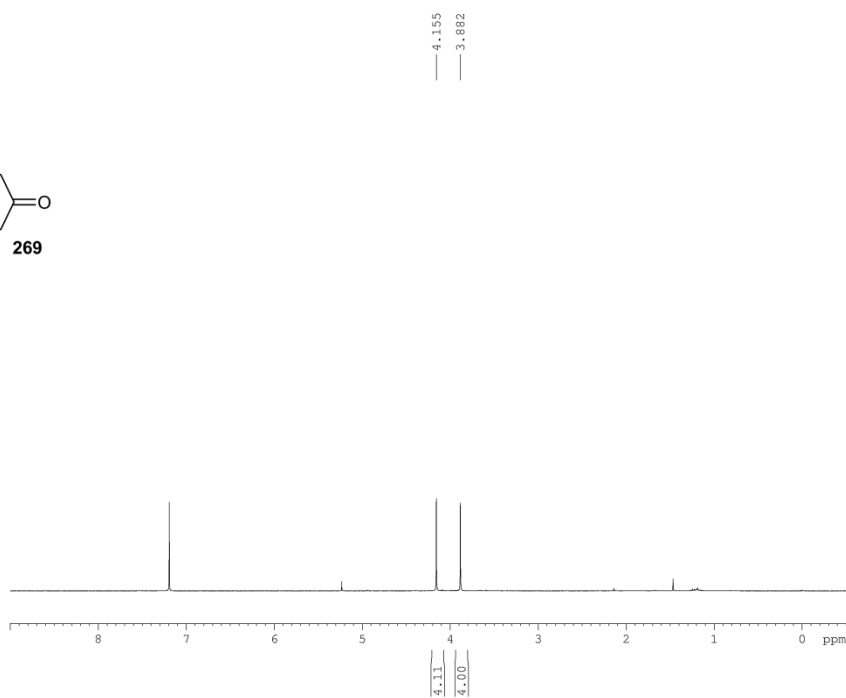
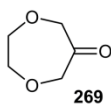
```

EXPNO 1
PROCNO 1
Date_ 20131216
Time 17.40
INSTRUM spect
PROBHD 5 mm PABBO BB-
PULPROG zgpg30
TD 65536
SOLVENT CDC13
NS 1024
DS 4
SWH 18028.846 Hz
FIDRES 0.275098 Hz
AQ 1.8175818 sec
RG 203
DW 27.733 usec
DE 6.50 usec
TE 298.0 K
D1 2.0000000 sec
D11 0.0300000 sec
TDO 1
    
```

```

===== CHANNEL f1 =====
NUC1 13C
P1 10.82 usec
PL1 0.00 dB
PL1W 30.14263725 W
SFO1 75.4778101 MHz

===== CHANNEL f2 =====
CPDPRG2 waltz16
NUC2 1H
PCPD2 100.00 usec
PL2 1.90 dB
PL12 19.17 dB
PL13 23.94 dB
PL2W 8.36853981 W
PL12W 0.15690966 W
PL13W 0.05231782 W
SFO2 300.1412006 MHz
SI 32768
SF 75.4702836 MHz
WDW EM
SSB 0
LB 1.00 Hz
GB 0
PC 1.40
    
```



```

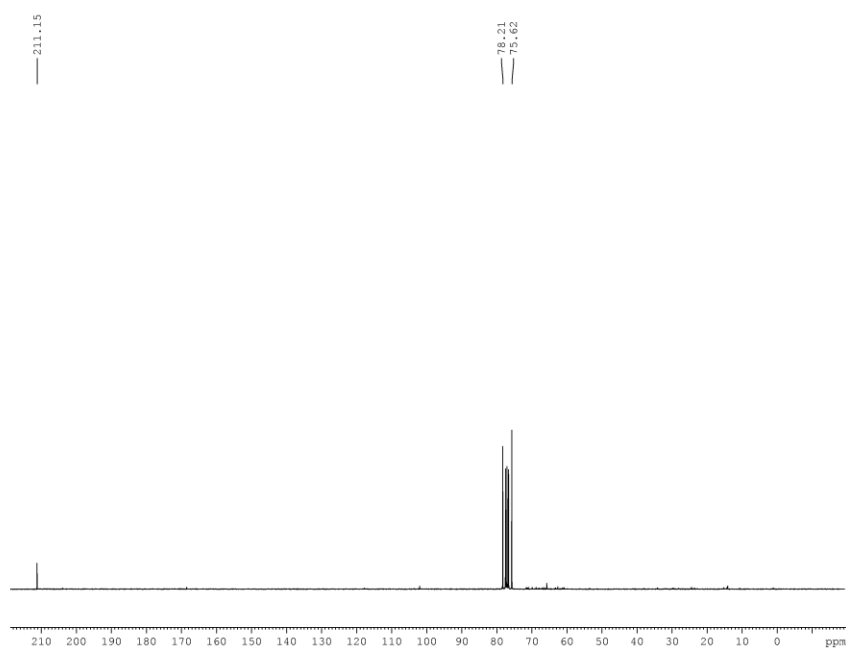
EXPNO          2
PROCNO         1
Date_          20140220
Time          14.37
INSTRUM       spect
PROBHD        5 mm PABBO BB-
PULPROG       zg30
TD            65536
SOLVENT       CDC13
NS            32
DS            2
SWH           6188.119 Hz
FIDRES        0.094423 Hz
AQ            5.2953587 sec
RG            203
DW            80.800 usec
DE            6.50 usec
TE            298.0 K
D1            1.0000000 sec
TDO           1

```

```

===== CHANNEL f1 =====
NUC1           1H
P1            13.70 usec
PL1           1.90 dB
PL1W          8.36853981 W
SFO1          300.1418535 MHz
SI            32768
SF            300.1400264 MHz
WDW           EM
SSB           0
LB            0.30 Hz
GB            0
PC            1.00

```



```

EXPNO          1
PROCNO         1
Date_          20140220
Time          6.02
INSTRUM       spect
PROBHD        5 mm PABBO BB-
PULPROG       zgpg30
TD            65536
SOLVENT       CDC13
NS            13000
DS            4
SWH           18028.846 Hz
FIDRES        0.275098 Hz
AQ            1.8175818 sec
RG            203
DW            27.733 usec
DE            6.50 usec
TE            298.0 K
D1            2.0000000 sec
D11           0.0300000 sec
TDO           1

```

```

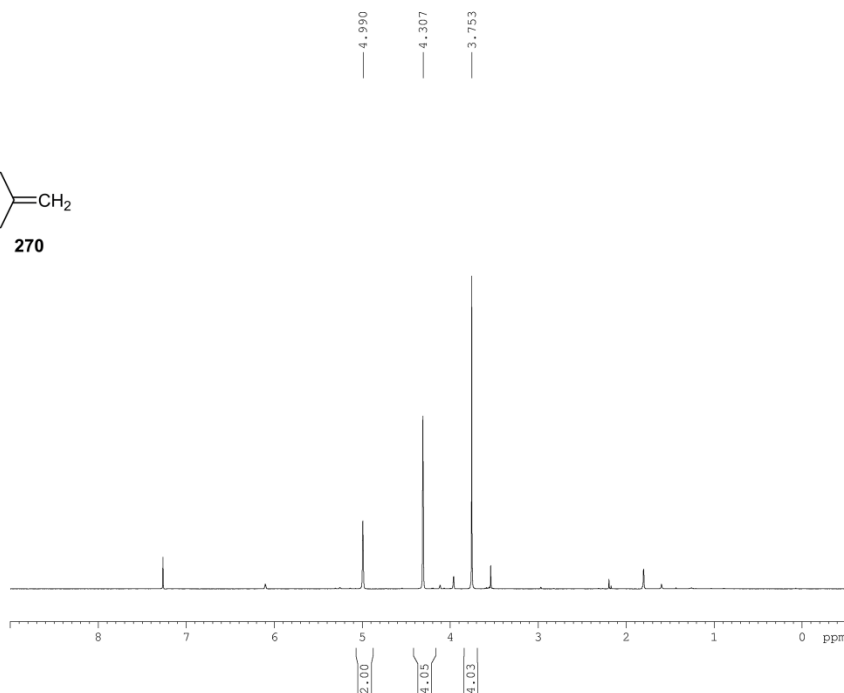
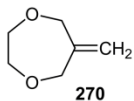
===== CHANNEL f1 =====
NUC1           13C
P1            10.82 usec
PL1           0.00 dB
PL1W          30.14263725 W
SFO1          75.4778101 MHz

```

```

===== CHANNEL f2 =====
CPDPRG2       waltz16
NUC2           1H
PCPD2         100.00 usec
PL2           1.90 dB
PL12          19.17 dB
PL13          23.94 dB
PL2W          8.36853981 W
PL12W         0.15690966 W
PL13W         0.05231782 W
SFO2          300.1412006 MHz
SI            32768
SF            75.4702667 MHz
WDW           EM
SSB           0
LB            1.00 Hz
GB            0
PC            1.40

```

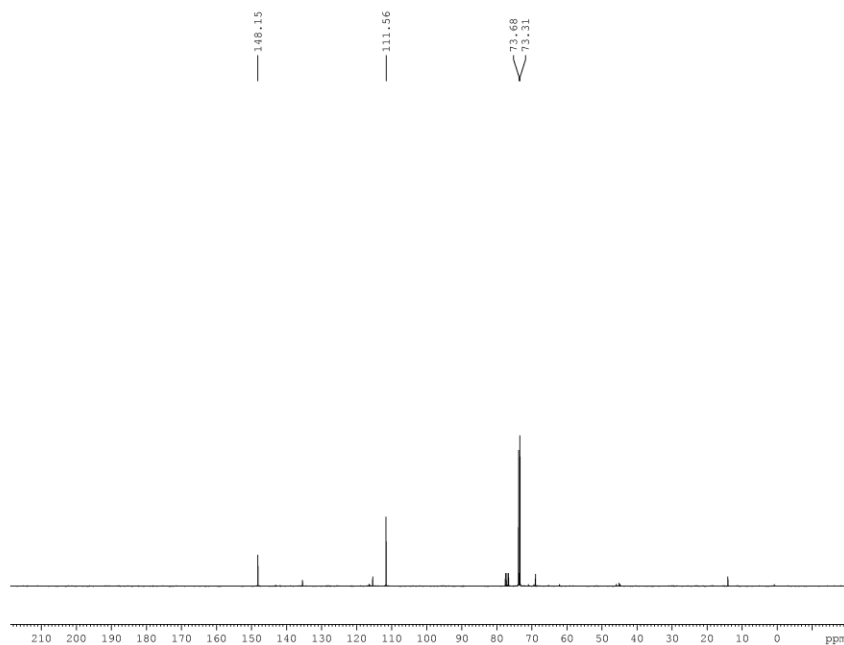


```

EXPNO 1
PROCNO 1
Date_ 20090309
Time 23.04
INSTRUM spect
PROBHD 5 mm PABBO BB-
PULPROG zg30
TD 65536
SOLVENT CDC13
NS 16
DS 2
SWH 6188.119 Hz
FIDRES 0.094423 Hz
AQ 5.2953587 sec
RG 203
DW 80.800 usec
DE 6.50 usec
TE 298.0 K
D1 1.0000000 sec
TDO 1
    
```

```

===== CHANNEL f1 =====
NUC1 1H
P1 13.70 usec
PL1 1.90 dB
PL1W 8.36853981 W
SFO1 300.1418535 MHz
SI 32768
SF 300.1400051 MHz
WDW EM
SSB 0
LB 0.30 Hz
GB 0
PC 1.00
    
```



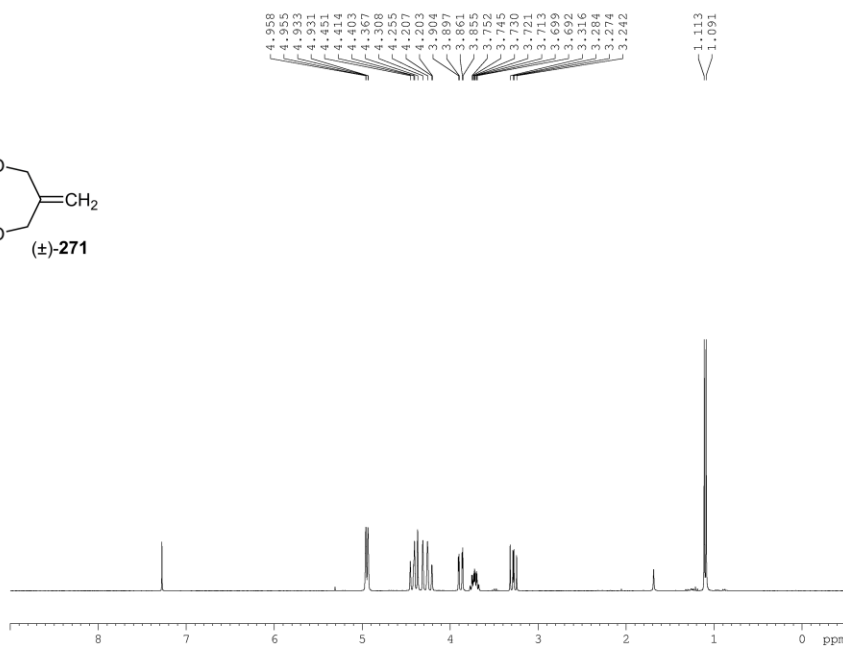
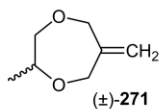
```

EXPNO 2
PROCNO 1
Date_ 20090310
Time 0.15
INSTRUM spect
PROBHD 5 mm PABBO BB-
PULPROG zgpg30
TD 65536
SOLVENT CDC13
NS 392
DS 4
SWH 18028.846 Hz
FIDRES 0.275098 Hz
AQ 1.8175818 sec
RG 203
DW 27.733 usec
DE 6.50 usec
TE 298.0 K
D1 2.0000000 sec
D11 0.0300000 sec
TDO 1
    
```

```

===== CHANNEL f1 =====
NUC1 13C
P1 10.82 usec
PL1 0.00 dB
PL1W 30.14263725 W
SFO1 75.4778101 MHz

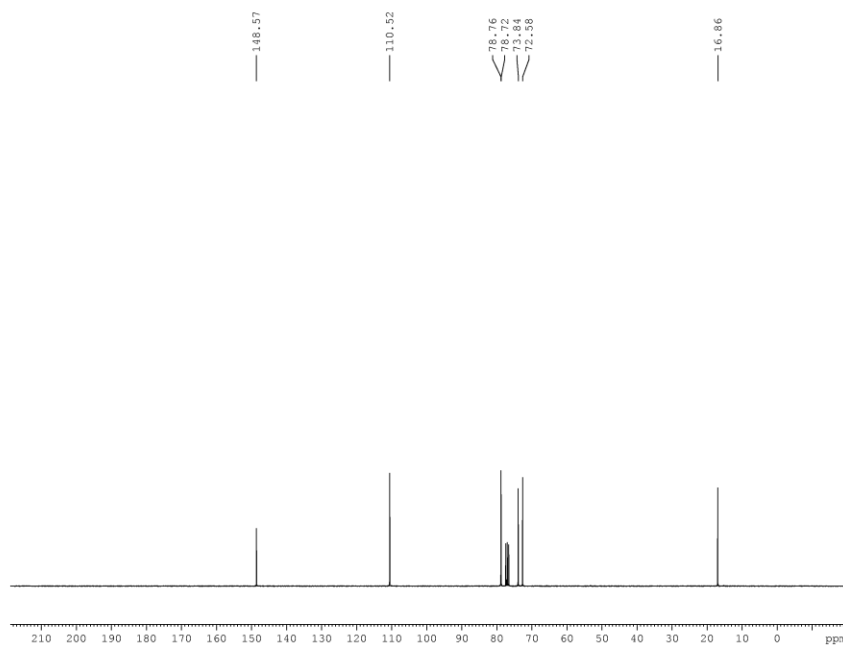
===== CHANNEL f2 =====
CPDPRG2 waltz16
NUC2 1H
PCPD2 100.00 usec
PL2 1.90 dB
PL12 19.17 dB
PL13 23.94 dB
PL2W 8.36853981 W
PL12W 0.15690966 W
PL13W 0.05231782 W
SFO2 300.1412006 MHz
SI 32768
SF 75.4702770 MHz
WDW EM
SSB 0
LB 1.00 Hz
GB 0
PC 1.40
    
```



```

EXPNO 1
PROCNO 1
Date_ 20150204
Time 11.28
INSTRUM spect
PROBHD 5 mm PABBO BB-
PULPROG zg30
TD 65536
SOLVENT CDC13
NS 16
DS 2
SWH 6188.119 Hz
FIDRES 0.094423 Hz
AQ 5.2953587 sec
RG 80.6
DW 80.800 usec
DE 6.50 usec
TE 294.0 K
D1 1.00000000 sec
TDO 1

===== CHANNEL f1 =====
NUC1 1H
P1 13.70 usec
PL1 1.90 dB
PL1W 8.36853981 W
SFO1 300.1418535 MHz
SI 32768
SF 300.1400016 MHz
WDW EM
SSB 0
LB 0.30 Hz
GB 0
PC 1.00
    
```

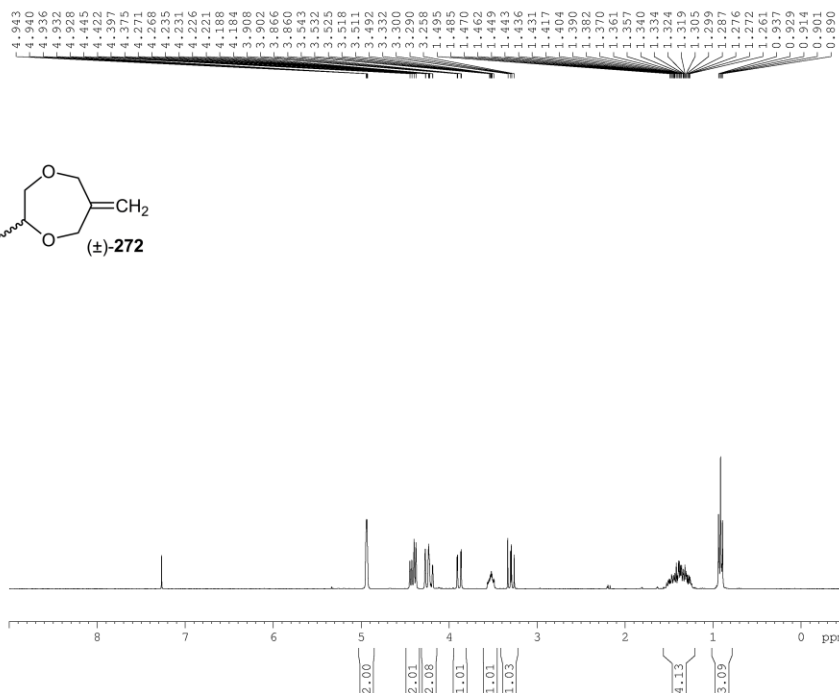
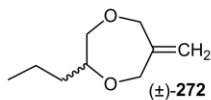


```

EXPNO 1
PROCNO 1
Date_ 20150204
Time 13.11
INSTRUM spect
PROBHD 5 mm PABBO BB-
PULPROG zgpg30
TD 65536
SOLVENT CDC13
NS 1024
DS 4
SWH 18028.846 Hz
FIDRES 0.275098 Hz
AQ 1.8175818 sec
RG 203
DW 27.733 usec
DE 6.50 usec
TE 294.2 K
D1 2.00000000 sec
D11 0.03000000 sec
TDO 1

===== CHANNEL f1 =====
NUC1 13C
P1 10.82 usec
PL1 0.00 dB
PL1W 30.14263725 W
SFO1 75.4778101 MHz

===== CHANNEL f2 =====
CPDPRG2 waltz16
NUC2 1H
PCPD2 100.00 usec
PL2 1.90 dB
PL12 19.17 dB
PL13 23.94 dB
PL2W 8.36853981 W
PL12W 0.15690966 W
PL13W 0.05231782 W
SFO2 300.1412006 MHz
SI 32768
SF 75.4702757 MHz
WDW EM
SSB 0
LB 1.00 Hz
GB 0
PC 1.40
    
```

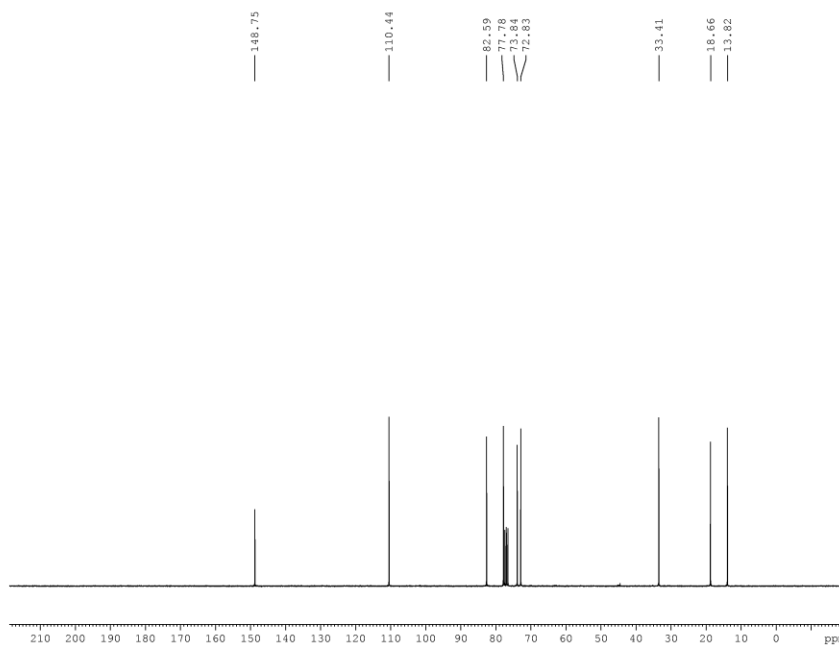


```

EXPNO 1
PROCNO 1
Date_ 20140506
Time 15.38
INSTRUM spect
PROBHD 5 mm PABBO BB-
PULPROG zg30
TD 65536
SOLVENT CDC13
NS 15
DS 2
SWH 6188.119 Hz
FIDRES 0.094423 Hz
AQ 5.2953587 sec
RG 80.6
DW 80.800 usec
DE 6.50 usec
TE 298.0 K
D1 1.0000000 sec
TDO 1
    
```

```

===== CHANNEL f1 =====
NUC1 1H
P1 13.70 usec
PL1 1.90 dB
PL1W 8.36853981 W
SF01 300.1418535 MHz
SI 32768
SF 300.1400037 MHz
WDW EM
SSB 0
LB 0.30 Hz
GB 0
PC 1.00
    
```



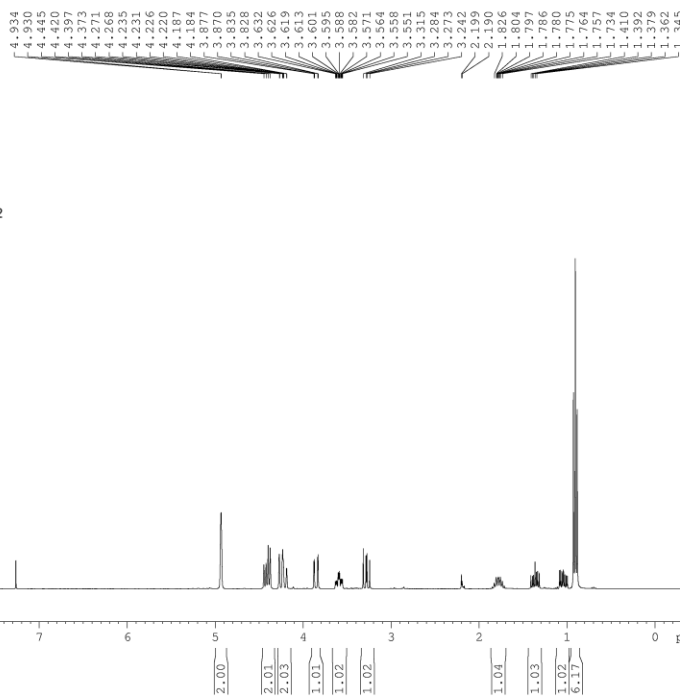
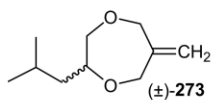
```

EXPNO 2
PROCNO 1
Date_ 20140506
Time 17.51
INSTRUM spect
PROBHD 5 mm PABBO BB-
PULPROG zgpg30
TD 65536
SOLVENT CDC13
NS 605
DS 4
SWH 18028.846 Hz
FIDRES 0.275098 Hz
AQ 1.8175818 sec
RG 203
DW 27.733 usec
DE 6.50 usec
TE 298.0 K
D1 2.0000000 sec
D11 0.0300000 sec
TDO 1
    
```

```

===== CHANNEL f1 =====
NUC1 13C
P1 10.82 usec
PL1 0.00 dB
PL1W 30.14263725 W
SF01 75.4778101 MHz

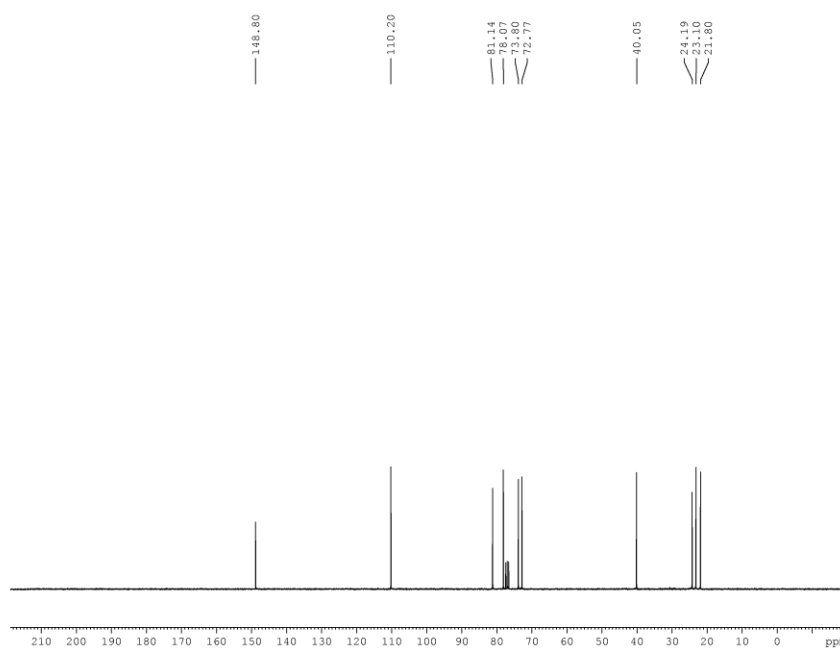
===== CHANNEL f2 =====
CPDPRG2 waltz16
NUC2 1H
PCPD2 100.00 usec
PL2 1.90 dB
PL12 19.17 dB
PL13 23.94 dB
PL2W 8.36853981 W
PL12W 0.15690966 W
PL13W 0.05231782 W
SF02 300.1412006 MHz
SI 32768
SF 75.4702740 MHz
WDW EM
SSB 0
LB 1.00 Hz
GB 0
PC 1.40
    
```



```

EXPNO 1
PROCNO 1
Date_ 20140805
Time 13.33
INSTRUM spect
PROBHD 5 mm PABBO BB-
PULPROG zg30
TD 65536
SOLVENT CDC13
NS 16
DS 2
SWH 6188.119 Hz
FIDRES 0.094423 Hz
AQ 5.2953587 sec
RG 71.8
DW 80.800 usec
DE 6.50 usec
TE 298.0 K
D1 1.0000000 sec
TDO 1

===== CHANNEL f1 =====
NUC1 1H
P1 13.70 usec
PL1 1.90 dB
PL1W 8.36853981 W
SFO1 300.1418535 MHz
SI 32768
SF 300.1400045 MHz
WDW EM
SSB 0
LB 0.30 Hz
GB 0
PC 1.00
    
```

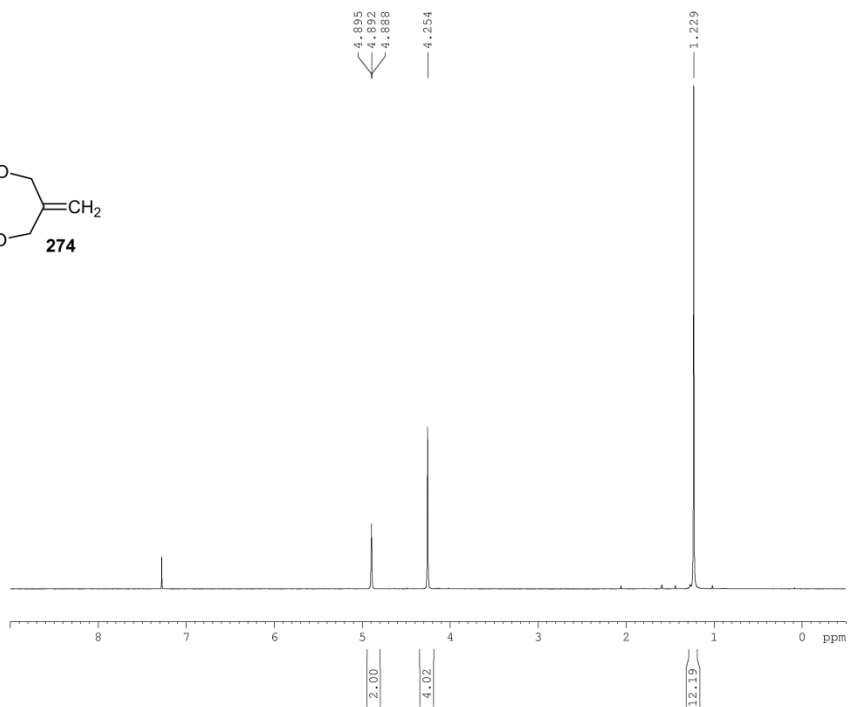
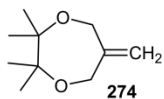


```

EXPNO 2
PROCNO 1
Date_ 20140611
Time 11.06
INSTRUM spect
PROBHD 5 mm PABBO BB-
PULPROG zgpg30
TD 65536
SOLVENT CDC13
NS 84
DS 4
SWH 18028.846 Hz
FIDRES 0.275098 Hz
AQ 1.8175818 sec
RG 203
DW 27.733 usec
DE 6.50 usec
TE 298.0 K
D1 2.0000000 sec
D11 0.0300000 sec
TDO 1

===== CHANNEL f1 =====
NUC1 13C
P1 10.82 usec
PL1 0.00 dB
PL1W 30.14263725 W
SFO1 75.4778101 MHz

===== CHANNEL f2 =====
CPDPRG2 waltz16
NUC2 1H
PCPD2 100.00 usec
PL2 1.90 dB
PL12 19.17 dB
PL13 23.94 dB
PL2W 8.36853981 W
PL12W 0.15690966 W
PL13W 0.05231782 W
SFO2 300.1412006 MHz
SI 32768
SF 75.4702742 MHz
WDW EM
SSB 0
LB 1.00 Hz
GB 0
PC 1.40
    
```

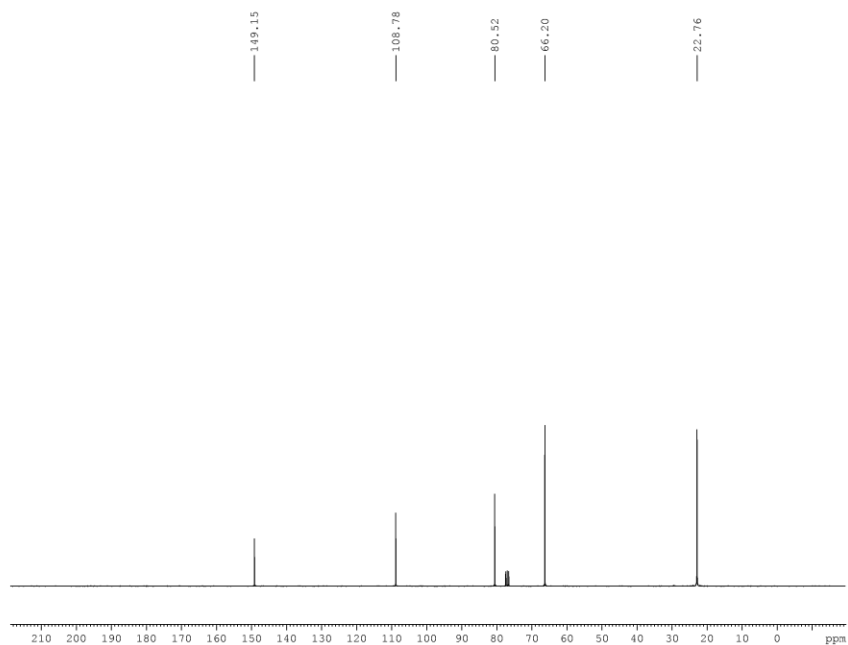


```

EXPNO 2
PROCNO 1
Date_ 20140807
Time 16.10
INSTRUM spect
PROBHD 5 mm PABBO BB-
PULPROG zg30
TD 65536
SOLVENT CDC13
NS 16
DS 2
SWH 6188.119 Hz
FIDRES 0.094423 Hz
AQ 5.2953587 sec
RG 191
DW 80.800 usec
DE 6.50 usec
TE 298.0 K
D1 1.0000000 sec
TDO 1
    
```

```

===== CHANNEL f1 =====
NUC1 1H
P1 13.70 usec
PL1 1.90 dB
PL1W 8.36853981 W
SFO1 300.1418535 MHz
SI 32768
SF 300.1400009 MHz
WDW EM
SSB 0
LB 0.30 Hz
GB 0
PC 1.00
    
```



```

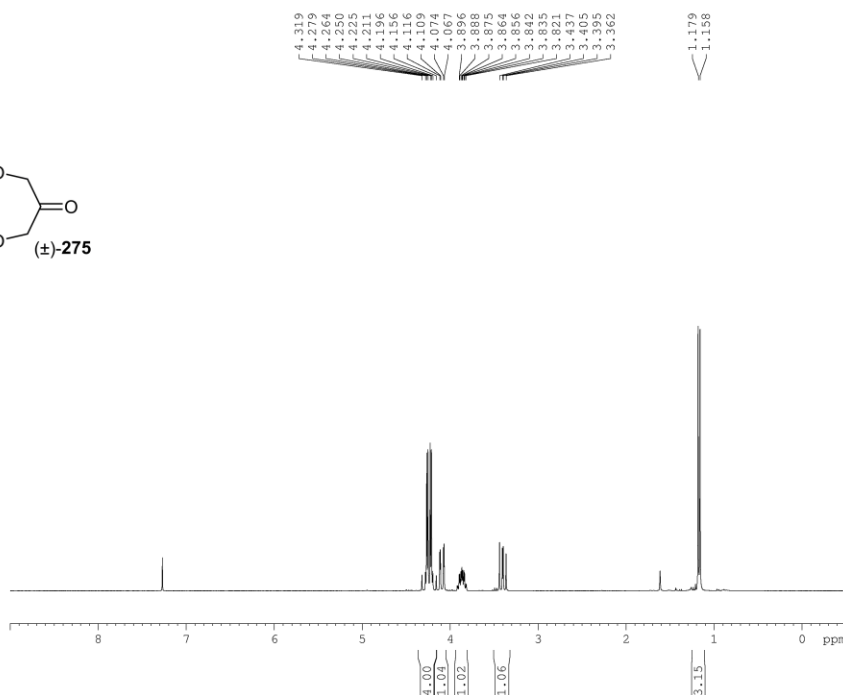
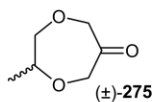
EXPNO 1
PROCNO 1
Date_ 20140807
Time 14.20
INSTRUM spect
PROBHD 5 mm PABBO BB-
PULPROG zgpg30
TD 65536
SOLVENT CDC13
NS 360
DS 4
SWH 18028.846 Hz
FIDRES 0.275098 Hz
AQ 1.8175818 sec
RG 203
DW 27.733 usec
DE 6.50 usec
TE 298.0 K
D1 2.0000000 sec
D11 0.0300000 sec
TDO 1
    
```

```

===== CHANNEL f1 =====
NUC1 13C
P1 10.82 usec
PL1 0.00 dB
PL1W 30.14263725 W
SFO1 75.4778101 MHz
    
```

```

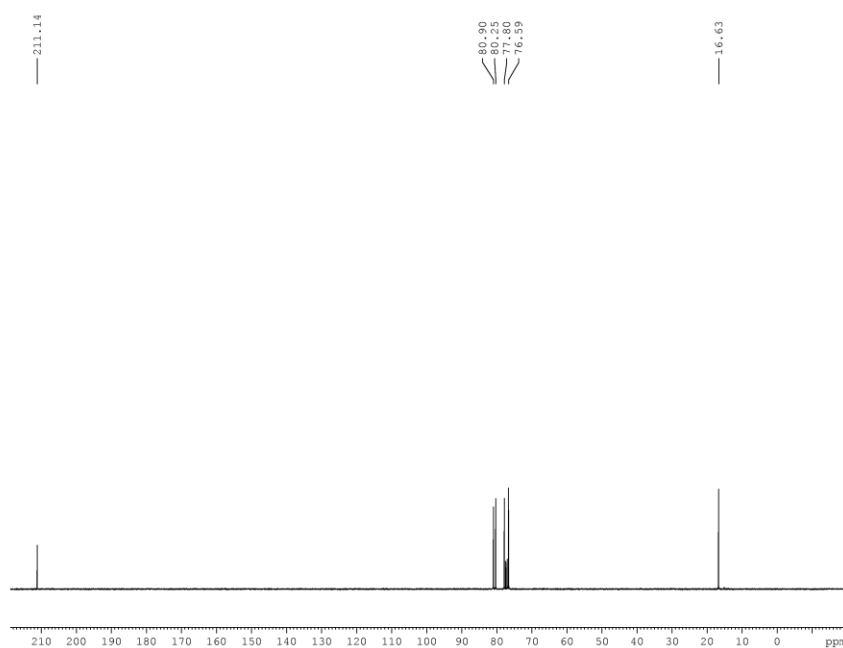
===== CHANNEL f2 =====
CPDPRG2 waltz16
NUC2 1H
PCPD2 100.00 usec
PL2 1.90 dB
PL12 19.17 dB
PL13 23.94 dB
PL2W 8.36853981 W
PL12W 0.15690966 W
PL13W 0.05231782 W
SFO2 300.1412006 MHz
SI 32768
SF 75.4702765 MHz
WDW EM
SSB 0
LB 1.00 Hz
GB 0
PC 1.40
    
```



```

EXPNO 2
PROCNO 1
Date_ 20150220
Time 9.17
INSTRUM spect
PROBHD 5 mm PABBO BB-
PULPROG zg30
TD 65536
SOLVENT CDC13
NS 16
DS 2
SWH 6188.119 Hz
FIDRES 0.094423 Hz
AQ 5.2953587 sec
RG 114
DW 80.800 usec
DE 6.50 usec
TE 298.0 K
D1 1.0000000 sec
TDO 1

===== CHANNEL f1 =====
NUC1 1H
P1 13.70 usec
PL1 1.90 dB
PL1W 8.36853981 W
SFO1 300.1418535 MHz
SI 32768
SF 300.1400031 MHz
WDW EM
SSB 0
LB 0.30 Hz
GB 0
PC 1.00
    
```

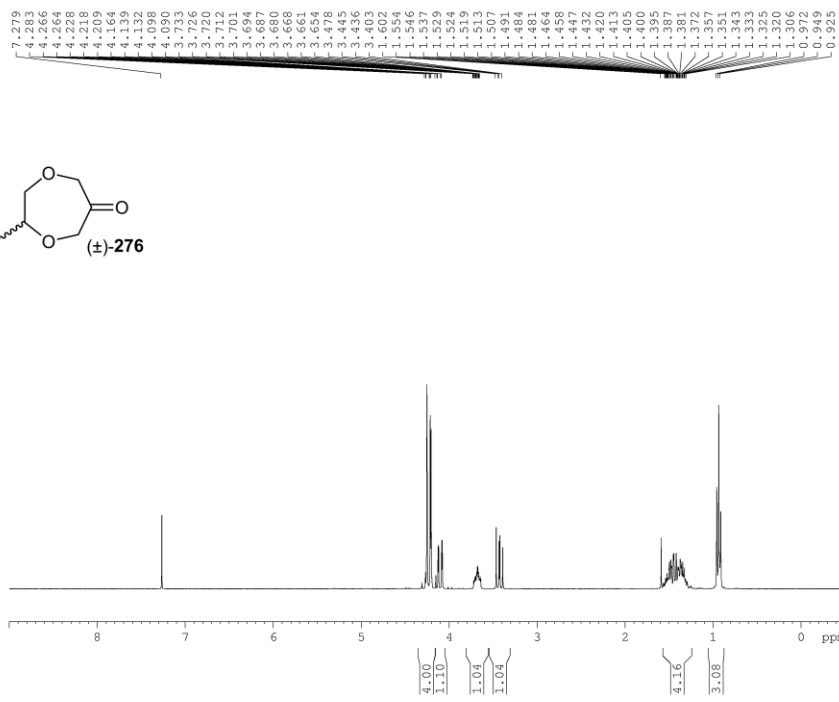
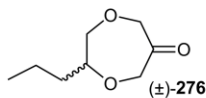


```

EXPNO 1
PROCNO 1
Date_ 20150219
Time 17.42
INSTRUM spect
PROBHD 5 mm PABBO BB-
PULPROG zgpg30
TD 65536
SOLVENT CDC13
NS 78
DS 4
SWH 18028.846 Hz
FIDRES 0.275098 Hz
AQ 1.8175818 sec
RG 203
DW 27.733 usec
DE 6.50 usec
TE 298.0 K
D1 2.0000000 sec
D11 0.0300000 sec
TDO 1

===== CHANNEL f1 =====
NUC1 13C
P1 10.82 usec
PL1 0.00 dB
PL1W 30.14263725 W
SFO1 75.4778101 MHz

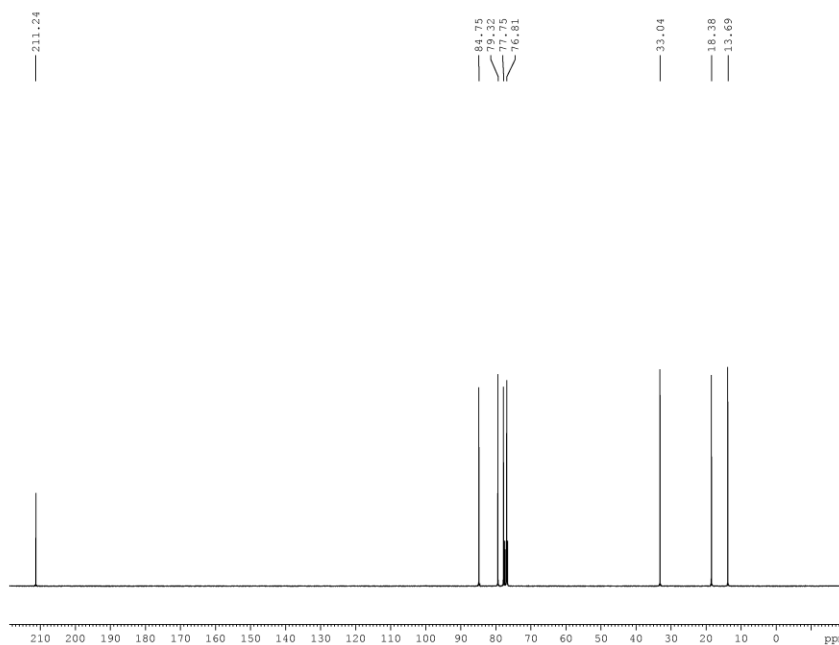
===== CHANNEL f2 =====
CPDPRG2 waltz16
NUC2 1H
PCPD2 100.00 usec
PL2 1.90 dB
PL12 19.17 dB
PL13 23.94 dB
PL2W 8.36853981 W
PL12W 0.15690966 W
PL13W 0.05231782 W
SFO2 300.1412006 MHz
SI 32768
SF 75.4702761 MHz
WDW EM
SSB 0
LB 1.00 Hz
GB 0
PC 1.40
    
```

```

EXPNO 2
PROCNO 1
Date_ 20140509
Time 16.32
INSTRUM spect
PROBHD 5 mm PABBO BB-
PULPROG zg30
TD 65536
SOLVENT CDC13
NS 16
DS 2
SWH 6188.119 Hz
FIDRES 0.094423 Hz
AQ 5.2953587 sec
RG 161
DW 80.800 usec
DE 6.50 usec
TE 673.2 K
D1 1.0000000 sec
TDO 1

===== CHANNEL f1 =====
NUC1 1H
P1 13.70 usec
PL1 1.90 dB
PL1W 8.36853981 W
SFO1 300.1418535 MHz
SI 32768
SF 300.1400045 MHz
WDW EM
SSB 0
LB 0.30 Hz
GB 0
PC 1.00
    
```

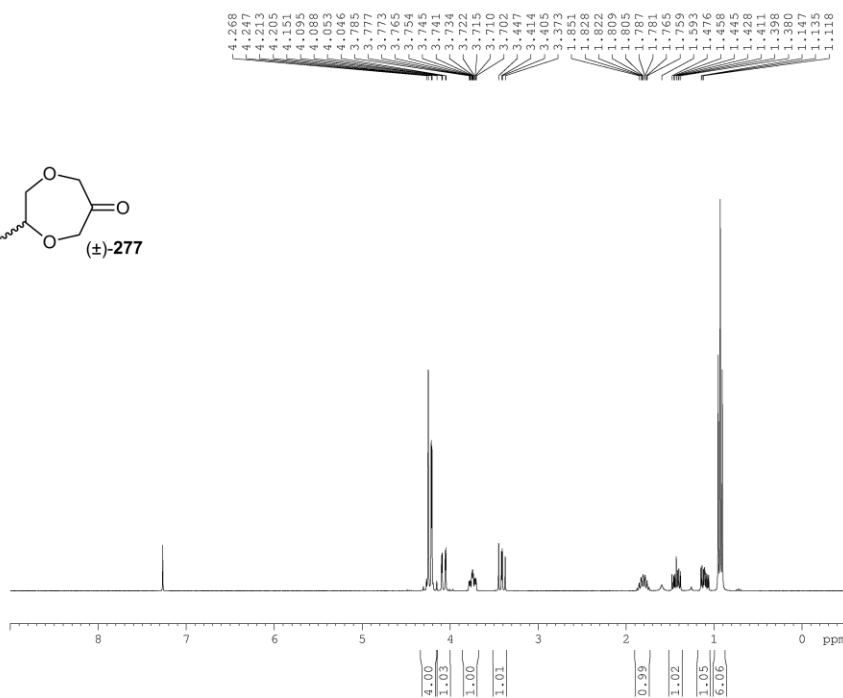
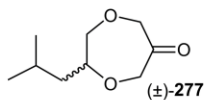


```

EXPNO 1
PROCNO 1
Date_ 20140509
Time 17.51
INSTRUM spect
PROBHD 5 mm PABBO BB-
PULPROG zgpg30
TD 65536
SOLVENT CDC13
NS 1024
DS 4
SWH 18028.846 Hz
FIDRES 0.275098 Hz
AQ 1.8175818 sec
RG 203
DW 27.733 usec
DE 6.50 usec
TE 673.2 K
D1 2.0000000 sec
D11 0.0300000 sec
TDO 1

===== CHANNEL f1 =====
NUC1 13C
P1 10.82 usec
PL1 0.00 dB
PL1W 30.14263725 W
SFO1 75.4778101 MHz

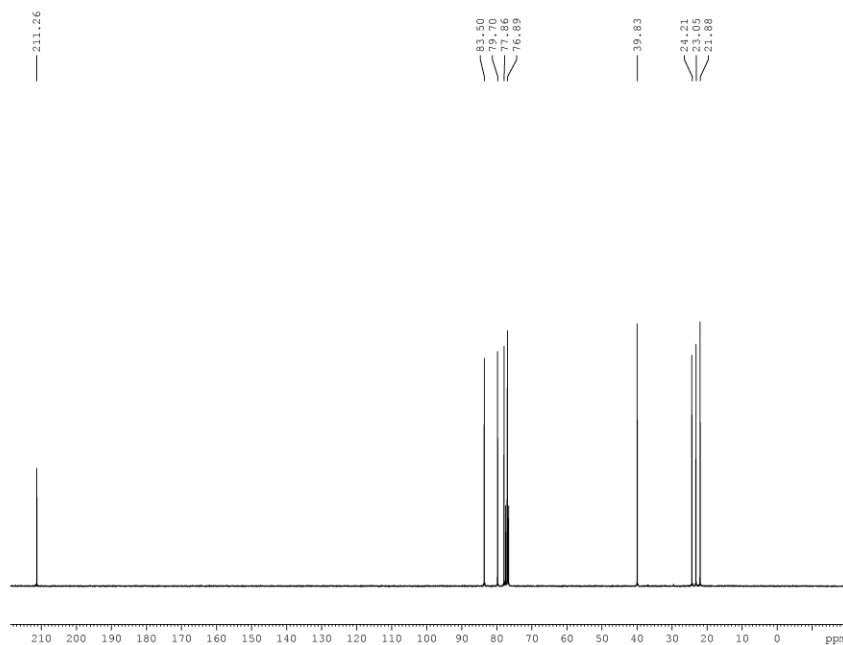
===== CHANNEL f2 =====
CPDPRG2 waltz16
NUC2 1H
PCPD2 100.00 usec
PL2 1.90 dB
PL12 19.17 dB
PL13 23.94 dB
PL2W 8.36853981 W
PL12W 0.15690966 W
PL13W 0.05231782 W
SFO2 300.1412006 MHz
SI 32768
SF 75.4702773 MHz
WDW EM
SSB 0
LB 1.00 Hz
GB 0
PC 1.40
    
```



```

EXPNO 1
PROCNO 1
Date_ 20141009
Time 14.57
INSTRUM spect
PROBHD 5 mm PABBO BB-
PULPROG zg30
TD 65536
SOLVENT CDC13
NS 16
DS 2
SWH 6188.119 Hz
FIDRES 0.094423 Hz
AQ 5.2953587 sec
RG 144
DW 80.800 usec
DE 6.50 usec
TE 298.0 K
D1 1.0000000 sec
TDO 1

===== CHANNEL f1 =====
NUC1 1H
P1 13.70 usec
PL1 1.90 dB
PL1W 8.36853981 W
SFO1 300.1418535 MHz
SI 32768
SF 300.1400041 MHz
WDW EM
SSB 0
LB 0.30 Hz
GB 0
PC 1.00
    
```

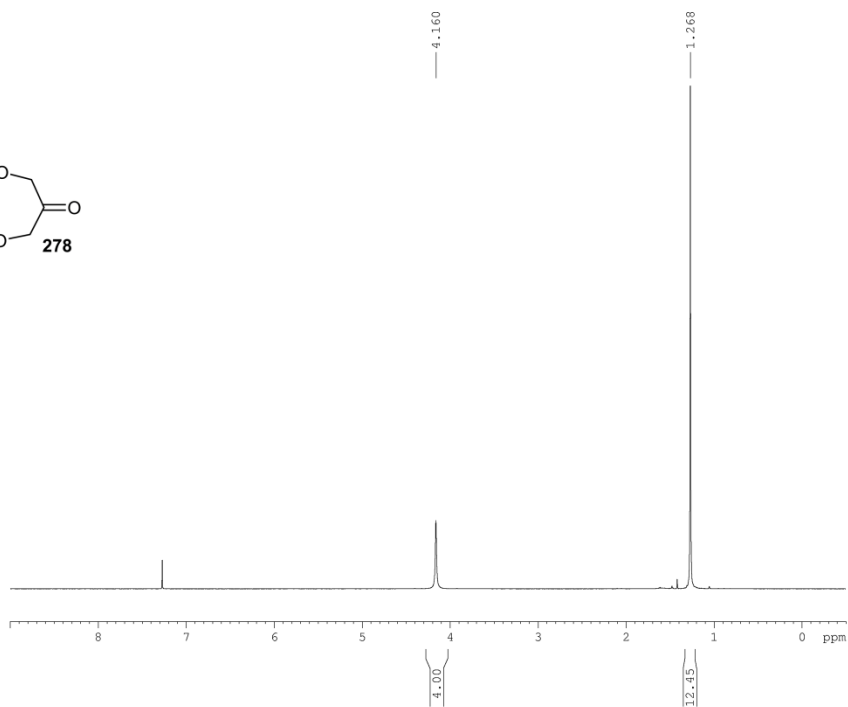
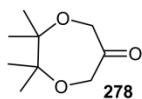


```

EXPNO 1
PROCNO 1
Date_ 20141009
Time 17.24
INSTRUM spect
PROBHD 5 mm PABBO BB-
PULPROG zgpg30
TD 65536
SOLVENT CDC13
NS 1024
DS 4
SWH 18028.846 Hz
FIDRES 0.275098 Hz
AQ 1.8175818 sec
RG 203
DW 27.733 usec
DE 6.50 usec
TE 298.0 K
D1 2.0000000 sec
D11 0.0300000 sec
TDO 1

===== CHANNEL f1 =====
NUC1 13C
P1 10.82 usec
PL1 0.00 dB
PL1W 30.14263725 W
SFO1 75.4778101 MHz

===== CHANNEL f2 =====
CPDPRG2 waltz16
NUC2 1H
PCPD2 100.00 usec
PL2 1.90 dB
PL12 19.17 dB
PL13 23.94 dB
PL2W 8.36853981 W
PL12W 0.15690966 W
PL13W 0.05231782 W
SFO2 300.1412006 MHz
SI 32768
SF 75.4702723 MHz
WDW EM
SSB 0
LB 1.00 Hz
GB 0
PC 1.40
    
```

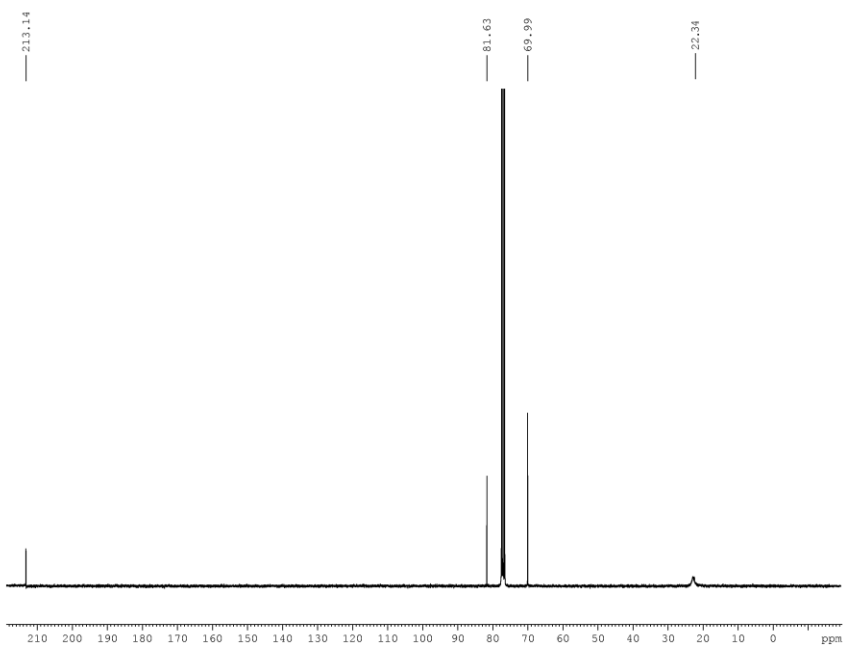


```

EXPNO 1
PROCNO 1
Date_ 20090310
Time 5.23
INSTRUM spect
PROBHD 5 mm PABBO BB-
PULPROG zg30
TD 65536
SOLVENT CDCl3
NS 16
DS 2
SWH 6188.119 Hz
FIDRES 0.094423 Hz
AQ 5.2953587 sec
RG 203
DW 80.800 usec
DE 6.50 usec
TE 298.0 K
D1 1.0000000 sec
TDO 1
    
```

```

===== CHANNEL f1 =====
NUC1 1H
P1 13.70 usec
PL1 1.90 dB
PL1W 8.36853981 W
SFO1 300.1418535 MHz
SI 32768
SF 300.1400027 MHz
WDW EM
SSB 0
LB 0.30 Hz
GB 0
PC 1.00
    
```



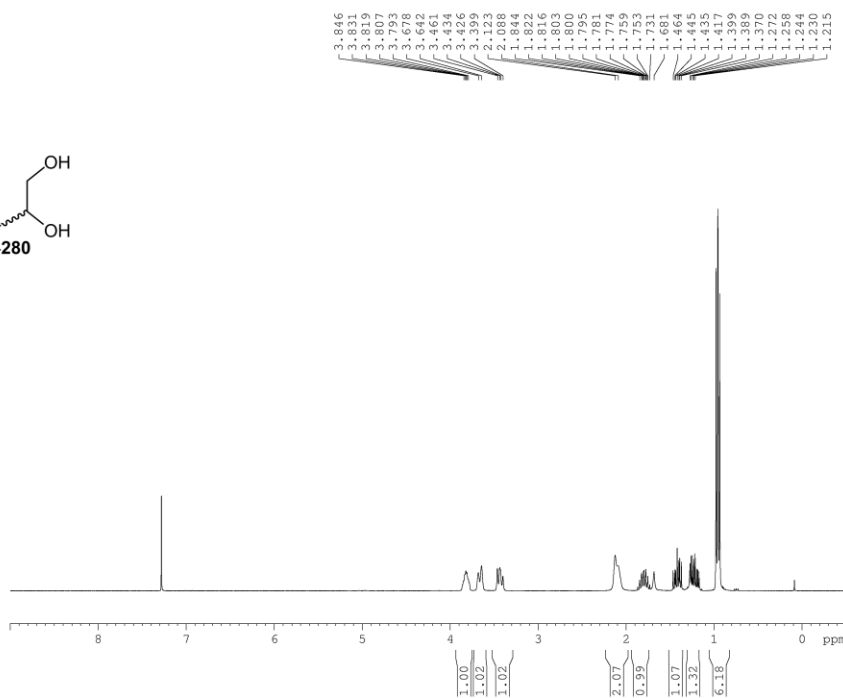
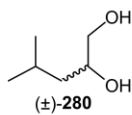
```

EXPNO 2
PROCNO 1
Date_ 20090310
Time 15.51
INSTRUM spect
PROBHD 5 mm PABBO BB-
PULPROG zgpg30
TD 65536
SOLVENT CDCl3
NS 8390
DS 4
SWH 18028.846 Hz
FIDRES 0.275098 Hz
AQ 1.8175818 sec
RG 203
DW 27.733 usec
DE 6.40 usec
TE 298.1 K
D1 2.0000000 sec
D11 0.0300000 sec
TDO 1
    
```

```

===== CHANNEL f1 =====
NUC1 13C
P1 10.82 usec
PL1 0.00 dB
PL1W 30.14263725 W
SFO1 75.4778101 MHz

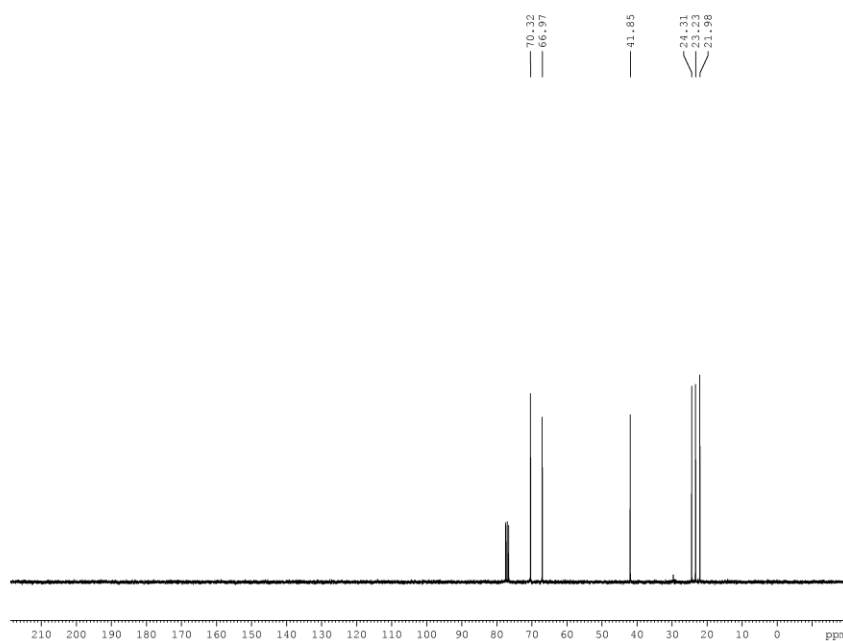
===== CHANNEL #2 =====
CPDPRG2 waltz16
NUC2 1H
PCPD2 100.00 usec
PL2 1.90 dB
PL12 19.17 dB
PL13 23.94 dB
PL2W 8.36853981 W
PL12W 0.15690966 W
PL13W 0.05231782 W
SFO2 300.1412006 MHz
SI 32768
SF 75.4702648 MHz
WDW EM
SSB 0
LB 1.00 Hz
GB 0
PC 1.40
    
```



```

EXPNO 2
PROCNO 1
Date_ 20140523
Time 15.18
INSTRUM spect
PROBHD 5 mm PABBO BB-
PULPROG zg30
TD 65536
SOLVENT CDCl3
NS 16
DS 2
SWH 6188.119 Hz
FIDRES 0.094423 Hz
AQ 5.2953587 sec
RG 114
DM 80.800 usec
DE 6.50 usec
TE 298.0 K
D1 1.0000000 sec
TDO 1

===== CHANNEL f1 =====
NUC1 1H
P1 13.70 usec
PL1 1.90 dB
PL1W 8.36853981 W
SF01 300.1418535 MHz
SI 32768
SF 300.1399996 MHz
WDW EM
SSB 0
LB 0.30 Hz
GB 0
PC 1.00
    
```

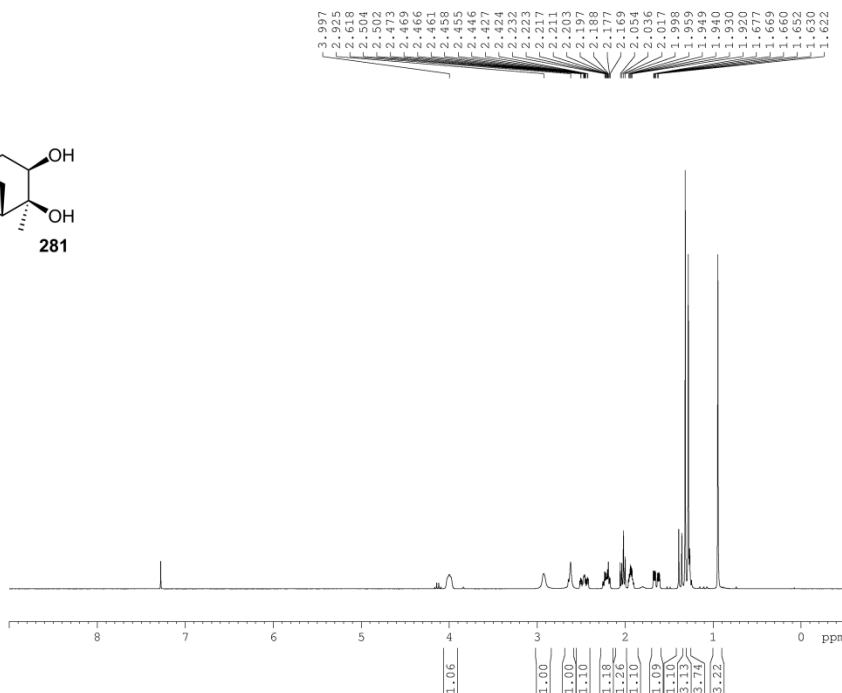
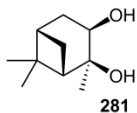


```

EXPNO 1
PROCNO 1
Date_ 20140522
Time 17.28
INSTRUM spect
PROBHD 5 mm PABBO BB-
PULPROG zgpg30
TD 65536
SOLVENT CDCl3
NS 43
DS 4
SWH 18028.846 Hz
FIDRES 0.275098 Hz
AQ 1.8175818 sec
RG 203
DM 27.733 usec
DE 6.50 usec
TE 298.1 K
D1 2.0000000 sec
D11 0.0300000 sec
TDO 1

===== CHANNEL f1 =====
NUC1 13C
P1 10.82 usec
PL1 0.00 dB
PL1W 30.14263725 W
SF01 75.4778101 MHz

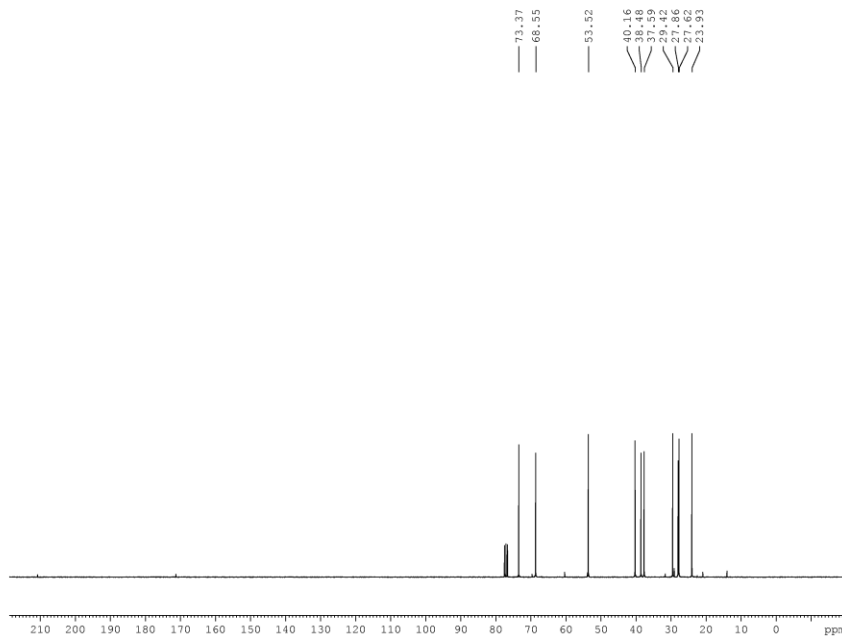
===== CHANNEL f2 =====
CPDPRG2 waltz16
NUC2 1H
PCPD2 100.00 usec
PL2 1.90 dB
PL12 19.17 dB
PL13 23.94 dB
PL1W 8.36853981 W
PL12W 0.15690966 W
PL13W 0.05231782 W
SF02 300.1412006 MHz
SI 32768
SF 75.4702687 MHz
WDW EM
SSB 0
LB 1.00 Hz
GB 0
PC 1.40
    
```



```

EXPNO 1
PROCNO 1
Date_ 20150115
Time 14.13
INSTRUM spect
PROBHD 5 mm PABBO BB-
PULPROG zg30
TD 65536
SOLVENT CDC13
NS 16
DS 2
SWH 6188.119 Hz
FIDRES 0.094423 Hz
AQ 5.2953587 sec
RG 80.6
DW 80.800 usec
DE 6.50 usec
TE 294.2 K
D1 1.0000000 sec
TDO 1

===== CHANNEL f1 =====
NUC1 1H
P1 13.70 usec
PL1 1.90 dB
PL1W 8.36853981 W
SFO1 300.1418535 MHz
SI 32768
SF 300.1400009 MHz
WDW EM
SSB 0
LB 0.30 Hz
GB 0
PC 1.00
    
```

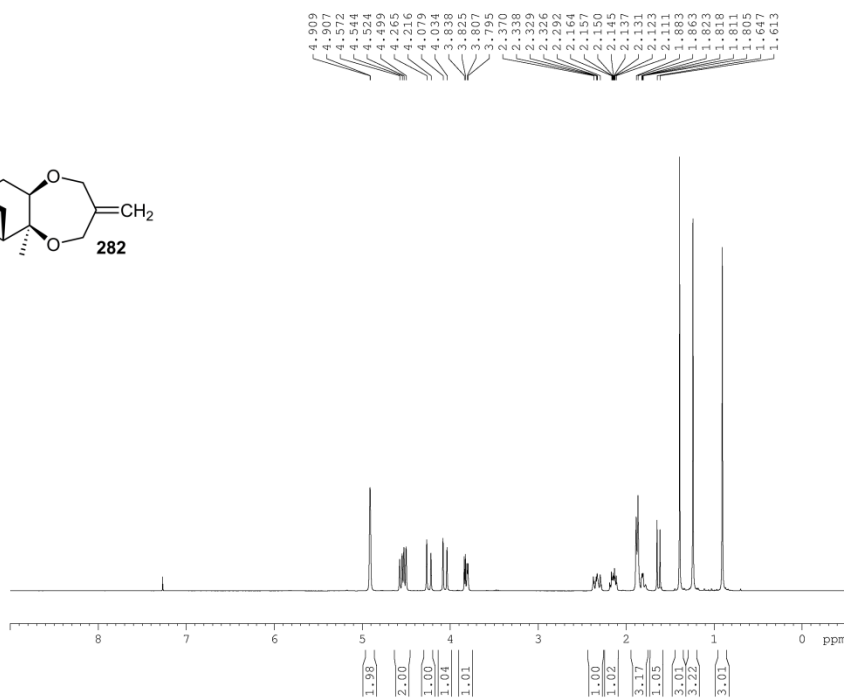
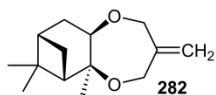


```

EXPNO 1
PROCNO 1
Date_ 20150115
Time 15.30
INSTRUM spect
PROBHD 5 mm PABBO BB-
PULPROG zgpg30
TD 65536
SOLVENT CDC13
NS 807
DS 4
SWH 18028.846 Hz
FIDRES 0.275098 Hz
AQ 1.8175818 sec
RG 203
DW 27.733 usec
DE 6.50 usec
TE 294.4 K
D1 2.0000000 sec
D11 0.0300000 sec
TDO 1

===== CHANNEL f1 =====
NUC1 13C
P1 10.82 usec
PL1 0.00 dB
PL1W 30.14263725 W
SFO1 75.4778101 MHz

===== CHANNEL f2 =====
CPDPRG2 waltz16
NUC2 1H
PCPD2 100.00 usec
PL2 1.90 dB
PL12 19.17 dB
PL13 23.94 dB
PL2W 8.36853981 W
PL12W 0.15690966 W
PL13W 0.05231782 W
SFO2 300.1412006 MHz
SI 32768
SF 75.4702783 MHz
WDW EM
SSB 0
LB 1.00 Hz
GB 0
PC 1.40
    
```

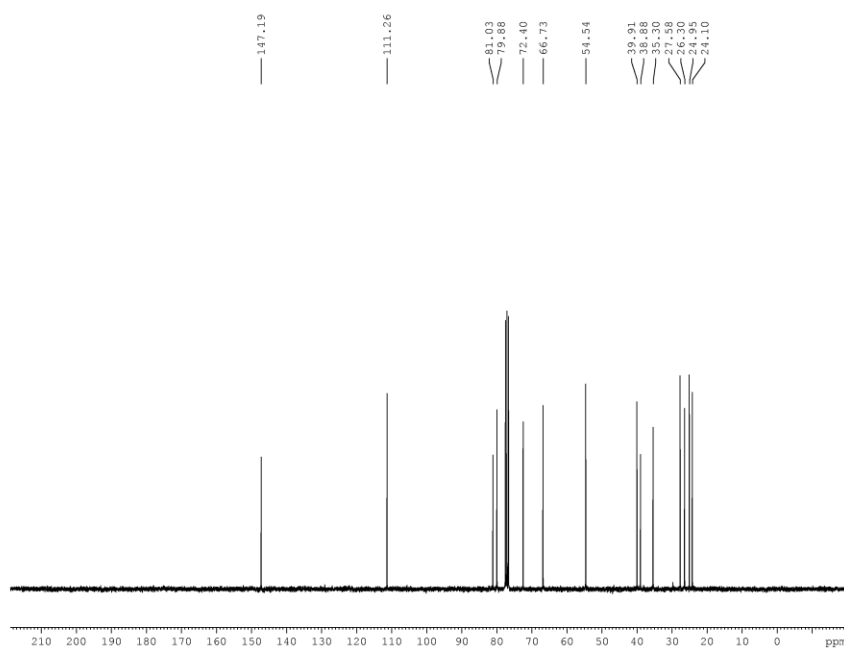


```

EXPNO 1
PROCNO 1
Date_ 20150206
Time 16.29
INSTRUM spect
PROBHD 5 mm PABBO BB-
PULPROG zg30
TD 65536
SOLVENT CDC13
NS 16
DS 2
SWH 6188.119 Hz
FIDRES 0.094423 Hz
AQ 5.2953587 sec
RG 40.3
DW 80.800 usec
DE 6.50 usec
TE 294.2 K
D1 1.0000000 sec
TDO 1
    
```

```

===== CHANNEL f1 =====
NUC1 1H
P1 13.70 usec
PL1 1.90 dB
PL1W 8.36853981 W
SFO1 300.1418535 MHz
SI 32768
SF 300.1400041 MHz
WDW EM
SSB 0
LB 0.30 Hz
GB 0
PC 1.00
    
```



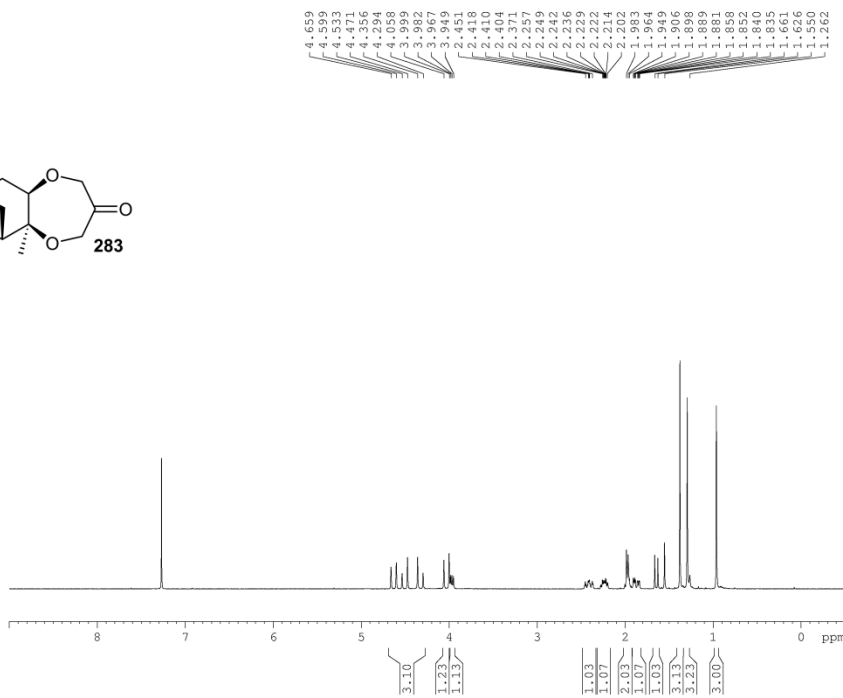
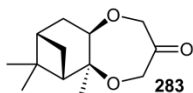
```

EXPNO 2
PROCNO 1
Date_ 20150206
Time 16.54
INSTRUM spect
PROBHD 5 mm PABBO BB-
PULPROG zgpg30
TD 65536
SOLVENT CDC13
NS 367
DS 4
SWH 18028.846 Hz
FIDRES 0.275098 Hz
AQ 1.8175818 sec
RG 203
DW 27.733 usec
DE 6.50 usec
TE 294.7 K
D1 2.0000000 sec
D11 0.0300000 sec
TDO 1
    
```

```

===== CHANNEL f1 =====
NUC1 13C
P1 10.82 usec
PL1 0.00 dB
PL1W 30.14263725 W
SFO1 75.4778101 MHz

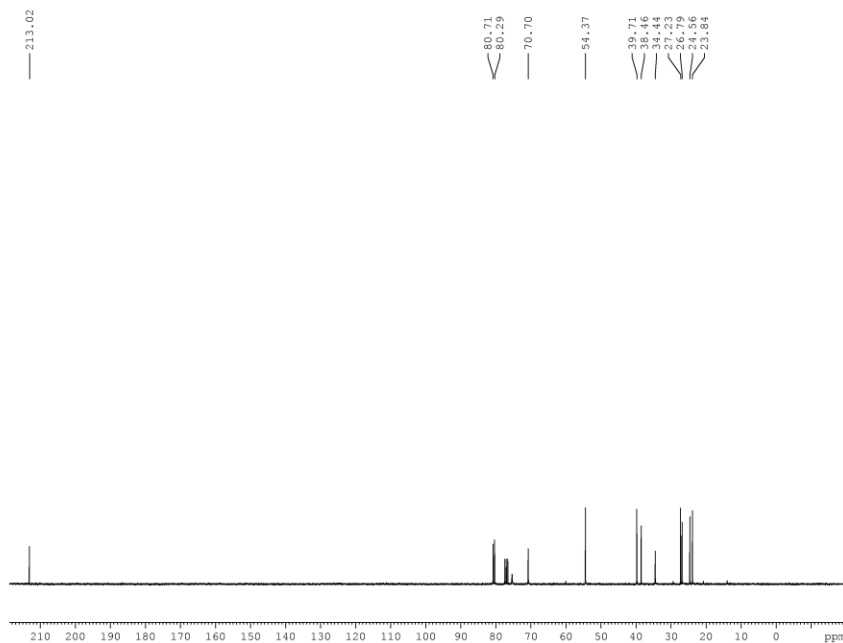
===== CHANNEL f2 =====
CPDPRG2 waltz16
NUC2 1H
PCPD2 100.00 usec
PL2 1.90 dB
PL12 19.17 dB
PL13 23.94 dB
PL2W 8.36853981 W
PL12W 0.15690966 W
PL13W 0.05231782 W
SFO2 300.1412006 MHz
SI 32768
SF 75.4702661 MHz
WDW EM
SSB 0
LB 1.00 Hz
GB 0
PC 1.40
    
```



```

EXPNO          2
PROCNO         1
Date_          20150316
Time           12.23
INSTRUM       spect
PROBHD        5 mm PABBO BB-
PULPROG       zg30
TD             65536
SOLVENT       CDC13
NS             16
DS             2
SWH           6188.119 Hz
FIDRES       0.094423 Hz
AQ           5.2953587 sec
RG            203
DW            80.800 usec
DE             6.50 usec
TE            298.0 K
D1            1.0000000 sec
TDO           1

===== CHANNEL f1 =====
NUC1           1H
P1             13.70 usec
PL1            1.90 dB
PL1W          8.36853981 W
SFO1          300.1418335 MHz
SI             32768
SF            300.1400036 MHz
WDW            EM
SSB            0
LB             0.30 Hz
GB             0
PC             1.00
    
```

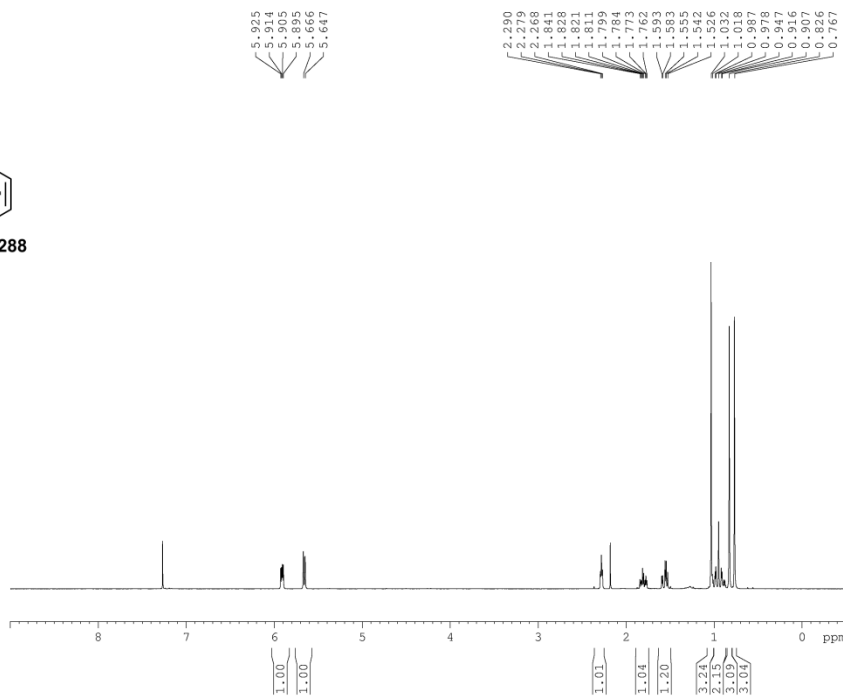


```

EXPNO          1
PROCNO         1
Date_          20150313
Time           13.05
INSTRUM       spect
PROBHD        5 mm PABBO BB-
PULPROG       zgpg30
TD             65536
SOLVENT       CDC13
NS             39
DS             4
SWH           18028.846 Hz
FIDRES       0.275098 Hz
AQ           1.8175818 sec
RG            203
DW            27.733 usec
DE             6.50 usec
TE            298.0 K
D1            2.0000000 sec
D11           0.0300000 sec
TDO           1

===== CHANNEL f1 =====
NUC1           13C
P1             10.82 usec
PL1            0.00 dB
PL1W          30.14263725 W
SFO1          75.4778101 MHz

===== CHANNEL f2 =====
CPDPRG2       waltz16
NUC2           1H
PCPD2         100.00 usec
PL2            1.90 dB
PL12          19.17 dB
PL13          23.94 dB
PL1W          8.36853981 W
PL12W         0.15690966 W
PL13W         0.05231782 W
SFO2          300.1412006 MHz
SI             32768
SF            75.4702800 MHz
WDW            EM
SSB            0
LB             1.00 Hz
GB             0
PC             1.40
    
```

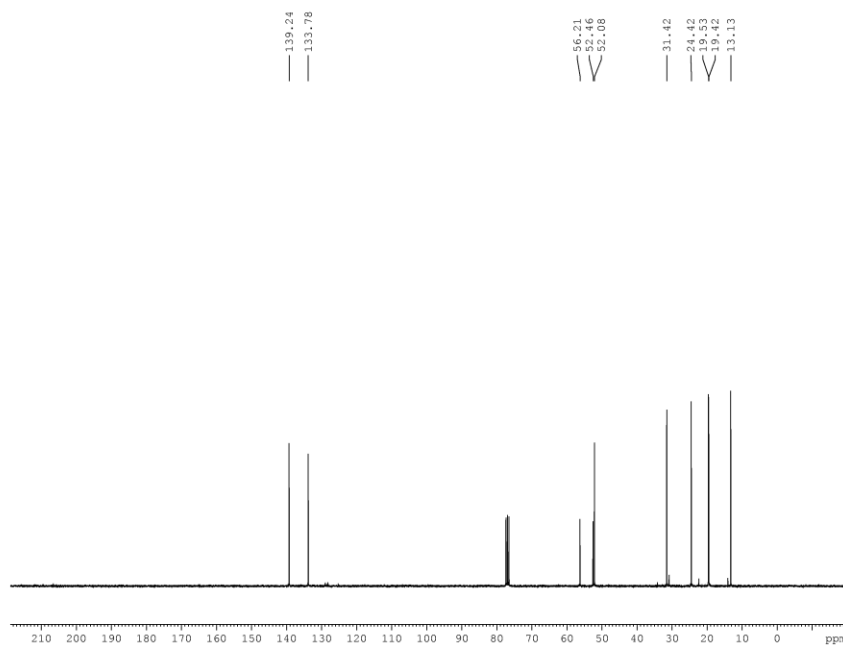


```

EXPNO      2
PROCNO     1
Date_      20140529
Time       13.09
INSTRUM    spect
PROBHD     5 mm PABBO B8-
PULPROG    zg30
TD          65536
SOLVENT    CDCl3
NS          16
DS          2
SWH         6188.119 Hz
FIDRES     0.094423 Hz
AQ          5.2953587 sec
RG          90.5
DW          80.800 usec
DE          6.50 usec
TE          298.0 K
D1          1.00000000 sec
TDO         1
    
```

```

----- CHANNEL f1 -----
NUC1        1H
P1          13.70 usec
PL1         1.90 dB
PL1W        8.36853981 W
SF01        300.1418535 MHz
SI          32768
SF          300.1400039 MHz
WDW         EM
SSB         0
LB          0.30 Hz
GB          0
PC          1.00
    
```



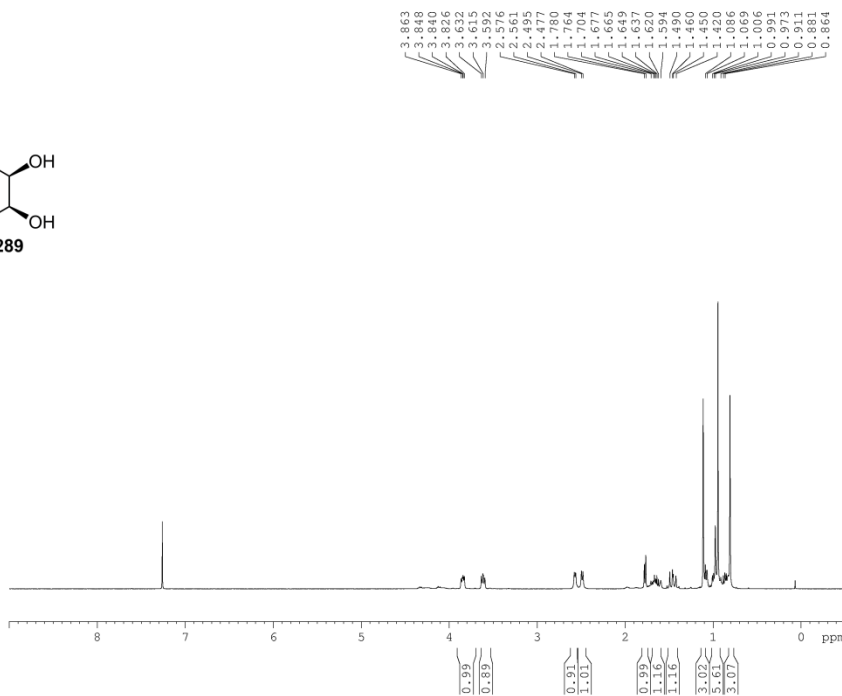
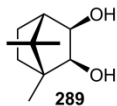
```

EXPNO      1
PROCNO     1
Date_      20140529
Time       12.17
INSTRUM    spect
PROBHD     5 mm PABBO B8-
PULPROG    zgpg30
TD          65536
SOLVENT    CDCl3
NS          236
DS          4
SWH         18028.846 Hz
FIDRES     0.275098 Hz
AQ          1.8175818 sec
RG          203
DW          27.733 usec
DE          6.50 usec
TE          298.0 K
D1          2.00000000 sec
D11         0.03000000 sec
TDO         1
    
```

```

----- CHANNEL f1 -----
NUC1        13C
P1          10.82 usec
PL1         0.00 dB
PL1W        30.14263725 W
SF01        75.4778101 MHz

----- CHANNEL f2 -----
CPDPRG2    waltz16
NUC2        1H
PCPD2      100.00 usec
PL2         1.90 dB
PL12        19.17 dB
PL13        23.94 dB
PL1W        8.36853981 W
PL12W       0.15690966 W
PL13W       0.05231782 W
SF02        300.1412006 MHz
SI          32768
SF          75.4702697 MHz
WDW         EM
SSB         0
LB          1.00 Hz
GB          0
PC          1.40
    
```

3.863
3.848
3.830
3.815
3.615
3.592
2.576
2.561
2.495
2.480
1.780
1.764
1.704
1.677
1.665
1.649
1.630
1.620
1.594
1.490
1.460
1.450
1.430
1.420
1.389
1.369
1.006
0.991
0.973
0.911
0.881
0.861

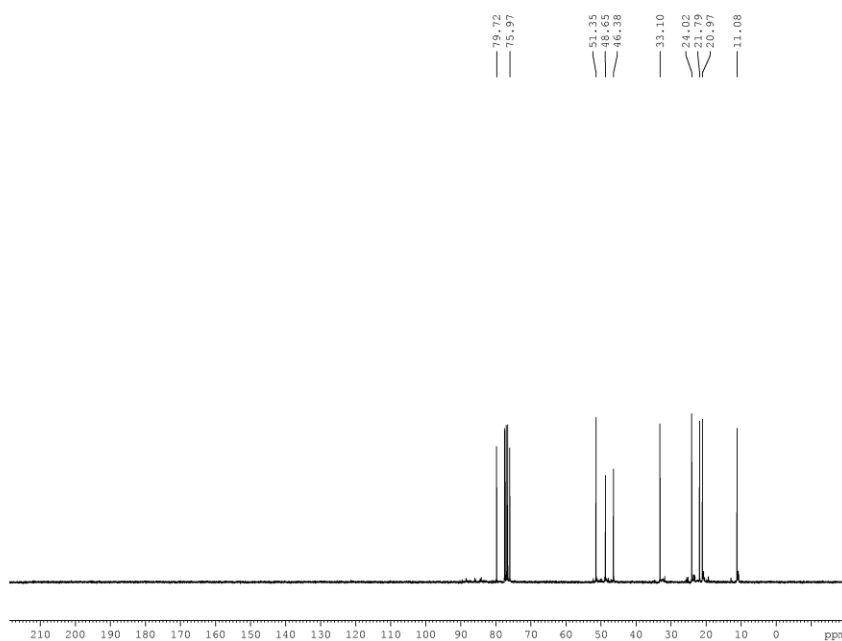


```

EXPNO          2
PROCNO         1
Date_          20140804
Time          15.07
INSTRUM       spect
PROBHD        5 mm PABBO BB-
PULPROG       zg30
TD            65536
SOLVENT       CDCl3
NS            16
DS            2
SWH           6188.119 Hz
FIDRES       0.094423 Hz
AQ           5.2953587 sec
RG           191
DW           80.800 usec
DE           6.50 usec
TE           298.0 K
D1           1.0000000 sec
TDO          1
    
```

```

===== CHANNEL f1 =====
NUC1          1H
P1           13.70 usec
PL1          1.90 dB
PL1W        8.36853981 W
SFO1        300.1418535 MHz
SI          32768
SF          300.1400060 MHz
WDW         EM
SSB          0
LB           0.30 Hz
GB           0
PC           1.00
    
```



79.72
75.97
51.35
48.08
45.98
33.10
21.02
20.97
11.08



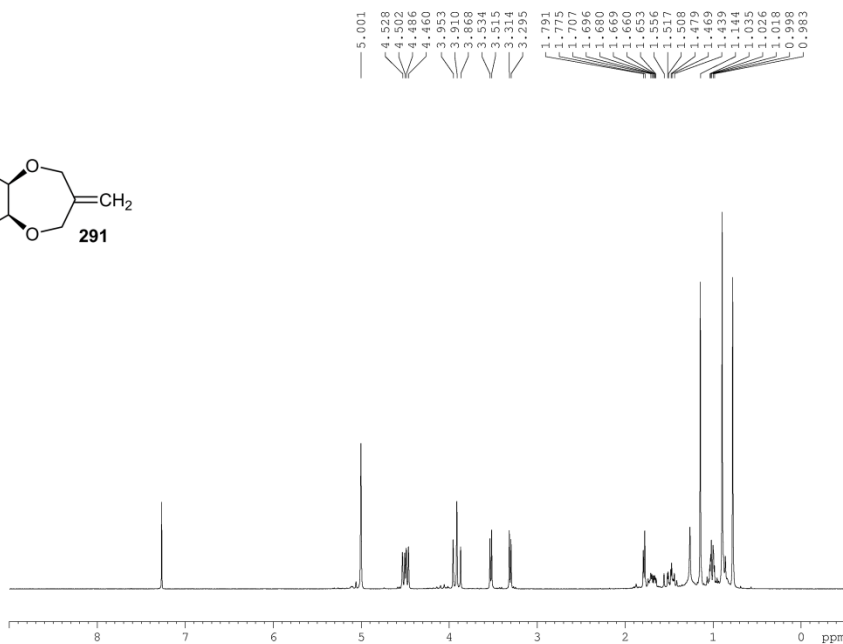
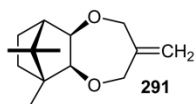
```

EXPNO          1
PROCNO         1
Date_          20140804
Time          14.39
INSTRUM       spect
PROBHD        5 mm PABBO BB-
PULPROG       zgpg30
TD            65536
SOLVENT       CDCl3
NS            4
DS            4
SWH           18028.846 Hz
FIDRES       0.275098 Hz
AQ           1.8175818 sec
RG           203
DW           27.733 usec
DE           6.50 usec
TE           298.0 K
D1           2.0000000 sec
D11          0.0300000 sec
TDO          1
    
```

```

===== CHANNEL f1 =====
NUC1          13C
P1           10.82 usec
PL1          0.00 dB
PL1W        30.14263725 W
SFO1        75.4778101 MHz

===== CHANNEL f2 =====
CPDPRG2       waltz16
NUC2          1H
PCPD2        100.00 usec
PL2          1.90 dB
PL12        19.17 dB
PL13        23.94 dB
PL1W        8.36853981 W
PL12W       0.15690966 W
PL13W       0.05231782 W
SFO2        300.1412006 MHz
SI          32768
SF          75.4702680 MHz
WDW         EM
SSB          0
LB           1.00 Hz
GB           0
PC           1.40
    
```

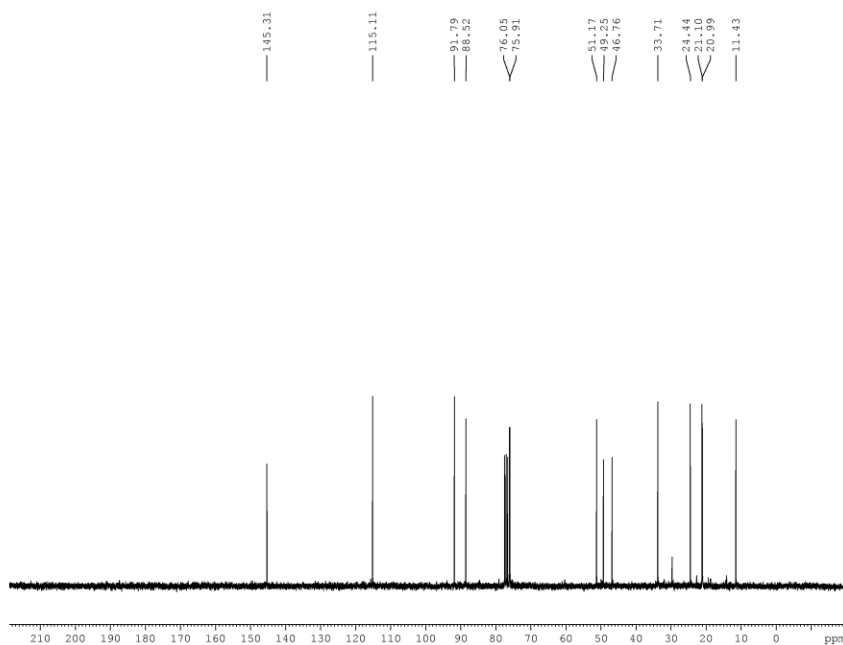


```

EXPNO 1
PROCNO 1
Date_ 20141125
Time 19.56
INSTRUM spect
PROBHD 5 mm PABBO BB-
PULPROG zg30
TD 65536
SOLVENT CDC13
NS 13
DS 2
SWH 6188.119 Hz
FIDRES 0.094423 Hz
AQ 5.2953587 sec
RG 191
DW 80.800 usec
DE 6.50 usec
TE 298.0 K
D1 1.0000000 sec
TDO 1
    
```

```

===== CHANNEL f1 =====
NUC1 1H
P1 13.70 usec
PL1 1.90 dB
PL1W 8.36853981 W
SFO1 300.1418535 MHz
SI 32768
SF 300.1400041 MHz
WDW EM
SSB 0
LB 0.30 Hz
GB 0
PC 1.00
    
```



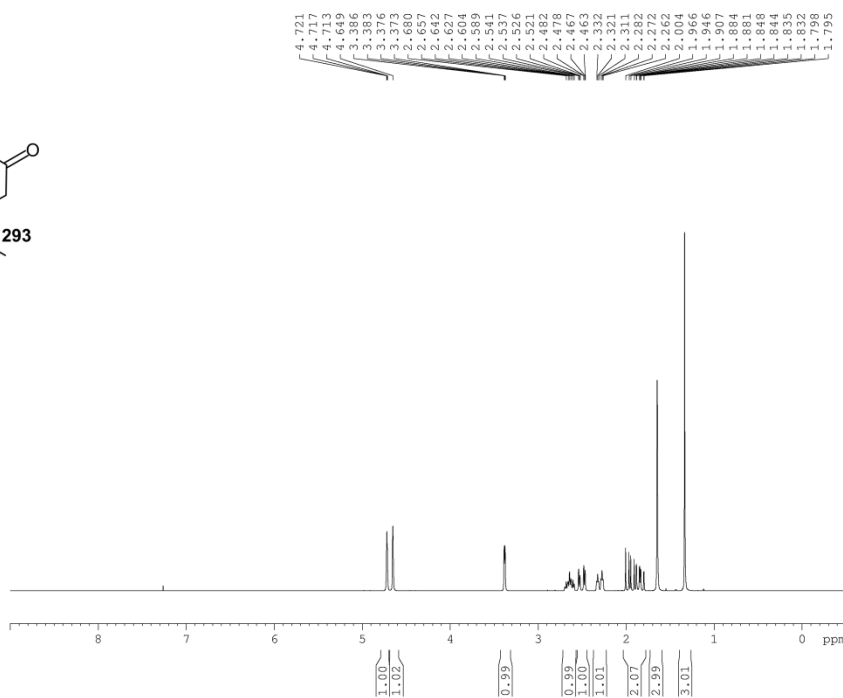
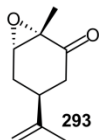
```

EXPNO 1
PROCNO 1
Date_ 20141124
Time 16.29
INSTRUM spect
PROBHD 5 mm PABBO BB-
PULPROG zgpg30
TD 65536
SOLVENT CDC13
NS 50
DS 4
SWH 18028.846 Hz
FIDRES 0.275098 Hz
AQ 1.8175818 sec
RG 203
DW 27.733 usec
DE 6.50 usec
TE 298.0 K
D1 2.0000000 sec
D11 0.0300000 sec
TDO 1
    
```

```

===== CHANNEL f1 =====
NUC1 13C
P1 10.82 usec
PL1 0.00 dB
PL1W 30.14263725 W
SFO1 75.4778101 MHz

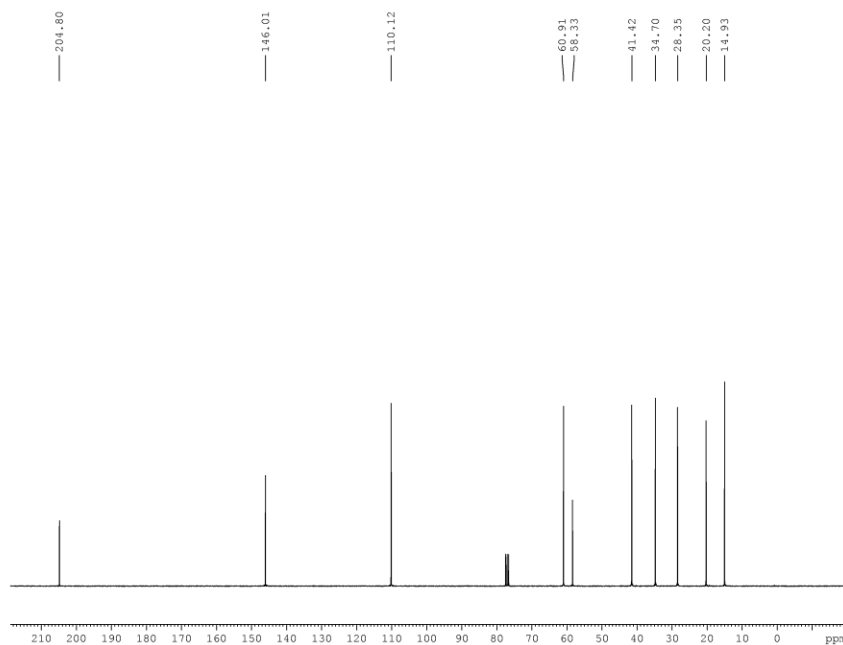
===== CHANNEL f2 =====
CPDPRG2 waltz16
NUC2 1H
PCPD2 100.00 usec
PL2 1.90 dB
PL12 19.17 dB
PL13 23.94 dB
PL2W 8.36853981 W
PL12W 0.15690966 W
PL13W 0.05231782 W
SFO2 300.1412006 MHz
SI 32768
SF 75.4702676 MHz
WDW EM
SSB 0
LB 1.00 Hz
GB 0
PC 1.40
    
```

```

EXPNO 1
PROCNO 1
Date_ 20120628
Time 9.46
INSTRUM spect
PROBHD 5 mm PABBO B8-
PULPROG zg30
TD 65536
SOLVENT CDCl3
NS 16
DS 2
SWH 6188.119 Hz
FIDRES 0.094423 Hz
AQ 5.2953587 sec
RG 20.2
DW 80.800 usec
DE 6.50 usec
TE 298.0 K
D1 1.00000000 sec
TDO 1

===== CHANNEL f1 =====
NUC1 1H
P1 13.70 usec
PL1 1.90 dB
PL1W 8.36853981 W
SF01 300.1418535 MHz
SI 32768
SF 300.1400052 MHz
WDW EM
SSB 0
LB 0.30 Hz
GB 0
PC 1.00
    
```

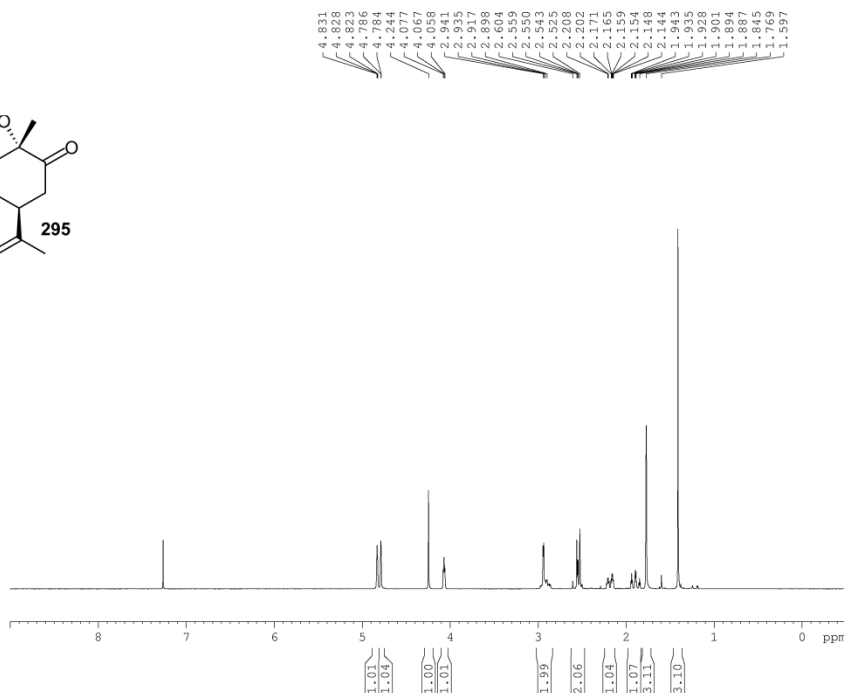
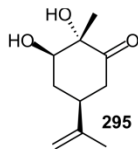


```

EXPNO 3
PROCNO 1
Date_ 20120628
Time 11.11
INSTRUM spect
PROBHD 5 mm PABBO B8-
PULPROG zgpg30
TD 65536
SOLVENT CDCl3
NS 888
DS 4
SWH 18028.846 Hz
FIDRES 0.275098 Hz
AQ 1.8175818 sec
RG 203
DW 27.733 usec
DE 6.50 usec
TE 298.0 K
D1 2.00000000 sec
D11 0.03000000 sec
TDO 1

===== CHANNEL f1 =====
NUC1 13C
P1 10.82 usec
PL1 0.00 dB
PL1W 30.14263725 W
SF01 75.4778101 MHz

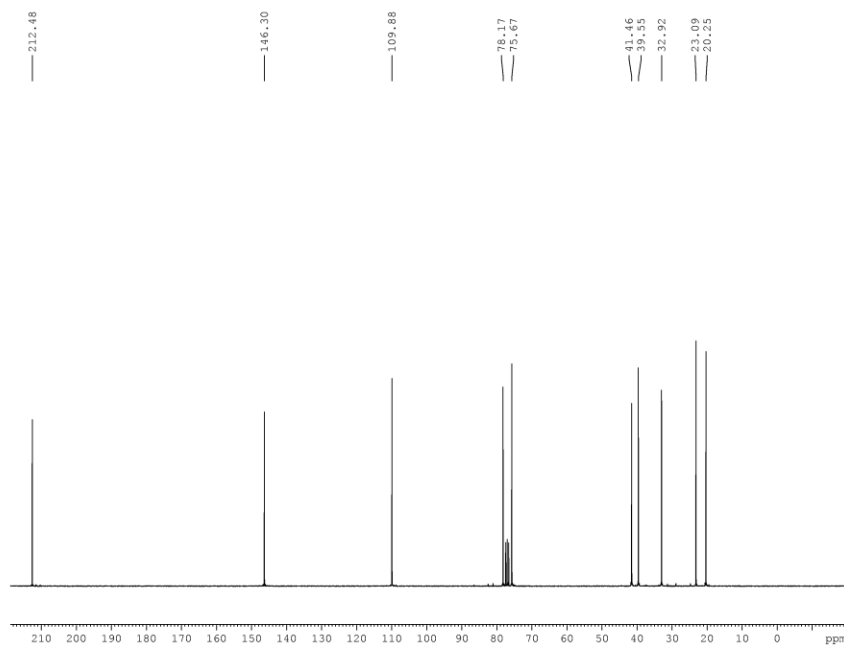
===== CHANNEL f2 =====
CPDPRG2 waltz16
NUC2 1H
PCPD2 100.00 usec
PL2 1.90 dB
PL12 19.17 dB
PL13 23.94 dB
PL1W 8.36853981 W
PL12W 0.15690966 W
PL13W 0.05231782 W
SF02 300.1412006 MHz
SI 32768
SF 75.4702799 MHz
WDW EM
SSB 0
LB 1.00 Hz
GB 0
PC 1.40
    
```



```

EXPNO 1
PROCNO 1
Date_ 20121019
Time 14.13
INSTRUM spect
PROBHD 5 mm PABBO BB-
PULPROG zg30
TD 65536
SOLVENT CDC13
NS 32
DS 2
SWH 6188.119 Hz
FIDRES 0.094423 Hz
AQ 5.2953587 sec
RG 101
DW 80.800 usec
DE 6.50 usec
TE 298.0 K
D1 1.0000000 sec
TDO 1

===== CHANNEL f1 =====
NUC1 1H
P1 13.70 usec
PL1 1.90 dB
PL1W 8.36853981 W
SFO1 300.1418335 MHz
SI 32768
SF 300.1400054 MHz
WDW EM
SSB 0
LB 0.30 Hz
GB 0
PC 1.00
    
```

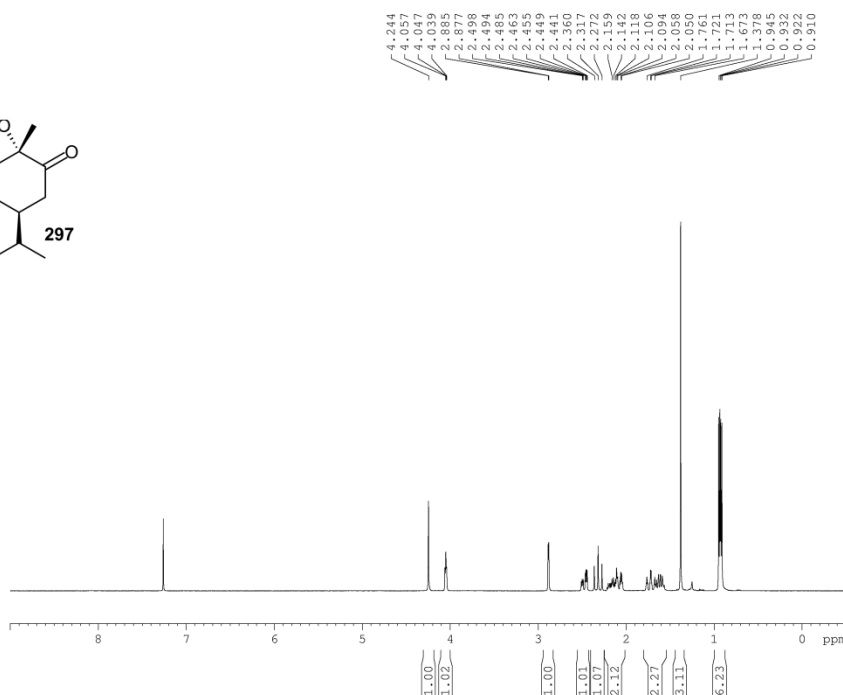
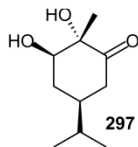


```

EXPNO 1
PROCNO 1
Date_ 20121019
Time 15.31
INSTRUM spect
PROBHD 5 mm PABBO BB-
PULPROG zgpg30
TD 65536
SOLVENT CDC13
NS 1024
DS 4
SWH 18028.846 Hz
FIDRES 0.275098 Hz
AQ 1.8175818 sec
RG 203
DW 27.733 usec
DE 6.50 usec
TE 298.0 K
D1 2.0000000 sec
D11 0.0300000 sec
TDO 1

===== CHANNEL f1 =====
NUC1 13C
P1 10.82 usec
PL1 0.00 dB
PL1W 30.14263725 W
SFO1 75.4778101 MHz

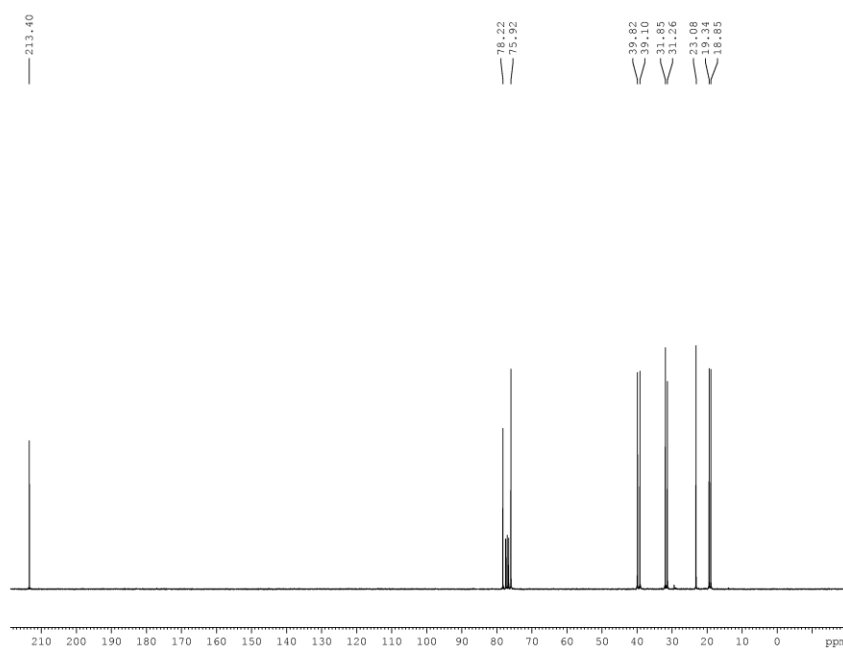
===== CHANNEL f2 =====
CPDPRG2 waltz16
NUC2 1H
PCPD2 100.00 usec
PL2 1.90 dB
PL12 19.17 dB
PL13 23.94 dB
PL2W 8.36853981 W
PL12W 0.15690966 W
PL13W 0.05231782 W
SFO2 300.1412006 MHz
SI 32768
SF 75.4702837 MHz
WDW EM
SSB 0
LB 1.00 Hz
GB 0
PC 1.40
    
```



```

EXPNO 1
PROCNO 1
Date_ 20140913
Time 16.02
INSTRUM spect
PROBHD 5 mm PABBO BB-
PULPROG zg30
TD 65536
SOLVENT CDC13
NS 16
DS 2
SWH 6188.119 Hz
FIDRES 0.094423 Hz
AQ 5.2953587 sec
RG 203
DW 80.800 usec
DE 6.50 usec
TE 294.8 K
D1 1.0000000 sec
TDO 1

===== CHANNEL f1 =====
NUC1 1H
P1 13.70 usec
PL1 1.90 dB
PL1W 8.36853981 W
SFO1 300.1418535 MHz
SI 32768
SF 300.1400061 MHz
WDW EM
SSB 0
LB 0.30 Hz
GB 0
PC 1.00
    
```

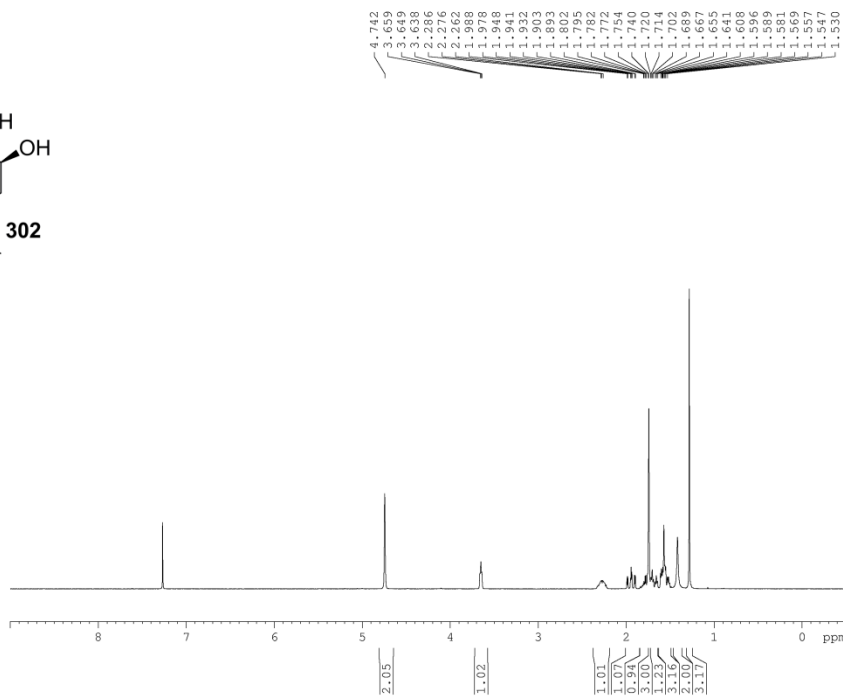
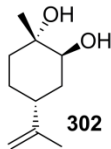


```

EXPNO 1
PROCNO 1
Date_ 20140913
Time 16.49
INSTRUM spect
PROBHD 5 mm PABBO BB-
PULPROG zgpg30
TD 65536
SOLVENT CDC13
NS 643
DS 4
SWH 18028.846 Hz
FIDRES 0.275098 Hz
AQ 1.8175818 sec
RG 203
DW 27.733 usec
DE 6.50 usec
TE 295.2 K
D1 2.0000000 sec
D11 0.0300000 sec
TDO 1

===== CHANNEL f1 =====
NUC1 13C
P1 10.82 usec
PL1 0.00 dB
PL1W 30.14263725 W
SFO1 75.4778101 MHz

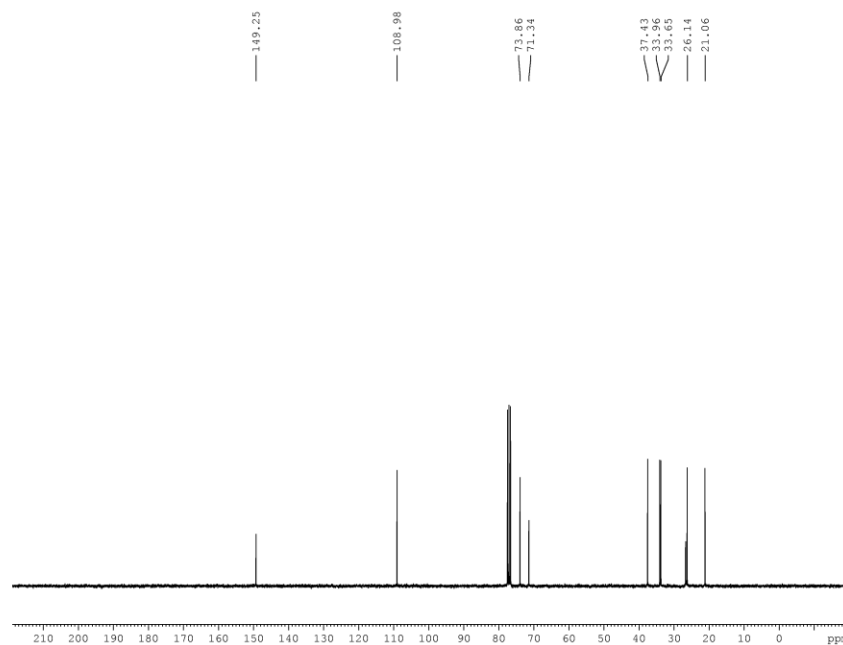
===== CHANNEL f2 =====
CPDPRG2 waltz16
NUC2 1H
PCPD2 100.00 usec
PL2 1.90 dB
PL12 19.17 dB
PL13 23.94 dB
PL2W 8.36853981 W
PL12W 0.15690966 W
PL13W 0.05231782 W
SFO2 300.1412006 MHz
SI 32768
SF 75.4702806 MHz
WDW EM
SSB 0
LB 1.00 Hz
GB 0
PC 1.40
    
```



```

EXPNO 1
PROCNO 1
Date_ 20090316
Time 23:51
INSTRUM spect
PROBHD 5 mm PABBO BB-
PULPROG zg30
TD 65536
SOLVENT CDC13
NS 16
DS 2
SWH 6188.119 Hz
FIDRES 0.094423 Hz
AQ 5.2953587 sec
RG 203
DW 80.800 usec
DE 6.50 usec
TE 298.1 K
D1 1.0000000 sec
TDO 1

===== CHANNEL f1 =====
NUC1 1H
P1 13.70 usec
PL1 1.90 dB
PL1W 8.36853981 W
SFO1 300.1418335 MHz
SI 32768
SF 300.1400040 MHz
WDW EM
SSB 0
LB 0.30 Hz
GB 0
PC 1.00
    
```

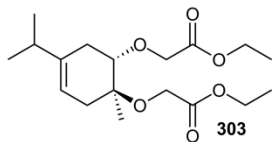


```

EXPNO 1
PROCNO 1
Date_ 20141118
Time 13:27
INSTRUM spect
PROBHD 5 mm PABBO BB-
PULPROG zgpg30
TD 65536
SOLVENT CDC13
NS 583
DS 4
SWH 18028.846 Hz
FIDRES 0.275098 Hz
AQ 1.8175818 sec
RG 203
DW 27.733 usec
DE 6.50 usec
TE 298.0 K
D1 2.0000000 sec
D11 0.0300000 sec
TDO 1

===== CHANNEL f1 =====
NUC1 13C
P1 10.82 usec
PL1 0.00 dB
PL1W 30.14263725 W
SFO1 75.4778101 MHz

===== CHANNEL f2 =====
CPDPRG2 waltz16
NUC2 1H
PCPD2 100.00 usec
PL2 1.90 dB
PL12 19.17 dB
PL13 23.94 dB
PL1W 8.36853981 W
PL12W 0.15690966 W
PL13W 0.05231782 W
SFO2 300.1412006 MHz
SI 32768
SF 75.4702659 MHz
WDW EM
SSB 0
LB 1.00 Hz
GB 0
PC 1.40
    
```

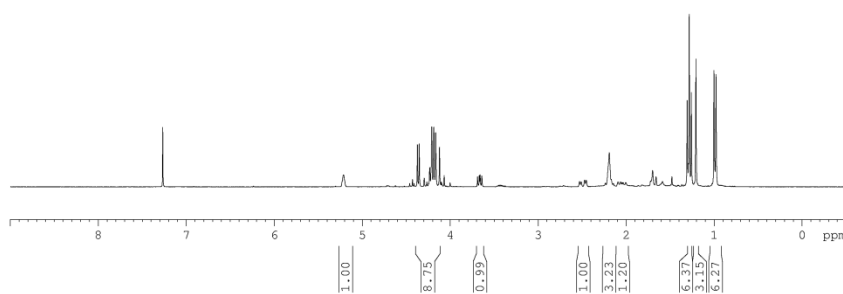


5.210
4.426
4.371
4.329
4.299
4.231
4.208
4.184
4.162
4.119
4.086
4.062
3.687
3.657
3.637
2.527
2.489
2.451
2.233
2.190
2.167
2.144
2.086
2.063
2.056
2.046
2.036
2.028
2.008
1.999
1.999
1.305
1.281
1.257
1.205
0.999
0.976



```

EXPNO 1
PROCNO 1
Date_ 20141127
Time 14.11
INSTRUM spect
PROBHD 5 mm PABBO BB-
PULPROG zg30
TD 65536
SOLVENT CDC13
NS 16
DS 2
SWH 6188.119 Hz
FIDRES 0.094423 Hz
AQ 5.2953587 sec
RG 203
DW 80.800 usec
DE 6.50 usec
TE 298.0 K
D1 1.0000000 sec
TDO 1
    
```



```

===== CHANNEL f1 =====
NUC1 1H
P1 13.70 usec
PL1 1.90 dB
PL1W 8.36853981 W
SFO1 300.1418335 MHz
SI 32768
SF 300.1400043 MHz
WDW EM
SSB 0
LB 0.30 Hz
GB 0
PC 1.00
    
```

171.00
170.95
140.86
115.07
81.22
68.18
60.67
60.41
60.33
36.01
34.09
30.98
21.23
20.88
14.00
13.96



```

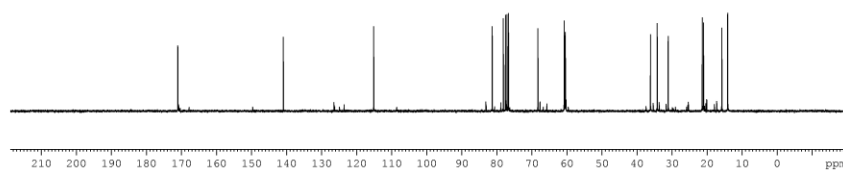
EXPNO 1
PROCNO 1
Date_ 20141127
Time 14.52
INSTRUM spect
PROBHD 5 mm PABBO BB-
PULPROG zgpg30
TD 65536
SOLVENT CDC13
NS 282
DS 4
SWH 18028.846 Hz
FIDRES 0.275098 Hz
AQ 1.8175818 sec
RG 203
DW 27.733 usec
DE 6.50 usec
TE 298.0 K
D1 2.0000000 sec
D11 0.0300000 sec
TDO 1
    
```

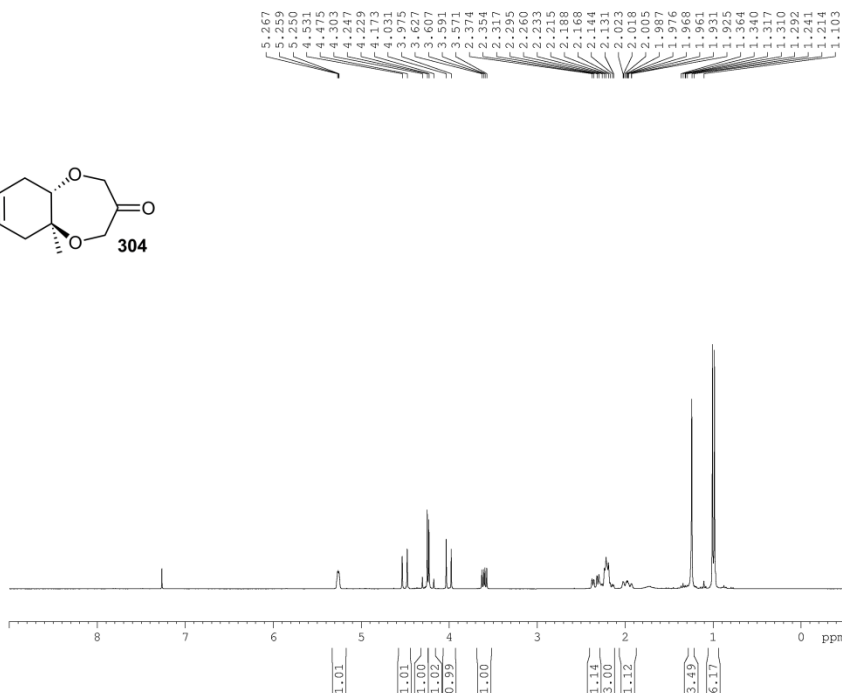
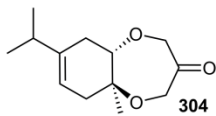
```

===== CHANNEL f1 =====
NUC1 13C
P1 10.82 usec
PL1 0.00 dB
PL1W 30.14263725 W
SFO1 75.4778101 MHz
    
```

```

===== CHANNEL f2 =====
CPDPRG2 waltz16
NUC2 1H
PCPD2 100.00 usec
PL2 1.90 dB
PL12 19.17 dB
PL13 23.94 dB
PL1W 8.36853981 W
PL12W 0.15690966 W
PL13W 0.05231782 W
SFO2 300.1412006 MHz
SI 32768
SF 75.4702732 MHz
WDW EM
SSB 0
LB 1.00 Hz
GB 0
PC 1.40
    
```



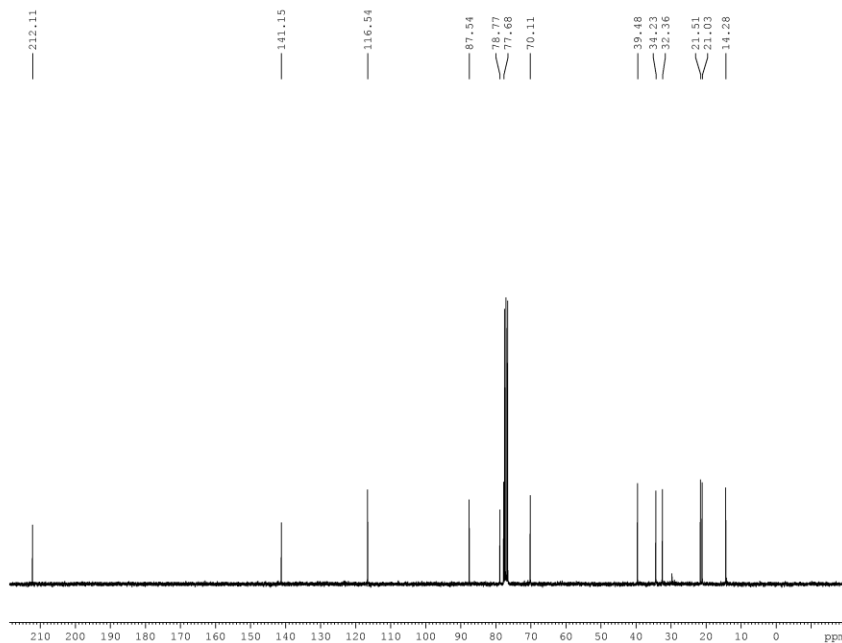


```

EXPNO 1
PROCNO 1
Date_ 20150225
Time 16.11
INSTRUM spect
PROBHD 5 mm PABBO BB-
PULPROG zg30
TD 65536
SOLVENT CDC13
NS 16
DS 2
SWH 6188.119 Hz
FIDRES 0.094423 Hz
AQ 5.2953587 sec
RG 64
DW 80.800 usec
DE 6.50 usec
TE 298.0 K
D1 1.0000000 sec
TDO 1
    
```

```

===== CHANNEL f1 =====
NUC1 1H
P1 13.70 usec
PL1 1.90 dB
PL1W 8.36853981 W
SFO1 300.1418335 MHz
SI 32768
SF 300.1400048 MHz
WDW EM
SSB 0
LB 0.30 Hz
GB 0
PC 1.00
    
```



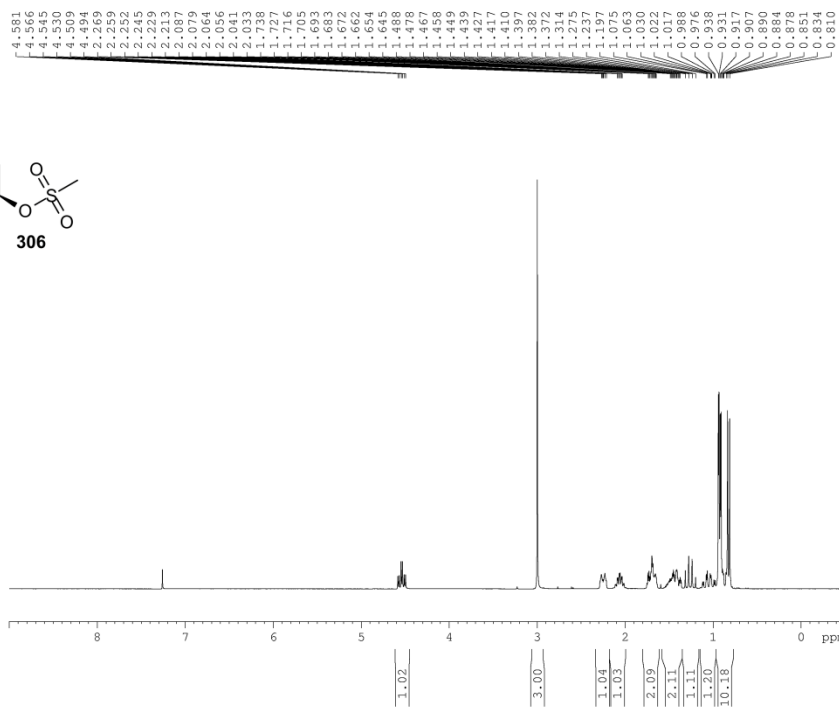
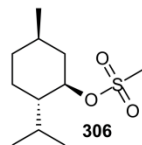
```

EXPNO 1
PROCNO 1
Date_ 20150226
Time 10.09
INSTRUM spect
PROBHD 5 mm PABBO BB-
PULPROG zgpg30
TD 65536
SOLVENT CDC13
NS 1024
DS 4
SWH 18028.846 Hz
FIDRES 0.275098 Hz
AQ 1.8175818 sec
RG 203
DW 27.733 usec
DE 6.50 usec
TE 298.0 K
D1 2.0000000 sec
D11 0.0300000 sec
TDO 1
    
```

```

===== CHANNEL f1 =====
NUC1 13C
P1 10.82 usec
PL1 0.00 dB
PL1W 30.14263725 W
SFO1 75.4778101 MHz

===== CHANNEL f2 =====
CPDPRG2 waltz16
NUC2 1H
PCPD2 100.00 usec
PL2 1.90 dB
PL12 19.17 dB
PL13 23.94 dB
PL2W 8.36853981 W
PL12W 0.15690966 W
PL13W 0.05231782 W
SFO2 300.1412006 MHz
SI 32768
SF 75.4702650 MHz
WDW EM
SSB 0
LB 1.00 Hz
GB 0
PC 1.40
    
```

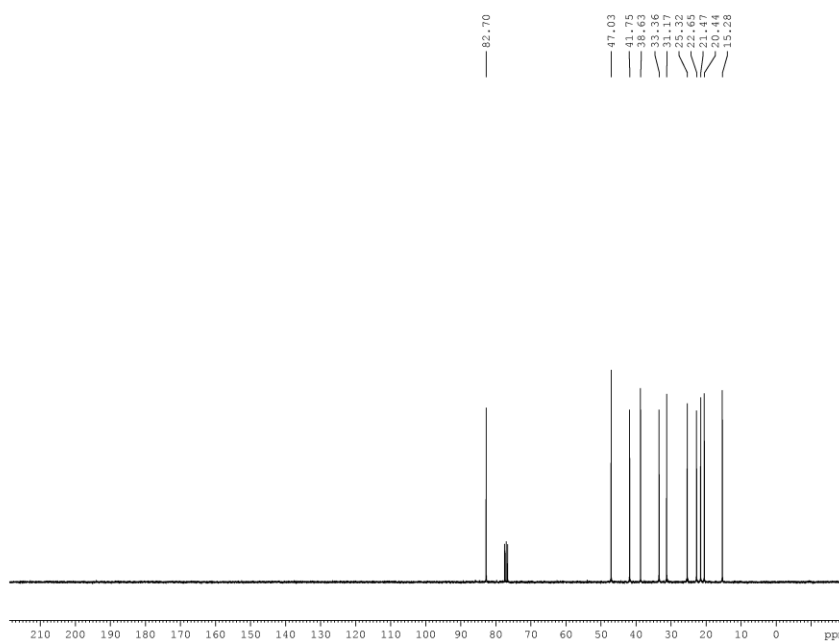


```

EXPNO 1
PROCNO 1
Date_ 20140822
Time 14.16
INSTRUM spect
PROBHD 5 mm PABBO BB-
PULPROG zg30
TD 65536
SOLVENT CDC13
NS 16
DS 2
SWH 6188.119 Hz
FIDRES 0.094423 Hz
AQ 5.2953587 sec
RG 57
DW 80.800 usec
DE 6.50 usec
TE 673.2 K
D1 1.0000000 sec
TDO 1
    
```

```

===== CHANNEL f1 =====
NUC1 1H
P1 13.70 usec
PL1 1.90 dB
PL1W 8.36853981 W
SF01 300.1418535 MHz
SI 32768
SF 300.1400064 MHz
WDW EM
SSB 0
LB 0.30 Hz
GB 0
PC 1.00
    
```



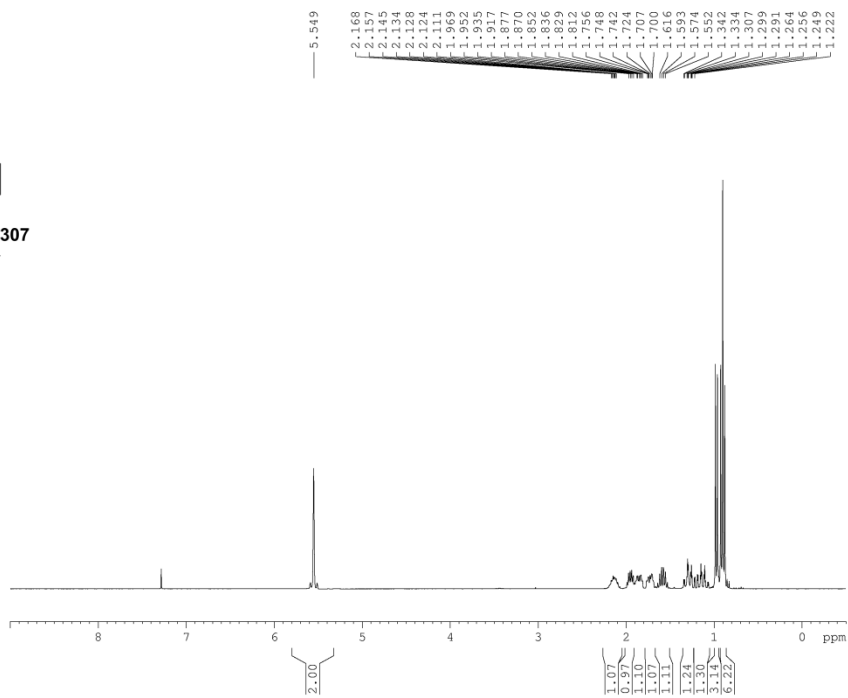
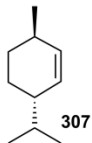
```

EXPNO 1
PROCNO 1
Date_ 20140822
Time 11.19
INSTRUM spect
PROBHD 5 mm PABBO BB-
PULPROG zgpg30
TD 65536
SOLVENT CDC13
NS 94
DS 4
SWH 18028.846 Hz
FIDRES 0.275098 Hz
AQ 1.8175818 sec
RG 203
DW 27.733 usec
DE 6.50 usec
TE 673.2 K
D1 2.0000000 sec
D11 0.0300000 sec
TDO 1
    
```

```

===== CHANNEL f1 =====
NUC1 13C
P1 10.82 usec
PL1 0.00 dB
PL1W 30.14263725 W
SF01 75.4778101 MHz

===== CHANNEL f2 =====
CPDPRG2 waltz16
NUC2 1H
PCPD2 100.00 usec
PL2 1.90 dB
PL12 19.17 dB
PL13 23.94 dB
PL2W 8.36853981 W
PL12W 0.15690966 W
PL13W 0.05231782 W
SF02 300.1412006 MHz
SI 32768
SF 75.4702867 MHz
WDW EM
SSB 0
LB 1.00 Hz
GB 0
PC 1.40
    
```

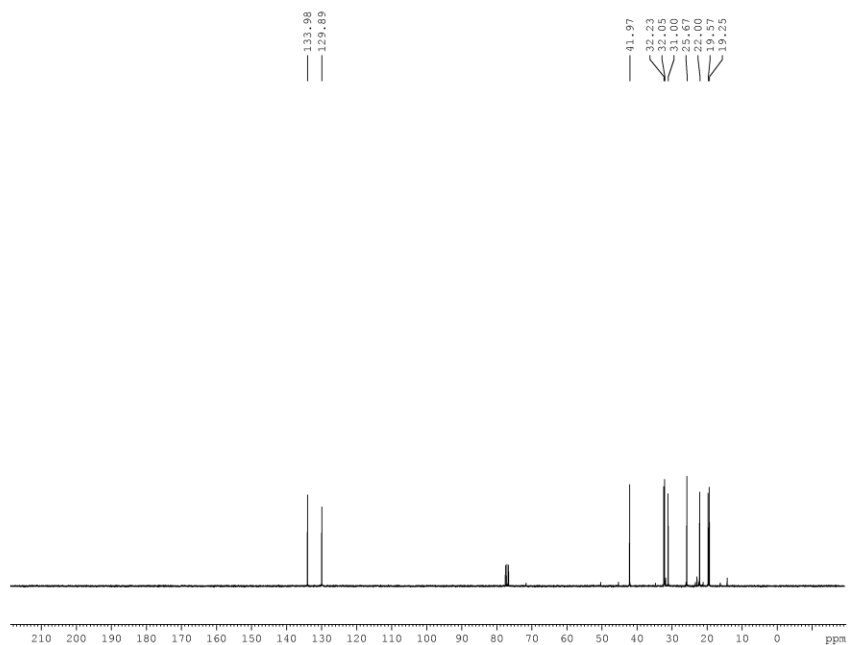


```

EXPNO 1
PROCNO 1
Date_ 20150304
Time 13.07
INSTRUM spect
PROBHD 5 mm PABBO BB-
PULPROG zg30
TD 65536
SOLVENT CDC13
NS 16
DS 2
SWH 6188.119 Hz
FIDRES 0.094423 Hz
AQ 5.2953587 sec
RG 64
DW 80.800 usec
DE 6.50 usec
TE 298.0 K
D1 1.0000000 sec
TDO 1
    
```

```

===== CHANNEL f1 =====
NUC1 1H
P1 13.70 usec
PL1 1.90 dB
PL1W 8.36853981 W
SFO1 300.1418535 MHz
SI 32768
SF 300.1399992 MHz
WDW EM
SSB 0
LB 0.30 Hz
GB 0
PC 1.00
    
```



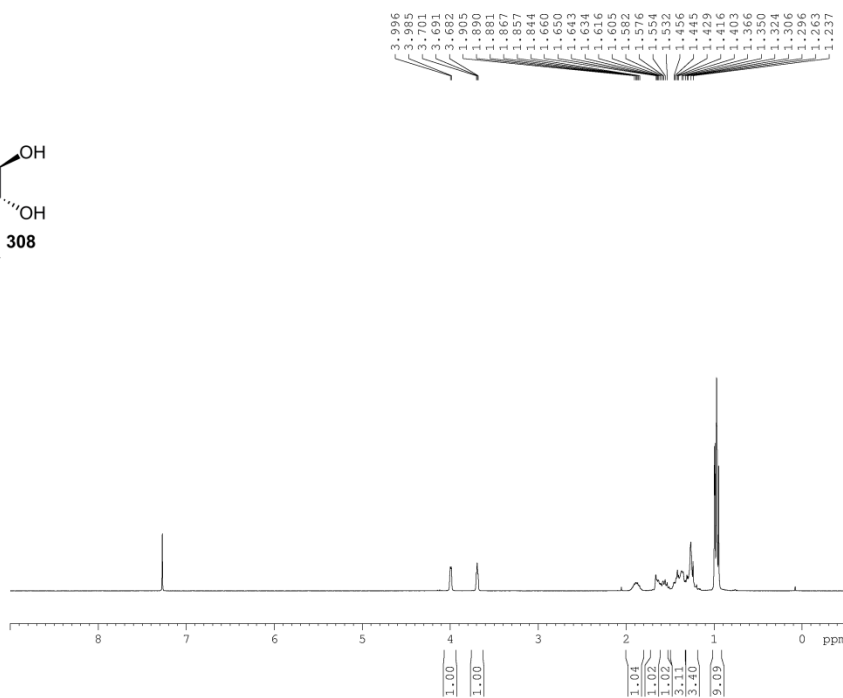
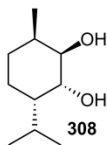
```

EXPNO 1
PROCNO 1
Date_ 20150304
Time 15.58
INSTRUM spect
PROBHD 5 mm PABBO BB-
PULPROG zgpg30
TD 65536
SOLVENT CDC13
NS 38
DS 4
SWH 18028.846 Hz
FIDRES 0.275098 Hz
AQ 1.8175818 sec
RG 203
DW 27.733 usec
DE 6.50 usec
TE 295.2 K
D1 2.0000000 sec
D11 0.0300000 sec
TDO 1
    
```

```

===== CHANNEL f1 =====
NUC1 13C
P1 10.82 usec
PL1 0.00 dB
PL1W 30.14263725 W
SFO1 75.4778101 MHz

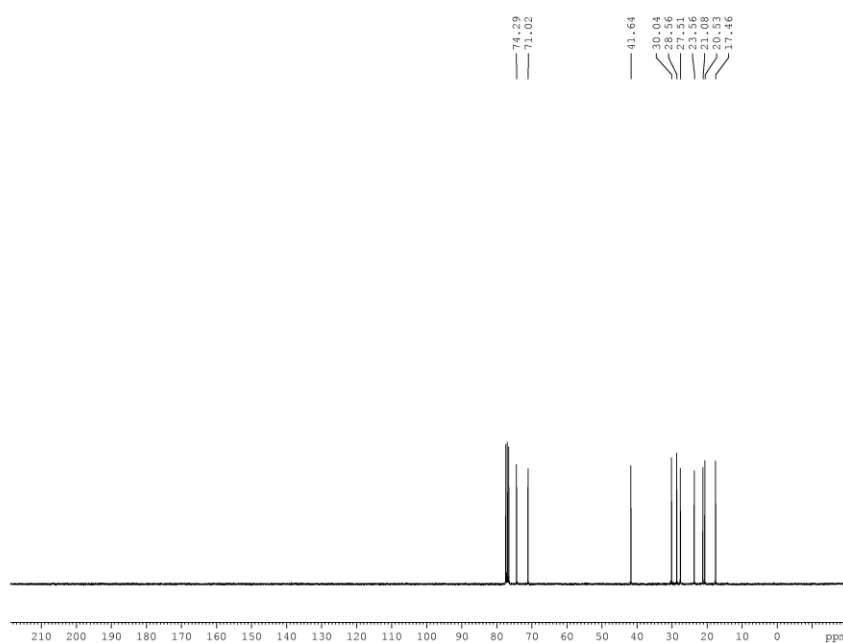
===== CHANNEL f2 =====
CPDPRG2 waltz16
NUC2 1H
PCPD2 100.00 usec
PL2 1.90 dB
PL12 19.17 dB
PL13 23.94 dB
PL2W 8.36853981 W
PL12W 0.15690966 W
PL13W 0.05231782 W
SFO2 300.1412006 MHz
SI 32768
SF 75.4702602 MHz
WDW EM
SSB 0
LB 1.00 Hz
GB 0
PC 1.40
    
```



```

EXPNO 3
PROCNO 1
Date_ 20141124
Time 12.24
INSTRUM spect
PROBHD 5 mm PABBO BB-
PULPROG zg30
TD 65536
SOLVENT CDCl3
NS 16
DS 2
SWH 6188.119 Hz
FIDRES 0.094423 Hz
AQ 5.2953587 sec
RG 203
DW 80.800 usec
DE 6.50 usec
TE 298.0 K
D1 1.0000000 sec
TDO 1

===== CHANNEL f1 =====
NUC1 1H
P1 13.70 usec
PL1 1.90 dB
PL1W 8.36853981 W
SFO1 300.1418535 MHz
SI 32768
SF 300.1400030 MHz
WDW EM
SSB 0
LB 0.30 Hz
GB 0
PC 1.00
    
```

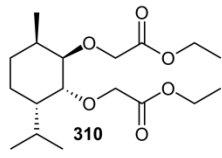
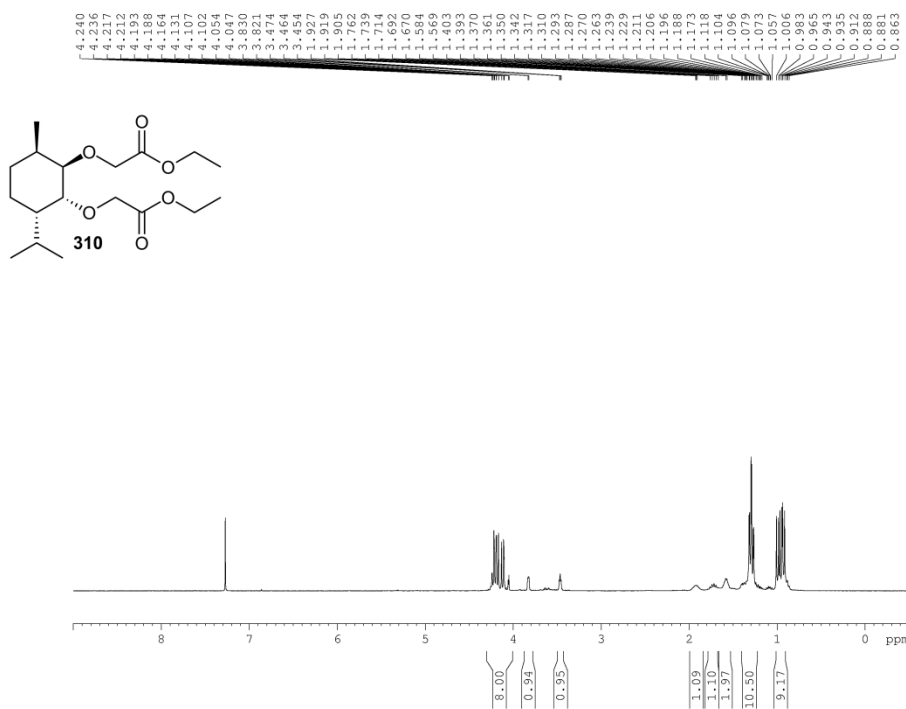


```

EXPNO 1
PROCNO 1
Date_ 20141124
Time 11.18
INSTRUM spect
PROBHD 5 mm PABBO BB-
PULPROG zgpg30
TD 65536
SOLVENT CDCl3
NS 800
DS 4
SWH 18028.846 Hz
FIDRES 0.275098 Hz
AQ 1.8175818 sec
RG 203
DW 27.733 usec
DE 6.90 usec
TE 298.1 K
D1 2.0000000 sec
D11 0.0300000 sec
TDO 1

===== CHANNEL f1 =====
NUC1 13C
P1 10.82 usec
PL1 0.00 dB
PL1W 30.14263725 W
SFO1 75.4778101 MHz

===== CHANNEL f2 =====
CPDPRG2 waltz16
NUC2 1H
PCPD2 100.00 usec
PL2 1.90 dB
PL12 19.17 dB
PL13 23.94 dB
PL2W 8.36853981 W
PL12W 0.15690966 W
PL13W 0.05231782 W
SFO2 300.1412006 MHz
SI 32768
SF 75.4702712 MHz
WDW EM
SSB 0
LB 1.00 Hz
GB 0
PC 1.40
    
```

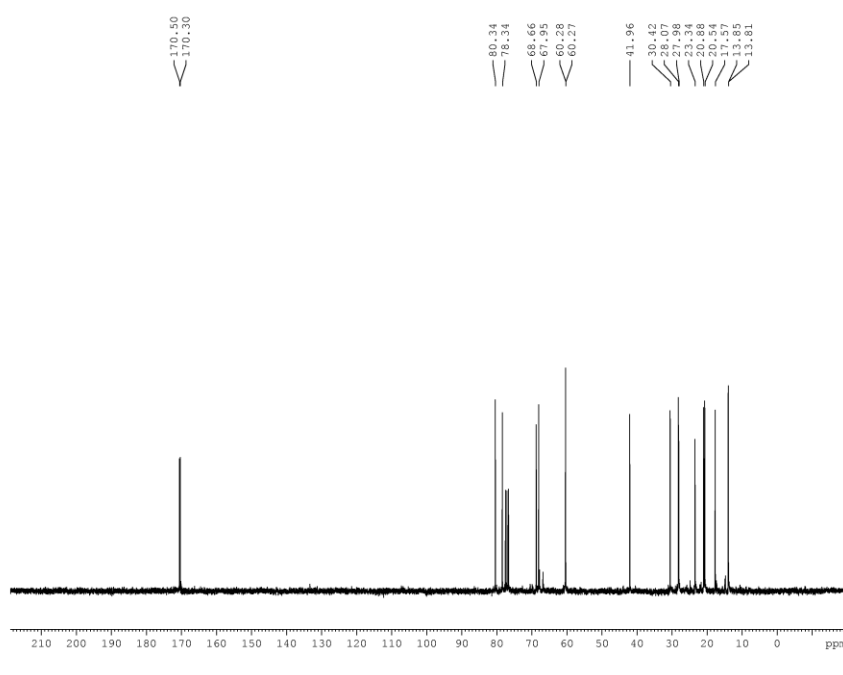


```

EXPNO 1
PROCNO 1
Date_ 20150213
Time 10.00
INSTRUM spect
PROBHD 5 mm PABBO BB-
PULPROG zg30
TD 65536
SOLVENT CDC13
NS 16
DS 2
SWH 6188.119 Hz
FIDRES 0.094423 Hz
AQ 5.2953587 sec
RG 203
DW 80.800 usec
DE 6.50 usec
TE 294.8 K
D1 1.0000000 sec
TDO 1
    
```

```

===== CHANNEL f1 =====
NUC1 1H
P1 13.70 usec
PL1 1.90 dB
PL1W 8.36853981 W
SF01 300.1418335 MHz
SI 32768
SF 300.1400030 MHz
WDW EM
SSB 0
LB 0.30 Hz
GB 0
PC 1.00
    
```



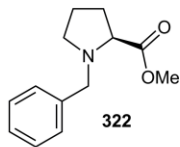
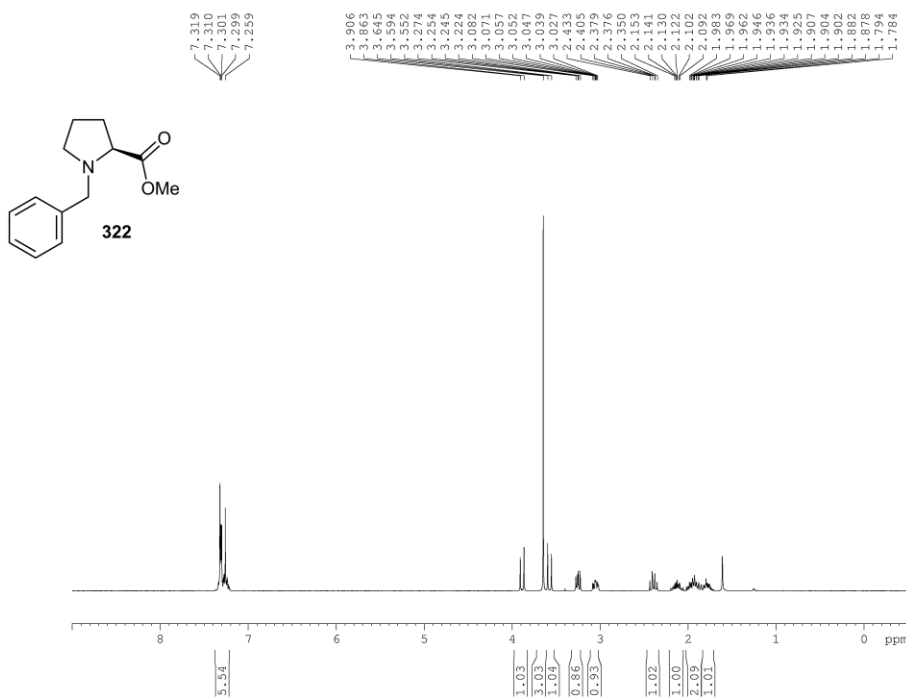
```

EXPNO 1
PROCNO 1
Date_ 20150210
Time 16.29
INSTRUM spect
PROBHD 5 mm PABBO BB-
PULPROG zgpg30
TD 65536
SOLVENT CDC13
NS 39
DS 4
SWH 18028.846 Hz
FIDRES 0.275098 Hz
AQ 1.8175818 sec
RG 203
DW 27.733 usec
DE 6.50 usec
TE 294.5 K
D1 2.0000000 sec
D11 0.0300000 sec
TDO 1
    
```

```

===== CHANNEL f1 =====
NUC1 13C
P1 10.82 usec
PL1 0.00 dB
PL1W 30.14263728 W
SF01 75.4778101 MHz

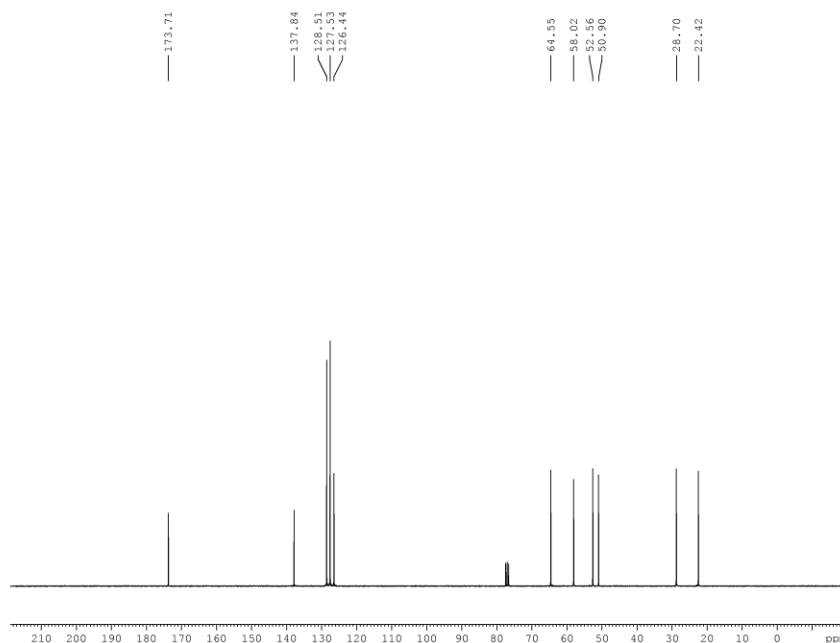
===== CHANNEL f2 =====
CPDPRG2 waltz16
NUC2 1H
PCPD2 100.00 usec
PL2 1.90 dB
PL12 19.17 dB
PL13 23.94 dB
PL1W 8.36853981 W
PL12W 0.15690966 W
PL13W 0.05231782 W
SF02 300.1412006 MHz
SI 32768
SF 75.4702779 MHz
WDW EM
SSB 0
LB 1.00 Hz
GB 0
PC 1.40
    
```



```

EXPNO 1
PROCNO 1
Date_ 20120319
Time 19.23
INSTRUM spect
PROBHD 5 mm PABBO BB-
PULPROG zg30
TD 65536
SOLVENT CDCl3
NS 32
DS 2
SWH 6188.119 Hz
FIDRES 0.094423 Hz
AQ 5.295387 sec
RG 114
DW 80.800 usec
DE 6.50 usec
TE 298.0 K
D1 1.0000000 sec
TDO 1

===== CHANNEL f1 =====
NUC1 1H
P1 13.70 usec
PL1 1.90 dB
PL1W 8.36853981 W
SF01 300.1418535 MHz
SI 32768
SF 300.1400058 MHz
WDW EM
SSB 0
LB 0.30 Hz
GB 0
PC 1.00
    
```

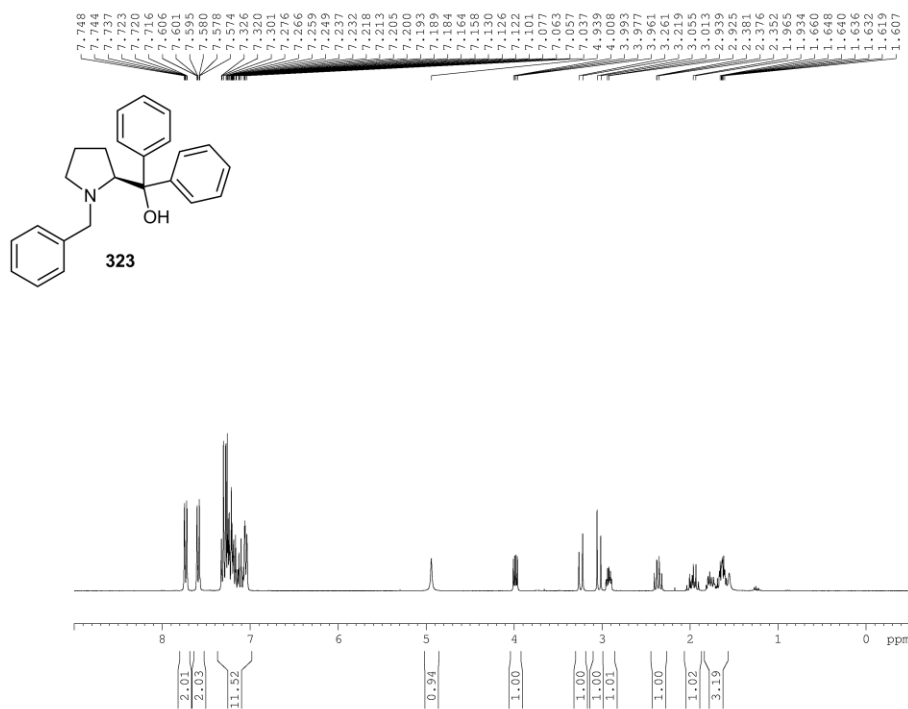


```

EXPNO 2
PROCNO 1
Date_ 20120319
Time 19.31
INSTRUM spect
PROBHD 5 mm PABBO BB-
PULPROG zgpg30
TD 65536
SOLVENT CDCl3
NS 136
DS 4
SWH 18028.846 Hz
FIDRES 0.275098 Hz
AQ 1.8175818 sec
RG 203
DW 27.733 usec
DE 6.50 usec
TE 298.0 K
D1 2.0000000 sec
D11 0.0300000 sec
TDO 1

===== CHANNEL f1 =====
NUC1 13C
P1 10.82 usec
PL1 0.00 dB
PL1W 30.14263725 W
SF01 75.4778101 MHz

===== CHANNEL f2 =====
CPDPRG2 waltz16
NUC2 1H
PCPD2 100.00 usec
PL2 1.90 dB
PL12 19.17 dB
PL13 23.94 dB
PL1W 8.36853981 W
PL12W 0.15690966 W
PL13W 0.05231782 W
SF02 300.1412006 MHz
SI 32768
SF 75.4703040 MHz
WDW EM
SSB 0
LB 1.00 Hz
GB 0
PC 1.40
    
```

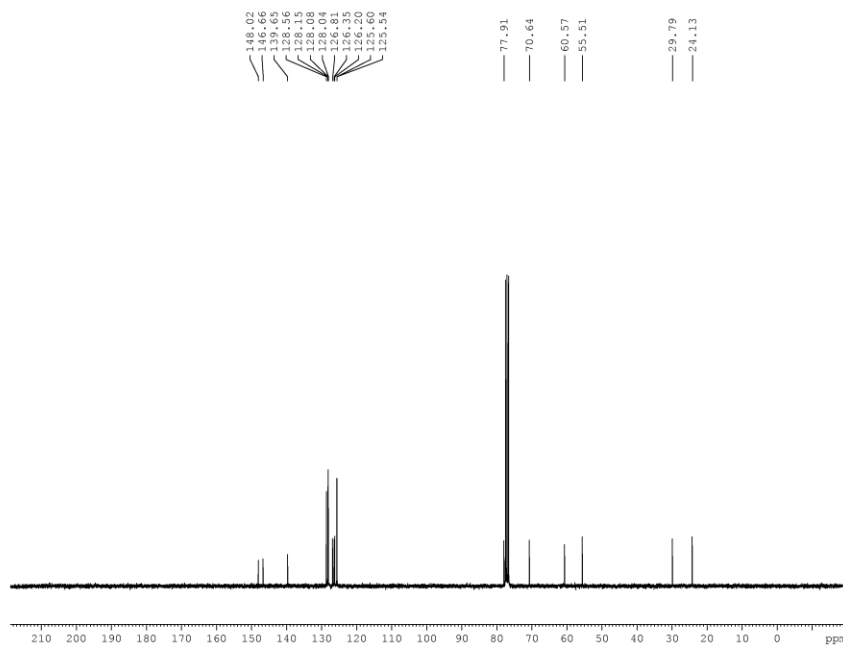


```

EXPNO          3
PROCNO         1
Date_          20120402
Time           15.19
INSTRUM       spect
PROBHD        5 mm PABBO BB-
PULPROG       zg30
TD            65536
SOLVENT       CDCl3
NS            64
DS            2
SWH           6188.119 Hz
FIDRES        0.094423 Hz
AQ           5.295387 sec
RG            101
DW            80.800 usec
DE            6.50 usec
TE            298.0 K
D1            1.0000000 sec
TDO           1
    
```

```

===== CHANNEL f1 =====
NUC1          1H
P1            13.70 usec
PL1           1.90 dB
PL1W          8.36853981 W
SF01          300.1418535 MHz
SI            32768
SF            300.1400057 MHz
WDW           EM
SSB           0
LB            0.30 Hz
GB            0
PC            1.00
    
```



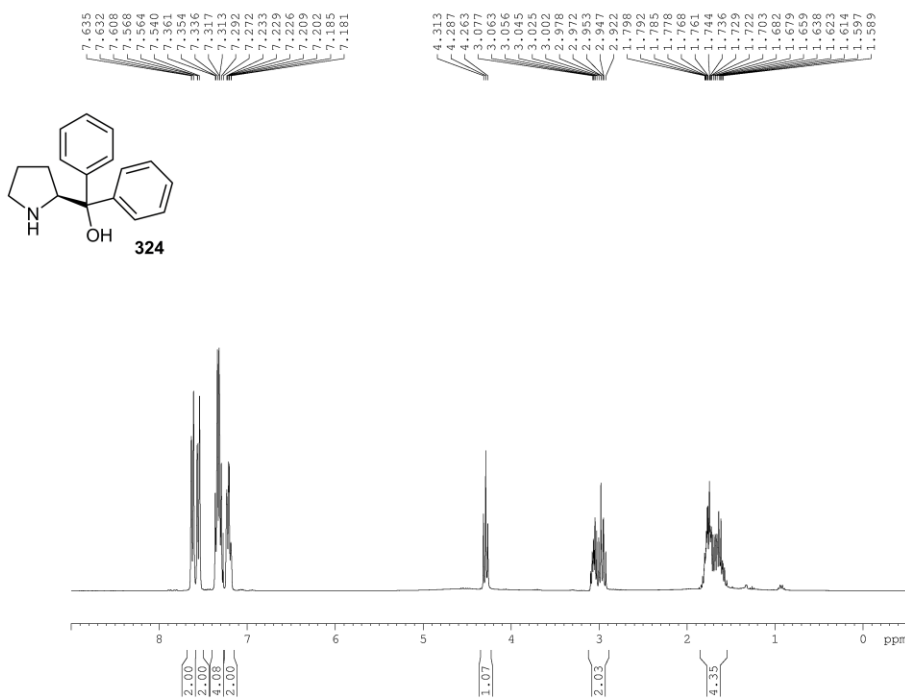
```

EXPNO          2
PROCNO         1
Date_          20120402
Time           14.46
INSTRUM       spect
PROBHD        5 mm PABBO BB-
PULPROG       zgpg30
TD            65536
SOLVENT       CDCl3
NS            1024
DS            4
SWH           18028.846 Hz
FIDRES        0.275098 Hz
AQ           1.8175818 sec
RG            203
DW            27.733 usec
DE            6.50 usec
TE            298.0 K
D1            2.0000000 sec
D11           0.03000000 sec
TDO           1
    
```

```

===== CHANNEL f1 =====
NUC1          13C
P1            10.82 usec
PL1           0.00 dB
PL1W          30.14263725 W
SF01          75.4778101 MHz

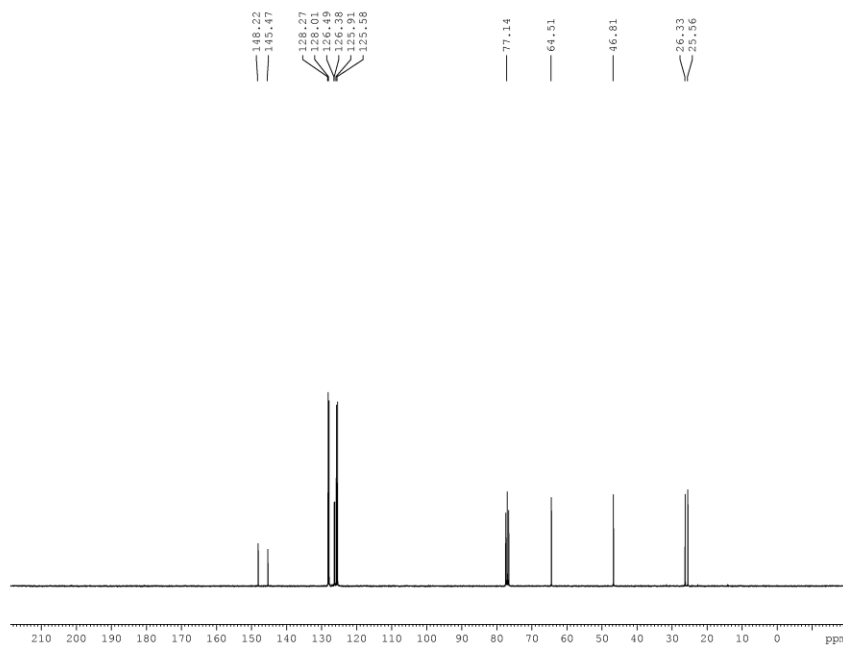
===== CHANNEL f2 =====
CPDPRG2       waltz16
NUC2          1H
PCPD2         100.00 usec
PL2           1.90 dB
PL12          19.17 dB
PL13          23.94 dB
PL1W          8.36853981 W
PL12W         0.15690966 W
PL13W         0.05231782 W
SF02          300.1412006 MHz
SI            32768
SF            75.4702662 MHz
WDW           EM
SSB           0
LB            1.00 Hz
GB            0
PC            1.40
    
```



```

EXPNO 1
PROCNO 1
Date_ 20120508
Time 10.05
INSTRUM spect
PROBHD 5 mm PABBO BB-
PULPROG zg30
TD 65536
SOLVENT CDCl3
NS 64
DS 2
SWH 6188.119 Hz
FIDRES 0.094423 Hz
AQ 5.295387 sec
RG 40.3
DW 80.800 usec
DE 6.50 usec
TE 294.7 K
D1 1.0000000 sec
TDO 1

===== CHANNEL f1 =====
NUC1 1H
P1 13.70 usec
PL1 1.90 dB
PL1W 8.36853981 W
SF01 300.1418535 MHz
SI 32768
SF 300.1400018 MHz
WDW EM
SSB 0
LB 0.30 Hz
GB 0
PC 1.00
    
```

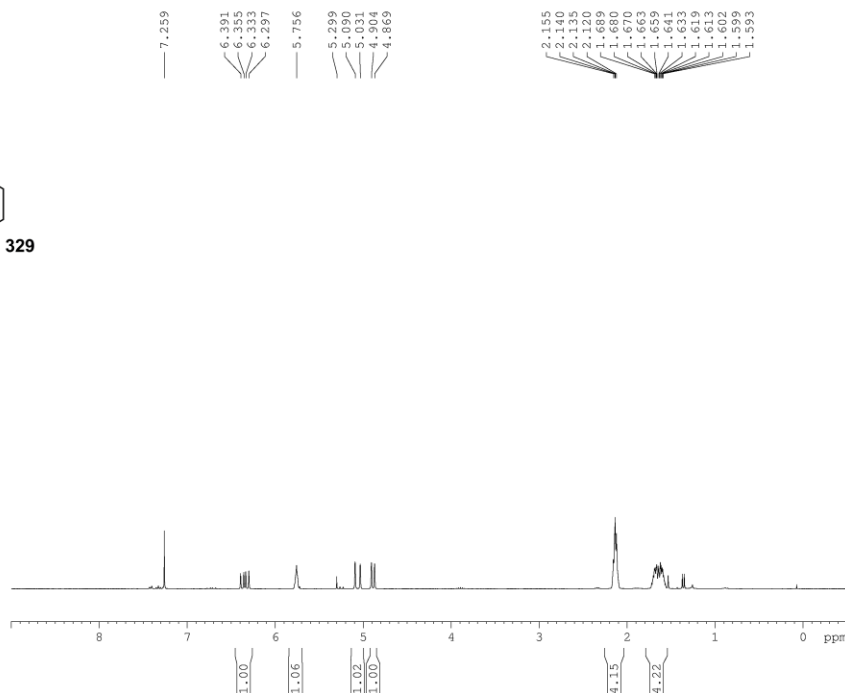
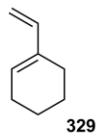


```

EXPNO 1
PROCNO 1
Date_ 20120508
Time 11.13
INSTRUM spect
PROBHD 5 mm PABBO BB-
PULPROG zgpg30
TD 65536
SOLVENT CDCl3
NS 1024
DS 4
SWH 18028.846 Hz
FIDRES 0.275098 Hz
AQ 1.8175818 sec
RG 203
DW 27.733 usec
DE 6.50 usec
TE 295.2 K
D1 2.0000000 sec
D11 0.0300000 sec
TDO 1

===== CHANNEL f1 =====
NUC1 13C
P1 10.82 usec
PL1 0.00 dB
PL1W 30.14263725 W
SF01 75.4778101 MHz

===== CHANNEL f2 =====
CPDPRG2 waltz16
NUC2 1H
PCPD2 100.00 usec
PL2 1.90 dB
PL12 19.17 dB
PL13 23.94 dB
PL1W 8.36853981 W
PL12W 0.15690966 W
PL13W 0.05231782 W
SF02 300.1412006 MHz
SI 32768
SF 75.4702756 MHz
WDW EM
SSB 0
LB 1.00 Hz
GB 0
PC 1.40
    
```

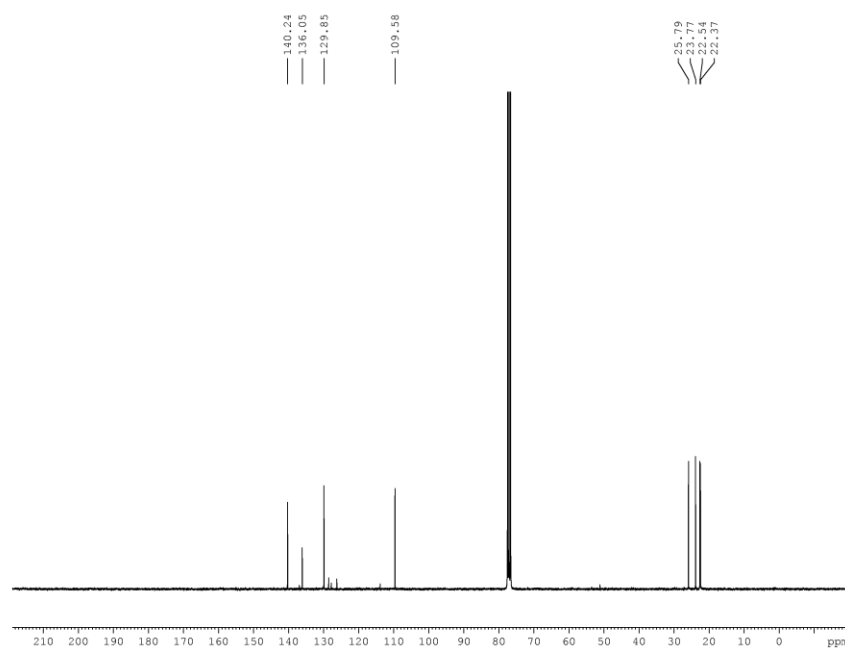



```

EXPNO 1
PROCNO 1
Date_ 20121130
Time 17.10
INSTRUM spect
PROBHD 5 mm PABBO BB-
PULPROG zg30
TD 65536
SOLVENT CDC13
NS 32
DS 2
SWH 6188.119 Hz
FIDRES 0.094423 Hz
AQ 5.2953987 sec
RG 128
DW 80.800 usec
DE 6.50 usec
TE 298.0 K
D1 1.0000000 sec
TDO 1
    
```

```

===== CHANNEL f1 =====
NUC1 1H
P1 13.70 usec
PL1 1.90 dB
PL1W 8.36853981 W
SF01 300.1418535 MHz
SI 32768
SF 300.1400060 MHz
WDW EM
SSB 0
LB 0.30 Hz
GB 0
PC 1.00
    
```



```

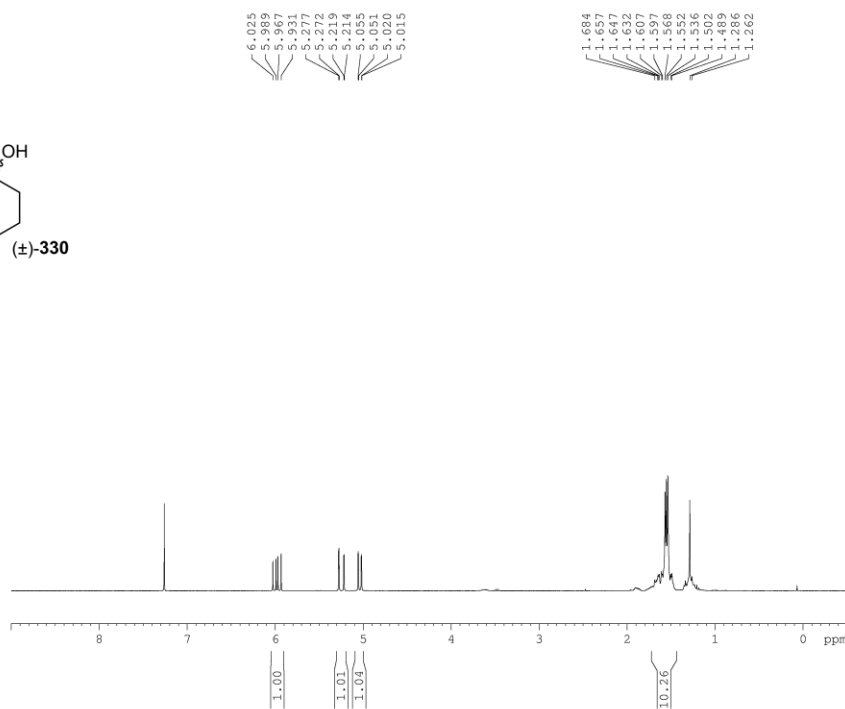
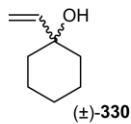
EXPNO 1
PROCNO 1
Date_ 20121130
Time 17.17
INSTRUM spect
PROBHD 5 mm PABBO BB-
PULPROG zgpg30
TD 65536
SOLVENT CDC13
NS 18000
DS 4
SWH 18028.846 Hz
FIDRES 0.275098 Hz
AQ 1.8175818 sec
RG 203
DW 27.733 usec
DE 6.50 usec
TE 298.0 K
D1 2.0000000 sec
D11 0.0300000 sec
TDO 1
    
```

```

===== CHANNEL f1 =====
NUC1 13C
P1 10.82 usec
PL1 0.00 dB
PL1W 30.14263725 W
SF01 75.4778101 MHz
    
```

```

===== CHANNEL f2 =====
CPDPRG2 waltz16
NUC2 1H
PCPD2 100.00 usec
PL2 1.90 dB
PL12 19.17 dB
PL13 23.94 dB
PL1W 8.36853981 W
PL12W 0.15690966 W
PL13W 0.05231782 W
SF02 300.1412006 MHz
SI 32768
SF 75.4702633 MHz
WDW EM
SSB 0
LB 1.00 Hz
GB 0
PC 1.40
    
```

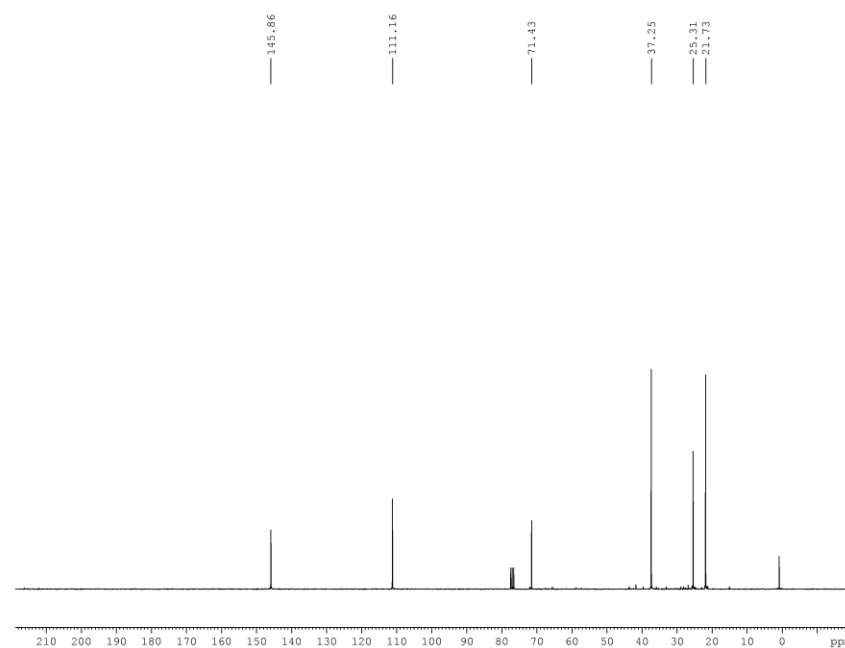


```

EXPNO 1
PROCNO 1
Date_ 20120726
Time 13.58
INSTRUM spect
PROBHD 5 mm PABBO BB-
PULPROG zg30
TD 65536
SOLVENT CDCl3
NS 25
DS 2
SWH 6188.119 Hz
FIDRES 0.094423 Hz
AQ 5.2953897 sec
RG 203
DW 80.800 usec
DE 6.50 usec
TE 298.0 K
D1 1.0000000 sec
TDO 1
    
```

```

===== CHANNEL f1 =====
NUC1 1H
P1 13.70 usec
PL1 1.90 dB
PL1W 8.36853981 W
SF01 300.1418535 MHz
SI 32768
SF 300.1400058 MHz
WDW EM
SSB 0
LB 0.30 Hz
GB 0
PC 1.00
    
```



```

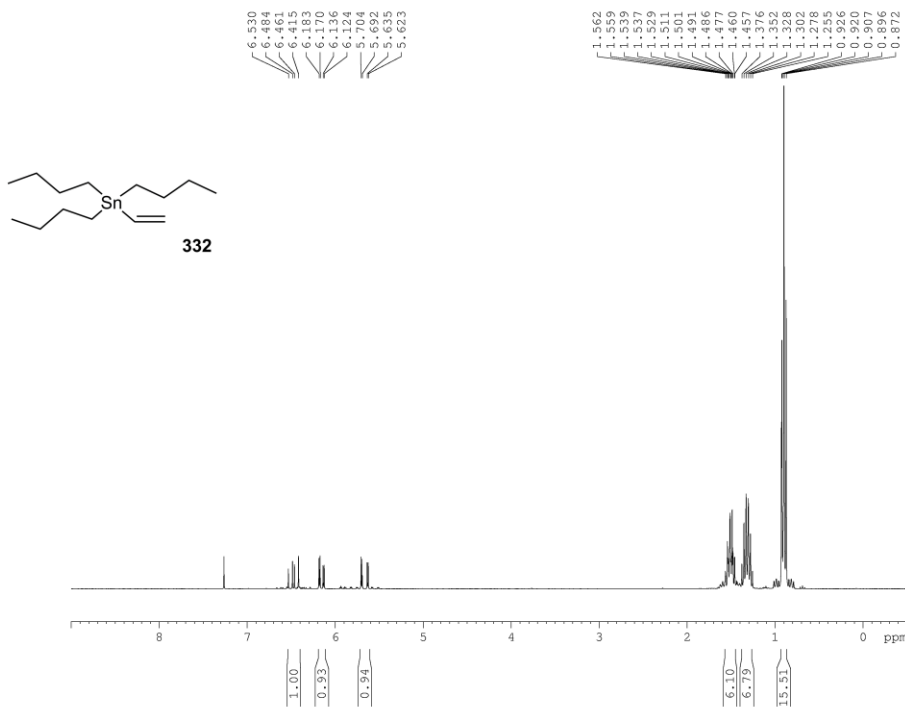
EXPNO 1
PROCNO 1
Date_ 20120626
Time 13.32
INSTRUM spect
PROBHD 5 mm PABBO BB-
PULPROG zgpg30
TD 65536
SOLVENT CDCl3
NS 631
DS 4
SWH 18028.846 Hz
FIDRES 0.275098 Hz
AQ 1.8175818 sec
RG 203
DW 27.733 usec
DE 6.50 usec
TE 298.1 K
D1 2.0000000 sec
D11 0.0300000 sec
TDO 1
    
```

```

===== CHANNEL f1 =====
NUC1 13C
P1 10.82 usec
PL1 0.00 dB
PL1W 30.14263725 W
SF01 75.4778101 MHz
    
```

```

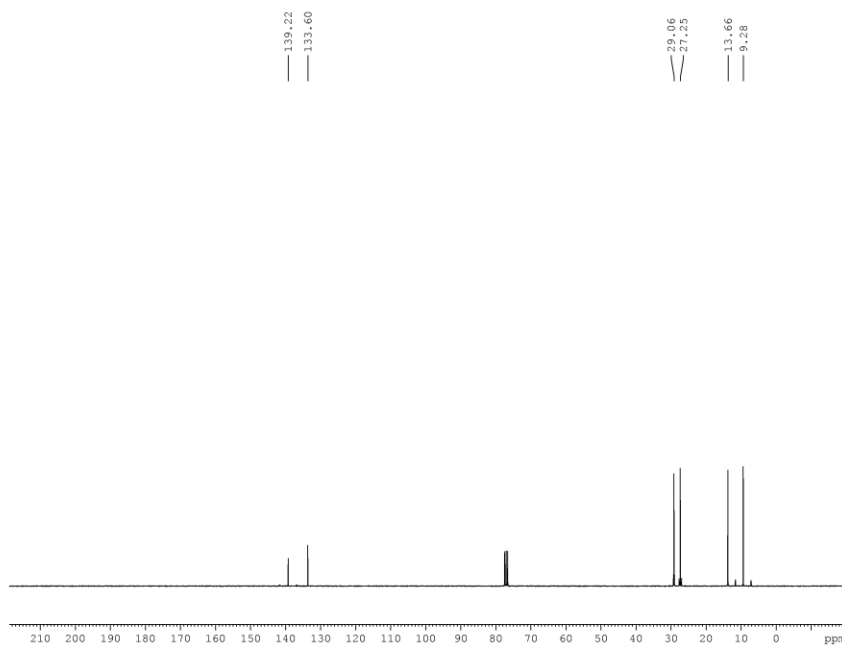
===== CHANNEL f2 =====
CPDPRG2 waltz16
NUC2 1H
PCPD2 100.00 usec
PL2 1.90 dB
PL12 19.17 dB
PL13 23.94 dB
PL1W 8.36853981 W
PL12W 0.15690966 W
PL13W 0.05231782 W
SF02 300.1412006 MHz
SI 32768
SF 75.4702774 MHz
WDW EM
SSB 0
LB 1.00 Hz
GB 0
PC 1.40
    
```



```

EXPNO 1
PROCNO 1
Date_ 20120729
Time 16.12
INSTRUM spect
PROBHD 5 mm PABBO BB-
PULPROG zg30
TD 65536
SOLVENT CDCl3
NS 16
DS 2
SWH 6188.119 Hz
FIDRES 0.094423 Hz
AQ 5.295387 sec
RG 64
DW 80.800 usec
DE 6.50 usec
TE 298.0 K
D1 1.0000000 sec
TDO 1

===== CHANNEL f1 =====
NUC1 1H
P1 13.70 usec
PL1 1.90 dB
PL1W 8.36853981 W
SF01 300.1418535 MHz
SI 32768
SF 300.1400049 MHz
WDW EM
SSB 0
LB 0.30 Hz
GB 0
PC 1.00
    
```

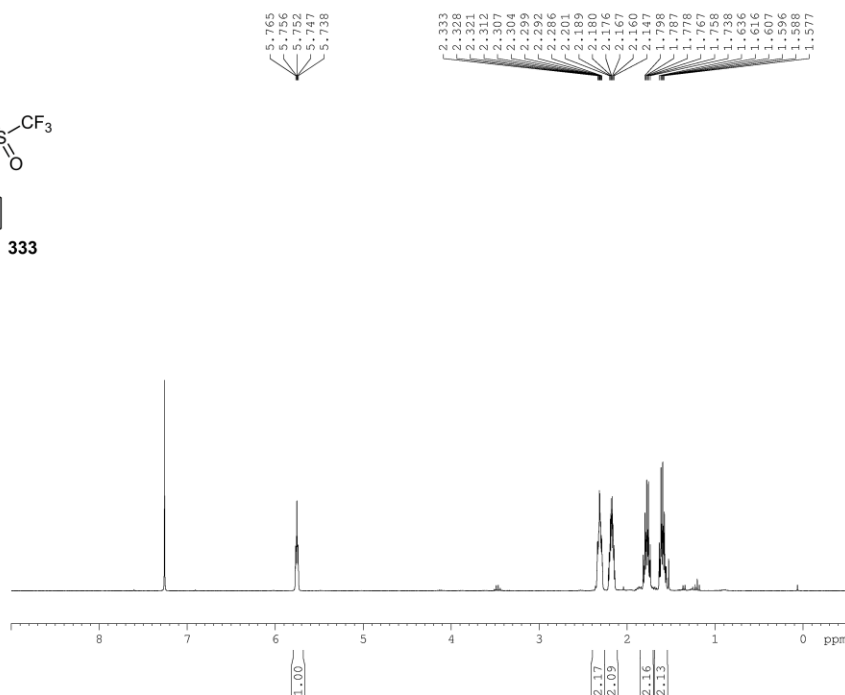
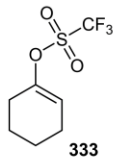


```

EXPNO 1
PROCNO 1
Date_ 20120729
Time 17.17
INSTRUM spect
PROBHD 5 mm PABBO BB-
PULPROG zgpg30
TD 65536
SOLVENT CDCl3
NS 930
DS 4
SWH 18028.846 Hz
FIDRES 0.275098 Hz
AQ 1.8175818 sec
RG 203
DW 27.733 usec
DE 6.50 usec
TE 298.0 K
D1 2.0000000 sec
D11 0.0300000 sec
TDO 1

===== CHANNEL f1 =====
NUC1 13C
P1 10.82 usec
PL1 0.00 dB
PL1W 30.14263725 W
SF01 75.4778101 MHz

===== CHANNEL f2 =====
CPDPRG2 waltz16
NUC2 1H
PCPD2 100.00 usec
PL2 1.90 dB
PL12 19.17 dB
PL13 23.94 dB
PL1W 8.36853981 W
PL12W 0.15690966 W
PL13W 0.05231782 W
SF02 300.1412006 MHz
SI 32768
SF 75.4702647 MHz
WDW EM
SSB 0
LB 1.00 Hz
GB 0
PC 1.40
    
```

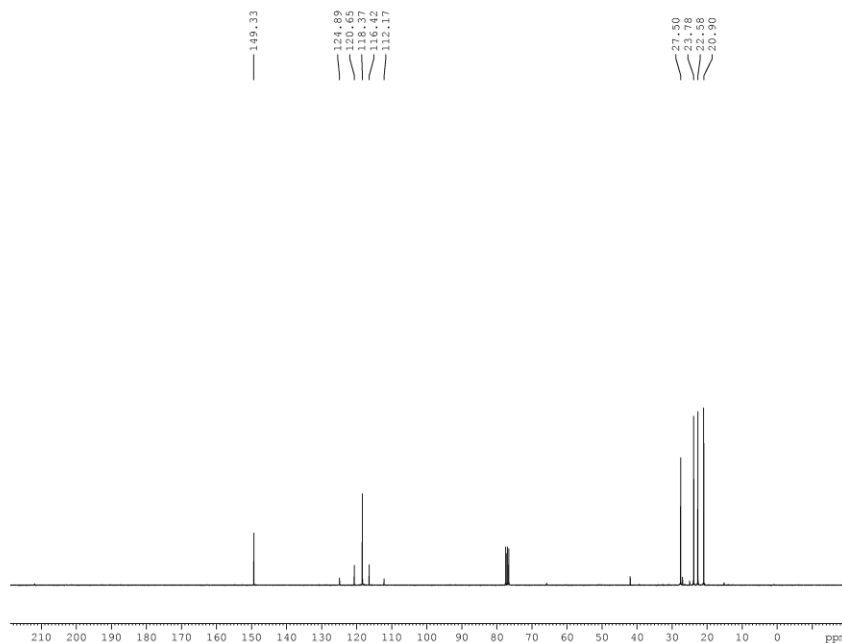


```

EXPNO 1
PROCNO 1
Date_ 20120817
Time 14.58
INSTRUM spect
PROBHD 5 mm PABBO BB-
PULPROG zg30
TD 65536
SOLVENT CDC13
NS 32
DS 2
SWH 6188.119 Hz
FIDRES 0.094423 Hz
AQ 5.2953587 sec
RG 203
DW 80.800 usec
DE 6.50 usec
TE 298.0 K
D1 1.00000000 sec
TDO 1
    
```

```

===== CHANNEL f1 =====
NUC1 1H
P1 13.70 usec
PLL 1.90 dB
PL1W 8.36853981 W
SFO1 300.1418535 MHz
SI 32768
SF 300.1400069 MHz
WDW EM
SSB 0
LB 0.30 Hz
GB 0
PC 1.00
    
```



```

EXPNO 1
PROCNO 1
Date_ 20120817
Time 16.12
INSTRUM spect
PROBHD 5 mm PABBO BB-
PULPROG zgpg30
TD 65536
SOLVENT CDC13
NS 1024
DS 4
SWH 18028.846 Hz
FIDRES 0.275098 Hz
AQ 1.8175818 sec
RG 203
DW 27.733 usec
DE 6.50 usec
TE 298.0 K
D1 2.00000000 sec
D11 0.03000000 sec
TDO 1
    
```

```

===== CHANNEL f1 =====
NUC1 13C
P1 10.82 usec
PL1 0.00 dB
PL1W 30.14263725 W
SFO1 75.4778101 MHz

===== CHANNEL f2 =====
CPDPRG2 waltz16
NUC2 1H
PCPD2 100.00 usec
PL2 1.90 dB
PL12 19.17 dB
PL13 23.94 dB
PL2W 8.36853981 W
PL12W 0.15690966 W
PL13W 0.05231782 W
SFO2 300.1412006 MHz
SI 32768
SF 75.4702628 MHz
WDW EM
SSB 0
LB 1.00 Hz
GB 0
PC 1.40
    
```